**Medical Radiology · Diagnostic Imaging**
*Series Editors:* H.-U. Kauczor · H. Hricak · M. Knauth

Samuel Stafrace
Johan G. (Hans) Blickman *Editors*

# Radiological Imaging of the Digestive Tract in Infants and Children

*Second Edition*

Springer

# Medical Radiology

## Diagnostic Imaging



For further volumes:
http://www.springer.com/series/4354

Samuel Stafrace • Johan G. (Hans) Blickman
Editors

# Radiological Imaging of the Digestive Tract in Infants and Children

Second Edition

Springer

*Editors*
Samuel Stafrace
Department of Radiology
Sidra Medical and Research Center
Doha
Qatar

Johan G. (Hans) Blickman
Radiologist-in-Chief
Golisano Childrens Hospital, URMC
Rochester, NY
USA

ISSN 0942-5373 ISSN 2197-4187 (electronic)
Medical Radiology
ISBN 978-3-319-18433-3 ISBN 978-3-319-18434-0 (eBook)
DOI 10.1007/978-3-319-18434-0

Library of Congress Control Number: 2016944465



Printed on acid-free paper

This Springer imprint is published by Springer Nature
The registered company is Springer International Publishing AG Switzerland

# Preface

As a pediatric radiologist, I often meet clinical colleagues who "just don't get it": who do not seem to see the cardinal differences involved when investigating and treating the next generation(s). This may be a fact of life that I have learnt to accept but as a pediatric radiologist brings the added responsibility of highlighting that children are different at every occasion possible: simply not small adults!

This second edition of *Diagnostic Imaging: Radiological Imaging of the Digestive Tract in Infants and Children* hopefully brings this across. It is targeted to generalists and specialists alike – although it is not exhaustive, it offers a broad practical approach to the clinical diagnostic issues encountered.

In the second edition, the number of chapters has been extended. After a brief chapter on modalities, the next couple of chapters target the emergency conditions encountered in infants and young children. The remaining chapters then follow a more traditional anatomical division. A practical chapter on interventional techniques completes the project.

Newer chapters brought along a good number of new authors: specifically picked from different parts of the world and of different professional stature. This surely adds to the variety offered and gives the completed book a more international reach. We have to thank each and every colleague and friend who have put in time to bring this together. I am very grateful especially for sharing the rare pathologies they encounter in their respective practices to broaden our knowledge base.

Chapters can now be acquired and downloaded individually. In view of this, we have tried our best to make each chapter a "stand alone." This surely resulted in some overlap – and occasionally some challenging ideas by different authors. We have chosen to leave this and see this as a strength of the project – allowing different experienced colleagues to share their interpretations of their personal experiences backed by the published literature.

Finally on a personal level:

When approached by my good friend Rick van Rijn to introduce me to Hans about this project, I have to admit I was delighted. I felt honored to the prospect of working with Hans and more so of being asked to lead this. Hans did warn that this is like building a new house or department – "twice as

expensive and twice as long!" His experience in such projects had surely nailed this equation. Hans – it has been such a pleasure!

Finally, I cannot but thank my immediate family – Mandy, Maya, and Elena. The time opportunity cost of a book project is very large – and the family is the one who pays for this. Your understanding and sacrifice humbles me.

Enjoy the book.

Doha, Qatar Sam Stafrace

To me, the most important part of being the senior author of any academic writing endeavor is to have the distinct pleasure of seeing the next generations of pediatric imagers grow and mature. Throughout my career, I have relished the joy and satisfaction of sharing an idea, nurturing the project, mentoring the colleagues in question, and finally rejoicing in the final "product."

When I was asked to undertake a second edition of *Diagnostic Imaging: Radiological Imaging of the Digestive Tract in Infants and Children*, I must confess to a less than enthusiastic reaction. Especially as our jobs have gotten busier, our academic time has shrunk and it was difficult to conceive of once more marshaling the energy to set up, manage, and complete such a project.

As mentioned above, our wonderful colleague (and my mentoree) Prof. Rick van Rijn would not hear of such drivel and suggested I contact Dr. Sam Stafrace, whom he described as a young and energetic colleague who would "surely jump at the chance!"

The result is before you. Sam and the most wonderful and knowledgeable crew of contributors have done an outstanding job. Thank you all, you especially Sam, as well as the excellent team at Springer, for going above and beyond.

All you readers now need to do is do well by our pediatric patients (and their parents, and their doctors, etc.). What more satisfying "job" is there?

Rochester, NY, USA Johan G. (Hans) Blickman
February 2016

# Contents

# Contributors

**Nazanin Ahmadi** Department of Radiology, Vrije Universiteit Medisch Centrum, Amsterdam, The Netherlands

**Teresa Berrocal** Pediatric Radiology Section, Department of Radiology, University Hospital La Paz, Madrid, Spain

**Johan G. (Hans) Blickman** Department of Radiology, Golisano Childrens Hospital, URMC, Rochester, NY, USA

**Apeksha Chaturvedi** Department of Radiology, Golisano Childrens Hospital, URMC, Rochester, NY, USA

**Gloria del Pozo** Pediatric Radiology Section, Department of Radiology, University Hospital 12 de Octubre, Madrid, Spain

**Melanie P. Hiorns** Department of Radiology, Great Ormond Street Hospital, London, UK

**Deepak R. Kaura** Department of Radiology, Sidra Medical and Research Center, Doha, Qatar

**Gurdeep S. Mann** Department of Radiology, Sidra Medical and Research Center, Doha, Qatar

**Manuel Parrón** Pediatric Radiology Section, Department of Radiology, University Hospital La Paz, Madrid, Spain

**Aisha Rizvi** Doha, Qatar

**Avez A. Rizvi** Department of Radiology, Sidra Medical and Research Center, Doha, Qatar

**Abdusamea G. Shabani** Department of Radiology, Sidra Medical and Research Center, Doha, Qatar

**Samuel Stafrace** Department of Radiology, Sidra Medical and Research Center, Doha, Qatar

**K. P. van Lienden** Department of Radiology, Academic Medical Centre/Emma Children's Hospital Amsterdam, Amsterdam Zuid-Oost, The Netherlands

**R. R. van Rijn** Department of Radiology, Academic Medical Centre/Emma Children's Hospital Amsterdam, Amsterdam Zuid-Oost, The Netherlands

# Imaging Techniques

## Kids are not Small Adults: Techniques and Helpful Hints

Johan G. (Hans) Blickman

## Contents




**Abstract**

Imaging techniques utilized in pediatric children very much spreads across the whole spectrum of the modalities available. The 'devil lies in the detail' where the emphasis and focus lies in reducing the radiation burden on the child whilst still answering the clinical questions. This chapter outlines the different techniques utilized highlighting their relative strengths and weaknesses.


## 1 Conventional Radiography

In a child with abdominal symptoms, conventional radiographs of the abdomen are usually the initial imaging study performed today utilizing computed radiographic or digital radiographic technology.

Although many clinicians request ultrasound (US) or computed tomography (CT) as the first abdominal imaging examination, conventional radiographs are still recommended by the American College of Radiology (ACR) appropriateness guidelines.

Appropriateness guidelines may often provide useful information if tailored to the individual patient's problem. Abdominal radiographs in infants and neonates are typically obtained in supine position, but after the age 1–2 years (when the child has started to walk) are often combined with a horizontal beam examination, preferably upright if needed. The left side down decubitus view may be obtained in newborns and ill or uncooperative patients. Single supine examinations may

J.G. (Hans) Blickman, MD, PhD FACR, FAAP
Department of Radiology, Golisano Childrens Hospital, URMC, Rochester, NY, USA
e-mail: johan_blickman@urmc.rochester.edu



S. Stafrace, J.G. (Hans) Blickman (eds.), *Radiological Imaging of the Digestive Tract in Infants and Children*, Medical Radiology, DOI 10.1007/978-3-319-18434-0_1

be obtained when the clinical suspicion is constipation or foreign body ingestion or if the examination is being performed for tube or catheter localization hence keeping the overall dose down.

The cross-table lateral view is less useful as it may be difficult to differentiate intraluminal air from extraluminal air. This is however useful if the baby/child should rather not be moved.

There are pertinent points of difference between the abdominal radiograph of an adult and that of a child: the liver takes up a relatively larger space in the peritoneal cavity of a child; the spleen may not be visible and usually does not displace the gastric contour in a child and it is often hard to differentiate large from small bowel, particularly when the bowel is slightly dilated.

Likewise, the retroperitoneal fat "stripes" (psoas shadows) are frequently not seen on the abdominal radiograph of a child because of the relative paucity of fat in the infant's and small child's retroperitoneum. The lack of fat in the capsules of the solid organs also makes evaluation of their size nearly impossible on abdominal radiographs. In contrast, the pro-peritoneal fat stripes are visible from infancy. A soft tissue pseudo-mass in the abdomen may be the urinary bladder, the fluid-filled stomach or intestine, or an umbilical hernia (Fig. 1).

In the newborn there should be air in the stomach at birth. By 6 h at the latest, the stomach and greater portion of the small bowel should be filled with air, by 12 h air should fill most of the (small) bowel, and by 24 h of life air should appear in the rectum, the so-called "rule of 6's."

However, the appearance of air throughout the gastrointestinal (GI) tract is usually more rapid than the above sequence in normal newborns and, unlike adults, children up to the toddler age group typically have air throughout the entire GI tract most of the time.

A variation in this sequence, such as absence of air in the stomach at 1 h, should raise the possibility of an esophageal obstruction. On the other hand, no air in the rectum need not herald intestinal obstruction like in the adult patient and should not be used to suggest bowel obstruction.

The most common cause of a lack of intestinal air in the newborn results from crying and/or less swallowing in ill babies, especially those with newborn lung disease.

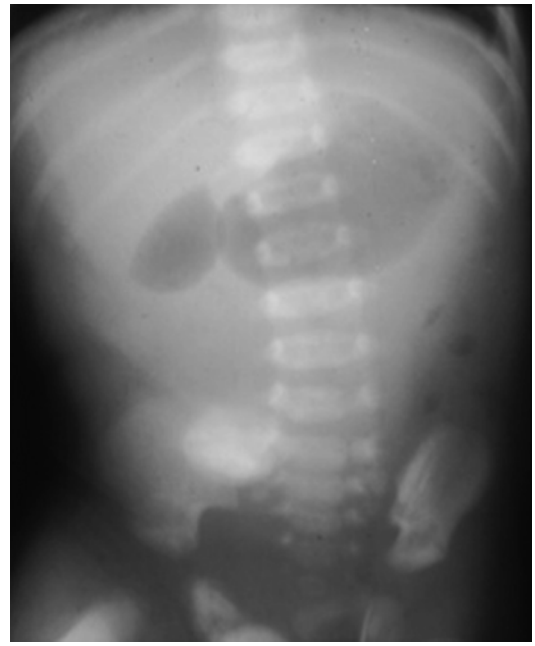

**Fig. 1** Soft tissue density at L4 region: an "outy," umbilical hernia. There is also evidence of a descending duodenal stenosis

Likewise, the neonate in whom an orogastric (OG) or nasogastric (NG) tube has been placed may have a relatively gasless abdomen without other underlying pathology. Other causes of a gasless abdomen are vomiting, medication that decreases peristalsis, and obstruction of a fluid-filled viscus. Peritoneal irritation (peritonitis) or ascites may also displace abdominal air.

Absence of meconium passage by 24 h is abnormal, and abdominal distention or marked dilatation of any viscus in the first day of life should lead to further imaging evaluation. As noted above, in neonates and infants, it is often impossible to differentiate small from large bowel, especially if the bowel becomes dilated. A prone film sometimes may be helpful because air then "rises" into the rectum to illustrate that distal obstruction is not present.

## 1.1 Tube and Catheter Positions

Most tubes and catheters are placed by the clinical team, but radiographs are often used for confirmation of position.

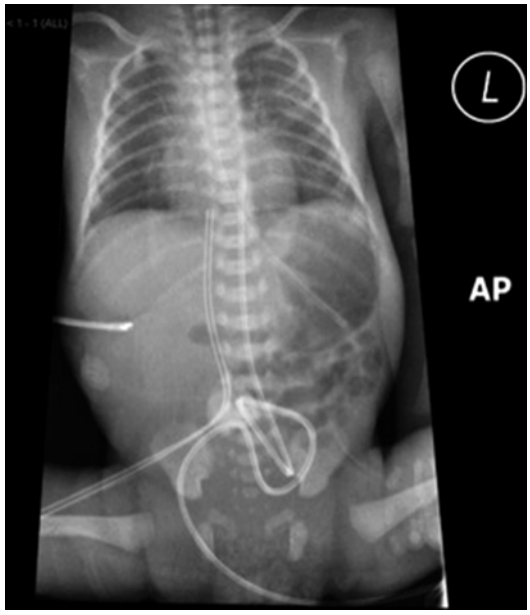


**Fig. 2** Plain chest and abdomen radiograph in a neonate demonstrating the appropriate position of the arterial and venous umbilical catheters. The left-sided arterial umbilical catheter (UAC) courses caudal to its junction with the internal iliac artery following which it travels cephalad through the iliac system and the aorta. The right-sided umbilical venous catheter (UVC) travels cephalad from the umbilical vein through the ductus venosus into the inferior cavo-atrial junction (Image courtesy of Dr. Gurdeep Mann, Sidra Medical and Research Center, Qatar)

In the (premature) newborn, abdominal radiographs are commonly used to assess the positions of umbilical catheters, enteric tubes, and vascular access catheters.

Umbilical artery and vein catheters can be distinguished on the basis of their anatomic positions (Fig. 2).

The umbilical artery catheter (UAC) enters one of the umbilical arteries and courses caudal to its junction with the internal iliac artery. It then turns cephalad, coursing through the iliac system to the abdominal aorta.

The tip should be either in the thoracic descending aorta or, preferably, in the abdominal aorta below the origin of the great vessels and above the aortic bifurcation.

The preferred position in the former instance is between T7 and T11("T7 is 'heaven', T8 is great, T9 is fine"), in the latter, below the inferior endplate of L3(the renal arteries originate at L2).

The major complication of malposition of these lines is embolization of a great vessel or lower extremity artery by the thrombus that invariably forms at the tip of the umbilical artery catheter or simply due to vascular spasm.

The umbilical vein catheter (UVC) courses from the umbilicus cephalad through the umbilical vein and ductus venosus into the inferior cavo-atrial junction. Because the umbilical vein catheter shares sinusoids with the portal vein, it may enter the portal vein, the splenic vein, or the superior mesenteric vein (SMV) and in those cases should be replaced. The tip's optimal position is just within the right atrium, just above the confluent shadows of the RA and the right hemidiaphragm.

In older infants and children, venous access is often achieved through the iliac vein. The major complication is venous thrombosis with the risk of subsequent pulmonary embolism. Perforation by a vascular catheter is fortunately quite rare but potentially fatal. OG tubes are more commonly used in the newborn and NG tubes in older children. The tip of such a tube should project over the stomach. Common complications of the use of orogastric or NG tubes are tracheal intubation, coiling of the tube in the pharynx or esophagus, and, rarely, perforation of the esophagus or stomach.

## 1.2 Radiation Considerations

When imaging children, we have a choice among many modalities; the ones that do not use radiation include ultrasound and MRI. Modalities using ionizing to radiation include conventional radiographs (relatively low dose), fluoroscopy (mid-range dose), and computed tomography (CT) (possibly high dose although doses are reducing significantly with newer technologies).

An unfortunate by-product of the disappearance of hard copy (film) is that we are no longer able to tell inadvertent higher dose by tracking the repeat rate of images of lesser quality easily.

Post-processing algorithms make all the images appear "nice" and the repeat examinations may not be obvious as there is no excess film. For that reason a short review of the current understanding of radiation versus pediatric imag-

ing also known as "imaging gently" or As Low As Reasonably Achievable(ALARA) follows.

The fetus and the young infant are at greatest risk for radiation-induced abnormalities as the effects of radiation are greatest on faster-growing organisms that are abundant in the fetus, infant, and young child. In addition, the effects of this radiation may not be obvious until later age. Evidence for carcinogenesis in the infant was first suggested in 1958 in a study of X-ray exposure during pregnancy. Subsequently, the survivors of the atomic bomb in Japan showed the age-related risk of radiation to be very much more obvious in children in the first decade of life. Thus, we know that ionizing radiation can be deleterious, but we do not know exactly how much and when. Pulse-fluoroscopy and digital imaging are two advances of the former decreasing exposure 30–50 % by changing from continuous to intermittent fluoroscopy. CT delivers the largest dose of ionizing radiation. Worrisome is that the use of CT examinations has increased at a rapid rate and in most non-pediatric radiology departments the technical factors are not adjusted for children. Fortunately the manufacturers are working diligently with us pediatric imagers to drastically lower the absorbed dose due to CT imaging and the rate of increase in CT utilization has slowed.

It is clear that we must reduce radiation dose to children as often as possible. We should actively screen the use of CT examinations as to whether the examination is really necessary in the clinical approach when making the diagnosis and question if another non-radiating modality could be used instead. We must always seek to use *that* protocol that gives the answer to the clinical question asked using the lowest dose.

## 1.3 Contrast Examinations

Indications for contrast examinations of the gastrointestinal tract are discussed subsequently in the appropriate chapters.

### 1.3.1 Barium Compounds

Guiding principles for contrast use should always include appropriate temperature and low or iso-osmolarity and always following ("watching with fluoroscopy") the administered contrast to reduce any possible complications.

There are two relative contraindications to using barium as a contrast agent: suspected bowel perforation and predisposition for pulmonary aspiration of barium. Neither one is an absolute contraindication. These compounds are inert thus they traverse the bowel lumen unaltered, flocculation being a thing of the past, as is the old-wives tale of barium "hardening to concrete" in an obstructed viscus.

Barium in the retroperitoneum, mediastinum, or peritoneal cavity that is removed shortly after entering these spaces holds only a minimal risk for sequelae such as granuloma formation, adhesions, and peritonitis. However, successful removal is not always possible and barium is generally contraindicated when the probability of perforation exists. Likewise, aspirated barium provokes a cough reflex. Thus, when routine care is taken, barium constitutes the most useful and safe contrast agent in the pediatric age group.

### 1.3.2 Water-Soluble Contrast Agents

The most commonly used water-soluble contrast agents are diatrizoate meglumine/sodium (Gastrografin or Gastroview), Iopamidol (Gastromiro), and, less commonly these days, diatrizoate meglumine (Hypaque), Iothalamate meglumine (Conray; Cysto-Conray) are also used.

These agents are hyperosmolar water-soluble media and should not be used routinely in the upper GI tract as there is a serious risk of pulmonary edema (or death) when these agents are aspirated. The aspirated contrast medium causes a release of histamine or histamine-like substances in the lung. In addition, hyperosmolar agents may be toxic to the bowel mucosa, and their hydrophilic nature can result in massive fluid shifts, especially in neonates.

Also these hyperosmolar contrast agents draw fluid into the GI lumen during their passage, often resulting in their marked dilution, sometimes as early as the third portion of the duodenum, thus severely limiting their diagnostic use for the rest of the GI tract.

In the large bowel, on the other hand, these agents are still used in an enema to exploit their hyperosmolar quality (e.g., to facilitate meconium plug evacuation by absorbing fluid into the bowel lumen, thus having a "lubricating" effect,

especially when mixed with a wetting agent such as polysorbate 80).

Through appropriate dilution of these agents, near isotonicity can be achieved. The package insert usually provides easy directions to accomplish this. A 3:1 water to contrast solution is the most commonly used dilution formula.

The risk of the preparation of these agents going wrong and the knowledge that simply doing an enema will often lead to evacuation of the meconium has lessened the preference for "lubricating" agents.

It is also for these reasons that many pediatric imaging departments do not even stock these agents any longer.

Isotonic contrast agents are very useful when perforation is suspected or when the anatomic integrity must be evaluated in the sick neonate. Indications include necrotizing enterocolitis (NEC) and bowel anastomoses after surgery.

Low-osmolar, water-soluble contrast agents have the advantages of not being diluted upon passage through the GI tract, of having virtually no effect on the lungs or peritoneum and of not being absorbed into the tissues. Their major disadvantage is their cost, which is many times higher than that of conventional agents.

### 1.3.3 Use of Contrast Studies

Performance and indications of contrast studies of the small and large bowel of a child do differ significantly from those of an adult. Clinical circumstances to a large degree dictate which study is to be performed and in what fashion.

Congenital abnormalities of the bowel, such as malrotation, occur more frequently in children, whereas inflammatory bowel disease (IBD) is uncommon in children younger than 10 years. It is therefore important that the radiologist be aware of the potential yield of an examination, its risks, and the implications of their results on possible therapeutic regimens to follow.

In pediatric upper GI (UGI) studies, the imager assesses the swallowing mechanism and for the presence or absence of nasopharyngeal reflux, laryngeal penetration, and tracheal aspiration. The contours and motility pattern of the esophagus and gastroesophageal junction, as well as the anatomic and functional integrity of the stomach, duodenum, and proximal jejunum, should be evaluated. It is thus an *anatomical* study, with limited answers to functional questions.

The location of the duodenojejunal junction is the end point in assessment of normal rotation and positioning of the GI tract. Normally, the duodenojejunal junction is located to the left of the spine, behind the stomach, at the level of the duodenal bulb.

It may be located as medially as the left pedicle or slightly lower than the level of the duodenal bulb. The ligament of Treitz forms properly when the duodenojejunal junction is appropriately located but is not or partially present in cases of bowel malposition. There is some discussion as to the reproducibility of these findings.

The duodenal C-loop is usually smooth but may contain undulations (e.g., Z-loop). On occasion, especially in children younger than 1 year, the duodenal sweep is on a mesentery and is redundant, mimicking malrotation. Double-contrast views of the stomach and duodenum arc worthwhile for evaluation of the mucosa but are not mandatory as they are (were) in the adult population.

The radiographic evaluation of gastroesophageal reflux (GER) in children is controversial. There are some who assess the presence or absence of GER over 5 min while intermittently performing fluoroscopy, whereas others rely on an incidental observation of GER during the upper GI study.

A pH probe study is the most reliable diagnostic tool for GER, but nuclear medicine evaluation ("milk scan") may be used to evaluate GER also. All infants younger than 9–12 months experience reflux from time to time, likely because the G-E junction is maturing.

The imaging for GER thus often serves to objectify the subjective and should be seen as such; in other words, therapy for symptoms possibly caused by GER should be guided by the clinical findings (e.g., visualized aspiration, recurrent pneumonias, or failure to thrive).

The contrast enema examination is performed *in neonates* primarily for anatomic evaluation of suspected "low" obstructions, neonatal small left colon syndrome, meconium plug, or ileal atresia. *In infants and children*, it is used most often to assess the location of the transition zone in Hirschsprung disease in order to guide the biopsy. Hirschsprung is however a pathological not radiological diagnosis.

Rigorous preparatory cleansing of the colon, as is done in adults, is not usually necessary in children because intraluminal lesions (carcinoma, polyps) are less common. However, when the clinical concern is for polyps or tumors, double-contrast enemas can be successfully performed in patients of virtually any age. Note that in the evaluation of Hirschsprung disease, there should be no preparation of the colon because it may flatten out or obscure a transition zone, especially in the rectum. For this reason, a straight-tipped non-bulbous catheter is often also used to minimize disturbance of the anorectal anatomy.

On the other hand, to evaluate the colonic mucosa in patients in whom IBD or polyps are suspected, adequate preparation is mandatory.

The use of a balloon-type enema tip is contraindicated in virtually all lower GI tract examinations in children. Proper taping into position of a soft, malleable, bulbous enema tip is almost always sufficient and virtually a-traumatic.

Whether fluoroscopy should be performed with the patient in the prone or supine position is a personal preference; however, at the outset of the study, the patient should be in the (left) lateral position so that the presacral space as well as the puborectalis sling can be adequately evaluated. Spot films of the splenic and hepatic flexures and the sigmoid colon are necessary only in specific instances, for instance, in older teenage boys with symptoms that may be caused by mucinous carcinomas of the colon.

A post-evacuation film is mandatory, especially after reduction of intussusception, to check for recurrence, and after all other single-contrast enema examinations to evaluate for mucosal detail. The film can be omitted after double-contrast examinations. A 24-h post-evacuation film is no longer utilized because it cannot differentiate Hirschsprung disease from other causes of prolonged retention of contrast material and stool.

### 1.3.4 Air

Air has been a useful contrast agent for decades (more than a century in fact). In pediatric imaging, air has been used with increasing frequency in the reduction of intussusception. Reluctance to use air has been attributed to its being more cumbersome to use. (It actually becomes easier to use with experience.) Additionally, there is reluctance to use air because the pressure of the insufflated air must be regulated, the absorbed radiation dose is somewhat higher, and the monitoring of the progression of the air column may be difficult.

More importantly, the perforation rate with air has been noted to be as high as 2.5 %, as opposed to 0.5 % with positive contrast materials.

On the other hand, air can be very useful, although rarely needed, as a contrast agent in suspected esophageal atresia. One needs only a small amount administered through an esophageal tube to outline the atretic pouch, without the risk of aspiration that would be present if a positive contrast agent were used.

## 2 Ultrasound

Ultrasound (US) is the screening modality of choice in the child in whom intra-abdominal or retroperitoneal pathology such as a mass, urinary calculi, pyloric stenosis, or an intussusception is suspected.

US is easy and quick to perform (can be done at the bedside and with minimal if any patient preparation) and uses no ionizing radiation. There is no known risk associated with the procedure, and the lack of fat in infants and children allows for better visualization of intra-abdominal and retroperitoneal structures than can be achieved in the adult.

In general, a directed approach (e.g., “right upper quadrant pain”) leads to a higher diagnostic yield than one guided by vague symptoms (e.g., “abdominal pain”). High-resolution transducers should always be used.

A variety of transducers is necessary to deal with children, who vary extensively in size. Color-flow Doppler US evaluation of all major vessels should be routine.

## 3 Computed Tomography

Computed tomography (CT) has proved to be an extremely accurate and fast imaging modality. Few children of any age require sedation when newer faster multidetector scanners (MDCT) are used.

An abdominal/pelvic CT scan should be performed with intravenous (IV) contrast agent except in cases assessing for renal calculi; oral contrast is optional, particularly in trauma settings. Sedation is rarely necessary when performing CT in kids. Child life assistance allows for most kids to be scanned quickly and easily without adding risk to the study.

Important to note that the requirement for informed consent with use of intravenous (IV) agents varies from institution to institution.

It is strongly suggested that low-osmolar, water-soluble contrast agents (physician-administered or physician-supervised) be used because contrast reactions and discomfort in case of extravasation are much less with such agents than the reactions experienced with hyperosmolar water-soluble contrast agents. Power injection at a rate of 1 mL/kg is recommended. IV administration of contrast agents is not recommended for patients in sickle cell crisis.

The advantages of CT lie in the superior tissue plane resolution compared with that achieved with conventional radiographs. Multiplanar reconstructions and three-dimensional (3D) rendering have improved the diagnostic accuracy of CT in children as well as in adults. Disadvantages are relative. The radiation dose per slice from the average abdominal CT scan compares favorably with that of very few chest radiographs or abdominal films. However, publicly reported concerns about the long-term effects of radiation from CT have significantly and appropriately raised parent and physician apprehension. In all but the largest children, the radiation dose can be significantly reduced by decreasing both mAs and kVp, made easier by the development of low-dose software protocols by all CT manufacturers. Much of the potentially harmful radiation in children comes from the use of settings appropriate to adults, increasing emergency department scanning and the ill-advised repeat study.

It is incumbent on the radiologist to assess the indication for the examination and the technical factors used. Indications for the use of CT include the evaluation of intra- abdominal solid masses, abscesses, trauma, and hepato-biliary abnormalities as well as tumor staging. It is also helpful in the guidance of percutaneous biopsies, placement of drainage catheters, and establishment of radiation therapy portals.

## 4 Magnetic Resonance Imaging

Advantages of magnetic resonance imaging (MRI) are superior multiplanar capabilities, absence of ionizing radiation, excellent soft tissue contrast, and high-resolution imaging of the vasculature.

The disadvantages include the need for sedation in younger patients. Sedation of older patients is determined on a case-by-case basis (see 1.1). Sedation regimens are influenced by the availability of pediatric anesthesia monitoring and child life services (Tyson et al. 2014).

The general trend is that sedation is administered and monitored by anesthesia or the pediatric intensivists, rarely by the radiologist.

Motion artifacts related to breathing and bowel peristalsis also limit the use of MRI in this setting. The total scan time for MRI is typically considerably longer than that for CT (although the scan times are decreasing steadily with improving software applications). Claustrophobia is also an issue in the use of MRI with pediatric patients. MRI is usually more expensive than CT or US.

### 4.1 Protocols

The MRI protocols for evaluating gastrointestinal disorders in children are, for the most part, similar to those used for imaging the adult patient, with the following important caveats: (1) the need to adapt the sequences for free-breathing acquisition and (2) the requirement for higher spatial and temporal resolution due to the small size and rapid hemodynamic status of children. The following are some specific considerations for imaging pediatric patients:

*Motion*: Techniques used to minimize artifacts secondary to physiologic respiratory and cardiovascular motion include respiratory ordered-phase encoding, respiratory triggering, navigator

respiratory gating, cardiac gating, gradient moment nulling ("flow comp") and pre-saturation. Peristalsis may be temporarily halted by the intravenous administration of glucagon, used less and less today.

*Spatial resolution*: In order to achieve adequate resolution, the smallest coil that provides optimal coverage of the region of interest should be used. For infants and newborns, the head or shoulder coil can sometimes be used to image the abdomen. Small phased-array surface coils are an ideal choice in small children, providing excellent spatial resolution along with the ability to reduce scan time by means of parallel imaging.

For larger children, phased-array coils with larger coverage (body coil) are optimal. The field of view, matrix, slice thickness and slice spacing determine the spatial resolution of any given study and should be tailored to the specific demands of the clinical situation.

### 4.2 Contrast Agents

#### 4.2.1 Oral Agents

To opacify the bowel, children may be administered baby formula with ferrous sulfate 2 h before imaging.

The paramagnetic effect of iron results in a positive contrast effect within bowel. In order to create a negative contrast effect, diamagnetic substances like barium sulfate or a manganese-rich drink such as blueberry or pineapple juice or bismuth subsalicylate (Kaopectate) may be used. Negative contrast agents diminish artifacts related to peristalsis, thereby significantly improving the quality of studies like MR cholangiopancreatography.

#### 4.2.2 Intravenous Agents

The usual pediatric dose and agent administered intravenously to children undergoing MRI of the abdomen is gadolinium-diethylene-triamine pentaacetic acid (Gd-DTPA) at a dose of 0.05–0.1 mmol/kg.

**Table 1** Common pediatric gastrointestinal nuclear medicine procedures

| Procedure | Radioisotope | Dose |
|---|---|---|
| Meckel scan | Technetium Tc 99 m pertechnetate | 1–5 mCi IV |
| Liver/spleen scan | Technetium Tc 99 m sulfur colloid | 0.5–5 mCi IV |
| Biliary scan | Technetium Tc 99 m diisopropyl iminodiacetic acid | 0.5–3 mCi IV |
| | Gastric Emptying Study Technetium Tc 99 m sulfur colloid in standard meal | 1 mCi PO or by NG tube |

Courtesy of Dr. Vaseem Chengazi, Director of Nuclear Medicine, URMC, Rochester, N.Y. USA

## 5 Radionuclide Studies

Radioisotope examinations, much less commonly than before, performed in the pediatric abdomen are studies to assess for GER (gastroesophageal reflux; milk scan) and gastric emptying, liver and spleen scans, and studies for ectopic gastric mucosa in Meckel diverticulae (Table 1). Some protocols encourage the use of H2 blockers to increase the sensitivity of detecting ectopic gastric mucosa (Spottswood et al. 2014). The gastric emptying halftime rates assessed with milk formulae in neonates are generally below 35–40 min but can be quite delayed (Fig. 3). GER can be imaged with a dedicated protocol if needed. There are no contraindications to these studies.

## 6 Miscellaneous Techniques

### 6.1 Placement of Tubes

A long tube can be placed either through the nose or through an existing gastrostomy with or without the help of a guidewire. Placement of these tubes into the jejunum seldom leads to complications, although perforation has been reported. Fluoroscopic monitoring is usually sufficient. The position of the tube should be checked before

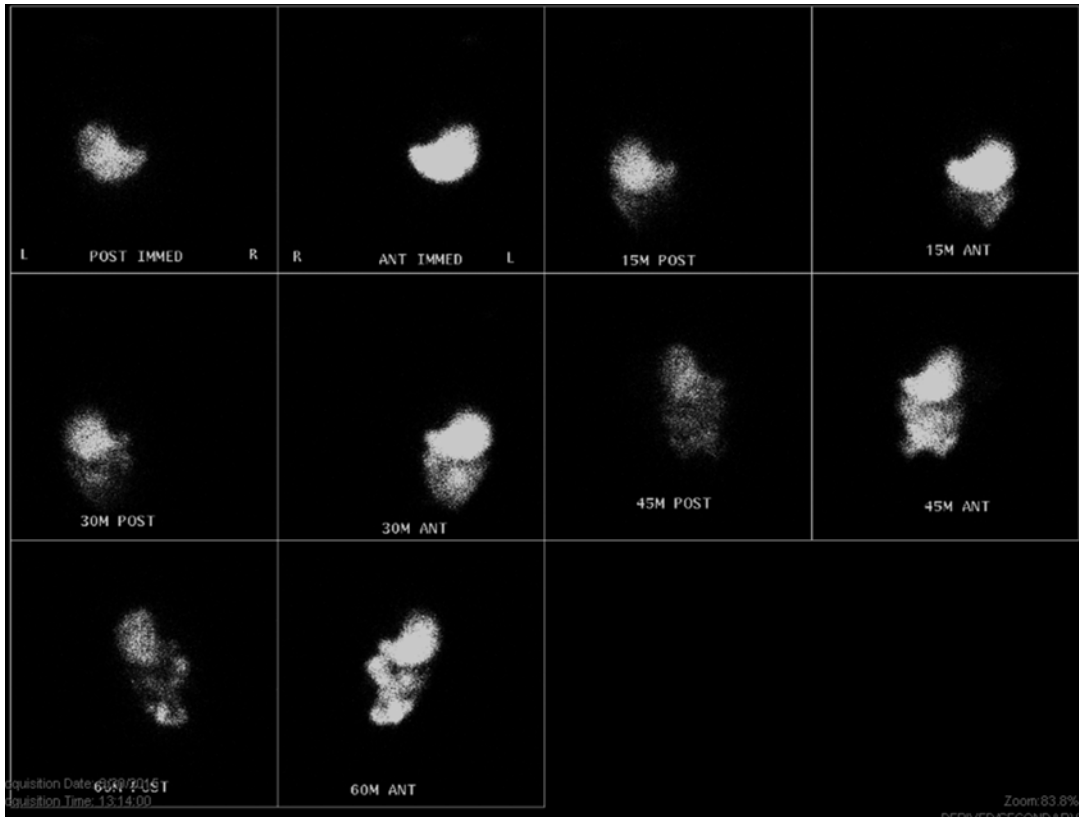


**Fig. 3** Normal gastric emptying study in a neonate (Courtesy of Dr. Vaseem Chengazi, Director of Nuclear Medicine, URMC, Rochester, N.Y. USA)

the procedure is ended, with contrast material injected through the line. A horizontal beam abdominal radiograph (or lower dose fluoroscopy image grab) should also be obtained to ascertain whether or not perforation or aberrant positioning has occurred. Complications of gastrostomy tube placement include malposition, higher incidence of GER, and tube migration. All of these complications can be assessed by instillation of a few milliliters of isotonic contrast under fluoroscopic guidance. Gastrostomies, placement of gastroduodenal and gastrojejunal tubes, and cecostomies in children should be performed by experienced interventional (pediatric) radiologists.

## References

Spottswood SE, Pfluger T, Bartold SP et al (2014) SNMMI and EANM practice guideline for Meckel Diverticulum Scintigraphy 2.0. J Nucl Med Technol 42:163–169

Tyson ME, Bohl DD, Blickman JG (2014) A randomized controlled trial: child life services in pediatric imaging. Pediatr Radiol 44(11):1426–1432

# Gastrointestinal Emergencies in the Neonate

Teresa Berrocal, Manuel Parrón, and Gloria del Pozo

## Contents



**Abstract**

Gastrointestinal emergencies in the neonate often necessitate one or more radiological assessments to assist in the diagnosis and successful management. This chapter systematically reviews the aetiology, investigative pathways and the specific imaging findings of intestinal pathologies presenting in the neonatal period.

## 1 Neonatal Intestinal Obstruction

Intestinal obstruction is the most common abdominal emergency in the neonatal period. It is almost always the result of a congenital anomaly of the gastrointestinal tract, which must be rectified surgically if the infant is to survive. Mortality in surgically untreated patients is close to 100 %, and the rate of survival is closely related to the time of surgical intervention (Subbarao 2008). The most common clinical findings are abdominal distension, vomiting, and sometimes failure to pass meconium, depending on the level of the obstruction.

These findings usually prompt the clinician to consult the radiologist, who must answer three major questions: Is the obstruction present? What is the location of the obstruction? What is the etiology?

The most valuable means of determining whether or not obstruction is present is the plain abdominal radiograph. Plain radiographs are often diagnostic. When not diagnostic, they may provide important clues suggesting the subsequent

T. Berrocal, MD, PhD • M. Parrón, MD (✉)
Pediatric Radiology Section,
Department of Radiology,
University Hospital La Paz,
Madrid, Spain
e-mail: manuel.parron@salud.madrid.org

G. del Pozo, MD, PhD
Pediatric Radiology Section,
Department of Radiology,
University Hospital 12 de Octubre, Madrid, Spain
e-mail: gloria.pozo@salud.madrid.org



S. Stafrace, J.G. (Hans) Blickman (eds.), *Radiological Imaging of the Digestive Tract in Infants and Children*, Medical Radiology, DOI 10.1007/978-3-319-18434-0_2

most valuable diagnostic procedure (Vinocur et al. 2012). Knowledge of the many variations in both the distribution and quantity of intestinal air in infants is useful in the interpretation of pathologic findings. In a healthy neonate, air can usually be identified in the stomach within minutes after birth and reaches the proximal portion of the small bowel during the first 6 h of life. By 6–12 h, the entire small bowel usually contains air, and after 12–24 h, normal neonates show rectosigmoid air in a plain abdominal radiograph.

About 80 % of the air that is seen in the alimentary tract is due to swallowed atmospheric air (Subbarao 2008). When an intestinal obstruction is present, since air proceeds distally in the gastrointestinal tract until stopped at the obstruction, an abdominal radiograph will show dilated air-filled loops proximal to the obstruction and no air distal to it. The amount/number of dilated loops depends on the site of obstruction: the lower the obstruction, the greater the number of dilated loops.

Once established that an intestinal obstruction is present, the radiologist should still determine the location of the obstruction and, if possible, the etiology.

In order to arrive at a pertinent differential diagnostic list of possible etiologies, neonatal obstructions can be classified as "high" or "low" obstruction.

*High or upper intestinal obstructions* are those that occur proximal to the mid-ileum and include obstructions involving the stomach, duodenum, jejunum, and proximal ileum.

Obstructions that involve the distal ileum or colon are called *low intestinal obstructions*. The distinction between high and low obstruction is also critical since children with high obstructions usually need little or no radiologic evaluation after plain radiograph, and the specific diagnosis is made in the operating room. Newborns with low obstructions need a contrast enema, which usually provides a specific diagnosis and may be therapeutic (Buonomo 1997; Subbarao 2008).

Thus, in summary, plain radiographs in neonates with *high* obstruction reveal one, two, or a few dilated air-filled bowel loops, depending on the level of the obstruction, while radiographs in *low* obstructions show multiple dilated air-filled bowel loops.

Abdominal ultrasound (US) may have a role here. With US, one can distinguish dilated from collapsed loops. One can often distinguish ileal loops from colon, and it is also possible to distinguish the dilated fluid-filled loop proximal to an atresia from the dilated meconium-filled loop of a meconium ileus. It may be possible to proceed directly to surgery for jejunal or ileal atresia or to proceed to reduction of a meconium ileus by contrast enema (Ryan and Donoghue 2010).

Disorders of the intestinal tract in the neonatal period usually present with abdominal distension and dilatation of the bowel. However, not all intestinal dilatations represent obstruction. Infants with medical disorders such as sepsis, electrolyte imbalance, or necrotizing enterocolitis may present ileus characterized by uniform dilatation of the bowel to the rectum. Also, infants on continuous positive airway pressure may swallow an excessive amount of air and exhibit important intestinal dilatation. This dilatation must be distinguished from mechanical obstruction, because the treatment is completely different. The differentiation between these two categories can usually be made on the basis of clinical history, laboratory tests, and appropriate radiographs (Hernanz-Schulman 1999).

## 1.1 High Obstruction

### 1.1.1 Gastric Outlet Obstruction

Complete obstruction involving the gastric outlet is a rare condition that is usually due to gastric atresia, although it may be caused by extrinsic pressure from congenital peritoneal bands or by annular pancreatic tissue in the gastric wall. Gastric atresia accounts for less than 1 % of all congenital intestinal obstructions and is limited to the antrum and pyloric region. It is thought to be due to localized vascular occlusion in fetal life rather than to failed recanalization because there is no epithelial perforation in the stomach comparable to that in the esophagus or duodenum (Okoye et al. 2000; Juang and Snyder 2012). The atresia is usually produced by a membranous diaphragm that only affects the mucosa, although there may be more extensive obliteration of the lumen.

Gastric atresia may be familial or associated with epidermolysis bullosa (Toma et al. 2002; Veyrac et al. 2012). The predominant symptom is

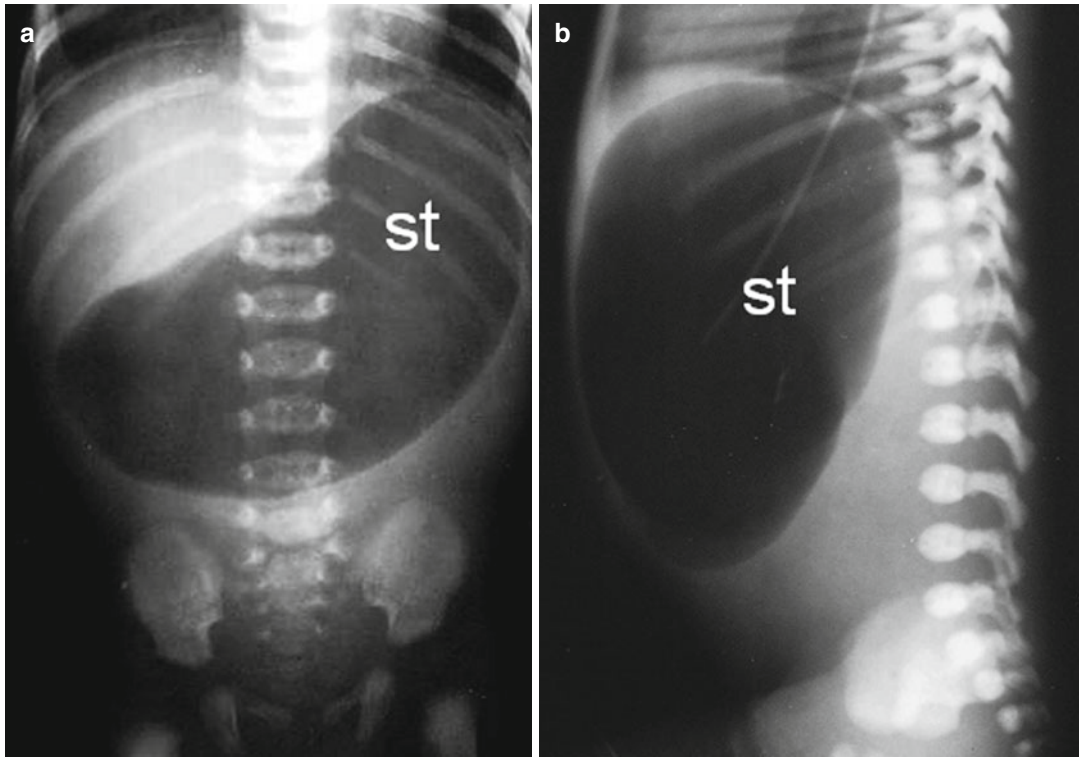


**Fig. 1** Pyloric atresia. (**a**) Anteroposterior and (**b**) lateral plain abdominal radiographs in a newborn infant that show distension of the stomach (*st*) and absence of air in the small bowel and colon, resulting in the characteristic "single bubble" image

vomiting within the first hours after birth, the vomits being free of bile. The absence of bile in the vomitus indicates that the obstruction is above the ampulla of Vater.

Abdominal radiograph shows distention of the stomach proximal to the obstruction and the absence of air in the small bowel and colon, resulting in a "single bubble" appearance (Vinocur et al. 2012) (Fig. 1). When a single bubble is observed, examination with contrast material is unnecessary, and most patients are taken directly to surgery (Buonomo 1997). The membranous atresia may perforate after birth, leaving variable degrees of stenosis. In these cases, plain radiograph shows radiological findings similar to that of partial gastric outlet obstruction. In partial gastric outlet obstruction, symptoms may not appear until childhood or even adulthood. The most common presenting symptoms are cyclic postprandial vomiting and episodes of transient vomiting. The most frequent cause is incomplete prepyloric diaphragm. Antral stenosis, aberrant pancreatic tissue in the gastric antrum, and antral duplication cysts can also cause partial gastric outlet obstruction.

Pyloric hypertrophy usually presents beyond the neonatal period; however, it has been diagnosed in utero and can be seen in the neonatal period after administration of prostaglandin E to infants with ductus-dependent congenital heart defect. The resultant stenosis is produced by central foveolar hyperplasia, and usually, mucosal thickening often with polypoid or lobular appearance is observed (Peled et al. 1992; Babyn et al. 1995) (Fig. 2).

In these conditions, a plain radiograph shows distention of the stomach and decreased air in the small bowel, the extent of which depends on the degree of obstruction. After plain radiograph, an abdominal US or barium studies are needed to identify the underlying defect. US is useful to differentiate the muscular thickening observed in hypertrophic pyloric stenosis from mucosal thickening often with polypoid or lobular appearance

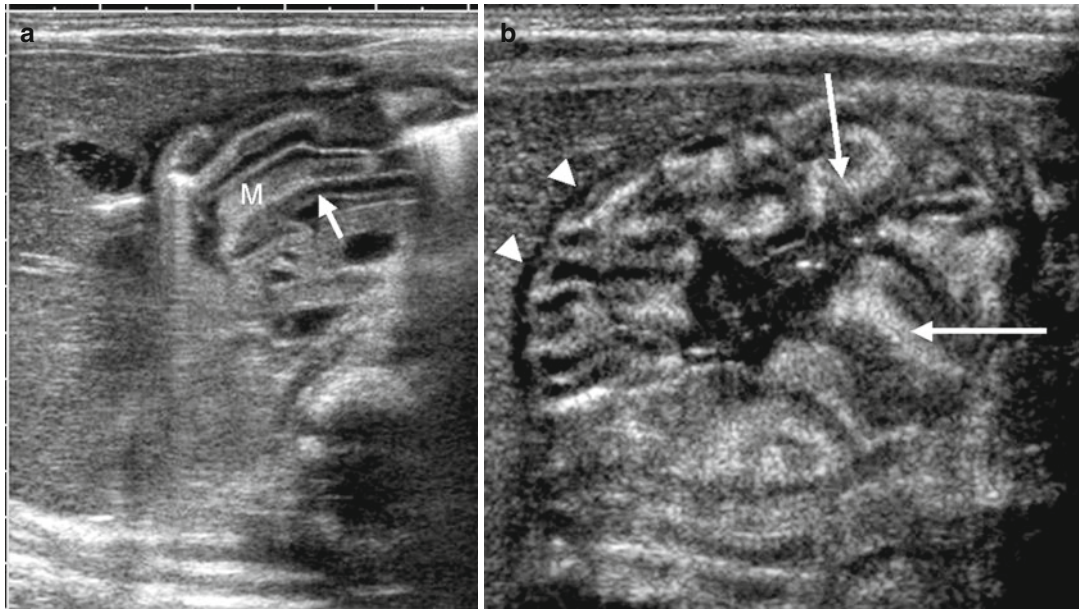


**Fig. 2** Prostaglandin therapy-induced gastric outlet obstruction. Neonate with ductus-dependent congenital heart disease treated with prostaglandin E to keep the ductus open. (**a**) Longitudinal US scan through the pyloric channel shows mucosal thickening (*M*) and a thin muscular layer (*arrows*), different from the muscular thickening seen in hypertrophic pyloric stenosis. (**b**) Axial scan through the gastric antrum reveals markedly hypertrophic mucosa (*arrows*) and an undulating appearance. The thickness of the muscular layer of the gastric wall is normal (*arrowheads*)

produced by central foveolar hyperplasia in neonates after administration of prostaglandin E. In barium studies, an incomplete prepyloric membrane (diaphragm) is seen as a thin (2–3-mm), linear-filling defect traversing the barium column (Fig. 3). At US, the diaphragm appears as an echogenic band extending centrally from the lesser and greater curvatures in the prepyloric region (Hayden 1996). Ectopic pancreatic tissue may be found at various sites in the gastrointestinal tract, most commonly the gastric antrum. An upper gastrointestinal series shows a smooth, dome-shaped filling defect 1–3 cm in diameter on the larger curvature (Fig. 4), and at times, central umbilication may be seen; pancreatic ectopic tissue may prolapse into the pylorus, producing intermittent obstruction (Allison et al. 1995).

### 1.1.2 Duodenal Obstruction

Complete duodenal obstruction is much more frequent than congenital gastric obstruction. Persistent vomiting is the cardinal presenting sign, but abdominal distension may not be a conspicuous feature.

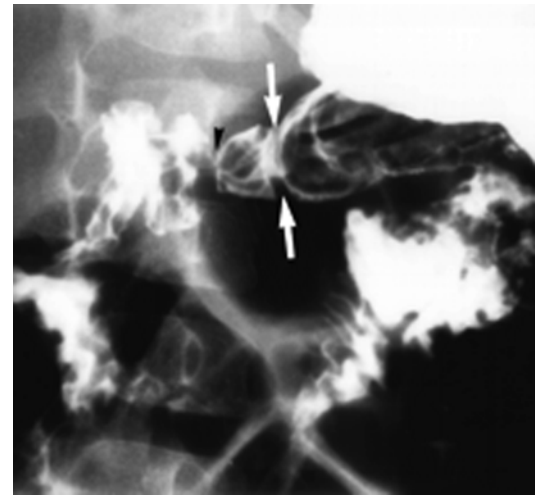

**Fig. 3** Incomplete antral web. Radiograph from a barium study (anterior oblique view) shows a concentric radiolucent band (*arrows*) producing discrete antral lumen reduction. *Arrowhead* indicates the pylorus

The vomiting is bile stained when the obstruction is below the ampulla of Vater (70 % of cases) and clear but persistent in supra-ampullary lesions.

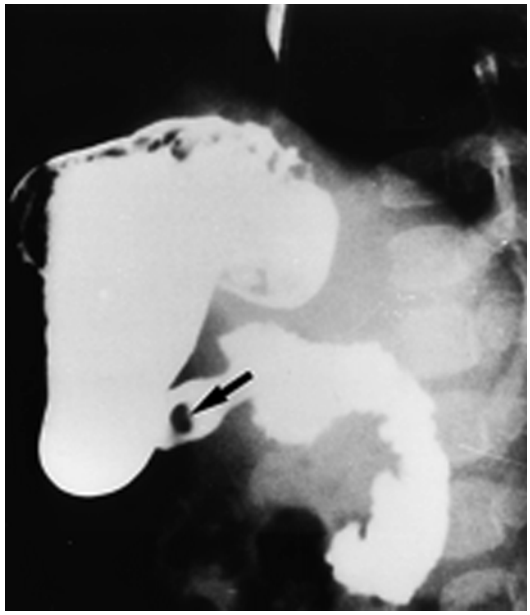

**Fig. 4** Ectopic pancreas in the gastric antrum. Image from an upper gastrointestinal series shows a rounded nodular defect in the gastric antrum with central umbilication identified by a fleck of barium (*arrow*). The diagnosis was confirmed at surgery

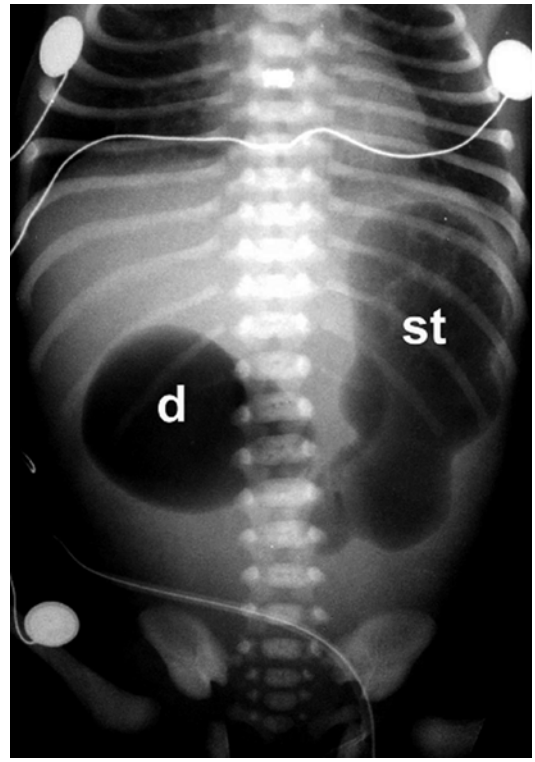


**Fig. 5** Complete duodenal obstruction caused by a congenital duodenal web. The stomach (*st*) and duodenum (*d*) are dilated, and there is no air more distally in the gastrointestinal tract, producing the classical "double bubble" image

The classic plain radiographic finding is the so-called double bubble image (Vinocur et al. 2012; Gilbertson-Dahdal et al. 2009) (Fig. 5). The higher, more leftward, and larger bubble is the stomach, and the other bubble is the dilated proximal duodenum, above the area of obstruction. Two distinct air–fluid levels are usually demonstrated on erect or horizontal beam radiographs. There is no air more distally in the gastrointestinal tract. Newborns showing evidence of complete duodenal obstruction on their abdominal radiograph rarely require further radiologic investigation. An upper gastrointestinal (UGI) series provides no additional information, and there is a potential hazard of vomiting with barium aspiration. Sometimes, vomiting can result in a lack of air in the obstructed segment; in these cases, a small amount of air can be injected via a nasogastric tube to depict more clearly the site of obstruction (Fig. 6). A contrast enema is not necessary when the diagnosis is obvious, although it can be performed to exclude additional more distal areas of atresia (Hernanz-Schulman 1999). In the case of isolated, proximal duodenal obstruction, the colon should be normal. The main causes for a "double bubble" in neonates are duodenal atresia, annular pancreas, and midgut volvulus although the latter is unlikely to result in significant duodenal dilatation. Less frequently it may be secondary to a duodenal web, Ladd bands, or the presence of a preduodenal portal vein (Etienne et al. 2012; Singal et al. 2009; Gilbertson-Dahdal et al. 2009).

*Duodenal atresia* is the most important cause of complete duodenal obstruction (Fig. 6). It occurs in approximately 1 in 10,000 births, and 60 % of the infants are premature. The etiology of this condition is thought to be failure of recanalization of the duodenum, approximately between the 9th and 11th week of gestation. Unlike jejunal and ileal atresia, this condition does not appear to be related to intrauterine vascular accidents (Lee et al. 2010). Major associated anomalies are present in about 50 % of the

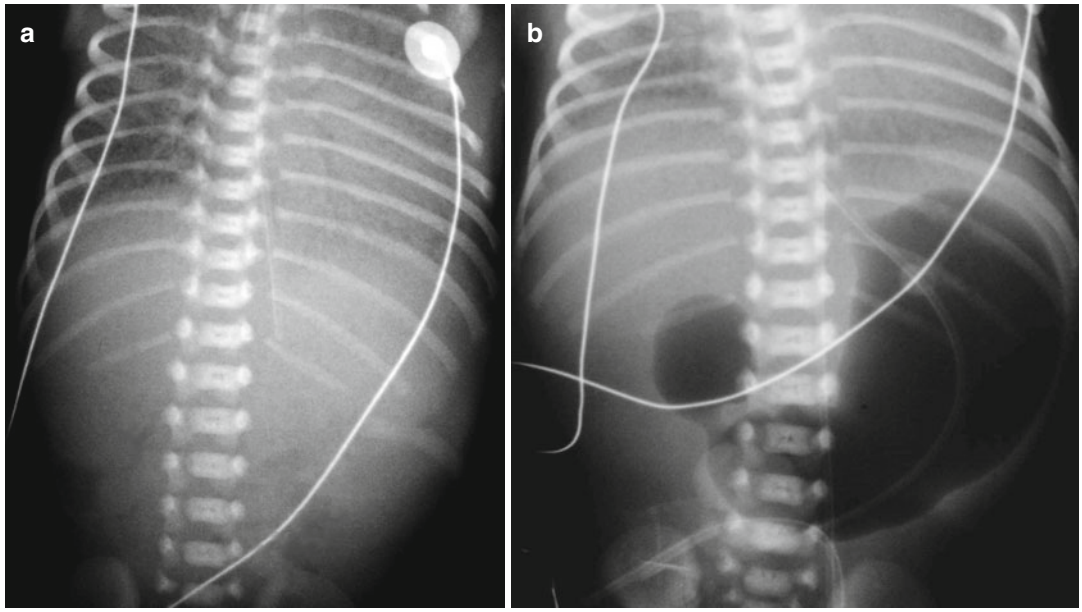


**Fig. 6** Duodenal atresia. (**a**) Plain radiograph obtained 6 h after birth shows absence of air in the gastrointestinal tract of this neonate with severe lung disease. (**b**) Radiograph made after inflation of the stomach through a nasogastric tube demonstrates complete duodenal obstruction ("double bubble" sign)

patients. Approximately 30 % have Down's syndrome; congenital cardiac defects are found in another 30 %, and 25 % have other GI anomalies. Renal, skeletal, and central nervous system anomalies are less common associations. Malrotation is found in up to 30 % of patients with congenital duodenal obstruction (Juang and Snyder 2012).

*Annular pancreas* is an anomalous band of pancreatic tissue, which arises from the head of the pancreas and encircles the second portion of the duodenum to a variable extent, giving rise to a variable degree of duodenal obstruction. This anatomy results if two ventral pancreatic buds arise from the ventral mesentery and rotate in opposite directions to fuse with the dorsal pancreatic bud (Etienne et al. 2012; Jimenez et al. 2004). If a complete ring is formed, there may be complete obstruction of the duodenum at the time of birth; if the ring is incomplete, obstruction may occur later in life or may never produce symptoms. When a complete ring is formed, radiological findings are indistinguishable from duodenal atresia with the typical double bubble sign, and the diagnosis is made at surgery (Hernanz-Schulman 1999; Jimenez et al. 2004) (Fig. 7).

*Midgut volvulus* is the most dramatic consequence of intestinal malposition. When present at birth, the classic finding on a plain film is partial obstruction of the duodenum, but evidence of complete obstruction may also be present. In such cases, it is impossible to distinguish midgut volvulus from duodenal atresia or annular pancreas (Fig. 8). Past the immediate postnatal period, any duodenal obstruction should be assumed to be midgut volvulus until proven otherwise (Buonomo 1997; Berrocal et al. 1999). It is the only condition mentioned above that may actually lead to the death of the patient. Antenatal diagnosis of duodenal obstruction would ideally reduce perinatal morbidity and mortality by allowing a planned delivery and prompt surgical intervention. The prenatal diagnosis usually occurs during the second trimester and is based on sonographic demonstration of polyhydramnios in conjunction with a fluid-filled "double bubble" in the fetal abdomen corresponding to the double bubble sign seen on postpartum radiographs (Shawis and Antao 2006; Rubesova 2012;

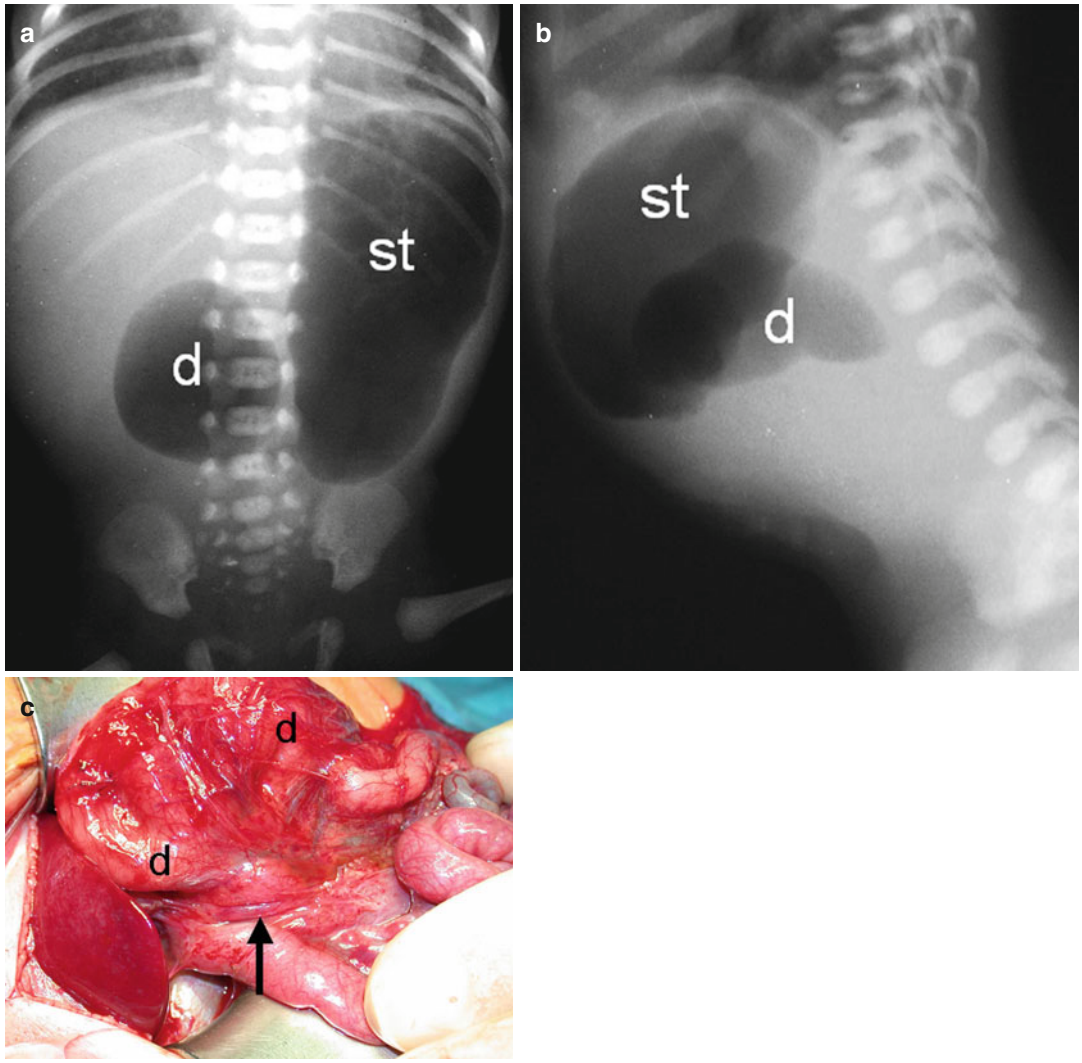


**Fig. 7** Annular pancreas. (**a**) Supine and (**b**) lateral views of the abdomen show complete obstruction at duodenal level identical to that seen in duodenal atresia. The stomach (*st*) and duodenal bulb (*d*) are distended and there is no distal air. (**c**) Surgical image shows the pancreatic tissue (*arrow*) encircling the duodenum (*d*)

Kul et al. 2012). Since there is a high incidence of associated anomalies, identification of a double bubble sign should prompt consideration of fettle karyotyping and a careful search for other fetal anomalies (Juang and Snyder 2012).

*Partial duodenal obstruction* may be produced by duodenal stenosis, duodenal web, Ladd bands, midgut volvulus, annular pancreas, preduodenal portal vein, and duplication cysts. Plain radiographs show gaseous distension of the stomach and duodenum with a normal or diminished quantity of air in the small bowel. Contrast studies are necessary to differentiate between midgut volvulus and partial duodenal obstruction caused by a web or stenosis (Vinocur et al. 2012). Duodenal web refers to a small congenital obstructing membrane with a central pinhole aperture that constitutes a functional web. Long-term pressure of peristalsis against the stenotic segment of the duodenum may lead to distal stretching of the web, forming an intraluminal pseudo-diverticulum (windsock diverticulum).

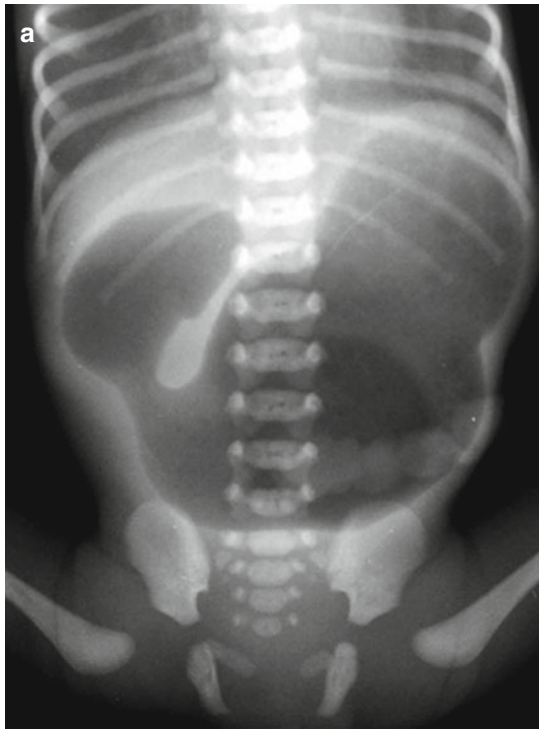


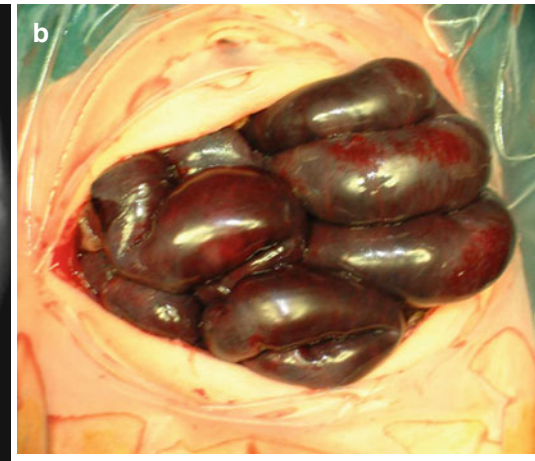


**Fig. 8** Midgut volvulus. Five-day-old neonate infant with severe vomiting. (**a**) Abdominal plain radiograph shows marked distension of the stomach and duodenal bulb and absence of air more distally. (**b**) Surgery demonstrated midgut volvulus with necrosis of the entire midgut

The characteristic upper gastrointestinal finding is a faint radiolucent membrane, produced by barium filling the lumen and around the diaphragm. In duodenal stenosis, upper gastrointestinal studies show the duodenal bulb distended and slow transit of oral contrast material through the stenotic segment of the duodenum to the distal bowel. Preduodenal portal vein is a rare anomaly in which the portal vein passes anterior to the duodenum rather than posteriorly. An UGI study usually shows a dilated stomach, the first part of the duodenum with an abrupt cutoff, some distal runoff of contrast, and a corkscrew appearance of the duodenum distal to the cutoff (Singal et al. 2009). In cases of duplication cysts, US is helpful by demonstrating a sonolucent-rounded structure with a characteristic echogenic inner mucosal layer and an hypoechoic underlying muscular layer located on the mesenteric side of the second portion of the duodenum. Because of the partial obstruction, affected pediatric patients may present later in life more commonly than those with duodenal atresia.

### 1.1.3 Malrotation and Midgut Volvulus

Malrotation is a general term that includes a wide spectrum of anomalies that occur when intestinal rotation and fixation happen in an abnormal way: malposition of the bowel.

Failure of completion of the normal intestinal rotation leads to a continuum of anatomic abnormalities with a common clinical denominator consisting of malposition of bowel and resulting obstruction with the potential for midgut volvulus. Only its presentation as an abdominal emergency in the neonatal period is discussed here.

Anomalies of rotation and their complications are best understood in light of the normal process of intestinal rotation. In normal bowel rotation, which occurs in the 5th to 12th weeks of gestation, the

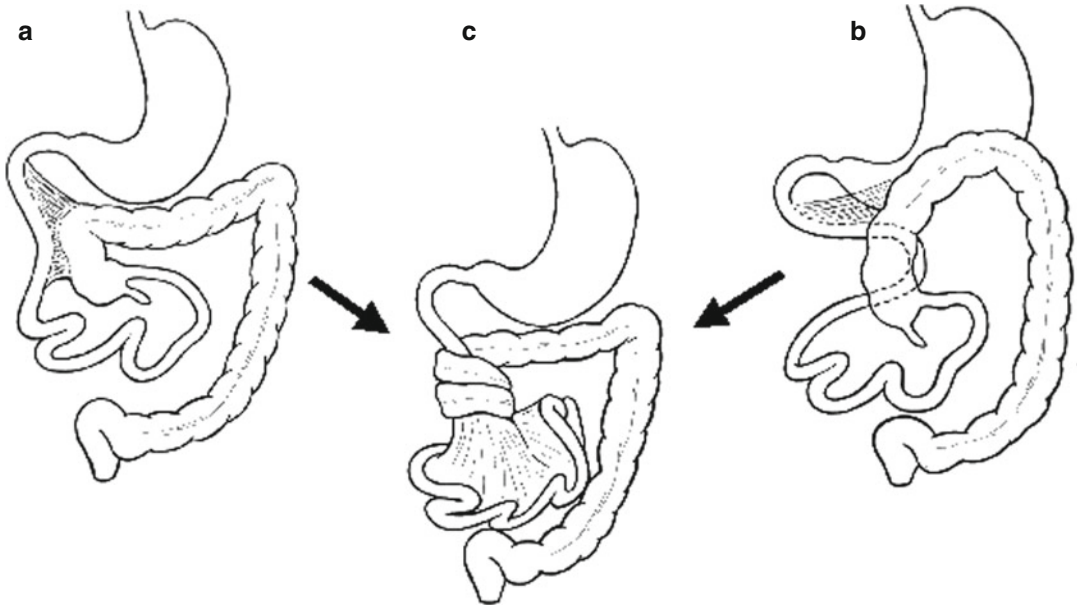


**Fig. 9** Schematic drawing that shows midgut volvulus (**c**) developing from non-rotation (**a**) or incomplete rotation (**b**). The lack of normal fixation due to short mesentery permits the bowel to volve

bowel herniates into the umbilical cord and rotates counterclockwise around the superior mesenteric artery (SMA) before returning to the peritoneal cavity. The duodenojejunal junction, anchored by the ligament of Treitz, is located in the left upper quadrant, and the mesenteric fixation is broad, extending to the cecum in the right lower quadrant. In classic malrotation, the duodenojejunal junction is located inferior and to the right of the normal position, and the cecum is often high and medially positioned. When the duodenojejunal junction and the cecum are not in their usual location, the mesenteric attachment is shortened to a narrow pedicle. Because the entire length of the midgut is attached to this narrow pedicle, there is a tendency for the intestines to twist around the pedicle. The twisting of malfixed intestines around the short mesentery results in midgut volvulus (Fig. 9) (Lampl et al. 2009; Strouse 2004).

With volvulus, the small bowel wraps around the axis of the SMA, with rotations of 720° and greater often reported. Increasing degrees of volvulus will obstruct the bowel lumen, but also the lymphatic drainage, the venous drainage, and eventually, the arterial supply.

Obstruction of this vascular supply and drainage of the entire small bowel is a life-threatening condition requiring immediate surgical intervention (Pickhardt and Bhalla 2002; Juang and Snyder 2012). One needs at least 3 in. of small bowel to survive in life.

A patient with malrotation may also develop dense peritoneal bands, termed Ladd bands, which originate in an attempt to "fix" the bowel positioning. These bands extend from the cecum to the hilum of the liver, posterior peritoneum, or abdominal wall across the duodenum and can cause extrinsic duodenal obstruction. Volvulus of the midgut may occur at any age, but it is more common in the first month of life, most of them presenting in the first week of life (Shew 2009; Daneman 2009). In general, the symptoms are those of obstruction. The child with obstruction secondary to midgut volvulus typically presents with a sudden onset of bilious vomiting often preceded by initial toleration of feeding. The sudden onset of bilious emesis in a neonate who has been normal for the first few days of life should be considered to be due to a midgut volvulus until proven otherwise (Buonomo 1997). In the early stages, prior to the onset of ischemia, the abdomen is not distended. Patients presenting with shock have a worse prognosis. This manifests as abdominal

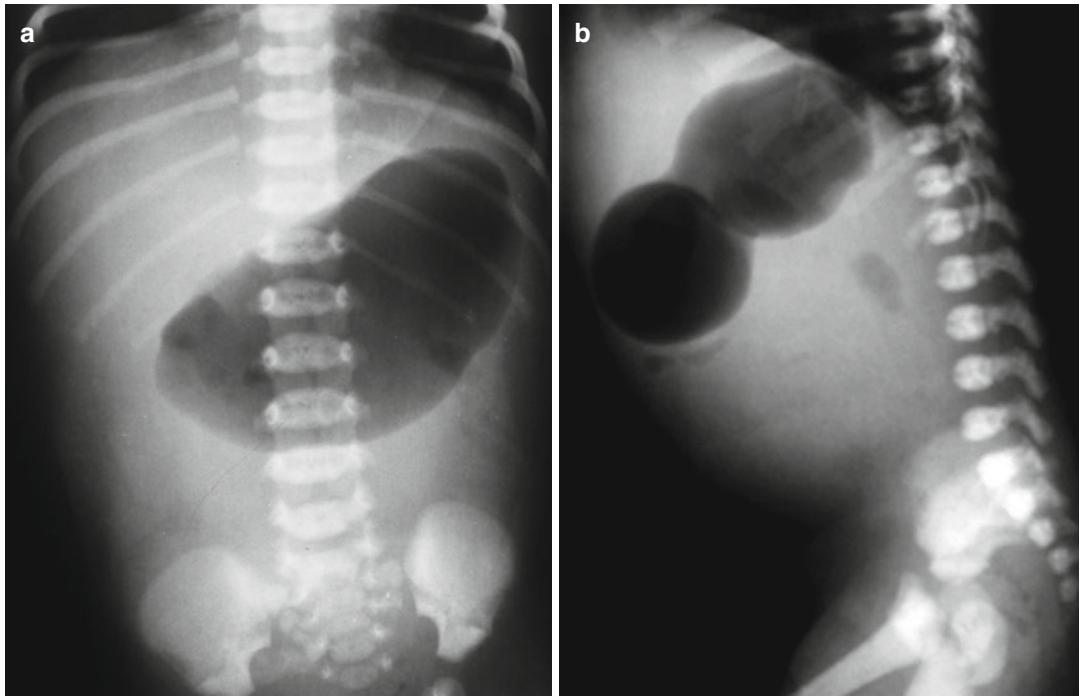


**Fig. 10** Midgut volvulus. (**a**) Supine and (**b**) lateral radiographs show distension of the stomach and duodenum with some distal intestinal air in a 12-day-old infant with severe vomiting

distension with peritonitis, bloody stools, and hemodynamic compromise (Shew 2009).

The imaging work-up often begins with a plain radiograph. An anteroposterior supine view and either an upright view or cross-table lateral view should be obtained. Although the use of the upright/decubitus radiograph has been debated, with some calling for its abandonment, many authors believe that the upright/decubitus radiograph is useful for the assessment of air–fluid levels and free air in the setting of bowel obstruction (Hryhorczuk and Lee 2012). The abdominal plain radiograph can show evidence of obstruction, usually in the third portion of the duodenum but, occasionally, higher or even lower. The stomach and proximal portion of the duodenum are dilated, and some air is usually seen in the jejunum and ileum (Fig. 10). These cases are frequently similar in appearance to duodenal stenosis and other incomplete congenital duodenal obstructions. As already noted, complete duodenal obstruction with the double bubble sign may also be a presentation form, this pattern being indistinguishable from other causes of complete congenital duodenal obstruction (Gilbertson-Dahdal et al. 2009). The abdominal radiograph may be normal if the obstruction is recent, intermittent, or incomplete or may demonstrate a relative paucity of bowel air. The significance of these findings must be recognized in the context of an infant with bilious vomiting, because they are much more alarming than multiple dilated loops of bowel, which denote a more distal obstruction from a cause other than midgut volvulus. A gasless abdomen associated with abdominal distension or tenderness may be a sign of strangulated midgut volvulus. Diffuse gaseous distension of the bowel with a "low obstruction" pattern is uncommon and correlates with gangrenous bowel, perhaps because vascular occlusion interferes with resorption of air (Strouse 2004) (Fig. 11).

An upper gastrointestinal series is classically the following imaging modality for the radiologic diagnosis of a midgut volvulus and should be performed in all patients with bilious emesis,

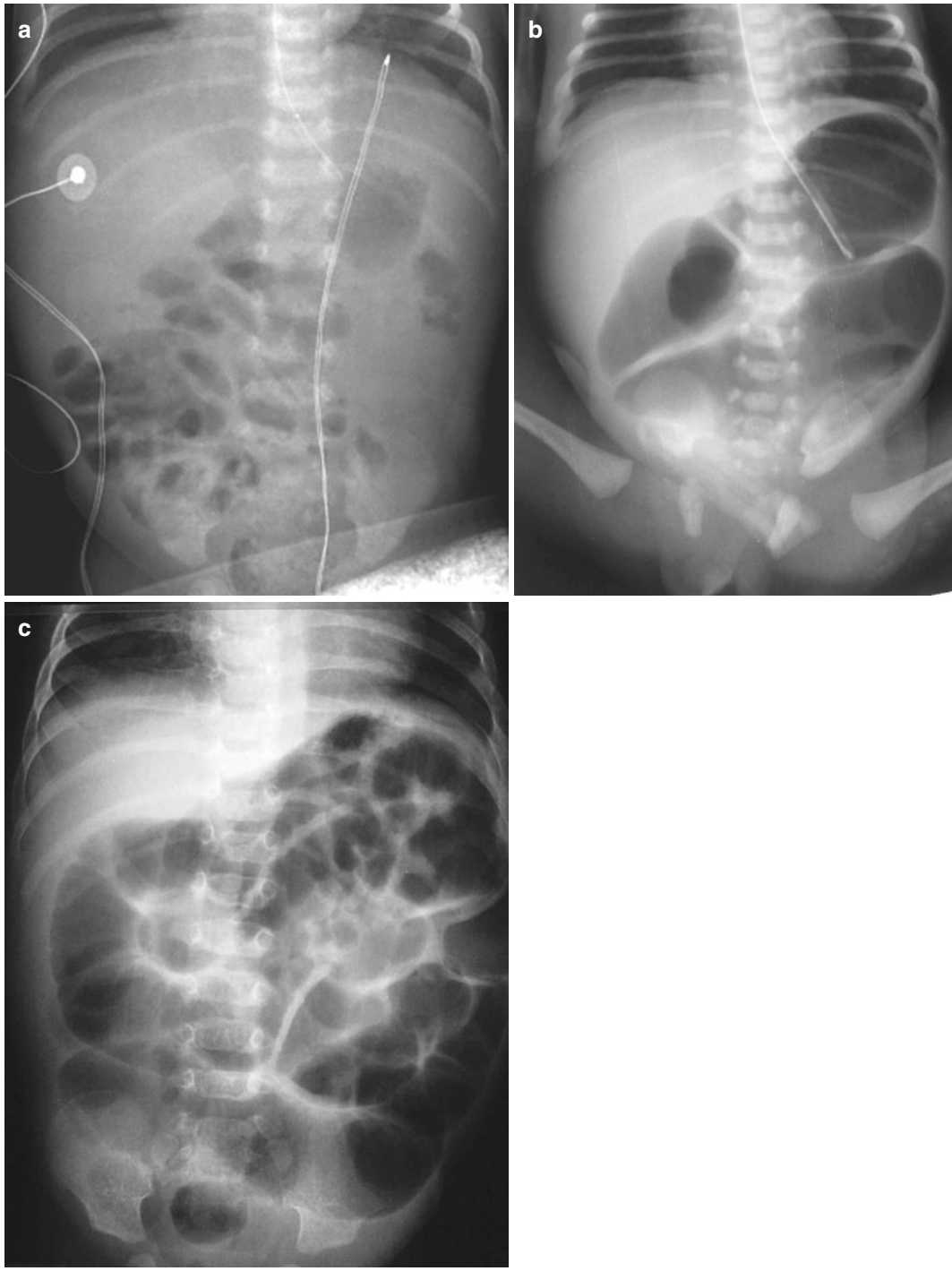


**Fig. 11** Different patterns of midgut volvulus in plain abdominal radiographs. (**a**) Normal air pattern in a neonate with bilious vomiting. (**b**) Another neonate patient with bilious vomiting. There are a few dilated bowel loops suggesting high intestinal obstruction. (**c**) Obstructed distended air pattern suggesting devitalized bowel probably due to venous obstruction and infarction

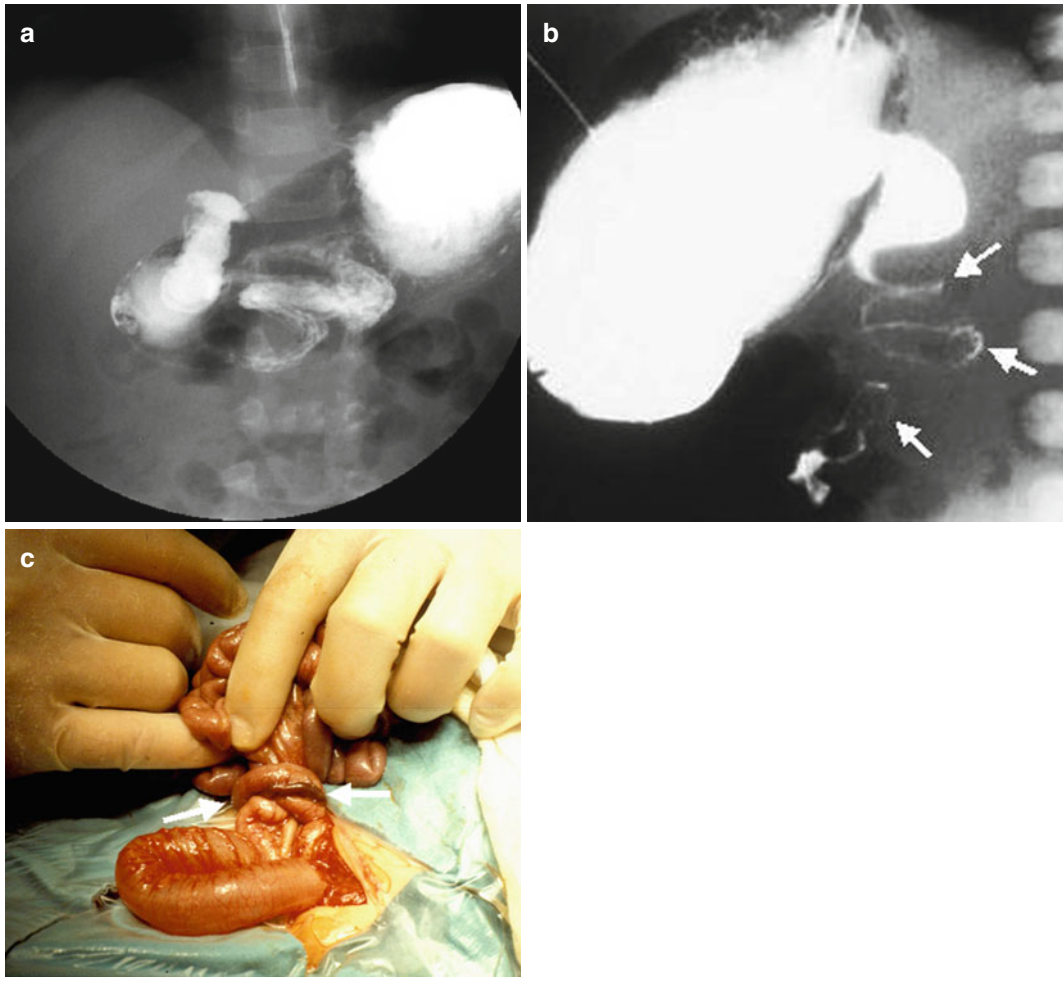


**Fig. 12** Midgut volvulus in a 16-day-old male infant with bilious vomiting. (**a**) Upper gastrointestinal study, anteroposterior projection. Radiograph demonstrates the corkscrew configuration of the duodenum and proximal jejunum. (**b**) Lateral projection. The spiral or corkscrew appearance of the duodenum and jejunum is again shown (*arrows*). The anterior course of the distal duodenum is demonstrated. (**c**) Midgut volvulus (*arrows*) without ischemia was found at surgery

except in those with evidence of complete duodenal obstruction in the plain radiograph or in critically ill infants.

A nonionic, water-soluble contrast medium is often the contrast of choice, although barium can be used, and being denser helps identify the DJ flexure better. Ionic hypertonic solutions, such as Gastrografin, are to be avoided as aspiration causes pulmonary edema that may be fatal.

The contrast medium may be administered orally or, even better, through a nasogastric tube to control the amount of contrast, because a contrast-filled, distended stomach may obscure the course and configuration of the duodenum. The pathognomonic finding of midgut volvulus in the upper gastrointestinal examination is a spiral or "corkscrew appearance" of the twisted distal duodenum and jejunum that is located in the middle of the abdomen (Strouse 2004; Applegate 2009) (Fig. 12). The bowel lumen is narrowed and the duodenum proximal to the obstruction may be mildly dilated. The contrast passes from the stomach to the duodenum and jejunum showing the characteristic corkscrew course both in the anteroposterior and lateral views. In the lateral view, the distal duodenum will exhibit a

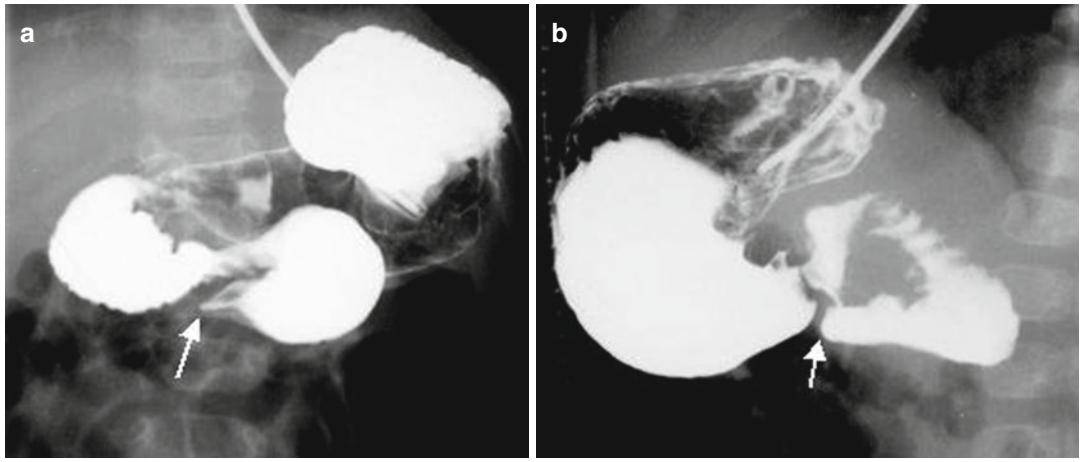


**Fig. 13** Midgut volvulus in a 7-day-old female infant with bilious vomiting. Upper gastrointestinal series. (**a**) Anteroposterior and (**b**) lateral projections. The distal duodenum courses anteriorly and tapers to a "beaked" obstruction (*arrow*). No contrast material is observed beyond the obstruction, but there is distal air indicating a recent complete obstruction

characteristic anterior course (Fig. 12) (Koplewitz and Daneman 1999). When there is complete obstruction, the contrast medium cannot enter the volved loops to show the "corkscrew" and only the entrance to the volvulus is identified, with a tapered or "beaked" appearance (Fig. 13). In cases of recent complete obstruction, distal air may be seen; however, the contrast cannot enter the volved segment, so the corkscrew image cannot be seen. Once the findings of volvulus are confirmed, no further imaging studies are necessary. Surgical intervention is mandatory immediately following the diagnosis.

Obstruction due to Ladd bands produces a Z-shaped configuration, outlining the lack of normal rotation and fixation of the duodenum. The Z-configuration may appear similar to the "corkscrew" of volvulus, but it does not indicate volvulus itself (Fig. 14). It must be stressed, however, that in most children with malrotation, obstruction is caused by the volvulus with the band playing a lesser role or no role at all (Lampl et al. 2009).

Currently, a contrast enema has fallen out of favor for the diagnosis of malrotation. This is because the cecum can be normal in up to 20–30 % of infants with malrotation, and, therefore, a normal cecum does not exclude malrotation. On the other hand, approximately 15 % of patients with normal rotation have a mobile cecum that could be misinterpreted as malfixation (Applegate 2009). Nevertheless, demonstration of an unequivocally abnormal cecal position in the setting of an equivocal upper gastrointestinal series may be helpful (Strouse 2004).

In fact, many authors currently recommend routine US examination before performing a gastrointestinal series in any patient with bilious vomiting if surgery is going to be delayed, for several reasons: (1) it can be performed at the bedside with lack of need for preparation; (2) it provides information about the outside part of the bowel loops and the abdominal cavity not provided by the contrast examination; (3) in complete obstruction, it provides information about the intestinal loops beyond the obstruction; and (4) lack of ionizing radiation (Babcock 2002; Ryan and Donoghue 2010). The first step is to determine the location of mesenteric vessels at their origin and follow their course in the mesenteric root. In normal patients, serial US demonstrate the superior mesenteric vein running on the right side of the superior mesenteric artery until their division (Couture 2008). Moreover, the third portion of the duodenum may be seen crossing the midline, posterior to the superior mesenteric pedicle, and the duodenojejunal angle is depicted on the left side, posterior to the stomach

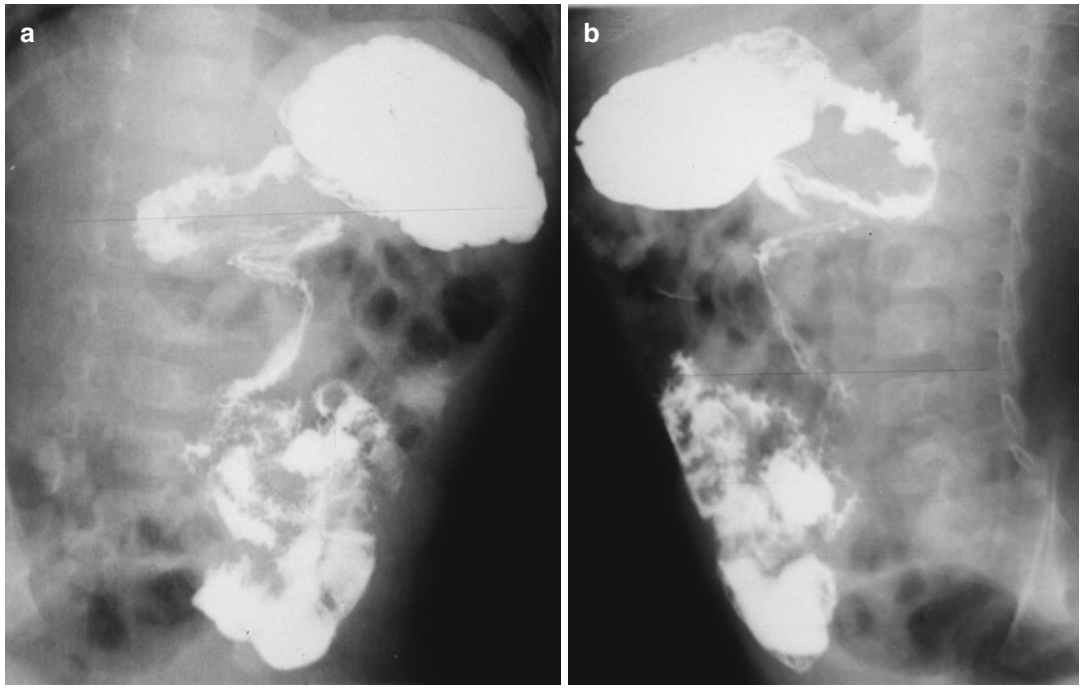


**Fig. 14** Malrotation with Z-shape of the duodenum and jejunum. Upper gastrointestinal series. (**a**) Anteroposterior and (**b**) lateral projections show a central, downward, Z-course of the duodenum. No volvulus was found at surgery. Surgery demonstrated the partial obstruction to be produced by Ladd bands

(Menten et al. 2012). Recently, based on anatomical and embryological principles, Yousefzadeh 2009 has suggested that a retroperitoneal third portion of the duodenum between the aorta and the SMA is an indicator for normal rotation rather than the position of the duodenojejunal flexure. Therefore, the demonstration of a retromesenteric duodenum is the reference standard of imaging in the work-up of malrotation, not any other previously published criteria (Yousefzadeh 2009). However, for some authors, the diagnosis of malrotation continues to be a challenge, as the third portion of the duodenum located behind the SMA has been described in cases of surgically repaired malrotation (Taylor 2011).

The characteristic finding of midgut volvulus in the US examination is the "whirlpool" sign produced by the twisting of the bowel, mesentery, and superior mesenteric vein around the axis of the superior mesenteric artery (Fig. 15). The whirlpool sign, proposed by Pracros et al. (1992), directly indicates the anatomic alteration caused by midgut volvulus. The SMV and tributaries wrap around the SMA as a result of the volvulus, resulting in a partial or complete blockage of the blood supply to the midgut. The whirlpool sign represents this characteristic pattern of the SMV and SMA on sonograms (Pracros et al. 1992; Shimanuki et al. 1996). Color Doppler reveals a circle of vascularity representing the superior mesenteric vein twisting around the superior mesenteric artery (Patino and Munden 2004). Other described findings such as dilated thick-walled bowel loops, mainly to the right of the spine, increased peritoneal fluid, a dilated duodenum, a truncated SMA, and a solitary hyperdynamic pulsating SMA are also useful findings in a proper clinical setting but are nonspecific (Sze et al. 2002). Dilated bowel loops, thickened bowel walls, and aperistaltic loops suggest intestinal ischemic damage, but ischemic loops may be thinned walled, and morphological US criteria cannot exclude bowel ischemic injury. Absence of flow within the spiral twist at color Doppler suggests ischemia, but it is an extremely rare occurrence (Veyrac et al. 2012). A rare

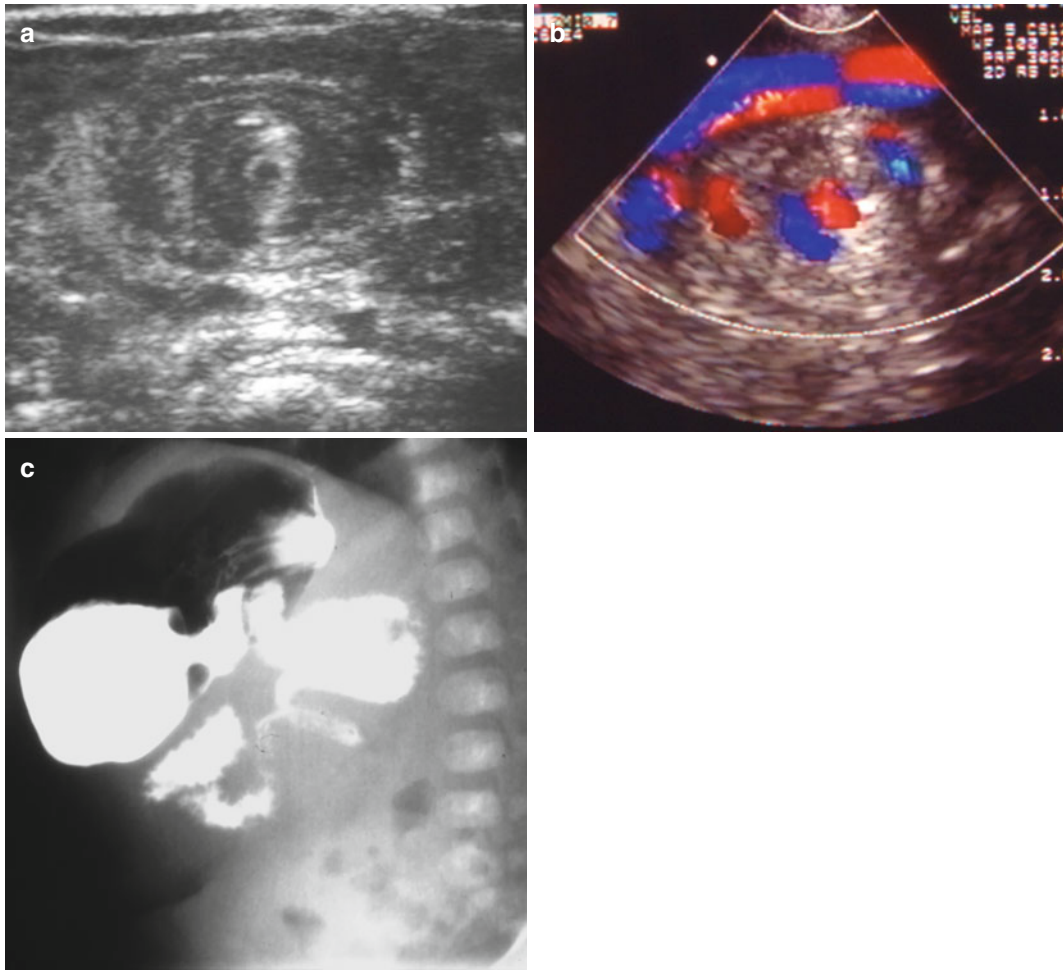


**Fig. 15** "Whirlpool" sign of midgut volvulus. Twelve-day-old female infant with bilious vomiting. (**a**) Transverse B-mode sonography of the upper abdomen shows the twisting of bowel, mesentery, and superior mesenteric vein around axis of superior mesenteric artery. (**b**) Color Doppler image demonstrates a circle of vascularity that represents the superior mesenteric vein twisting around the superior mesenteric artery, producing the characteristic "whirlpool sign." (**c**) Upper gastrointestinal series confirms midgut volvulus

normal variant of midgut rotation is the counterclockwise rotation of the SMV around the SMA. In this condition, counterclockwise SMV/SMA configuration may appear similar to whirlpool sign of volvulus, but it does not indicate volvulus itself, and an upper gastrointestinal series shows a normally located duodenal–jejunal junction. The so-called counterclockwise barber-pole sign is usually seen in asymptomatic patients, and the significance of these findings must be recognized in the context of an asymptomatic infant under review for another reason (Clark and Ruess 2005).

### 1.1.4 High Small Bowel Obstruction

High small bowel obstruction includes atresia or stenosis of the jejunum or proximal ileum. It is now generally accepted that intestinal atresia and stenosis below the duodenum are caused by an intra-abdominal vascular accident during intrauterine life. The vascular accident may be primary or secondary to a mechanical obstruction, as in the case of in utero volvulus. This results not merely in a hindrance of growth, but also in an actual disappearance of the affected portion of the fetal bowel (Juang and Snyder 2012).

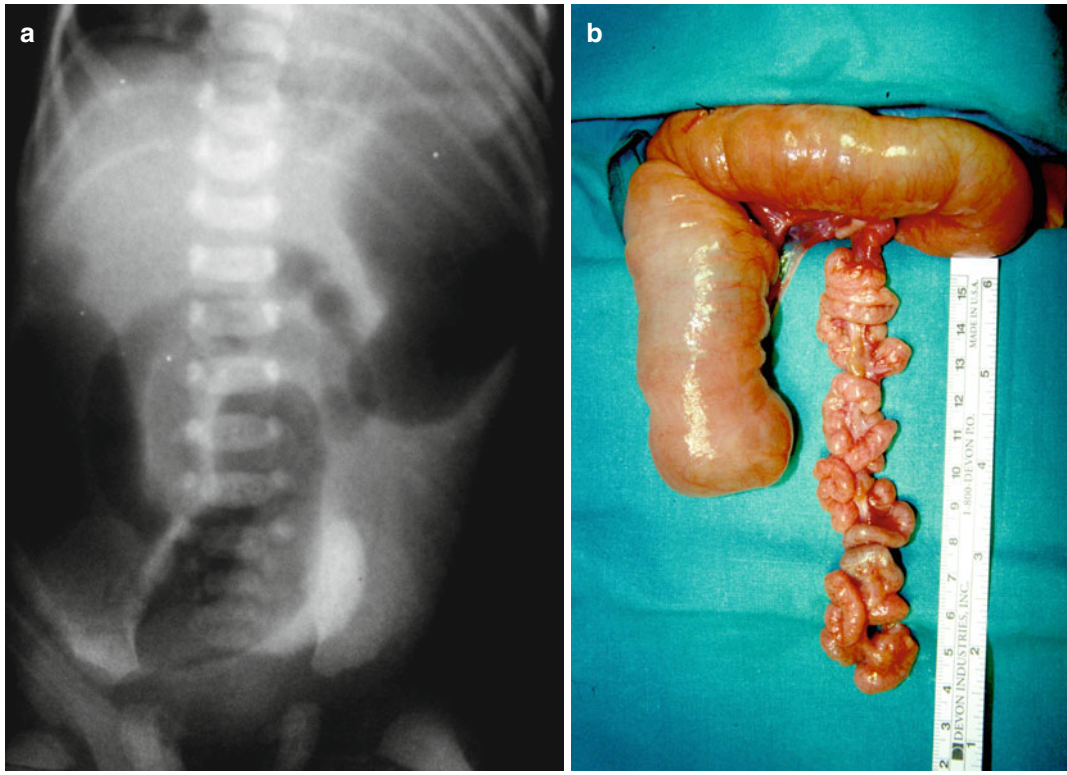


**Fig. 16** "Apple-peel" mesentery. (**a**) Plain radiograph showing dilated proximal loops suggesting high obstruction. (**b**) Surgical specimen shows the dilated proximal segment and the collapsed distal segment, which spirals around its vascular supply and resembles an "apple peel." The mesentery is short

Jejunoileal atresias are classified into four types based on their anatomic appearance (Juang and Snyder 2012). Type I is a simple intraluminal diaphragm and accounts for 32 % of jejunal atresias. In type II, the proximal bowel terminates in a blind end and the distal bowel commences similarly, the two ends being joined by a fibrous band. In type III, the proximal and distal blind ends are completely separated with no connecting band. The adjoining mesentery always has a V-shaped defect corresponding to the missing segment. The familial form of multiple atresias is considered type IV. A rare form of inherited jejunal atresia is the "apple-peel mesentery," also called the "Christmas tree mesentery." This abnormality is the result of a catastrophic in utero vascular accident, producing an interruption of the distal superior mesenteric artery that leads to atresia of a large segment of small bowel and mesentery. The proximal segment is dilated, whereas the collapsed distal segment is spiraled around its vascular supply and resembles an apple peel. The blood supply is retrograde through the anastomotic arcade of the inferior mesenteric artery (Patil et al. 2011). This defect has historically been associated with high mortality, although recent reports suggest an improved prognosis (Lee et al 2012). The apple-peel type of atresia does not have distinctive findings on plain film (Fig. 16).

Jejunal atresias comprise approximately 50 % of small bowel atresias, and in 10 % of the cases, there are multiple areas of atresia (Lee et al. 2012). Jejunal atresia is clinically characterized by bilious vomiting, frequently delayed until after the first feeding, and abdominal distension. The lower the obstructive lesion in the small bowel, the more severe the abdominal distension and the more difficult the accurate localization of the site of obstruction becomes (Godbole and Stringer

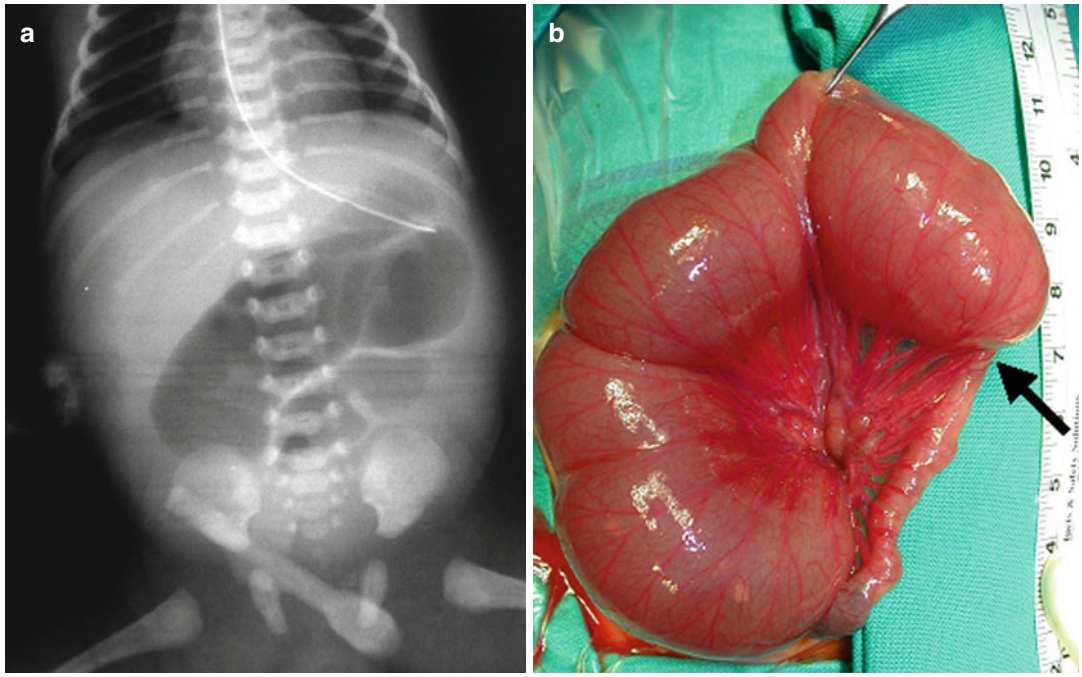


**Fig. 17** Jejunal atresia. (**a**) Supine radiograph shows a few dilated air-filled intestinal loops, about four "bubbles," which indicate a high obstruction. (**b**) Surgical image demonstrates the location of the atresia (*arrow*), the dilated proximal jejunum, and the small caliber of the bowel distal to the atresia

2002). The diagnosis is usually apparent on the plain films. The abdominal radiograph shows a few dilated bowel loops (three or four air bubbles), more than in the case of duodenal atresia and fewer than in ileal atresia or in other causes of low bowel obstruction (Fig. 17). The loop just proximal to the site of the atresia is frequently disproportionately dilated with a bulbous end. There is no air in the lower portion of the abdomen; this is observed most clearly in the upright film (Fig. 18). The colon cannot be identified and air is not found in the rectum. These signs indicate an obstructive lesion in the small intestine, and surgery is mandatory. Here, also when the obstruction can be definitely identified in the small intestine, there is no need to delay surgery to give contrast material orally. An upper gastrointestinal series is clearly not indicated. In fact, flocculation and dispersion of the contrast given orally may occur, due to the high mucus content of the distended segment, and little information is obtained. Occasionally, the dilated bowel loops may be fluid filled giving an airless abdomen. In cases of doubt, aspiration and insufflation of air through a nasogastric tube should be carried out (Fig. 19). Although a patient with jejunal or proximal ileal atresia usually needs no further radiologic investigation, contrast material enema examinations are commonly performed to attempt to exclude second and third areas of atresia lower in the bowel. The colon in isolated jejunal and proximal ileal atresia, as in duodenal atresia, is normal or near normal in size. If a microcolon is encountered, additional distal atresia should be suspected (Hernanz-Schulman 1999). Contrast enema is especially indicated when the scout radiograph shows distension of the flanks and elevation of the diaphragms indicating the presence of multiple dilated loops of the bowel filled with fluid distal to the obstruction. If the ischemic event that produced the atresia caused a perforation, there may be evidence of meconium peritonitis with peritoneal calcification.

Severe congenital stenosis of the small bowel is usually accompanied by vomiting and

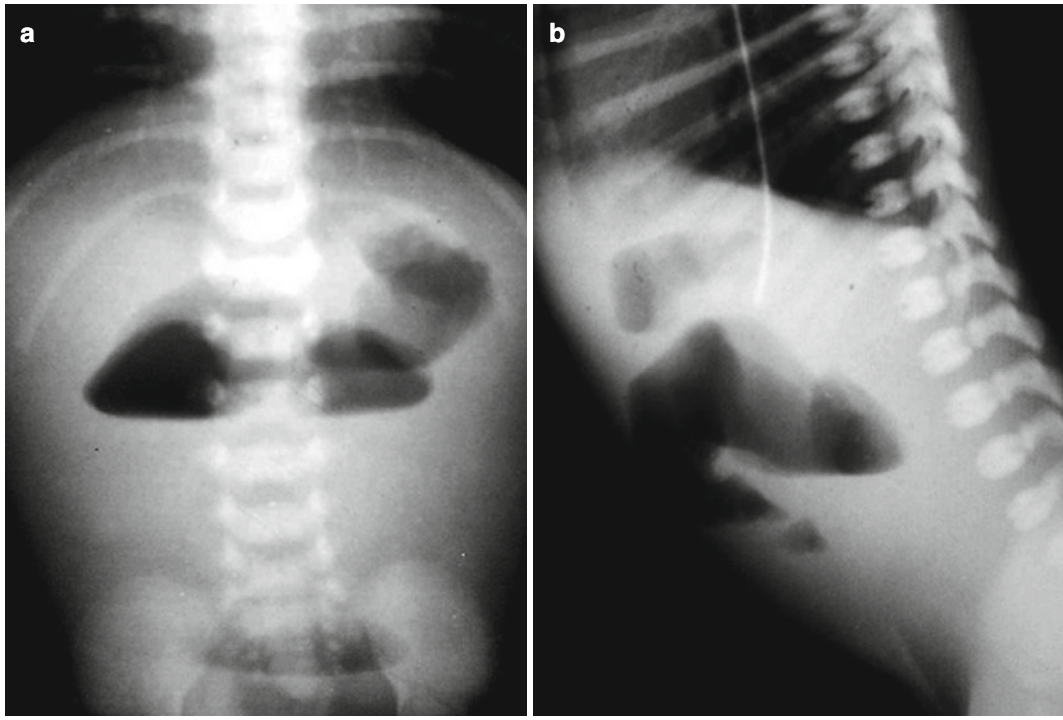


**Fig. 18** Jejunal atresia. (**a**) Anteroposterior and (**b**) lateral upright radiographs show a few central air–fluid levels indicating high obstruction

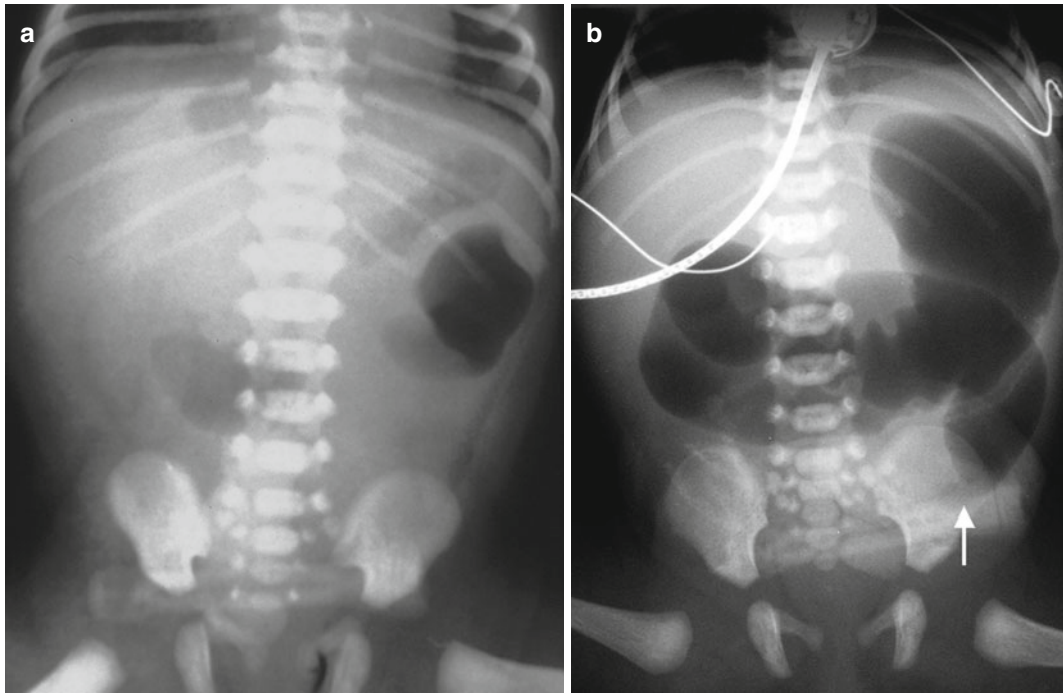


**Fig. 19** Jejunal atresia. (**a**) Supine radiograph shows a gasless abdomen. (**b**) Aspiration and insufflation of air through a nasogastric tube were carried out that adequately demonstrate the point of obstruction (*arrow*). Massively dilated loops of jejunum but only about three "bubbles" are seen indicating a high obstruction

abdominal distension, identical in severity to that seen in atresia. In less severe cases, these symptoms may be mild or even delayed for several days or weeks. Plain abdominal radiographs reveal dilatation of bowel loops proximal to the stenosis and normal or decreased quantity of air in the small bowel distal to the stenosis (Juang and Snyder 2012).

## 1.2 Low Obstruction

Low intestinal obstruction is defined as obstruction occurring in the distal ileum or colon. The symptoms are vomiting, abdominal distension, and failure to pass meconium. For practical purposes, the differential diagnosis of low intestinal obstruction in the neonate consists of five conditions. Two conditions involve the distal ileum and include ileal atresia and meconium ileus, and three involve the colon, which are colonic atresia, Hirschsprung disease, and functional immaturity of the colon that include meconium plug syndrome and small left colon syndrome.

A low obstruction is usually obvious on the plain film. Plain radiographs in low obstructions are characteristic, always showing multiple dilated air-filled bowel loops, with air–fluid levels in the upright or horizontal beam radiographs. It is usually impossible to determine the level of obstruction from the plain radiograph (if the affected segment is the distal ileum or any part of the colon). The dilated loops occupy the entire abdominal cavity, and the small and large bowel cannot be distinguished from each other. This distinction can be readily made with a contrast enema. Virtually all neonates with evidence of low obstruction require a contrast enema, which usually provides a specific diagnosis and may be therapeutic (Buonomo 1997; Vinocur et al. 2012). The critical differential diagnostic finding on the contrast enema of a newborn with low obstruction is the presence or absence of a microcolon. The term microcolon is synonymous with "unused colon." The colon in low intestinal obstruction is small, owing to a lack of use rather than anatomic or functional abnormality (Subbarao 2008). The caliber of the colon depends on the passage of intestinal fluid and desquamated mucosal cells from the jejunum and proximal ileum. These small intestinal contents are termed succus entericus. If little or no succus entericus reaches the colon, it is tiny. In low intestinal obstructions, the fetal colon does not receive sufficient contents from the small intestine to assume its normal caliber, and, therefore, at birth, the colon is usually of very small caliber, generally less than 1 cm, and nondistensible. Proximal obstructions such as duodenal or jejunal atresias maintain normal colonic caliber by virtue of passage of succus entericus produced by the remaining small bowel distal to the atresia (Hernanz-Schulman 1999). Normally, meconium reaches the cecum in the fourth month of intrauterine life and is in the rectum by the fifth month. The development of obstruction at an early period will consequently prevent the passage of meconium into the colon, leaving this structure collapsed and narrowed, although potentially distensible. In cases of distal small bowel obstruction of relatively recent onset, the colon has had time to attain a normal caliber, and therefore, a microcolon is not present. Thus, the presence of a microcolon is diagnostic of a long-standing distal small bowel obstruction, but a normal colon does not exclude this condition in all cases (Dalla Vecchia et al. 1998). The degree of microcolon in complete obstruction is variable, presumably due to the variable amount of meconium formed by internal secretions below the obstruction. The choice of contrast medium varies among different medical centers although a low osmolar water-soluble contrast is preferable to barium.

Currently, abdominal US is useful in low intestinal obstruction since it distinguishes dilated from collapsed loops or ascites (Fig. 20) and can often distinguish ileal loops from colon. It is also possible to distinguish the dilated fluid-filled loop proximal to an atresia from the dilated meconium-filled loop of a meconium ileus and to demonstrate associated anomalies in the abdominal organs. It may be possible to proceed directly to surgery for ileal atresia or to proceed to reduction of a meconium ileus by contrast enema. Therefore, in many centers, it is routinely used before or instead of contrast enema (Ryan and Donoghue 2010).

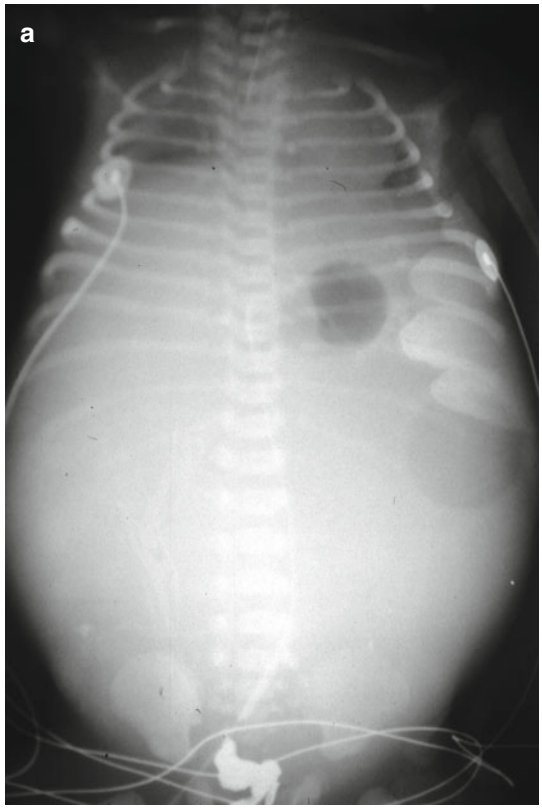


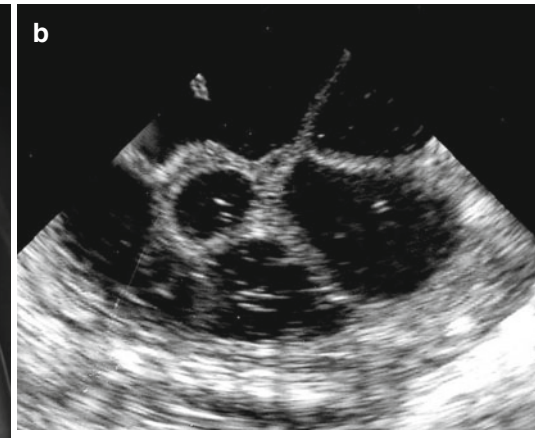


**Fig. 20** High intestinal obstruction. (**a**) Plain radiograph of a newborn infant that shows a gasless abdomen with air seen only in the stomach. Despite the lack of intestinal air, there is distension of the flanks and elevation of the diaphragms. (**b**) Sonography demonstrates the abdominal distension to be produced by fluid-filled intestinal loops. At surgery, a proximal ileal atresia was found

### 1.2.1 Distal Small Bowel Obstruction

Ileal atresia is an important cause for low intestinal obstruction, representing approximately 50 % of small bowel atresias. It occurs in approximately 1 in 5,000 live births and affects male and female infants equally. Approximately 1 in 3 infants is premature. Most cases of ileal atresia occur secondary to vascular disruption during fetal life. The ischemic insult to the midgut can affect single or multiple segments of the already developed intestine, and the resulting ischemic necrosis of the bowel can lead to subsequent resorption of the affected segment. Approximately 25 % have a history of polyhydramnios (Juang and Snyder 2012).

Plain abdominal film shows numerous dilated loops of bowel occupying the entire abdominal cavity, including the pelvic portion, and multiple air–fluid levels in an upright film (Fig. 21). With this degree of distension, the mucosal pattern of the small bowel is effaced, and it is impossible to differentiate the small bowel from the colon. Examination of the colon is then warranted to disclose the presence or absence of a colonic lesion (Subbarao 2008). In ileal atresia, the colon is normally placed but has an abnormally small caliber, the so-called functional microcolon typical of distal small bowel obstruction (Fig. 21 d, e). The presence of pneumoperitoneum indicates that perforation has occurred and a colon examination is contraindicated. Intraperitoneal calcifications, indicative of meconium peritonitis, are not uncommon in ileal atresia. US can demonstrate severe distension of the proximal bowel loops (16–40 mm in diameter), filled with fluid and punctuated with echodense particles of

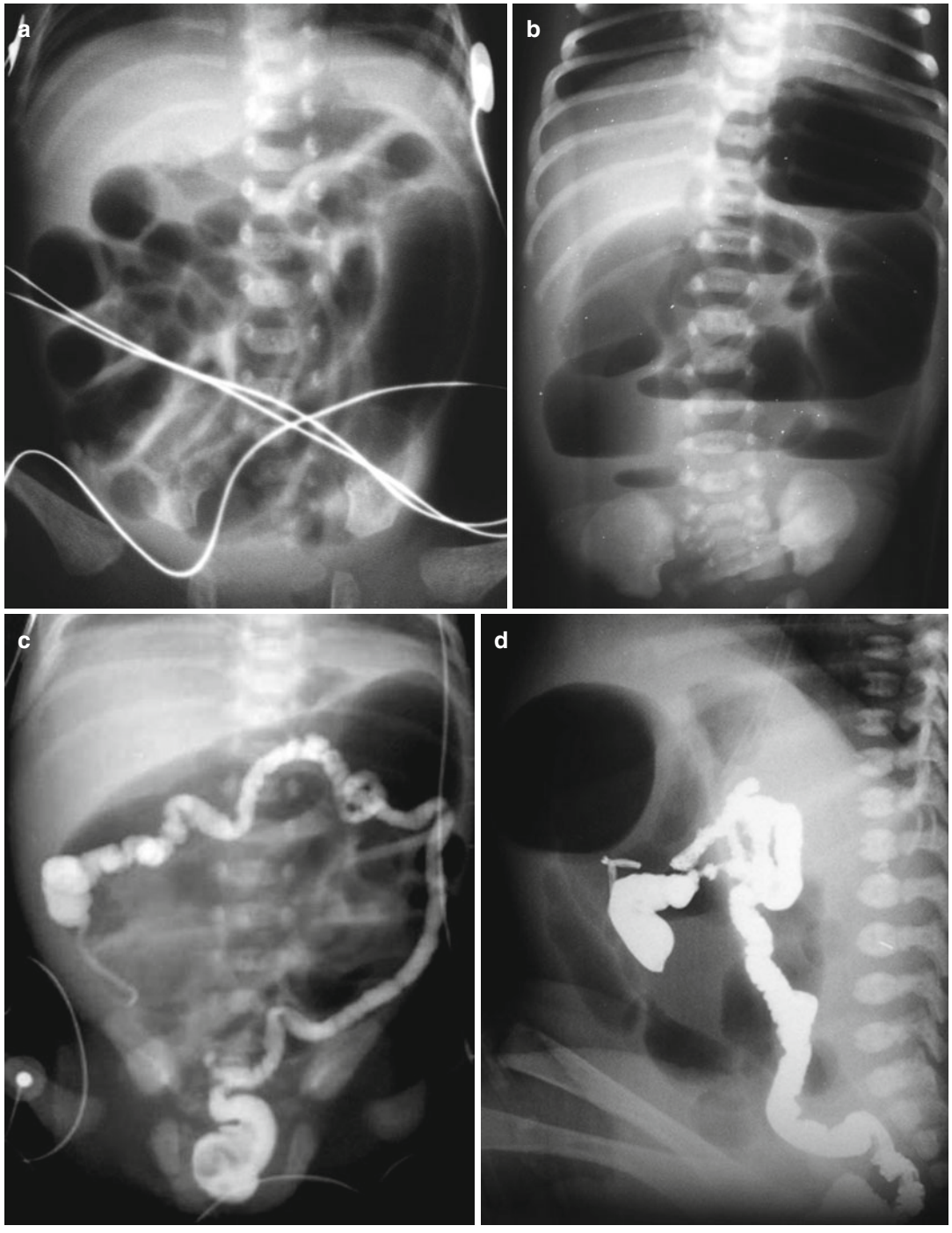


**Fig. 21** Ileal atresia. (**a**, **b**) Supine and upright abdominal radiographs show multiple dilated air-filled bowel loops occupying the entire abdominal cavity, with air–fluid levels in the upright radiograph. With this degree of distension, it is impossible to differentiate the small bowel from the colon. (**c**, **d**) Contrast enema outlines the minute size of the colon corresponding to an unused colon

air. The loops have thin walls and increased peristalsis (Cuture et al. 2008). It is important to depict the bowel loops distal to the atresia, but this can be difficult in patients with markedly distended, air-filled loops of proximal bowel. Distal bowel is small in size (3–4 mm), with echodense or target-like meconial content. The microcolon is easily recognized as the unused colon ranges from 3 to 6 mm size and does not contain any air. In rare cases, calcified enteroliths may be detected in the collapsed distal loops (Veyrac et al. 2012). On fetal US, approximately 50 % of the patients have no abnormal findings, and the rest shows multiple dilated loops of bowel, ascites, single large cysts, and polyhydramnios with or without associated anomalies (Jo et al. 2012).

Meconium ileus is a low intestinal obstruction produced by impaction of abnormal meconium in the distal ileum. Meconium, being the colonic contents at birth and made up of desquamated cells, lanugo hair, and proteinaceous material, may obstruct like in meconium plug syndrome (neonatal small left colon). It is "sticky" in cystic fibrosis (CF) due to abnormal proteins (see below). This leads to impaction at the narrowest portion of the small bowel, the ileocecal valve, although this association is not invariable. In 1999, Kubota (Kubota et al. 1999) proposed the term meconium-related ileus to comprehend different forms of meconium obstruction not associated to cystic fibrosis, like meconium plug syndrome and meconium disease. These relatively frequent and benign conditions need prompt recognition to exclude other forms of neonatal intestinal obstruction; among them, meconium disease is frequently associated to severe prematurity and low birth weight (Paradiso et al. 2011).

In cystic fibrosis, the defective secretion of $HCO_3$ creates an altered luminal environment that is more acidic and dehydrated than seen within the normal intestine and causes the meconium to become abnormally viscous and thick. The effects on the gastrointestinal tract range from temporary meconium retention with delayed but spontaneous evacuation of the meconium, to complete obstruction. When obstruction occurs, the narrow distal ileum is obstructed by concretions of gray inspissated meconium pellets (Paradiso et al. 2011). Proximal to this, the ileum is grossly distended by thick, tenacious, chewing gum-like meconium due to the viscid, abnormal mucus. Meconium ileus is the earliest manifestation of cystic fibrosis and occurs in 10–15 % of patients. A family history is often elicited. Symptoms usually commence on the first day of life and consist of bile-stained vomiting and abdominal distension. The abdomen may have a doughy feel, and it is sometimes possible to indent the bowel contents on pressure. The diagnosis may be confirmed by finding an increased concentration of sodium chloride in the sweat (Burge and Drewett 2004). Meconium ileus can be uncomplicated or complicated by volvulus, perforation, or peritonitis. The plain radiograph in uncomplicated meconium ileus usually demonstrates low obstruction. The abdomen is filled with air-distended loops, and occasionally, there is a relative absence of air–fluid levels (Fig. 22). In general, patients with meconium ileus have fewer air–fluid levels than patients with small bowel atresias. The sticky, viscid meconium prevents rapid movement of air shadows during changes of posture so that fluid levels do not easily develop. Sometimes, a mixture of air and meconium may be visualized as coarse, granular, ground–glass shadows, giving rise to a "soap bubble" appearance similar to the fecal pattern of the colon in older patients. However, a similar fecal pattern may also be seen in ileal atresia and aganglionosis of the terminal ileum, so these findings are not of much use in the differential diagnosis of low obstruction.

Contrast enema classically demonstrates a microcolon, and multiple small filling defects consisting of meconium pellets may be seen within the microcolon and in the collapsed distal ileum if there is reflux of contrast material beyond the ileocecal valve, with dilated small bowel proximal to the obstruction (Fig. 23). These findings are diagnostic of meconium ileus. Once the diagnosis is made, these patients should undergo a therapeutic enema to help the passage of the sticky meconium and to relieve the obstruction avoiding surgery. The type of contrast to be used in this examination should be considered carefully, especially given the fact that the etiology of the distal obstruction is not known prior to this examination. Barium is not ideal in patients with meconium ileus and impacted meconium pellets.

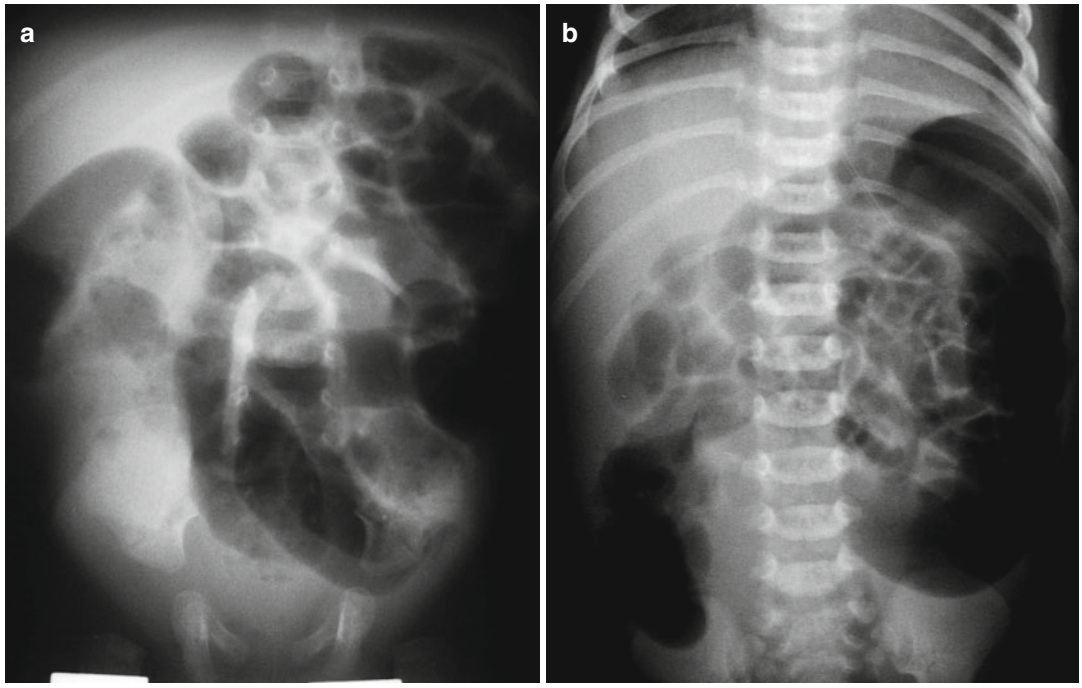


**Fig. 22** Meconium ileus. (**a**) Supine plain radiograph shows marked bowel distension with suggestive evidence of mottled air and feces in ascending colon and terminal ileum. (**b**) Upright film shows absence of well-defined air–fluid levels

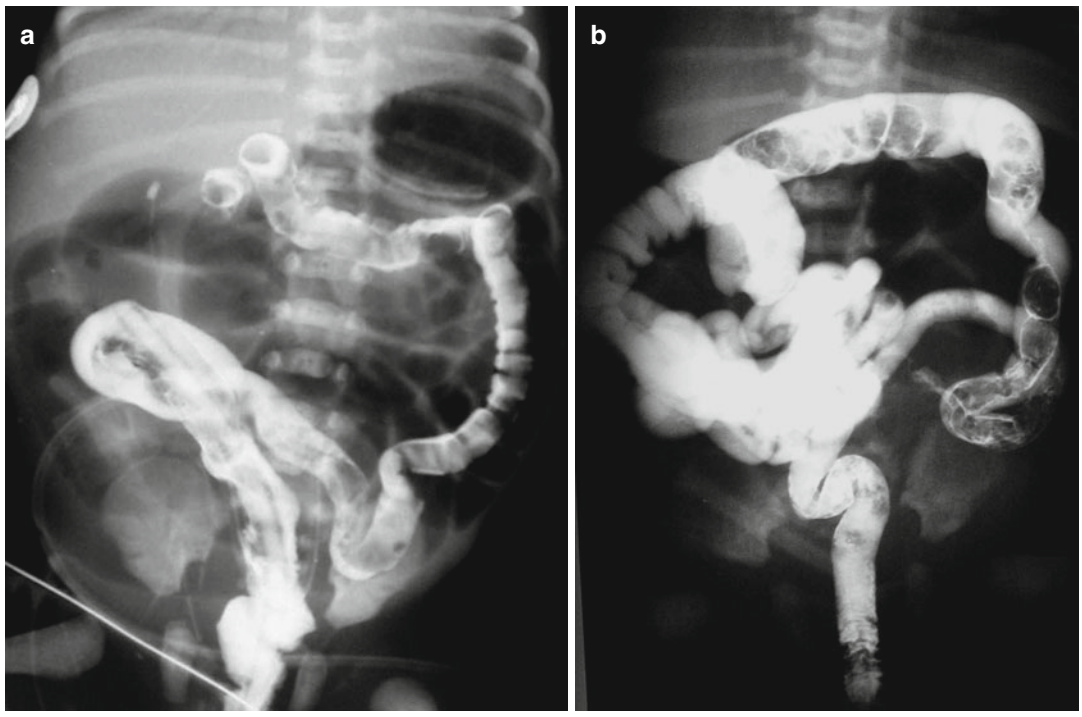


**Fig. 23** Meconium ileus. (**a**) Water-soluble contrast enema showing a microcolon with scattered filling defects that correspond to inspissated meconium. (**b**) The enema was continued with reflux of the contrast medium into the terminal ileum, showing filling defects that represent meconium pellets. The patient was discharged within 48 h of successful treatment

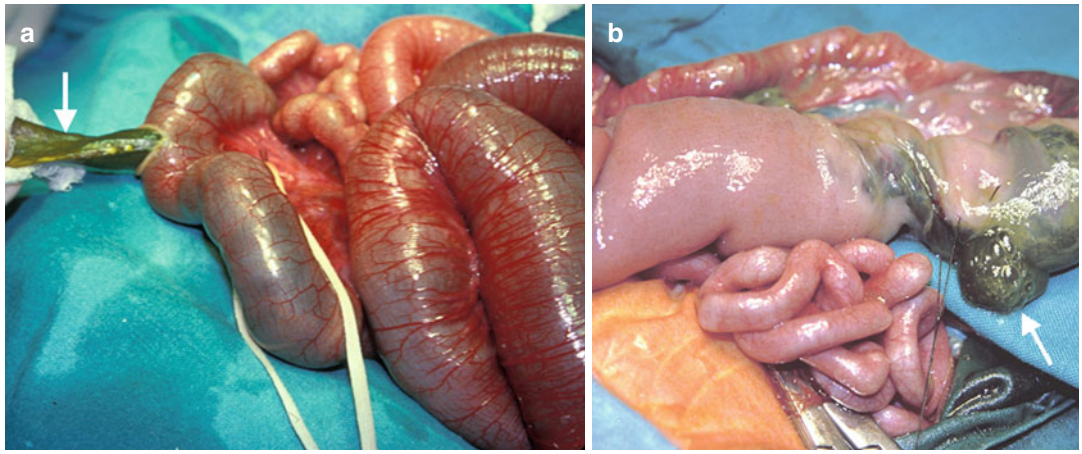


**Fig. 24** Meconium ileus. (**a**, **b**) Intraoperative views illustrating the tenacious nature of the meconium impacted within the distal small bowel loops (*arrows*) in a patient in which contrast enema failed to solve the obstruction

It is preferable to begin the enema examination with a water-soluble contrast medium. Low osmolar, nonionic water-soluble agents are the best choice to avoid large fluid shifts into the bowel. These agents are expensive, so a relatively dilute isosmolar ionic water-soluble contrast medium may also be acceptable. Hyperosmolar agents such as Gastrografin continue to be used by many radiologists (Veyrac et al 2012; Juang and Snyder 2012) although many have ceased using it because of its risks. The success rate of enema resolution of meconium ileus is less than 40 % (Buonomo 1997).

Gastrografin is meglumine diatrizoate; a water-soluble, radiopaque solution containing 0.1 % polysorbate 80 (Tween 80) and 37 % organically bound iodine. The solution's osmolarity is 1,900 Osm/L. This very hyperosmolar agent decreases the tenacity of the meconium by drawing water into the bowel lumen. Before proceeding with this therapy, the infant must show signs of uncomplicated meconium ileus and no clinical or radiologic evidence of complicating factors (e.g., volvulus, gangrene, perforation, peritonitis). An expert group convened by the Cystic Fibrosis Foundation Consensus Conference found no scientific evidence that Gastrografin was superior to other low osmolar water-soluble contrast media in the treatment of meconium ileus. As Gastrografin may cause hypotension or circulatory collapse in newborn infants, currently, the best choice is the use of low osmolar agents in these infants. The flow of the contrast through the thick meconium is slow, and usually several enemas are required. Efforts must be taken to reflux contrast into the ileum and if possible back into the dilated proximal bowel (Fig. 23). Care should be taken that the patient is well hydrated because of fluid shifts. The patient's electrolyte balance must be attended to before, during, and after each enema (Veyrac et al. 2012). Meconium ileus may be complicated by volvulus of a distal intestinal loop, perforation, or atresia. All patients with complicated meconium ileus require surgical intervention (Fig. 24); therefore, radiographs need to be read carefully for the presence of calcification or pneumoperitoneum which indicates in utero perforation and the need for surgical intervention without further imaging (Minato et al. 2012).

US may demonstrate a specific pattern different from that of small bowel atresia. Severe microcolon is present, but the small bowel is less dilated and less peristaltic. The most important finding is the characteristic appearance of the dilated bowel loops, which contain abnormal meconium. The thick meconium sticks on the bowel walls resulting in a pseudo-thickening; the dessicated meconium forms a hyperechogenic layer against the bowel mucosa, producing a stratified appearance; elsewhere, air bubbles are trapped within the abnormal meconium in the

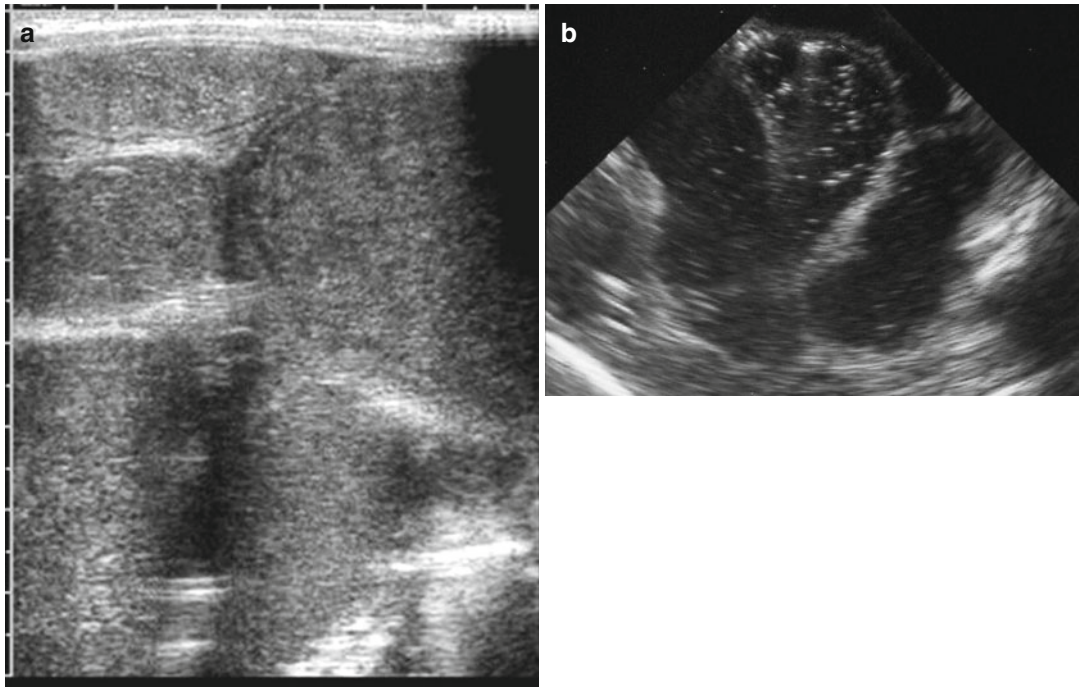


**Fig. 25** (**a**) Neonate with cystic fibrosis. Sonography shows intestinal loops filled with hyperechoic thick meconium. (**b**) Neonate with ileal atresia. Intestinal loops are filled with hypoechoic fluid and air

outer area of the intestinal lumen. The distal bowel loops, in the right lower quadrant, are small (3–4 mm), with target-like appearance due to impacted meconial pellets (Veyrac et al. 2012). In ileal atresia, the bowel is filled with hypoechoic fluid and air (Fig. 25).

*Meconium peritonitis* is a condition that is the result of in utero perforation of the fetal gastrointestinal tract during the last 6 months of pregnancy. Sterile meconium escapes through the perforation into the peritoneal cavity producing a marked reaction with dense adhesions, which usually calcify rapidly, in some cases as early as 24 h after it leaves the intestinal lumen. Yellow-green nodules form on the bowel wall, and the perforation may be sealed off so well that at birth there may not be any macroscopic evidence of the leak. However, if the perforation is still present after birth and meconium still escapes into the peritoneal cavity, secondary septic peritonitis will develop. Very often, a pseudocyst is formed by adjacent loops of the intestine, which tend to wall off the perforation. The wall of this pseudocyst is lined by a thick plaque of greenish-yellow material with areas of calcification (Minato et al. 2012). The intrauterine perforation may be due to any obstructing lesion such as atresia, meconium ileus, volvulus, a Meckel diverticulum, internal hernia, or bands (Douglas 2010). In such cases, the causative lesion will be found at laparotomy. Frequently, however, no obvious cause for the perforation can be found. Such idiopathic perforations may be produced by localized areas of intestinal infarction due to minute emboli from the placenta (Eckoldt et al. 2003). The diagnosis is usually obvious on the plain radiographs of the abdomen and is characterized by linear or punctate calcifications over the serosal surfaces of the abdominal viscera. The calcification may consist of a few irregular scattered areas or may be more extensive, consisting of continuous linear depositions of calcium localized underlying the anterior or posterior abdominal walls, in the flanks, or beneath the diaphragm (Lang et al. 1997) (Fig. 26). Calcifications may also be observed in the scrotal sac of males owing to communication

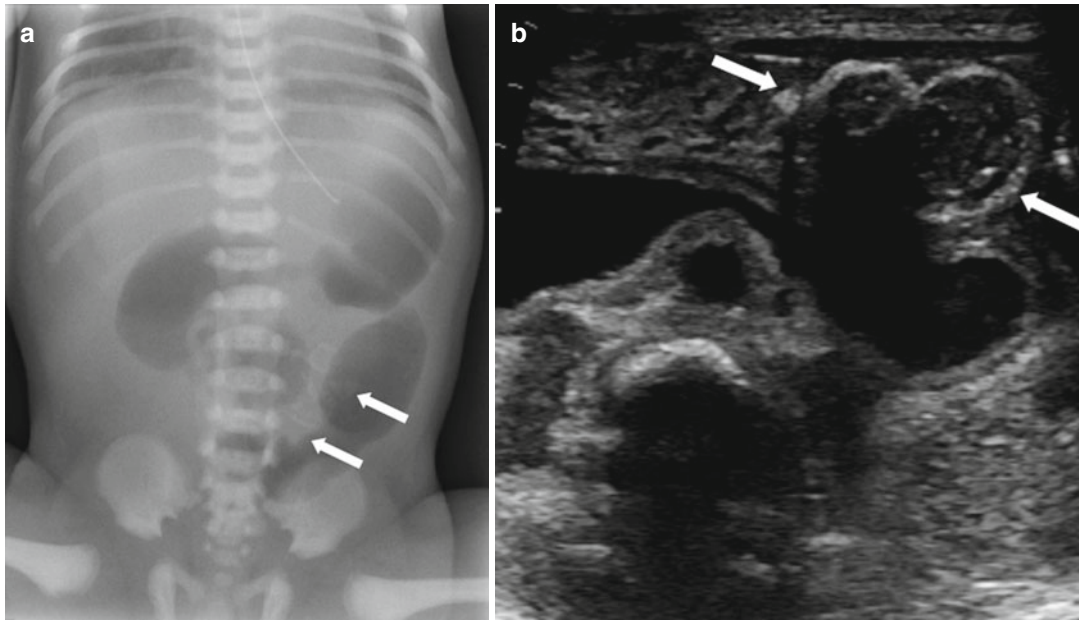


**Fig. 26** Meconium peritonitis. (**a**) Abdominal radiograph in a neonate demonstrating proximal bowel obstruction with dilated duodenum and jejunal loops. Focal calcifications (*arrows*) can be seen in the midline of the radiograph indicating calcified meconium contents. There is no free air. (**b**) Transverse US image at the level of the third part of the duodenum demonstrating the dilated duodenum deep to the calcified foci of meconium (*arrows*). At surgery, there was jejunal atresia and distal colonic atresia possibly related to antenatal vascular events

through a patent processus vaginalis (Salman et al. 1999) (Fig. 27). Pseudocyst also may be seen as a mass effect on plain radiographs. In addition, distended loops of the bowel with air–fluid levels may be present due to the underlying intestinal obstruction. Where the perforation is still patent, free air will be seen in the peritoneal cavity (Fig. 28) or trapped in a walled-off loculus or pseudocyst. Decubitus radiographs to determine the presence or absence of free air with a persistent perforation are essential. The typical appearances of pneumoperitoneum, however, are not usually seen because of the presence of adhesions, which obliterate most of the peritoneal cavity (Minato et al. 2012).

Ultrasound may be useful in these patients, especially in the presence of a relatively airless abdomen. Meconium peritonitis predominantly presents two ultrasound appearances: general or cystic abnormality. With the generalized condition, highly echogenic material spreads throughout the abdomen and around the bowel loops (Fig. 29), sometimes producing a characteristic "snowstorm appearance" (Veyrac et al. 2012). The cystic form is characterized by localized, cystic collections of meconium (meconium pseudocysts) ranging from a few centimeters in size to huge cysts occupying most of the abdominal cavity. The cyst is usually well defined and predominantly echogenic, but may also be less well defined and markedly heterogeneous. The walls are echogenic and may be thick or thin (Doodnath and Puri 2010) (Figs. 27 and 30). Calcified foci may be demonstrated with posterior shadowing in many cases. Meconium peritonitis may also be diagnosed by prenatal ultrasound. It can present as fetal meconium ascites, giant pseudocysts, small pseudocysts, and calcifications. Associated polyhydramnios is a common finding (Rubesova 2012).

### 1.2.2 Colonic Obstruction

Colonic atresia similar to small bowel atresia, is believed to result from an intrauterine vascular insult. The colon is the least frequent location, representing 5–15 % of all intestinal atresias.

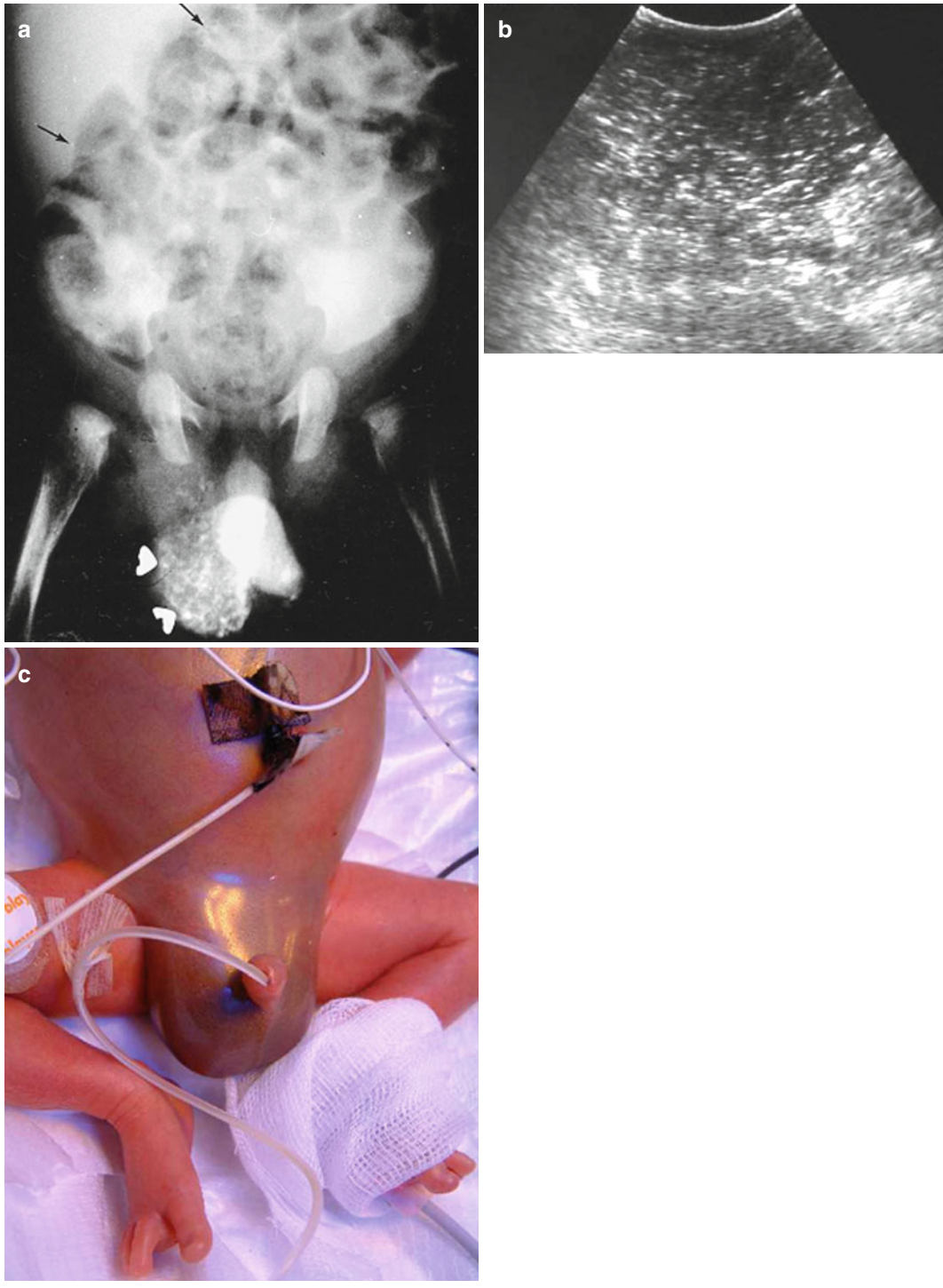


**Fig. 27** Meconium peritonitis with calcified meconium in the scrotum. (**a**) Plain radiograph at birth showing scattered areas of calcification in the scrotum (*arrowhead*). Small flakes of intra-abdominal calcifications are also observed (*arrows*). (**b**) Sonography of the same patient shows an intrascrotal pseudocyst-containing fluid and echogenic debris and calcium. (**c**) Clinical picture of the same patient showing the enlarged scrotum

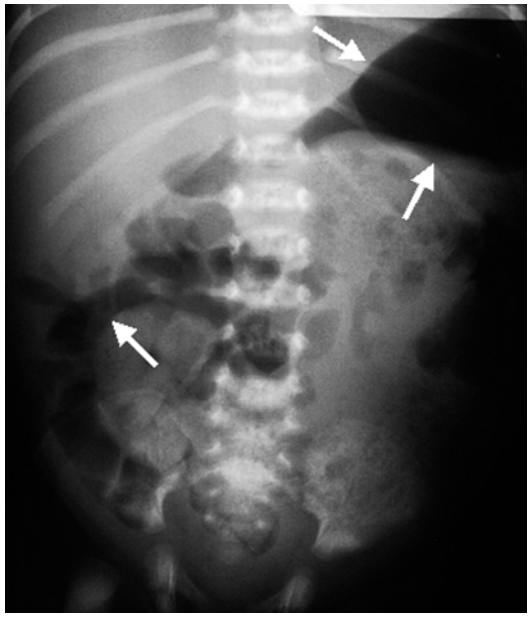

**Fig. 28** Meconium peritonitis with intrauterine bowel perforation. Free air within the peritoneal cavity is observed (*arrows*) in this neonate with ileal atresia. No bowel distension is observed. A patent bowel perforation was found at surgery

Colonic atresia is classified into three types: type I consists of mucosal atresia with an intact bowel wall and mesentery (web); type II consists of atretic ends separated by a fibrous cord; and type III consists of atretic ends separated by a V-shaped mesenteric gap. In the ascending and transverse colon, colonic atresia type III predominates. Types I and II are seen more commonly distal to the splenic flexure. Type III lesions are easily the most common variant overall. Proximal location is more common than distal, with atresia beyond the splenic flexure being unusual. In one review of 118 cases, approximately one fourth occurred in each of these locations: ascending, transverse, splenic flexure, and descending/sigmoid colon. The hepatic flexure was an uncommon site (Juang and Snyder 2012). Multiple atresia syndromes may involve the colon in addition to the small bowel. The diagnosis may be suspected prenatally, but the US findings cannot usually be distinguished from other forms of intestinal atresia. Polyhydramnios is uncommon due to the distal nature of the obstruction. Most infants are born at term. Clinical presentation may be delayed up to 48 h after birth. The abdominal scout radiograph, in particular when the atresia is in the ascending colon, is often indistinguishable from obstruction of the distal ileum.

Plain abdominal radiography is usually unclear prior to 12–24 h of age so that an adequate amount of air can reach the site of obstruction (Hajivassiliou 2003). Sonography can determine the cause of distension before air is present in the distal bowel. The sonographic features are dilated distal small bowel and proximal colon, which often is markedly echogenic secondary to retained meconium. Contrast enema usually reveals a microcolon distal to the atresia, with obstruction to the retrograde flow of barium at the site of the atresia (Fig. 31). A "windsock" appearance may be observed with membranous atresias. Calcification of meconium peritonitis due to in utero bowel perforation is present in about 12 % of atresia cases and can be diagnosed antenatally by sonography. Diagnosis of colonic atresia is an indication for urgent surgical intervention because this anomaly has a higher risk of perforation (10 % incidence) than seen in other intestinal atresias, presumably as a result of a closed loop obstruction from the intact ileocecal valve (Juang and Snyder 2012).

*Hirschsprung disease* is a form of low intestinal obstruction caused by the absence of normal myenteric ganglion cells in the submucosal and intermuscular myenteric plexuses of a segment of the colon. Clusters of enlarged, unmedullated nerve fibers have taken their place. In normal intrauterine development, neuroenteric cells migrate from the neural crest to the upper end of the gastrointestinal tract by 5 weeks and proceed in a caudal direction. These cells reach the rectum by 12 weeks and commence the intramural migration from the myenteric plexus (Auerbach plexus) to the submucosal plexus (Meissner plexus). Hirschsprung disease is caused by abnormal neural crest cell migration resulting in arrested distal migration of these cells (Gershon and Ratcliffe 2004; Juang and Snyder 2012). The length of the aganglionic segment is variable but always commences at the lower end of the rectum and extends proximally for a variable distance. In

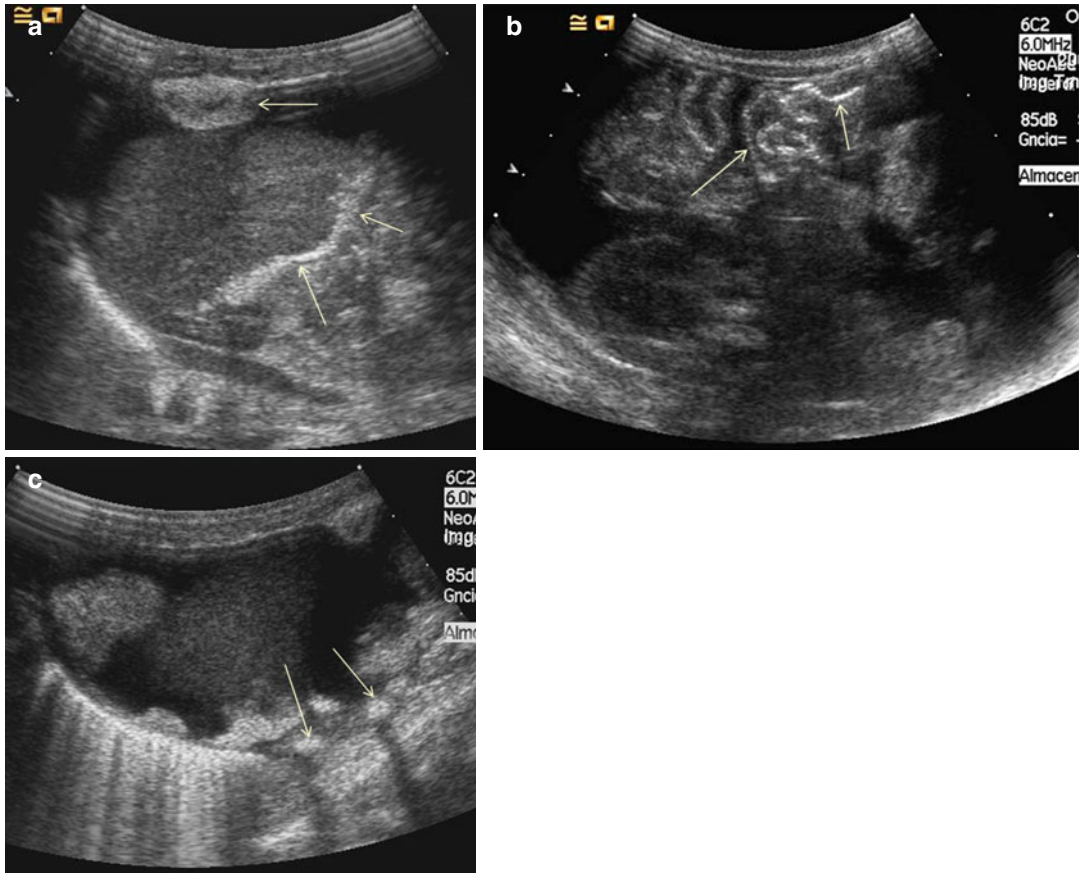


**Fig. 29** Meconium peritonitis in a neonate with cystic fibrosis. Sonography demonstrates intra-abdominal calcifications (**a**) around the liver surface (*arrows*). (**b**) Calcifications around the bowel loops (*arrows*). (**c**) In this case, the ribs should not be misinterpreted as inspissated meconium in the bowel loops (*arrows*)

about 80 % of cases, the anomaly does not extend beyond the sigmoid (short segment), while in the remainder it extends proximally to involve variable lengths of the colon and may even involve the terminal ileum (long segment). Ultrashort segment disease (with aganglionosis essentially limited to the region of the internal sphincter) and aganglionosis involving the entire alimentary tract are very rare presentations (Laughlin et al. 2012).

In children with Hirschsprung disease, the absence of ganglion cells results in the failure of the distal intestine to relax normally; peristaltic waves do not pass through the aganglionic segment, and there is no normal defecation leading to a functional obstruction. The aganglionic segment remains unexpanded, and the proximal colon becomes distended and hypertrophied. Hirschsprung disease is responsible for approximately 15–20 % of cases of neonatal bowel obstruction. Short segment disease is more common in males at a ratio of 4:1. In long segment aganglionosis, male preponderance diminishes to 2.8:1. Gender distribution is almost equal in the cases with extensive involvement. A positive family history is encountered in about 10 % of patients with short segment disease and in 25 % of patients with total colonic aganglionosis. Hirschsprung disease is associated with esophageal dysmotility syndromes, malrotation, and ileal or colonic atresia. Approximately 3 % of patients with Down syndrome have Hirschsprung disease. It has also been associated with other neurocristopathies (neuroblastoma, pheochromocytoma, MEN IIA syndrome) and is thought to be related to their

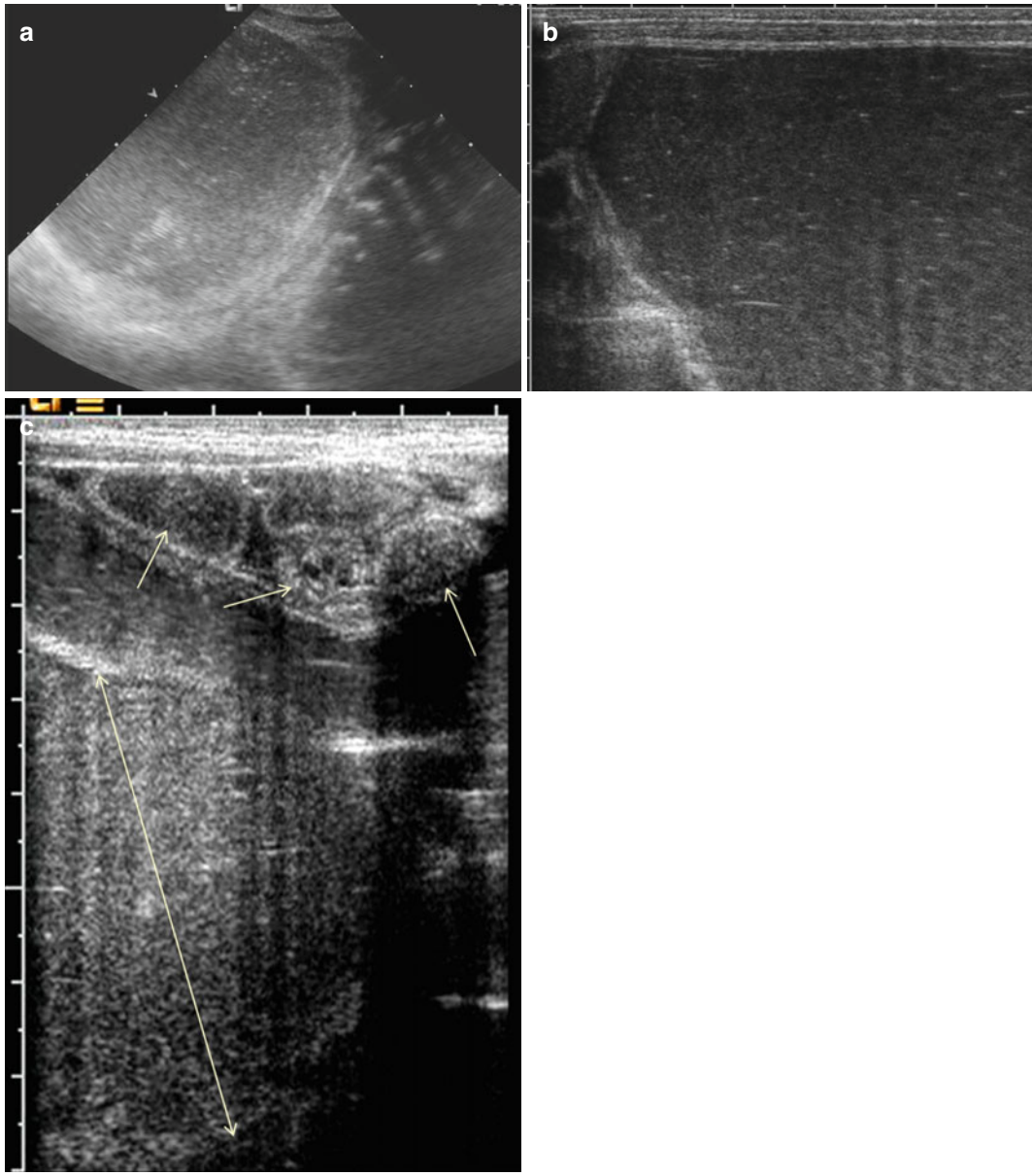


**Fig. 30** Meconium pseudocyst. (**a**) Sonography of the right side of the abdomen shows a large fluid-filled mass with echogenic contents. (**b**) Same patient; high resolution US scan demonstrates a well-defined walled cyst with striking echogenic content consistent with inspissated meconium. (**c**) The intestinal loops are filled with hyperechogenic content (thick meconium) (*arrows*) and marked dilatation of some loops (*arrowheads*)

common neuroblastic origin (Quedas et al. 2012). The severity of the symptoms does not depend entirely on the length of the aganglionic segment. Abdominal distension, failure to pass meconium in the first 24 h of life, constipation, and bilious vomiting are the predominant symptoms, with the signs of obstruction appearing within a few days after birth.

A plain abdominal radiograph of infants with this condition is similar to that of other forms of low small bowel obstruction. The abdomen is filled with several distended loops of the colon

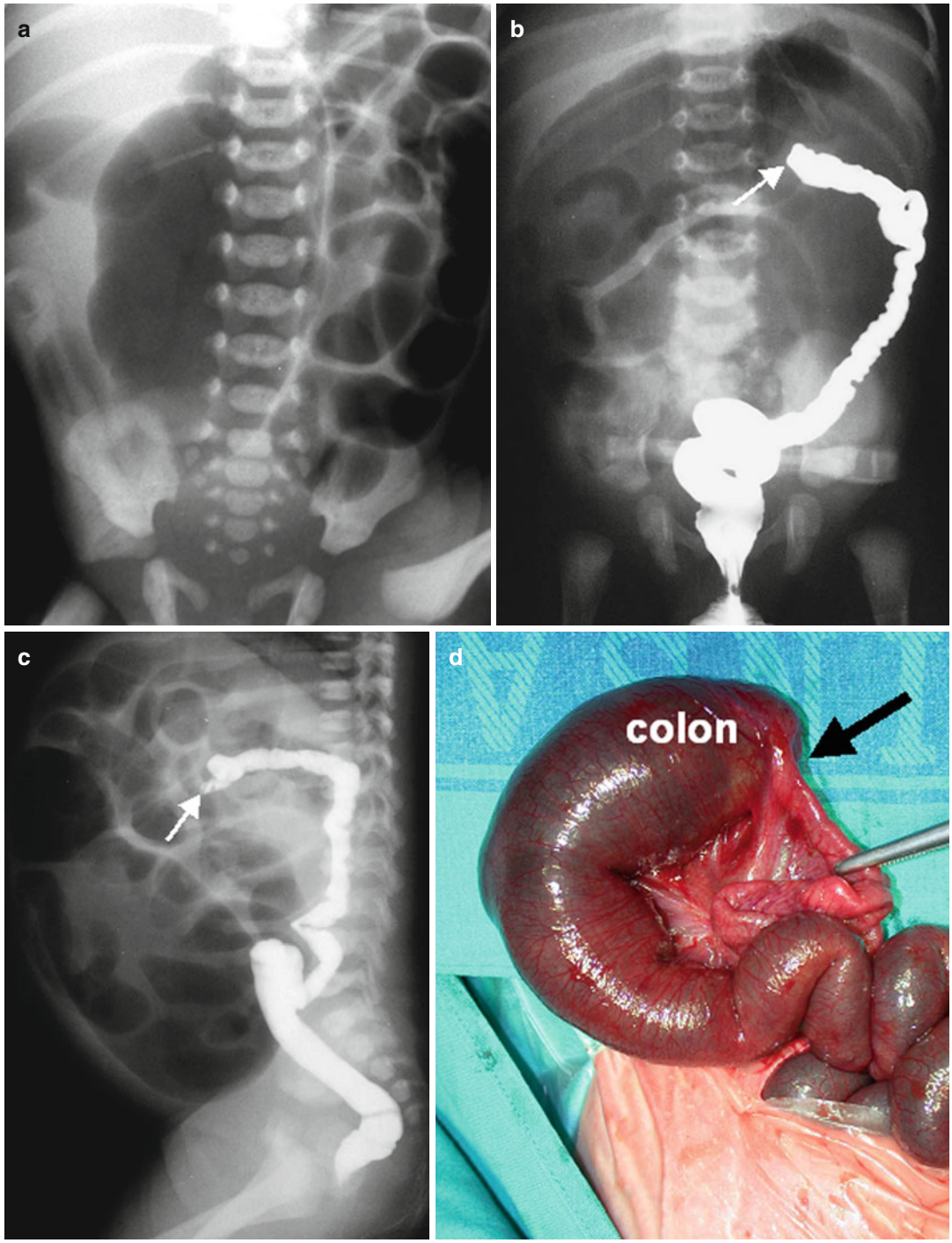


**Fig. 31** Colonic atresia. (**a**) Supine radiograph shows gaseous distension of bowel. (**b**, **c**) Contrast enema; anteroposterior and lateral views show an abnormally small colon (microcolon) with complete obstruction to retrograde flow of contrast material proximal to the mid-transverse portion of colon (*arrows*). (**d**) Photograph at surgery shows a distended colon up to the site of the atresia (*arrow*) and a microcolon distal to it

and the small bowel often with air–fluid levels. The colon is usually difficult to identify accurately, and air is usually absent in the rectum (Fig. 32). About 5 % of patients may present with pneumoperitoneum secondary to perforation (Doodnath and Puri 2010). Most of these patients have long segment or total colonic aganglionosis. As in other cases of low intestinal obstruction, a contrast enema is needed. Rectal examination should not be performed prior to the enema as this may mask a low-lying transition zone. The enema examination is started with the patient in a lateral position. The catheter should be placed barely within the rectum, so as not to obscure a transition zone. Balloon catheters should never been used as they may obscure a transition zone or even perforate the aganglionic rectum. Although the contrast enema has classically been performed with barium sulfate, currently, low osmolar water soluble is the preferred contrast medium because of the risk of barium peritonitis in the event of colonic perforation. There are many signs of Hirschsprung disease on contrast enema studies.

The most important is the transition zone between the normal or relatively narrow aganglionic segment and the dilated bowel proximal to it, usually in the shape of an inverted cone (Figs. 32 and 33). This finding is present in about 65 % of neonates (Doodnath and Puri 2010). When this is observed, the examination should be discontinued, especially if barium is being used, as filling of the more proximal dilated bowel beyond the transition zone may lead to impaction and does not alter further management. The transition zone may, however, be difficult to see in newborns. In such cases, the rectosigmoid index may be useful. Normally, the rectum is 20–40 % larger than the sigmoid in diameter. In Hirschsprung disease, this ratio may equilibrate or reverse. The pathologic transition zone is usually somewhat more proximal than the radiographic one (Jamieson et al. 2004).

Abnormal contractions and irregular peristaltic activity of the aganglionic portion of the colon may also be seen, occurring in about 20 % of infants, and should not suggest mucosal ulceration.

Retention of contrast medium at 24 h with colonic distension may be a helpful sign, but is nonspecific, as it can be observed in 60 % of patients without Hirschsprung disease. On the other hand, good evacuation does not rule out the disease (Juang and Snyder 2012). US shows normal or increased size of the colon, which contains normal hypoechogenic meconium punctuated with air bubbles. According to Veyrac et al. (2012), along the colon, a transition zone may be detected by US. However, the sonographic transition zone does not correlate with enema findings or pathology making it an unreliable finding.

The radiologic diagnosis of total colonic aganglionosis is much more difficult. Findings may include a normal barium enema, a short colon of normal caliber, a microcolon, rounding of the colonic flexures, or a transition zone in the ileum (Fig. 34). Clinical suspicion should be heightened in patients presenting with clear signs and symptoms of distal obstruction, in whom the contrast enema does not demonstrate a specific cause (Hayakawa et al. 2003). US findings may be variable from distended right colon contrasting with normal sized or slightly dilated left colon and rectum to homogeneous normal colonic size. This highlights the difficulty in diagnosing this form of Hirschsprung disease, whatever imaging is used (Cowles et al. 2006). Histological confirmation is obtained by means of rectal biopsy.

Enterocolitis is the major cause of death in patients with Hirschsprung disease, with a mortality rate as high as 30 %. The patients may present with diarrhea, hypovolemia, and prostration. Enterocolitis of Hirschsprung disease can be diagnosed on plain radiograph by the irregular contour of the dilated colonic wall caused by the edema, spasm, and ulceration of the intestinal wall. Patients who present with perforation typically do not have enterocolitis. Enema is contraindicated in patients with suspected enterocolitis because of the possibility of perforation.

*Functional immaturity of the colon* is a common cause of neonatal obstruction, particularly in premature infants and in those whose mothers were treated during labor with magnesium preparation or high doses of opiates or other sedatives.

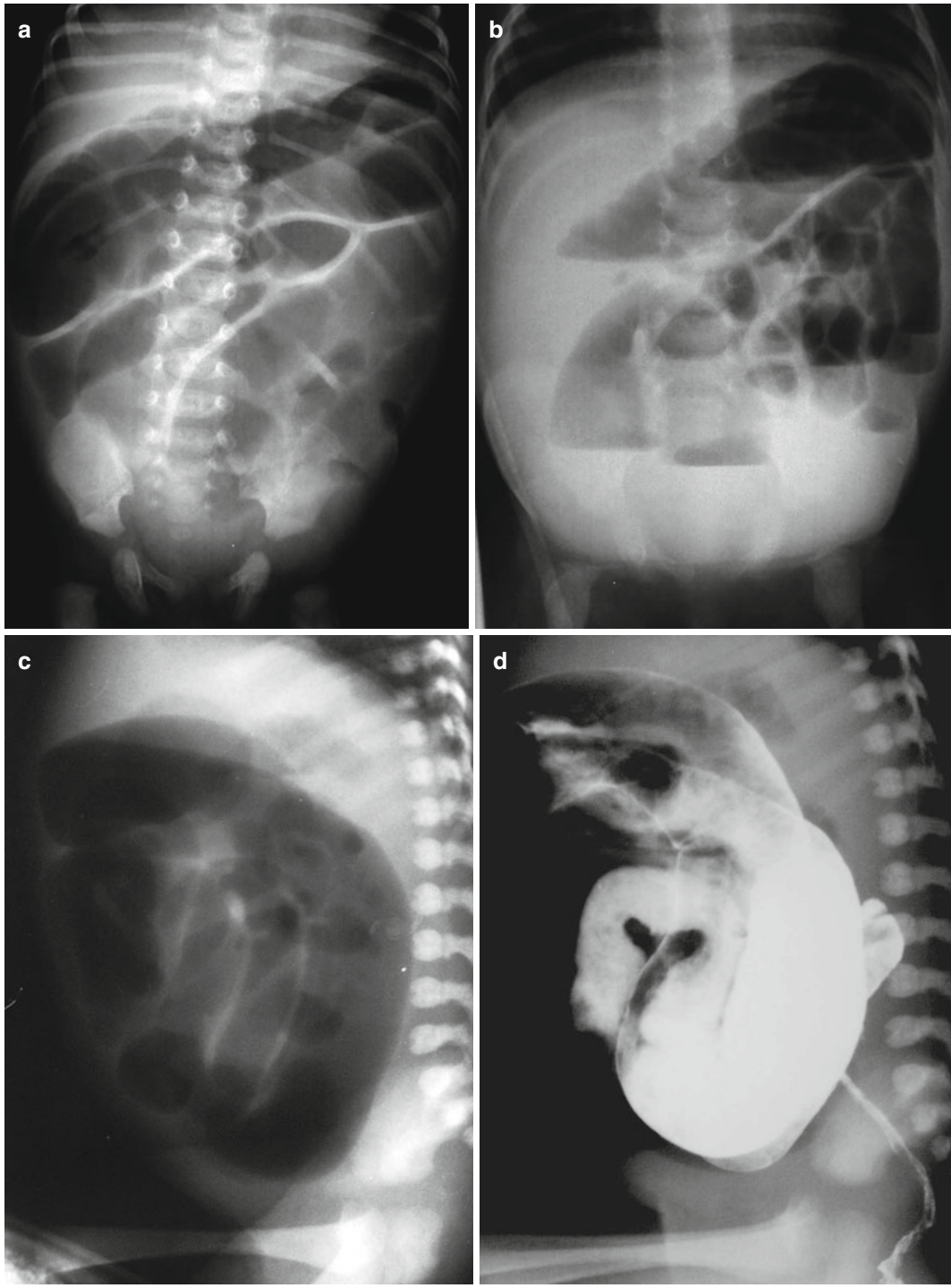


**Fig. 32** Hirschsprung disease. (**a**) Supine, (**b**) upright, and (**c**) lateral plain radiographs show distension of the bowel corresponding to a low obstruction, with air–fluid levels in the upright film and absence of air in the rectum in the lateral film. (**d**, **e**) Contrast enema showing a distended colon with an obvious zone of transition (*arrows*) in the rectosigmoid junction. The caliber of the rectum is very small

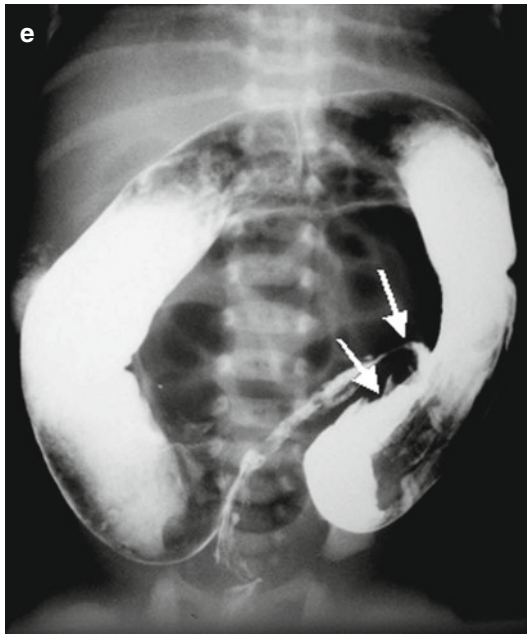


**Fig. 32** (continued)

The condition has also been encountered in children of diabetic mothers, or children with septicemia, hypothyroidism, or hypoglycemia. It is a typically benign and self-limited transient functional colonic obstruction in neonates.

The term includes meconium plug syndrome and small left colon syndrome, and both entities are associated with dysmotility of the colon. The underlying cause is thought to be related to immaturity of the colonic ganglion cells (myenteric nerve plexus) (Vinocur et al. 2012). These infants have difficulty in initiating evacuation, abdominal distension, and sometimes vomiting, but, in general, bowel distension usually is less severe than in organic obstruction.

Abdominal radiographs typically show multiple dilated bowel loops, an appearance that is characteristic for low intestinal obstruction. The condition is both diagnosed and treated with contrast material enemas.

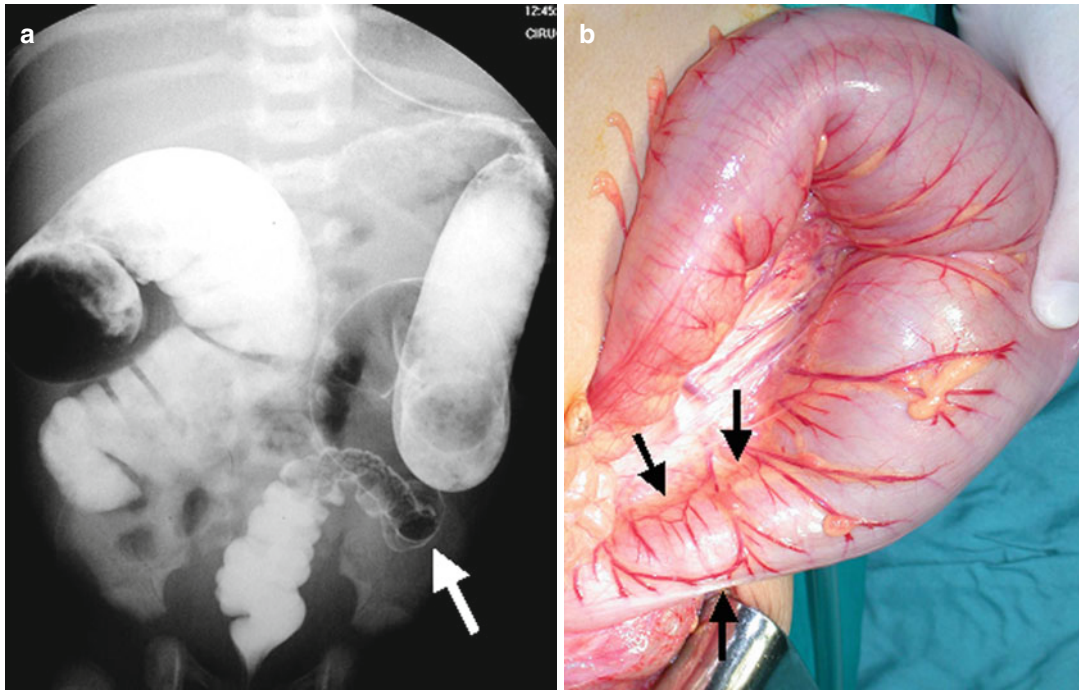


**Fig. 33** Hirschsprung disease. (**a**) Contrast enema shows a distended colon and a small rectum and sigmoidportion of the colon(*arrow*). The rectosigmoid index is abnormal

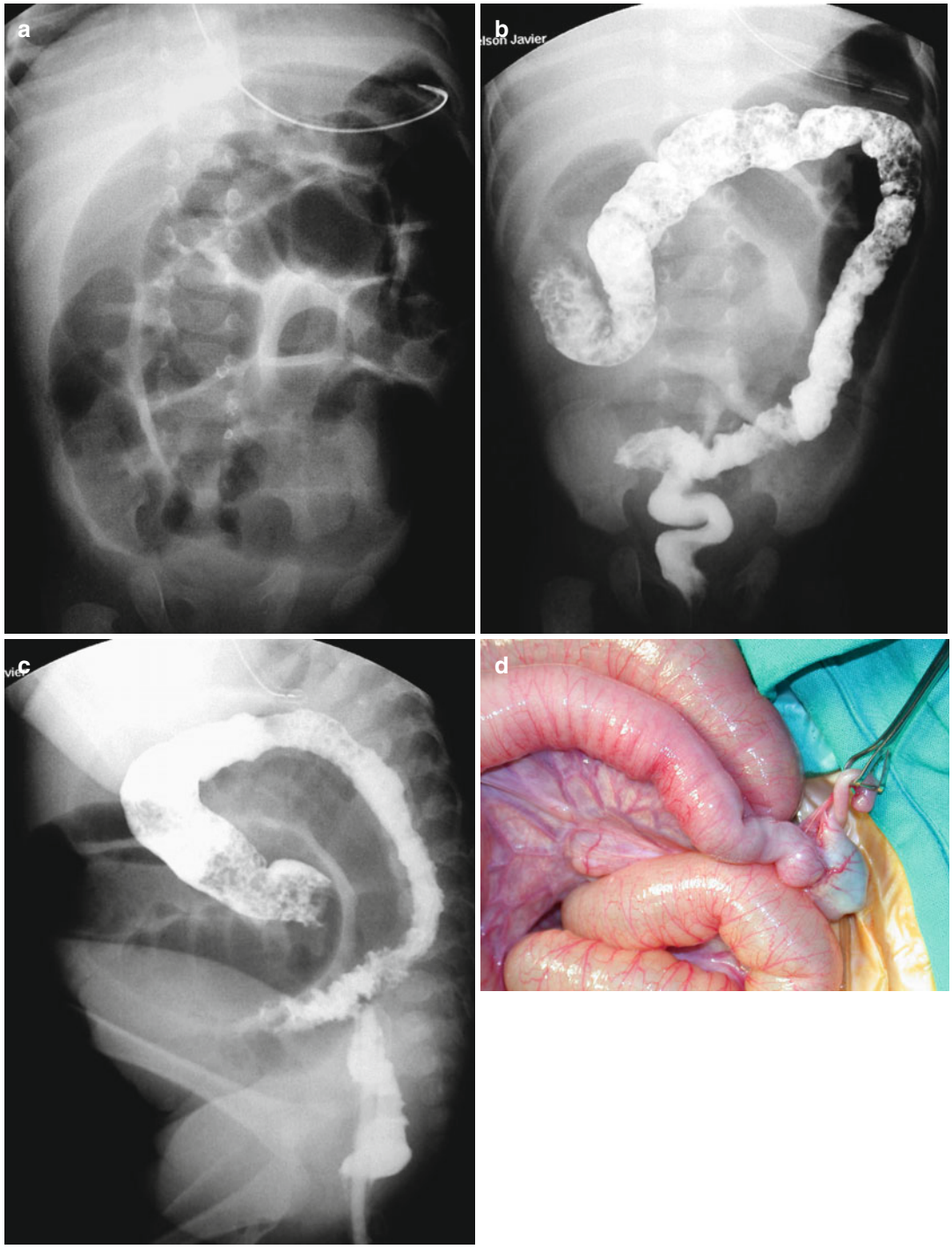


**Fig. 34** Total colonic aganglionosis. (**a**) Plain radiograph of the abdomen demonstrates low obstruction. (**b**, **c**) Anteroposterior and lateral views during contrast enema show a shortened colon (compared with the normal redundancy of the neonatal colon) with the flexures appearing a lower location than expected. There is a normal rectosigmoid index. (**d**) Intraoperative photograph shows dilated bowel loops with the transition zone at the distal ileum

In cases of *meconium plug syndrome*, the meconium forms a long, thick, snakelike plug, which obstructs the colon. The contrast enema reveals a large meconium plug as a translucent filling defect surrounded by opaque material filling the rectosigmoid, often extending into the descending colon (Fig. 35). The contrast medium will sometimes stream around the plug to give a double contrast appearance, with the contrast-lined colonic walls showing up against the negative filling defect of the plug. The large plug is usually evacuated during or soon after the enema examination. Typically, following the enema, there is clinical improvement, and over the course of hours to days, radiographic and clinical signs of obstruction subside. The only problem is that a few cases of meconium ileus and a few cases of Hirschsprung disease may be incorrectly lumped into this group. Then, if the difficulty is not promptly and completely cured, a sweat test for cystic fibrosis and further observation for Hirschsprung disease should be carried out (Burge and Drewett 2004). The US findings are characteristic showing a severe microcolon (3–5 mm) and microileum (1.5–3 mm), with echodense or target-like content. The bowel loops proximal to the meconial impaction are dilated, with variable severity (9–20 mm). An ampulla-like segmental bowel loop dilatation has been observed. These loops are filled with meconium mixed with air bubbles (Saguintaah et al. 2010). When the infant cannot be transported to the department of radiology due to instability, the enema may be performed at bedside with sonographic guidance. US can follow the progression of contrast fluid into the colon and terminal ileum lumen, surrounding the dessicated meconium (Veyrac et al. 2012).

*Neonatal small left colon syndrome* is a functional lower intestinal obstruction of unknown etiology, but a significant association has been noted between maternal diabetes and the disease (an incidence of 40–50 % of reported cases being infants of diabetic mothers). The clinical presentation of patients with small left colon syndrome is very similar to that of patients with meconium plug syndrome. Air–fluid levels are often absent in the upright radiograph, particularly prior to 48 h of life. "Soap bubble" meconium is typically seen in the collapsed left colon on the plain radiograph, and the distended bowel tends to be less than that seen in atresias. The contrast enema reveals a normal or slightly dilated colon and rectum, but the left colon up to the splenic flexure is very small, resembling a microcolon (Fig. 36). The amount of meconium present in the colon is variable, and discrete plugs of meconium at the point of transition may or may not be seen (Amat et al. 2011). Typically, after the enema, there is clinical improvement, and over the course of hours to days, radiographic and clinical signs of obstruction resolve. The only important differential diagnosis in babies with these findings is Hirschsprung disease with a transition zone at the splenic flexure. There are several findings that can be helpful. The distal rectosigmoid colon is of normal caliber and larger than the left colon, the proximal colon is less dilated than in Hirschsprung disease, and the transition zone of small left colon syndrome tends to be quite abrupt, whereas in Hirschsprung disease, it tends to be cone shaped and gradual. However, the distinction between both entities is not always possible on the basis of radiological findings, and a rectal biopsy must then be performed (Ellis et al. 2009). The US findings are variable. The rectum usually has a normal diameter and the left colon may be smaller distally or along its entire length. The proximal colon shows a progressive increase in size. In a third of patients, the colon has a homogeneous normal or slightly dilated diameter. In all cases, the colon contains normal meconium that is hypoechogenic and punctuated with air bubbles (Veyrac et al. 2012).

## 2 Necrotizing Enterocolitis

Necrotizing enterocolitis (NEC) is the leading gastrointestinal emergency of the premature neonate associated with significant morbidity and mortality. In many cases, it happens in apparently healthy premature neonates or infants who have no other medical problems. Although it affects mostly premature, 10 % of affected infants are born at term. Its incidence varies between 0.3 and 2.4 infants/1,000 births and between 3.9 and 22.4 % among infants of less than 1,500 g. Males and females are equally affected. Most infants develop NEC within the first 2 weeks of life

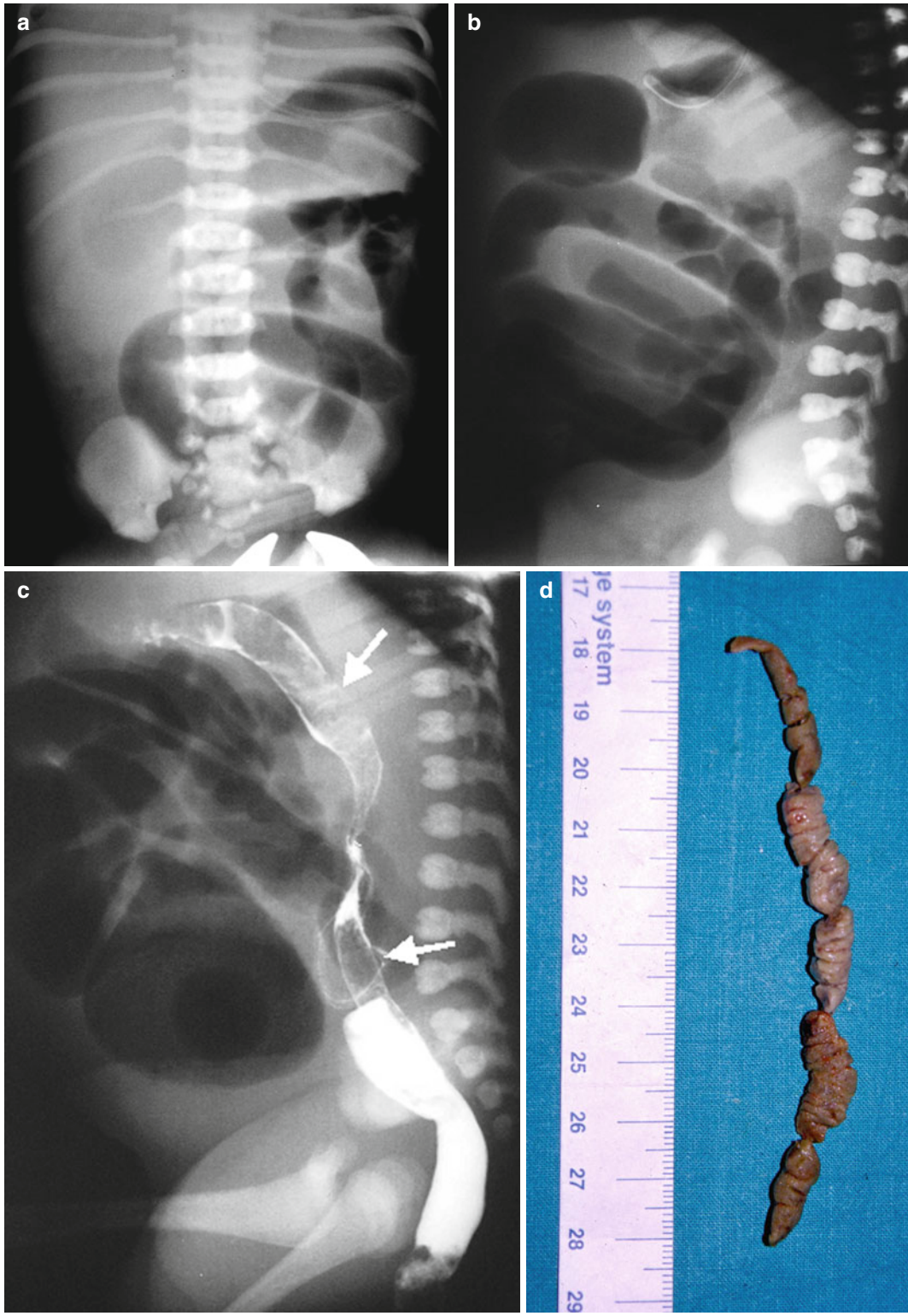


**Fig. 35** Meconium plug syndrome. (**a**) Anteroposterior and (**b**) lateral plain radiographs show distension of bowel loop consistent with low obstruction. (**c**) Isosmolal water-soluble contrast enema; the lateral view outlines the characteristic long-filling defect (*arrows*) within the colon. (**d**) Clinical image of a meconium plug surgically obtained in a patient in whom several attempts to conservatively solve the obstruction failed

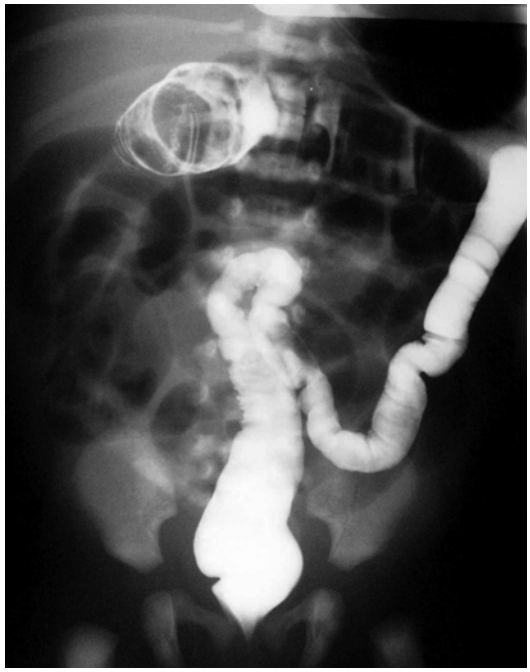

**Fig. 36** Small left colon syndrome. Isosmolal water-soluble contrast enema in a newborn with low obstruction demonstrates a normal rectum and distal rectosigmoid and a relatively narrow proximal sigmoid and descending colon with a transition to a more dilated colon at the splenic flexure. In 1 week, radiographic and clinical signs of obstruction resolved

(Lin and Stoll 2006). Its precise cause remains unclear, but it is thought that factors such as ischemia, decreased mucus production, and diminished immune response of the premature neonate may lead to invasion of the intestinal mucosa by intestinal flora resulting in air into the bowel wall. Some experimental work suggests that translocation of intestinal flora across an incompetent mucosa may play a role in spreading the disease and systemic involvement. Such a mechanism would account for the apparent protection breastfed infants have against fulminant NEC (Horton 2005). The terminal ileum and the proximal colon are most commonly affected, though any portion of the intestines may be involved. The clinical signs are nonspecific and consist of feeding intolerance, increased gastric retention, vomiting, abdominal distension, and the presence of blood in the stools.

The mainstay of diagnostic imaging is currently abdominal radiograph. The timing of follow-up plain abdominal radiographs depends on the severity of the NEC and may vary from 6 to 24 hourly. Because of the possibility of perforation of the necrotic bowel, the supine radiograph should be supplemented with a horizontal beam (cross-table lateral or, preferably, a left-lateral decubitus) radiograph.

The radiographic findings of NEC are nonspecific, especially in early stages. Diffuse nonspecific gaseous distension and thickened bowel walls suggesting edema and inflammation are the most common pattern (Fotter and Sorantin 1994; Faingold et al. 2005) (Fig. 37). The dilatation is usually due to an ileus and may be generalized or focal, depending on the extent of bowel involvement. It is the commonest sign, being present in over 90 % of patients. It is often called the "jumbled pattern" of NEC.

The degree of dilatation usually correlates well with the clinical severity of the disease, and the distribution of the dilated loops in serial examinations is related to clinical progression (Epelman et al. 2007). An asymmetric bowel air pattern or distension localized to focal loops only may also be seen, and the change from generalized dilatation to an asymmetric distribution where dilatation is confined to a more localized area of the abdomen is a threatening sign that suggests the development of bowel necrosis and progression to peritonitis. Radiographs can sometimes reveal scarce or absent intestinal air, which is more worrisome than diffuse distension that changes over time.

But the characteristic finding of NEC is pneumatosis intestinalis, consisting of submucosal or subserosal air (Epelman et al. 2007). Although intramural air may be present in other neonatal conditions, it is most commonly seen in NEC and thus has been considered a virtually pathognomonic sign of NEC. Pneumatosis intestinalis appears as a characteristic train–track lucency configuration within the bowel wall and may be linear or cystic (Fig. 38). The cystic collections are usually submucosal, whereas the linear form is usually subserosal. The linear lucencies are often observed curvilinear and appear as black lines on the radiograph. The rounded, cystic lucencies when extensive may have a bubbly appearance,

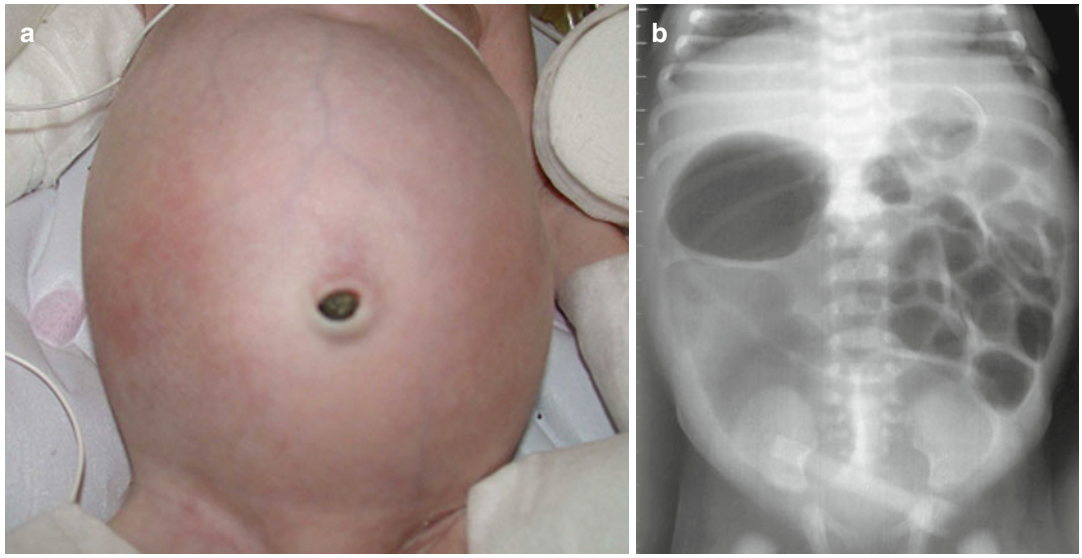


**Fig. 37** Necrotizing enterocolitis. (**a**) Photograph of a 3-week-old premature neonate showing significant abdominal distension. (**b**) Plain abdominal radiograph shows diffuse nonspecific gaseous distension of the bowel loops

which should not be confused with intraluminal stool. Pneumatosis intestinalis is due to the production of small bubbles of hydrogen by bacteria within the intestinal wall (Lin and Stoll 2006). Intramural air bubbles may also represent extravasated air from within the intestinal lumen. Intramural air is more commonly present in the distal small bowel and proximal large bowel and is therefore most commonly seen in the right lower quadrant. However, it may involve any part of the gastrointestinal tract including the stomach and rectum. The amount of intramural air does not always relate to the clinical severity of NEC. Serial radiographs help assess disease progression.

Another diagnostic hallmark of NEC is portal vein air. Like pneumatosis intestinalis, it was considered a pathognomonic sign of NEC, but some reports have shown that they might also be present in viral enteritis and cow's milk protein allergy (Lin and Stoll 2006). Portal vein air is more frequent and less ominous than was previously thought. It is an extension of intramural air that enters the veins of the bowel wall and passes into the portal venous system. The origin is the fermentation of substrates in milk feedings by bacteria present in the gastrointestinal lumen. The amount of portal venous air is not always related to the amount of intramural air present, and the portal venous air may be more obvious than the intramural air. On a supine plain abdominal radiograph, portal venous air appears as branching, linear, radiolucent vessels that may extend from the region of the main portal vein toward the periphery of both hepatic lobes, and the extent depends on the amount of portal venous air present (Fig. 39). Occasionally, it is more easily appreciated on the horizontal beam view of the abdomen than on the supine view. Portal venous air must be differentiated from air in the biliary tree, which is uncommon in the neonatal period and is classically more centrally located in the larger ducts, in contrast to portal venous air, which may extend more peripherally (Epelman et al. 2007).

Free air in the peritoneal cavity or pneumoperitoneum is the result of bowel perforation (Fig. 40), and it is the only universally accepted indication for surgery. The presence of abdominal free air can be difficult to discern on a flat radiograph, which is why decubitus radiographs are recommended when the clinical deterioration suggests perforation. The football sign is characteristic of intraperitoneal air on a flat plate and manifests as a subtle oblong lucency over the liver shadow. It represents the air bubble that has risen to the most anterior aspect of the abdomen in a baby lying in a supine

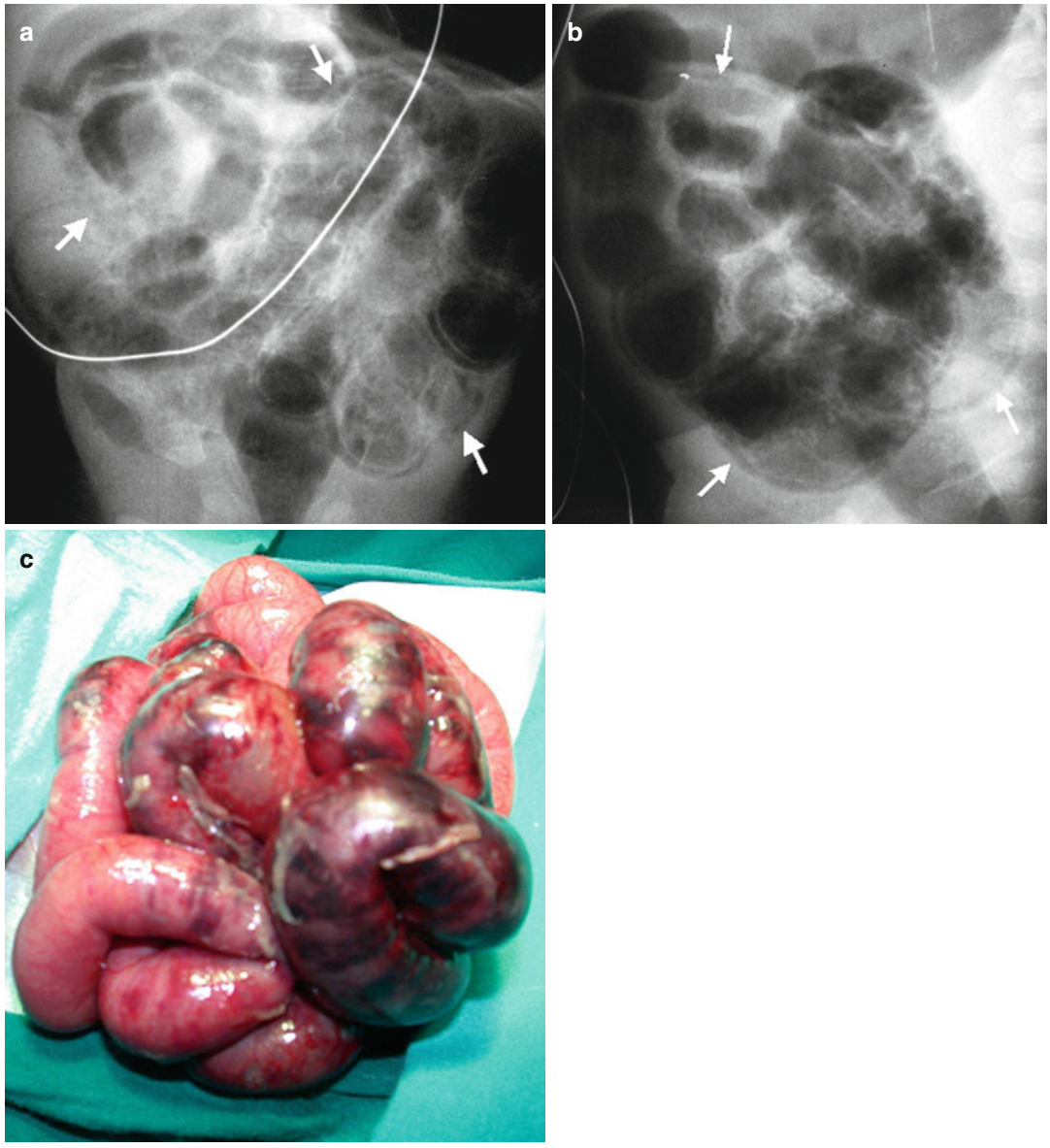


**Fig. 38** Pneumatosis intestinalis in a 1-week-old infant. (**a**) Anteroposterior and (**b**) lateral plain radiographs show small and large bowel loops sharply outlined by collections of air in the bowel wall (*arrows*). Most of these collections of intramural air are linear indicating a subserosal location. (**c**) Surgical image of the same patient demonstrates diffuse bowel necrosis

position and can be demonstrated by left-lateral decubitus imaging (Buonomo 1999). Perforation most commonly occurs in the distal ileum and proximal colon. Although free air in the abdominal cavity confirms it, bowel wall perforation might be present in the absence of free air in one third of the cases. Ascites is a late finding that usually develops some time after perforation when peritonitis is present. Ascites is observed on an AP radiograph as centralized bowel loops that appear to be floating on a background of density. It is better observed on US.

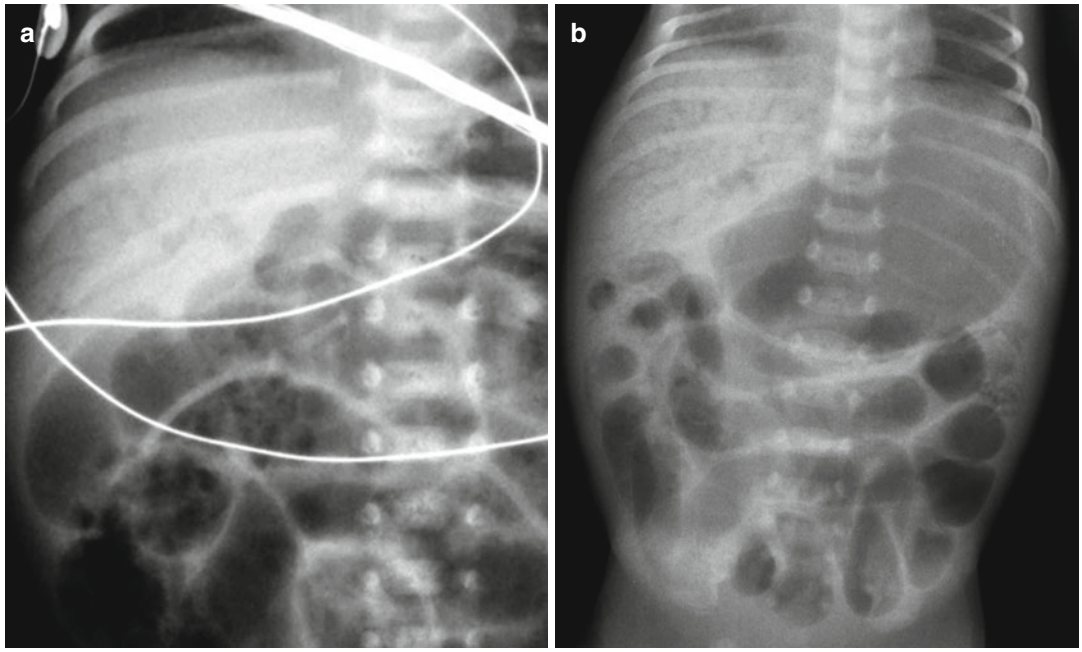


**Fig. 39** Portal vein air. Plain radiographs. (**a**) Air is observed within the portal vein branches complicating pneumatosis intestinalis in a 3-week-old premature infant. (**b**) Another premature infant with pneumatosis intestinalis and air within the portal vein

Abdominal US is a relatively new technology for evaluating suspected NEC in neonates. The major advantages of abdominal US in NEC are that it provides, in real time, direct images of abdominal structures, particularly the bowel, and fluid in the peritoneal cavity. Studies by Faingold and Kim (Faingold et al. 2005; Kim et al. 2005) showed that abdominal US including color Doppler sonography was extremely helpful for facilitating patient management in this disease. Although abdominal US may show intraluminal bowel air, it does not display the pattern of gaseous distention as well as plain abdominal radiograph. However, abdominal US offers several other clear advantages over plain abdominal radiograph, as the ability to depict bowel wall thickness and echogenicity as well as free and focal fluid collections and their character. US displays peristalsis not shown in plain radiograph and by means of color and power Doppler imaging can also give additional information on viability of bowel wall.

Intramural air is seen as hyperechoic foci in the bowel wall. The amount of intramural air may vary considerably from single or scattered hyperechoic foci in the wall (Fig. 41) to complete circumferential involvement of the wall of one or many bowel loops. Large amounts of intramural air may give the wall a speckled or granular appearance, which can be confused with dense calcification. However, the latter usually has a much sharper posterior acoustic shadowing than intramural air. Small amounts of intramural air in the nondependent portions of a bowel loop have to be differentiated from small amounts of intraluminal air floating between the intraluminal fluid and the nondependent portion of the bowel wall. In contrast to intraluminal air, intramural air will not change position because of peristalsis, respiratory movement, changes of the patient's position, or abdominal compression with the transducer (Epelman et al. 2007).

Portal vein air (PVG) is an extension of intramural air that enters the veins of the bowel wall and passes into the portal venous system. On abdominal US, portal vein air may be seen in the

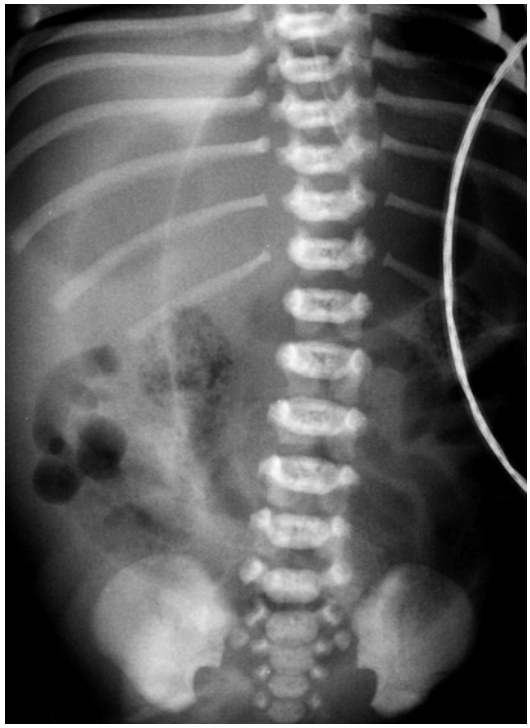

**Fig. 40** Pneumoperitoneum complicating necrotizing enterocolitis. Supine radiograph in a 1-month-old premature infant shows intramural air in the small bowel and free intraperitoneal air secondary to bowel perforation. Central lucency and the outlined falciform ligament are clearly demonstrated

main portal vein and its major branches as bright, shifting echogenic foci moving within the veins with the blood flow (Dilli et al. 2011). This finding has been termed informally the "champagne sign" because of its similar appearance to a champagne flute. Eventually, portal vein air is trapped in the small branches of the portal vein inside the liver and is identifiable as dense granular echogenicities in the liver parenchyma that, when sufficient enough, form a linear, branching pattern (Dordelmann et al. 2009). This pattern may be seen diffusely throughout the liver or may have a more focal distribution in either lobe (Fig. 42). One of the limitations of abdominal US in the diagnosis of portal vein air is that during NEC, the presence of air in the portal vein is not persistent and may be detectable only for a short time interval. Portal vein air may also be missed on abdominal US, because necrotic bowel tissue is poorly perfused, thus reducing the transport of intramural air to the portal vein. Lastly, abdominal US may occur as a rather late finding since the traceability of PVG could be seen as a disease extension with comparatively large amounts of intramural air (Dordelmann et al. 2009). Regarding Doppler US, portal branches will show a typical artifact at spectral analysis caused by the air in the blood, which can be appreciated audibly as a crackle and visually on the spectral tracing as sharp bidirectional spikes of Doppler shift superimposed on the portal venous waveforms (Epelman et al. 2007).

Abdominal US has not been the standard method used to detect free air or pneumoperitoneum. However, this technique may indeed show small or large volumes of free air (Faingold et al. 2005). Small volumes may be detected as hyperechoic foci with "dirty" shadowing either between the anterior surface of the liver and the abdominal wall, between bowel loops, or floating on free peritoneal fluid just deep to the abdominal wall (Epelman et al. 2007). It may sometimes be possible to visualize small hyperechoic foci of free air leaking out of necrotic bowel loops and rising to the nondependent aspect of free fluid just deep to the abdominal wall. Larger amounts of free air may be difficult to differentiate from intraluminal air. However, it is indeed possible to differentiate the two, as the larger amounts of free air appear as sheets of echogenicity just deep to the abdominal wall and do not conform to the shape of bowel loops as intraluminal air does. Also, the free air is not subject to changes in shape due to peristalsis as intraluminal air is (Epelman et al. 2007).

One of the greatest contributions of the ultrasound supplemented with power and color Doppler to the diagnosis of NEC is related to the characteristics of the intestinal wall. With abdominal US, it is possible to visualize the bowel wall directly and to assess bowel wall thickness, echogenicity, and peristalsis that are altered in this disease. According to Faingold et al. (2005), thickening of the bowel wall (normal bowel wall thickness ranged from 1.1 to 2.6 mm in neonates) is seen in all patients with

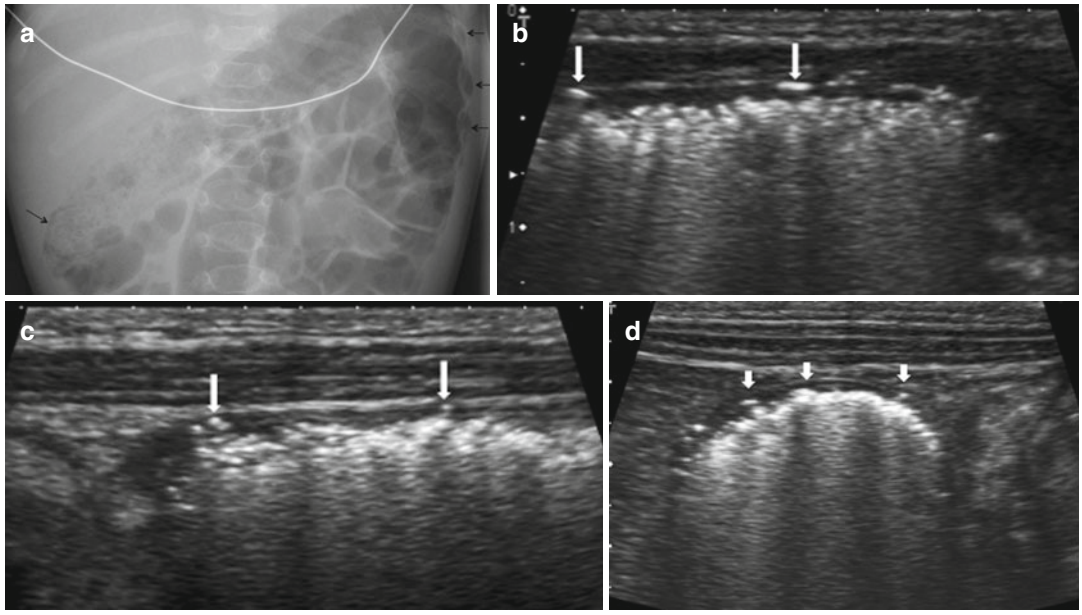


**Fig. 41** Necrotizing enterocolitis. (**a**) Plain radiograph, (**b**, **c**) longitudinal ,and (**d**) transverse US scans show air bubbles (*arrows*) within the colonic wall corresponding to pneumatosis intestinalis. The intramural air has a typical hyperechoic pattern with posterior reverberation artifacts. With this amount of intramural air, it is difficult to assess the thickness of the bowel wall

NEC, while thinning (less than 1 mm in thickness) is seen in those with severe NEC. With both bowel wall thickening and thinning, the normal echogenicity of the bowel wall is lost, and it may be difficult to distinguish the bowel wall from echogenic intraluminal contents in more severely affected loops. Bowel wall thickening is accompanied by an increase in echogenicity of the full wall thickness, often associated with a hyperechoic rim along the damaged mucosa (Fig. 43). Thickening and increased echogenicity of the valvulae conniventes of the small bowel may give rise to a gray-scale "zebra" pattern. However, bowel wall thickening associated with increased echogenicity is a nonspecific sign, as also seen in these neonates with other causes of diffuse edema in the absence of inflammation or ischemia. Peristaltic activity is lost in all of the more severely affected neonates and in approximately 30 % of those less severely affected.

A variety of patterns of bowel wall perfusion may be depicted at color Doppler US. Increased bowel wall perfusion may be shown as a marked increase in color Doppler signals in the bowel wall and/or mesentery that reflect marked hyperemia due to vasodilatation (Fig. 44). The absence of bowel wall perfusion at color Doppler US is more sensitive and specific than the presence of free air at abdominal radiograph in the detection of necrotic bowel in NEC. The absence of color Doppler signals in the bowel wall is thought to reflect absence of perfusion to the involved loop. The absence of color Doppler signals correlated well with transmural bowel necrosis (Faingold et al. 2005).

The true major advantage of abdominal US over abdominal radiograph in NEC is its ability to evaluate abdominal fluid, whether this is intraluminal or extraluminal and whether it is free in the peritoneal cavity or a more localized fluid collection. It has to be remembered that perforation may be associated with the accumulation of intraperitoneal fluid in the absence of free air on the abdominal radiograph (McBride et al. 2010), and in this regard, abdominal US plays a major role as it is much more accurate in depicting

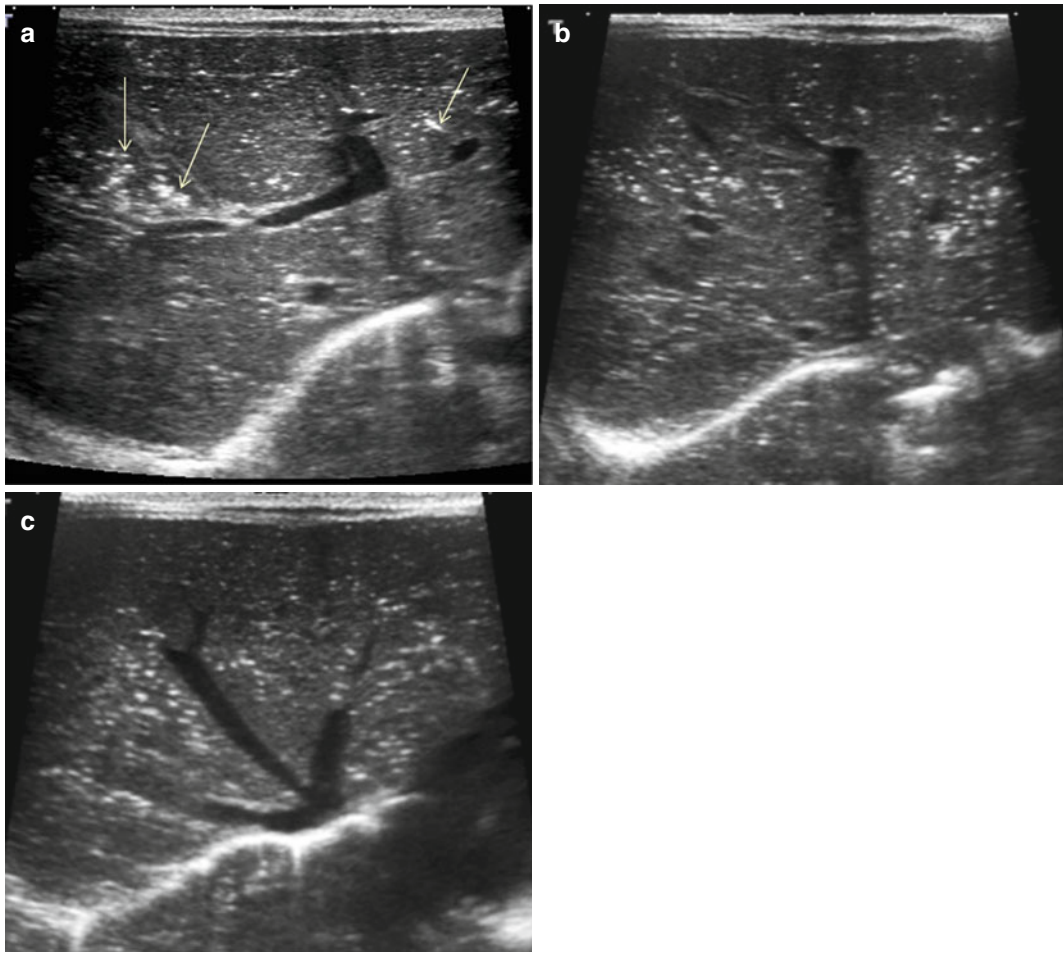


**Fig. 42** Portal vein air. (**a**) Hepatic US shows portal venous air, which is depicted as punctate and linear branching areas of echogenicity in the portal branches within the liver (*arrows*). Note the air bubble in the left portal vein air. (**a**–**c**) Transverse sonograms of the liver show multiple punctate and linear echogenic areas (*arrows*) corresponding to extensive air within the portal vein branches

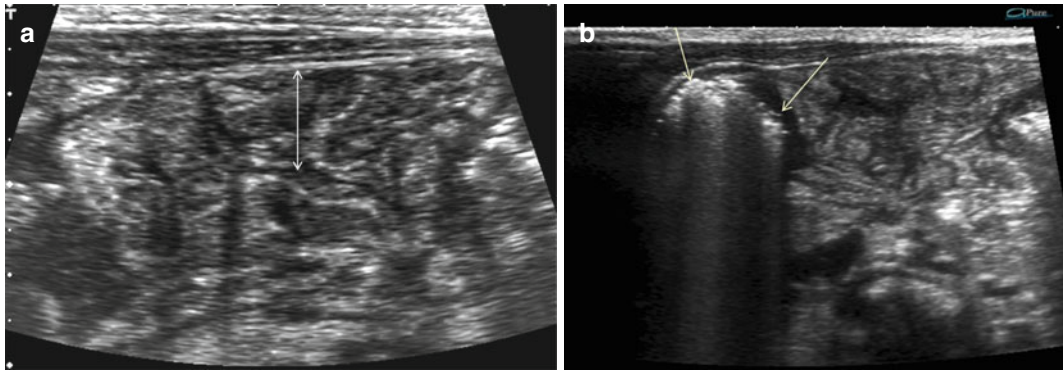


**Fig. 43** Necrotizing enterocolitis. Bowel wall. (**a**) Longitudinal US scan at the level of a small bowel loop showing a thickened wall (*arrowheads*) accompanied by a generalized increase in the mural echogenicity with a thin hyperechoic rim along the damaged mucosa. (**b**) Same patient. Axial US image of the right side of the abdomen shows pneumatosis intestinalis in the ascending colon (*arrowheads*) and small bowel wall thickening with a somewhat layered appearance

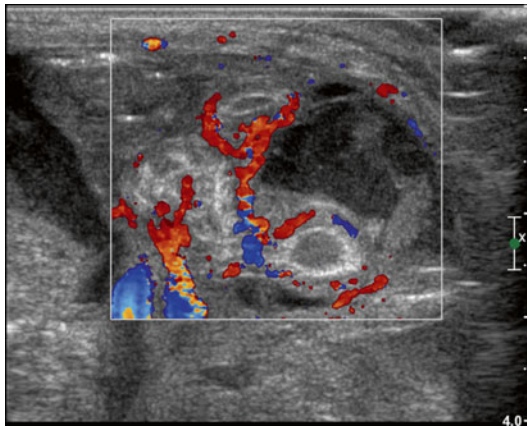

**Fig. 44** Necrotizing enterocolitis. Color Doppler sonogram shows thickened, hyperechoic bowel loops with a "Y" pattern of increased flow outlining the mesenteric and subserosal vessels of the bowel loops. In addition, there is a focal fluid collection of echogenic fluid and debris (Courtesy of Dr. Epelman, Children's Hospital of Philadelphia)

small or even larger amounts of free fluid than abdominal radiograph. Furthermore, abdominal US can show localized fluid collections and abscess formation, which are not uncommonly seen in severe NEC. Abscesses often contain septations and echogenic material (Epelman et al. 2007; McBride et al. 2010).

NEC mortality ranges from 9 to 28 % and is due to refractory shock, disseminated intravascular coagulation, multiple organ failure, intestinal perforation, sepsis, extensive bowel necrosis, and complication of short bowel syndrome. Proper selection of patients for medical versus surgical managements has resulted in significant improvement in survival of infants with NEC. About 20 % of patients treated medically or surgically develop one or multiple strictures at previously affected sites, especially in the large bowel. The strictures may be asymptomatic but may also cause bowel obstruction several weeks or months after the episode of NEC (Arnold et al. 2010; Martinez-Ferro et al. 2010) (Fig. 45). Strictures may develop even in patients whose NEC was not severe. Therefore, any patient with symptoms of obstruction after completion of treatment for necrotizing enterocolitis should undergo a contrast enema.

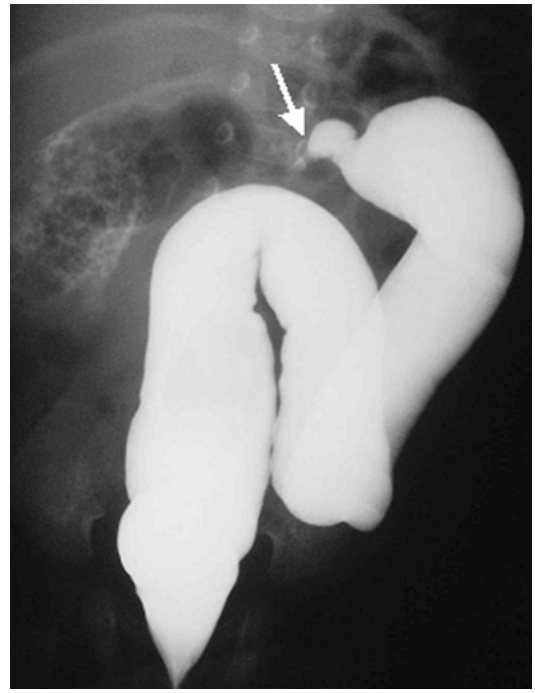

**Fig. 45** Contrast enema performed 6 months after surgery for NEC demonstrates a solitary short stricture at the transverse colon (*arrow*)

## 3 Pneumoperitoneum

Pneumoperitoneum or free intraperitoneal air in the neonatal period is usually the result of a hollow viscus perforation. In healthy neonates, the perforation is usually iatrogenic, secondary to the insertion of a tube or a rectal thermometer (Fig. 46). Necrotizing enterocolitis is the most common cause of pneumoperitoneum in the neonatal intensive care unit. Intestinal atresia is also an important cause, the perforation usually occurring in the dilated loops above the atresia. Ruptured or perforated Meckel, sigmoid and jejunal diverticula, toxic megacolon, perforation by a nasogastric tube, and idiopathic gastric perforation in premature infants are also common causes of pneumoperitoneum in the neonatal period. At times, free intraperitoneal air may be seen in neonates supported by mechanical ventilation. It occurs following a path through the normal diaphragmatic foramina. There is no perforation of the gastrointestinal tract in these cases.

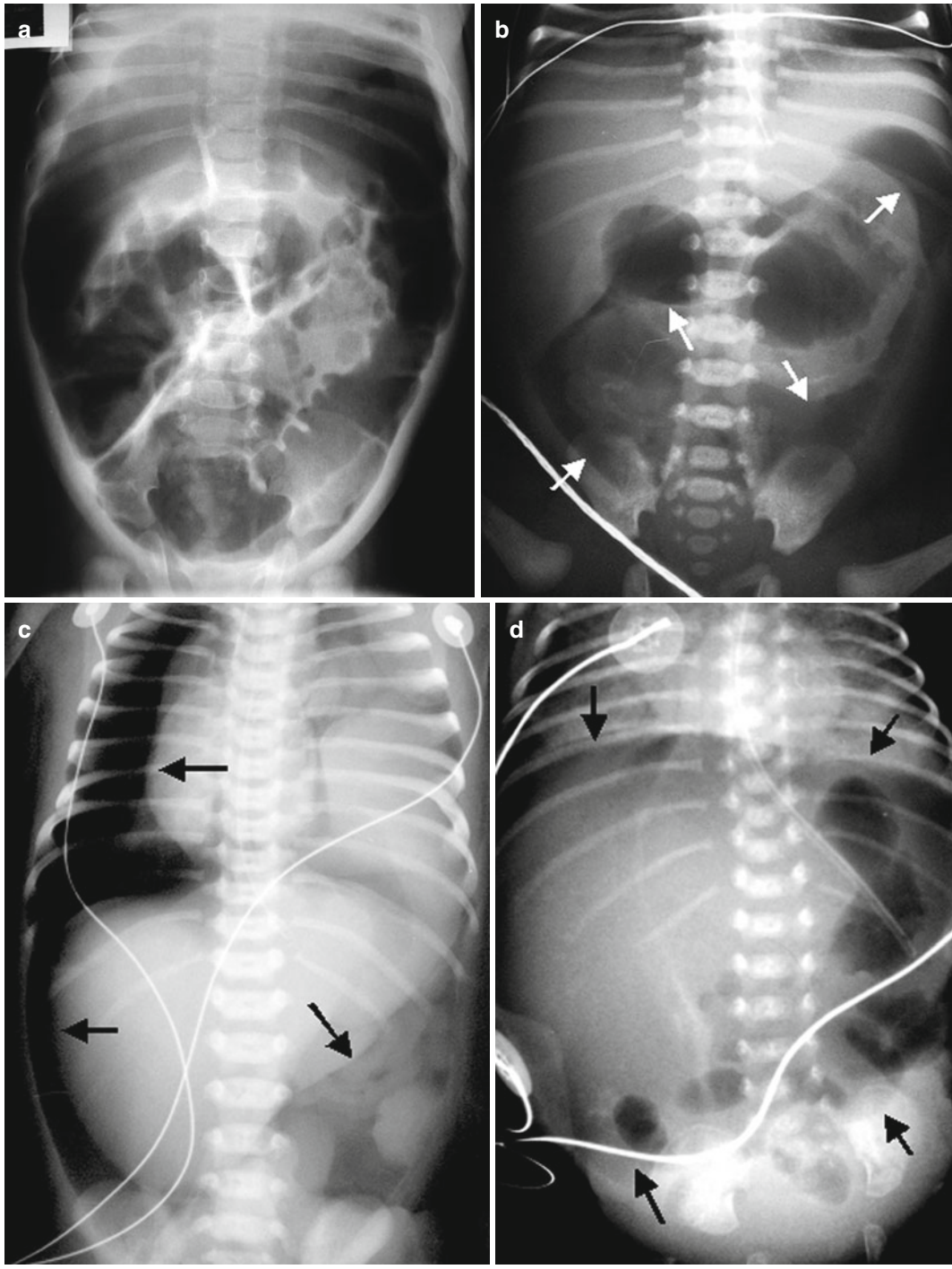


**Fig. 46** Pneumoperitoneum. (**a**) Massive pneumoperitoneum complicating the insertion of a rectal tube. (**b**) Pneumoperitoneum (*arrows*) in a newborn with ileal atresia. (**c**) Massive pneumothorax, pneumomediastinum, and pneumoperitoneum (*arrows*) in a patient that had been supported by mechanical ventilation. (**d**) Neonate with abdominal distension following the insertion of a rectal thermometer. A supine radiograph shows a lucency occupying the entire abdominal cavity (*arrows*) with the falciform ligament outlined by air

## References


Allison JW, Johnson JF III, Barr LL et al (1995) Induction of gastroduodenal prolapse by antral heterotopic pancreas. Pediatr Radiol 25:50–51

Amat VS, Núñez Núñez R, Enríquez Zarabozo E et al (2011) Small left colon syndrome: a review of our experience. Cir Pediatr 24(3):156–160

Applegate KE (2009) Evidence-based diagnosis of malrotation and volvulus. Pediatr Radiol 39(Suppl 2): S161–S163

Arnold M, Moore SW, Sidler D et al (2010) Long-term outcome of surgically managed necrotizing enterocolitis in a developing country. Pediatr Surg Int 26:355–360

Babcock DS (2002) Sonography of the acute abdomen in the pediatric patient. J Ultrasound Med 21:887–899

Babyn P, Peled N, Manson D et al (1995) Radiologic features of gastric outlet obstruction in infants after long-term prostaglandin administration. Pediatr Radiol 25:41–43

Berrocal T, Lamas M, Gutiérrez J et al (1999) Congenital anomalies of the small intestine, colon and rectum. Radiographics 19:1219–1236

Buonomo C (1997) Neonatal gastrointestinal emergencies. Radiol Clin North Am 35:845–864

Buonomo C (1999) The radiology of necrotizing enterocolitis. Radiol Clin North Am 37:1187–1198

Burge D, Drewett M (2004) Meconium plug obstruction. Pediatr Surg Int 20:108–110

Clark P, Ruess L (2005) Counterclockwise barber-pole sign on CT: SMA/SMV variance without midgut malrotation. Pediatr Radiol 35:1125–1127

Couture A (2008) Bowel obstruction in neonates and children. In: Couture A, Baud C, Ferran JL et al (eds) Gastrointestinal tract sonography in fetuses and children, Medical radiology. Diagnostic imaging. Springer, Berlin/Heidelberg, pp 131–251

Cowles AR, Berdon WE, Holt PD et al (2006) Neonatal intestinal obstruction simulating meconium ileus in infants with long segment intestinal aganglionosis: radiographic findings that prompt the need for rectal biopsy. Pediatr Radiol 36:1–5

Dalla Vecchia LK, Grosfeld JL, West KW et al (1998) Intestinal atresia and stenosis. Arch Surg 133:490–497

Daneman A (2009) Malrotation: the balance of evidence. Pediatr Radiol 39(Suppl 2):S164–S166

Dilli D, Oguz S, Erol R et al (2011) Does abdominal sonography provide additional information over abdominal plain radiography for diagnosis of necrotizing enterocolitis in neonates? Pediatr Surg Int 27:321–327

Doodnath R, Puri P (2010) A systematic review and meta-analysis of Hirschsprung's disease presenting after childhood. Pediatr Surg Int 26:1107–1110

Dordelmann M, Rau GA, Bartels D et al (2009) Evaluation of portal venous gas detected by ultrasound examination for diagnosis of necrotizing enterocolitis. Arch Dis Child Fetal Neonatal Ed 94:F183–F187

Douglas D (2010) Meconium pseudocyst. Pediatr Radiol 40(Suppl 1):S105

Eckoldt F, Heling KS, Woderich KS, Bollmann R, Mau HR (2003) Meconium peritonitis and pseudo-cyst formation: prenatal diagnosis and post-natal course. Prenat Diagn 23:904–908

Ellis H, Kumar R, Kostyrka B (2009) Neonatal small left colon syndrome in the offspring of diabetic mothers-an analysis of 105 children. J Pediatr Surg 44(12):2343–2346

Epelman M, Daneman A, Navarro OM et al (2007) Necrotizing enterocolitis: review of state-of the-art imaging findings with pathologic correlation. Radiographics 27:285–305

Etienne D, John A, Menias CO, Ward R, Tubbs RS, Loukas M (2012) Annular pancreas: a review of its molecular embryology, genetic basis and clinical considerations. Ann Anat 194(5):422–428

Faingold R, Daneman A, Tomlinson G et al (2005) Necrotizing enterocolitis: assessment of bowel viability with color Doppler US. Radiology 235:587–594

Fotter R, Sorantin E (1994) Diagnostic imaging in necrotizing enterocolitis. Acta Paediatr 396(Suppl):41–44

Gershon MD, Ratcliffe EM (2004) Developmental biology of the enteric nervous system: pathogenesis of Hirschsprung's disease and other congenital dysmotilities. Semin Pediatr Surg 13:224–235

Gilbertson-Dahdal DL, Dutta S, Varich LJ et al (2009) Neonatal malrotation with midgut volvulus mimicking duodenal atresia. AJR Am J Roentgenol 192:1269–1271

Godbole P, Stringer MD (2002) Bilious vomiting in the newborn: how often is it pathologic? J Pediatr Surg 37:909–911

Hajivassiliou CA (2003) Intestinal obstruction in neonatal/pediatric surgery. Semin Pediatr Surg 12:241–253

Hayakawa K, Hamanaka Y, Suzuki M et al (2003) Radiological findings in total colon aganglionosis and allied disorders. Radiat Med 21:128–134

Hayden CK Jr (1996) Ultrasonography of the acute pediatric abdomen. Radiol Clin North Am 34:791–806

Hernanz-Schulman M (1999) Imaging of neonatal gastrointestinal obstruction. Radiol Clin North Am 37:1163–1186

Horton KK (2005) Pathophysiology and current management of necrotizing enterocolitis. Neonatal Netw 24:37–46

Hryhorczuk AL, Lee EY (2012) Imaging evaluation of bowel obstruction in children: updates in imaging techniques and review of imaging findings. Semin Roentgenol 47(2):159–170

Jamieson DH, Dundas SE, Belushi SA et al (2004) Does the transition zone reliably delineate aganglionic bowel in Hirschsprung's disease? Pediatr Radiol 34:811–815

Jimenez JC, Emil S, Podnos Y et al (2004) Annular pancreas in children: a recent decade's experience. J Pediatr Surg 39:1654–1657

Juang D, Snyder CL (2012) Neonatal bowel obstruction. Surg Clin North Am 92:685–711

Kim WY, Kim WS, Kim IO et al (2005) Sonographic evaluation of neonates with early-stage necrotizing enterocolitis. Pediatr Radiol 35(11):1056–1061

Koplewitz BZ, Daneman A (1999) The lateral view: a useful adjunct in the diagnosis of malrotation. Pediatr Radiol 29:144–145

Kubota A, Imura K, Yagi M et al (1999) Functional ileum in neonates: Hirschsprung's disease-allied disorders versus meconium related ileus. Eur J Pediatr Surg 9(6):392–395

Kul S, Korkmaz HAA, Aysegul Cansu A et al (2012) Contribution of MRI to Ultrasound in the Diagnosis of Fetal Anomalies. J Magn Reson Imaging 35:882–890

Lampl B, Levin TL, Berdon WE, Cowles RA (2009) Malrotation and midgut volvulus: a historical review and current controversies in diagnosis and management. Pediatr Radiol 39(4):359–366

Lang I, Daneman A, Cutz E et al (1997) Abdominal calcification in cystic fibrosis with meconium ileus: radiologic-pathologic correlation. Pediatr Radiol 27:523–527

Laughlin DM, Friedmacher F, Puri P (2012) Total colonic aganglionosis: a systematic review and meta-analysis of long-term clinical outcome. Pediatr Surg Int 28(8): 773–779

Lee NK, Kim S, Jeon TY et al (2010) Complications of congenital and developmental abnormalities of the gastrointestinal tract in adolescents and adults: evaluation with multimodality imaging. Radiographics 30:1489–1507

Lee SH, Cho YH, Kim HY et al (2012) Clinical experience of complex jejunal atresia. Pediatr Surg Int 28(11):1079–1083

Lin PW, Stoll BJ (2006) Necrotising enterocolitis. Lancet 368:1271–1283

Martinez-Ferro M, Rothenberg S, St Peter S et al (2010) Laparoscopic treatment of postnecrotizing enterocolitis colonic strictures. J Laparoendosc Adv Surg Tech A 20(5):477–480

McBride WJ, Roy S, Brudnicki A et al (2010) Correlation of complex ascites with intestinal gangrene and perforation in neonates with necrotizing enterocolitis. J Pediatr Surg 45(5):887–889

Menten R, Reding R, Godding V et al (2012) Sonographic assessment of the retroperitoneal position of the third portion of the duodenum: an indicator of normal intestinal rotation. Pediatr Radiol 42(8):941–945

Minato M, Okada T, Miyagi H et al (2012) Meconium pseudocyst with particular pathologic findings: a case report and review of the literature. J Pediatr Surg 47:E9–E12

Okoye BO, Parikh DH, Buick RG et al (2000) Pyloric atresia: five new cases, a new association, and a review of the literature with guidelines. J Pediatr Surg 35: 1242–1245

Paradiso VF, Briganti V, Oriolo L et al (2011) Meconium obstruction in absence of cystic fibrosis in low birth weight infants: an emerging challenge from increasing survival. Ital J Pediatr 37:55

Patil RT, Gupta R, Parelkar SV et al (2011) A rare case of duodenal atresia with apple-peel configuration of the small intestine and malrotation. Eur J Pediatr Surg 21(5):340–342

Patino MO, Munden MM (2004) Utility of the sonographic whirlpool sign in diagnosing midgut volvulus in patients with atypical clinical presentations. J Ultrasound Med 23:397–401

Peled N, Dagan O, Babyn P et al (1992) Gastric-outlet obstruction induced by prostaglandin therapy in neonates. N Engl J Med 327:505–511

Pickhardt PJ, Bhalla S (2002) Intestinal malrotation in adolescents and adults: spectrum of clinical and imaging features. AJR Am J Roentgenol 179(6): 1429–1435

Pracros JP, Sann L, Genin G et al (1992) Ultrasound diagnosis of midgut volvulus: the "whirlpool" sign. Pediatr Radiol 22:18–20

Quedas EPS, Longuini VC, Sekiya T et al (2012) RET haplotype, not linked to the C620R activating mutation, associated with Hirschsprung disease in a novel MEN2 family. Clinics 67(S1):57–61

Rubesova E (2012) Fetal bowel anomalies – US and MR assessment. Pediatr Radiol 42(Suppl 1): S101–S106

Ryan S, Donoghue V (2010) Gastrointestinal pathology in neonates: new imaging strategies. Pediatr Radiol 40: 927–931

Saguintaah M, Veyrac C, Prodhomme O et al (2010) Meconium obstruction in extremely-low-birth-weight premature infant: US contribution to diagnosis and management. Pediatr Radiol 40:1091–1092, Abstract 65

Salman AB, Karaoglanoglu N, Suma S (1999) Abdominal, scrotal, and thoracic calcifications owing to healed meconium peritonitis. J Pediatr Surg 34:1415–1416

Shimanuki Y, Aihara T, Takano H et al (1996) Clockwise whirlpool sign at color Doppler US: an objective and definite sign of midgut volvulus. Radiology 199: 261–264

Shawis R, Antao B (2006) Prenatal bowel dilatation and the subsequent postnatal management. Early Hum Dev 82(5):297–303

Shew SB (2009) Surgical concerns in malrotation and midgut volvulus. Pediatr Radiol 39(Suppl 2):S167–S171

Singal AK, Ramu C, Paul S et al (2009) Preduodenal portal vein in association with midgut malrotation and duodenal web—triple anomaly? J Pediatr Surg 44:E5–E7

Strouse PJ (2004) Disorders of intestinal rotation and fixation ("malrotation"). Pediatr Radiol 34:837–851

Subbarao K (2008) Roentgenological diagnosis of alimentary tract emergencies in the new born. Indian J Radiol Imaging 18(3):198–203

Jo YS, Jang DG, Nam SY, Choi SK, Shin JC, Lee G (2012) Antenatal sonographic features of ileal atresia. J Obstet Gynaecol Res 38(1):215–219

Sze RW, Guillerman RP, Krauter D et al (2002) A possible new ancillary sign for diagnosing midgut volvulus: the

truncated superior mesenteric artery. J Ultrasound Med 21:477–480

Taylor GA (2011) CT appearance of the duodenum and mesenteric vessels in children with normal and abnormal bowel rotation. Pediatr Radiol 41(11): 1378–1383

Toma P, Mengozzi E, Dell'Acqua A et al (2002) Pyloric atresia: report of two cases (one associated with epidermolysis bullosa and one associated with multiple intestinal atresias). Pediatr Radiol 32:552–555

Veyrac C, Baud C, Prodhomme O et al (2012) US assessment of neonatal bowel (necrotizing enterocolitis excluded). Pediatr Radiol 42(Suppl 1):S107–S114

Vinocur DN, Lee EY, Eisenberg RL (2012) Neonatal intestinal obstruction. AJR Am J Roentgenol 198(1): W1–W10

Yousefzadeh DK (2009) The position of the duodenojejunal junction: the wrong horse to bet on in diagnosing or excluding malrotation. Pediatr Radiol 39: S172–S177

# Gastrointestinal Emergencies in the Infant and Young Child

Gloria del Pozo and Teresa Berrocal

## Contents




**Abstract**

Abdominal pain in children is a common presentation. When severe, differentiating surgical from medical causes is required. This chapter systematically reviews the causes of gastrointestinal emergencies past the neonatal period outlining the imaging algorithms and multi-modality imaging findings of the most common causes.


## 1 Introduction

Acute abdominal pain is a common complaint in the pediatric age group. Approximately up to 10 % of school-age children have recurrent abdominal pain, and in only 10 % of these children, the etiology can be detected. The majority of these children have self-limited disease. The most common associated conditions include upper respiratory tract


G. del Pozo, MD, PhD (✉)
Pediatric Radiology Section,
Department of Radiology,
University Hospital 12 de Octubre, Madrid, Spain
e-mail: gpozo.hdoc@salud.madrid.org

T. Berrocal, MD, PhD
Pediatric Radiology Section,
Department of Radiology,
University Hospital La Paz, Madrid, Spain
e-mail: tberrocalf@hotmail.com




S. Stafrace, J.G. (Hans) Blickman (eds.), *Radiological Imaging of the Digestive Tract in Infants and Children*, Medical Radiology, DOI 10.1007/978-3-319-18434-0_3

infection, pharyngitis, viral syndrome, gastroenteritis, and constipation (Henderson et al. 1992).

Acute abdomen is defined as a severe abdominal pain that starts suddenly so that the possibility of immediate surgery should be considered. The causes of acute abdomen in children vary depending on the age of the child and can be divided into diseases that can be treated with medical care and those in which emergency surgical intervention may be necessary. The most frequent surgically treated causes of acute abdomen are appendicitis, intussusception, adhesions causing bowel obstruction, incarcerated hernia, midgut volvulus, and complicated Meckel diverticulum. Nonsurgically treated conditions frequently have a digestive origin and include gastroenteritis, severe constipation, mesenteric lymphadenitis, ileocecitis, Henoch-Schönlein purpura, inflammatory bowel disease, or paralytic ileus, among others. Furthermore, many intra-abdominal or extra-abdominal disorders can cause acute abdominal pain. Intra-abdominal causes may have a genitourinary (urinary tract infection, ovarian torsion) or pancreaticobiliary origin (cholecystitis, pancreatitis, etc.). Extra-abdominal causes include abdominal pain referred from non-abdominal organs (pneumonia, discitis) and abdominal pain related to a systemic disease, such as diabetic ketoacidosis, hypothyroidism, lead poisoning, sickle cell anemia, and porphyria. Fortunately, these causes differ with the age group, thus simplifying the differential diagnosis (Table 1).

**Table 1** Possible causes of abdominal pain in children (not exhaustive)

| |
|---|
| *Abdominal* |
| *Gastrointestinal* |
| *Surgical* |
| Appendicitis |
| Intussusception |
| Small bowel obstruction |
| Adhesions |
| Incarcerated hernia |
| Volvulus |
| Meckel diverticulum |
| *Nonsurgical* |
| Gastroenteritis |
| Terminal ileitis |
| Crohn disease |
| Henoch-Schönlein purpura |
| Mesenteric adenitis |
| Primary fat epiploic lesions |
| Peritonitis |
| Constipation |
| Paralytic ileus |
| *Genitourinary* |
| Urinary tract infection |
| Calculi |
| Pelviureteric junction obstruction |
| Ovarian cyst |
| Ovarian torsion |
| Hydrometrocolpos |
| *Pancreaticobiliary* |
| Cholecystitis |
| Calculi |
| Choledochal cyst |
| Pancreatitis |
| *Extra-abdominal* |
| Referred pain |
| Thorax: pneumonia, pleural effusion |
| Musculoskeletal: disc pathology |
| Systemic |
| Endocrine: diabetes, hypothyroidism |
| Porphyria |

The role of diagnostic imaging is to determine whether the acute abdominal pain is due to a surgically or medically treated disease and, if possible, to diagnose the exact nature of the pain. Since intussusception or appendicitis are the main surgically treated causes to keep in mind, imaging tests should be targeted to rule out intussusceptions in infants and young children and appendicitis in older children. Plain abdominal radiographs have been used traditionally as the initial imaging examination in children with acute abdominal pain of unknown (equivocal) etiology, but they are usually unhelpful in establishing the cause of the acute abdominal pain as an isolated symptom. The traditional indications for plain abdominal radiography – bowel obstruction, pneumoperitoneum, and the search for ureteral calculi – have been questioned by cross-sectional imaging (Marincek 2002). However, in many centers, plain radiographs serve as the initial radiological approach. The presence of an appendicolith in the right iliac fossa supports the diagnosis of acute appendicitis. If the abdominal pain is accompanied by vomiting, or if there is any clinical suspicion of bowel obstruction or perforation, a supine plain film of the abdomen can be useful, with an additional decubitus or upright view to exclude perforation where indicated. If abdominal pain is accompanied by fever, a chest radiograph may also be obtained, since pneumonia is a well-recognized

cause of abdominal pain (Hayes 2004). The principal imaging technique used for evaluating acute abdominal pain in children is sonography. In most cases, an ultrasound (US) can provide a specific diagnosis, whereas, in others, valuable supplemental information can be obtained. It is a widely available investigation that is relatively inexpensive. It does not involve the use of ionizing radiation, a major advantage in pediatric practice. However, US of the gastrointestinal tract requires experience and patience. Computed tomography (CT) should be reserved for selected patients when further information is needed. Magnetic resonance imaging (MRI) is seldom required as a primary imaging technique but can supplement CT and ultrasound in select cases (jaundice, malignancy) (Carty 2002). The use of MRI is increasing in emergency or semi-emergency situations in some instances including suspected appendicitis, anomaly of the internal genitalia, ovarian torsion, and congenital biliary dilatation (Nosaka 2000; Carty 2002).

## 2 Intussusception

Intussusception (IT) is the most common cause of intestinal obstruction in young children, and delayed diagnosis may lead to bowel perforation. IT occurs when a portion of the digestive tract invaginates into the adjacent bowel segment. The portion of bowel that invaginates into the distal bowel is referred to as the intussusceptum, whereas the distal segment is referred to as intussuscipiens. This condition, with an estimated incidence of 56 children per 100,000 per year in the USA (Parashar et al. 2000), usually occurs in children between 3 months and 2 years of age, more commonly in well-nourished males. Although any intestinal portion can be involved, 90 % of symptomatic intussusceptions are ileocolic. Almost all intussusceptions in children are "idiopathic" (95 %), without a recognizable anatomical abnormality that could function as a lead point except for hypertrophy of Peyer patches in the lymphoid-rich terminal ileum. Hyperplastic areas can be picked up by a peristaltic wave and become intussuscepted. Lymphoid hyperplasia may be stimulated by viral, bacterial, or parasitic infections. This possibility seems to be supported by the seasonal variation of IT and an increased incidence associated with the rotavirus vaccine. For an individual child there is a low-level increased risk of IT associated with rotavirus vaccination (rates <1 in 50,000) (Lepage and Vergison 2012). In the first week after the first vaccine dose, the relative risk is 5.3 (95 % CI, 3.0–9.3). Despite the greater severity of these intussusceptions, from a public health perspective, there has been a significant reduction in rotavirus disease worldwide as a result of indirect protection after mass infant vaccination (herd immunity effect) strengthening the argument favoring its use (Desai et al. 2012).

There are other types of intussusceptions; some may be asymptomatic and usually limited to the small bowel and others secondary to pathological lead points or gastrojejunostomy tubes, and others occur in the postoperative period or after blunt abdominal trauma.

### 2.1 Diagnosis

Less than half the children with IT have the classic triad of colicky abdominal pain with drawing-up of the legs, palpable abdominal mass, and bloody mucous stool or hematochezia. The onset of nonspecific abdominal symptoms in which vomiting predominates with an initial absence of rectal bleeding, as well as atypical presentations with diarrhea, neurological symptoms (seizures or lethargy), or shock of uncertain origin, may result in the diagnosis of IT being disregarded. On the other hand, only 30–68 % of children with suspicious clinical findings actually have the condition (del-Pozo et al. 1999). Therefore, it is desirable to use diagnostic tools that are as innocuous as possible in both the affected children and particularly in children who do not have intussusceptions, in order to decrease any possible discomfort and avoid possible adverse effects on their actual diseases. US is the current imaging modality of choice; it is a highly accurate diagnostic test for IT that can also make alternative diagnoses such as urinary tract pathology, appendicitis, ovarian torsion, and volvulus. Plain abdominal radiographs do not have the required accuracy for this life-threatening condition and are reported as normal in 40–50 % of the cases (Meradji et al. 1994; Hernandez et al. 2004). The radiation exposure during a fluoroscopy, its limitation to document other pathologies unrelated to IT, and the subsequent diagnostic delays in children who eventually turn

out to be affected by another pathology do not justify the performance of a diagnostic enema.

The imaging goal in children with suspected IT is to confirm the diagnosis, distinguish IT from other entities, and determine what type of IT they have, because management can be different. In ileocolic IT cases US can also assess risk predictors of irreducibility and ischemia before undertaking reduction.

### 2.1.1 US

US is a highly sensitive (97.9–100 %) and specific (88–100 %) test for IT (Pracros et al. 1987; Wang and Liu 1988). IT can be identified readily on US even by inexperienced users and nonpediatric radiologists with a reported 100 % negative predictive value (Hryhorczuk and Strouse 2009). Because deep penetration of the ultrasound beam is not necessary in small children, a high-resolution transducer (5–12 MHz) can be used to improve image definition. The ileocolic IT mass is a large structure, usually greater than 5×2.5 cm, that often displaces adjacent bowel loops. The probe is held in a transverse plane and the route of the colon is traced distally to the rectum. The majority of ileocolic intussusceptions are located underneath the liver and can easily be detected using the liver as an acoustic window. An additional lateral abdominal approach avoiding intestinal air interposition may be necessary, particularly in obstructive cases. The invaginated ileum is located inside the recipient loop, so ileocolic intussusceptions are not usually detected in the right lower quadrant (RLQ), but along the course of the colon, mostly the ascending and transverse colon. On rare occasions, a severe IT can even protrude from the rectum.

The ultrasound image of IT is complex. Although we generally speak of two bowel loops, three bowel walls and the mesentery are in fact involved. The intussuscipiens ("receiving loop") contains the infolded intussusceptum ("donor loop"), which has two components: a central entering limb of bowel and a thick more peripherally everted returning limb. The attached mesentery is dragged between these two limbs (Fig. 1). The invagination of the bowel into itself is not a true "telescoping" of independent segments and requires one of them (the returning limb) to turn inside out, leaving its opposite serosal surfaces facing each other (Fig. 2). The appearance of an IT, described as a donut (Swischuck et al. 1985), target, or multiple concentric ring signs (Holt and Samuel 1978), varies depending on the scanning level and the amount and arrangement of the enclosed mesentery. The thickest component of the IT is the everted returning limb, which, together with the thin intussuscipiens, forms the hypoechoic outer ring or donut seen on axial US scans. At the center of the IT, the hyperechoic mesentery progressively increases toward the base surrounding the central entering limb of the intussusceptum eccentrically, like a flag hanging on its pole. On axial US scans, the IT changes gradually as the study proceeds from the apex toward the base and the center size increases while the outer rim of the donut decreases. At its apex, where the mesentery is absent, just a hypoechoic center is seen, corresponding to the central entering limb of the intussusceptum, while at the base, where the amount of enclosed mesentery is maximal, a hyperechoic

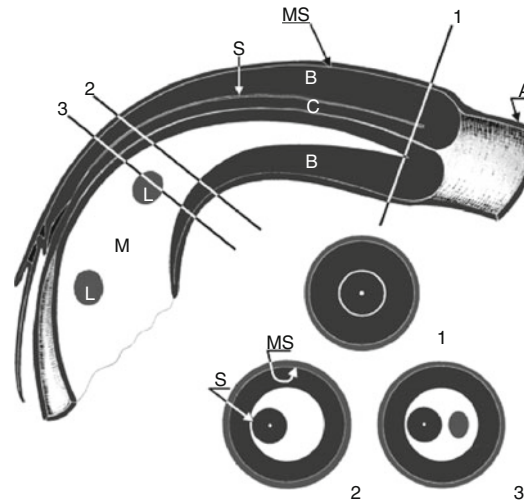


**Fig. 1** Structure of an intussusception. Diagram shows a longitudinal view and three axial views of an intussusception; three bowel loops and the mesentery can be seen. The intussuscipiens (*A*) contains the two limbs of the intussusceptum: the everted returning limb (*B*), which is edematous, and the central entering limb (*C*), which is located at the center of the intussusception with the accompanying mesentery (*M*). The mesentery contains some lymph nodes (*L*) (*MS* contacting mucosal surfaces of the intussuscipiens and everted limb, *S* contacting serosal surfaces of the everted limb and central limb) (From reference del-Pozo 1999)

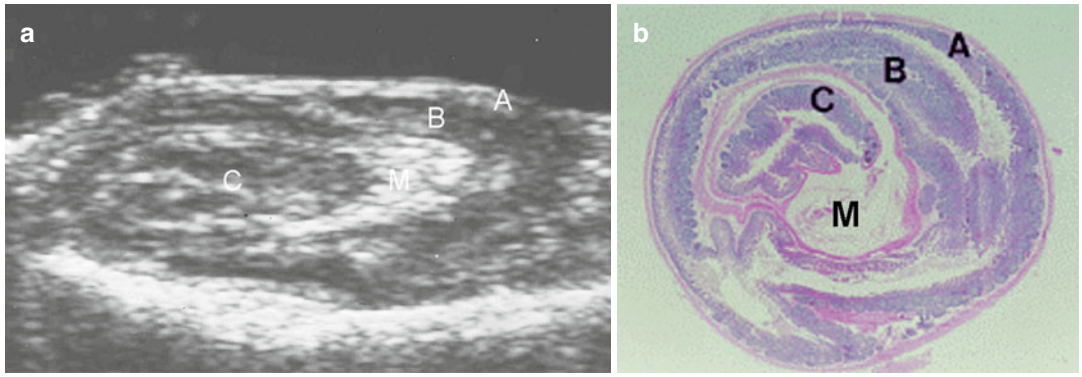


**Fig. 2** Correlation of sonographic and pathologic findings in intussusceptions in pigs. (**a**) axial US scan; (**b**) corresponding pathological specimen. Axial sections at the base show a donut sign with a peripheral hypoechoic ring (formed by the everted limb of the intussusceptum and the intussuscipiens) and a hyperechoic crescent shaped center due to the mesentery enclosing the hypoechoic central limb of intussusceptum (crescent-in-donut sign) (*A* intussuscipiens, *B* everted limb of intussusceptum, *C* central limb of intussusceptum, *M* mesentery) (From reference del Pozo (1996a))

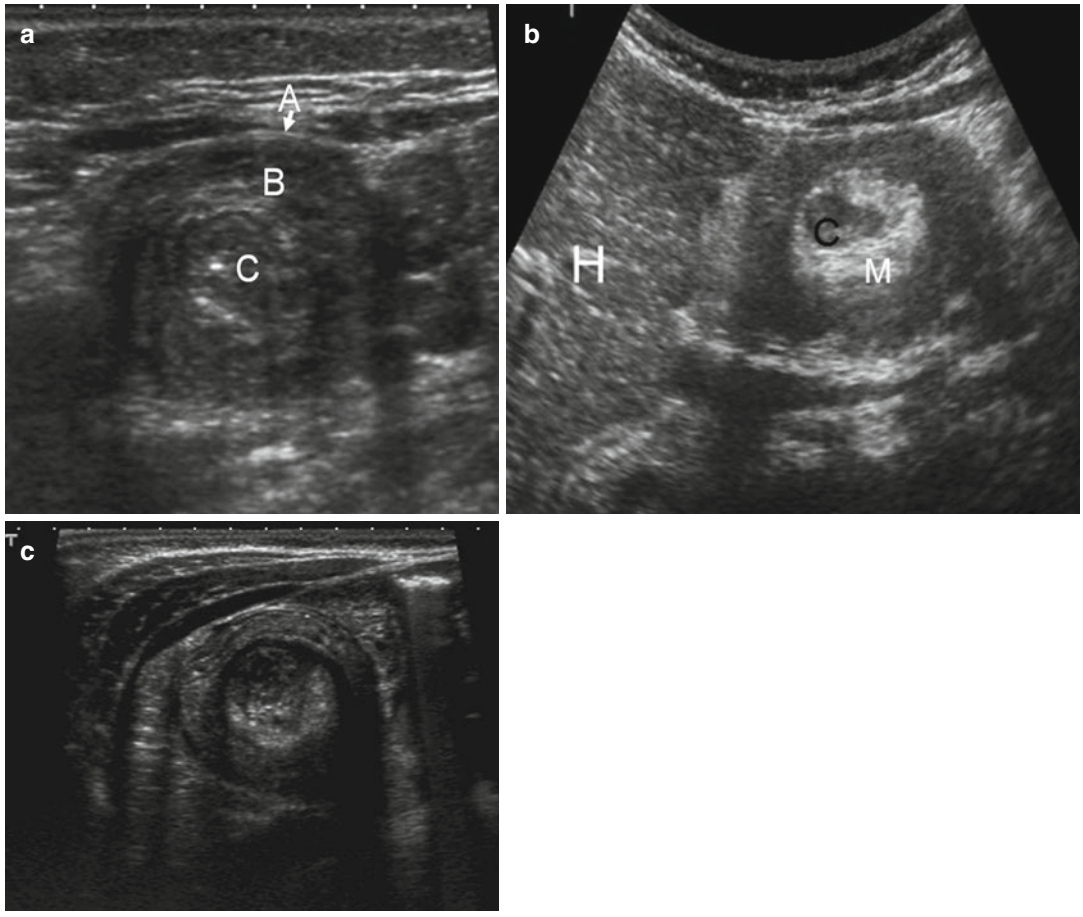


**Fig. 3** The crescent-in-donut sign. Axial US scans obtained (**a**) at the apex, (**b**) at the middle (apex proximal regions), and (**c**) at the base of an intussusception, show the central limb of the intussusceptum (*C*) eccentrically surrounded by the hyperechoic mesentery a situation that produces the crescent-in-donut sign (**a**: From reference del-Pozo (1999). *A* intussuscipiens, *B* everted limb of intussusceptum, *C* central limb of intussusceptum, *M* mesentery, *H* liver)

crescentic center is visible (the crescent-in-donut sign) (del-Pozo et al. 1996a) (Fig. 3). On longitudinal US scans, a bowel-within-bowel appearance may also be visualized as a sandwich sign (Pracros et al. 1987; Montali et al. 1983) formed by three nearly parallel hypoechoic bands separated by two mesenteric hyperechoic bands, which is the longitudinal view of the crescent-in-donut sign (Fig. 4a). The pseudokidney sign occurs if the IT is curved or it is imaged obliquely and the mesentery is just visualized at one side of the central limb of the intussusceptum (Fig. 4b).

The different components of the IT image may vary. At the apex of the ileocolic IT, the outer ring of the "donut," mostly created by the everted returning limb of the intussusceptum, is hypoechoic, resulting from the lymphoid hyperplasia of the invaginated terminal ileum, and at the base of the IT, there is an "onion-skin" image due to the differentiation of the multiple layers of the colon wall involved at this level. The donut may rarely appear hyperechoic during episodes of pain. Occasionally, air is seen as dotted hyperechoic areas in the thickness of the returning limb of the intussusceptum; this observation has been linked to irreducibility and ischemia (Stranzinger et al. 2009) (Fig. 5) and should not be confused with air in the lumen of the colon trapped between the mucosal surfaces of the two facing bowel loops, the intussuscipiens and the returning limb of the intussusceptum. The hyperechoic mesentery may contain hypoechoic areas that correspond to lymph nodes, the dragged cecoappendiceal complex or vessels (del-Pozo et al. 1999) (Fig. 6).

To summarize, the US appearance of the intussusceptions depends on two factors: (1) the length of the IT (the longer the IT, the greater the amount of mesentery included and dragged cecum and appendix) and (2) the level where the section is obtained (the closer to the base, the smaller the donut and the greater the thickness and nonhomogeneity of the enclosed mesentery). The hyperechoic crescent of the intussusceptum mesentery characterizes the image of the IT and differentiates it from any other pathologic conditions of the gastrointestinal tract that cause bowel wall thickening, such as inflammation, edema, hematoma, or tumor (simple image of donut or pseudokidney appearance) or an area of volvulus (whirlpool

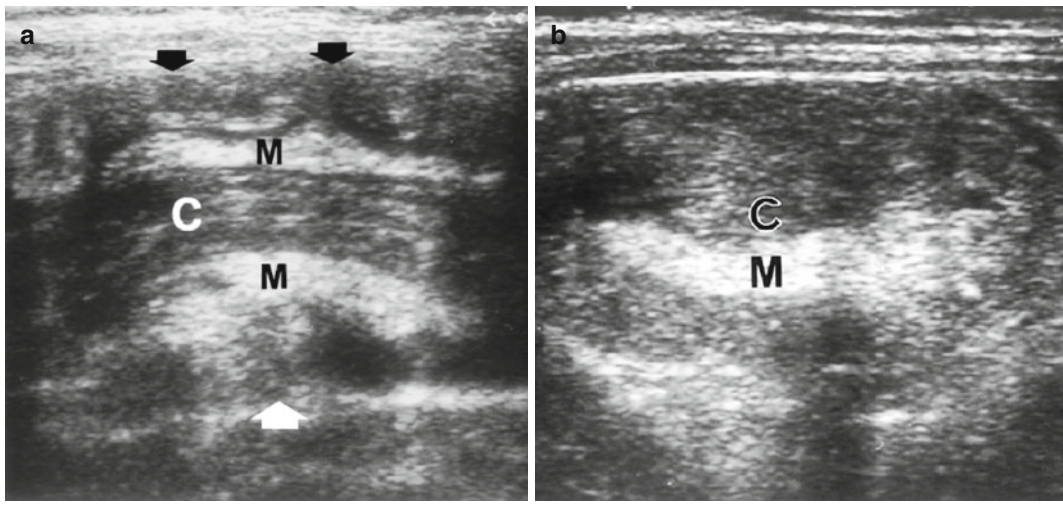


**Fig. 4** Intussusception on longitudinal US scans. Variable appearance of intussusception on longitudinal US scans depending on which side of the central limb of the intussusceptum the mesentery is imaged. It may be depicted at one side (pseudokidney) or at both sides (sandwich). (**a**) US scan obtained in the strict longitudinal plane of an intussusception slightly away from the apex shows the sandwich sign. The outer hypoechoic bands (*arrows*) represent the everted limb of the intussusceptum beside the intussuscipiens. The two hyperechoic bands represent the mesentery. The central hypoechoic band represents the central limb of the intussusceptum. (**b**) US scan shows the pseudokidney sign. The mesentery is demonstrated on one side of the central limb of the intussusceptum. *C* central limb of the intussusceptum, *M* mesentery (From reference del-Pozo (1999))

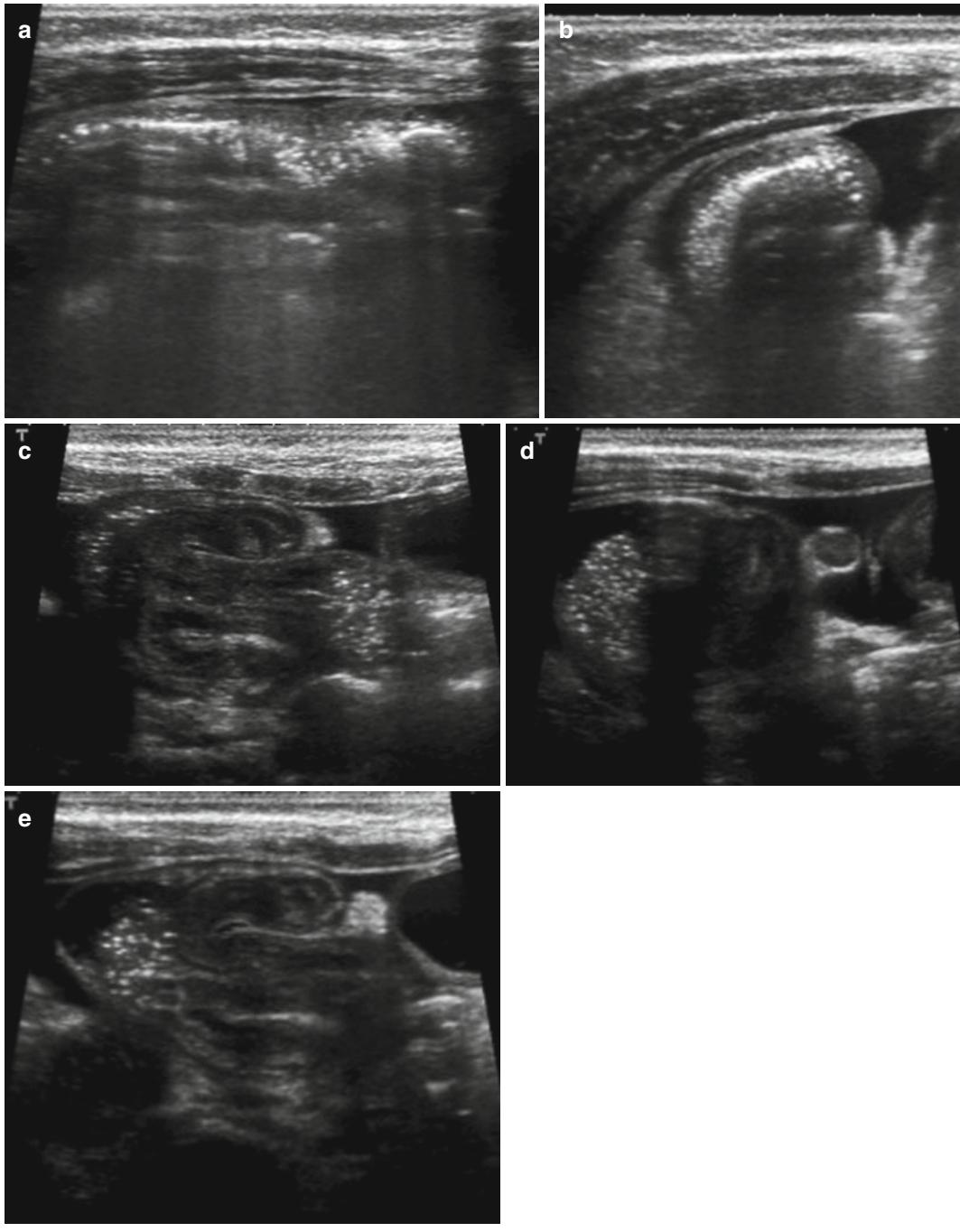


**Fig. 5** Air in the intussusceptum (**a**–**e**). Multiplanar US scan images show air as linear and dotted hyperechoic foci in the thickened wall of the returning limb of the intussusceptum in an ileocolic intussusception. This intussusception was successfully reduced by enema therapy. Air passing from the bowel wall into the lumen of the terminal ileum was observed on US-guided saline enema during the reduction process. Compare images **c** and **e**

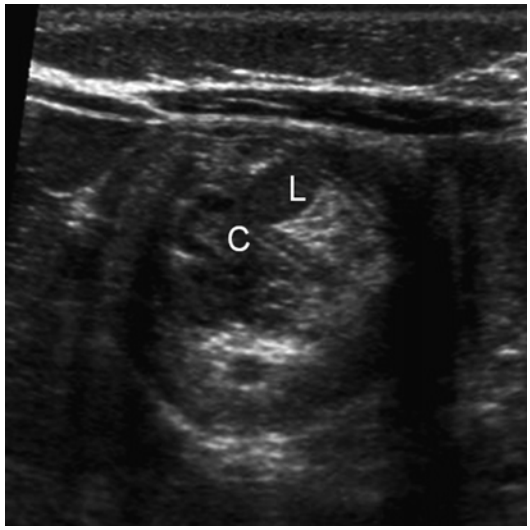


**Fig. 6** Longitudinal/oblique scan of the subhepatic region demonstrating an ileocolic intussusception. (*C* Central intussusceptum, *L* mesenteric lymph nodes)

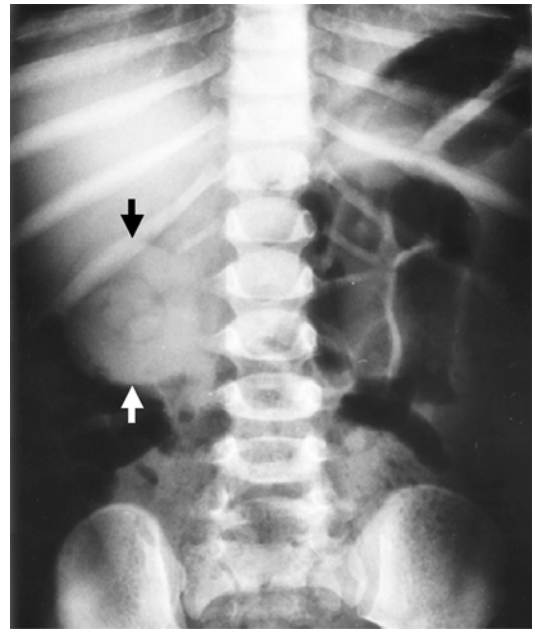

**Fig. 7** Target sign. Plain radiograph shows a round soft tissue mass in the right upper quadrant (*arrows*). The mass contains a ringlike area of lucency (From reference del-Pozo (1999))

sign). The mesentery also helps differentiate the IT from normal findings such as stool or psoas muscle that may occasionally be mistaken for an IT.

### 2.1.2 Other Imaging Modalities

An IT can be recognized on abdominal x-rays, contrast barium studies (upper GI series, enema), CT, or MRI. These two latter modalities may also identify the cause.

The diagnostic reliability of abdominal x-rays is a subject of great controversy in the literature. In some institutions, if there is a low pretest probability for the diagnosis of IT, plain abdominal x-ray is used as screening test, and it can reliably exclude the diagnosis when interpreted by expert radiologists (Roskind et al. 2012). Patients younger than 5 months with a negative abdominal x-ray are at low risk for IT, as are those older than 5 months who have a negative abdominal x-ray, absence of bilious emesis, and presence of diarrhea (Weihmiller et al. 2011). However, when clinical suspicion of IT is high, US is recommended and plain abdominal x-ray would not be necessary as a first examination (Verschelden et al. 1992; Riebel et al. 1993; Daneman and Alton 1996). Furthermore, abdominal x-rays have a low sensitivity and specificity for diagnosing IT when interpreted by pediatric emergency physicians, as often occurs during the clinical decision-making process (Morrison et al. 2009). Many plain radiographic signs of intussusceptions have been described. The most common is a soft tissue mass, which is most often seen in the right upper quadrant effacing the adjacent hepatic contour. The most specific plain radiographic findings are the "target sign" and "meniscus sign." The "target sign" consists of a soft tissue mass that contains concentric circular or nearly circular areas of lucency, which are due to the mesenteric fat of the intussusceptum (Ratcliffe et al. 1992) (Fig. 7). The "meniscus sign" consists of a crescent of air within the colonic lumen that outlines the apex of the intussusceptum (Fig. 8). Other signs include reduced air in the small intestine or a gasless abdomen and obstruction of the small bowel. Conversely, identification of a cecum filled with air or feces in the normal location is the finding that allows exclusion of intussusceptions with the most confidence (Sargent et al. 1994). However, the sigmoid colon

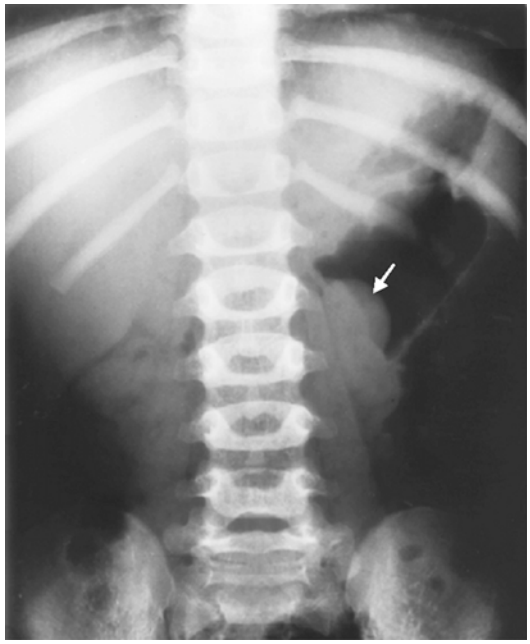

**Fig. 8** Meniscus sign. Plain radiograph shows the meniscus sign: a rounded soft tissue mass (the intussusceptum) protruding into the air-filled transverse colon (*arrow*) (From reference del-Pozo, (1999))

is often positioned in the right lower quadrant (RLQ) in infants and young children and can therefore be mistaken for the cecum, leading to a false-negative result (Fiorella and Donnelly 2001).

Barium enema examination has been the standard of reference for the diagnosis of IT for many years. The classic signs of IT at enema examination are the "meniscus" sign and "coiled spring" sign. The "meniscus" sign at enema examination is analogous to the "meniscus" sign at plain radiography and is produced by the rounded apex of the intussusceptum protruding into the column of contrast material. The "coiled spring" sign is produced when the edematous mucosal folds of the returning limb of the intussusceptum are outlined by contrast material in the lumen of the colon (Fig. 9).

CT is reserved for patients in whom other imaging modalities are unrevealing or in the workup for pathological lead points of IT detected by ultrasound (Navarro and Daneman 2004). An IT can be recognized on CT, but CT cannot be used to reduce the IT and can be time consuming in children who may require sedation. Radiation exposure concerns should be particularly kept in mind in these small children.

## 2.2 Assessment of Reducibility: Risk Predictors of Irreducibility and Ischemia

The only absolute contraindications for enema reduction of IT are the presence of perforation, peritonitis, or shock. Criteria that are linked to a lower reduction rate and a higher perforation rate, especially if more than one is present, include patient age under 3 months or greater than 5 years, a long duration of symptoms, rectal bleeding, dehydration, signs of small bowel obstruction, and the presence of the "dissection sign" on a contrast study (Katz et al. 1993). The dissection sign refers to contrast material within the lumen of the intussuscipiens that "dissects" it for a long distance over the surface of the intussusceptum. US findings have also been evaluated in an attempt to predict the presence of bowel necrosis and the reducibility of the IT by enema, including the presence of trapped peritoneal fluid within the IT, the absence of blood flow on US Doppler, the presence of enlarged lymph nodes, the presence of a thick peripheral hypoechoic rim of the donut, and the presence of air in the returning limb of the intussusceptum. The presence of these features, although associated with increased necrosis and failed reduction, does not preclude an attempted reduction by enema. The presence of free intraperitoneal fluid has not been associated with irreducibility.

Trapped peritoneal fluid within the IT is present in 14–23 % of the cases and it is easily detected on US. It is broadly accepted that substantial amounts of fluid (more than 15 × 5 mm on axial US scans) correlates significantly with bowel ischemia at surgery and lower rates of successful reduction by enema, originally reported using a low enema pressure (<88.8 mmHg) (del-Pozo et al. 1996b). One more recent paper reports that reduction rates are not influenced by the presence of trapped liquid (Caro et al. 2011), but the enema

pressures used in this cohort were higher than in the earlier paper. The vascular impairment in an IT is maximal at the apex. The initial venous stasis causes progressive edema and transudation throughout the surfaces of the returning limb of the intussusceptum. Because this segment is inside out, the transudate through the mucosal surface flows directly into the colon lumen and

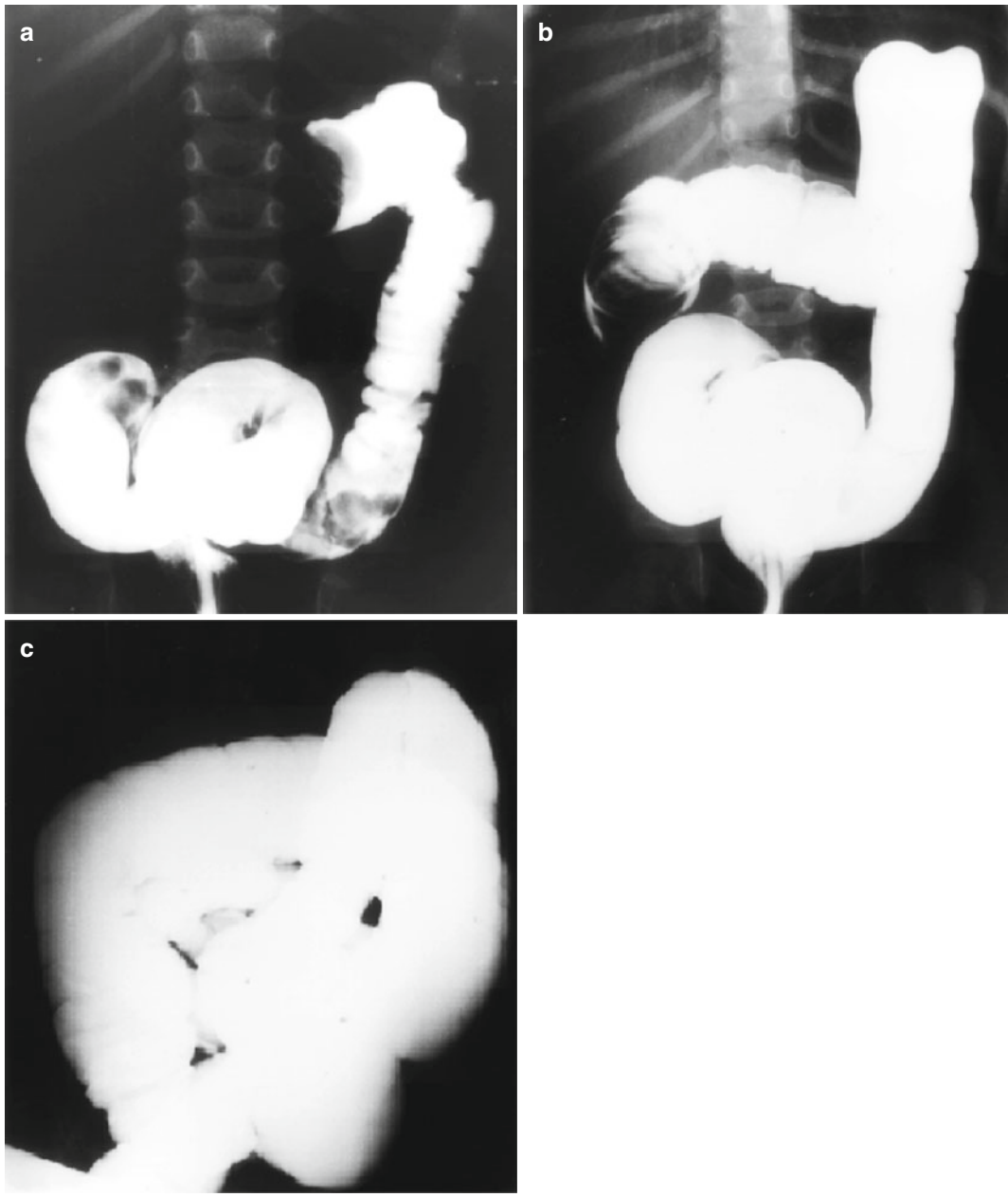


**Fig. 9** Contrast enema reduction. 'Meniscus' and 'coiled spring' signs. (**a**) Image from a barium enema study shows the meniscus sign in the contrast material-filled distal transverse colon. (**b**) Image from a barium enema study performed after partial reduction of the intussusception shows the coiled spring sign. Contrast material outlines the facing mucosal surfaces of the intussuscipiens and the intussusceptum. (**c**) Image from a barium enema study performed after complete reduction of the intussusception shows barium flowing freely into the ileum (From reference del-Pozo (1999))

will be eliminated easily. Conversely, the transudate through the serosal layer is trapped between both serosal layers of the limbs of the intussusceptum. This fluid may not flow freely into the peritoneal cavity because the edematous mesentery acts as a wedge preventing fluid from leaking through the neck of the IT (Fig. 10). This situation may explain why free peritoneal fluid is detected in less than 50 % of cases of IT, and its presence has not been related to ischemia or an increased risk of perforation (Swischuk and Stansberry 1991). On axial US scans, the trapped fluid appears as the double-crescent-in-donut sign, because it has adapted to the mesentery crescent, which is attached at just one side of the loop. In addition to the mesenteric crescent-in-donut appearance, there is an anechoic crescent that represents trapped ascites accumulated between the serosal layers of both enfolded intussusceptum limbs. In advanced stages, the apex of the intussusceptum becomes thinner and asymmetrically dilated at its antimesenteric side, adopting a

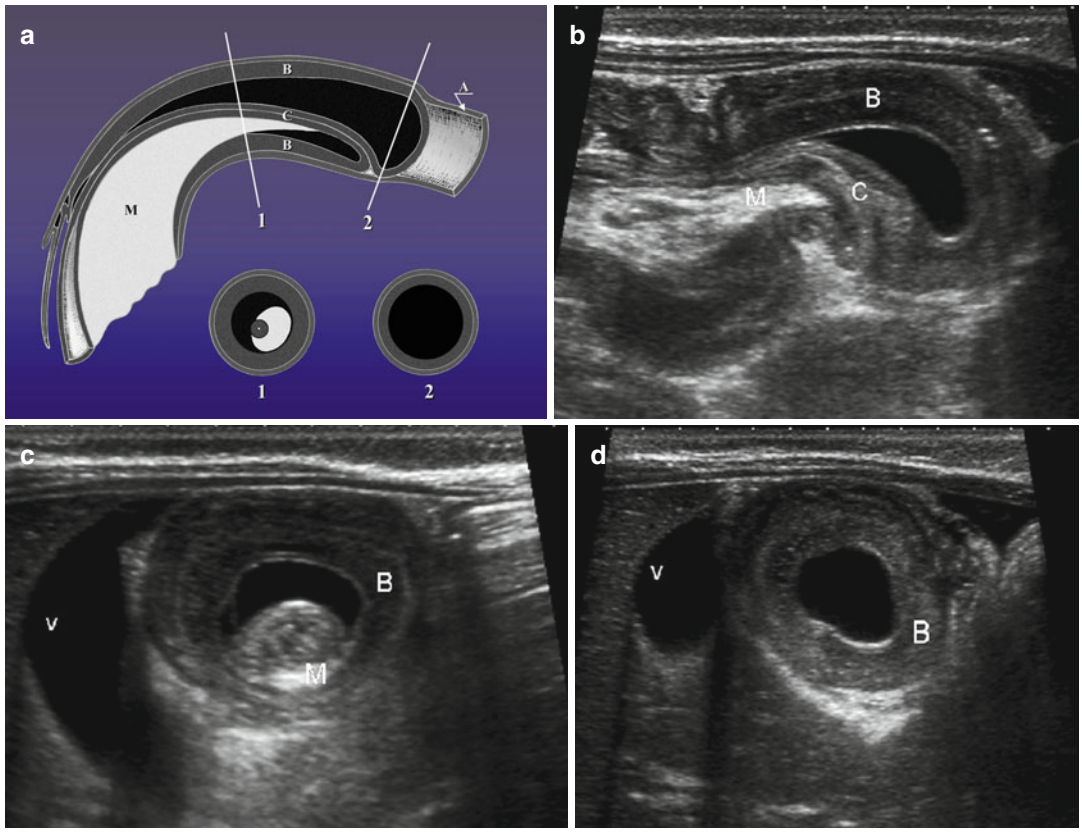


**Fig. 10** Intussusception with trapped peritoneal fluid. (**a**) Schematic representation of an intussusception with the presence of fluid. Sagittal and axial images were obtained at different levels. Fluid collects between the serosal layers of both limbs of the intussusceptum; the returning limb is everted and compromised. The mesentery acts as a wedge which makes the exit of fluid into the peritoneum difficult. Dilatation at the apex of the intussusceptum, probably secondary to ischemia and to the increase in trapped fluid, occurs mainly at the antimesenteric border. This fact results in the asymmetric disposition of the area of fluid, which explains the appearance on axial US images. *1* crescent-in-donut sign with additional anechoic crescent, *2* everted intussusceptum filled with peritoneal fluid, *A* intussuscipiens, *B* returning limb of the intussusceptum, *C* entering limb of the intussusceptum, *M* mesentery. The *black areas* represent fluid in the intussusception (From reference Del Pozo (1996b)). (**b**) Longitudinal and (**c**, **d**) US axial scans of an intussusception with trapped peritoneal fluid. Axial US scan shows the double-crescent-in-donut sign. This is the crescent-in-donut sign with an additional echo-free crescent that represents the trapped fluid (*V* gallbladder, *M* mesentery)

pyriform "cul-de-sac" morphology that can be confused with a duplication cyst or with fluid in the lumen of an obstructed bowel loop (Fig. 10). The trapped fluid contributes to irreducibility by increasing bowel loop size. During an enema reduction, the pressure applied at the apex of the IT results in deformation of the incarcerated intussusceptum accentuating its cuneiform wedge-shaped morphology as the longitudinal diameter is decreased and the transverse diameter increased, like a balloon filling with fluid. This behavior emphasizes its wedge-shaped morphology, hindering reduction. If a maximum quantity of fluid is accumulated or excessive pressure is applied, the increase in the transverse diameter of the intussusceptum may overdistend the intussuscipiens, leading to rupture. As a matter of fact, many of the perforations described in the literature occur in the colon, even if the vasculature of this part of the bowel was not affected (Mitra et al. 1982; del-Pozo et al. 1996b).

The absence of blood flow within the IT on Doppler US correlates with irreducibility but not definitely with bowel necrosis. Kong et al. (1997) have shown that 31 % of intussusceptions without detectable blood flow could be reduced by air enema in comparison to a 90 % reduction rate when flow was detectable. On the other hand, the presence of flow has been observed in an IT that had necrosis and perforation at surgery (Hanquinet et al. 1998) (Fig. 11).

None of the factors related with irreducibility contraindicate attempting a therapeutic enema although their presence does indicate a need for more precise handling and progressive pressures.

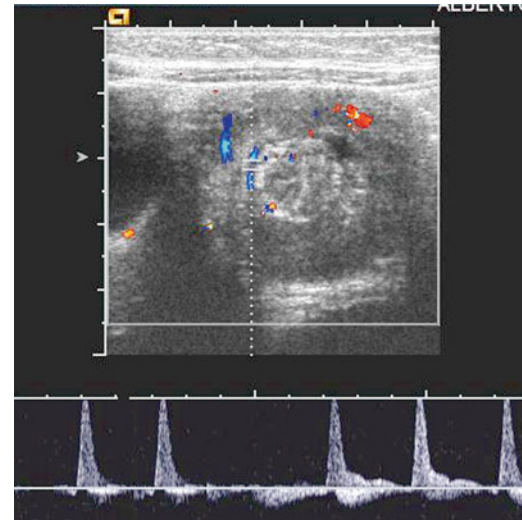

**Fig. 11** Intussusception with duplex Doppler sonography. Color Doppler indicates wall vascularity. High resistive index is observed in the vessels within the intussusception. This intussusception could be reduced

## 2.3 Small Bowel Intussusceptions and Intussusceptions Secondary to Lead Points

Nowadays, small bowel intussusceptions are more frequent and less severe than in early reports, probably due to the wider use of abdominal US and CT studies and the improvements in image quality (Navarro and Daneman 2004; Strouse et al. 2003). Most are asymptomatic, transient, and detected as an incidental finding, but they can also be seen in the context of predisposing diseases that affect the thickness and motility of the bowel wall such as viral infections, Henoch-Schönlein purpura, Peutz-Jeghers syndrome, celiac disease, postoperative abdominal surgery, and the presence of feeding tubes. The management of small bowel intussusceptions is different to that of ileocolic IT. This difference is important because they often resolve spontaneously, not requiring further imaging tests. They can be distinguished by their smaller size, with a mean diameter of 1.5 cm (range 1.1–2.5 cm) and length of 2.5 cm (range 1.5–6.0 cm), which contrast to those of ileocolic intussusceptions, which have a mean diameter of 3.7 cm and a mean length of 8.2 cm (Wiersma et al. 2006) (Fig. 12). Additional features include active peristalsis, atypical location (in the central abdominal region or in the left side of the abdomen), the presence of a homogeneous mesentery without lymph nodes, and, when identified, a normally free ileocecal valve. On the other hand, in the symptomatic patient with small bowel IT, US features that warrant closer monitoring and suggest surgical intervention include lack of peristalsis, a larger longitudinal diameter, trapped peritoneal fluid, small bowel obstruc-

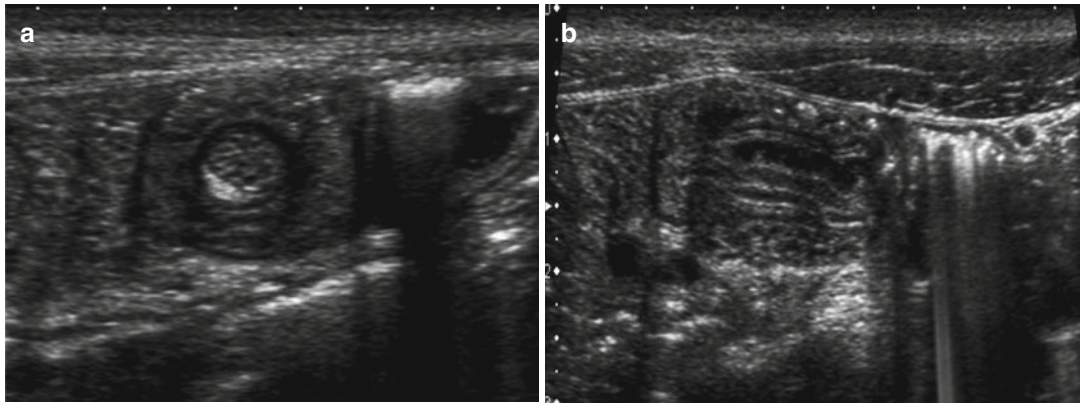


**Fig. 12** Small bowel intussusception. (**a**) Axial and (**b**) sagittal US scans showing a bowel-within-bowel appearance. In (**a**) small concentric ring image and the characteristic hyperechoic mesentery crescent is identified

tion, or the presence of lead points. In one series of patients with isolated small bowel IT, all cases in which the intussusceptum was shorter than 3.5 cm resolved spontaneously while the children who required surgery had a mean intussusceptum length of 7.3 cm (95 % CI 4.8–9.7 cm) (Munden et al. 2007). In ileoileal IT located near the ileocecal valve, a total or partial enema reduction may be attempted.

IT is secondary to a focal lead point (Meckel diverticulum, duplication cyst, polyp, or lymphoma) or a diffuse underlying abnormality (celiac disease, Henoch-Schönlein purpura, cystic fibrosis, enteritis, hemophilia, or Kawasaki syndrome) in less than 5 % of cases. Except for the neonatal period, the frequency of this type of IT increases with age and when there are recurrent episodes. The presence of lead points in an IT should be evaluated before taking a therapeutic approach. Contrast enema can reduce IT with lead points (63.6 %) that have been overlooked. The advantage of a US over a conventional contrast enema, which only depicts the bowel lumen, is the ability of the former to detect and characterize many of the lead points by analyzing the apex of the intussusceptum (66 % US versus 11 % air enema or 40 % contrast enema) (Miller et al. 1995; Navarro and Daneman 2004). An inverted Meckel diverticulum is the most common pathological lead point promoting an IT. It can be seen on US as a segment of blind-ending bowel, with a bulbous, elongated, or teardrop shape projecting for a variable distance from the apex of the intussusceptum. The central serosal surface may surround hyperechoic mesenteric fat or anechoic fluid appearing on axial US scans as a rounded shape at the center of the IT apex (Fig. 13). This appearance differentiates it from the eccentrically located crescent shape of the mesentery or the fluid trapped within the IT. Nevertheless, both images may coexist at different levels of the IT. IT due to lymphoma can be difficult to differentiate from the follicular lymphoid hyperplasia present in idiopathic IT, since a homogeneously hypoechoic thickening at the apex of the intussusceptum can be observed in both cases. A larger lesion and enlarged mesenteric lymph nodes are essential features in assessing a diagnosis of lymphoma, which is also supported by an age older than 3 years and longer duration of symptoms accompanied with weight loss. The partial or total reduction by enema could avoid an en bloc resection in selected cases (Fig. 14).

Although multiple recurrences may be a predictor of the presence of a lead point, most patients with a lead point will only have a single episode of IT. In consultation with the referring surgeon, image-guided reduction can also be attempted in those patients with focal lead points in whom surgery will eventually be required to remove the lead point. Nonoperative reduction may facilitate eventual surgery by diminishing the length of the IT and thus the amount of bowel manipulation required at surgery (Navarro and Daneman 2004).

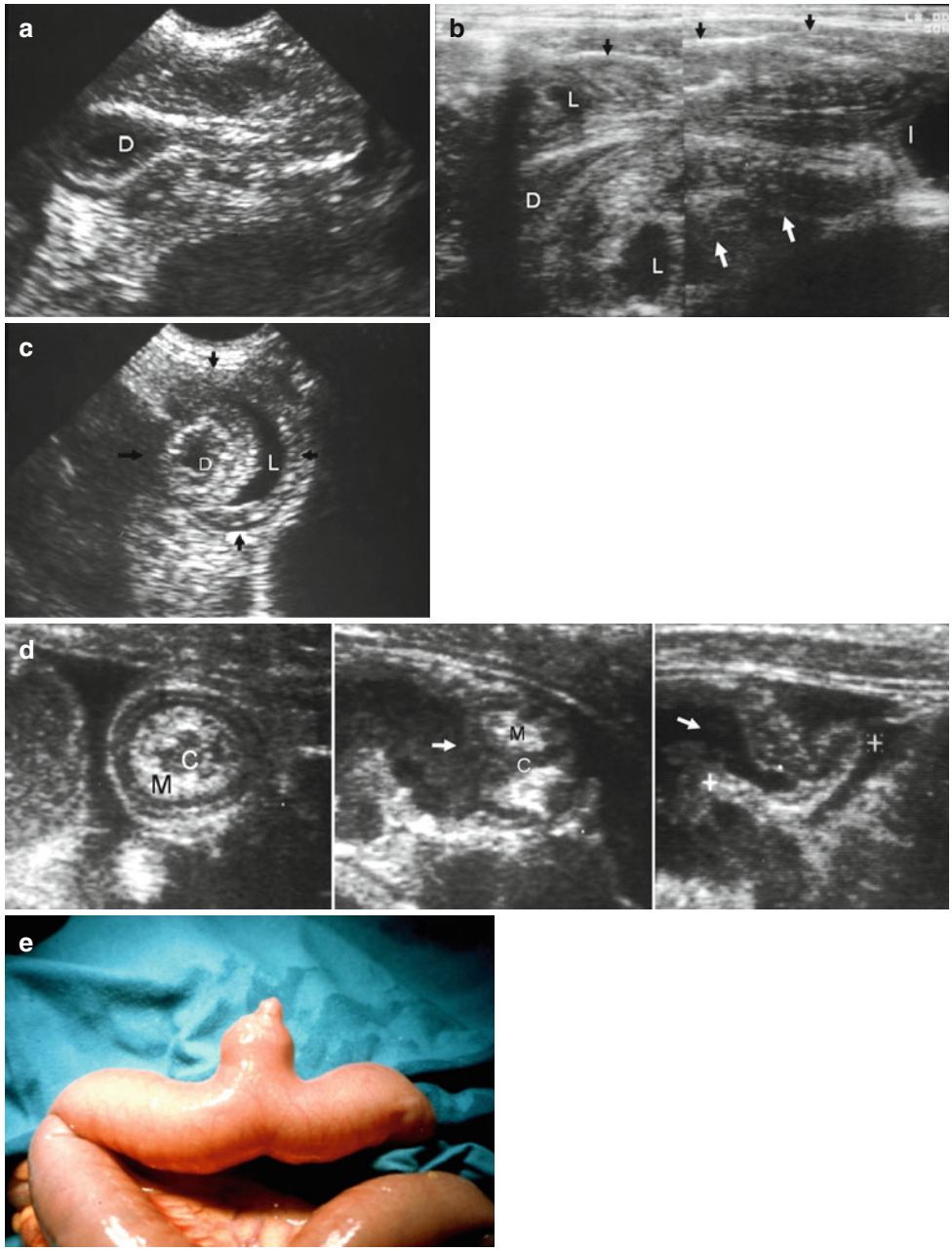


**Fig. 13** Intussusceptions secondary to Meckel diverticulum. *Case 1*: Longitudinal (**a**) (at the apex) and (**b**) and axial (**c**) US scans of an intussusception detected in the hypogastrium (*arrows*). Central sonolucent pyriform mass at the apex of the intussusceptum corresponding to inverted diverticulum (*D*). *L* trapped fluid in intussuscepted ileum. *I* proximal dilated ileum entering into the intussusception. US-guided saline enema demonstrated a normal ileocecal valve and a proximal ileoileal intussusception that was reduced (not showed), leaving a residual partially intussuscepted diverticulum that finally was also reduced (between calipers). (**d**) Sequence show partially intussuscepted diverticulum reduction: *M* Meckel diverticulum mesentery, C, central limb of the intussuscepted diverticulum. *Arrow*, saline enema. The enema (*arrow*) pushes the intussuscepted diverticulum. In the post-reduction view the saline enema fills the diverticulum (between calipers), which is finally surrounded by ascites. (**e**) Interval surgery was performed. *Case 2*: (**f**) Axial US and (**g**) in vitro (surgical specimen) US showing a central hyperechoic mesentery (*M*). Note that the trapped fluid (case 1) or the mesentery (*M*) (case 2) in the intussuscepted inverted diverticulum (*D*) adopts a central position and spherical morphology at the intussusceptions apex, unlike the crescent shape of the trapped peritoneal fluid in the intussusceptum (*L*)

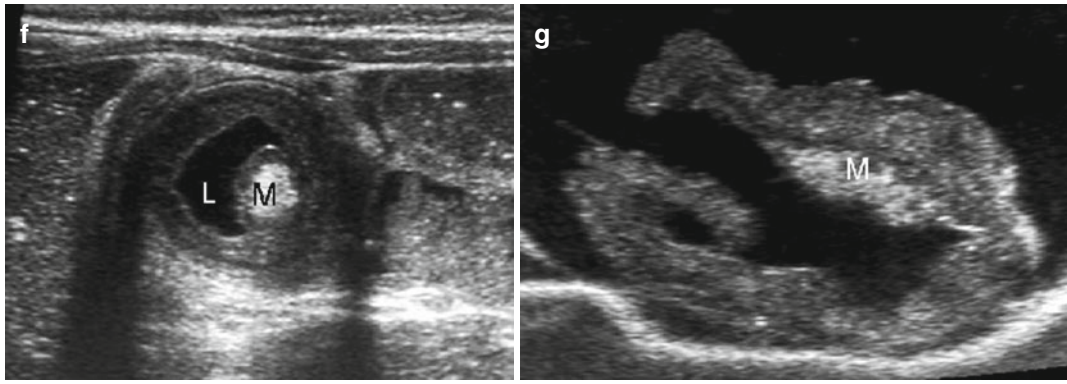


**Fig. 13** (continued)

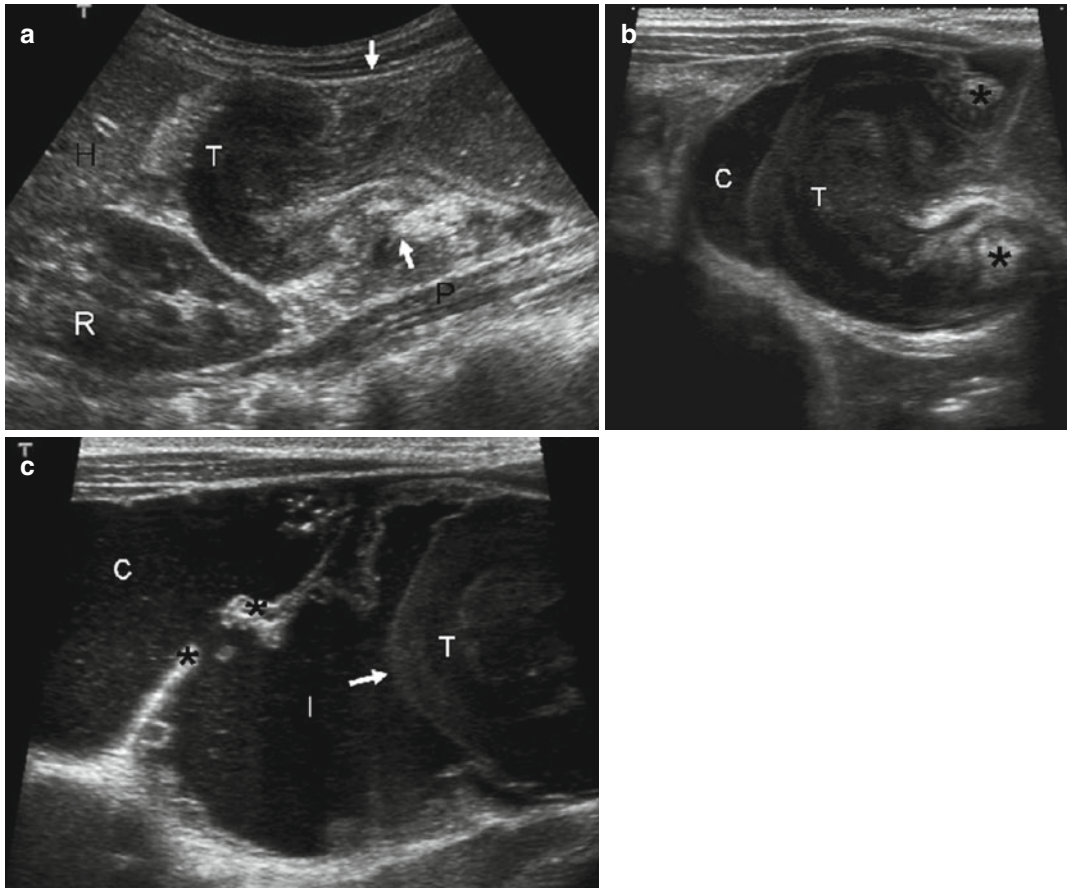


**Fig. 14** Ileocolic intussusception secondary to Burkitt lymphoma. (**a**) Longitudinal US scans show a hypoechoic mass (*T*) at the intussusception apex (*arrows*). (**b**, **c**) Sequential images of US-guided saline enema show partial reduction of the intussusception, leaving a residual ileoileal intussusception (*arrow*), which could not be reduced at surgery or in the pathological department. (**c**) Fluid enema passes from the cecum (*C*) into the ileum (*I*) leaving the ileocecal valve lip-free (*) (*T* tumor, *H* liver, *R* kidney, *P* psoas muscle)

## 2.4 Treatment

Enema therapy monitoring the reduction process in real time using contrast agents was standardized and popularized in the 1940s (Ravitch and McCune 1948), and it is accepted as the treatment of choice for the reduction of ileocolic intussusceptions. Currently, several techniques are performed using hydrostatic (contrast or saline) or pneumatic (air) enema, under either sonographic or fluoroscopic guidance.

There is continuing discussion without general agreement about which type of enema is the best to reduce an IT. In the absence of large series and the conflicting results of two randomized studies (Meyer et al. 1993; Hadidi and El Shal 1999), the reported differences in reduction and perforation rates are more probably related to the complications that occurred before enema therapy, the intracolonic pressures employed, and the patient selection criteria for direct surgery, than to the type of enema used. These factors have changed at different institutions and countries through time over the history of IT therapy. The different published series have not assessed these factors, hampering the possibility of an objective comparison between series. Reduction rates can be low in complicated IT cases. Applying a higher pressure can increase the reduction rate. Lastly, a selective election of patients going directly to surgery may indirectly increase the reduction rate of enema therapy by avoiding complicated intussusceptions. In fact, a recent study from a large US database containing records for over 3 million pediatric admissions reported a national average of 85 % rate of successful radiological reduction, but interestingly also showed a high rate of patients that went directly to surgery, indicating how surgery could be indirectly related with high enema reduction rates. Rates of surgical intervention varied from 61 % at children's hospitals to 74 % at general hospitals (Jen and Shew 2009).

### 2.4.1 Technical Factors

The goal of any type of enema therapy is to reduce the IT by exerting pressure on the apex of the intussusceptum and push it from the pathologic position back to the original position. The reduction and perforation rates for a specific type of enema therapy are directly proportional to the pressure applied. Ravitch (1986) found that the intracolonic pressure achieved by placing the barium enema bag 3.5 ft (105 cm) above the table did not reduce any IT in which the intestine was necrotic or incarcerated. Further studies found that a pressure that did not exceed 120 mmHg for hydrostatic enemas and 108 mmHg for air enemas did not perforate the colon in animals (Shiels et al. 1993). Pressure can be controlled by measuring the height of the bag containing the fluid for a hydrostatic enema or using a manometer for an air enema. A pressure of 120 mmHg is equivalent to a 100-cm column of barium or a 150-cm column of water or water-soluble contrast material (Kuta and Benator 1990). This theoretical pressure is reached during liquid enema therapy only if the diameter of the tubing of the system is large enough to easily transmit the pressure. In hydrostatic enema therapy, the use of a rectal tube of large caliber may be more effective in increasing the actual intracolonic pressure than the use of an increased column height (Schmitz-Rode et al. 1991). According to some experimental studies, the likelihood of perforation is smaller with the use of liquid compared to air enemas, because the intraluminal pressure is more constant than that exerted during air insufflation, which tends to produce oscillations that can surpass the pressure threshold (Zambuto et al. 1995). However, the perforations demonstrated by air enema are small compared with those demonstrated by liquid enema, which produces larger colonic tears and greater peritoneal contamination (Shiels et al. 1993; Daneman et al. 1995).

There is no agreement on the number and duration of reduction attempts, the efficacy of premedication or sedation, the use of rectal tubes with inflatable retention balloons, or the use of transabdominal manipulation (Meyer 1992; Katz and Kolm 1992). This lack of agreement reflects the fact that no large studies have demonstrated a definite improvement in the reduction rate with any of these factors. According to the classic "rule of threes," the barium bag is suspended 3 ft above the examination table and three attempts over a maximum of 3 min are performed for reduction. This rule has been discarded at some institutions, and some authors even use delayed attempts, that is,

they repeat the reduction attempt after the patient rests for a time interval that varies from 30 min up to several hours. Delayed attempts in previously partially reduced IT may be successful in up to 50 % of cases, improving the reduction rate (Gonzalez-Spinola et al. 1999; Navarro et al. 2004). Use of US guidance permits an even more liberal approach to enema therapy due to the lack of radiation exposure. Use of sedation may improve the reduction rate (Ilivitzki et al. 2012). However, sedation prevents the patient from performing the Valsalva maneuver during straining. This maneuver increases the intraluminal pressure (by approximately 60 mmHg) and decreases the intracolonic/extracolonic pressure gradient, improving the effectiveness of enema therapy and protecting against perforation, particularly during air enema therapy (Shiels et al. 1993; Bramson et al. 1997). These pressure effects may also be increased by placing the patient in a prone position. Use of a rectal balloon catheter is not a universal practice. It may increase the speed and effectiveness of enema therapy, creating a closed system that transmits the pressure of the enema material (liquid or air) without leaking. It works in the same way as securely taping the catheter to the patient's buttocks with abundant tape (Applegate 2009). One critical safety issue is that the balloon must be inflated gently and progressively in order to prevent mucosal ischemia in the rectum.

### 2.4.2 Types of Enema Therapies

In any type of enema, before attempting the reduction, the patient should be stabilized, and the surgical team should be notified because of the risk of perforation and the possibility of subsequent surgical intervention if enema reduction fails. Successful reduction is indicated by the free flow of contrast or air into the small bowel, and it is usually accompanied by a clinical resolution of symptoms. After successful reduction of an IT, the patient has an increased risk of developing recurrent IT in the near future, so the child should be observed in the hospital for 12–24 h.

Barium enema has been validated as a simple, safe, and efficacious therapy by extensive experience over a long period (Fig. 9). It remains the most commonly employed therapy among general radiologists and in institutions that deal with few IT cases per year. However, there is a continued tendency to replace barium with other contrast agents, because of sequelae (granulomas, adhesions, loculated ascites) if perforation occurs during barium enema therapy (Bramson and Blickman 1992; Meyer 1992). Water-soluble agents reduce the risk of electrolyte disturbances and chemical peritonitis in patients in whom perforation occurs. On the other hand, hypertonic ionic water-soluble agents may induce rapid fluid shifts and should be diluted to iso-osmolar concentrations, which will still allow appropriate anatomical delineation (Daneman and Navarro 2004).

Air enema therapy under fluoroscopy is now very popular (Guo et al. 1986; Shiels et al. 1991; Daneman and Navarro 2004), being the current standardized method for IT reduction in North America. This method is quick and clean with a high reduction rate (73–95 %) and less radiation exposure than the barium enema therapy. The decreased radiation exposure is related to the shortened time required to achieve reduction and the milder radiographic technique used. The average dose to reduce an IT by air enema under fluoroscopy is roughly estimated as 2,567 mRads (Henrikson et al. 2003). Reduction is considered complete only when a good portion of the distal ileum is filled with air, which also excludes the possibility of an ileoileal IT (Fig. 15). A disadvantage of the pneumatic technique under fluoroscopy is seen in patients with marked amounts of air in the small bowel proximal to the IT before the enema is performed. In these patients, it may be more difficult to visualize both the IT and the reduction because of the multiple air-filled loops. Occasionally, the passage of air into the terminal ileum without complete reduction of the ileocolic IT can be erroneously interpreted as a complete successful reduction (Daneman and Navarro 2004). The pneumatic reduction technique provides an advantage if perforation occurs, because air is generally less harmful in the peritoneal cavity than other contrast materials, as mentioned above. Air enema therapy requires precise control of the threshold pressure and a thorough knowledge of the technique and potential complications. Immediate paracentesis using a large-caliber needle may be necessary if tension pneumoperitoneum is produced secondary to

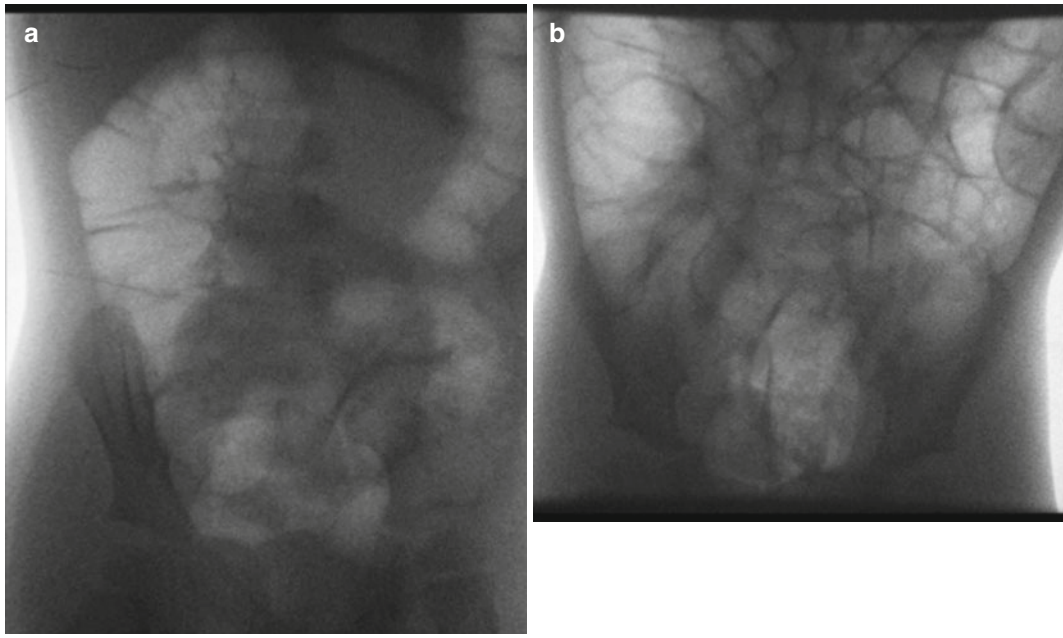


**Fig. 15** Air enema intussusception reduction. (**a**) Image obtained at the beginning of the reduction with soft tissue mass seen in the ascending colon. (**b**) Image obtained just after complete reduction showing air distention of multiple loops of small bowel

perforation (Kirks 1994). The advantages and disadvantages of air enema therapy under fluoroscopy are summarized in Table 2.

The most important studies of US guidance of IT reduction have been performed in Asian countries and Europe (Woo et al. 1992; Rohrschneider and Tröger 1995). The procedure is usually performed with a warm saline solution, but several other fluids can be used (Fig. 16). Studies have shown a high reduction rate (76–95.5 %) with few complications (0.17 %) (Bai et al. 2006). The primary advantage of this technique is the lack of radiation exposure. As a result, there is no limit to either the procedure time or the number of attempts, something that improves the success rate, though it may prolong the process (Gonzalez-Spinola et al. 1999). US has a high accuracy and reliability for monitoring the reduction process and for the visualization of all components of the IT, with easy recognition of pathological lead points (Figs. 13 and 14) and residual intussusceptions (Fig. 17), when they exist. To easily visualize the reduction process on a US-guided enema, the pressure can be progressively increased from 60 to 120 mmHg by raising the saline bag. Disappearance of the crescent-in-donut sign and visualization of fluid refluxing through the free ileocecal valve are proof of a successful reduction (del- Pozo 2005). The axial tracing over the thickened terminal ileum from the ileocecal valve up until it has a normal thickness, the passage of abundant fluid into the ileal loops, and the reestablishment of the antegrade

**Table 2** Advantages and disadvantages of the air enema technique for reduction of intussusception

| |
|---|
| *Advantages* |
| Excellent results (70–95.6 % of cases) |
| Less exposure to radiation than with contrast enema |
| Easy, quick, and clean technique |
| *Disadvantages* |
| X-ray exposure required thus limiting procedure time |
| Risk of tension pneumoperitoneum |
| Visualization limited to intraluminal content |
| Less control of residual ileoileal intussusceptions |

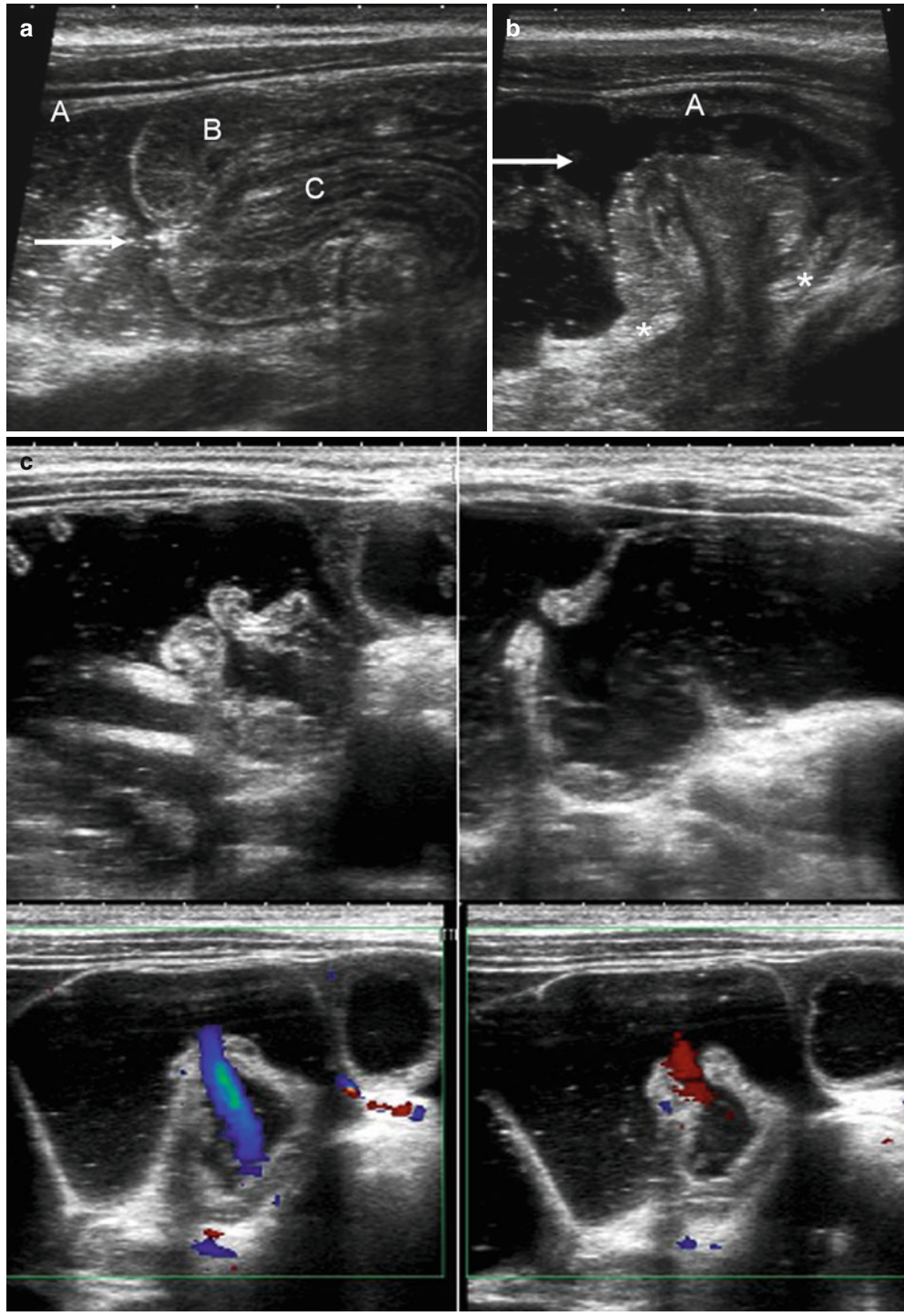


**Fig. 16** Reduction of an ileocolic intussusception with sonographically guided saline enema. (**a**) The fluid in the colon (*arrow*) outlines the intussusceptum in the ascending colon. This is the sonographic equivalent of the meniscus sign. (**b**) The enema pushes the intussusceptum into the ileocecal valve (*asterisks*), which eventually passes through the valve. (**c**) Serial images of the free ileocecal valve after intussusception reduction (four sequences: closed, open, with retrograde and anterograde passage of fluid depicted on color Doppler US) (*A* intussuscipiens, *B* returning limb of the intussusceptum, *C* entering limb of the intussusceptum)

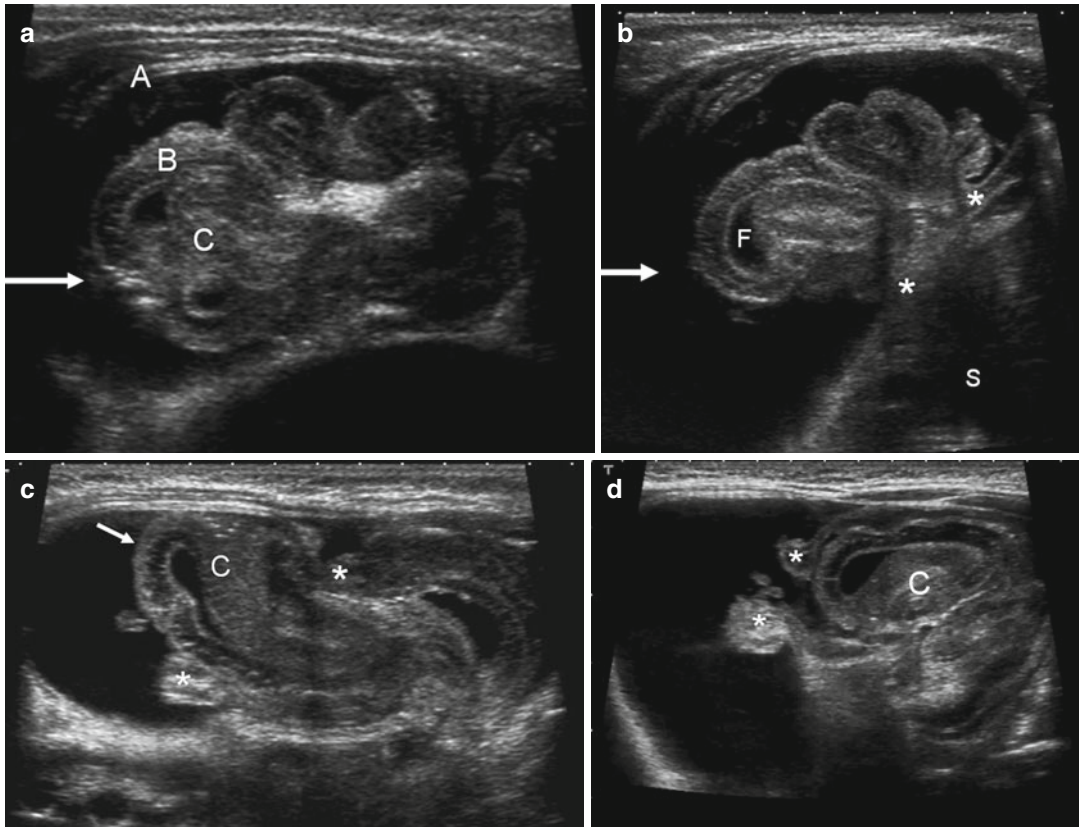


**Fig. 17** Reduction with sonographically guided saline enema of an intussusception in two attempts (ileoileal residual). (**a**) The fluid in the colon (*arrow*) outlines the intussusceptum in the ascending colon. (**b**) The enema pushes the intussusceptum into the ileocecal valve (*asterisks*) and finally in (**c**) can be seen passing through the valve. Image (**d**) shows a residual ileoileal intussusception that finally could also be reduced (*S* sigmoid colon, *F* trapped peritoneal fluid within the intussusceptum, *A* intussuscipiens, *B* returning limb of the intussusceptum, *C* entering limb of the intussusceptum)

flow through the ileocecal valve verified on Doppler US help to exclude the presence of residual ileoileal IT (Fig. 18). Perforation is easily recognized when fluid inside the colon suddenly decreases while substantial amounts of free fluid appear in the peritoneal cavity (Wang and Liu 1988; Hadidi et al. 1999) with increasing echogenicity. The main potential disadvantage of US is the need for a radiologist who is comfortable with this modality for enema guidance and is available on a 24-h basis. However, because of the widespread support for use of US for IT diagnosis, its use to guide enema therapy has also been increasingly advised: "We, as pediatric radiologists, should familiarize ourselves with this technique to conform to the ALARA (as low as reasonably achievable) principle of radiation exposure in our practice" (Khanna and Applegate 2008). The procedure should be attempted at any hospital with a surgical team and can present a benefit with respect to the risk of delaying patient transfer to another center, since even partial reductions may improve the outcome at a tertiary hospital. The advantages and disadvantages of US-guided saline enema therapy are summarized in Table 3.

US-guided air enema therapy attempts to unite the advantages of air enema therapy (a quick and clean method with high reduction rate) and those of US guidance (no radiation exposure). There has been little experience with this modality, probably because the excellent sonographic visualization of fluid is markedly reduced by the reverberation artifacts from the insufflated

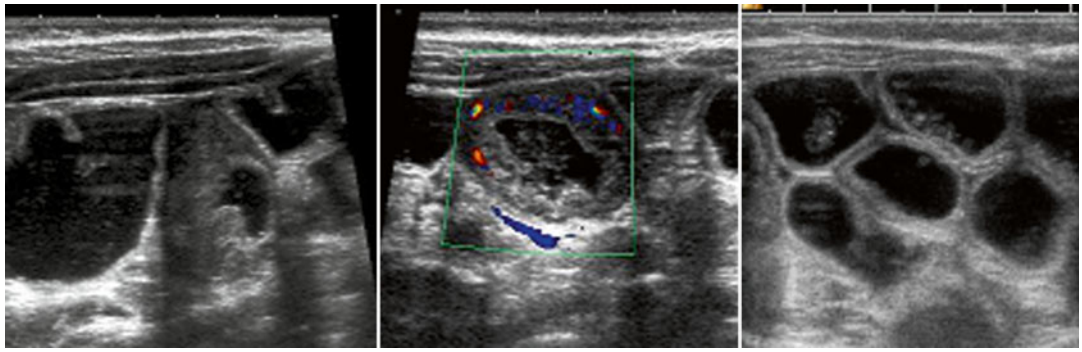

**Fig. 18** US findings after successful US-guided enema reduction. The sequence shows asymmetrical thickening of the terminal ileum wall in the area in which the intussusceptum was folded; postischemic bowel wall increased flow and multiple bowel loops filled with fluid verifying the complete reduction

**Table 3** Advantages and disadvantages of US-guided saline enema technique for intussusception reduction

| |
|---|
| *Advantages* |
| No X-ray exposure, thus procedure time is not limited |
| Excellent results (76–95.5 % of cases) |
| Visualization of all the components of the intussusception |
| Easier recognition of lead points and residual intussusceptions |
| Low perforation rate (0.26 %) |
| *Disadvantages* |
| Less clean technique |

air (Ko et al. 2007). Despite that, good results have been reported. Adequate visualization of the ileocecal valve and demonstration of an abrupt transition between the edematous terminal ileum and the proximal normal ileal loop, visible on the scan along the long axis of the ileum, are reliable signs of successful reduction. Detection of perforation with pneumoperitoneum has been also reported (Gu et al. 2000; Yoon et al. 2001). However, small residual ileoileal intussusceptions may be obscured by the presence of large amounts of intraluminal air, and this could also interfere with a subsequent US study, if required.

### 2.4.3 Complications

Untreated IT evolves to small bowel obstruction followed by perforation, peritonitis, and septic shock. The overall mean perforation rate in developed countries is lower than 1 %. Perforation may already have occurred before enema therapy or may occur during the reduction process. In the latter case, perforation has been reported in both ischemic and normal bowel segments. As far as we know, pneumoperitoneum has not been reported in childhood IT before enema therapy, probably because perforations are covered or located distal to the obstructive point. Perforations may occur in the gangrenous ileum (the intussusceptum) or in the overdistended colon (the intussuscipiens) (Mitra et al. 1982). In the former case the perforation is covered by the intussuscipiens, which does not allow air to escape into the peritoneal cavity; in the latter, the edematous intussuscepted ileum prevents the exit of the proximal intestinal air through the colonic perforation.

IT recurrence rates average 10 % (4–19 %) after enema reduction and 1–3 % after surgery. If nonsurgical reduction fails, it should be attempted again, since most recurrences occur in idiopathic intussusceptions (77–100 %) (Navarro and Daneman 2004). However, one should be aware of the increased frequency of the lead points in recurrent IT episodes. Some authors recommend performing stool culture in recurrent cases (Dugougeat et al. 2000). Treatment with glucocorticoids has been suggested to prevent recurrence when the only imaging finding is ileal lymphoid hyperplasia (Lin et al. 2000). Rarely, IT complications can include bacteremia and delayed hypovolemic shock caused by a possible third-space fluid loss within the lumen of the intestinal loops.

In conclusion, plain radiography is of limited value in the diagnosis of IT. US, an accurate and safe modality, may predict reducibility, detect lead points, and permit alternative diagnoses. Nonsurgical treatment of IT is possible in most cases. Pneumatic reduction under fluoroscopic guidance and hydrostatic reduction under US monitoring are the preferred techniques. The reported differences in reduction and perforation rates are probably due more to complications that occurred before enema therapy, the pressures exerted, and the patient selection criteria than to the type of enema used. However, air enema may produce higher intraluminal pressures that result in higher reduction rates. Liquid agents appear to cause fewer perforations, but if they occur they are larger and more harmful than with air. Use of US guidance eliminates the drawback of radiation exposure, thus allowing a greater number of attempts.

## 3 Appendicitis

Acute appendicitis is the most common reason for emergency abdominal surgery in children. Appendicitis occurs in all age groups but has a higher incidence in children between 5 and 15 years old. Epidemiologic studies reveal that lifetime risk of appendicitis is 8.6 % for males and 6.7 % for females. Appendectomy lifetime risk before the pediatric imaging advances was 12.0 % for males and 23.1 % for females (Addiss et al. 1990). In the last several decades, both the diagnosis and management of appendicitis as well as pediatric imaging and laparoscopy have all undergone significant improvements (Pepper et al. 2012).

Appendicitis pathogenesis is conditioned by the specific "cul-de-sac" anatomy of the appendix, which is prone to develop ectasia, fecalith formation, obstruction, and/or infection followed by ischemia, necrosis, and perforation (Gray and Ashley 1986). Diagnosis is based on clinical symptoms including periumbilical pain that migrates to the right lower quadrant (RLQ), anorexia, nausea, vomiting, low-grade fever, McBurney's point tenderness, and leukocytosis. Nevertheless, more than 30 % of cases of appendicitis have atypical clinical presentations (Lewis et al. 1975), and this is more frequent in small children and cases of unusual appendiceal location. This is a possible explanation for why there is a higher prevalence of ruptured appendicitis in children (30–74 % of cases) (Williams et al. 2009). In addition, the clinical presentation of many nonsurgical conditions of abdominal pain may mimic those of acute appendicitis. In fact most of the children with suspected appendicitis do not have it. Cross-sectional imaging has contributed to reduce both unnecessary laparotomies and the complications caused by delayed or wrong diagnoses (Ooms et al. 1991; Kosloske et al. 2004). Early surgical intervention in patients with acute appendicitis prevents appendiceal perforation, which is associated with increased morbidity and mortality. Surgical findings of appendiceal disruption and pus or feces in the abdominal cavity indicate perforated appendicitis (Ooms et al. 1991). Pathological diagnosis determines the grade of parietal polymorphonuclear infiltration and necrosis, differentiating between catarrhal, phlegmonous, suppurative, or gangrenous appendicitis (Cotran et al. 1989).

### 3.1 Appendicitis Imaging

Plain abdominal radiographs are of limited value, no longer being used as the first imaging test. More than 50 % are normal, and when positive, radiological findings consist in perforation, making them useless for early diagnosis (Johnson and Coughlin 1989). Moreover, it adds unnecessary cost and ionizing radiation. The presence of an appendicolith is the only specific sign of appendicitis, but it is only detected in 10 % of cases. When this finding is associated with abdominal pain, the chance of having appendicitis is 90 %, and at least 50 % of these patients already have a perforated or gangrenous appendicitis (Holgersen and Stanley-Brown 1971).

US is a widely available, accurate, and inexpensive imaging modality in suspected acute appendicitis with a reported pooled sensitivity and specificity of 88 % and 94 %, respectively (Doria et al. 2006). US accuracy rate varies widely between European and American published series (Holscher and Heij 2009). In an

acute abdominal pain setting, US is an interactive technique with higher accuracy when performed by a pediatric radiologist who integrates both clinical and imaging findings than when images, usually limited to the RLQ, are taken by a sonographer and then interpreted by a pediatric radiologist. The usefulness of US lies in establishing the diagnosis of appendicitis in children with equivocal clinical findings and aiding to detect other abdominal or pelvic conditions that may mimic appendicitis. However, the prevalence of disease in a patient population affects the positive predictive value of a test. When disease prevalence is low, false-positive rates increase (van Randen et al. 2008). With heavy reliance on CT, patients undergoing US for evaluation of appendicitis are often patients in whom the suspicion for the disorder is low or patients with an atypical presentation, mimicking other processes. In addition, when prevalence is low, sonographers and radiologists, not having seen the "classic" appendicitis cases, may lose diagnostic skills over time (Strouse 2010). Furthermore, US is an operator-dependent technique that requires more effort and time to achieve a negative diagnosis than a positive one, since all sorts of transducers and approaches must be tested; this is why US sensitivity usually decreases with the decreased prevalence of the disease. US operators can feel like frustrated fishermen and a "cry wolf" effect may occur, leading to discouragement in following studies that could misdiagnose an actual appendicitis. Therefore, high US accuracy depends on appropriate screening by the surgical team.

The graded compression US technique described by Puylaert (1986) is helpful in positioning the appendix into the most focused area of the ultrasonographic beam and in displacing and compressing bowel loops, but this is not always required in children. In fact, compression can increase the pain making proper US examination that much more difficult. High-resolution transducers (5 and 15 MHz), knowledge of RLQ anatomy, experience, and patience are desirable. The peritoneal cavity is screened to detect bowel pathology with five or six vertically orientated, overlapping lanes using a broad-based probe. Puylaert (2003) refers to this as "mowing the lawn." When the child can cooperate by pointing to the area with maximum tenderness, it should be chosen as the starting point for imaging, because it is often the site of the inflamed appendix (Cogley et al. 2012). Normal appendix can be identified by US in more than 80 % of asymptomatic patients (Rioux 1992; Wiersma et al. 2005). It may be visualized as a tubular, mobile, and blind-ended structure. The traditionally accepted upper limit diameter of 6 mm or less (Jeffrey et al. 1988; Vignault et al. 1990) has recently been suggested to be closer to 7 mm (Goldin et al. 2011). Anteroposterior diameter should be measured perpendicular to the longitudinal appendiceal axis on a sagittal scan, avoiding potential overestimation resulting from an oblique axial scan ("bezel effect") or an ovoid axial appendiceal shape. In children, there is significant overlap of diameters between normal and pathological appendices (Rettenbacher et al. 2001; Goldin et al. 2011; Simonovský 2001). Increased size is therefore not a reliable isolated criterion for appendicitis diagnosis. Normal appendices can measure more than 6 mm either due to fecal material within the lumen (Simonovský 1999) or to follicular lymphoid hyperplasia of the mucosal layer. In fact, more than half of negative appendectomies with US diameters of over 6 mm ($7 \pm 13$ mm) that were confirmed by the pathologist have been reported to be due to lymphoid hyperplasia in the appendix wall (Hahn et al. 1998). Similarly, and although this is difficult to measure, using either an appendiceal wall thickness <3 mm as normal (Simonovský 2002) or >1.7 mm as an appendicitis criterion (Goldin et al. 2011) has limited value, since the wall is thinned in dilated obstructed appendices. Analysis of morphological criteria may add enough information to avoid the limitation of the nonspecific numerical criteria for appendicitis diagnosis.

The normal appendix has five concentric alternating hyperechoic and hypoechoic layers just like any intestinal bowel loop. From inside to outside we can recognize the hyperechoic mucosal surface, hypoechoic mucosa, hyperechoic submucosa (due to vessels, connective tissue, and fat content), hypoechoic muscular, and hyperechoic serosa layers (Kimmey et al. 1989) (Fig. 19). Basically, the intestinal bowel wall is a hypoechoic structure limited by two hyperechoic surfaces

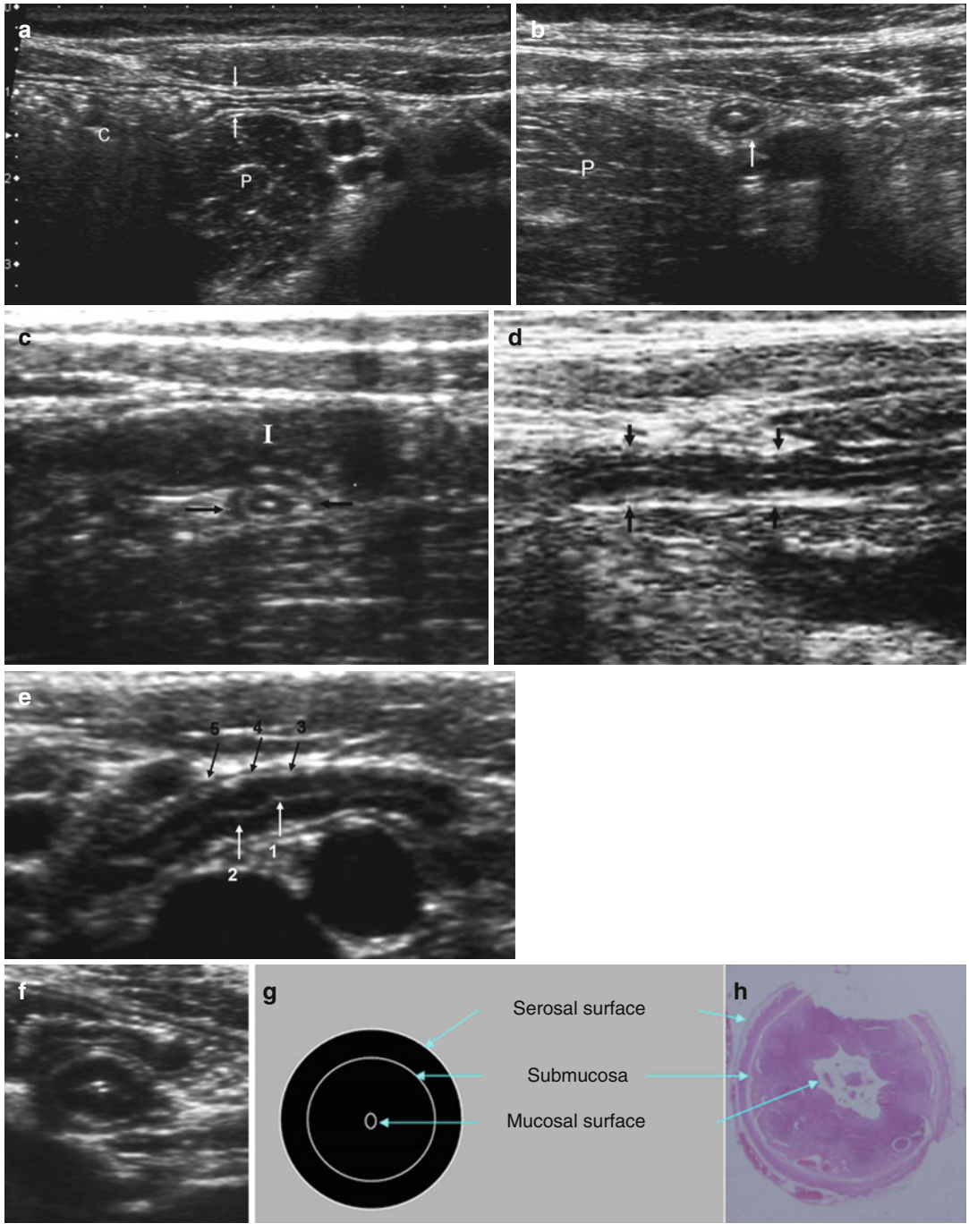


**Fig. 19** Normal appendix: spectrum of appearances. (**a**) Longitudinal and (**b**) axial (tiny intraluminal air) appendiceal views of the normal appendix (*P* psoas muscle, *C* cecum). (**c**) Axial scan of the rounded proximal part of a normal appendix (*arrow*) behind the terminal ileum (*I*).“Target” appearance with preserved concentric layers of “gut signature.” (**d**, **e**) Longitudinal sections of normal appendices (*arrows*) showing five layers that are alternately hyperechoic and hypoechoic from inner to outer: hyperechoic mucosal surface (*1*), hypoechoic mucosa (*2*), thin hyperechoic submucosa (*3*), hypoechoic muscular (*4*), and hyperechoic serosa (*5*). The hypoechogenicity of the mucosa corresponds to the follicular lymphoid tissue of the mucosal lamina propria, the most prominent layer of the normal appendix in children. (**f**–**h**) Collapsed appendix with associated cross-sectional diagram and histological specimen shows the hyperechoic appendiceal layers as three concentric rings. The histological specimen demonstrates lymphoid hyperplasia

(serosa and mucosa) and crossed by another hyperechoic line: the submucosa. The mucosa is the thickest and most prominent layer of the normal appendix in children. Its hypoechogenicity is due to the presence of follicular lymphoid tissue of the mucosal lamina propria (Spear et al. 1992).

Several patterns of appendicitis based on "in vitro" US-pathological correlations (del Pozo et al. 1994) and appendiceal anatomic considerations (Spear et al. 1992; Borushok et al. 1990) have been described depending on whether the appendiceal lumen is dilated or not as well as the appearance of the appendiceal submucosal layer (thin, thicker, or lost). Appendicular patterns help to differentiate normal from pathological appendix regardless of its diameter and both of them from the normal terminal ileum. Distinctive axial US patterns of appendicitis have been systematized as thin rings or three/two/one ring. Each of the three rings correlates to one of the hyperechoic appendiceal layers, from inner to outer: mucosal surface, submucosa, and serosa layers. Like a countdown, the progressive loss of those rings leads to perforation (three rings, two rings, one ring, perforation) (Fig. 20).

In early appendicitis, the appendiceal lumen may be collapsed or dilated. On axial US scans, when the appendix is obstructed, distal dilatation and thinned appendiceal wall are seen. The usually hypoechoic luminal content expands the layers of the appendiceal wall giving a thin-ring pattern (Fig. 21). When the appendix is collapsed, the transmural inflammation stresses the concentric layered appearance. The relative mucosal predominance of the normal appendix changes to a submucosal predominance, giving a three-ring pattern (Fig. 22a, b). Submucosal thickness, described in children under 14 years old as an appendicitis finding (del Pozo et al. 1994), may be a normal finding in appendices of older children and adults, probably related to the submucosal fat content (Kimmey et al. 1989). In the more

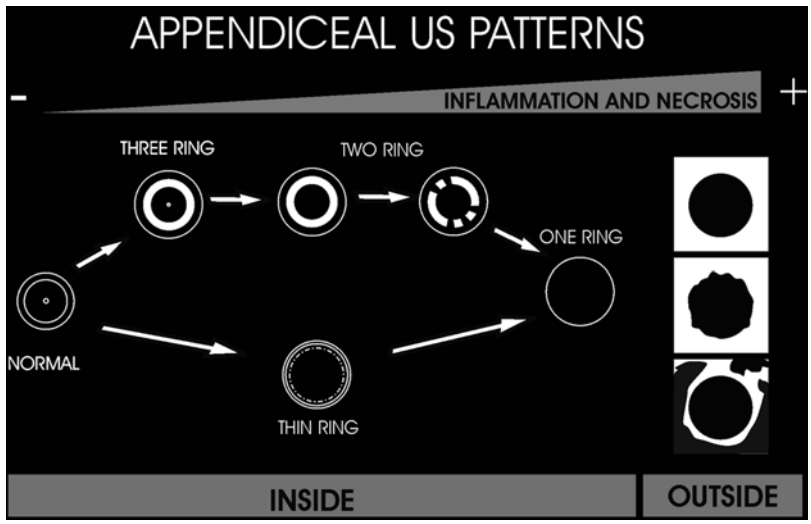


**Fig. 20** The illustration represents US axial slides of the appendix. The hyperechoic layers (rings) correspond to the mucosal surface (MS), submucosa (SB), and serosa layers (SE). These rings gradually disappear as the inflammation progresses, from inner to outer. Normal appendix: AP diameter ≤ than 6 mm, mucosal predominance. Three-ring pattern: AP diameter > than 6 mm, collapsed lumen, and submucosal prominence. Thin-ring pattern: AP diameter > than 6 mm, dilated lumen, thinned wall. and patent SB and SE with subtle mucosal surface. Two-ring pattern: non-visible central spot or inner ring (*MS*). The appendiceal center may represent either the inflamed mucosa or hypoechoic content. Both the submucosa and serosa are preserved. One-ring pattern: Appendix homogeneously hypoechoic. Only the serosal layer is preserved. Mucosal and submucosal layers are non-visible. Outside the appendix, as inflammation increases, prominence of Periappendiceal fat, appendicular contour irregularity, and, finally, presence of loculated collections or echogenic ascites are observed. Like in a countdown, the progressive loss of those rings leads to perforation (3–2–1–perforation) (From reference del Pozo (1994))

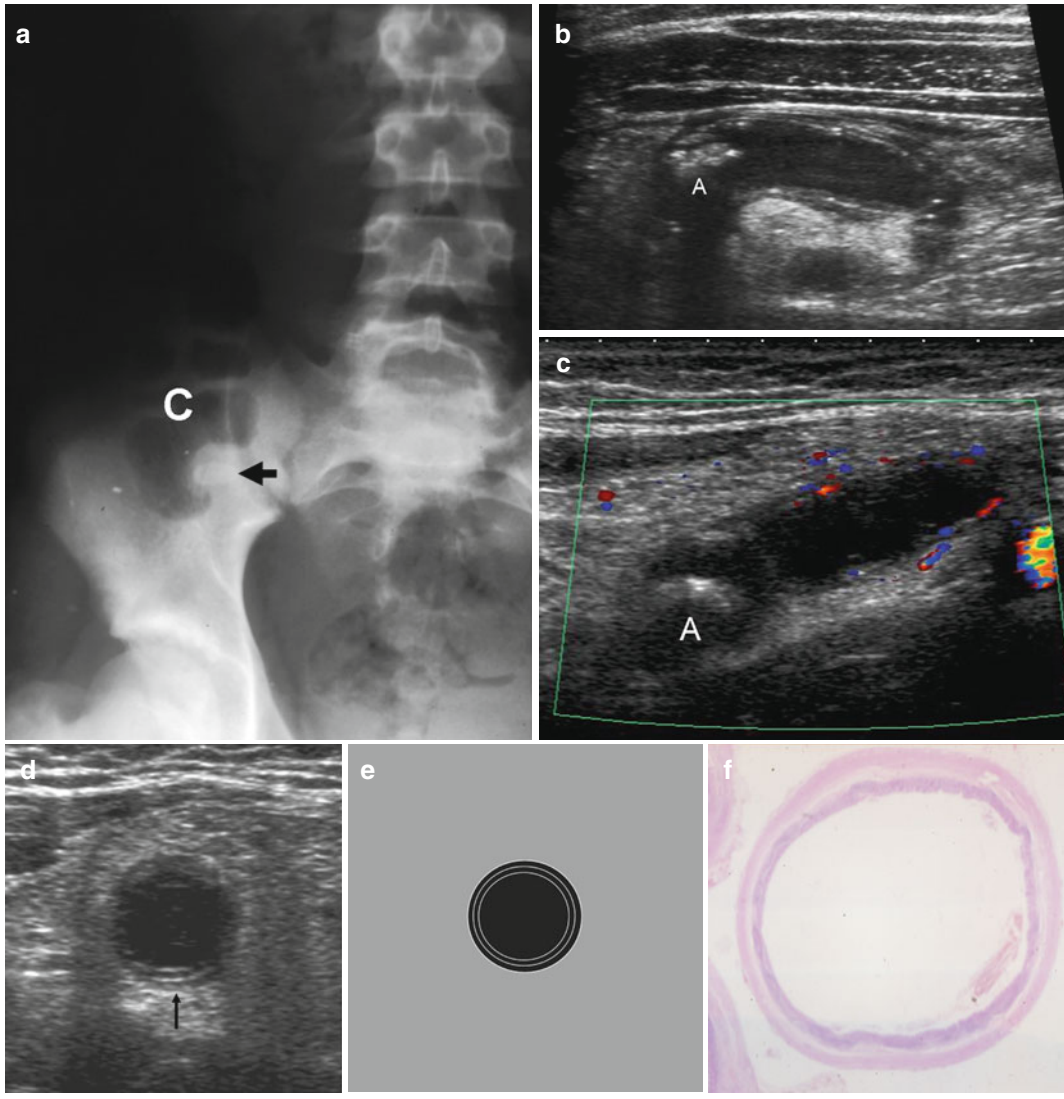


**Fig. 21** Obstructive appendicitis. (**a**) Plain abdominal radiograph showing an appendicolith (*arrow*) indenting the cecal lumen (*C*). (**b**, **c**) Longitudinal US and Doppler US scans show typical obstructive appendicitis produced by an appendicolith (*A*) causing distal appendiceal dilatation (*arrows*). (**d**) Axial US scan shows how the purulent luminal content expands the five layers of the appendiceal wall producing a thin concentric ring pattern (*arrow*). (**e**) Diagram showing the thin-ring pattern. (**f**) Histological specimen shows a dilated appendix

**Fig. 22** Patterns of appendicitis with the lumen collapsed: axial US scans, diagrams, "in vitro" axial US scan, and histological specimen. Early appendicitis. (**a**) Axial US and (**b**) diagram showing a three-ring pattern. The three hyperechoic rings represent the mucosal surface, the thickened submucosa (*SB*), and the serosa (*S*) layers. The relative mucosal predominance of the normal appendix changes to a submucosal predominance. Advanced appendicitis. (**c**) Axial US and (**d**) diagram showing a two-ring pattern. Notice the preserved SM and S layers and the associated prominent Periappendiceal fat. The central ring or "spot" that represents the mucosal surface cannot be identified. (**e**) Axial US and (**f**) diagram showing a one-ring pattern corresponding to the serosa (*arrows*). Note the thickened omentum (*O*) and the intraperitoneal echogenic free fluid (*A*). The appendix appears homogeneously hypoechoic due to the loss of the submucosa hyperechogenicity. (**g**) "In vitro" axial US scan of appendicitis showing a two-ring pattern: hyperechoic submucosa (SM) and serosa (*S*) (*MA* hyperechoic mesoappendix, *M* muscular, *m* mucosa). (**h**) The specimen corroborates US findings showing inflamed appendix with the lumen collapsed

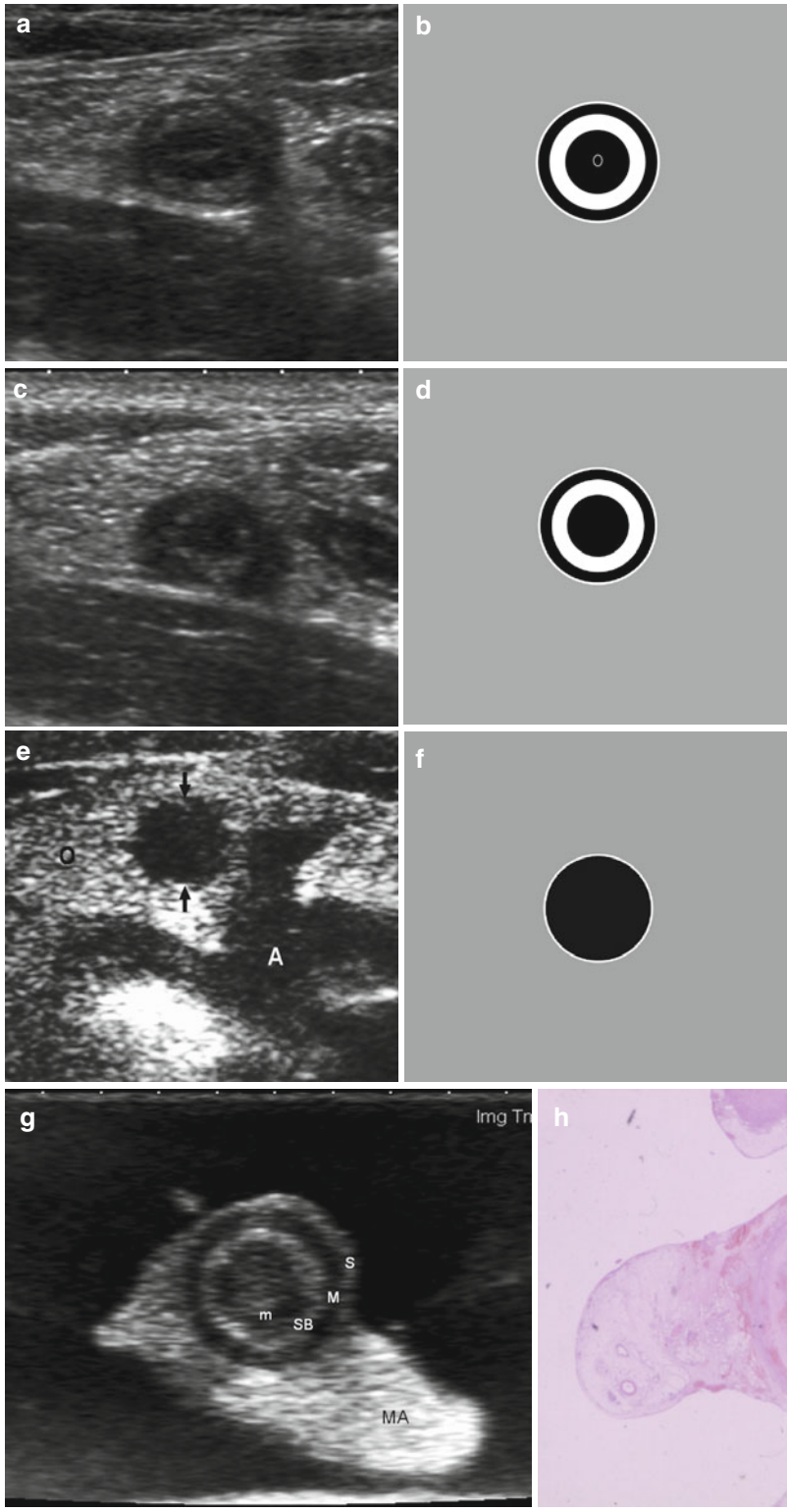
a
b
c
d
e
O
A
f
g
Img Tn
S
M
m
SB
MA
h

advanced inflammatory stage, the central ring or "spot," which represents the mucosal surface, cannot be identified making it difficult to evaluate whether the hypoechoic center corresponds to an inflamed mucosa or to intraluminal content. The preserved submucosa and serosa originate a two-ring pattern (Fig. 22c, d). Finally, necrosis and suppuration lead to the loss of submucosal hyperechogenicity, and the appendix tends to appear as a homogeneously hypoechoic circle outlined by the serosa giving a one-ring pattern. The serosa may not be clearly identifiable itself due to its similar hyperechogenicity with the inflamed surrounding periappendiceal fat in these advanced stages ("silhouette sign") (Figs. 22e–h and 23). The accurate identification of the different appendiceal layers demands a careful technique. Otherwise, the thin-ring and one-ring patterns may be easily confused, resulting in misinterpreting as a higher grade of involvement than really exists. All the patterns may coexist in the same appendix (del Pozo et al. 1992) (Fig. 23). Furthermore, one of the appendiceal ends may remain normal, while the opposite, particularly the tip ending, is swollen, thus stressing the importance of imaging the full appendix (Nghiem and Jeffrey 1992) (Fig. 24). Appendicoliths appear as hyperechoic foci with sharp distal

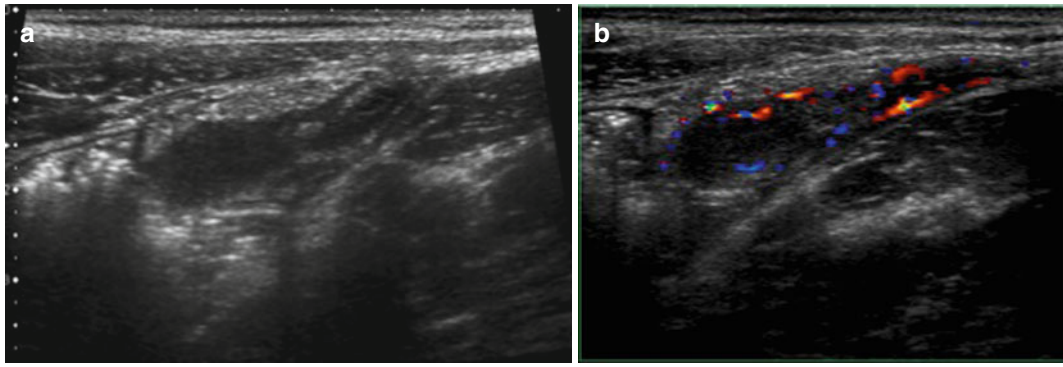


**Fig. 23** Several patterns of appendicitis in the same appendix. (**a**) B-mode US and (**b**) color Doppler longitudinal US scans, from the right lower quadrant summarizing all the different appearances of appendicitis, showing at the base the five conspicuous appendiceal layers with the patent mucosal surface and the prominent submucosa layer. These layers begin disappearing from the appendiceal base to the tip. Notice the associated thickened omentum encircling the appendix physiologically preventing the dissemination of the process

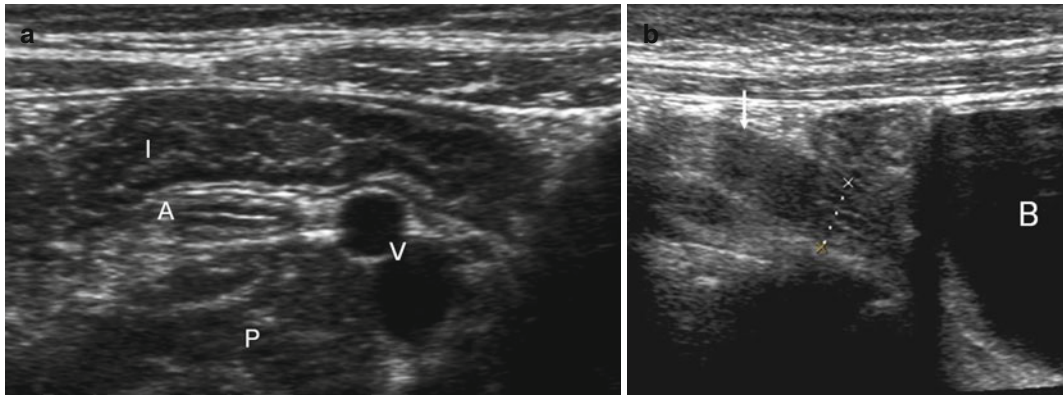


**Fig. 24** Tip ending appendicitis in the pelvis. (**a**) Axial US scan shows a retroileal not enlarged appendix but with subtle submucosal thickening. (**b**) Enlarged appendiceal tip (*arrow*) ending in the pelvis with blurring of the wall layers (measurement, 7.1 mm). Histopathological analysis demonstrated phlegmonous appendicitis at the tip (*I* lymphoid hyperplasia of the terminal ileum with patent ileal lumen, *V* iliac vessels, *P* psoas muscle *B* bladder *A* appendix)

acoustic shadowing. An appendicolith may be identified in any appendicular pattern and it supports a positive diagnosis, although it can also be seen in normal appendices (Fig. 21).

Perforated appendicitis may cause a phlegmon or abscess, originating complex images that are usually difficult to interpret. Circumferential loss of the submucosal layer of the appendix, prominent pericecal fat, and loculated pericecal fluid have been related to a higher perforation rate, giving a US sensitivity for the diagnosis of perforation of 86 % (Borushok et al. 1990) (Fig. 25). Perforation is more frequent in infants and small children, and at these ages, it is often free resulting in a purulent peritonitis. The lesser omentum in these children cannot cover a perforation as would happen in older children. Intraperitoneal echogenic free fluid is the most conspicuous US finding seen when free perforation takes place. The perforated appendix is difficult to identify as it tends to be collapsed, partially destroyed, and generally hidden behind the paralytic dilated bowel loops (Fig. 26). Generalized peritonitis may evolve to distant abscesses (Fig. 25c, d). Pneumoperitoneum secondary to an appendiceal perforation is extremely

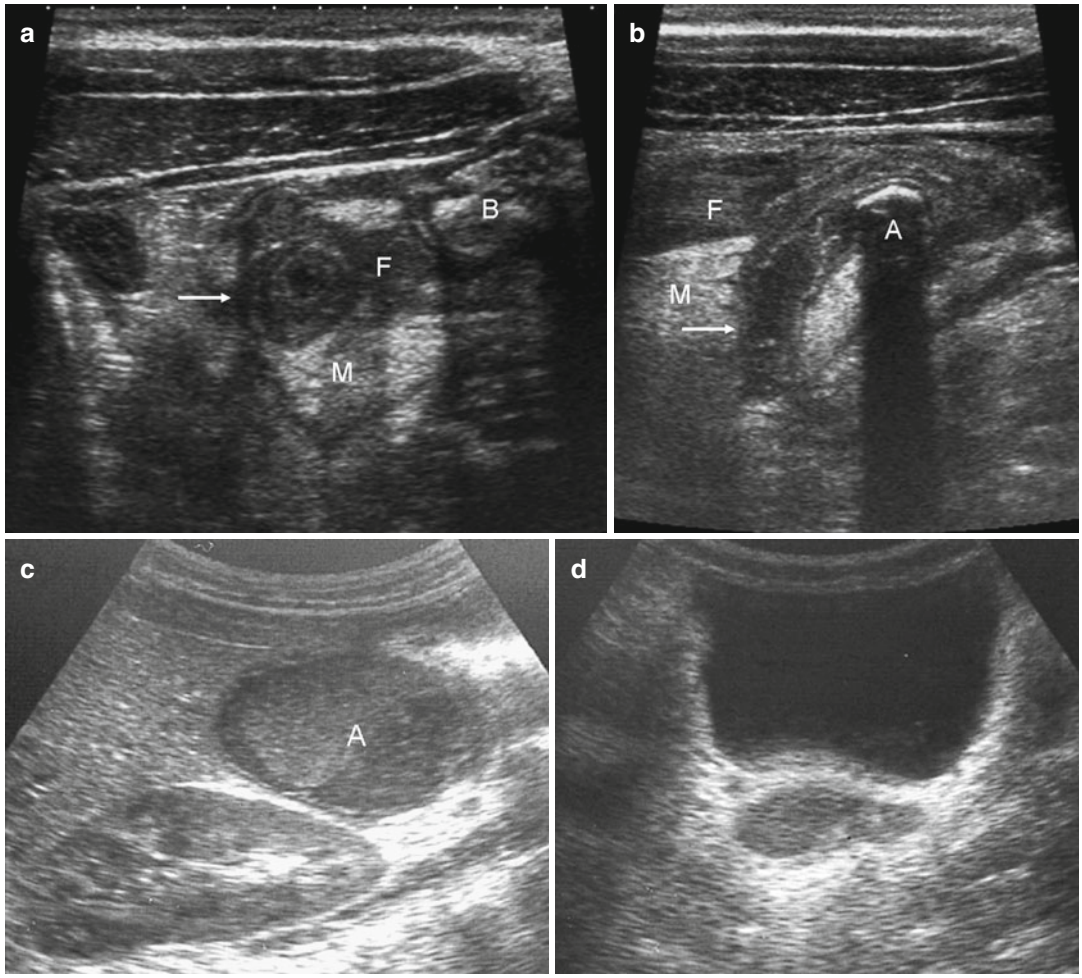


**Fig. 25** Perforated appendicitis: phlegmon and abscess. (**a**, **b**) Phlegmon. Inflammatory mass composed by a complex fluid collection (*F*), prominent mesenteric and omental fat (*M*), and adjacent thickened poorly defined intestinal bowel loops (*B*) just close to the appendiceal tip ending (*arrow*). At this level there is a one-ring pattern with loss of the submucosal layer (*A* appendicolith with sharp shadowing). (**c**, **d**) Abscesses. Distant multiple abscesses in the in the subhepatic region (**c**) and in the pouch of Douglas (**d**) (*A* abscess)

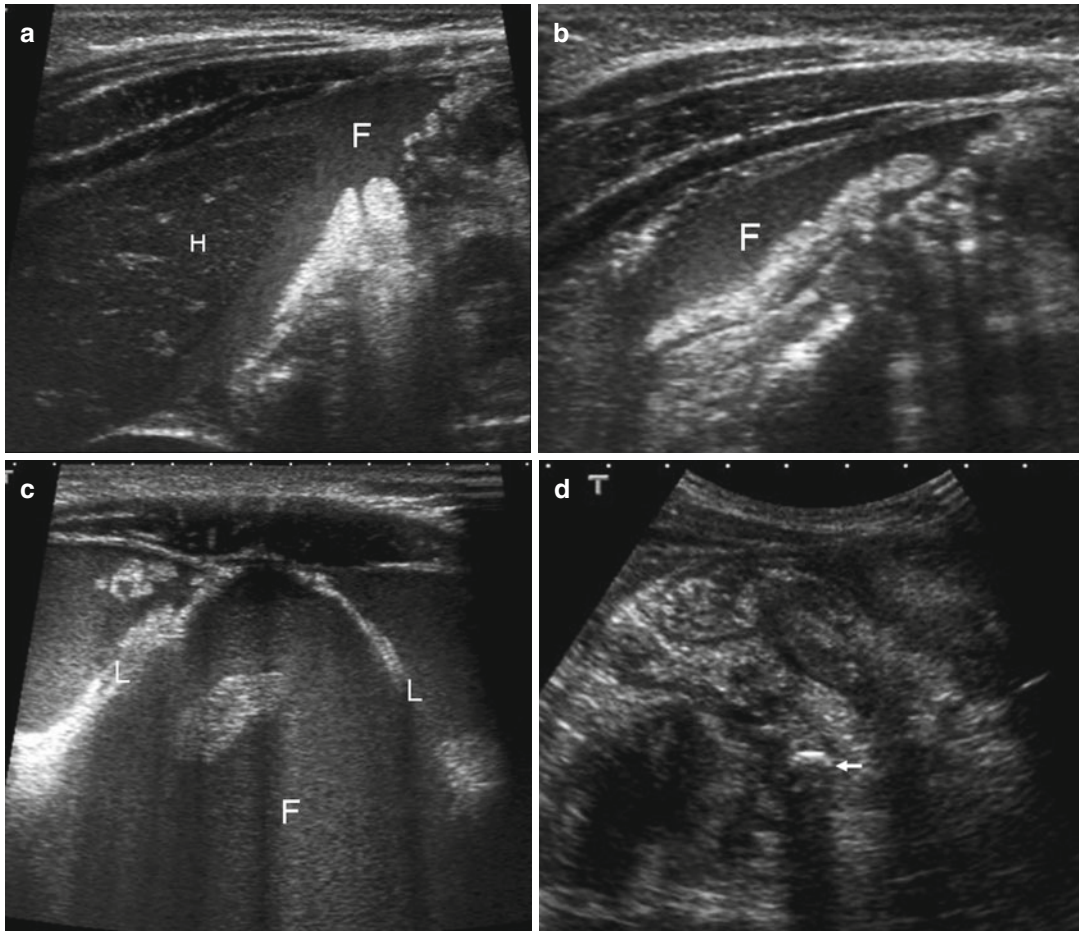


**Fig. 26** Peritonitis. Perforated appendicitis. US scans show echogenic free fluid in (**a**) the subhepatic region, (**b**) paracolic gutter, and (**c**) pelvis reflecting purulent peritonitis. (**d**) An appendicolith (*arrow*) is seen deeply behind intestinal bowel loops (*F* echogenic free fluid, *L* umbilical ligaments, *H* liver). Notice that the fluid surrounding the hepatic parenchyma exceeds its echogenicity

rare as the appendiceal lumen is obstructed and no longer connected to the colonic lumen.

Color Doppler US is useful as an additional positive finding of appendicitis in uncertain cases of borderline appendiceal size or ambiguous morphological US findings. Circumferential color in the wall of the inflamed appendix reflects inflammatory hyperperfusion and is evidence of active inflammation (Birnbaum and Wilson 2000) (Fig. 27). In cases with gangrenous appendicitis, color Doppler US may show decreased or no appendiceal flow. With appendix perforation, the hyperemia seen in the inflamed appendix extends to the also inflamed periappendiceal fat (Fig. 28).

In summary, high diagnostic accuracy when diagnosing appendicitis can be achieved only by considering several US criteria simultaneously, including localization of the tenderness, appendiceal compressibility, size, shape and pattern, presence of hyperechoic periappendiceal inflamed fatty tissue, appendicoliths, and blood flow in the appendiceal wall detected on color Doppler US. The centrifugal sequential loss of the hyperechoic appendiceal layers or rings, from the inner to the outer, enlargement of Periappendiceal fat, appendicular contour irregularity, and, finally, the presence of collections or echogenic ascites are correlated with the progres-

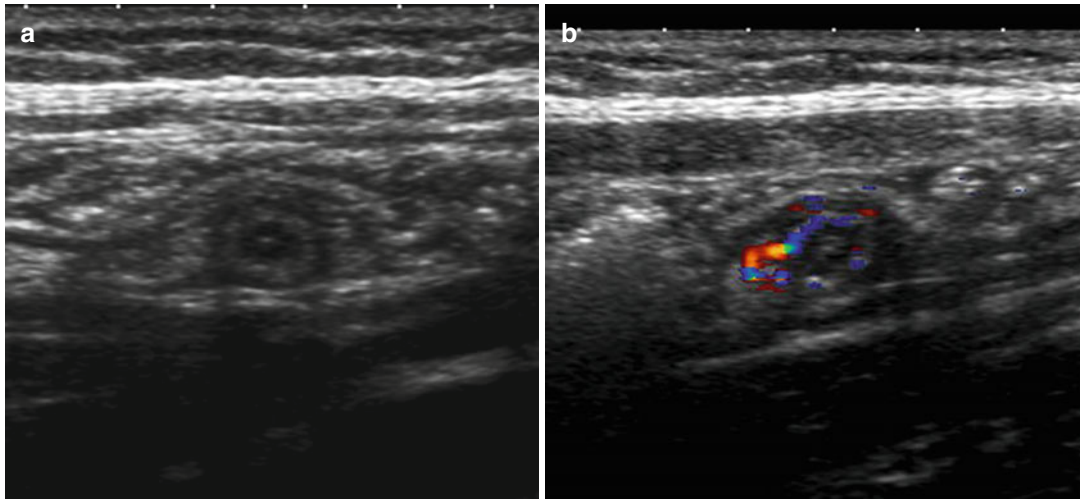


**Fig. 27** Acute appendicitis on color doppler US. (**a**, **b**) Mode US axial scan showing a three-ring-pattern appendicitis. (**b**) Color doppler demonstrates hyperemia of the mesoappendix and appendiceal wall

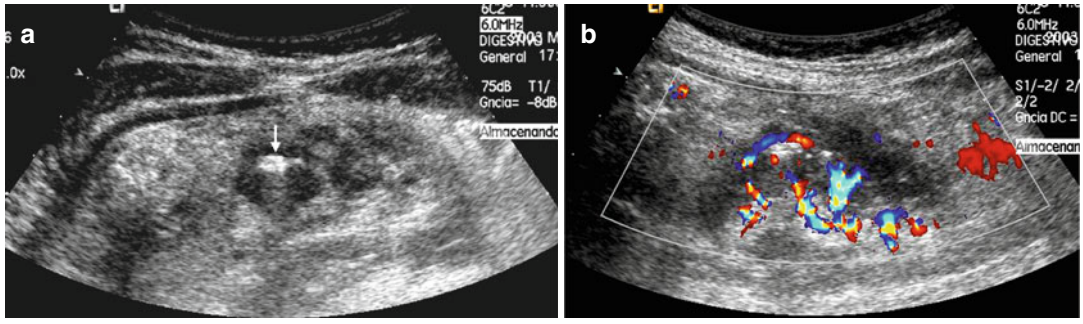


**Fig. 28** Perforated appendicitis on color Doppler US. (**a**) Axial US scan shows air within the appendiceal dilated lumen (*arrow*) and enlargement of the Periappendiceal fat. (**b**) Color Doppler demonstrates the enlarged periappendicular tissue corresponding to the inflammatory mass

sion from appendicular inflammation to necrosis and perforation. Ultrasonographic Blumberg sign (rebound tenderness), analogous to the sonographic Murphy sign tested in cholecystitis, can be evaluated at the end of the study when diagnosis remains unclear.

Appendicitis may resolve spontaneously in noncomplicated cases but only rarely in perforated forms. Serial US examinations have documented these infrequent spontaneous resolutions. They are considered as a false-positive diagnosis in most of the published series, due to inherent unavailability of surgical and pathological confirmation (Jeffrey et al. 1987). Spontaneously resolving appendicitis occurs in at least 1 in 13 cases of appendicitis and has an overall recurrence rate of 38 %, with the majority of cases recurring within the first year (Cobben et al. 2000). The fact that US findings cannot firmly predict the evolution of these cases means that nonoperative management may be considered. On the other hand, if the appendicitis is resolved without treatment, recurrence is not the rule, and an interval appendectomy may be unnecessary (Puylaert 1990).

A significant number of appendicitis cases may have an atypical location, producing a long-standing misdiagnosis process and, occasionally, may involve or even create fistulae, into other organs

such as the bladder, ureter, or colon. If the appendix is not identified in the RLQ, the entire abdomen should be systematically examined with appropriate transducers (Baldisserotto and Marchiori 2000), because this structure may be located retrocecally (20–25 % of cases) or in the pelvic area (7.9 % of cases) (Collins 1932) (Fig. 29). A lateral approach through the flank may facilitate US identification of a retrocecal appendix, which lies posterolaterally to the cecum and would be found hidden by the cecal air when using an anteroposterior approach (Ceres et al. 1990; Quigley and Stafrace 2013).

Most of the false-positive diagnoses of appendicitis are related to an increased diameter resulting from inspissated feces or noncompressible noninflammatory contents ("rod sign") (Simonovský 1992) (Fig. 30) or parietal lymphoid hyperplasia, as mentioned above. Patients with cystic fibrosis may also have a markedly enlarged appendix (>8 mm in diameter) filled with mucus or stool without acute appendicitis

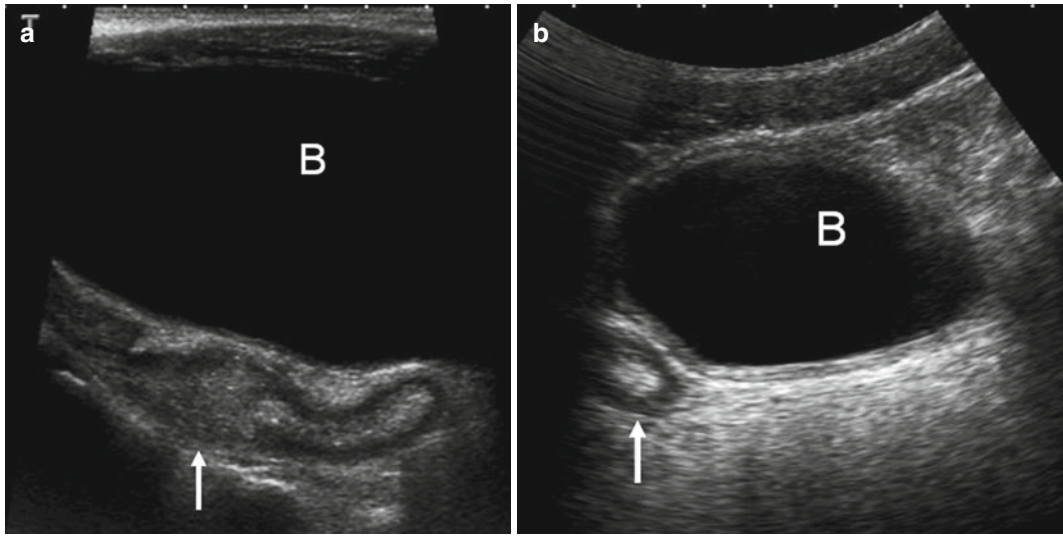


**Fig. 29** Pelvic appendicitis. (**a**) Longitudinal (7.5 MHz linear transducer) and (**b**) Axial (3.5 MHz convex transducer) US scans show an enlarged retrovesical appendix (*arrow*) with loss of the wall stratification at the mid-appendix and echogenic appendiceal content at the tip end abutting wall bladder (*B*). A well-filled bladder helps identify a pelvic appendix

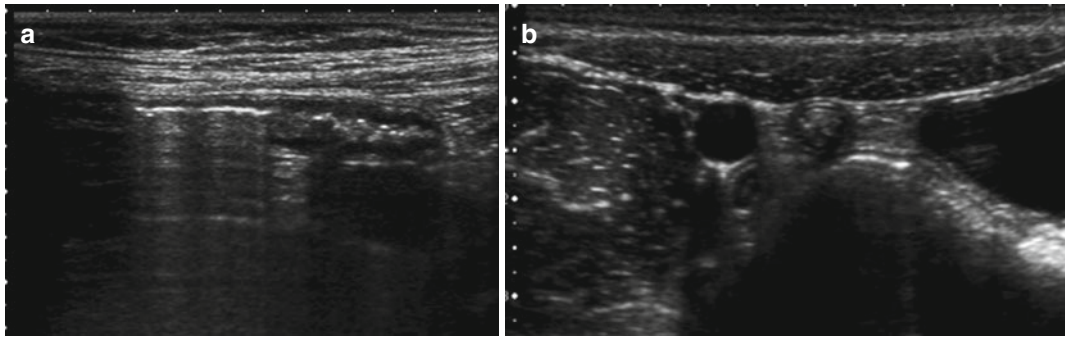


**Fig. 30** Enlarged feces-filled normal appendix. Asymptomatic 6-year-old boy. (**a**) Longitudinal and (**b**) transverse images. The appendix has preserved wall layering. The appendicular AP diameter measured 7.2 mm exceeding the accepted upper limit

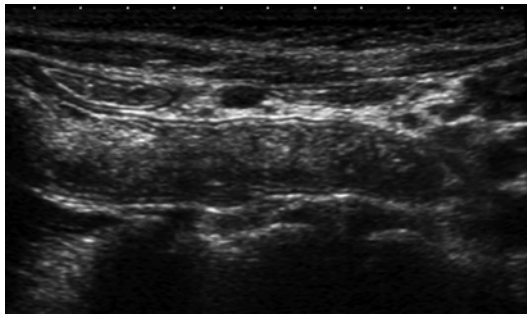

**Fig. 31** Normal appendix in a patient with cystic fibrosis. Asymptomatic 10-year-old boy. Longitudinal US scan showing an enlarged appendix (AP diameter measured 8.5 mm) filled with feces. No mural abnormality or secondary inflammatory changes were identified

(Menten et al. 2005) (Fig. 31). False-positive diagnoses may also result from misinterpretation of the normal terminal ileum as an inflamed appendix. The terminal ileum is easily compressible, displays active peristalsis, and presents a thin submucosal layer in contrast to the inflamed appendix. Nevertheless, the normal terminal ileum presents a similar pattern to that of the normal appendix with a thin submucosal layer and a thick hypoechoic mucosa layer, but instead of the nearly anechoic mucosa of the normal appendix with rectilinear mucosal surface, the mucosa of the terminal ileum has a nonhomogeneous appearance due to the presence of mucosal folds. In addition, the end of the small bowel is not "blind ending" and the proximal end of the ileum forms the lips of the ileocecal valve while the appendix emerges as a funnel from the cecum (Fig. 19a). Eventually, an inflamed Meckel diverticulum or a uterine tube with torsion can also be misinterpreted as an enlarged appendix. On the other hand, false-negative diagnoses are usually related to loss of appendix visualization due to obesity or abundant air interposition, which can occur with an atypical pelvic location and/or associated paralytic ileus. Another reason for false-negative results is partial visualization of a proximal normal appendix with focal appendicitis of the tip ending. Secondary changes due to appendicitis such as lymphadenopathies, fat thickness, or bowel loop wall thickening can be erroneously interpreted as mesenteric adenitis, omental infarct, or infectious ileocecitis, leading to a false-negative result.

Computed tomography (CT) is a highly accurate and effective cross-sectional imaging technique for diagnosing and staging acute appendicitis. Its advantages over US are reduced operator dependence; the capacity to view the entire range of air, soft tissue, fat, and bone attenuation values inherent to the abdomen; and better evaluation of complications such as phlegmon and abscess formation (Sivit et al. 2000). Although CT can help clinicians to rapidly diagnose or exclude acute appendicitis, recent enthusiasm for CT, supported by at least one meta-analysis (Doria et al. 2006), has been tempered because of widespread public concern about the potential risks of radiation exposure (Brenner and Hall 2007). These concerns are particularly relevant in children as a result of their life expectancy and increased susceptibility to radiation effects (Brenner et al. 2001; Hryhorczuk et al. 2012). Additional CT disadvantages include longer preparation times, use of contrast agents, and sedation in younger children. When CT is indicated, the technical parameters should be adjusted according to the child's age and weight, the body region of interest, and the clinical question. Low-dose CT protocols using an effective current-time product of 30 mAs have proven to be highly accurate (Keyzer et al. 2004). Low-dose CT has also shown to not be inferior to standard-dose CT with respect to the negative appendectomy rate among young adults with suspected appendicitis (Kim et al. 2012). Recent advances in multidetector CT allow image review with thinner collimation (Johnson et al. 2009) and the reconstruction of multiplanar reformats increasing the detectability of abnormal and normal appendices (Kim et al. 2008; Hernanz-Schulman 2010). However, the paucity of intra-abdominal fat in children compared to adults contributes to a relatively lower rate of normal appendix detection at CT (12 %) (Kaiser et al. 2002) (Fig. 32) and a poorer identification of periappendiceal fatty stranding, which lowers diagnostic accuracy (Harswick et al. 2006). This has led to current

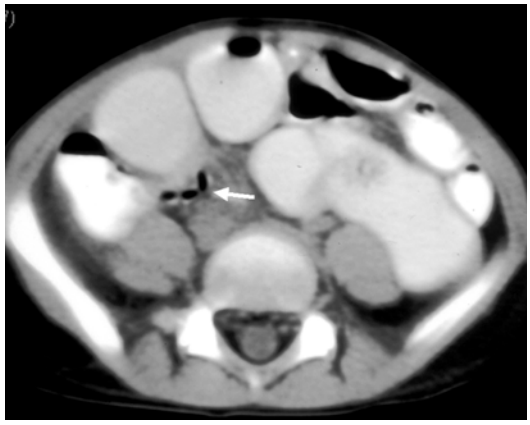

**Fig. 32** Normal appendix on CT. Normal air-filled appendix (*arrow*). Dilated bowel loops filled with oral contrast are depicted. Note the small amount of intra-abdominal fat that contributes to the children's lower rate of normal appendix detection on CT

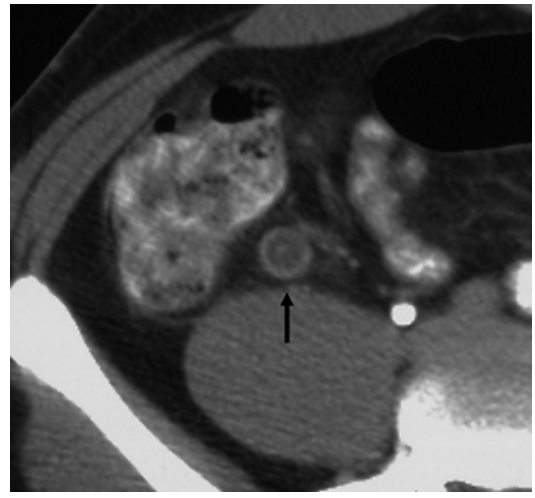

**Fig. 33** Phlegmonous appendicitis on CT. Axial CT scan showing a retrocecal enlarged and enhancing appendix (*arrow*) with subtle fatty stranding

standard imaging practices including the use of intravenous iodinated contrast (Jacobs et al. 2001; Kaiser et al. 2004; Iwahashi et al. 2005). Positive (high-attenuation) oral contrast and, sometimes, positive rectal contrast have also been recommended (Hershko et al. 2007; Stroman et al. 1999). The theoretical advantages of positive oral (and rectal) contrast in diagnosing appendicitis lie in their ability to highlight the lumen of the small bowel, cecum, and normal appendix in cases without appendicitis and in the absence of filling of an inflamed and obstructed appendix in cases with acute appendicitis (Kharbanda et al. 2007). The use of positive vs. neutral oral contrast does not affect the diagnostic utility of contrast-enhanced CT in identifying acute appendicitis irrespective of the experience or the familiarity of the reader with the type of oral contrast used (Naeger et al. 2011). When seen, the normal appendix appears as a tubular or ringlike pericecal structure that is either totally collapsed or partially filled with fluid, contrast material, or air. The periappendiceal fat should appear homogeneous, although a thin mesoappendix may be present. The appearance of the abnormal appendix varies with the stage and severity of the disease process. In patients with mild, non-perforating appendicitis, the appendix may appear as a minimally distended, fluid-filled, tubular structure 5 mm in diameter surrounded by the homogeneous fat attenuation of the normal mesentery. This appearance, however, occurs in less than 5 % of patients. Most patients demonstrate greater degrees of luminal distention and evidence of transmural inflammation. The inflamed appendix usually measures 7–15 mm in diameter. Circumferential and symmetric wall thickening is nearly always present and is best demonstrated on images obtained with intravenous contrast material enhancement (Birnbaum and Wilson 2000) (Fig. 33). The thickened wall is usually homogeneously enhancing, although mural stratification in the form of a target sign may be noted. Other common findings include an appendicolith, circumferential or focal apical cecal thickening, pericecal fat thickening, and the arrowhead sign. The latter finding occurs when cecal contrast material funnels symmetrically at the cecal apex to the point of the appendiceal occlusion (Rao et al. 1997). Perforated appendicitis is usually accompanied by pericecal phlegmon or abscess formation (Fig. 34). Associated findings include extraluminal air, marked ileocecal thickening, peritonitis, and small bowel obstruction.

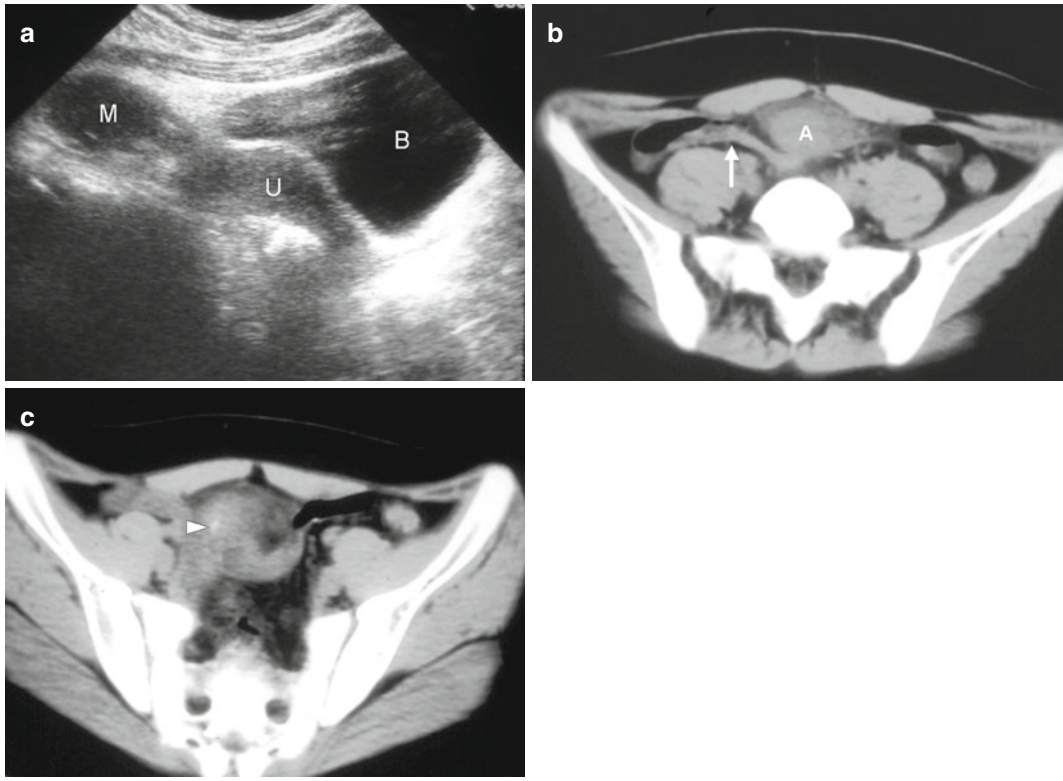


**Fig. 34** Perforated appendicitis on CT. 13-year-old girl treated with antibiotics for pelvic pain and fever. (**a**) US shows a nonspecific cystic mass (*M*) cranial to the uterus (*U*). No flow was observed on color Doppler US. (**b**, **c**) CT clearly demonstrates the close relation between the mass (*A*) and the enlarged appendix (*arrow*) with an appendicolith (*arrowhead* in **c**). An appendiceal abscess was demonstrated at surgery (*B* bladder, *A* abscess)

MRI is increasingly used as a non-radiation alternative to CT. MRI is a safe, reliable, and potentially cost-effective technique for the evaluation of patients suspected of having appendicitis – particularly after an equivocal US and when CT is contraindicated (Cobben et al. 2009). Studies have reported the visualization of a normal appendix on MRI in 43–63 % of the cases (Pedrosa et al. 2006; Nitta et al. 2005). Recent studies have demonstrated that the introduction of 3-T abdominal MRI increasing signal-to-noise ratio in combination with newer body coils and the use of parallel processing have significantly reduced scan times (median scan time for the entire examination of 5 min 40 s), making it possible to advocate the use of MRI with its reported results of 100 % sensitivity, 99 % specificity, 100 % negative predictive value, and 98 % positive predictive value in the diagnosis of acute appendicitis. Ultrafast 3-T MRI requires no sedation and no oral or IV contrast agent and has no associated radiation exposure risks (Johnson et al. 2012) (Figs. 35 and 36). The images performed at 1.5 T would have a lower signal-to-noise ratio and increased motion artifacts and may not be of diagnostic quality. Limited availability and high cost are still the main disadvantages of MRI.

## 3.2 Management

Most of the literature now focuses on a combination of analytical models such as the Alvarado score with sequential imaging. The Alvarado score

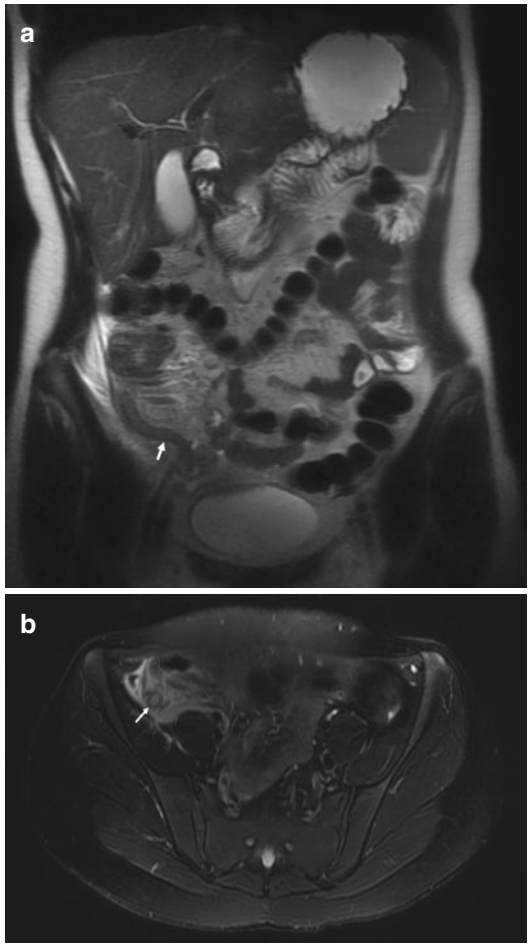


**Fig. 35** Appendicitis (3T MR images). 18-year-old girl with right lower quadrant pain. (**a**) Coronal T2 SSFSE (single-shot fast spin-echo) and (**b**) axial T2 FRFSE (fast-recovery fast spin-echo) images show a dilated tubular structure in the right lower quadrant corresponding to the thickened appendix and associated hyperintense inflammatory edema in the surrounding soft tissues (*arrow*) (Courtesy from George Wu. Geisinger PA)

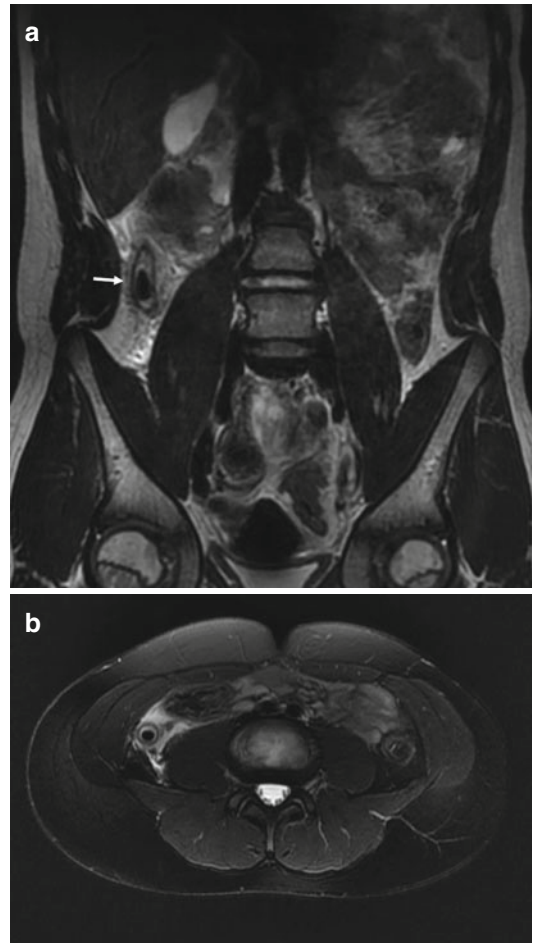


**Fig. 36** Appendicitis with appendicolith (3T MR images). 11-year-old boy with right lower quadrant pain. (**a**) Coronal high-resolution 512×512 3D fast-recovery fast spin-echo (FRFSE) CUBE and (**b**) axial T2 fast-recovery fast spin-echo MR images show a dilated tubular structure in the right lower quadrant corresponding to the appendix with a low-signal appendicolith in the lumen and associated hyperintense inflammatory edema in the surrounding soft tissues (*arrow*) (Courtesy from George Wu, Geisinger PA)

is a ten-point scoring system for the diagnosis of appendicitis based on clinical signs and symptoms and a differential leukocyte count. With an intermediate score of 5 to 8, further diagnostic studies are required (Douglas et al. 2000). In cases with a high clinical suspicion of appendicitis, direct surgery is indicated. Experienced pediatric surgeons can, with history and examination, differentiate appendicitis from other abdominal disorders with 92 % accuracy (Williams et al. 2009). Clinicians should therefore consult a surgeon with experience or transfer the patient to a large specialty center rather than obtaining imaging studies. When the clinical presentation is unclear, US should be performed, even if the result is negative, positive, or nonconclusive, as the primary modality of choice even in obese patients (Sulowski et al. 2011; Butler et al. 2011). A negative diagnosis

requires the whole identification of the normal appendix. However, in experienced hands, the nonvisualization of secondary changes may be considered a negative diagnosis even if the appendix was not identified with an NPV of 95 % (Pacharn et al. 2010). A positive diagnosis followed by an early appendectomy decreases the complication rate (Blakely et al. 2011). Patients who present late with a well-localized abscess or inflammatory mass (phlegmon) may initially be treated nonoperatively. Antibiotics occasionally followed by a delayed interval appendectomy in cases of phlegmon and percutaneous drainage through US or CT guidance in abscesses larger than 3 to 4 cm in diameter may be used. Nonoperative management has a recurrence rate of 8–43 %. Therefore, an interval appendectomy is only recommended in patients who present certain other criteria, such as the presence of an appendicolith (Puapong et al. 2007).

When US provides a nonconclusive diagnosis, different options should be considered depending on the clinical findings and on the resources available in each institution: options include an observation period followed by a delayed US examination or a CT or an early MRI in order to obtain a more accurate and prompt diagnosis (Kosloske et al. 2004; Krishnamoorthi et al. 2011). A staged imaging protocol for appendicitis that emphasizes US and proceeds to CT with IV contrast only if US is inconclusive has shown high sensitivity (96–99 %) and specificity (83–92 %), as well as the incremental cost-effectiveness ratios (Hagendorf et al. 2004). Furthermore, similar high accuracy in the diagnosis of appendicitis has been demonstrated by a protocol-based inpatient clinical evaluation by pediatric surgeons (with selective use of diagnostic imaging methods), with additional lower negative appendectomy (5 %) and perforation rates (17 %) achieved without the radiation exposure and potential costs derived from excessive use of radiological examinations (Kosloske et al. 2004; Ziegler 2004).

Several mostly nonsurgical abdominal processes such as enteritis (ileocecitis, inflammatory bowel disease), mesenteric adenitis, primary fat epiploic lesions (right segmental omental infarction and epiploic appendagitis), typhlitis, infectious peritonitis, and functional gynecological pathology may clinically simulate appendicitis. An accurate diagnosis to avoid non-necessary surgery is essential in these cases.

## 4 Small Bowel Obstruction

Besides perforated appendicitis and IT, the most common causes of small bowel obstruction are incarcerated hernias and adhesions. Other causes of small bowel obstruction comprise a miscellaneous group of rare conditions, such as midgut volvulus, Meckel diverticulum, advanced stages of Crohn disease, and bezoars. Adhesions usually result from prior surgery and are often multiple. There is an increasing tendency for initial conservative management rather than immediate operative intervention, as a proportion of cases will resolve spontaneously, management by nasogastric tube placement. The diagnosis of bowel obstruction is established on clinical grounds and usually confirmed with plain abdominal radiographs. Plain radiographs usually show distended bowel loops with air-fluid levels (Fig. 37). In inguinal incarcerated hernia, plain film will also show thickening of the right inguinoscrotal fold (Fig. 38a). Because of the diagnostic limitations of plain films, cross-sectional methods are increasingly used (Babcock 2002). On US, dilated, fluid-filled small bowel loops can be seen, which are recognized by the presence of the valvulae conniventes. The bowel wall may become edematous due to vascular and lymphatic blockage, and ascites may be an accompanying feature of intestinal obstruction. In patients with mechanical bowel obstruction, hyperperistalsis with a to-and-fro motion of the bowel contents is often observed during real-time imaging. Once the obstruction becomes high grade or complete, peristalsis may be absent (O'Malley and Wilson 2003). Intestinal bowel loops and mesenteric fat passing down the inguinal canal into the scrotum can be readily identified in inguinal hernias (Fig. 38c). On US or

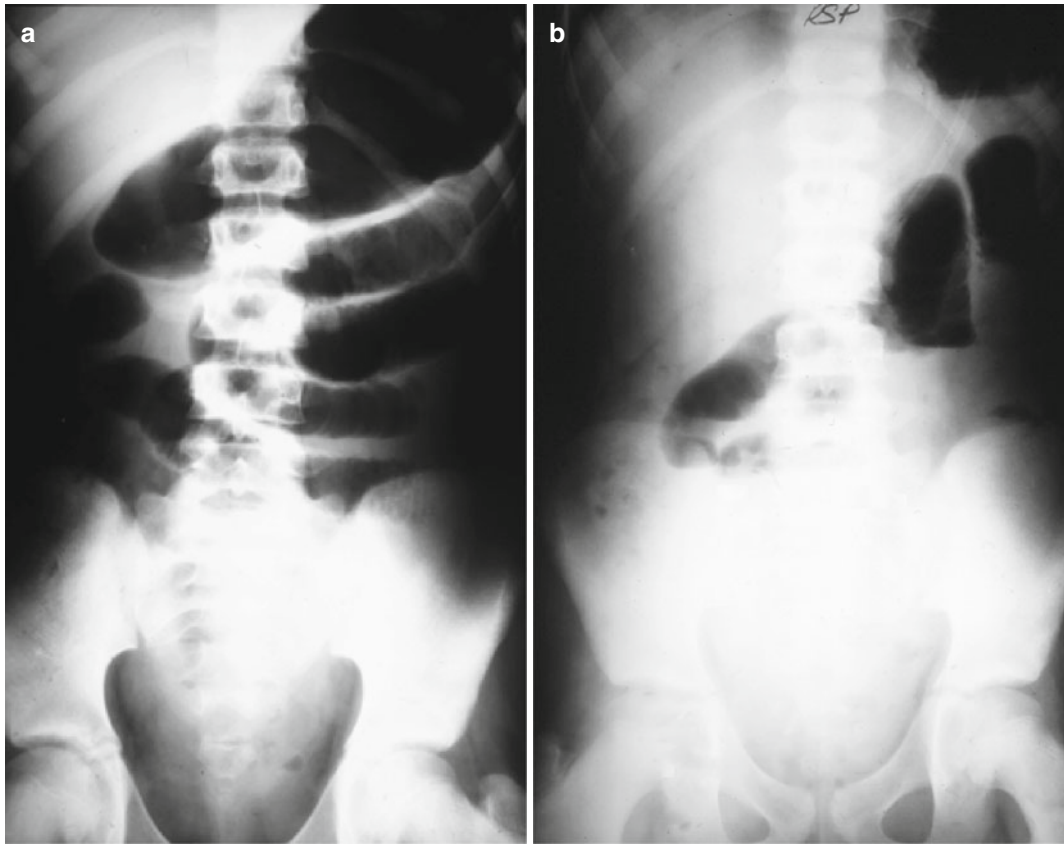


**Fig. 37** Small bowel obstruction due to adhesive band. (**a**) Supine plain radiograph shows multiple dilated loops of proximal small bowel with no distal passage of air. (**b**) Erect film demonstrates multiple air-fluid levels. Previous appendectomy

CT a diagnosis of adhesions is assumed when there is no identifiable lesion at the transition zone between the dilated and the collapsed bowel loops, because the adhesive band itself is not visualized (Marincek 2002). Closed-loop obstruction is a form of mechanical bowel obstruction in which two points along the course of the bowel are obstructed at a single point. It is usually secondary to an adhesive band or a hernia. Because a closed loop tends to involve the mesentery and is prone to produce a volvulus, it represents the most common cause of strangulation. Characteristic findings of closed-loop obstructions are a C-shaped, U-shaped, or "coffee bean" configuration of the bowel loop (Marincek 2002) (Fig. 39). Mechanical obstruction of the gut must be differentiated from paralytic ileus. Multiple causes exist for both diffuse and localized paralytic ileus and gaseous distention of the small and the large intestine are seen. Paralytic ileus is a common problem after abdominal surgery. It may be secondary to inflammatory or infectious disease; electrolyte, metabolite, and/or hormonal disturbances; drug therapies; or innervation defects. Plain radiographs may show generalized dilated bowel loops with distal air, as well as air-fluid levels in the upright or decubitus radiograph (Marincek 2002) (Fig. 40). Differentiation of paralytic from mechanical ileus can also be documented by M-mode US (Riccabona 2001).

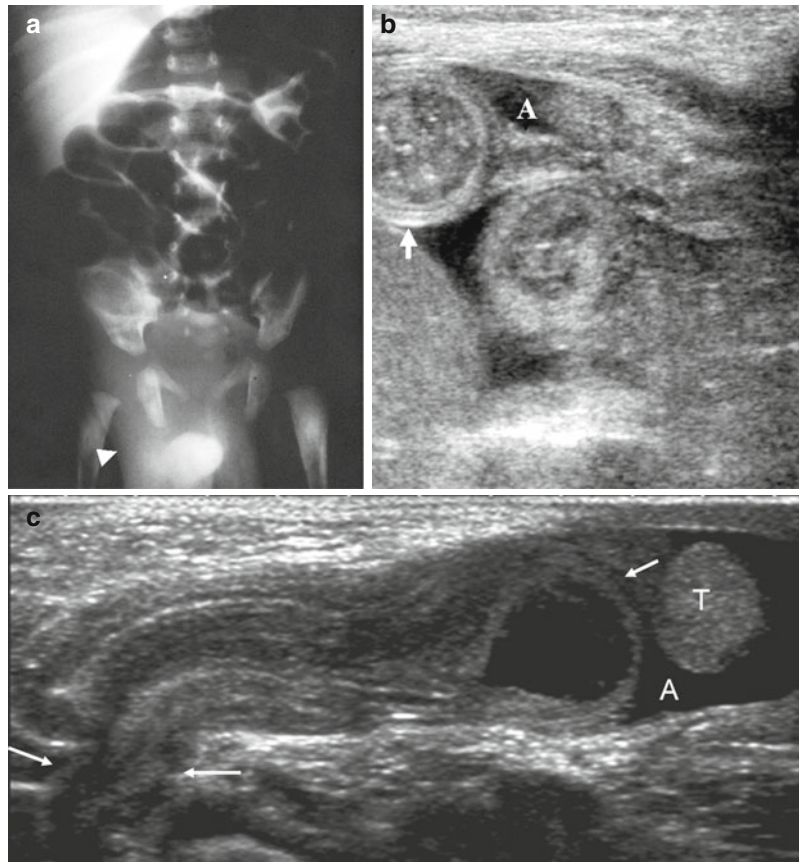


**Fig. 38** Incarcerated inguinal hernia. (**a**) Plain film shows dilated loops of small bowel and thickening of the right inguinoscrotal fold (*arrowhead*). (**b**) US scan shows dilated small bowel loops and ascites. Notice the stratified appearance of the bowel wall with 5 layers (*arrow*). (**c**) Longitudinal US scan shows fluid-filled bowel loops in the right inguinoscrotal canal (*arrows*), passing down into the scrotum. The testis (*T*) shows a normal appearance (*A* ascites)

## 5 Midgut Volvulus

Midgut volvulus is a complication of intestinal malrotation. Clockwise twisting of the bowel around the SMA axis can be induced because of a narrowed mesenteric attachment. This life-threatening condition is a clear indication for emergency surgery. Because among older children and adolescents presentation is usually nonspecific and malrotation is rarely considered, the diagnosis of midgut volvulus is difficult to establish. Patients with midgut volvulus may experience recurrent episodes of colicky abdominal pain and vomiting over a longer period of time which should result in an imaging request. Diarrhea and malabsorption from chronic venous and lymphatic obstruction may also develop (Berdon 1995). Findings on abdominal radiographs in midgut volvulus are usually abnormal but nonspecific. In older patients with acute symptoms, US or CT is generally performed instead of upper gastrointestinal series. US is currently the modality of choice. Identifying an abnormal position of the mesenteric vessels with the vein located to the left or to the front of the artery can raise the suspicion of malrotation. On the contrary, demonstration of the third duodenal segment between the aorta and the superior mesenteric artery in retroperitoneal location has been

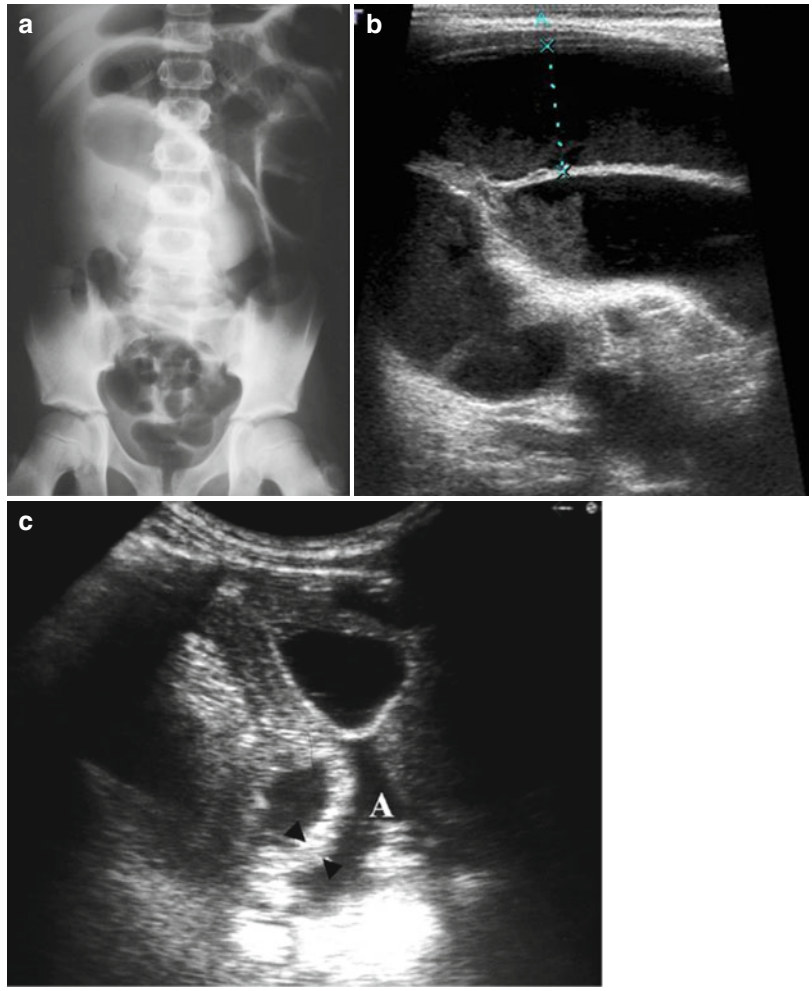


**Fig. 39** Mechanical small bowel obstruction. Volvulus secondary to adhesions from previous appendectomy. (**a**) Supine plain abdominal radiographs show characteristic C-shaped configuration of bowel loop in the mesogastrium with presence of distal air, due to a short evolution time. (**b**, **c**) US scans show dilated bowel loops. Distance between calipers measures 24 mm. Some bowel loops demonstrate a thickened wall (*arrowheads*) and ascites (*A*), suggesting strangulation

recently proposed as a method to exclude malrotation (Yousefzadeh 2009) (Fig. 41). It showed 0 % false-positive rates versus up to 15 % with UGI (Yousefzadeh et al. 2010; Menten et al. 2012). However, for some authors, the diagnosis of malrotation continues to be a challenge, as the third portion of the duodenum located behind the SMA has been described in cases of surgically repaired malrotation (Snyder and Chaffin 1954; Taylor 2011).

When volvulus occurs, the twist of the bowel loops and the vessels around the mesenteric artery axis creates on US the clockwise "whirlpool sign" (Pracros et al. 1992), best shown in Doppler color studies (Patino and Munden 2004). In the final stage of the process, the presence of free fluid and wall thickening indicates vascular compromise. A similar appearance can be seen on CT (Bernstein and Russ 1998; Pickhardt and Bhalla 2002). Additional CT findings include duodenal obstruction, congestion of the mesenteric vasculature, and evidence of underlying malrotation. The presence of intestinal ischemia or necrosis is an ominous sign. On the other hand, the counterclockwise rotation of the SMV over the SMA (barber-pole sign) seen in

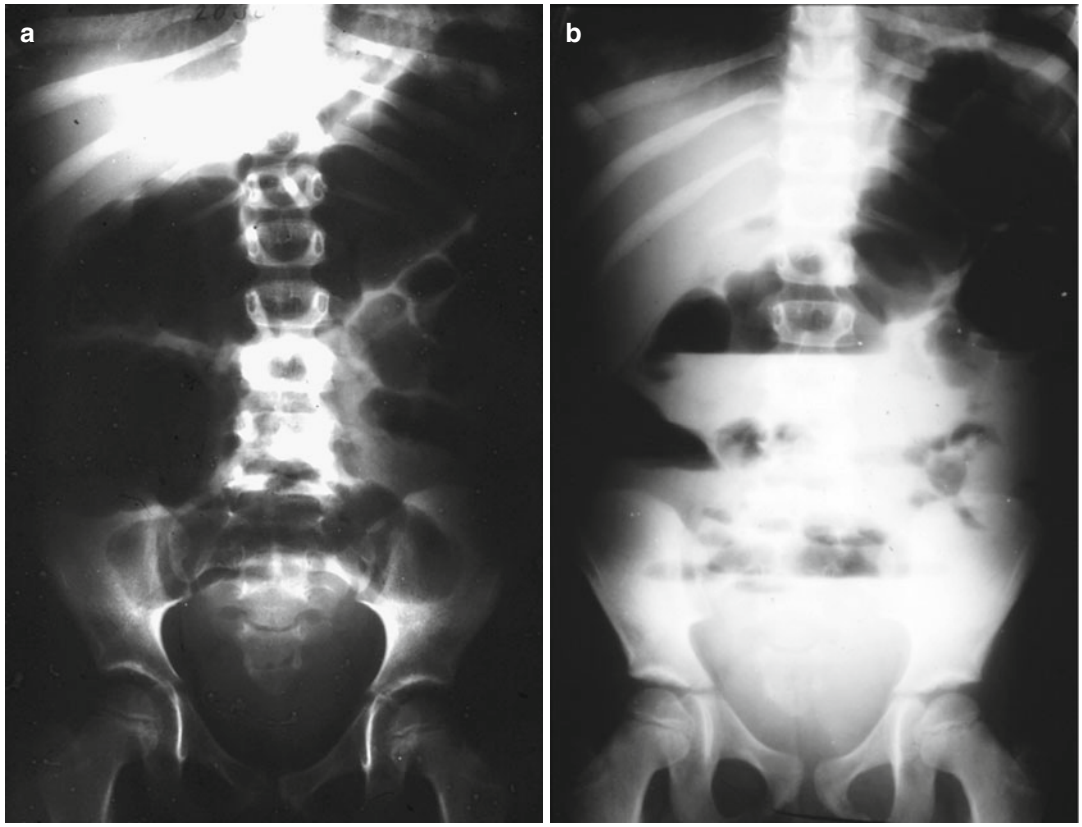


**Fig. 40** Paralytic ileus due to gastroenteritis. (**a**) Supine film shows generalized dilated bowel loops and distal air. (**b**) Upright film demonstrates multiple air-fluid levels

patients with normal midgut rotation is a normal variant and nonspecific finding, present in up to 10 % of normal patients (Taylor 2011). Even though the clockwise whirlpool sign warrants surgery for midgut malrotation and volvulus, the counterclockwise barber-pole sign might only warrant UGI series to confirm normal midgut rotation (Clark and Ruess 2005).

Internal hernia caused by abnormal peritoneal bands is an under-recognized complication of malrotation (Maxson et al. 1995). This condition may also be life-threatening because of the risk of bowel obstruction and strangulation. CT findings of malrotation and small bowel obstruction (without volvulus) may be seen in patients with this complication (Pickhardt and Bhalla 2002). Evidence of ischemic bowel again portends a poor prognosis. Some patients may present a combination of midgut volvulus and internal hernia.

Such a life-threatening combination in otherwise healthy adolescents underscores the importance of early detection and treatment.

## 6 Meckel Diverticulum

Meckel diverticulum is a remnant of the omphalomesenteric duct. It is located in the antimesenteric side of the ileum, usually not more than 60 cm from the ileocecal valve. This anomaly occurs in 0.5–4 % of the population, being usually asymptomatic. Meckel diverticulum can present clinically with rectal bleeding, inflammation (Fig. 42), or obstruction. Intestinal obstruction can be produced by small bowel volvulus around an associated omphalomesenteric band or herniation of bowel loops through a mesentery diverticulum defect. The diverticulum may also act as a lead

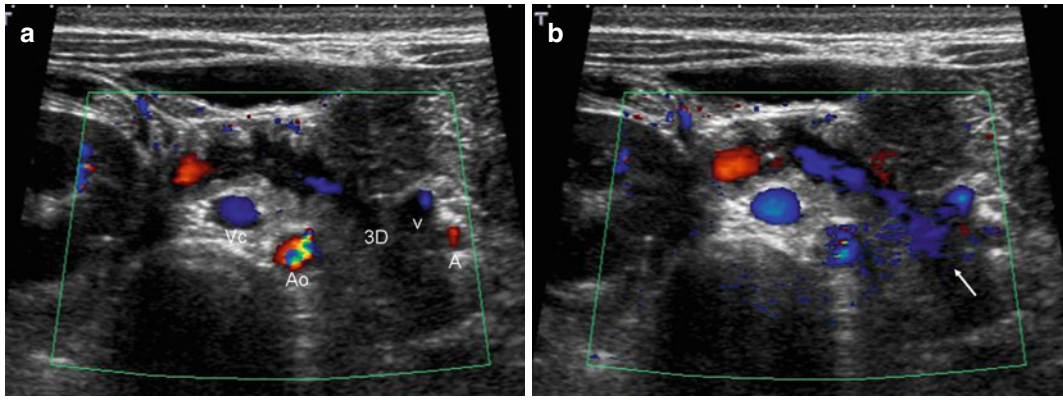


**Fig. 41** Normal third duodenal segment and mesenteric vessel anatomy. (**a**, **b**) Axial Doppler US scans demonstrating the normal position of the mesenteric vessels (*V* vein, *A* artery) with the vein located to the right of the artery and showing the third duodenal segment (*3D*) between the aorta (*Ao*) and the superior mesentery artery in a retroperitoneal location excluding malrotation (*Vc* inferior vena cava). (**b**) Intestinal content passing through 3D (*arrow*) depicted on Doppler US. Note image obtained through the right lateral approach, avoiding gaseous interposition

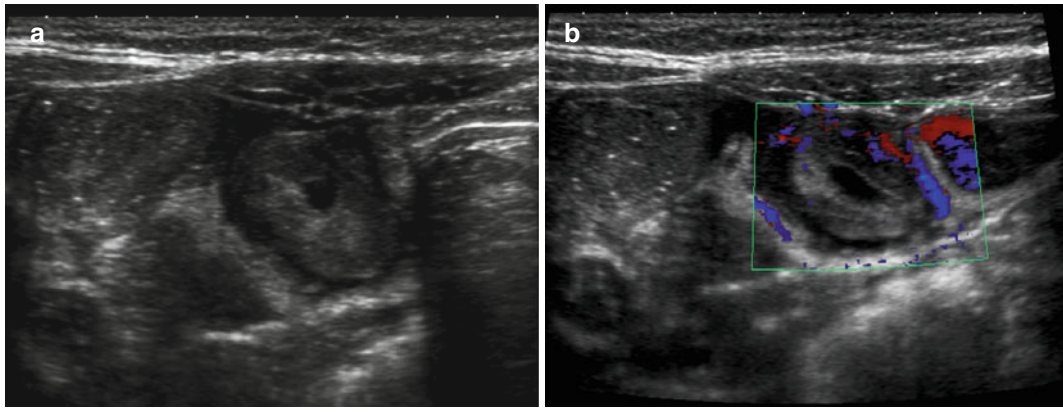


**Fig. 42** (**a**) Surgically proven Meckel diverticulum. High frequency transverse US images. Segment of ileum with thickening of the wall, increased vascularization (**b**), inflammatory changes in the adjacent fat and surrounding free fluid (Courtesy of Dr. Miguel Rasero)

point for IT or become incarcerated in a hernia. The most frequent form of presentation is painless bleeding in children younger than 5 years old. Bleeding is related to ulceration of heterotopic gastric mucosa, present in the diverticulum in less than 25 % of cases. The 99 m-Tc pertechnetate scan has demonstrated high accuracy for detecting a diverticulum when isotope is taken up by ectopic gastric mucosa (Hayes 2004). It is difficult to make a diagnosis of Meckel diverticulum as the cause of abdominal pain, despite the wide variety of imaging techniques available, particularly if symptoms are relieved and the diverticulum bowel wall regains its normal appearance becoming indistinguishable from the adjacent bowel loops. Radiographic findings are nonspecific in most cases of intestinal obstruction. In cases of Meckel diverticulum acting as a lead point, US may be useful in showing a cystic or echogenic pyriform inverted diverticulum at the apex of the IT (Fig. 13). US may also detect an inflamed or torsioned diverticulum mimicking appendicitis. In these cases, the unusual location of the enlarged diverticulum far from the cecum, as well as an anteroposterior diameter greater than 2.5 cm, can help to make an accurate diagnosis (Gallego et al.

1998) (Fig. 42). On the other hand, and as in the appendix, fecaliths may produce obstruction of the diverticulum and inflammation.

## 7 Enteritis

Gastroenteritis is the most frequent cause of abdominal pain in children. Different organisms may cause this entity, which is usually a self-limiting disease in developed countries. Diarrhea, vomiting, and abdominal pain are the most common symptoms. These symptoms can overlap with symptoms in some appendicitis cases and consequently imaging is required in patients with an atypical course. Plain film may show generalized small and large bowel distension, with air-fluid levels on positional views as a paralytic ileus (Fig. 40). US may detect generalized dilated bowel loops without wall thickening or significant ascites in noninvasive gastroenteritis cases (Fig. 43). In cases

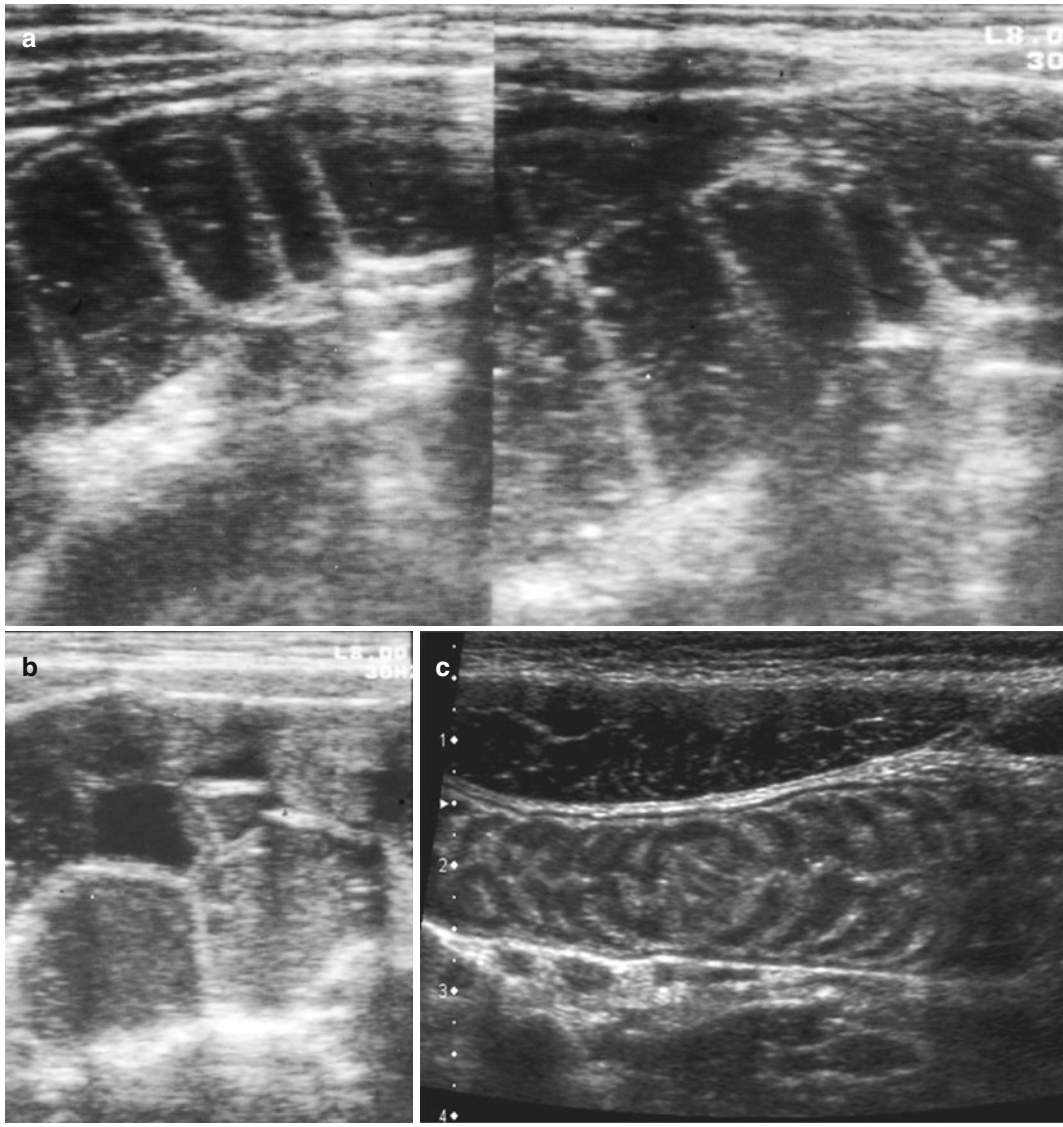


**Fig. 43** Several US appearances of gastroenteritis. (**a**, **b**) US images show dilated small bowel and colon without bowel wall thickening or ascites. (**c**) Prominent mucosal jejunal folds. Peristalsis was enhanced

of viral gastroenteritis, multiple air-filled and/or fluid-filled bowel loops, which usually display active peristalsis, can be observed on real-time US. Transient small bowel intussusceptions can be observed in patients with hyperperistalsis (Hayden 1996). The normal appendix is not usually seen due to the abundant interposed air. US differential diagnosis between gastroenteritis and appendicitis may be difficult because appendicitis may also produce associated dilatation of intestinal bowel loops due to adynamic or mechanical ileus, mostly in complicated cases. However, the absence of inflammatory secondary changes such as echogenic peritoneal fluid or enlarged omental fat makes the possibility of perforated appendicitis remote.

Acute terminal ileitis, or ileocecitis, is a bacterial enteritis limited to the ileocecal region. The term ileocecitis, as proposed by Puylaert et al. (1989), defines those bacterial infections that affect primarily the ileocecal region, clinically mimicking appendicitis. *Yersinia*, *Campylobacter*, and *Salmonella* are the most frequent infective organisms. In these cases, diarrhea is often absent or moderate. US diagnosis of these entities may avoid a significant number of unnecessary laparotomies. US findings include mural thickening of the terminal ileum, ileocecal valve, and cecum, as well as the presence of multiple enlarged mesenteric lymph nodes. The thickened ileum appears mostly hypoechoic due to the abundant mucosal lymphoid hyperplasia. This finding may help to differentiate acute infectious ileitis from Crohn disease, which characteristically exhibits a transmural inflammatory thickening. In both entities inflammation often extends along the proximal colon, giving rise to a prominent haustral pattern on the longitudinal view ("accordion" sign) (Fig. 44). In many cases the appendix cannot be visualized. Nevertheless, the exclusion of appendicitis is justified when US reveals pathology other than lymph nodes that could explain the patient's symptoms (Puylaert et al. 1989). Crohn disease may also be confused with bacterial infection of the ileocecal region. In this case no surgical dilemma will ensue since appendectomy is not indicated in either case (Puylaert et al. 1989).

## 8 Inflammatory Bowel Disease

Crohn disease may affect any part of the gastrointestinal tract, with the ileocecal region being the most commonly involved area. In children, 20 % of Crohn disease cases present with acute abdominal pain mimicking acute appendicitis (Hayes 2004). Only rarely Crohn disease may involve the appendix. Parietal inflammation is often discontinuous in Crohn disease with areas of preserved normal bowel wall, producing "skip lesions." Another characteristic of the disease is the transmural inflammation extending through all layers of the intestinal wall and also involving the mesentery (Valette et al. 2001). Axial US scans show a target image related to the stratified transmural thickening of the bowel wall usually involving the distal ileum and proximal colon, as well as an enlargement and increased echogenicity of the mesentery and omental fat. The transmural pattern of the disease is often associated with an irregular thickening of the submucosa and muscular layers. The involved segment appears rigid and displays no peristalsis on US (Fig. 45) (Hayes 2004). Ileal transmural wall thickening and inflammation of the surrounding fatty tissue aid the distinction between Crohn and infectious terminal ileitis (Puylaert 2001). Characteristic CT findings include terminal ileal thickening with or without a target sign enhancement pattern on contrast-enhanced CT, fibrofatty proliferation of the ileal mesentery, reactive adenopathy, and perienteric sinus tracts and mesentery abscesses in cases of severe extramural inflammation (Birnbaum and Jeffrey 1998). When Crohn disease involves the appendix, the inflamed appendix usually appears collapsed with transmural thickening of the wall.

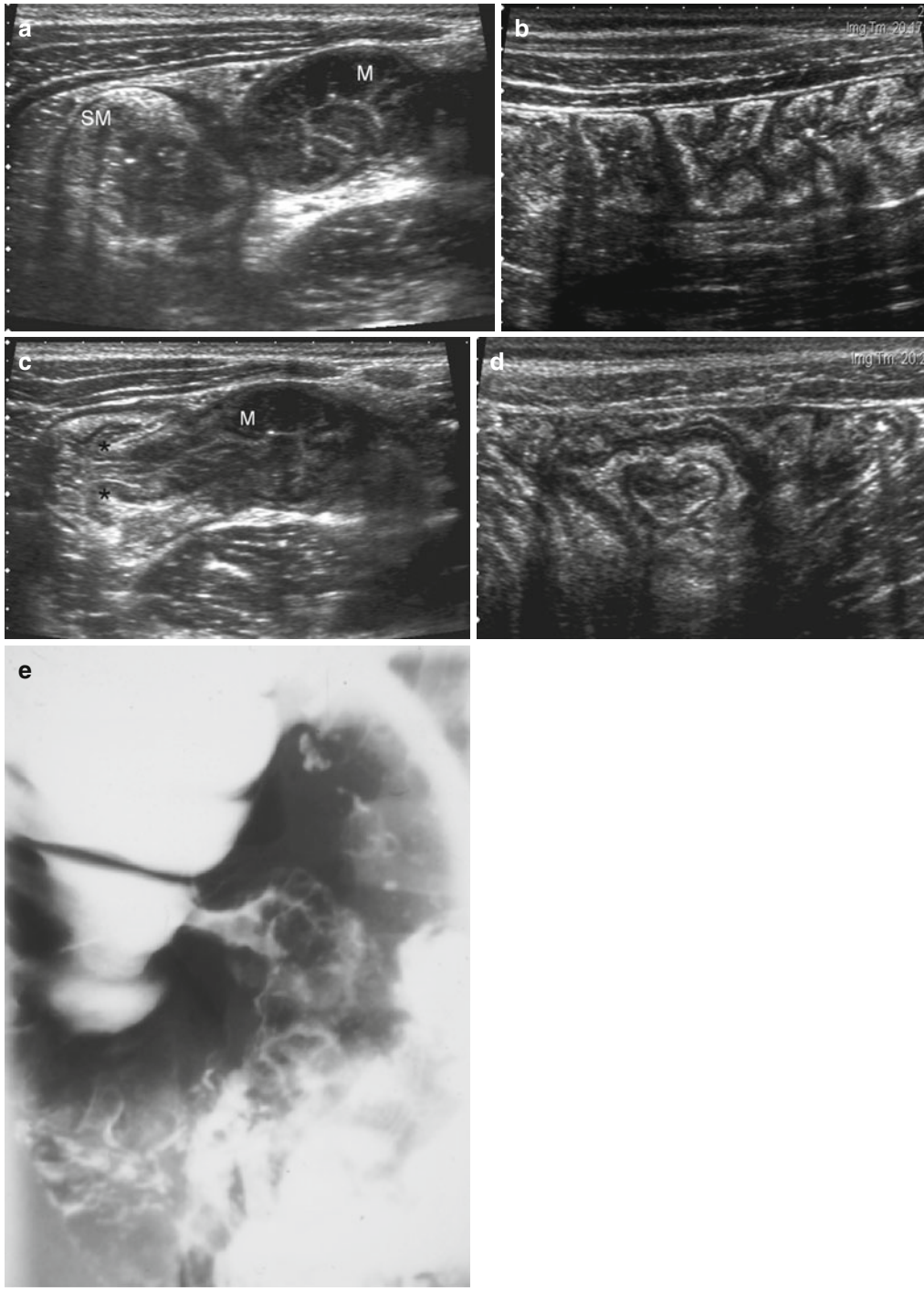


**Fig. 44** Ileocecitis due to *Yersinia enterocolitica* infection. (**a**–**d**); US images at the right iliac fossa show thick-walled bowel representing the ascending colon, terminal ileum, and ileocecal valve. (**a**) Axial US scan. There is mural stratification with a predominant bright submucosa in the colonic wall (*SM*) and lymphoid hyperplasia of the mucosa within the terminal ileum (*M*). (**b**) Longitudinal US scan showing the "accordion" sign in the ascending colon. (**c**, **d**) Longitudinal and axial US scans depicting the thickened ileocecal valve (*asterisks*). (**e**) Barium examination shows nodularity of the terminal ileum

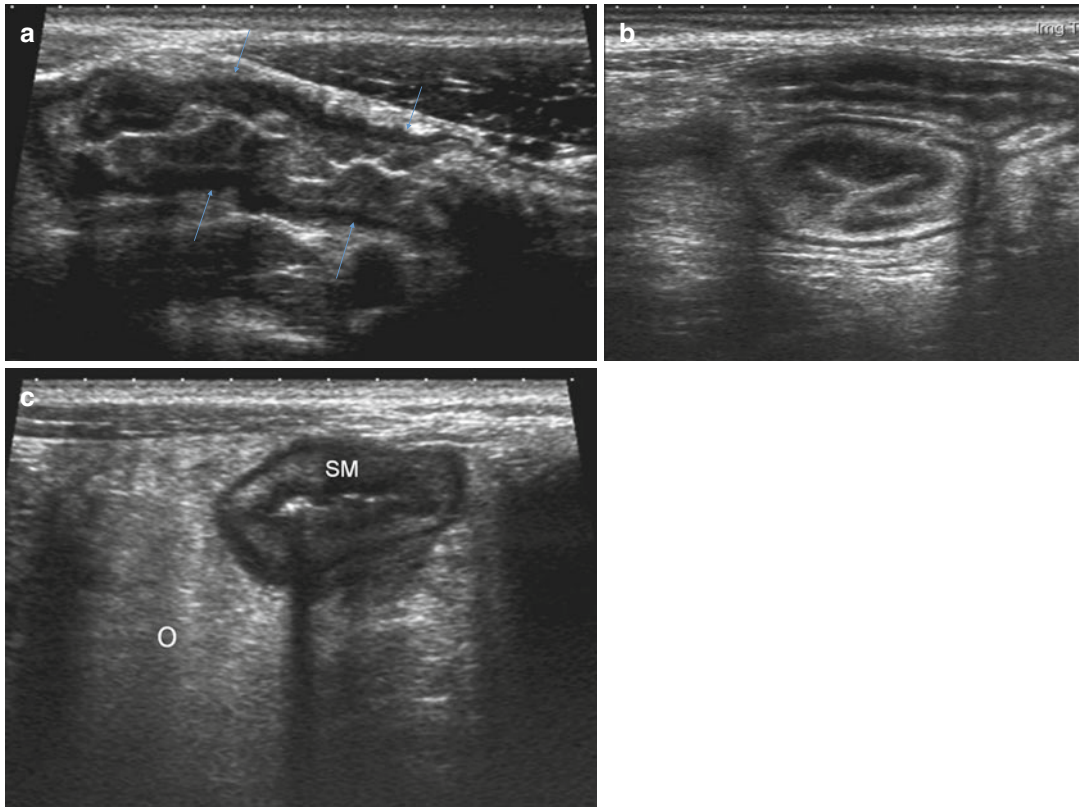


**Fig. 45** Crohn disease. (**a**) Longitudinal US scan of the terminal ileum (*arrows*) shows irregular transmural wall thickening with mucosal surface discontinuity. Mural stratification is lost in some areas. (**b**, **c**) Axial US scans show a target image with stratified transmural thickening, as well as hyperechogenicity of the enlarged omental fat (*O*). The hyperechoic submucosa (*SM*) is enlarged, helping to make the distinction with acute infectious ileitis

## 9 Henoch-Schönlein Purpura

Henoch-Schönlein syndrome (HSP), or anaphylactoid purpura, is a vasculitic disease of unknown origin although it is possibly secondary to viral-induced, allergic, or hypersensitive reactions. HSP usually occurs in children under 10 years old and may involve the skin, joints, gut, and/or kidney. More than 50 % of cases have abdominal symptoms, which may precede the cutaneous rash and cause a diagnostic dilemma (Hayden 1996). On US, different degrees of localized or diffuse involvement can be observed in the small bowel loops. Symmetrical transmural thickening of the bowel wall secondary to submucosal edema and hemorrhage is often seen (Hayden 1996) (Fig. 46). Luminal bowel narrowing and significant amounts of ascites may be present. Transient small bowel intussusceptions can also be observed. In general, the condition is a self-limiting process with a good clinical outcome.

## 10 Mesenteric Lymphadenitis

Mesenteric lymphadenitis is a consequence of an enteric infection, usually viral, that predominantly affects mesenteric lymph nodes. It is the most frequent diagnosis in children who are found to have a normal appendix at surgery.

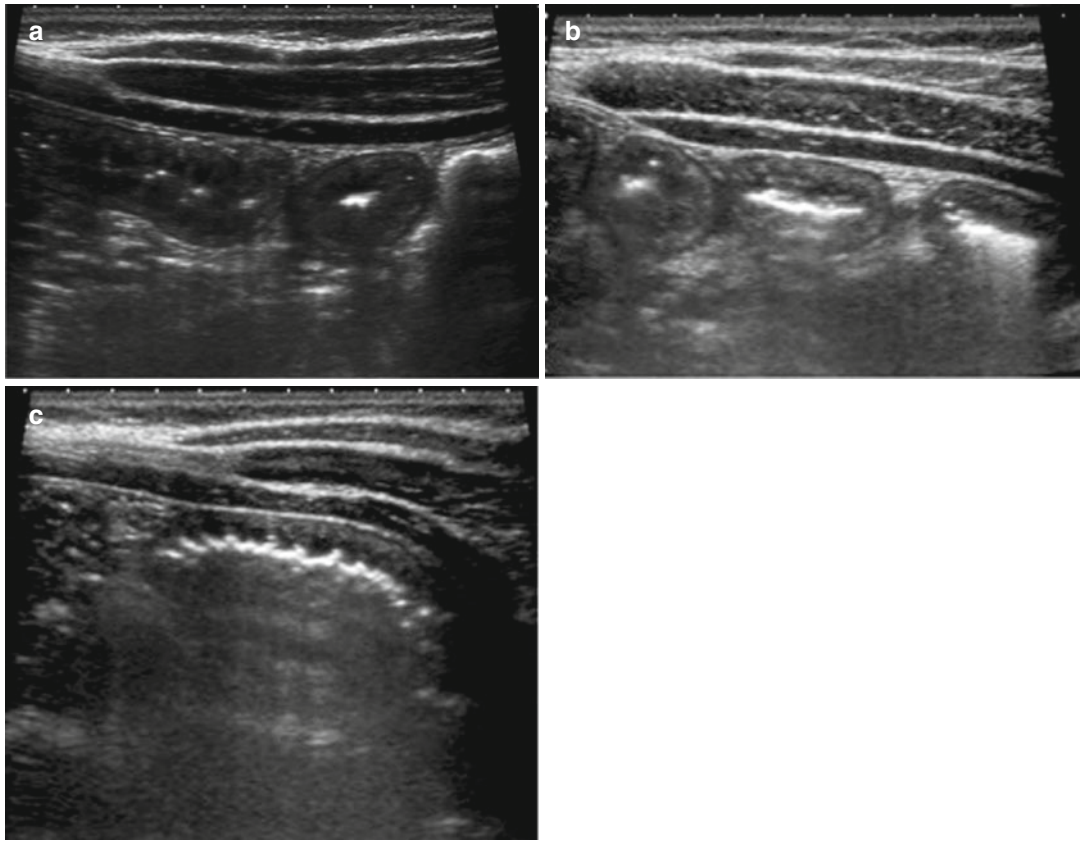


**Fig. 46** Henoch Schonlein Purpura. (**a**–**c**) Sonography shows symmetrical and continuous transmural small bowel wall thickening and ill-defined wall layers in a number of small bowel loops. The colon was normal

Mesenteric lymphadenitis is a self-limiting process. Mesenteric lymph nodes located in the central abdomen, or less frequently at the RLQ, are visualized on US as oval, hypoechoic lesions that are increased in number and size (Fig. 47a). In nearly 25 % of asymptomatic patients, more than five lymph nodes can be observed (Wiersma et al. 2005). Otherwise, a short-axis diameter of 8 mm on CT and 10 mm on US has been proposed as the upper limit for normal mesenteric lymph node size (Karmazyn et al. 2005; Wiersma et al. 2005). Lymphadenopathy due to the normal immunization process can be seen in almost 50 % of asymptomatic children as well as associated with multiple abdominal and pelvic disorders. Increased color Doppler flow in otherwise tender enlarged lymph nodes reflects its abnormal nature (Fig. 47b). Although exuberant blood flow can be demonstrated in inflamed lymph nodes, it is a nonspecific finding that can not differentiate the cause of the inflammation (Hayden 1996). On the other hand, moderately enlarged mesenteric lymph nodes can be seen associated with appendicitis in about half of the cases (Puylaert 1990). These nodes are rarely prominent, but when they occur, a diagnosis of mesenteric lymphadenitis cannot be established, except when a normal appendix is unequivocally identified. Therefore, mesenteric adenitis is an exclusion diagnosis that can only be established when appendicitis and other digestive pathologies are excluded.

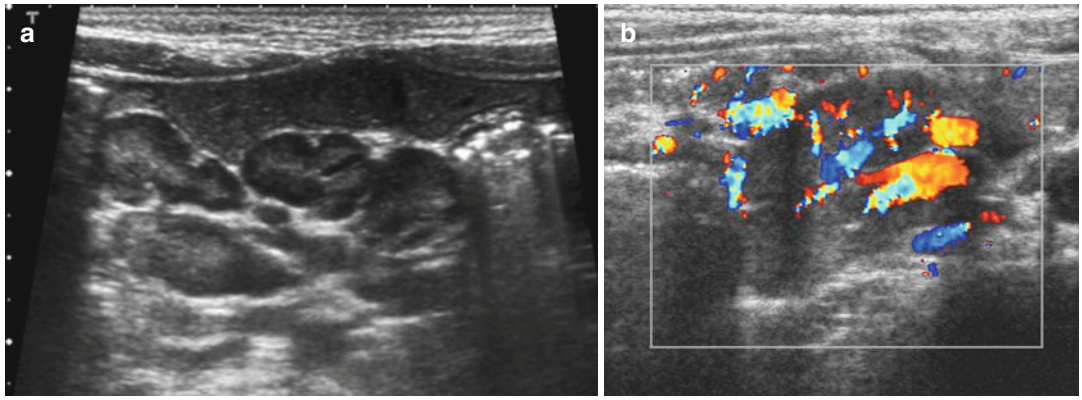


**Fig. 47** Mesenteric lymphadenitis. (**a**) US image shows multiple enlarged mesenteric lymph nodes in the mesogastrium. The appendix was normal. (**b**) No normal Doppler signal but increased flow reflecting hyperemia

## 11 Primary Fat Epiploic Lesions: Right Segmental Omental Infarction and Epiploic Appendagitis

Epiploic appendagitis and omental infarction are benign self-limiting conditions that are more frequent than initially reported. Both disorders frequently mimic symptoms of an abdominal surgical emergency, often leading to clinical misdiagnosis of appendicitis. Discriminating between either condition is of no practical relevance in children since treatment and prognosis are identical (van Breda Vriesman and Puylaert 2002). Spontaneous and complete resolution of symptoms, typically within 2 weeks, is the rule. Obesity seems to be an important risk factor for primary omental torsion in children. Varjavandi et al. (2003) postulated that the increased fat deposition in obese children outstrips the blood supply to the developing omentum. This could lead to either relative ischemia as the inciting event, increased omental weight leading to torsion, or traction to the most distal parts of the omentum. On gray-scale US and color Doppler US, the most frequent appearance is that of a hyperechoic mass containing poorly defined nodular or linear hypoechoic areas with few vessels within the mass and sometimes hyperemia in the peripheral area. The hyperechoic area corresponds to preserved omental tissue with edema and vascular congestion, the avascular hypoechoic areas corresponding to infarcted tissue (Baldisserotto et al. 2005). Sometimes a progressive increased attenuation is detected in the fatty mass (Fig. 48). Small amounts of free peritoneal fluid between the bowel loops and in the pelvic cul-de-sac are routinely observed (Theriot et al. 2003). The lesion is more conspicuous on CT studies, appearing as a well-circumscribed fatty mass of inflamed omentum interspersed with hyperattenuating stripes and inflammatory stranding. The underlying colon, terminal ileum, and appendix remain unaffected (Birnbaum and Jeffrey 1998).

Epiploic appendices are pedunculated adipose structures protruding from the serosal surface of the colon. An epiploic appendix might incidentally undergo infarction because of torsion or spontaneous venous thrombosis. The condition has been called epiploic appendagitis (van Breda Vriesman and Puylaert 2002). It is considered, as is segmental omental infarction, a self-limiting process, with a nonoperative management. The hyperechoic inflamed appendage is often delineated by a hypoechoic ring on US scans. CT findings of a small pedunculated fat-attenuation mass with a hyperattenuating rim can differentiate epiploic appendagitis from the broader and poorly defined segmentary infarcted omentum mass (Birnbaum and Jeffrey 1998).

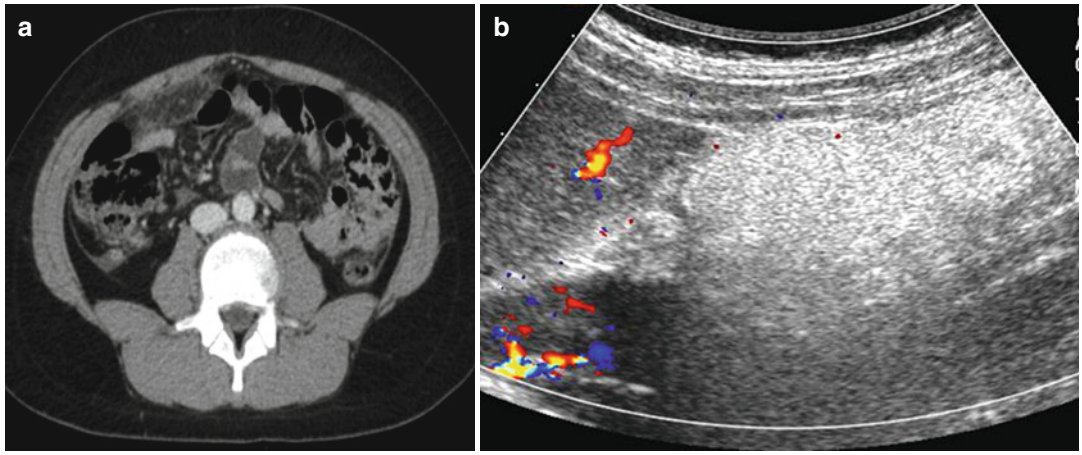


**Fig. 48** Omental infarction. (**a**) Axial CT image shows an area of fat stranding just under the right rectus abdominis muscle indicating inflamed mesenteric fat. (**b**) Another patient showing the hyperechoic mass inferior to the liver

## 12 Peritonitis

Peritonitis is often secondary to perforated appendicitis. Primary bacterial peritonitis is an inflammatory process of the peritoneum without an identifiable intra-abdominal source. Although this rare entity has been typically associated with underlying systemic processes such as nephrotic syndrome, liver failure, and the presence of a ventriculoperitoneal shunt catheter, primary bacterial peritonitis may also occur in otherwise healthy children. An US and CT finding of complex ascites is relatively nonspecific, most commonly thought to be associated with perforated appendicitis or a hollow viscus perforation. However, when the imaging findings of peritonitis are disproportionately greater than the degree of abnormal appendiceal changes or are associated with visualization of a normal appendix, the diagnosis of primary bacterial peritonitis should be considered. The diagnosis can be confirmed by paracentesis and demonstration of a single species of gram-positive cocci on stained smears, findings that would be highly unlikely to be caused by appendicitis. The demonstration of multiple bacterial species, especially if gram-negative bacilli are present, still warrants exclusion of hollow viscus perforation (Dann et al. 2005). Inflammation of the peritoneum caused by *Mycobacterium tuberculosis* can be produced by direct spread from gastrointestinal tuberculosis or after hematogenous dissemination from a pulmonary focus. On US and CT scans, the involvement of the omentum in peritoneal tuberculosis is often diffuse, unlike the focal involvement of the omentum in appendicitis or in omental infarction. Additional findings such as lymphadenopathy, involvement of the mesentery, bowel wall thickening, or loculated ascites suggest the diagnosis of gastrointestinal tuberculosis (van Breda Vriesman and Puylaert 2002).

Post-laparoscopic appendectomy complication (PLAC) has been reported as a complication of laparoscopic appendectomy that appears in children after an uneventful postoperative period. PLAC is characterized by RLQ abdominal pain and tenderness associated with US features and responsivity to antibiotic treatment. US findings described at hospital readmission are peritoneal fluid, edematous mesenteric fat, and thickening of the bowel wall. PLAC may be the result of a slow development of local interstitial infection in the ileocecal area due to mesothelial damage caused by $CO_2$ pneumoperitoneum and a local thermal effect produced by energized systems. This may explain its delayed appearance and the efficacy of the antibiotic treatment (Serour et al. 2005).

## 13 Hepatobiliary Causes of Acute Abdominal Pain

Hepatitis, focal hepatic lesions, and biliary pathology such as cholecystitis or biliary conditions more characteristic of childhood (hydrops, choledochal cyst) may also cause abdominal pain. Acute cholecystitis in children is relatively rare, but certain pediatric patients are prone to these diseases. Acute cholecystitis may be calculous or acalculous. The triad of right upper quadrant pain, vomiting, and fever is the usual clinical presentation (Huang and Yang 2011). Jaundice occurs in 25–45 % of patients probably secondary to inflammation around the bile duct. US should be the primary screening in patients with these symptoms. US findings include gallbladder wall thickening and distension and, sometimes, gallstones. A gallbladder wall thickness over 3 mm is abnormal, although it can be observed in many conditions unrelated to cholecystitis such as hypoalbuminemia, ascites, and portal hypertension. The ultrasonographic Murphy's sign (maximal tenderness over the sonographically localized gallbladder) is a useful secondary sign. The presence of intraluminal membranes and echoes with or without gallbladder wall irregularity may indicate hemorrhagic or gangrenous cholecystitis (Charalel et al. 2011).

Until recently, biliary lithiasis was considered infrequent in childhood, but the frequency of the diagnosis has been increasing. In children, up to 75 % of gallstones are pigmented stones. Their etiology is often unknown (Svensson and Makin 2012).

Symptom-free stones usually have a benign course and spontaneous resolution can occur. The most frequent clinical presentation is abdominal pain, with or without vomiting. Ultrasound is very accurate in the detection of calculi in the gallbladder, but less so in the intrahepatic and extrahepatic ducts (Fig. 49). Magnetic resonance cholangiopancreatography (MRCP) can be used when choledocholithiasis needs to be excluded and ultrasound is negative.

Choledochal cysts are localized dilatations of the biliary ductal system. Five types have been described: type I (80–90 %), dilatation of the common bile duct (IA cystic, IB focal, IC fusiform); type II, diverticulum; type III, choledochocele; type IV, multiple cysts (IVA intra- and extrahepatic, IVB extrahepatic); and type V (intrahepatic biliary cyst) corresponding to Caroli disease. The pathogenesis is related to an anomalous relation of the common bile duct and the pancreatic duct, which allows reflux of pancreatic secretion into the biliary tree. It is more frequently seen in female and Asian infants. It may be found in all ages from neonate to adult, but is now frequently discovered during prenatal sonogram (Diao et al. 2012). Prenatally diagnosed choledochal cyst is a distinct group with a tendency of developing liver fibrosis immediately after birth. Early surgical intervention is warranted in the neonatal period. Clinical symptoms include episodic abdominal pain, jaundice, and a right upper quadrant mass. At US and MRCP this appears as a cyst in the porta hepatis, separated from the gallbladder and communicating with the biliary ductal system (to differentiate extrahepatic biliary atresia) (Fig. 50). Complications include cholelithiasis, choledocholithiasis, pancreatitis, malignant degeneration, and cirrhosis.

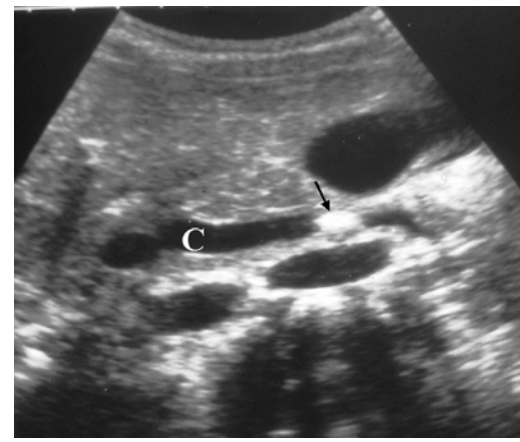


**Fig. 49** Choledocholithiasis presenting as an acute abdomen in an 8-year-old boy. US scan demonstrates a calculus (*arrow*) in the distal common bile duct (*C*) producing dilatation of the proximal component

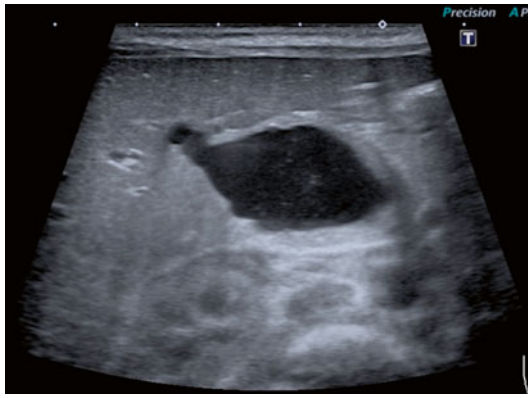


**Fig. 50** Choledochal cyst. Transverse US scan through the liver shows a cystic mass in the porta hepatis. Hepatobiliary scintigraphy confirmed communication of the cystic structure with the biliary system

## 14 Acute Pancreatitis

Acute pancreatitis is an uncommon clinical entity in children that is caused by a wide variety of etiological agents, the most common of which is blunt abdominal trauma. Other causes include viral infections, drugs, and hereditary abnormalities. Clinical presentation depends on the severity of the disease, but abdominal pain is invariable. Other symptoms are vomiting, fever, jaundice, and an abdominal mass if a pseudocyst is present. When pancreatitis is suspected in a child, US should be the primary imaging investigation (Darge and Anupindi 2009). The most common US finding is diffuse or focal glandular enlargement and decreased echogenicity, with poorly defined borders (Fig. 51). Dilatation of the pancreatic duct may be present. In cases of mild pancreatitis, the pancreas may appear normal on US. CT or MRI is usually reserved for patients with complications, especially those requiring intervention. CT shows diffuse pancreatic enlargement, heterogeneous attenuation, a poorly defined pancreatic contour, and peripancreatic fluid collections, which are most commonly found in the anterior pararenal space and lesser sac (Lautz et al. 2012). More than one third of patients with acute pancreatitis have an initially normal CT. MRI should be preferred to CT when available because of the lack of ionizing radiation. Pseudocyst formation is the most common complication of the acute pancreatitis and they are the most usual type of cysts occurring in the pancreas. Pseudocysts may be extrapancreatic (usually in the lesser sac) or intrapancreatic and generally require at least 4 weeks following an episode of acute pancreatitis. On US they appear as anechoic structures with well-defined borders and posterior reinforcement (Fig. 52). These lesions are usually homogeneous and of water signal intensity on T1-weighted and T2-weighted images (Ly and Miller 2002). Pancreatic abscesses can have imaging features similar to pseudocysts, but may be distinguished by means of the clinical history or when there is air within the collection (Balthazar 2002; Darge and Anupindi 2009) (Fig. 53).

## 15 Renal Causes of Acute Abdominal Pain

Renal causes of abdominal pain include upper urinary tract infection, particularly pyelonephritis, renal colic produced by a stone in the urinary tract, and pelviureteric junction obstruction. Urinary tract infections, which are usually related to vesicoureteral reflux, may cause symptoms similar to those of IT, mostly in young children. In most of these cases, the US is normal and only when there is a high-grade reflux (grades III–IV) may pyelocaliceal dilatation point to the correct urological origin of the pain. When evident, foci of infection are often hypoechoic with focal loss of the corticomedullary differentiation (Brader et al. 2008). A renal abscess appears as a heterogeneous mass lesion with central necrosis. Structural abnormalities of the urinary tract that may be found in children presenting with infection include duplex systems, renal ectopia, horseshoe kidney, and renal malrotation (Caiulo

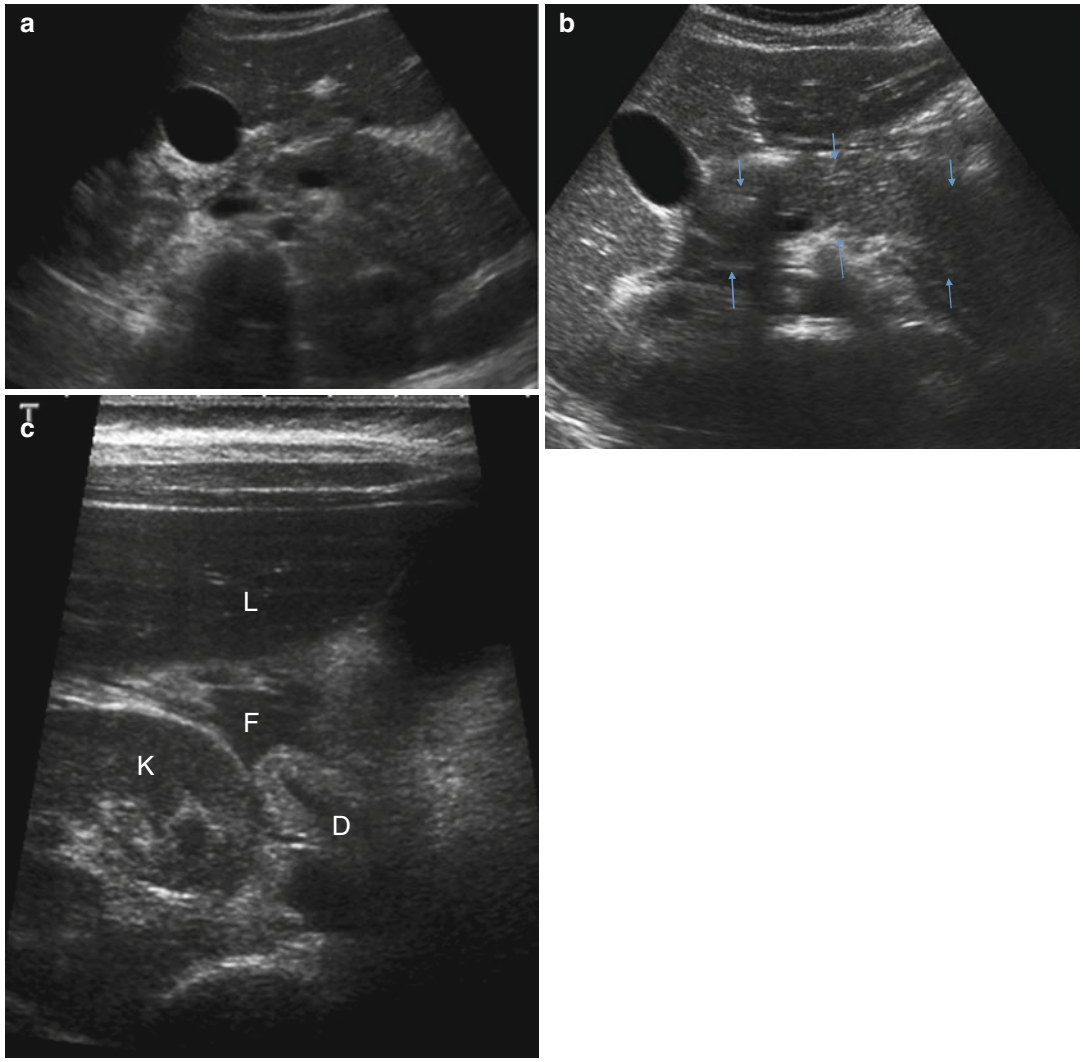


**Fig. 51** Diffuse acute pancreatitis. (**a**) and (**b**) Transverse US scan through the pancreas shows this to be globally enlarged. (**c**) Retroperitoneal fluid surrounding the second duodenal portion. This is an extremely helpful finding when suspecting acute pancreatitis. In children a normal or inflamed pancreas can demonstrate similar hypoechogenicities given the paucity of fat in the normal paediatric pancreas. The hepatic hypoechogenity linked to fasting and vomiting can also makes assessing pancreatic echogenicity challenging. *D* duodenum, *K* Kidney, *L* Liver, *F* Retroperitoneal fluid

et al. 2012). A VCUG is indicated in children presenting with an acute urinary tract infection, but should not be performed during acute phase. The child should remain on antibiotic prophylaxis and the VCUG should be done as a planned investigation (Pennington and Zerin 1999).

Renal lithiasis (stones, calculi) are more common in infants than in older children, and 20 % of cases manifest as renal colic. Underlying causes are multiple with *Proteus* being the most common pathogen. The role of imaging is to diagnose lithiasis, to detect any underlying anatomical

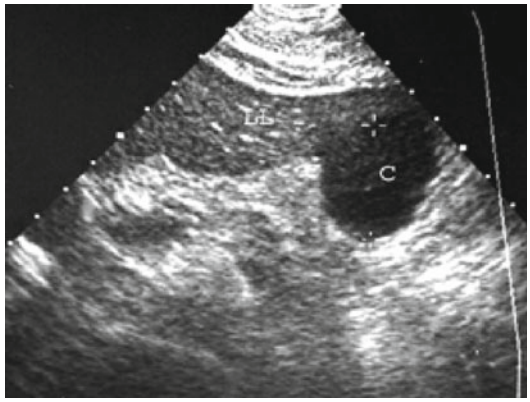


**Fig. 52** Pancreatic pseudocyst. Transverse US scan through the pancreas shows a cystic mass (*C*) with posterior acoustic enhancement just anterior to the pancreatic tail. *LL* left lobe of liver

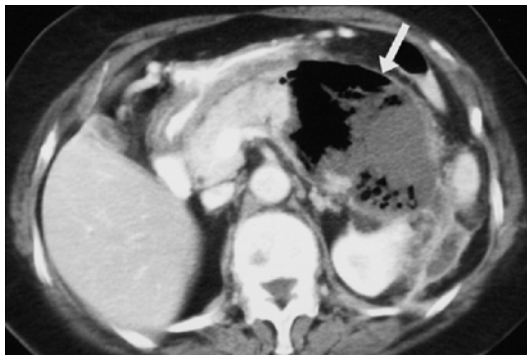

**Fig. 53** Pancreatic abcess. CT axial image showing a complex air containing fluid collection in the pancreatic tail (*arrow*)

abnormality, and to demonstrate the effect on the urinary tract so that treatment can be appropriate. Renal lithiasis can be detected radiographically or sonographically. The latter method may also substantiate the presence of obstructive uropathy and in many cases it may demonstrate its level and etiology. A calculus manifests as a hyperechoic area with acoustic shadowing located within the pelvicaliceal system or ureter (Fig. 54). In suspected obstruction by a calculus, US examination should include the kidneys, ureters, and bladder to determine the level of obstruction. On plain abdominal radiographs calculi are seen as radiopacities in the renal areas, the line of the ureters, or the bladder region. Differential diagnosis includes an appendicolith, an intracolic foreign body, a calcified ovarian mass, or an adenopathy. CT should not be used as a routine investigation tool due to its associated radiation dose; however, it is useful in patients with renal colic and a negative US study and in patients with US findings suggestive of ureteric obstruction in which US failed to demonstrate the calculus. In such cases, a non-contrast, low-dose CT scan usually allows demonstration of the stone, even a non- or poorly radiopaque stone (Moş et al. 2010).

Pelviureteric junction obstruction may be detected on prenatal US or on US examination of infants who have a urinary tract infection; however, a significant proportion of cases present later in childhood with abdominal pain. US demonstrates a dilated renal collecting system with no associated dilated ureter. There are multiple hypoechoic cystic spaces, the largest being medial and representing the dilated pelvis. The cysts intercommunicate and the infundibula and calyces, as well as surrounding renal parenchyma, can usually be identified (Ward et al. 1998). In severe cases the distended renal pelvis has a classically convex contour (Fig. 55). The patient should be well hydrated at the time of examination. Following an US diagnosis of pelviureteric junction obstruction, the patient should have a Mag 3 renogram after IV furosemide to assess the degree of obstruction and the relative filtration of the obstructed kidney. The excretion curves that are generated during this examination provide useful information regarding the degree of obstruction. They also provide a useful baseline for future follow-up in patients in whom immediate surgical treatment of their obstruction is not warranted. However, this imaging modality is being substituted by MR urography if facilities are available (Riccabona 2010). Most patients with severe pelviureteric junction obstruction are surgically treated with a dismembered pyeloplasty, while those with mild or moderate pelviureteric junction obstruction are followed up with periodic US.

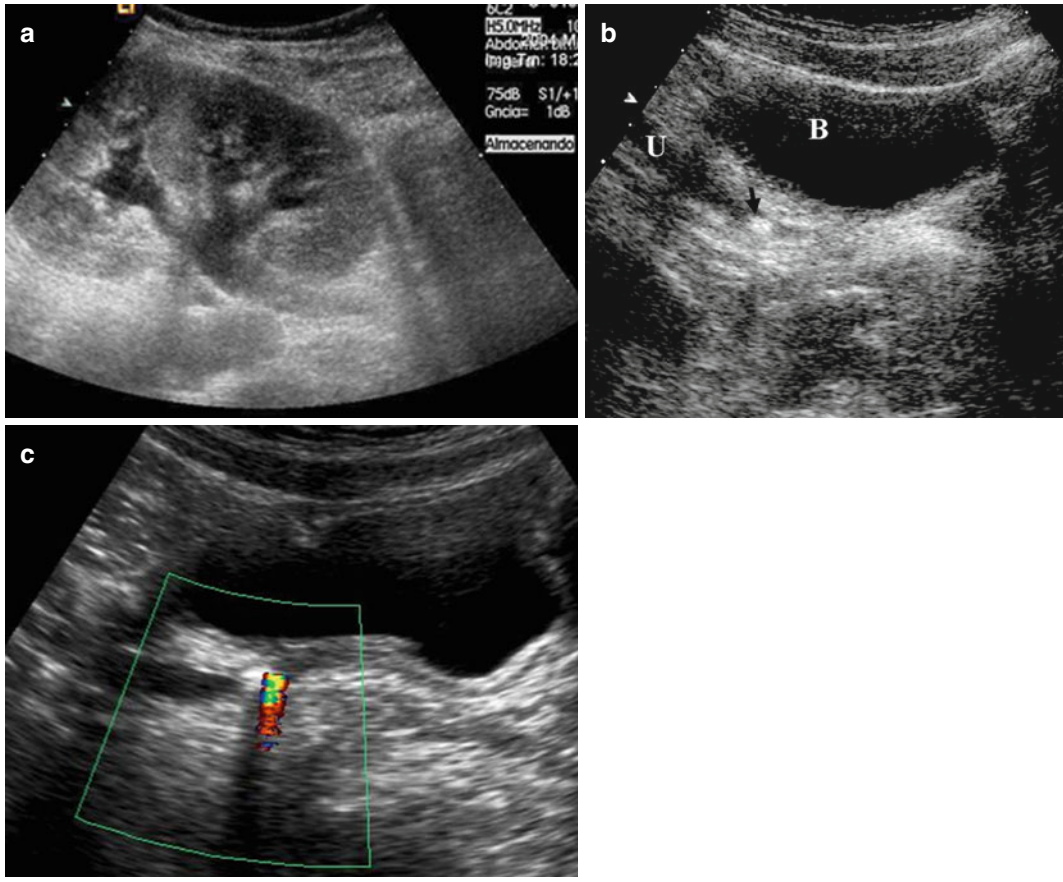


**Fig. 54** (**a**, **b**) Calculus in the distal ureter. Longitudinal US scan through the right kidney shows a dilated collecting system from a calculus (*arrow*) in the distal right ureter (*U*), bladder (*B*). (**c**) Sonographic twinkling demonstrated on interrogation with colour doppler

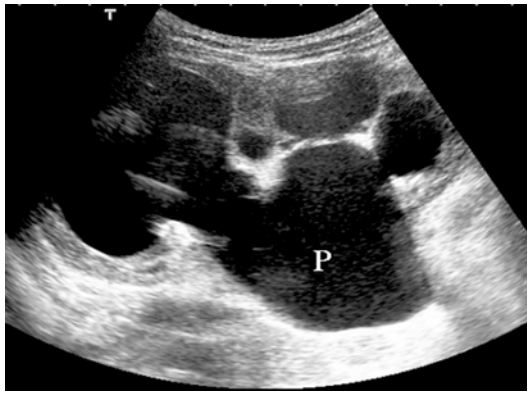


**Fig. 55** Uteropelvic junction obstruction. Longitudinal US scan of the right kidney demonstrates dilated calyces communicating with a markedly dilated renal pelvis (*P*). No dilated ureter is identified

## 16 Gynecological Causes of Acute Abdominal Pain

The main gynecological conditions causing acute abdominal pain are functional ovarian cysts, ovarian torsion, and hydrometrocolpos. Transabdominal US will commonly show the culprit pathology. Transvaginal US should not be routinely done as a primary investigation in adolescent girls but may supplement the abdominal examination in sexually active teenagers. Ovarian cysts usually result from failure of involution during the normal menstrual cycle. They may cause acute lower abdominal or pelvic pain in prepubertal and pubertal girls if they are complicated by rupture, torsion, or hemorrhage

or if they become significantly enlarged. Transabdominal US in uncomplicated cysts usually show a thin-walled, well-defined, echo-free ovarian mass and excellent through-transmission (Carty 2002). Simple cysts may be quite large, but most of them resolve spontaneously, only requiring clinical and sonographic follow-up. Rarely, there is a complication, the most common being ovarian torsion. Functional cysts may also rupture and result in free fluid in the pelvis. Despite the high frequency of presentation of these cysts, they should not be assumed to be the cause of the acute symptoms until other pathologies, especially appendicitis, have been excluded. Functional cysts may develop internal hemorrhage. Hemorrhagic ovarian cysts typically present with sudden and severe lower abdominal pain. On US, they may appear echogenic or hypoechoic (Fig. 56). Most of them are heterogeneous in echogenicity and show through-transmission due to their underlying cystic nature. They may contain internal clots, septations, as well as fluid-debris levels. The cyst wall may be thin or thick and irregular. A changing US appearance over time can help make the diagnosis. The initial bright echogenicity of acute hemorrhage, produced by fibrin deposition, becomes less echogenic and eventually fluidlike as the fibrin dissolves and the clot lyses (Yilmaz et al. 2001). A complex cystic ovarian mass may often be treated conservatively, particularly if there are no features suggesting the presence of torsion. In these cases, US follow-up is necessary until complete resolution.

In adnexal torsion, the ovary twists with the vascular pedicle. Ovarian torsion initially leads to impairment of lymphatic and venous drainage, later followed by arterial occlusion and thrombosis and eventually hemorrhagic infarction of the involved organ. It is most common in prepubertal girls, due to the increased adnexal mobility prior to menarche. Torsion is more common on the right side since the sigmoid colon prevents excessive movement of the left ovary and fallopian tube. Ovarian torsion is a surgical emergency that may clinically mimic acute appendicitis, gastroenteritis, or IT. The pain may be intermittent and localized to one of the lower quadrants, or it may be severe, acute, and generalized. Associated nausea, vomiting, or constipation may occur. A palpable abdominal mass and a paralytic ileus may also be present. US is the most important imaging modality for the diagnosis of adnexal torsion. The US findings are variable, but often the involved/affected ovary appears noticeably enlarged, with multiple enlarged peripheral follicles (Nizar et al. 2009) (Fig. 57), and it is

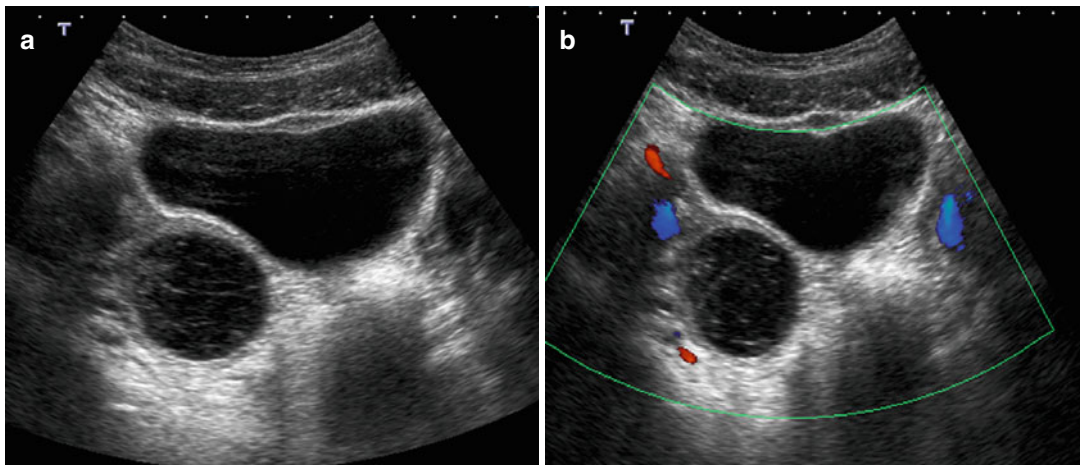


**Fig. 56** Symptomatic haemmorhagic ovarian cyst. (**a**) Complex cystic mass containing echoes located deep to the bladder. (**b**) No flow is identified on interrogation with colour doppler

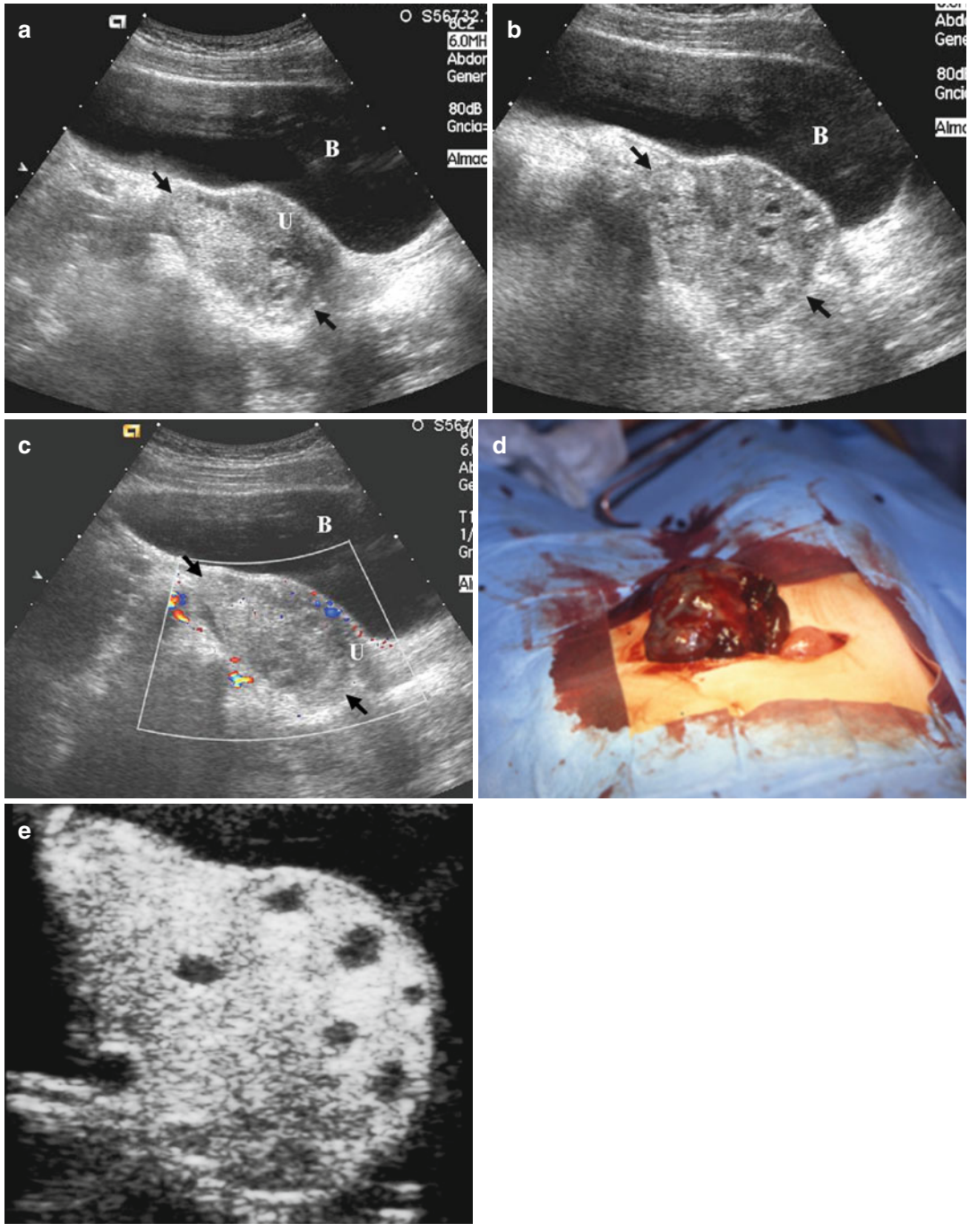


**Fig. 57** Ovarian torsion: (**a**, **b**) Longitudinal US scan shows an echogenic mass with tiny cysts behind the uterus (*U*). The small prepubertal uterus is displaced anteriorly; difficult to delineate separately from the mass (*arrows*). (**c**) Colour Doppler image showing the absence of flow in the center of the ovary. (**d**) Surgical specimen. (**e**) In vitro US study of the ovary. Multiple edematous immature follicles are visualized in the ovary both peripherally and centrally. *B* Bladder

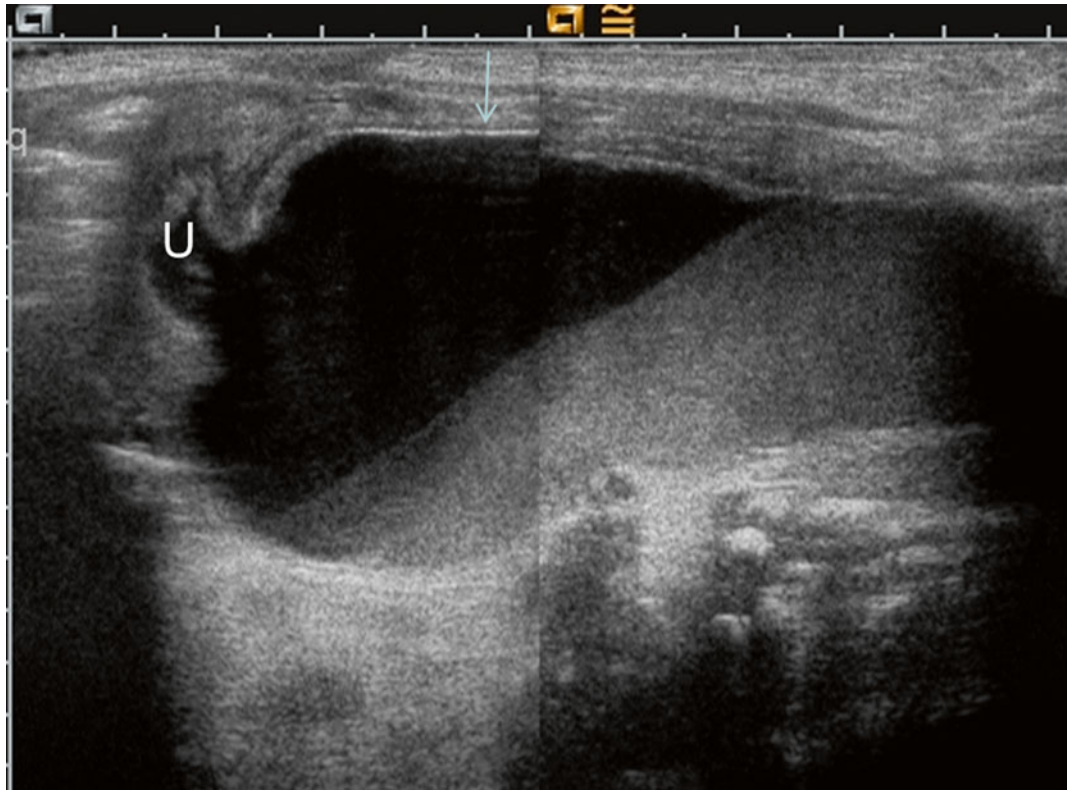


**Fig. 58** Hydrocolpos due to an imperforate hymen. Longitudinal US image in a neonate showing a dilated vagina with a fluid/fluid level (*arrow*). *U* uterus

difficult to delineate it from the small uterus, which is often anteriorly displaced. This occurs in 60–75 % of the cases of torsion in a previously normal ovary. However, the ovarian appearance may vary depending on the degree of internal hemorrhage, stromal edema, and infarction that have occurred by the time it is diagnosed. Other grayscale imaging appearances include a purely cystic, a mixed cystic-solid, or a solid adnexal mass lesion particularly when underlying ovarian pathology is present, which occurs rarely. Fluid may be present in the pouch of Douglas. Doppler studies may demonstrate absent or reduced central venous and arterial flow. However, complete absence of Doppler signal alone is not a specific finding as flow may be difficult to obtain even in normal ovaries. In addition, low-velocity peripheral arterial flow (less than 5 cm/s) may persist due to dual ovarian blood supply. The presence of dampened arterial and venous flow or absent arterial with a dampened venous flow has also been described in ovarian torsion (Nizar et al. 2009). Doppler US may be normal in intermittent or incomplete torsions.

Pelvic inflammatory disease is increasing in incidence in sexually active adolescents and is due to either *Chlamydia trachomatis* or *Neisseria gonorrhoeae* infection. Infection ascends from the cervix to involve the endometrium and fallopian tubes. The fallopian tubes become edematous and hyperemic and are filled with pus, which may spill over into the peritoneum causing peritonitis. If the fimbriated ends of the fallopian tubes become adherent to the ovaries, the tubes may obstruct and distend with fluid, resulting in a hydrosalpinx, or with pus resulting in a pyosalpinx. The infection may extend to the ovaries, resulting in a tubo-ovarian abscess. Clinically, patients with pelvic inflammatory

disease present with pelvic pain that may worsen during or just after menstruation. Dysfunctional uterine bleeding and dysuria may also appear. Ultrasound is the primary imaging modality, the sonographic findings varying according to the extent of the disease. Endometritis may lead to enlargement of the endometrium and fluid may be seen in the endometrial cavity. Pyosalpinx manifests as thickened and dilated fallopian tubes containing debris-laden fluid and septations. A tubo-ovarian abscess usually appears as a complex and heterogeneous adnexal mass, commonly accompanied by free fluid in the pouch of Douglas. Transvaginal US gives better anatomical detail of the inflamed adnexal structures and may obviate the need for laparoscopy in adolescents with pelvic inflammatory disease (Buchweitz et al. 2000). In severe cases, CT and MRI can be useful in demonstrating the extent of the disease throughout the abdomen and pelvis.

Genital tract obstruction may cause abdominal pain and amenorrhea in the adolescence and is usually due to an imperforate hymen but may also result from vaginal or cervical atresia. With an imperforate hymen, the menstrual products during menarche collect in the vagina and uterus, producing a hydrometrocolpos. In vaginal or cervical atresia, the products may collect in the fallopian tubes and broad ligament. The diagnosis is easily made on US when a fluid-filled vagina and dilated uterus are seen behind the bladder (Ayaz et al. 2011) (Fig. 58). It is not unusual that, after a urine culture for a suspected urinary tract infection, the patient will undergo US with an empty bladder. In these situations, special attention must be paid in order not to mistake a fluid-filled vagina for a full bladder. Identification of the dilated uterus in the cranial aspect of the cystic structure that occupies the pelvis can help make the correct diagnosis.

## References


Addiss DG, Shaffer N, Fowler BS et al (1990) The epidemiology of appendicitis and appendectomy in the United States. Am J Epidemiol 132(5):910–925

Applegate KE (2009) Intussusception in children: evidence-based diagnosis and treatment. Pediatr Radiol 39(Suppl 2):S140–S143

Ayaz UY, Dilli A, Api A (2011) Ultrasonographic diagnosis of congenital hydrometrocolpos in prenatal and newborn period: a case report. Med Ultrason 13(3):234–236

Babcock DS (2002) Sonography of the acute abdomen in the pediatric patient. J Ultrasound Med 21: 887–899

Bai YZ, Qu RB, Wang GD et al (2006) Ultrasound-guided hydrostatic reduction of intussusceptions by saline enema: a review of 5218 cases in 17 years. Am J Surg 192:273–275

Baldisserotto M, Marchiori E (2000) Accuracy of non-compressive sonography of children with appendicitis according to the potential positions of the appendix. AJR Am J Roentgenol 175:1387

Baldisserotto M, Maffazzoni DR, Dora MD (2005) Omental infarction in children: color Doppler sonography correlated with surgery and pathology findings. AJR Am J Roentgenol 184:156–162

Balthazar EJ (2002) Complications of acute pancreatitis: clinical and CT evaluation. Radiol Clin North Am 40:1211–1229

Berdon WE (1995) The diagnosis of malrotation and volvulus in the older child and adult: a trap for radiologists. Pediatr Radiol 25:101–103

Bernstein SM, Russ PD (1998) Midgut volvulus: a rare cause of acute abdomen in an adult patient. AJR Am J Roentgenol 171:639–641

Birnbaum BA, Jeffrey RB Jr (1998) CT and sonographic evaluation of acute right lower quadrant pain. AJR Am J Roentgenol 170:361–371

Birnbaum BA and Wilson SR (2000). Appencicitis at the millenium. Radiology 215:337–348

Blakely ML, Williams R, Dassinger MS et al (2011) Early vs interval appendectomy for children with perforated appendicitis. Arch Surg 146(6):660–665

Borushok FK, Jeffrey RB Jr, Laing FC et al (1990) Sonographic diagnosis of perforation in patients with acute appendicitis. AJR Am J Roentgenol 154: 275–278

Brader P, Riccabona M, Schwarz T, Seebacher U, Ring E (2008) Value of comprehensive renal ultrasound in children with acute urinary tract infection for assessment of renal involvement: comparison with DMSA scintigraphy and final diagnosis. Eur Radiol 18:2981–2989

Bramson RT, Blickman JG (1992) Perforation during hydrostatic reduction of intussusception: proposed mechanism and review of the literature. J Pediatr Surg 27:589–591

Bramson RT, Shiels WE II, Eskey CJ et al (1997) Intraluminal colon pressure dynamics with Valsalva maneuver during air enema study. Radiology 202:825–828

Brenner DJ, Hall EJ (2007) Computed tomography an increasing source of radiation exposure. N Engl J Med 357:2277

Brenner D, Elliston C, Hall E et al (2001) Estimated risks of radiation-induced fatal cancer from pediatric CT. AJR Am J Roentgenol 176:289

Buchweitz O, Malik E, Kressin P, Meyhoefer-Malik A, Diedrich K (2000) Laparoscopic management of tubo-ovarian abscesses: retrospective analysis of 60 cases. Surg Endosc 14(10):948–950

Butler M, Servaes S, Srinivasan A et al (2011) US depiction of the appendix: role of abdominal wall thickness and appendiceal location. Emerg Radiol 18(6): 525–531

Caiulo VA, Caiulo S, Gargasole C, Chiriacò G, Latini G, Cataldi L, Mele G (2012) Ultrasound mass screening for congenital anomalies of the kidney and urinary tract. Pediatr Nephrol 27(6):949–953

Caro P, Iqbal A, Donoghue V et al (2011) Interloop fluid in intussusception. Pediatr Radiol 41(11):1483

Carty HM (2002) Paediatric emergencies: non-traumatic abdominal emergencies. Eur Radiol 12:2835–2848

Ceres L, Alonso I, Lopez P et al (1990) Ultrasound study of acute appendicitis in children with emphasis upon the diagnosis of retrocecal appendicitis. Pediatr Radiol 20:258–261

Charalel RA, Jeffrey RB, Shin LK (2011) Complicated cholecystitis: the complementary roles of sonography and computed tomography. Ultrasound Q 27(3):161–170

Clark P, Ruess L (2005) Counterclockwise barber-pole sign on CT: SMA/SMV variance without midgut malrotation. Pediatr Radiol 35(11):1125–1127

Cobben LP, de Van Otterloo AM, Puylaert JB (2000) Spontaneously resolving appendicitis: frequency and natural history in 60 patients. Radiology 215:349–352

Cobben L, Groot I, Kingma L et al (2009) A simple MRI protocol in patients with clinically suspected appendicitis: results in 138 patients and effect on outcome of appendectomy. Eur Radiol 19(5):1175–1183

Cogley JR, O'Connor SC, Houshyar R et al (2012) Emergent pediatric US: what every radiologist should know. Radiographics 32(3):651–665

Collins DC (1932) The length and position of the vermiform appendix. A study of 4.680 specimens. Ann Surg 96:1044–1048

Cotran RS, Kumar V, Robbins SL (1989) Appendix. In: Saunders WB stall, (ed) Robbins pathologic basis of disease, 4th edn. Saunders, Philadelphia, pp 902–904

Daneman A, Alton DJ (1996) Intussusception. Issues and controversies related to diagnosis and reduction. Radiol Clin North Am 34:743–756

Daneman A, Navarro O (2004) Intussusception. Part 2: an update on the evolution of management. Pediatr Radiol 34:97–108

Daneman A, Alton DJ, Ein S et al (1995) Perforation during attempted intussusception reduction in children–a comparison of perforation with barium and air. Pediatr Radiol 25(2):81–88

Dann PH, Amodio JB, Rivera R et al (2005) Primary bacterial peritonitis in otherwise healthy children: imaging findings. Pediatr Radiol 35:198–201

Darge K, Anupindi S (2009) Pancreatitis and the role of US, MRCP and ERCP. Pediatr Radiol 39(Suppl 2): S153–S157

del- Pozo G (2005) Intussusception: still work in progress. Pediatr Radiol 35:92–94

del Pozo G, Sánchez L, Miralles M et al (1992) Appendicitis in children: usual and unusual appearances. Radiology 185:349–360. Supplement

del Pozo G, Miralles M, Sánchez L et al (1994) Apendicitis aguda en la infancia. Hallazgos ecográficos frecuentes e infrecuentes. Radiología 36:411–424

del-Pozo G, Albillos JC, Tejedor D (1996a) Intussusception: US findings with pathologic correlation. The crescent-in-doughnut sign. Radiol 199:688–692

del-Pozo G, González-Spinola J, Gómez-Ansón B et al (1996b) Intussusception: trapped peritoneal fluid detected with US-relationship to reducibility and ischemia. Radiol 201:379–386

del-Pozo G, Albillos JC, Tejedor D et al (1999) Intussusception in children: current concepts in diagnosis and enema reduction. RadioGraphics 19:299–319

Desai R, Cortese MM, Meltzer MI et al (2012) Potential intussusception risk versus benefits of rotavirus vaccination in the United States. Pediatr Infect Dis J 27

Diao M, Li L, Cheng W (2012) Timing of surgery for prenatally diagnosed asymptomatic choledochal cysts: a prospective randomized study. J Pediatr Surg 47:506–512

Doria AS, Moineddin R, Kellenberger CJ et al (2006) US or CT for diagnosis of appendicitis in children and adults? A meta-analysis. Radiology 241(1):83–94

Douglas CD, Macpherson NE, Davidson PM et al (2000) Randomised controlled trial of ultrasonography in diagnosis of acute appendicitis, incorporating the Alvarado score. BMJ 321(7266):919–922

Dugougeat F, Navarro O, Daneman A (2000) The role of sonography in children with abdominal pain after recent successful reduction of intussusception. Pediatr Radiol 30(9):654

Fiorella DJ, Donnelly LF (2001) Frequency of right lower quadrant position of the sigmoid colon in infants and young children. Radiology 219(1):91–94

Gallego C, del Pozo G, Marin C et al (1998) Torsion of a Meckel's diverticulum: sonographic findings. Pediatr Radiol 28:599–601

Goldin AB, Khanna P, Thapa M et al (2011) Revised ultrasound criteria for appendicitis in children improve diagnostic accuracy. Pediatr Radiol 41:993

Gonzalez-Spinola J, Del Pozo G, Tejedor D et al (1999) Intussusception: the accuracy of ultrasound-guided saline enema and the usefulness of a delayed attempt at reduction. J Pediatr Surg 34:1016–1020

Gray GF, Ashley P (1986) Surgical pathology of the vermiform appendix. In: Soumers SC, Rosen PP, Fechner RE (eds) Pathology annual, vol 21. Appleton-Century-Crofts, Norwalk, pp 111–144, Part 2

Gu L, Zhu H, Wang S et al (2000) Sonographic guidance of air enema for intussusception reduction in children. Pediatr Radiol 30:339–342

Guo JZ, Ma XY, Zhou QH (1986) Results of air pressure enema reduction of intussusception: 6,396 cases in 13 years. J Pediatr Surg 21:1201–1203

Hadidi AT, El Shal N (1999) Childhood intussusception: a comparative study of nonsurgical management. J Pediatr Surg 34(2):304–307

Hagendorf BA, Clarke JR, Burd RS (2004) The optimal initial management of children with suspected appendicitis: a decision analysis. J Pediatr Surg 39(6):880–885

Hahn HB, Hoepner FU, Kalle T, Macdonald EB, Prantl F, Spitzer IM, Faerber DR (1998) Sonography of acute appendicitis in children: 7 years experience. Pediatr Radiol 28(3):147–151

Hanquinet S, Anooshiravani M, Vunda A et al (1998) Reliability of color Doppler and power Doppler sonography in the evaluation of intussuscepted bowel viability. Pediatr Surg Int 13(5–6):360–362

Harswick C, Uyenishi AA, Kordick MF, Chan SB (2006) Clinical guidelines, computed tomography scan, and negative appendectomies: a case series. Am J Emerg Med 24(1):68–72

Hayden CK Jr (1996) Ultrasonography of the acute pediatric abdomen. Radiol Clin North Am 34:791–806

Hayes R (2004) Abdominal pain: general imaging strategies. Eur Radiol 14:L123–L137

Henderson J, Goldacre MJ, Fairweather JM (1992) Conditions accounting for substantial time spent in hospital in children age 1–14 years of age. Arch Dis Child 67:83–86

Henrikson S, Blane CE, Koujok K et al (2003) The effect of screening sonography on the positive rate of enemas for intussusception. Pediatr Radiol 33:190–193

Hernandez JA, Swischuk LE, Angel CA (2004) Validity of plain films in intussusception. Emerg Radiol 10(6):323–326

Hernanz-Schulman M (2010) CT and US in the diagnosis of appendicitis: an argument for CT. Radiology 255:3–7

Hershko DD, Awad N, Fischer D et al (2007) Focused helical CT using rectal contrast material only as the preferred technique for the diagnosis of suspected acute appendicitis: a prospective, randomised, controlled study comparing three different techniques. Dis Colon Rectum 50:1223–1229

Holgersen LO, Stanley-Brown EG (1971) Acute appendicitis with perforation. Am J Dis Child 122:288–293

Holscher HC, Heij HA (2009) Imaging of acute appendicitis in children: EU versus U.S. …or US versus CT? A European perspective. Pediatr Radiol 39:497–499

Holt S, Samuel E (1978) Multiple concentric ring sign in the ultrasonographic diagnosis of intussusception. Gastrointest Radiol 3:307–309

Hryhorczuk AL, Strouse PJ (2009) Validation of US as a first-line diagnostic test for assessment of pediatric ileocolic intussusception. Pediatr Radiol 39(10): 1075–1079

Hryhorczuk AL, Mannix RC, Taylor GA (2012) Pediatric abdominal pain: use of imaging in the emergency department in the United States from 1999 to 2007. Radiology 263(3):778–785

Huang SC, Yang YJ (2011) Septic shock and hypofibrinogenemia predict a fatal outcome in childhood acute acalculous cholecystitis. J Pediatr Gastroenterol Nutr 53:548–552

Ilivitzki A, Shtark LG, Arish K, Engel A (2012) Deep sedation during pneumatic reduction of intussusception. Pediatr Radiol 42(5):562–565

Iwahashi N, Kitagawa Y, Mayumi T et al (2005) Intravenous contrast-enhanced computed tomography in the diagnosis of acute appendicitis. World J Surg 29:83–87

Jacobs JE, Birnbaum BA, Macari M et al (2001) Acute appendicitis: comparison of helical CT diagnosis focused technique with oral contrast material versus nonfocused technique with oral and intravenous contrast material. Radiology 220:683–690

Jeffrey RB Jr, Laing FC, Lewis FR (1987) Acute appendicitis: high-resolution real-time ultrasound findings. Radiology 163:11–14

Jeffrey RB Jr, Laing FC, Townsend RR (1988) Acute appendicitis: sonographic criteria based on 250 cases. Radiology 167:327–329

Jen HC, Shew SB (2009) The impact of hospital type and experience on the operative utilization in pediatric intussusception: a nationwide study. J Pediatr Surg 44:241–246

Johnson JF, Coughlin WF (1989) Plain film diagnosis of appendiceal perforation in children. Semin Ultrasound CT MR 10:306–313

Johnson PT, Horton KM, Kawamoto S et al (2009) MDCT for suspected appendicitis: effect of reconstruction section thickness on diagnostic accuracy, rate of appendiceal visualization, and reader confidence using axial images. AJR Am J Roentgenol 192(4): 893–901

Johnson AK, Filippi CG, Andrews T et al (2012) Ultrafast 3-T MRI in the evaluation of children with acute lower abdominal pain for the detection of appendicitis. AJR Am J Roentgenol 198(6):1424–1430

Kaiser S, Frenckner B, Jorulf HK (2002) Suspected appendicitis in children: US and CT–a prospective randomized study. Radiology 223:633–638

Kaiser S, Finnbogason T, Jorulf HK et al (2004) Suspected appendicitis in children: diagnosis with contrast-enhanced versus nonenhanced helical CT. Radiology 231:427–433

Karmazyn B, Werner EA, Rejaie B et al (2005) Mesenteric lymph nodes in children: what is normal? Pediatr Radiol 35:774–777

Katz ME, Kolm P (1992) Intussusception reduction 1991: an international survey of pediatric radiologists. Pediatr Radiol 22:318–322

Katz M, Phelan E, Carlin JB et al (1993) Gas enema for the reduction of intussusception: relationship between clinical signs and symptoms and outcome. AJR Am J Roentgenol 160:363–366

Keyzer C, Tack D, Bohy P et al (2004) Acute appendicitis: comparison of low-dose and standard-dose unenhanced multi-detector row CT. Radiology 232: 164–172

Khanna G, Applegate K (2008) Ultrasound guided intussusception reduction: are we there yet? Abdom Imaging 33:38–40

Kharbanda AB, Taylor GA, Bachur RG (2007) Suspected appendicitis in children: rectal and intravenous contrast-enhanced versus intravenous contrast-enhanced CT. Radiology 243:520–526

Kim HC, Yang DM, Jin W et al (2008) Added diagnostic value of multiplanar reformation of multidetector CT data in patients with suspected appendicitis. RadioGraphics 28(2):393–405

Kim K, Kim YH, Kim SY et al (2012) Low-dose abdominal CT for evaluating suspected appendicitis. N Engl J Med 366(17):1596–1605

Kimmey MB, Martin RW, Haggitt RC et al (1989) Histologic correlates of gastrointestinal ultrasound images. Gastroenterology 96:433–441

Kirks DR (1994) Diagnosis and treatment of pediatric intussusception: how far should we push our radiologic techniques? Radiology 191:622–623

Ko HS, Schenk JP, Tröger J et al (2007) Current radiological management of intussusception in children. Eur Radiol 17(9):2411–2421. Epub 2007 Feb 17

Kong M-S, Wong H-F, Lin S-L et al (1997) Factors related to detection of blood flow by color Doppler ultrasonography in intussusception. J Ultrasound Med 16: 141–144

Kosloske AM, Love CL, Rohrer JE et al (2004) The diagnosis of appendicitis in children: outcomes of a strategy based on pediatric surgical evaluation. Pediatrics 113(1 Pt 1):29–34

Krishnamoorthi R, Ramarajan N, Wang NE et al (2011) Effectiveness of a staged US and CT protocol for the diagnosis of pediatric appendicitis: reducing radiation exposure in the age of ALARA. Radiology 259:231

Kuta AJ, Benator RM (1990) Intussusception: Hydrostatic pressure equivalents for barium and meglumine sodium diatrizoate. Radiology 175:125–126

Lautz TB, Turkel G, Radhakrishnan J, Wyers M, Chin AC (2012) Utility of the computed tomography severity index (Balthazar score) in children with acute pancreatitis. J Pediatr Surg 47(6):1185–1191

Lepage P, Vergison A (2012) Impact of rotavirus vaccines on rotavirus disease. Expert Rev Anti Infect Ther 10(5):547–561

Lewis FR, Holcroft JW, Boey J et al (1975) Appendicitis: a critical review of diagnosis and treatment in 1.000 cases. Arch Surg 110:677–684

Lin SL, Kong MS, Houng DS (2000) Decreasing early recurrence rate of acute intussusception by the use of dexamethasone. Eur J Pediatr 159:551

Ly JN, Miller FH (2002) MR imaging of the pancreas: a practical approach. Radiol Clin North Am 40:1289–1307

Marincek B (2002) Nontraumatic abdominal emergencies: acute abdominal pain: diagnostic strategies. Eur Radiol 12:2136–2150

Maxson RT, Franklin PA, Wagner CW (1995) Malrotation in the older child: surgical management, treatment, and outcome. Am Surg 61:135–138

Menten R, Lebecque P, Saint-Martin C et al (2005) Outer diameter of the vermiform appendix: not a valid sonographic criterion for acute appendicitis in patients with cystic fibrosis. AJR Am J Roentgenol 184:1901

Menten R, Reding R, Godding V et al (2012) Sonographic assessment of the retroperitoneal position of the third portion of the duodenum: an indicator of normal intestinal rotation. Pediatr Radiol 42(8):941–945

Meradji M, Hussain SM, Robben SGF et al (1994) Plain film diagnosis in intussusception. Br J Radiol 67:147–149

Meyer SE (1992) The current radiologic management of intussusception: a survey and review. Pediatr Radiol 22:323–325

Meyer JS, Dangman BC, Buonomo C et al (1993) Air and liquid contrast agents in the management of intussusception: a controlled, randomized trial. Radiology 188:507–511

Miller SF, Landes AB, Dautenhahn LW et al (1995) Intussusception: ability of fluoroscopic images obtained during air enemas to depict lead points and other abnormalities. Radiology 197:493–496

Mitra SK, Rao PLNG, Bhattacharyya NC et al (1982) Rupture of intussuscipiens. J Pediatr Surg 17:300–301

Montali G, Croce F, de Pra L et al (1983) Intussusception of the bowel: a new sonographic pattern. Br J Radiol 56:621–623

Morrison J, Lucas N, Gravel J (2009) The role of abdominal radiography in the diagnosis of intussusception when interpreted by pediatric emergency physicians. J Pediatr 155:556–559

Moş C, Holt G, Iuhasz S, Moş D, Teodor L, Hălbac M (2010) The sensitivity of transabdominal ultrasound in the diagnosis of ureterolithiasis. Med Ultrason 12(3): 188–197

Munden MM, Bruzzi JF, Coley BD et al (2007) Sonography of pediatric small-bowel intussusception: differentiating surgical from nonsurgical cases. AJR Am J Roentgenol 188:275–279

Naeger DM, Chang SD, Kolli P et al (2011) Neutral vs positive oral contrast in diagnosing acute appendicitis with contrast-enhanced CT: sensitivity, specificity, reader confidence and interpretation time. Br J Radiol 84(1001):418–426

Navarro O, Daneman A (2004) Intussusception. Part 3: diagnosis and management of those with an identifiable or predisposing cause and those that reduce spontaneously. Pediatr Radiol 34:305–312

Navarro OM, Daneman A, Chae A (2004) Intussusception: the use of delayed, repeated reduction attempts and the management of intussusceptions due to pathologic lead points in pediatric patients. AJR Am J Roentgenol 182:1169–1176

Nghiem HV, Jeffrey RB (1992) Acute appendicitis confined to the appendiceal tip: evaluation with graded compression sonography. J Ultrasound Med 11:205–207

Nitta N, Takahashi M, Furukawa A et al (2005) MR imaging of the normal appendix and acute appendicitis. J Magn Reson Imaging 21(2):156–165

Nizar K, Deutsch M, Filmer S et al (2009) Doppler studies of the ovarian venous blood flow in the diagnosis of adnexal torsion. J Clin Ultrasound 37(8):436– 439

Nosaka S (2000) Diagnostic radiology in acute pediatric abdomen. Nippon Igaku Hoshasen Gakkai Zasshi 60:5–13

O'Malley ME, Wilson SR (2003) US of gastrointestinal tract abnormalities with CT correlation. Radiographics 23:59–72

Ooms HWA, Koumans RKJ, Ho Kang You PJ et al (1991) Ultrasonography in the diagnosis of acute appendicitis. Br J Surg 78:315–318

Pacharn P, Ying J, Linam LE et al (2010) Sonography in the evaluation of acute appendicitis: are negative sonographic findings good enough? J Ultrasound Med 29(12):1749–1755

Parashar UD, Holman RC, Cummings KC et al (2000) Trends in intussusception-associated hospitalizations and deaths among US infants. Pediatrics 106: 1413–1421

Patino MO, Munden MM (2004) Utility of the sonographic whirlpool sign in diagnosing midgut volvulus in patients with atypical clinical presentations. J Ultrasound Med 23:397–401

Pedrosa I, Levine D, Eyvazzadeh AD et al (2006) MR imaging evaluation of acute appendicitis in pregnancy. Radiology 238(3):891–899

Pennington DJ, Zerin MJ (1999) Imaging of the UTI. Pediatr Ann 28:678–686

Pepper VK, Stanfill AB, Pearl RH (2012) Diagnosis and management of pediatric appendicitis, intussusception, and Meckel diverticulum. Surg Clin North Am 92:505–526

Pickhardt PJ, Bhalla S (2002) Intestinal malrotation in adolescents and adults: spectrum of clinical and imaging features. AJR Am J Roentgenol 179:1429–1435

Pracros JP, Tran-Minh VA, Morin de Finfe CH et al (1987) Acute intestinal intussusception in children. Contribution of ultrasonography (145 cases). Ann Radiol 30:525–530

Pracros JP, Sann L, Genin G et al (1992) Ultrasound diagnosis of midgut volvulus: the "whirlpool" sign. Pediatr Radiol 22:18–20

Puapong D, Lee SL, Haigh PI et al (2007) Routine interval appendectomy in children is not indicated. J Pediatr Surg 42(9):1500– 1503

Puylaert JBCM (1986) Acute appendicitis: US evaluation using graded compression. Radiology 158:355–360

Puylaert JBCM (1990) Diagnosis of appendicitis by ultrasound. In: Puylaert JBCM (ed) Ultrasound of appendicitis and its differential diagnosis. Springer, Berlin, pp 29–62

Puylaert JB (2001) Ultrasound of acute GI tract conditions. Eur Radiol 11:1867–1877

Puylaert JB (2003) Ultrasonography of the acute abdomen: gastrointestinal conditions. Radiol Clin North Am 41:1227–1248

Puylaert JB, Vermeijden RJ, Van der Werf SD et al (1989) Incidence and sonographic diagnosis of bacterial ileocaecitis masquerading as appendicitis. Lancet 2(8654): 84–86

Quigley AJ, Stafrace (2013) Ultrasound assessment of acute appendicitis in paediatric patients: methodology and pictorial overview of findings seen. Insights Imaging. 4(6):741–51

Rao PM, Rhea JT, Novelline RA et al (1997) Helical CT technique for the diagnosis of appendicitis: prospective evaluation of a focused appendix CT examination. Radiology 202:139–144

Ratcliffe JF, Fong S, Cheong I et al (1992) Plain film diagnosis of intussusception: prevalence of the target sign. AJR Am J Roentgenol 158:619–621

Ravitch MM (1986) Intussusception. In: Ravitch MM (ed) Pediatric Surgery, 4th edn. Year Book Medical, Chicago, pp 868–882

Ravitch MM, McCune RM Jr (1948) Reduction of intussusception by barium enema. Ann Surg 128:904–917

Rettenbacher T, Hollerweger A, Macheiner P et al (2001) Outer diameter of the vermiform appendix as a sign of acute appendicitis: evaluation at US. Radiology 218:757–762

Riccabona M (2001) Paediatric ultrasound. I. Abdominal. Eur Radiol 11:2354–2368

Riccabona M (2010) Obstructive diseases of the urinary tract in children: lessons from the last 15 years. Pediatr Radiol 40(6):947–955

Riebel TW, Nasir R, Weber K (1993) US-guided hydrostatic reduction of intussusception in children. Radiology 188:513–516

Rioux M (1992) Sonographic detection of the normal and abnormal appendix. AJR Am J Roentgenol 158: 773–778

Rohrschneider WK, Tröger J (1995) Hydrostatic reduction of intussusception under US guidance. Pediatr Radiol 25:530–534

Roskind CG, Kamdar G, Ruzal-Shapiro CB et al (2012) Accuracy of plain radiographs to exclude the diagnosis of intussusception. Pediatr Emerg Care 28(9): 855–858

Sargent MA, Babyn P, Alton DJ (1994) Plain abdominal radiography in suspected intussusception: a reassessment. Pediatr Radiol 24:17–20

Schmitz-Rode T, Müller-Leisse C, Alzen G (1991) Comparative examination of various rectal tubes and contrast media for the reduction of intussusceptions. Pediatr Radiol 21:341–345

Serour F, Witzling M, Gorenstein A (2005) Is laparoscopic appendectomy in children associated with an uncommon postoperative complication? Surg Endosc 19:919–922

Shiels WE II, Maves CK, Hedlung GL et al (1991) Air enema for diagnosis and reduction of intussusception: clinical experience and pressure correlates. Radiology 181:169–172

Shiels WE II, Kirks DR, Keller GL et al (1993) Colonic perforation by air and liquid enemas: comparison study in young pigs. AJR Am J Roentgenol 160: 931–935

Simonovský V (1992) Acute appendicitis: the false-positive observations prospective diagnosis – value of the 'rod' sign. Eur Radiol 2:511–516
Simonovský V (1999) Sonographic detection of normal and abnormal appendix. Clin Radiol 54(8):533–539
Simonovský V (2001) The specificity of appendiceal outer diameter at US. Radiol 220(3):828–830
Simonovský V (2002) Normal appendix: is there any significant difference in the maximal mural thickness at US between pediatric and adult populations? Radiology 224(2):333–337
Sivit CJ, Applegate KE, Stallion A et al (2000) Imaging evaluation of suspected appendicitis in a pediatric population: effectiveness of sonography versus CT. AJR Am J Roentgenol 175:977–980
Snyder WH, Chaffin L (1954) Embryology and pathology of the intestinal tract: presentation of 40 cases of malrotation. Ann Surg 140:368–379
Spear R, Kimmey MB, Wang KY et al (1992) Appendiceal US scans: histologic correlation. Radiology 183:831–834
Stranzinger E, Dipietro MA, Yarram S et al (2009) Intramural and subserosal echogenic foci on US in large-bowel intussusceptions: prognostic indicator for reducibility? Pediatr Radiol 39(1):42–46
Stroman DL, Bayouth CV, Kuhn JA et al (1999) The role of computed tomography in the diagnosis of acute appendicitis. Am J Surg 178:485–489
Strouse PJ (2010) Pediatric appendicitis: an argument for US. Radiology 255(1):8–13
Strouse PJ, DiPietro MA, Saez F (2003) Transient small-bowel intussusception in children on CT. Pediatr Radiol 33:316–320
Sulowski C, Doria AS, Langer JC et al (2011) Clinical outcomes in obese and normal-weight children undergoing ultrasound for suspected appendicitis. Acad Emerg Med 18(2):167–173
Svensson J, Makin E (2012) Gallstone disease in children. Semin Pediatr Surg 21(3):255–265
Swischuck LE, Hayden CK, Boulden T (1985) Intussusception: indications for ultrasonography and explanation of the doughnut and pseudokidney signs. Pediatr Radiol 15:388–391
Swischuk LE, Stansberry SD (1991) Ultrasonographic detection of free peritoneal fluid in uncomplicated intussusception. Pediatr Radiol 21:350–351
Taylor GA (2011) CT appearance of the duodenum and mesenteric vessels in children with normal and abnormal bowel rotation. Pediatr Radiol 41(11):1378–1383. Epub 2011 May 19
Theriot JA, Sayat J, Franco S et al (2003) Childhood obesity: a risk factor for omental torsion. Pediatrics 112(6 Pt 1), e460
Valette PJ, Rioux M, Pilleul F et al (2001) Ultrasonography of chronic inflammatory bowel diseases. Eur Radiol 11:1859–1866
van Breda Vriesman AC, Puylaert JBCM (2002) Epiploic appendagitis and omental infarction: pitfalls and lookalikes. Abdom Imaging 27:20–28
van Randen et al (2008) Acute appendicitis: meta-analysis of diagnostic performance of CT and graded compression US related to prevalence of disease. Radiol 249(1):97–106
Varjavandi V, Lessin M, Kooros K et al (2003) Omental infarction: risk factors in children. J Pediatr Surg 38:233–235
Verschelden P, Filiatrault D, Garel L et al (1992) Intussusception in children: reliability of US in diagnosis – a prospective study. Radiology 184:741–744
Vignault F, Filiatrault D, Brandt ML et al (1990) Acute appendicitis in children: evaluation with US. Radiology 176:501–504
Wang GD, Liu SJ (1988) Enema reduction of intussusception by hydrostatic pressure under ultrasound guidance: a report of 377 cases. J Pediatr Surg 23:814–818
Ward AM, Kay R, Ross JH (1998) Ureteropelvic junction obstruction in children. Unique considerations for open operative intervention. Urol Clin North Am 25: 211–217
Weihmiller SN, Buonomo C, Bachur R (2011) Risk stratification of children being evaluated for intussusception. Pediatrics 127:e296, 298–302
Wiersma F, Sramek A, Holscher HC (2005) US features of the normal appendix and surrounding area in children. Radiology 235:1018–1022
Wiersma F, Allema JH, Holscher HC et al (2006) Ileoileal intussusception in children: ultrasonographic differentiation from ileocolic intussusception. Pediatr Radiol 36(11):1177–1181
Williams RF, Blakely ML, Fischer PE et al (2009) Diagnosing ruptured appendicitis preoperatively in pediatric patients. J Am Coll Surg 208(5):819–828
Woo SK, Kim JS, Suh SJ et al (1992) Childhood intussusception: US-guided hydrostatic reduction. Radiology 182:77–80
Yilmaz E, Usal C, Kovanlikaya A, Karabay N (2001) Sonographic and MRI findings in prepubertal adnexal hemorrhagic cyst with torsion. J Clin Ultrasound 29(3):200–202
Yoon CH, Kim HJ, Goo HW (2001) Intussusception in children: US-guided pneumatic reduction–initial experience. Radiology 218:85–88
Yousefzadeh DK (2009) The position of the duodenojejunal junction: the wrong horse to bet on in diagnosing or excluding malrotation. Pediatr Radiol 39(Suppl 2):S172–S177
Yousefzadeh DK, Kang L, Tessicini L (2010) Assessment of retromesenteric position of the third portion of the duodenum: a US feasibility study in 33 newborns. Pediatr Radiol 40:1476–1484
Zambuto D, Bramson RT, Blickman JG (1995) Intracolonic pressure measurements during hydrostatic and air contrast barium enema studies in children. Radiology 196:55–58
Ziegler MM (2004) The diagnosis of appendicitis: an evolving paradigm. Pediatrics 113(1 Pt 1):130–132

# The Esophagus

Gurdeep S. Mann, Avez A. Rizvi,
Abdusamea G. Shabani, Aisha Rizvi,
and Samuel Stafrace

## Contents



**Abstract**

The esophagus is a dynamic conduit, which connects the oral cavity to the stomach. Esophageal secretions and antegrade peristalsis enable the passage of solids and liquids toward the stomach. Conversely, the esophagus enables prompt expulsion of gastrointestinal content during vomiting and passively with gastric reflux. The pediatric esophagus is subject to a number of congenital and acquired disorders. In this chapter, we review the embryology, applied anatomy, and diagnostic imaging appearances related to the normal pediatric esophagus and in infants and children with esophageal disease.

G.S. Mann, MBCHB, MRCP, FRCR (✉)
A.G. Shabani, MBBCh, FRCR
S. Stafrace, MD, MRCP, FRCR, FRCP Edin
Department of Radiology, Sidra Medical and Research Center, PO Box 26999, Doha, Qatar

Weill Cornell Medicine-Qatar, Doha, Qatar
e-mail: gmann@sidra.org; ashabani@sidra.org; sstafrace@sidra.org

A.A. Rizvi, MS, MD
Department of Radiology, Sidra Medical and Research Center, PO Box 26999, Doha, Qatar
e-mail: arizvi@sidra.org

A. Rizvi, MBBS
Doha, Qatar
e-mail: aisha.rizvi89@gmail.com



S. Stafrace, J.G. (Hans) Blickman (eds.), *Radiological Imaging of the Digestive Tract in Infants and Children*, Medical Radiology, DOI 10.1007/978-3-319-18434-0_4

# 1 Anatomy and Development of the Esophagus

## 1.1 Embryology

The esophagus and trachea are derived from a common tubular structure, which differentiates into the esophagus posteriorly and laryngotracheal groove anteriorly (Fig. 1). The respiratory diverticulum forms on the ventral wall of the primitive foregut at the border of the pharyngeal gut. The esophagus can be recognized as a structure distinct from the pharynx and stomach by the third gestational week at a fetal crown-rump-length (CRL) of 2.5 mm (Takubo 2009). Regional differentiation of the esophagus and stomach from the remainder of the gastrointestinal tract is specified by SOX2 genes (Sadler 2012). The mesodermal

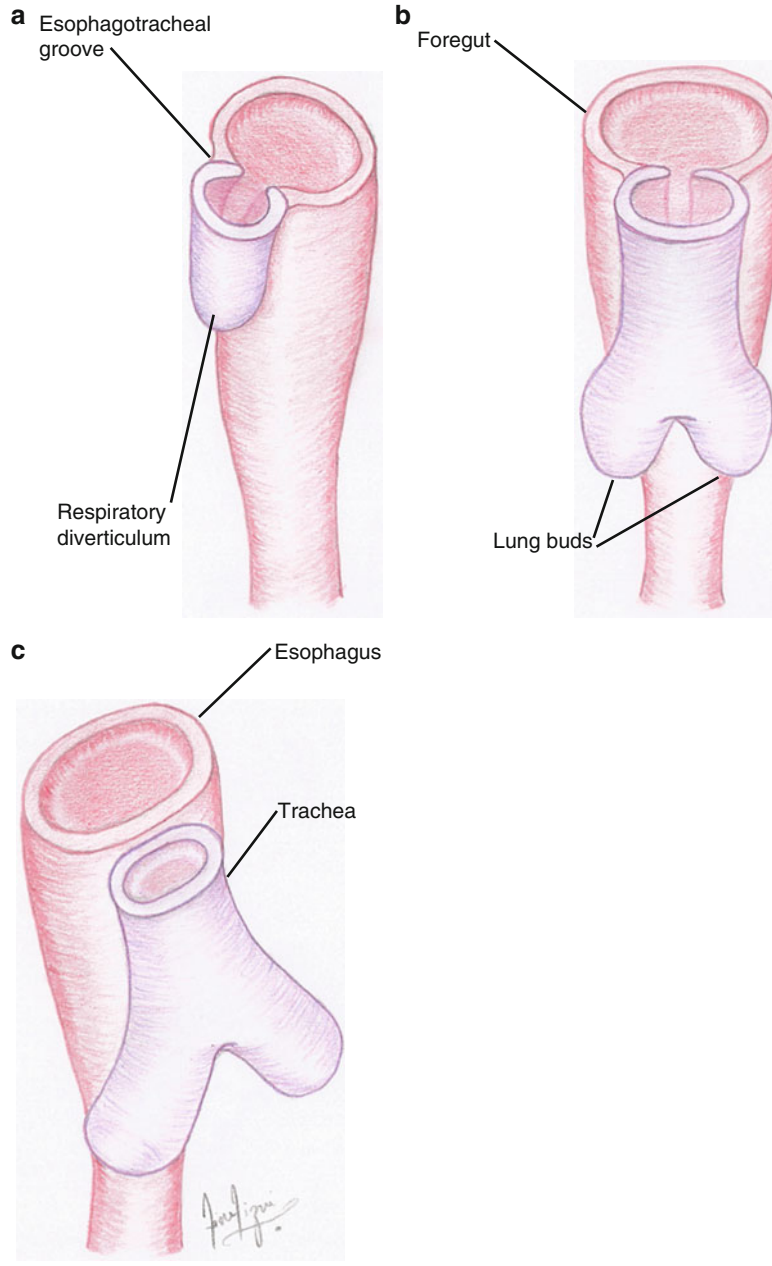


**Fig. 1** (**a**–**c**) Embryology of the esophagus. (**a**) The respiratory diverticulum arises from the ventral wall of the foregut at 4 weeks (**b**–**c**). The laryngotracheal groove partitions the trachea from the primitive foregut, the latter eventually differentiates into the esophagus. Image courtesy of Dr. Aisha Rizvi MBBS, Doha, Qatar

esophagotracheal septum undergoes progressive bilateral evagination partitioning the dorsal esophagus from the ventral respiratory epithelium. Most of the commonest congenital esophageal abnormalities relate to failure of this partitioning process. The esophagus is initially short and only attains normal relative length by the 7th week. Failure to elongate satisfactorily pulls the stomach cranially through the esophageal hiatus resulting in a congenital hiatus hernia.

## 1.2 Imaging Anatomy

The esophagus is a muscular conduit. It extends from the pharynx just left of midline at the level of the C6 vertebral body and inferior cricoid cartilage. Along the length of the neck, the esophagus lies posterior to the trachea and anterior to the cervical prevertebral muscles. The recurrent laryngeal nerves pass between the esophagus and trachea. Laterally it is bound by each carotid sheath (containing the vagus nerve, internal jugular vein, and common carotid artery) and the lateral lobes of the thyroid.

In the thorax the esophagus courses inferiorly and slightly obliquely to the left. It lies predominantly within the posterior mediastinum adjacent to the thoracic prevertebral muscles and anterior to the thoracic duct, posterior intercostal arteries, and azygos veins. The anterior surface of the esophagus abuts the aortic arch, left mainstem bronchus at around the T5 vertebral level, and left atrial parietal pericardium. The esophagus lies between the layers of the parietal pleura. The azygoesophageal recess (AER) is an anatomical space lying anterior to the spine and posterolateral to the lower thoracic esophagus. The AER extends from the level of the anterior turn of the azygos vein at T4 and inferiorly to the level of the aortic hiatus (Gibbs et al. 2007). The AER is formed by the interface of the azygos vein, lower thoracic esophagus, and posteromedial right lung lower lobe pleura. Distortion of the AER contour can be detected on a radiograph or cross-sectional imaging and may imply pathology such a hiatus hernia or bronchopulmonary foregut malformation.

The thoracic duct lies to the right and posterior aspect of the esophagus at T5 and extends cranially to the neck. The esophagus enters the abdomen through the diaphragmatic esophageal hiatus formed by a muscular sling from the right hemidiaphragmatic crus just to the left of the midline at T10. The intra-abdominal portion of the esophagus lies anterior to the left crus of the diaphragm and posterior to the left hepatic lobe. The esophagus terminates at the gastric cardia at T11. The distal end of the esophagus forms into a slightly dilated vestibule just above the gastroesophageal junction (GEJ). The upper limit of the vestibule is at the A-ring, the lower limit at the B-ring (Fig. 2). The A- and B-rings are usually only visualized in the presence of a small sliding hiatus hernia. The Z-line refers to the junction of the esophageal and gastric mucosa and may occasionally be seen as a subtle line on a double contrast barium study.

The esophagus is composed mainly of striated muscle in its upper third, smooth muscle in the distal third, and a mixture of the two in its

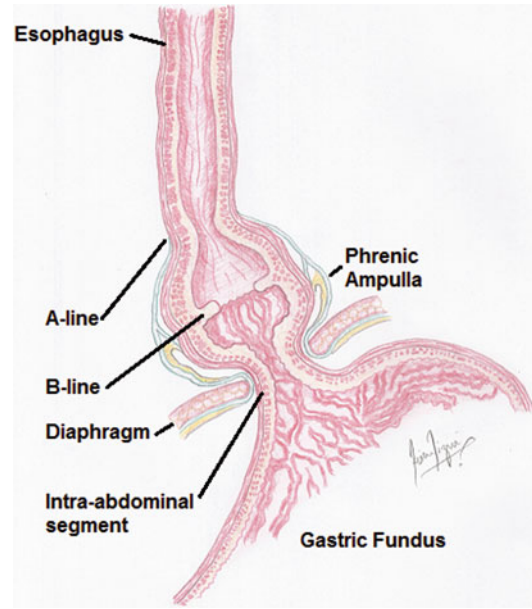


**Fig. 2** Esophageal rings. Line diagram showing the position of the muscular A-ring at the junction between the phrenic ampulla and tubular esophagus, and mucosal B-line demarcating the squamocolumnar junction. Image courtesy of Dr. Aisha Rizvi MBBS, Doha, Qatar

mid-portion. The upper esophageal sphincter (UES) and normal antegrade peristaltic activity are developed by 33 weeks gestation (Jadcherla et al. 2005). The muscularis propria is comprised of smooth muscle and its inner circular layer forms in the 6th week. The outer longitudinal layer is complete by the 10th week. Stratified muscle develops in the fourth month. The muscularis mucosae develops cranially from the distal esophagus in the fourth month and is complete by the 7th month. The circular muscle layer provides the sequential antegrade peristaltic contractions toward the stomach. It is continuous with the hypopharyngeal inferior constrictor muscle. The circular muscle layer courses transversely in the cranial and caudal regions of the esophagus and obliquely within the body of the esophagus and is continuous with the intrinsic component of the lower esophageal sphincter (see below). The UES is located between the pharynx and the cervical esophagus. It is comprised of the hyoid bone, the posterior aspects of the cricoid and thyroid cartilage, and three muscles: thyropharyngeus, inferior esophageal constrictors, and cricopharyngeus. The cricopharyngeus muscle is transversely oriented, while thyropharyngeus muscle is obliquely oriented. The region between these two muscles is the Killian triangle (dehiscence), from which a Zenker diverticulum may form; the latter almost exclusively develops in late adulthood. The cricopharyngeus muscle lies at C5–C6 and is normally relaxed on swallowing, hence not normally visualized on contrast esophagram but may be seen as a posterior horizontal impression in a small number of otherwise asymptomatic patients. Cricopharyngeal dysfunction however may cause dysphagia. The lower esophageal sphincter (LES) is located where the esophagus merges with the stomach. It is comprised of intrinsic and extrinsic components. The intrinsic component consists of esophageal muscle fibers under neurohormonal influence. The extrinsic component consists of the esophageal hiatus in the crural diaphragm and serves as an external sphincter. Malfunction of either component may result in gastroesophageal reflux (GER). The manometric location of the LES differs from the endoscopic location.

The arterial blood supply of the esophagus is extensive comprising of a segmental network of anastomotic vessels. Branches of the inferior thyroid artery supply the upper esophageal sphincter (UES) and cervical esophagus. Paired aortic esophageal arteries or terminal bronchial arteries supply the thoracic esophagus. The distal esophagus and LES are supplied by the left gastric artery and branches of the left phrenic artery. The venous drainage of the esophagus is derived from an extensive submucosal plexus that drains into the superior vena cava via the azygos system. Collaterals of the left gastric vein, a branch of the portal vein, receive venous drainage specifically from the mid-esophagus. Submucosal connections between the portal and systemic venous systems in the distal esophagus enable esophageal varices to form in portal hypertension resulting in submucosal varices. These are sources of major upper gastrointestinal hemorrhage in conditions such as liver cirrhosis (Kuo and Urma 2006). Esophageal lymphatic egress is derived from three interconnected drainage systems. The proximal third drains into the thoracic duct via deep cervical lymph nodes. The middle third drains into the superior and posterior mediastinal nodes. The distal third follows the venous drainage along the course of the left gastric artery to the gastric and celiac lymph nodes. The innervation of the esophagus includes the Meissner plexus, which provides vagal secretomotor parasympathetic innervation of the submucosa, and the Auerbach (myenteric) plexus which provides spinal motor innervation of the muscularis propria.

## 2 Imaging Techniques and Indications

### 2.1 Radiography

The non-distended esophagus is not visualized on plain radiography and can be difficult to assess on cross-sectional imaging. The position of the esophagus may be inferred on radiographs by the presence of intraluminal air. An air-filled esophagus typically results from aerophagia, during

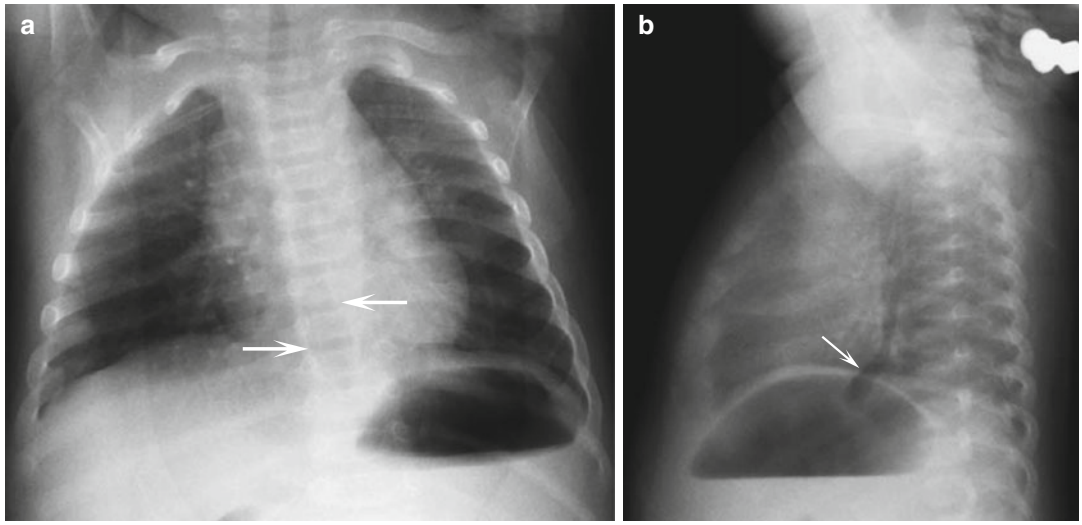


**Fig. 3** (**a**, **b**) Air outlining a normal esophagus. (**a**) AP and (**b**) lateral chest radiographs of a crying infant with an air-filled esophagus (*arrows*) secondary to aerophagia

crying, when large amounts of air are swallowed (Fig. 3). In neonates continuous positive pressure may result in marked gaseous distension of the esophagus and stomach requiring decompression via an orogastric tube. Segmental gaseous distension of the esophagus is seen in an atretic esophageal pouch or proximal to an esophageal stricture. Tracheoesophageal fistula is another cause of an air-filled esophagus. An air-fluid level may be visualized on an erect chest radiograph in esophageal stricture or achalasia. Radiographs are important in evaluating the course and termination of orogastric and nasogastric tubes (Figs. 4 and 5). The position of an intact esophagus may be inferred from the course of an indwelling enteric tube. Aberrant course raises the possibility of esophageal perforation (Fig. 6) or other pathology distorting the esophagus.

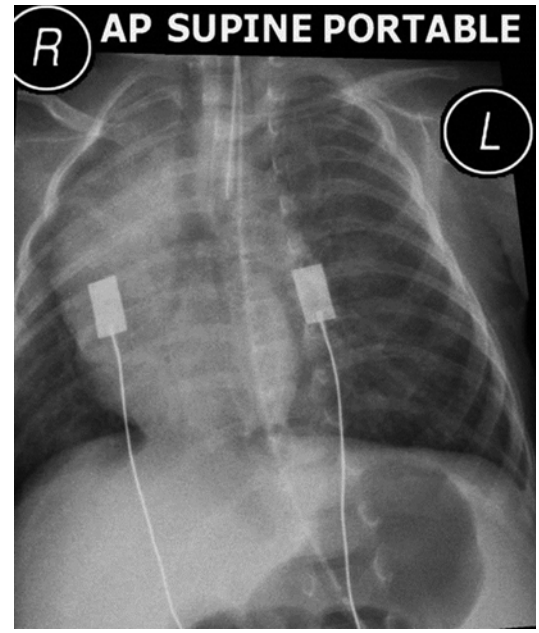


**Fig. 4** Malposition of endotracheal tube. Esophageal malposition of an endotracheal tube. Oblique frontal chest radiograph confirming inadvertent intubation of the esophagus with an endotracheal tube posterior to the airway

## 2.2 Fluoroscopy

Fluoroscopy remains the key imaging modality to assess the pediatric and adolescent esophagus. The contrast esophagram (or barium swallow) is the radiological imaging test of choice to evaluate the anatomy, dysphagia, and dysmotility. It is preferred in the initial work-up and follow-up of most surgical esophageal disorders. The esophagram provides comprehensive intraluminal anatomical information from which mural and extraluminal pathology may also be inferred. It

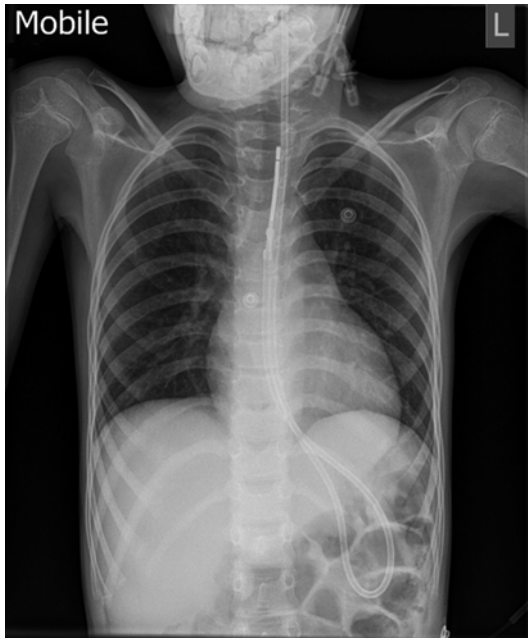


**Fig. 5** Esophageal termination of a nasogastric tube. Suboptimal enteric tube position with the tube coiling back on itself in the gastric cardia and terminating in the esophagus. This is not safe for feeding and should be removed and replaced

also yields detailed functional information regarding transit time and patency of the gastroesophageal sphincters. The esophagram can be coupled with an upper gastrointestinal (UGI) series (Fig. 7) to assess the stomach and proximal small bowel in order to detect GER and exclude structural abnormalities causing vomiting. Ideally the stomach and proximal small bowel should be imaged as part of the initial esophagram in a child to document gastric emptying and duodenojejunal flexure position. Follow-up studies should include the proximal stomach. The main indications for performing an esophagram in children are summarized in Table 1. The choice of contrast agent used is at the discretion of the radiologist who should be knowledgeable of any patient allergies and the specific clinical indication. Barium sulfate yields the highest-quality single and double contrast studies. Assessment of fine mucosal detail is rarely required in children and single contrast studies usually suffice. In sick neonates or where there is suspected contrast leakage, low-osmolar water-soluble contrast medium is preferable. Gastrografin by virtue of

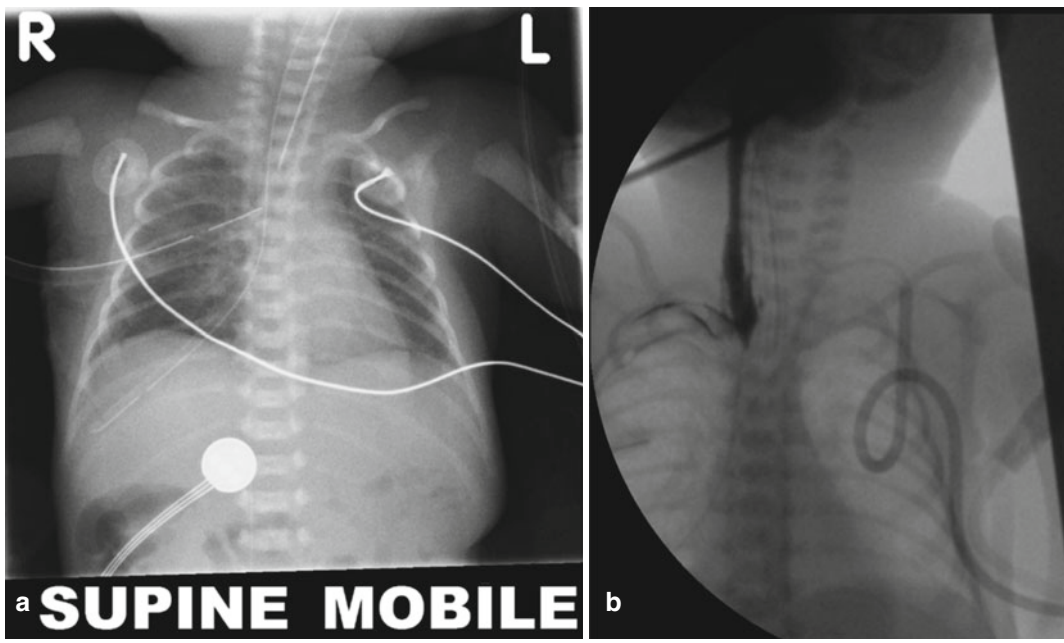


**Fig. 6** (**a**, **b**) Iatrogenic esophageal perforation. (**a**) Frontal chest radiograph showing abnormal course of the orogastric tube terminating in the right upper abdominal quadrant. (**b**) Water-soluble contrast series showing a contained extrapleural contrast leak

its high osmolality is to be avoided in all children and patients with neurological impairment, as pulmonary aspiration has been associated with fatal pulmonary edema. Gastromiro® is favored in Europe and gastrografin is not routinely used in UGI series. Oral intake of contrast medium is to be encouraged and can be made more palatable using a range of flavorings. Caution is required when opacifying the esophagus using an enteric tube. It may be difficult to control opacification with the risk of inadvertent pulmonary aspiration leading to transient hypoxia or even respiratory arrest in the labile child (Fig. 8). One scenario where such a technique is employed is the post-operative assessment of tracheoesophageal fistula (see Sect. 4.1). The infant is placed prone and lateral shoot-through or biplane fluoroscopy is performed at a high frame rate. The aim of the

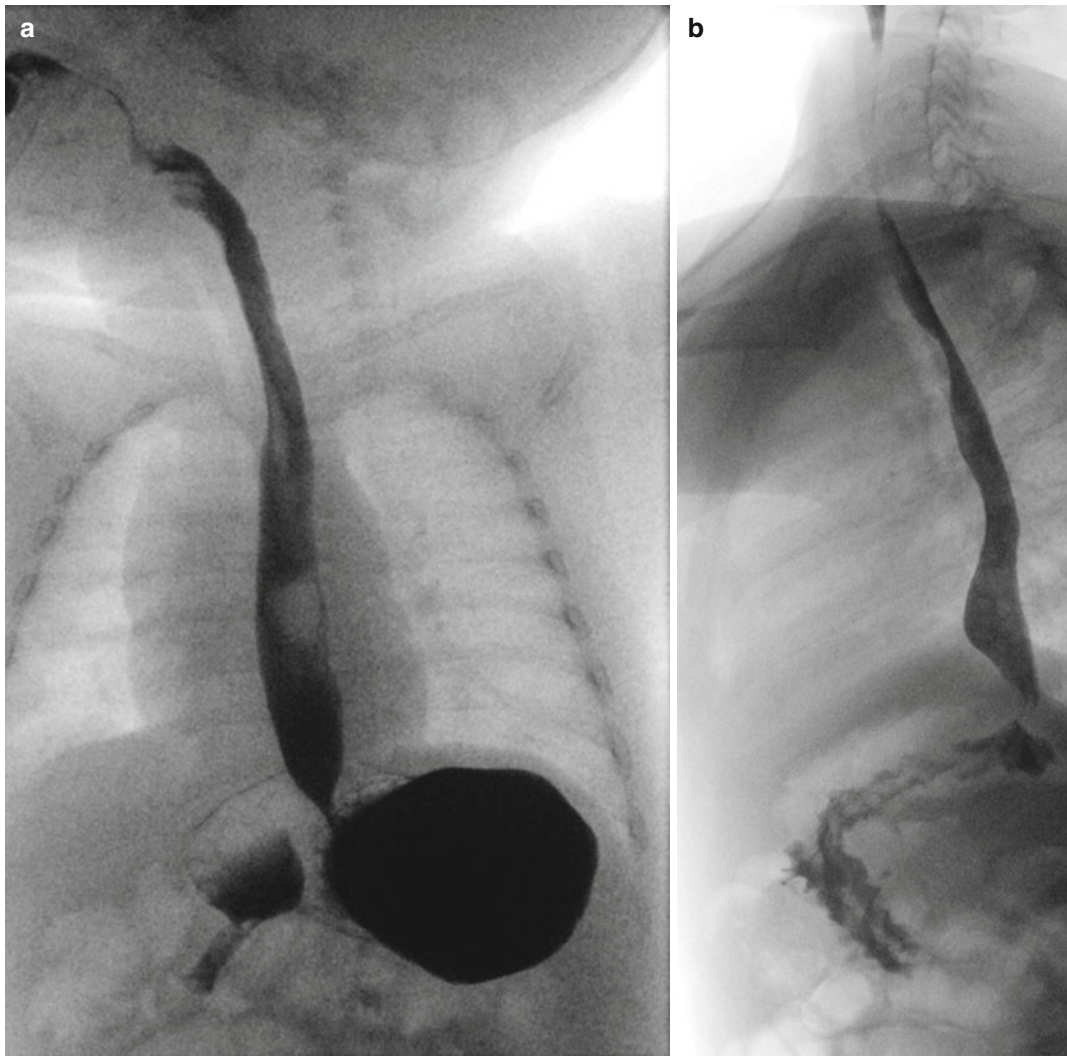


**Fig. 7** (**a**–**d**) Normal barium esophagram in an infant. (**a**) Oblique anteroposterior and (**b**) lateral barium esophagrams, the lateral esophagram shows normal anterior indentation of the esophagus by the aortic arch, left main bronchus, and left atrium. (**c**) AP esophagram in a 9-month-old child showing normal parallel orientation of the mucosal folds in the empty esophagus (*arrow*). The esophageal mucosal folds should be less than five in number with a maximal thickness of 3 mm. (**d**) Spurious mobile lucent gaseous filling defects due to excessive crying, these promptly cleared

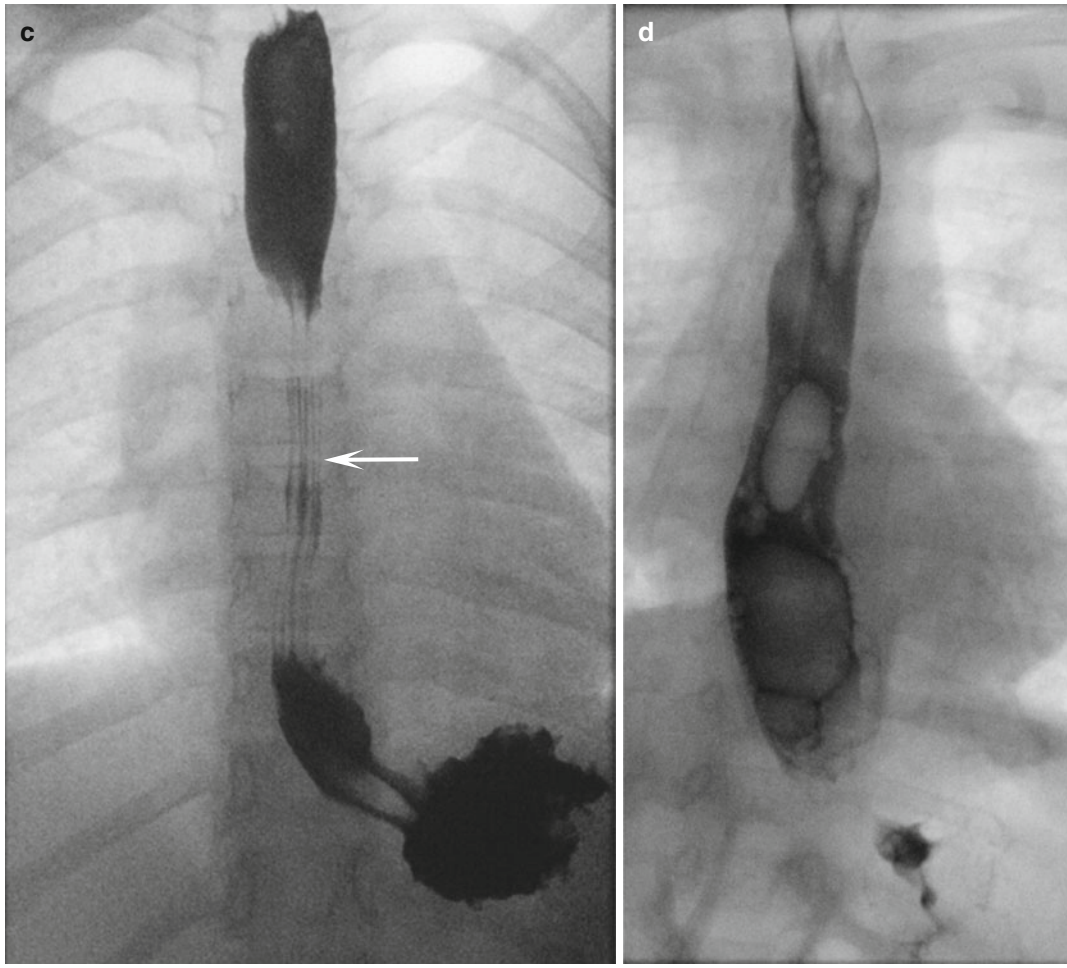


**Fig. 7** (continued)

**Table 1** Summary of the main indications for an esophagram

| |
|---|
| Dysphagia |
| Odynophagia |
| Dysmotility disorders |
| Recurrent pneumonia or chronic tracheobronchial inflammation (aspiration) |
| Strictures |
| Extrinsic compression (vascular or non-vascular) |
| Esophageal obstruction |
| Postsurgical evaluation |
| Esophagitis |
| Gastroesophageal reflux |
| Tracheoesophageal fistula |
| Chest pain of non-cardiac origin |
| Varices |
| Neoplasm |

esophagram is to adequately image the distended esophagus in two planes without aspiration. The cervical esophagus is assessed in the true antero-posterior (AP) and lateral planes. The AP and lateral planes should be used for the thoracic esophagus with obliquity as required to avoid overlap from the spine. In most cases normal feeding volumes are most appropriate. If the child refuses to drink adequate volumes of contrast, then the contrast volume as a last resort may be augmented with a more palatable drink such as juice or milk. The sated child may refuse to drink and ingestion of a recent meal may result in spurious intraluminal findings from retained ingested matter; hence a pre-procedural fast is essential. Aerophagia can mimic intraluminal

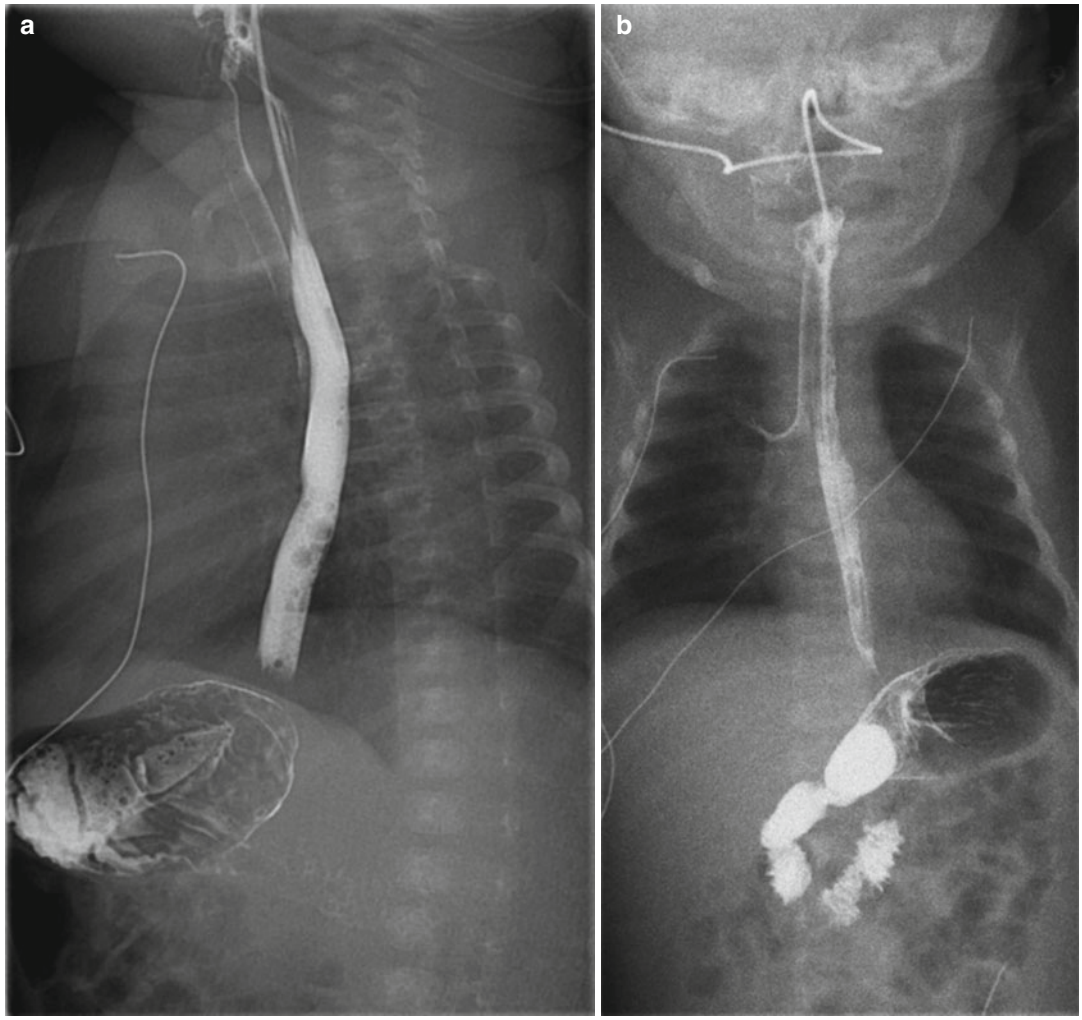


**Fig. 8** (**a**, **b**) Overflow aspiration during tube-esophagram study. (**a**) Lateral and (**b**) AP esophagography show high enteric tube position and overdistension of the esophagus with unintentional contrast overflow into the airway

filling defects (Fig. 7d). Fasting times depend on the child's age and should not exceed the child's routine feeding intervals. Age-appropriate fasting times are in the order of approximately 2–3 h for neonates and young infants, 4 h for older infants and children, and at least 6–8 h for adolescents (ACR 2014). Fasting children are best scheduled for early morning examinations to minimize patient distress and parental anxiety. Infants and younger children are examined recumbent and may require immobilization to reduce motion artifact and minimize fluoroscopy time. Older children and adolescents may prefer swallowing barium in the erect position. Esophageal transit is aided by gravity. A double contrast study may be performed in older children using barium sulfate and Carbex® and completed with the ingestion of a small absorbable barium tablet. The latter may be retained in subtle disorders of esophageal dysmotility.

As with all fluoroscopic imaging, radiation exposures must be as low as reasonably achievable using pediatric-specific protocols, employing low-dose, pulsed and cine-fluoroscopy with grabbed images and cine-loop capture. Fine mucosal detail and depiction of

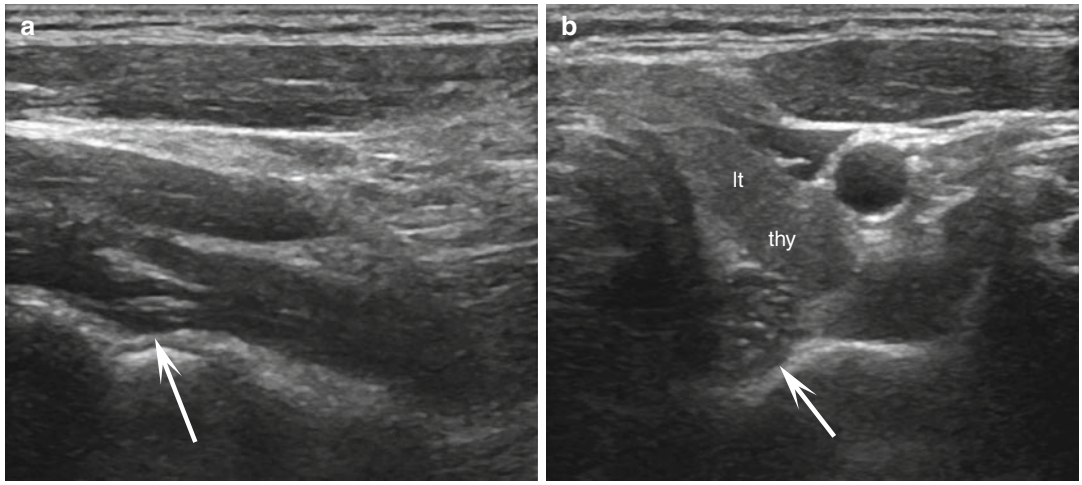


**Fig. 9** (**a**, **b**) Ultrasound of the cervical esophagus. (**a**) Longitudinal and (**b**) transverse views of the cervical esophagus (*arrow*) obtained using the left thyroid lobe (lt thy) as an acoustic window

subtle contrast leakage or fistulae may require higher dose exposures. The assessment of dysmotility is typically performed as part of a multidisciplinary team with a speech and language therapist attending the study. The child is assessed with different age-appropriate consistencies of food and liquid ranging from barium-coated solids (fruit or small cookie pieces), thickened puree or yogurt, and thin liquids (see Sect. 3).

## 2.3 Ultrasound

Ultrasound (US) is not an organ-specific imaging technique. It is, however, safe and widely available. US to date has not been widely adopted to assess the esophagus. Portions of the esophagus can be noninvasively imaged using high-frequency high-resolution linear transducers. The esophagus has five layers best appreciated using endoscopic US. Novel applications of conventional US include the assessment of swallowing and lower esophageal sphincter competency. US can be used to dynamically assess the tongue, oral cavity, hyoid, and larynx during swallowing using the midline anterior neck as an acoustic window (Miller and Kang 2007). The cervical esophagus can be assessed using the thyroid gland as an acoustic window (Fig. 9). The intra-abdominal portion of the esophagus may be evaluated through the left lobe of the liver (Fig. 10) to dynamically depict gastroesophageal reflux following a feed (Koumanidou et al. 2004). The esophagus itself serves as an important acoustic window for the echocardiographer using transesophageal echocardiography.

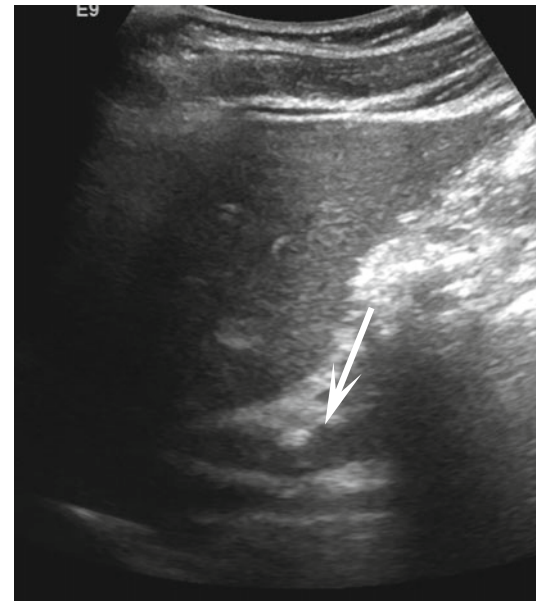

**Fig. 10** Ultrasound of the intra-abdominal esophagus. Longitudinal US image of the esophagus (*arrow*) obtained using the left lobe of the liver as an acoustic window

### 2.4 Computed Tomography

The esophagus is not primarily assessed using computed tomography (CT) in children. One specific exception is suspected extrinsic esophageal compression by a vascular ring or pulmonary arterial sling (see Sect. 4.6). Modern multi-detector CT (MDCT) enables rapid image acquisition with reduced sedation requirements. Imaging can be performed with free-breathing. 2–3 cc/kg of intravenous low-osmolar iodinated contrast medium is used; oral contrast medium is not required. Acquisition timing may be optimized using bolus tracking and threshold triggering. Weight-based exposure parameters should be used to ensure achieving as-low-as-reasonably possible radiation doses. MDCT can dynamically assess airway caliber. Two-dimensional (2D) multiplanar reformatted, maximum-intensity, minimum-intensity projection, and three-dimensional (3D) imaging reconstructions can be generated to improve diagnostic yield.

### 2.5 Magnetic Resonance Imaging

Magnetic resonance imaging (MRI) is not a first-line imaging strategy for the pediatric esophagus. The esophagus is subject to considerable cardiac and respiratory motion, and EKG-gated and respiratory-gated imaging techniques are required to optimally demonstrate the esophagus. MRI is an alternative to MDCT for assessing vascular rings but is more time-consuming and frequently requires sedation or general anesthesia. MRI can be useful for assessing esophageal involvement from (para)spinal pathology such as tumor. MR image post-processing uses techniques similar to those used for MDCT.

### 2.6 Scintigraphic Studies

In children scintigraphic studies may be used to (i) verify suspected gastroesophageal reflux or pulmonary aspiration, (ii) assess esophageal transit, and (iii) quantify the rate of gastric emptying of liquid meals. In infants and children, a gastroesophageal reflux study is typically combined with a liquid phase gastric emptying study ("milk scan"). Techniques are not well standardized across institutions. Practice parameter guidelines for performing gastrointestinal scintigraphy have been jointly issued by American College of Radiology, Society for Nuclear Medicine, and Society for Pediatric Radiology (ACR–SNM–SPR 2014) for use in children. A pre-procedural fast of approximately 4 h is required prior to administering a liquid meal consisting of a weight-based concentration of technetium-99 m (Tc-99 m) sulfur colloid and either milk, formula, or juice. The feed can be administered orally, by nasogastric tube, or via a percutaneous gastrostomy tube. Dynamic imaging of the chest and abdomen is obtained in the supine position for 60 min. The number of reflux events during the study, duration, and proximal extent of reflux can be reported (Fig. 11). Pulmonary aspiration is confirmed by activity within the lungs on delayed imaging. Gastric emptying is assessed at 1, 2, and 3 h after completion of feeding. Follow-up studies can be used to assess response to medical therapy. Contrast studies coupled with manometry in most cases have obviated need for dynamic supine esophageal scintigraphic transit studies; however, these can be performed before or after a combined milk scan.

## 3 Swallowing Disorders

### 3.1 Normal Swallowing and Esophageal Transit

Swallowing is a complex dynamic sequential process that consists of both voluntary and involuntary components. The voluntary phases include preparatory sucking and oral bolus formation. In the oral phase coordinated movement of the mandible along with elevation of the tongue toward the hard palate propels the ingested bolus posteriorly toward the oropharynx. The involuntary components comprise the pharyngeal and esophageal phases. In the pharyngeal phase elevation the soft palate by the arriving bolus causes the palatine constrictor muscles to contract and the bolus passes into the oropharynx. Simultaneously

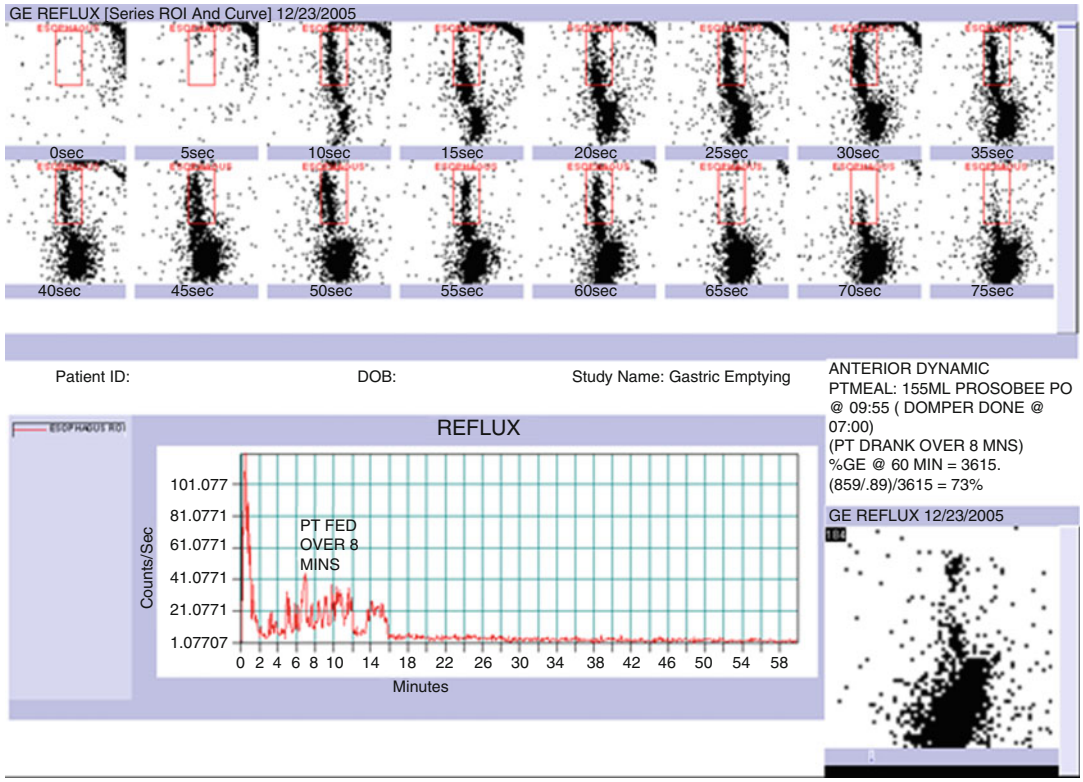


**Fig. 11** Tc99m radionuclide "milk" scan. Serial imaging demonstrates gastroesophageal reflux to the upper esophagus but no pulmonary aspiration on delayed imaging at 4 h

the velopharyngeal portal closes to prevent nasal escape of the bolus. The oropharyngeal constrictor muscles generate a peristaltic wave toward the larynx, closing the vocal cords, the arytenoids descend narrowing the laryngeal vestibule while depressing the epiglottis, clearing any laryngeal penetration and preventing pulmonary aspiration. Respiratory ventilation ceases. The bolus passes laterally around the epiglottis toward the piriform sinuses and then through the upper esophageal sphincter (UES). The UES comprises of the inferior pharyngeal constrictor muscles, cricopharyngeus muscle, and proximal cervical esophagus. The UES is normally tensioned at rest. Preceding bolus arrival, the cricopharyngeus muscle relaxes. The suprahyoid muscles and thyrohyoid muscles contract, the hyolaryngeal complex moves anteriorly opening the UES (Matsuo and Palmer 2008). As the bolus enters the UES, primary peristalsis consists of an initial rapid primary wave of relaxation to accommodate a bolus and a slower secondary wave of contraction that propels it toward the lower esophageal sphincter (LES). Gravity aids peristalsis in the upright position. The LES at rest prevents gastric reflux but relaxes during a swallow and allows bolus passage into the stomach. Secondary peristalsis ensures any residual bolus passes into the stomach and is initiated locally in the esophagus by luminal distension by the retained bolus. Tertiary contractions are abnormal non-propulsive contractions and signify esophageal dysmotility (Fig. 12).

## 3.2 Disorders of Swallowing

The prevalence of feeding disorders at any point in a developing child varies but is estimated to be between 25 and 40 % (Lefton-Greif and Arvedson 2007). Incidence levels are much higher in

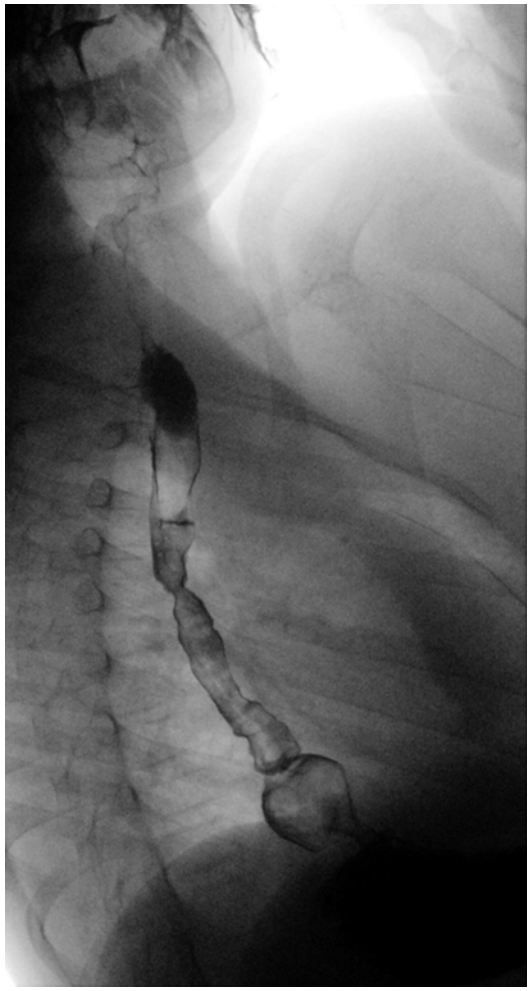

**Fig. 12** Esophageal dysmotility. Barium esophagram showing a corkscrew appearance to the esophagus in a child with diffuse esophageal spasm and tertiary contractions

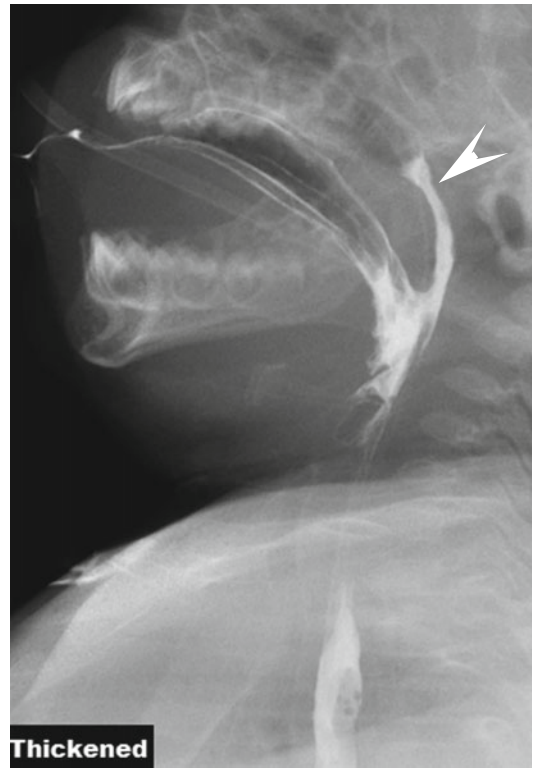


**Fig. 13** Nasal regurgitation. Lateral videofluoroscopic swallow study showing nasal regurgitation (*arrowhead*)

premature infants and children with neurological disability and more commonly persist in the latter group. The causes of pediatric swallowing dysfunction (dysphagia) are varied, often complex and multifactorial in etiology, and can be either physiologic or behavioral. The most common causes of pediatric dysphagia are neurological and include cerebral palsy, traumatic brain injury, cranial nerve palsies, and meningomyelocele. Other common causes include prematurity, craniofacial abnormalities, tracheotomy, long-term ventilator dependence, and failure to thrive (Prasse and Kikano 2009). Dysphagia with aspiration is common in full-term infants less than 1 month of age and improves with age (Vazquez and Buonomo 1999). Abnormalities can occur at all anatomic levels during the oral, pharyngeal, and esophageal phases of swallowing. Micrognathia or macroglossia predisposes to oral phase dysfunction and swallowing difficulties. Children on long-term tube feeding or intensive care in the neonatal period may be unused to feeding, and they may simply refuse to eat. Severely neurologically impaired children may be unable to suck or they may lack sufficient tongue control to latch onto and maintain control of the nipple or teat. Oral motor dysfunction occurs with moderate or severe cerebral palsy and developmental delay. Incomplete buccal closure leads to drooling and abnormal tongue and jaw motion (Kramer 1989). Those neurologically impaired children unable to elevate the soft palate experience nasopharyngeal incoordination and nasopharyngeal reflux (Fig. 13). Occasional nasopharyngeal

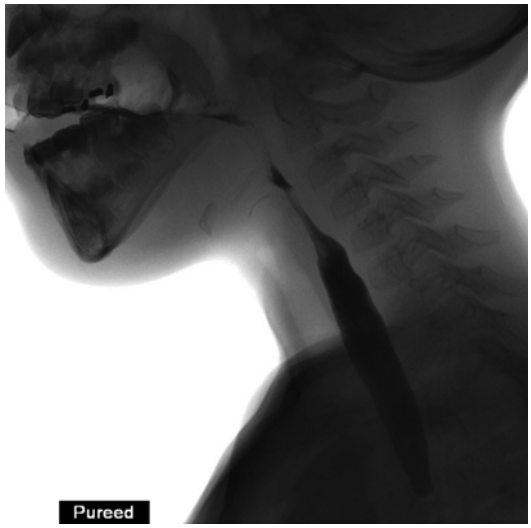


**Fig. 14** Laryngeal penetration. Lateral videofluoroscopic swallow study showing trace laryngeal penetration

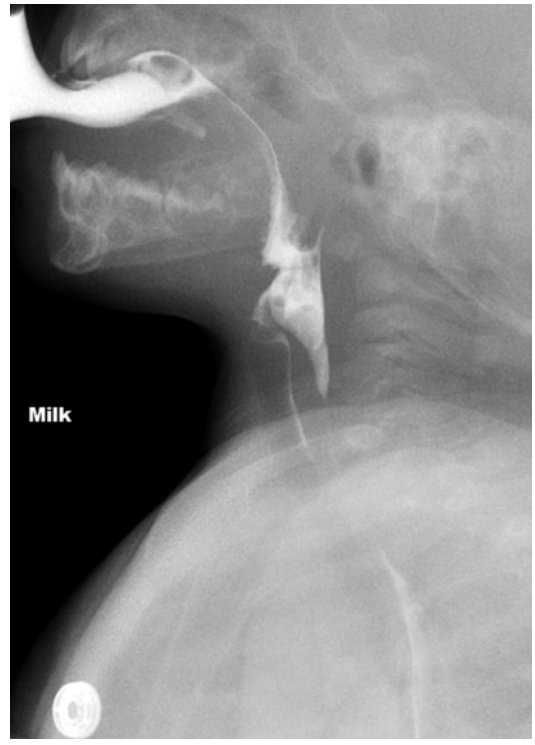


**Fig. 15** Pulmonary aspiration. Lateral videofluoroscopic swallow study showing trace pulmonary aspiration

incoordination is most commonly due to transient swallowing incoordination. Retropharyngeal masses such as teratoma, lymphoma, or abscess may rarely cause dysphagia. Cricopharyngeal achalasia, a failure of relaxation of the cricopharyngeus muscle, is most commonly secondary to GER. Signs of cricopharyngeal achalasia include absent, delayed, or incomplete opening or early closure of the upper esophageal sphincter. Laryngeal penetration occurs when a bolus enters the glottis to the level of the laryngeal vestibule above the true vocal folds (Fig. 14). This may be very subtle, intermittent, or transient and referred to as "flash penetration." Pulmonary aspiration occurs when a bolus enters an incompletely protected airway beyond the level of the vocal cords and soils the trachea (Fig. 15).

## 3.3 Imaging Assessment of Swallowing and Esophageal Transit

The assessment of feeding and swallowing disorders in infants and children requires a multidisciplinary approach of healthcare professionals in partnership with the child's caregivers. The standard technique is the videofluoroscopic swallow study (VFSS) also referred to as the "modified barium swallow" and can help determine the consistencies of feed that a child is able to safely ingest and thereby avoid those which would predispose to aspiration. VFSS is more sensitive than combined clinical assessment of aspiration (DeMatteo et al. 2005) and conventional UGI for the detection of aspiration (Vazquez and Buonomo 1999). VFSS principally assesses oropharyngeal function and may detect related anatomical pathology. VFSS may be combined with a subsequent UGI series to assess esophageal motility and transit. A scout chest radiograph can be obtained to assess for evidence of pulmonary aspiration if there is no recent chest radiograph. Assessment of swallowing is routinely performed in young children in the true lateral position only. In older children the AP plane should also be assessed. US can be used to dynamically assess the tongue, oral cavity, hyoid, and larynx (Miller and Kang 2007) but is not widely offered as a clinical service.

VFSS requires the patient to be stationary and often the child to be securely seated. Infants can be restrained in their own child safety seat if no dedicated infant feeding seat is available. Collimation is to the hard palate, to the anterior cervical spine, and to the level of the tips of the shoulders. Orbital exposure should be avoided where possible. Unfortunately VFSS does routinely expose the thyroid to radiation. The execution of swallowing occurs too rapidly to be observed fluoroscopically. Pulsed fluoroscopy cannot be used as during routine video esophagrams as it may prevent detection of fleeting episodes of laryngeal penetration and microaspiration (Mercado-Deane et al. 2001). A video recording of the entire cinefluoroscopic study should be obtained. This can be reviewed without additional radiation exposure and compared to other historical series by the multidisciplinary team at their convenience. It is the author's practice to only save cine-loops on PACS of any abnormal series for the radiologist to review prior to any subsequent VFSS. Children may tire as feeding progresses and may have difficulty maintaining their airway so the study should be continued after the first few uneventful swallows for any given consistency (Newman et al. 2001). The child's own speech therapist or feeding therapist should ideally be present during the examination to witness the study and determine the optimal volume and order of boluses of different consistencies that are to be fed. Participation of the parents and caregivers is actively encouraged, helping to recreate some aspect of daily feeding and to reassure the child. The therapist can advise on compensatory maneuvers that assist swallowing (Fernbach 1994). Young children are given various barium-impregnated liquids of differing density depending on the type of fluid and amount of added thickener. Older children are initially challenged with a mixture of barium thickened with pudding or pureed food, yogurt, then with thin liquid barium, and finally with more solid food such as barium-coated crackers or cookies. Barium density influences transit time and the swallowing mechanism. High-density barium has a slower transit time, causing the upper esophageal sphincter to open later, to remain open for longer and to delay its closure (Dantas et al. 1989). The examination must be terminated if aspiration occurs and any changes in vital signs should be monitored with appropriate airway suctioning and supplementary oxygen administered as required. It is important to document whether aspiration induces a cough reflex. Frank aspiration should be further assessed with a post-examination chest radiograph. Coordination of swallowing improves with age. Follow-up VFSS is an effective means to monitor progress.

# 4 Congenital Anomalies

## 4.1 Esophageal Atresia and Tracheoesophageal Fistula

Esophageal atresia (EA) is congenital disorder comprising of discontinuity of the esophageal lumen. In approximately 90 % of cases, EA is associated with a communication with the trachea or bronchus which is referred to as tracheoesophageal fistula (TEF). In around 7 % of cases, there is no fistula and in the remainder no EA (Spitz 2007). EA with or without TEF is the most common congenital malformation of the esophagus with a prevalence of approximately 2.5–3.5 per 10,000 births (Pedersen et al. 2012; Shaw-Smith 2006). The underlying etiology of EA/TEF is poorly understood but is fundamentally related to disruption of separation of the embryonic proximal foregut into ventral respiratory and dorsal gastrointestinal tubes (Felix et al. 2009).

The original anatomical classification of EA was proposed by Vogt (1929) and stratified based on the presence or absence of a TEF; this was subsequently adapted by Ladd (1944) and Gross (1953). The main classification systems for EA/TEF are summarized in Table 2. Regardless, it is important to accurately describe the underlying anatomical substrate (Fig. 16) to aid preoperative planning.

### 4.1.1 Antenatal Diagnosis

Antenatal diagnosis of EA should be considered when there is a small or absent fetal stomach in the setting of maternal polyhydramnios and

detection of amniotic fluid-filled distended atretic esophageal pouch. The latter sign is referred to as the upper neck "pouch sign" (Kalache et al. 1998) and is only visualized in a third of cases (Fig. 17). The detection rate of EA using antenatal US is quoted at 10–40 % with a PPV of only 50 % (Hochart et al. 2015). The imaging characteristics on fetal MRI (Fig. 18) associated with the highest positive predictive values for EA are an esophageal pouch (100 %) and a small stomach (75 %) (Ethun et al. 2014).

**Table 2** Summary of the different types of EA and TEF

| Classification | | | | |
|---|---|---|---|---|
| Vogt – Ladd type | | Gross – type | Description | Frequency (%) |
| 1 | | | Esophageal agenesis | Rare |
| 2 | I | A | "Long-gap" or "pure" EA | 7 |
| 3a | II | B | EA with proximal TEF | 1 |
| 3b | III, IV | C | EA with distal TEF | 86 |
| 3c | V | D | EA with both proximal and distal TEF | 2 |
| 4 | | E | H-type TEF without EA | 4 |
| | | F | Congenital esophageal stenosis | rare |
| | | | EA with distal fistula connecting to the right mainstem bronchus | rare |

Adapted from Vogt (1929), Ladd (1944), Gross (1953), and Spitz (2007)

### 4.1.2 Postnatal Diagnosis

Salivary secretions rapidly accumulate in infants with EA who typically present with drooling, cough, or respiratory distress on attempted feeding. Children with isolated TEF (H-type type fistula) are more clinically challenging to diagnose. They may present later in life with recurrent feed-related coughing, choking, cyanotic episodes, reflux, or silent aspiration pneumonia.

### 4.1.3 Radiological Appearances

The radiological appearance depends on the type of lesion and whether there is esophageal atresia, patent fistula(e), or both. In most cases a chest x-ray with an orogastric tube in situ will be sufficient to make the diagnosis of EA. The diagnosis of EA should be suspected when an orogastric tube is gently advanced in a neonate and resistance is unexpectedly encountered at a relatively short placement distance. The pouch length may be inferred from a radiograph if the esophageal tube coils (Fig. 19) within the atretic pouch. However, it should be noted that the pouch is distensible and this would likely underestimate the pouch size. Care should be taken not forcibly

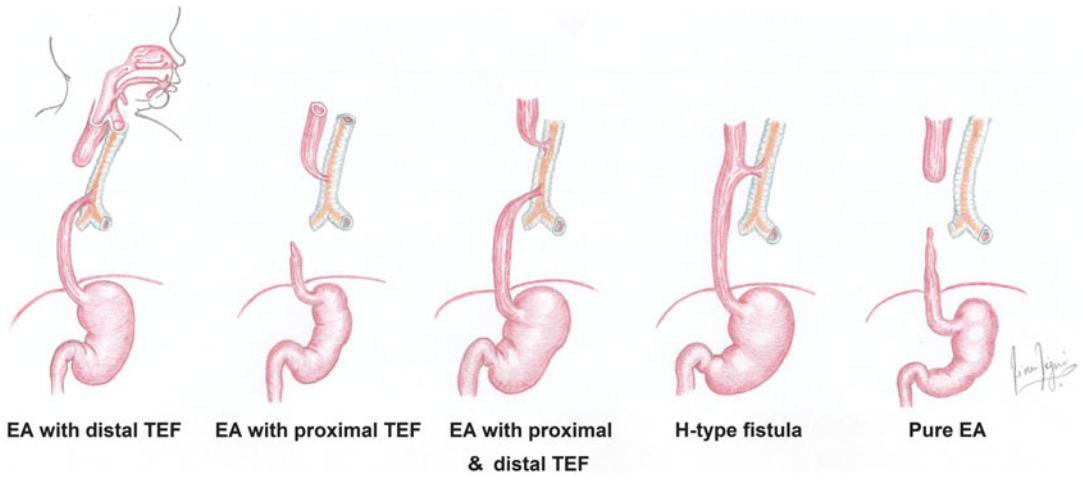


**Fig. 16** Line diagram summarizing the main types of esophageal atresia (*EA*) and tracheoesophageal fistulae (*TEF*). Image courtesy of Dr. Aisha Rizvi MBBS, Doha, Qatar

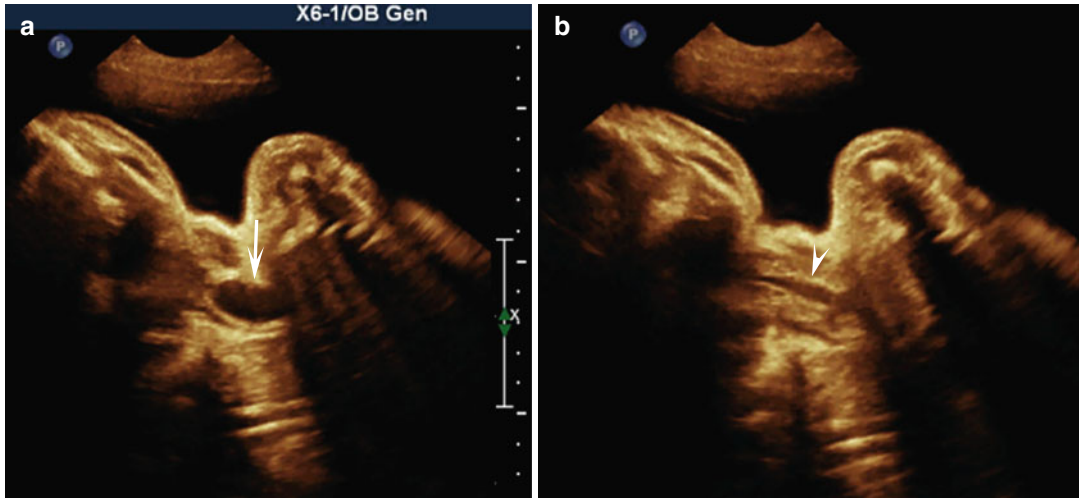


**Fig. 17** (**a**, **b**) Antenatal US of esophageal atresia (EA). (**a**) Longitudinal fetal sonogram demonstrating a characteristic distended upper-pouch sign (*arrow*) in pure EA and (**b**) normal trachea (*arrowhead*). Images courtesy of Dr. Karim D. Kalache MD, Division Chief of Fetal and Maternal Medicine, Sidra Medical and Research Center, Doha, Qatar

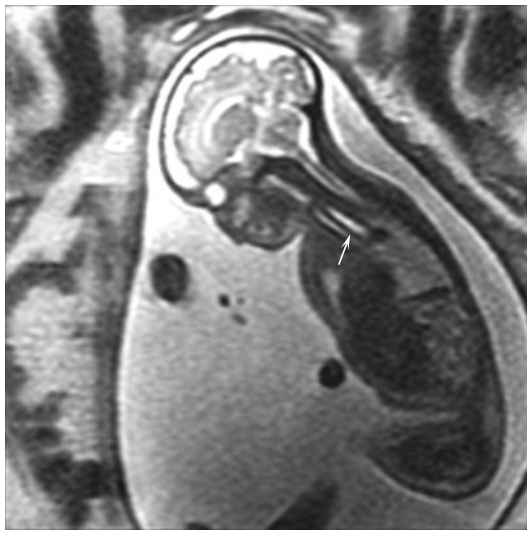

**Fig. 18** Fetal MRI of esophageal atresia. Sagittal T2W HASTE image showing a fluid-filled dilated esophagus (*arrow*), polyhydramnios, and absent stomach. Image courtesy of Dr. Ashley J. Robinson MBChB, Division Chief of Interventional Radiology, Doha, Qatar

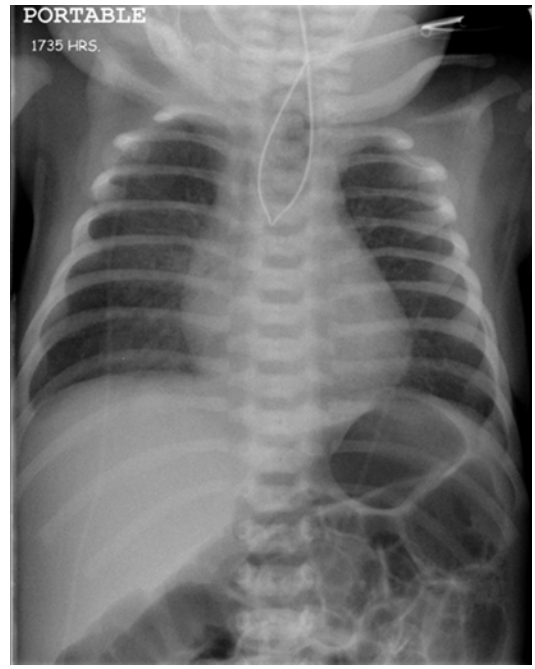


**Fig. 19** Esophageal atresia with distal tracheoesophageal fistula. The orogastric tube has coiled within the atretic esophageal pouch

advance the enteric tube which may result in perforation of the atretic segment. An oral Replogle tube should be placed to decompress the esophagus and freely drain the salivary secretions to minimize the risk of aspiration. The characteristic radiological features of EA include a radiolucent, air-filled, distended, proximal blind-ending pouch (Fig. 20a). The lateral chest radiograph

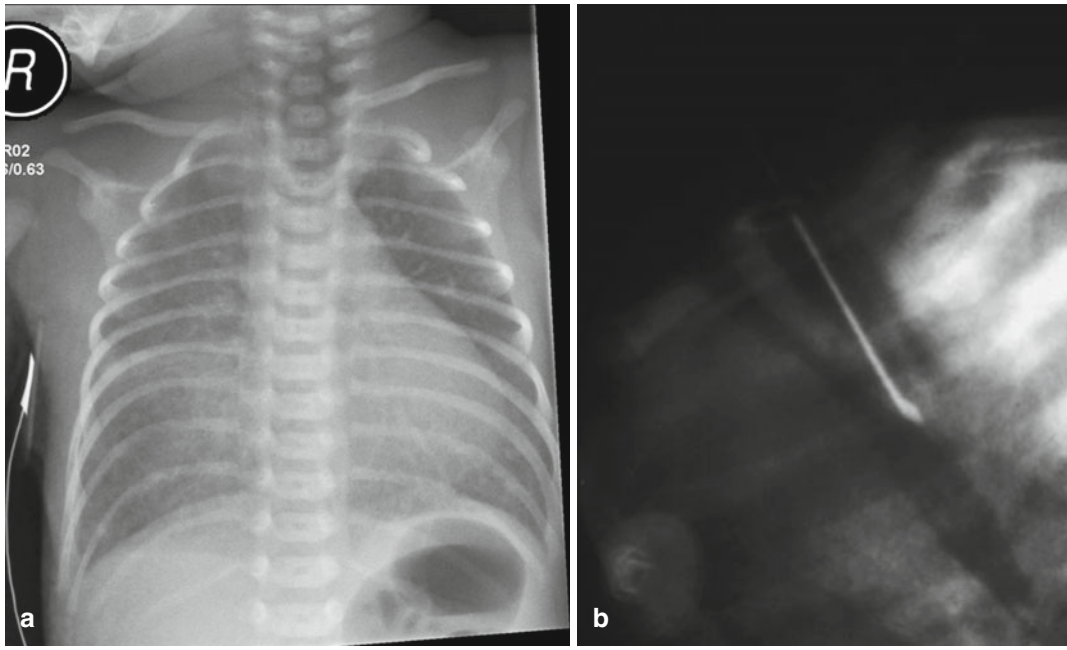


**Fig. 20** (**a**, **b**) Esophageal atresia with distal. (**a**) Initial radiograph with no enteric tube shows distension of the atretic esophageal pouch. (**b**) Tracheomalacia. Lateral radiograph with the orogastric tube in the distended atretic proximal esophagus and markedly decreased caliber of the airway at the same level

confirms the distended esophageal pouch, which displaces the airway anteriorly, effacing the tracheal lumen (Fig. 20b). The cervical esophagus can become quite distended in children on nasal continuous positive airway pressure (CPAP) and have a similar appearance to EA (Walor et al. 2005). Mechanical ventilation predisposes to gastric overinflation but can be avoided where possible by placing an endotracheal tube just beyond the most distal fistula (Spitz 2007). An initial radiograph must include the entire abdomen to assess for the presence of bowel air. A normal bowel air pattern is seen with a TEF (Figs. 21). A gasless abdomen implies the absence of a patent fistula and isolated EA (Fig. 22). The presence of 13 ribs is a predictor of long-gap atresia in TEF (Kulkarni et al. 1997).

A lateral "pouch-o-gram" of the atretic proximal esophagus is not usually necessary because of the low incidence of a fistula from the proximal pouch. A contrast pouch-o-gram can result in aspiration or respiratory compromise resulting from overdistension of the pouch and compression of the airway. Only 1–2 ml of non-ionic contrast medium or atmospheric air is required to adequately distend the pouch. Contrast medium must be removed at the end of the procedure. If primary surgical repair is deferred in a child with suspected long-gap esophageal atresia, then the patient is palliated with a percutaneous endoscopic gastrostomy (PEG). A lateral pouch-o-gram may be combined with a contrast series administered via the PEG tube to determine the esophageal gap to aid planning of definitive repair (Fig. 23). Occasionally contrast administered via a PEG will delineate a distal TEF (Fig. 24).

An H-type fistula is often very challenging to demonstrate on a contrast esophagram (Fig. 25). Where there is ongoing suspicion of TEF with a normal barium esophagram, a further contrast examination may rarely be requested, referred to as a tube esophagram. This study preoperatively has a high false-negative rate and bronchoscopy is preferable. During the tube esophagram, the infant can be placed on a board in the true lateral or prone position. The lateral position affords unobstructed views of the airway and esophagus

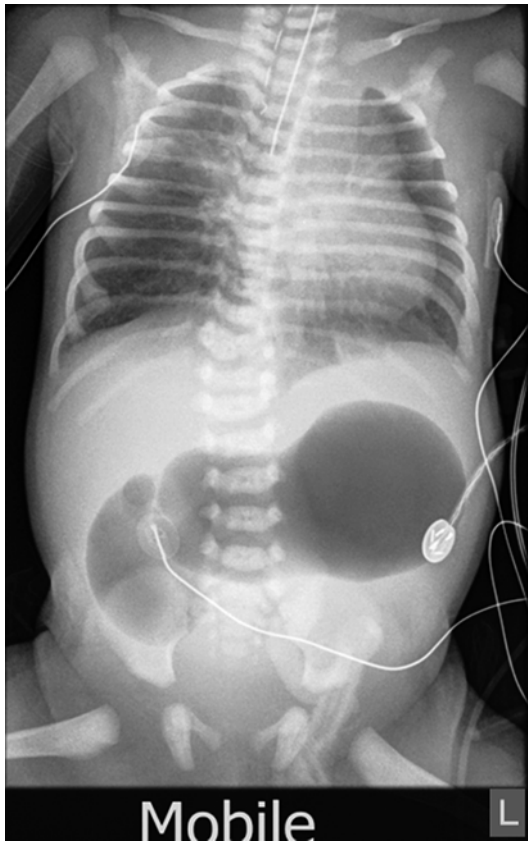


**Fig. 21** Esophageal atresia with distal tracheoesophageal and VACTERL association. An oral Replogel tube is in situ. The endotracheal tube is advanced to a relatively low termination beyond the distal fistula. Lower thoracic vertebral segmentation anomalies are present. There is a characteristic *double-bubble* sign with gaseous distension of the stomach and proximal stomach due to duodenal atresia

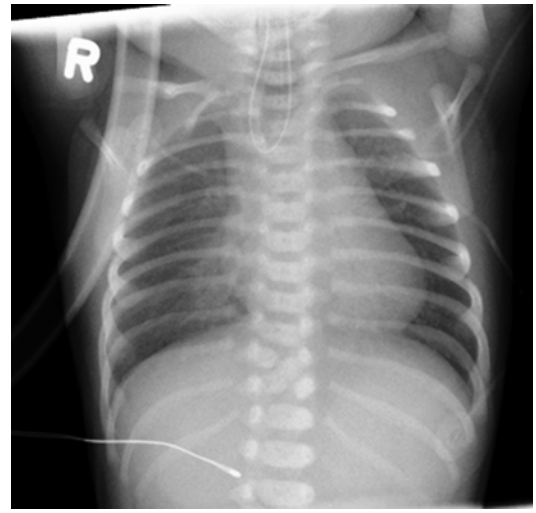


**Fig. 22** Esophageal atresia without tracheoesophageal fistula. The imaged abdomen is gasless, a full length abdominal radiograph was confirmatory

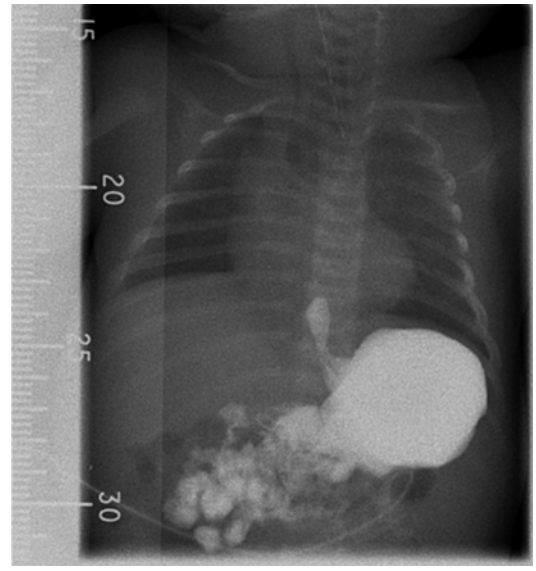


**Fig. 23** Long-gap esophageal atresia. The atretic proximal esophageal pouch is distended with a small amount of air while simultaneously the stomach is opacified with contrast via a gastrostomy. The gap is just under five vertebral bodies in length

and gives the best access for suctioning. Biplane or high-resolution lateral fluoroscopic screening using a high frame rate and video capture facilities are highly desirable in order to depict a subtle fistula. The examination is performed with an enteric tube inserted into the esophagus at the level of the carina. This is slowly withdrawn while low-osmolar non-ionic contrast medium is injected at a rate sufficient to adequately distend the esophagus. The field of view should include the larynx in order to confidently differentiate between contrast entering the trachea through a subtle fistulous connection and inadvertent soiling of the airway by overflow resulting in aspiration. Great care must be exercised as the child may develop cyanosis, respiratory distress, or even apnea following inadvertent pulmonary aspiration. The upper cervical esophagus is the most common location for an H-type fistula. TEF

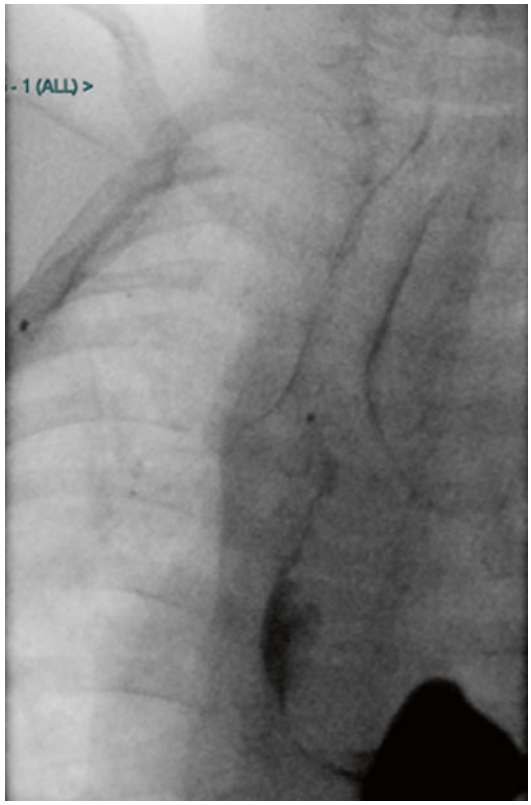


**Fig. 24** Distal tracheoesophageal fistula demonstrated by contrast administered via a gastrostomy catheter

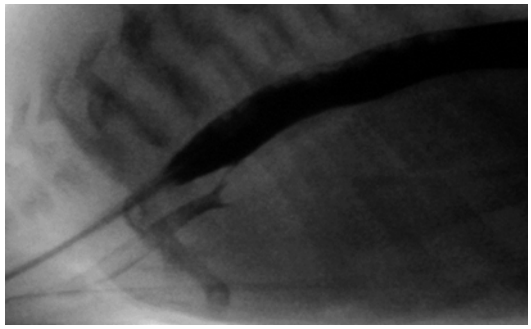

**Fig. 25** Prone tube esophagram showing an H-type tracheoesophageal fistula with oblique and cephalad course

are muscular tubes that are not consistently open. TEF are thought to open with swallowing or during respiration. A fistula may temporarily occlude with food or secretions. It is not uncommon for the fistula not to be demonstrated the first time on an initial screening run on a tube esophagram.

The differential for EA includes esophageal stricture and web. The differential for TEF includes laryngotracheoesophageal cleft, esophageal diverticulum, and tubular duplications.

### 4.1.4 Associated Abnormalities

EA may be isolated, associated with birth defects or form part of a syndrome. There is a high frequency of congenital abnormalities associated with EA/TEF which can have significant short- and long-term implications for the child. VACTERL association is a combination of congenital anomalies typically characterized by the presence of at least three of the following components: vertebral defects, duodenal and/or anal atresia, cardiac defects, TEF, renal anomalies, and limb abnormalities. Careful physical examination should be supplemented by preoperative echocardiography in these babies to exclude structural heart disease and confirm the laterality of the aortic arch. Thoracotomy or endoscopic access is obtained on the side contralateral to the aortic arch. Radiographs should be evaluated for aortic arch laterality and vertebral and limb anomalies. US screening of the renal tract is preferably performed prior to surgery. US evaluation of the spine is also performed to exclude tethered cord but should not delay surgical repair.

Autosomal recessive disorders associated with EA/TEF include Fanconi anemia, rarely Fryns syndrome and the X-linked recessive disorder Opitz G/BBB syndrome (Stoll et al. 2009). Autosomal dominant syndromic associations of EA/TEF include CHARGE syndrome (coloboma, heart, atresia choanal, retarded growth, genital hypoplasia, ear deformities) and AEG syndrome (anophthalmia-esophageal-genital). Feingold syndrome is associated with EA (Van Bokhoven et al. 2005). Chromosomal abnormalities associated with EA include trisomy 18, trisomy 21, trisomy 13, and trisomy X mosaicism (Felix et al. 2007).

### 4.1.5 Postoperative Appearances of EA/TEF Repair

Surgical repair typically involves a lateral thoracotomy, TEF ligation, and primary anastomotic repair of the proximal and distal esophagus;

however, rarely minimally invasive surgery may be offered (Holland and Fitzgerald 2010). Some surgeons may advocate use of a trans-anastomotic tube. Where the baby is not conditioned for primary repair or the gap is too long, temporary palliation with cervical esophagostomy with oversewing of the distal esophagus may be indicated (Spitz 2007), a feeding PEG tube is placed for a staged repair. Following repair the child is typically ventilated and recovered in the intensive care unit with the neck flexed to reduce anastomotic tension (Holland and Fitzgerald 2010). For long-gap EA, defined as a distance of more than four vertebral bodies while under tension, the surgical options include delayed primary repair or a gastric, colonic, or small bowel esophageal replacement conduit.

Early postoperative period complications following EA/TEF repair include anastomotic leak and sepsis secondary to mediastinitis. An UGI series using non-ionic water-soluble contrast medium is routinely indicated four to seven days following primary repair to look for evidence of a leak prior to commencing feeds. The surgical anastomosis is always narrower than the previously obstructed proximal pouch and should not be confused with a stricture (Fig. 26a, b). A normal anastomosis will not impede or obstruct the flow of contrast medium. Small, contained anastomotic leaks may be managed conservatively and most will resolve but a few children will go on to develop a recurrent fistula. Up to 50 % of children with a leak will go on to develop an anastomotic stricture (Kovesi and Rubin 2004).

Almost invariably, some degree of esophageal dysmotility is encountered following EA/TEF repair. Other common long-term complications following EA/TEF repair include feeding difficulties, tracheomalacia, and GER. Esophageal stricture is by far the most frequent long-term complication following EA repair requiring interventional therapy. Treatment involves serial intermittent pneumatic dilatation (Fig. 26c) to prevent foreign body impaction from solid feeds (see Sect. 4.5). Treatment is less successful when associated with reflux (Kovesi and Rubin 2004). A (barium) esophagram should be performed with new onset of dysphagia or altered eating pattern that may indicate a stricture. Drooling and refusal to eat are often symptoms of foreign body or food impaction.

## 4.2 Congenital Esophageal Stenosis

This rare anomaly of unknown etiology is found in 1 in 25,000 to 1 in 50,000 live births. Congenital esophageal stenosis (CES) is characterized by a focal 2–3 mm circumferential narrowing of the esophageal lumen present from birth typically located at the junction of the middle third and distal third of the esophagus. CES may occur at any level. Very rarely CES may be multiple. Three distinct histological subtypes have been described: fibromuscular hypertrophy with dysplasia of the muscularis or submucosa, ectopic tracheobronchial cartilaginous remnants, and finally incomplete membranous diaphragm (Nihoul-Fekete et al. 1987).

CES in the neonatal period is frequently associated with EA and is contended by some authors to be a mild variant of EA (Berrocal et al. 1999). Care should be taken to evaluate the distal esophagus for a coexisting congenital stenosis. TEF is seen in a third of cases and other congenital anomalies in 17–33 % (Vasudevan et al. 2002). The diagnosis should always be considered in an infant with dysphagia or with an impacted foreign body following EA repair. The incidence of postoperative anastomotic leaks in children with TEF is higher when associated with CES (Newman and Bender 1997).

Children typically present outside the neonatal period with recurrent vomiting or food impaction on introduction of solids (Michaud et al. 2013). This may be preceded by failure to thrive and aspiration pneumonitis. A diagnosis should be considered in any case of acute dysphagia. The differential diagnosis includes strictures due to reflux esophagitis, caustic ingestion, and sequelae of surgery.

### 4.2.1 Radiological Findings

On fluoroscopic studies a CES lesion appears as an aperistaltic, gradual tapered narrowing, or as

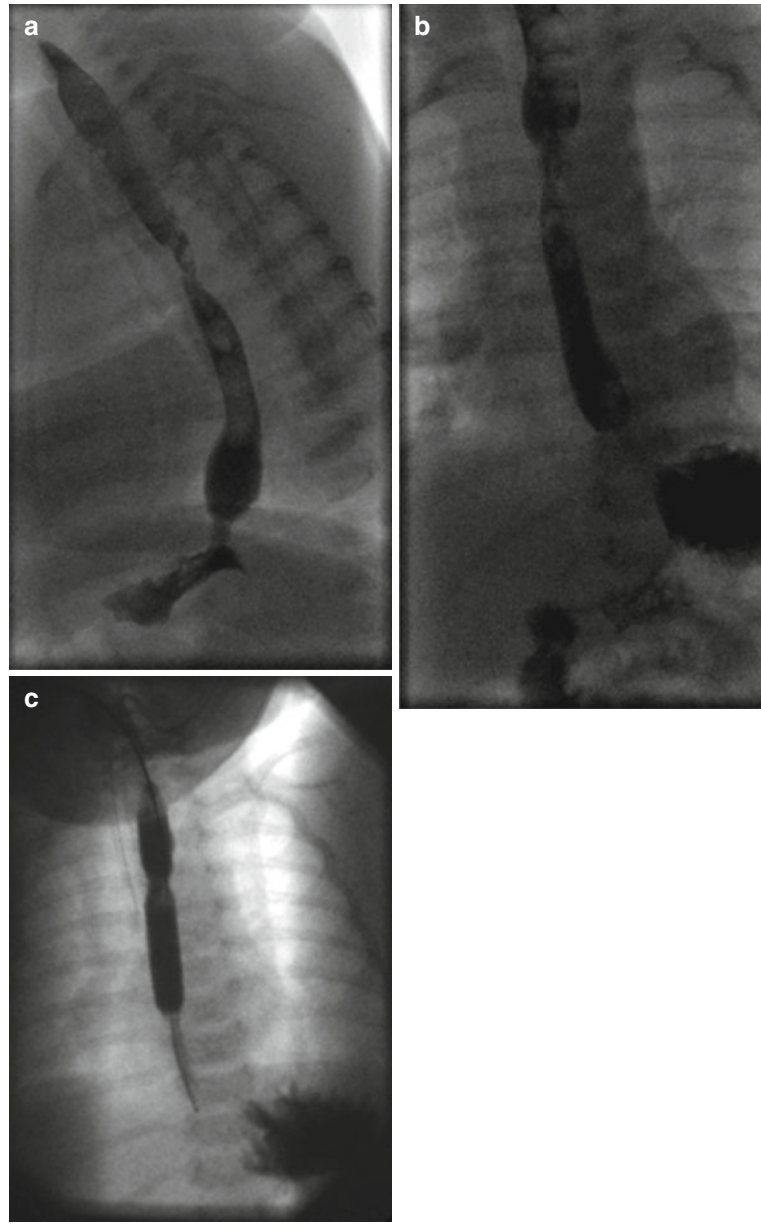


**Fig. 26** (**a**–**c**) Post-anastomotic narrowing of the esophagus. (**a**, **b**) Routine postoperative swallow with non-ionic isotonic contrast medium showing esophageal narrowing at the primary anastomosis without evidence of hold up. No leak was demonstrated. (**c**) Follow-up of uneventful fluoroscopic balloon dilatation of the stricture

a persisting abrupt oblique or transverse filling defect (Fig. 27). The esophagram findings do not predict the histological subtype and endoscopic biopsy is required (Amae et al. 2003). The stenosis is smooth with intact mucosa. This may be found at the same level as a TEF. Intraluminal filling defects may represent an impacted food bolus or other foreign body. Proximal esophageal dilatation reflects a higher-grade stenosis. The entire esophagus must be carefully scrutinized after surgical correction of EA to look for coexisting CES (Vasudevan et al. 2002). Esophageal dysmotility may accompany all forms of CES.

Initial treatment may include endoscopic or interventional balloon dilatation. There is higher incidence of esophageal perforation in those with tracheobronchial remnants (TBR), especially in young children; dilatation is more effective in other histological subtypes (Michaud et al. 2013).

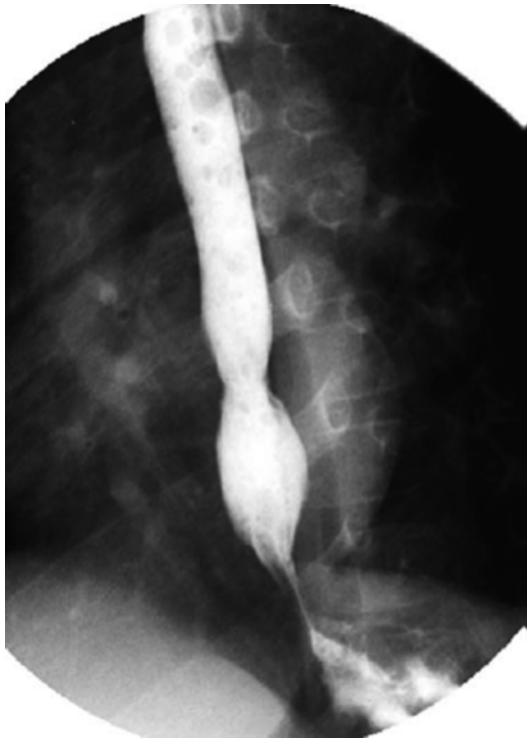

**Fig. 27** Congenital esophageal stenosis. Barium swallow showing discrete annular stenosis in distal esophagus. Tracheobronchial remnants were found during histopathology

Esophageal luminal diameter increases with age and patient growth but despite repeated dilatations will never be normal (Newman and Bender 1997).

## 4.3 Esophageal Duplication

Esophageal duplication cysts are rare and the true prevalence is unknown. They account for approximately 15–20 % of all gastrointestinal duplications and are typically solitary. Around 80 % of cases are detected in childhood, most are symptomatic at presentation, approximately 60 % are found in the lower third of the esophagus, and the remainder evenly distributed in the proximal and middle thirds (Yoshida et al. 2005). They very rarely affect the intra-abdominal esophagus. Esophageal duplications are defined by the presence of (1) attachment to the esophageal wall, (2) gastrointestinal epithelial lining, and (3) a smooth muscle wall. Spherical duplication cysts are the product of a foregut cystic malformation and are enteric cysts which abnormally pinch off from the foregut and incorporate in the wall of the developing gastrointestinal tract (Sharma et al. 2009). They may contain gastric mucosa, which can cause mural ulceration, bleeding, and rarely perforation. Secondary infection is uncommon. The differential is a bronchopulmonary foregut cyst. Spherical esophageal duplication cysts are treated by excision. Tubular duplications represent true microscopic and macroscopic duplication with a blind loop of the gut lying along the antimesenteric border. These typically communicate with the bowel lumen. Complete esophageal duplication is extremely rare and is often associated with gastric duplication (Herman et al. 1991). Tubular duplications require more complex surgical management.

### 4.3.1 Radiological Findings

Esophageal duplication cysts may be detected incidentally on chest radiographs as a posterior mediastinal mass. An esophagram demonstrates a smooth, well-defined extrinsic soft tissue mass displacing the esophagus. US may adequately demonstrate a distal esophageal cyst (Fig. 28). Cross-sectional imaging enables differentiation of the cyst from a solid mass such as neuroblastoma or pulmonary sequestration and to show its relationship to adjacent vital structures. CT reveals a well-defined round or ovoid fluid containing non-enhancing mass adjacent to the esophagus (Fig. 29). On MR cyst content reflects the amount of water and proteinacious material, with signal typically following water but may appear more complex if complicated by hemorrhage.

## 4.4 Esophageal Bronchus

Esophageal bronchus is a rare form of congenital bronchopulmonary foregut malformation (CBPFM) involving an abnormal cartilaginous fistulous connection between the foregut and an isolated portion of respiratory tissue. The most common variant is the esophageal bronchus whereby a portion of lung communicates with

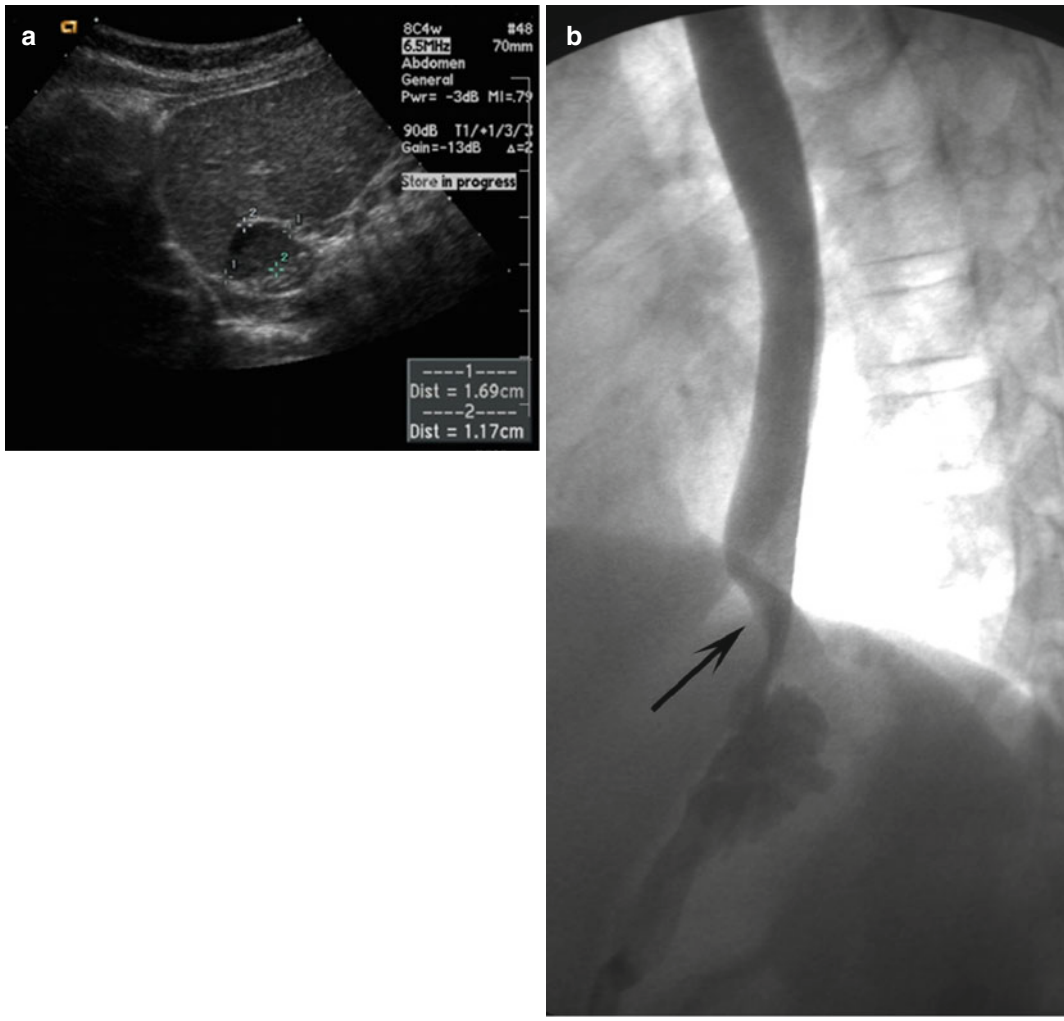


**Fig. 28** (**a**, **b**) Esophageal duplication cyst. (**a**) US image showing a thin-walled subdiaphragmatic cyst (between calipers) causing (**b**) smooth extrinsic compression of the distal esophagus as shown on a barium esophagram (*black arrow*)

the lower esophagus. The anomalous communication may involve a whole lung. Involvement of the stomach is rare. The embryological classification of these fistulae is summarized in Table 3. The fistula forms through a focal mesodermal defect when a portion of the lung bud covered by mesenchyme connects with the elongating foregut (Srikanth et al. 1992). The affected bronchus is absent from the native bronchial tree. The arterial supply of the affected lung arises from the pulmonary artery or both pulmonary and systemic circulations. Venous drainage is to the pulmonary vein, azygos, or portal venous system. There is a frequent association with other bronchopulmonary foregut malformations such as congenital pulmonary airway malformation, sequestered lung, and bronchogenic cyst. Other common associations include TEF with EA and cardiac anomalies which substantially increase morbidity and mortality. Symptoms include respiratory distress, coughing related to feeds, and recurrent lower respiratory tract infections. Whole lung involvement tends to present in the neonatal period, whereas lobar involvement may present later in life. Neonatal tracheal reimplantation is the treatment of choice. However, resection of the anomalous pulmonary tissue and fistula with

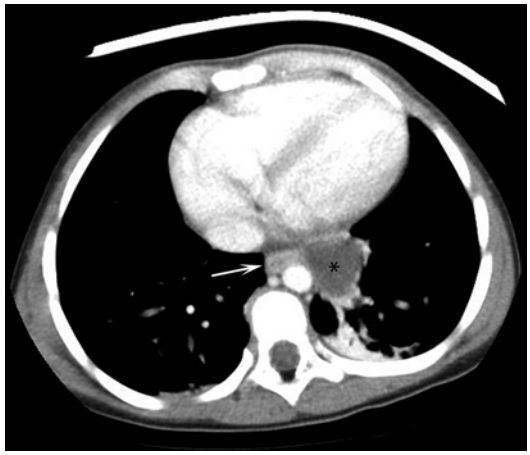

**Fig. 29** Axial CT of esophageal duplication cyst (*) adjacent to the esophagus (*arrow*) and descending thoracic aorta

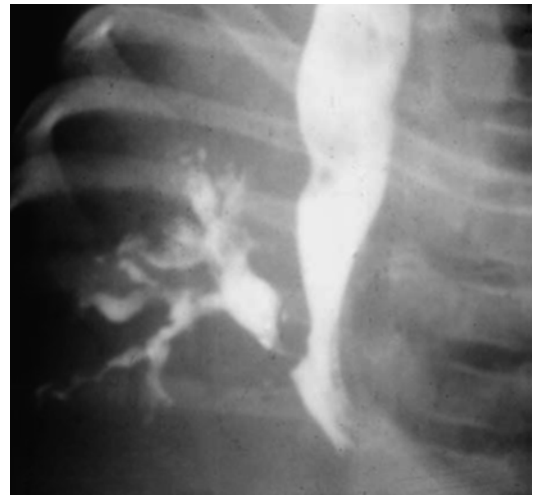

**Fig. 30** Esophageal bronchus. Barium esophagram demonstrates the right main bronchus arises from the esophagus. The right lung is completely opacified

**Table 3** Proposed classification of bronchopulmonary foregut fistulae

| Type | Subtype | |
|---|---|---|
| 1 | | CBPFM associated with esophageal atresia and tracheoesophageal fistula |
| | A | Entire lung arises from the esophagus or stomach |
| | B | Portion of one lung or lobe arises from the esophagus |
| 2 | | A lung originates from the distal esophagus |
| 3 | | Isolated anatomic lung, lobar or segmental fistula to esophagus or stomach |
| 4 | | Portion of the normal bronchial system communicates with the esophagus and receives systemic blood supply |

Adapted from Srikanth et al. (1992)

repair of the anomalous communication is required if the affected lung has been destroyed by recurrent infection (Sugandhi et al. 2011).

### 4.4.1 Radiological Findings

The chest radiograph is nonspecific, revealing opacification of the affected portion of lung. A water-soluble contrast examination of the esophagus and stomach using isotonic non-ionic contrast medium is sufficient to confirm an abnormal communication (Fig. 30). Unenhanced CT will reveal pulmonary parenchymal complications including atelectasis, bullae, and abscess formation and estimate percentage lung involvement. MDCT angiography (CTA) is preferable to depict adequacy of arterial blood supply and venous drainage.

## 4.5 Hiatal Hernia

A hiatus hernia is defined by the abnormal migration of an intra-abdominal structure in to the thoracic cavity through the esophageal hiatus. Hiatus hernia and intra-thoracic stomach are uncommon in children. They may be congenital or acquired. Most are sporadic. Associations include a short esophagus, Marfan's syndrome, and visceral heterotaxy (Al-Assiri et al. 2005). The anatomical classification of hiatal hernias is summarized in Fig. 31 and is as follows: Type I hiatal hernias, also referred to as sliding hiatal hernias, are by far the most common type. Type I hernias result from circumferential laxity of the phrenoesophageal membrane such that the gastroesophageal junction and a portion gastric cardia migrate through the widened muscular hiatal tunnel (Kahrilas et al. 2008). The

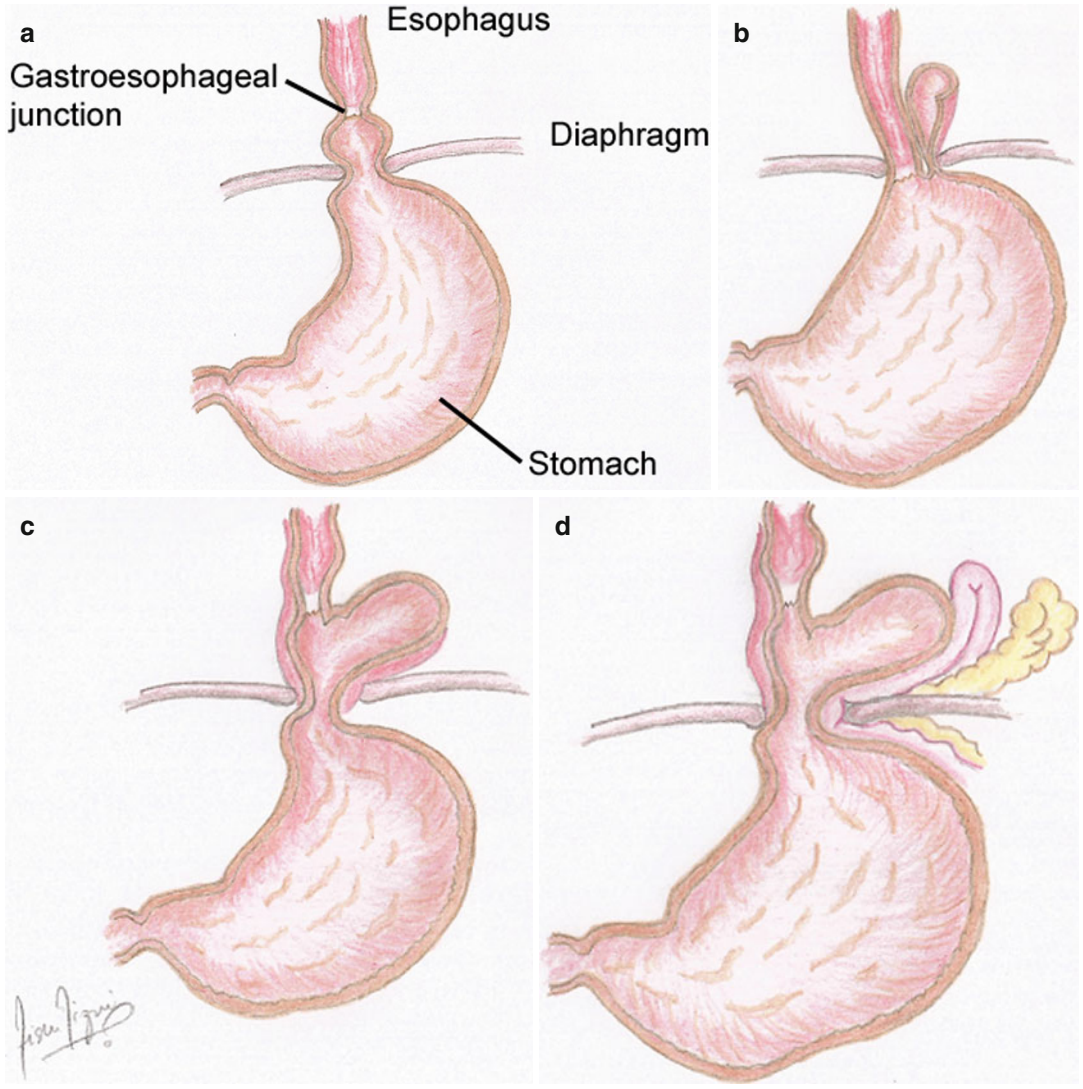


**Fig. 31** (**a**–**d**) The classification of hiatal hernias. (**a**) Type I (sliding) is the most common whereby the gastroesophageal junction herniates beyond the gastroesophageal junction. (**b**) In type II hernias the gastric fundus is the lead point for herniation and the gastroesophageal junction is normally positioned. (**c**) Type III is a mixture of types I and II. (**d**) Type IV hernias involve herniation of the stomach and other organs. Image courtesy of Dr. Aisha Rizvi MBBS, Doha, Qatar

stomach remains in its usual longitudinal alignment and the fundus remains below the gastroesophageal junction. These may be intermittent and are often found incidentally on an esophagram but can predispose to GER. Type II–IV hernias are referred to as paraesophageal hernias. Type II hernias occur when part of the gastric fundus herniates through the diaphragmatic hiatus adjacent to the esophagus. The gastroesophageal junction remains in normal anatomical position. Type III hernias are the most common type of paraesophageal hernia and are a combination of Types I and II, with the fundus lying above the gastroesophageal junction. Type IV hernias are characterized by the presence of a structure other than stomach such as colon, spleen, small intestine, or pancreas in the hernial sac.

Esophageal transit time and duration of GER are prolonged in children with hiatal hernia. In symptomatic children with recurrent gastroesophageal reflux disease, laparoscopic fundoplication is advocated (Bansal and Rothenberg 2014).

### 4.5.1 Radiological Findings

Depending on the size of the herniated portion of the intra-thoracic stomach, chest radiographs may reveal a air-filled lucency occasionally with compressive atelectasis of adjacent lung. An esophagram is confirmatory (Fig. 32). Ultrasound can demonstrate a short length of abdominal esophagus, loss of the acute gastroesophageal angle, and GER as well as transhiatal passage of omental fat (Westra et al. 1990; Koumanidou et al. 2004).

## 4.6 Vascular Rings and Sling Abnormalities

### 4.6.1 Vascular Rings

A "vascular ring" refers to an anomaly of the embryonic aortic arch complex and involves the paired 4th–6th aortic arches. Abnormal regression or persisting patency of these arches results in vascular and ligamentous derivatives encircling and compressing the trachea and esophagus. Vascular rings are uncommon but approximately one fifth are associated with congenital cardiac anomalies. The presentation of a vascular ring is varied, but predominantly related to the degree of airway compression. Symptoms include life-threatening respiratory compromise in the infant, stridor, and recurrent chest infections. Gastrointestinal symptoms such as dysphagia, particularly on the introduction of solids, are less common and are more often encountered with a left retroesophageal subclavian artery arising from a right aortic arch (Bonnard et al. 2003). Vascular rings may often be asymptomatic and detected as an incidental finding on a contrast esophagram or cross-sectional imaging. Rarely, ingested foreign bodies may declare a vascular ring as the foreign body will lodge just proximal to the ring (see Sect. 5.3).

Approximately 75 % of cases of double aortic arch are typically formed by a dominant superior right aortic arch and completed by a more inferior smaller or atretic left aortic arch. In approximately 20 % the left aortic is dominant (Fraser and Carberry 2012). A double aortic arch results in anterior and bilateral airway compression and posterior and bilateral indentation of the esophagus. A right aortic arch with aberrant left subclavian artery (LSCA) will give rise to a vascular ring if the left ductus arteriosus passes between the right descending aorta and the left pulmonary artery and results in posterior oblique compression of the esophagus. The aberrant LSCA will often arise from a diverticulum of Kommerell.

The traditional surgical treatment of a vascular ring is to relieve the constriction by open thoracotomy with division of non-functional or non-critical components of the ring, typically the atretic or nondominant segment (Alsenaidi et al. 2006). In cases with a right aortic arch and a left ligamentum arteriosum, the ductal remnant is divided, and the trachea and esophagus are released from fibroadhesive bands (Backer et al. 2005). Primary translocation of the aberrant left subclavian artery to the left carotid artery, with removal of the Kommerell diverticulum and division of the ligamentum through a left thoracotomy, is an alternative strategy (Shinkawa et al. 2012). Minimally invasive thoracoscopic division of a vascular ring avoids the morbidity associated with thoracotomy (Al-Bassam et al. 2007).

#### 4.6.1.1 Radiological Findings

A chest radiograph may demonstrate tracheomalacia and confirm the laterality of the aortic arch(es). A right-sided aortic arch in a child with respiratory symptoms is suspicious for a vascular ring. The next examination is typically a (barium) esophagram which best depicts extrinsic esophageal compression by an atretic or persistent aberrant vascular segment which are typically not well delineated by MDCT or MRI (Turner et al. 2005). The esophagram is a useful screening modality as it is widely available, may exclude other esophageal pathologies, and does not require sedation. An adequately distended normal esophagram will exclude a vascular ring.

A vascular ring caused by a double aortic arch system with bilateral arch patency causes significant focal narrowing and anterior indentation of

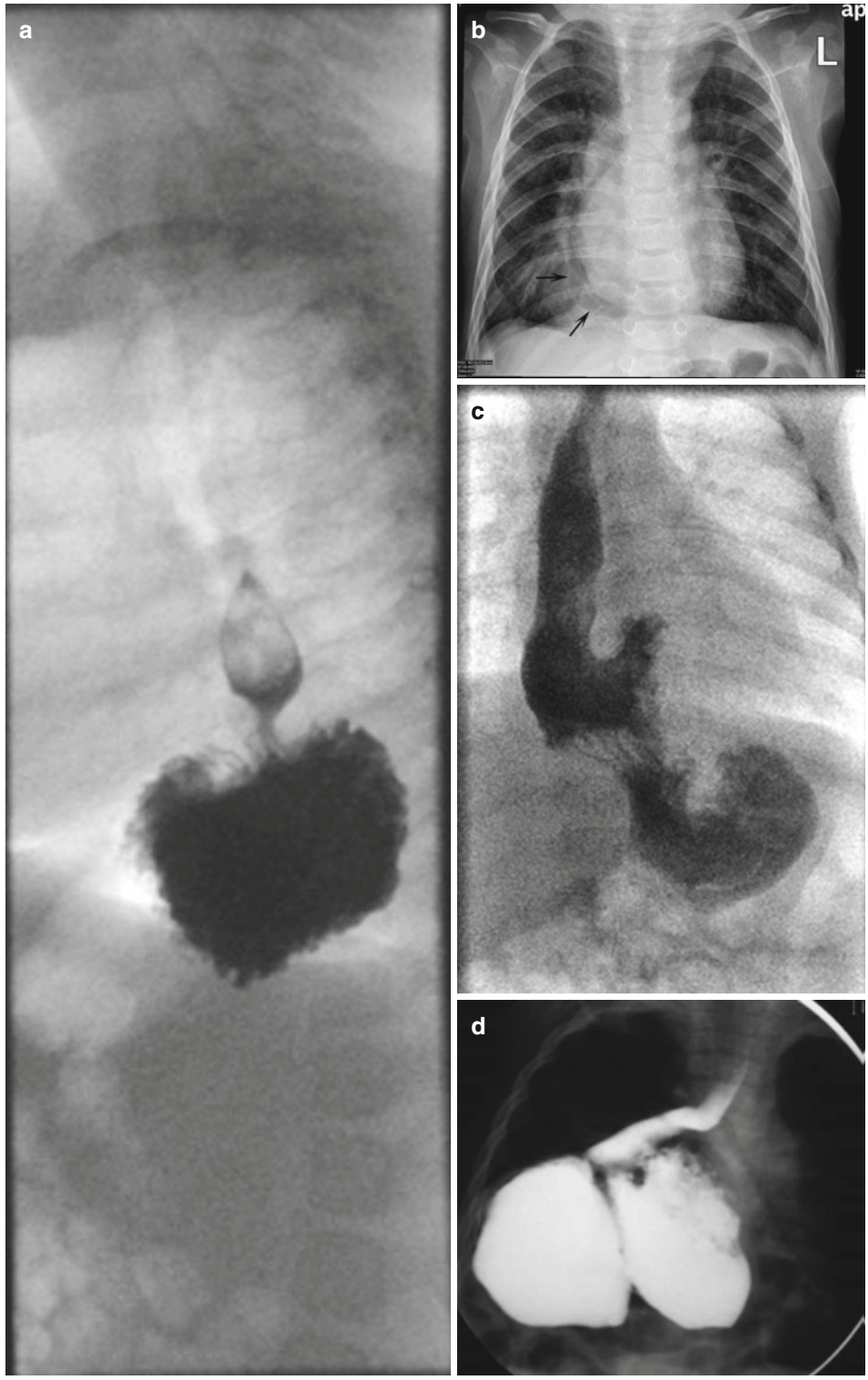


**Fig. 32** (**a**–**d**) Radiographic imaging of hiatal hernias. (**a**) Barium swallow demonstrating a type I hiatus hernia. (**b**) Frontal chest radiograph showing a retrocardiac lucency (*arrows*) (**c**) confirmed on a barium swallow to be a type III hiatus hernia. (**d**) Intra-thoracic herniation of the stomach in a child with Marfan's syndrome

the trachea, which can be appreciated on the lateral chest radiograph and barium esophagram (Fig. 33a, b). A characteristic S-shaped configuration of right- and left-sided lateral indentations is present on the frontal projection. A barium esophagram can depict the right arch and a posterior esophageal impression that is frequently associated with congenital heart disease. A contrast

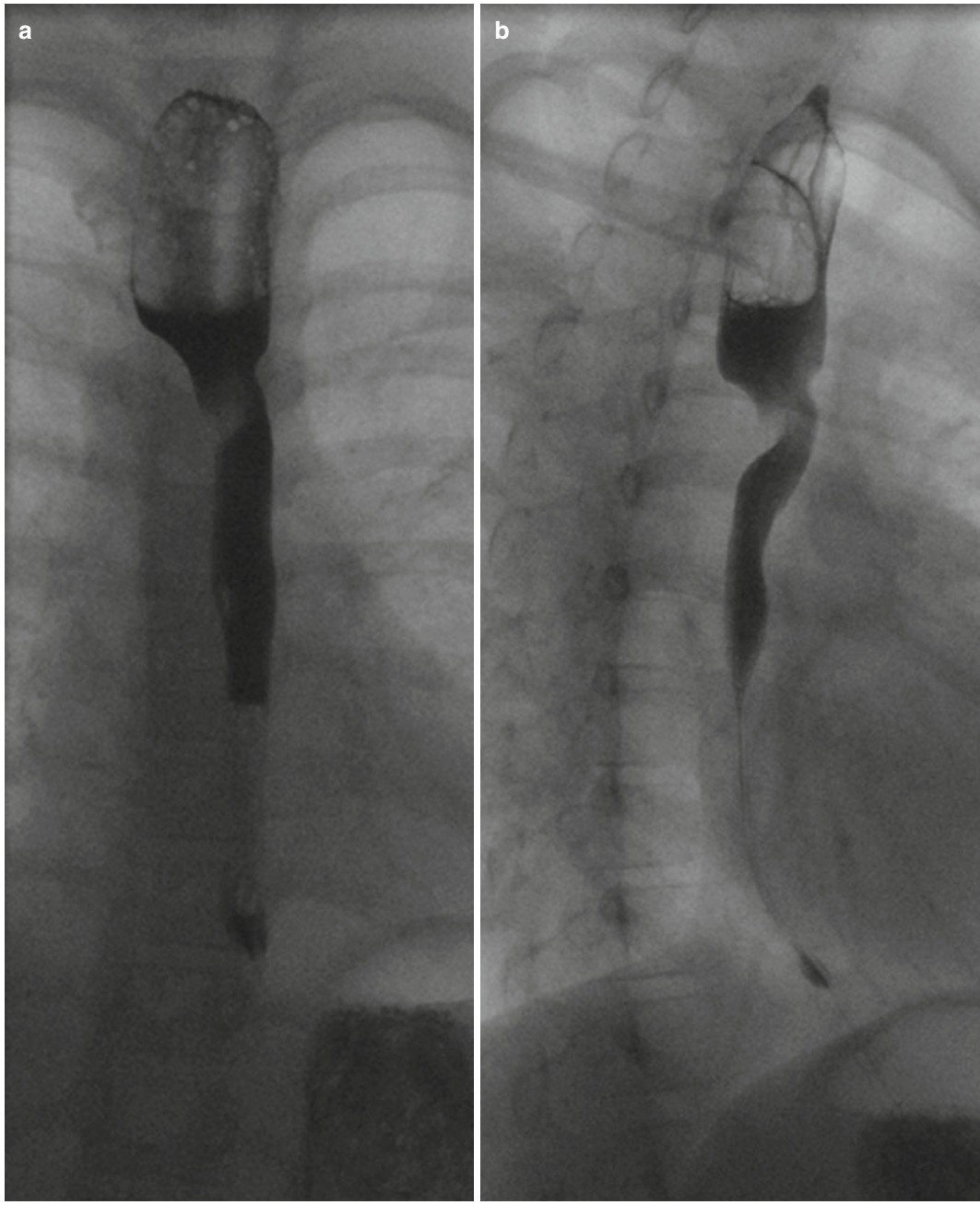


**Fig. 33** (**a**–**e**) Double aortic arch. Barium esophagram (**a**) AP view showing bilateral extrinsic impressions upon the esophagus and (**b**) the lateral view showing a posterior indentation. (**c**) Axial contrast-enhanced maximum-intensity projection CT showing a complete double aortic arch encircling the trachea and esophagus, (**d**) corresponding 3D volume-rendered image and (**e**) coronal minimum-intensity projection image showing tight compression of the trachea

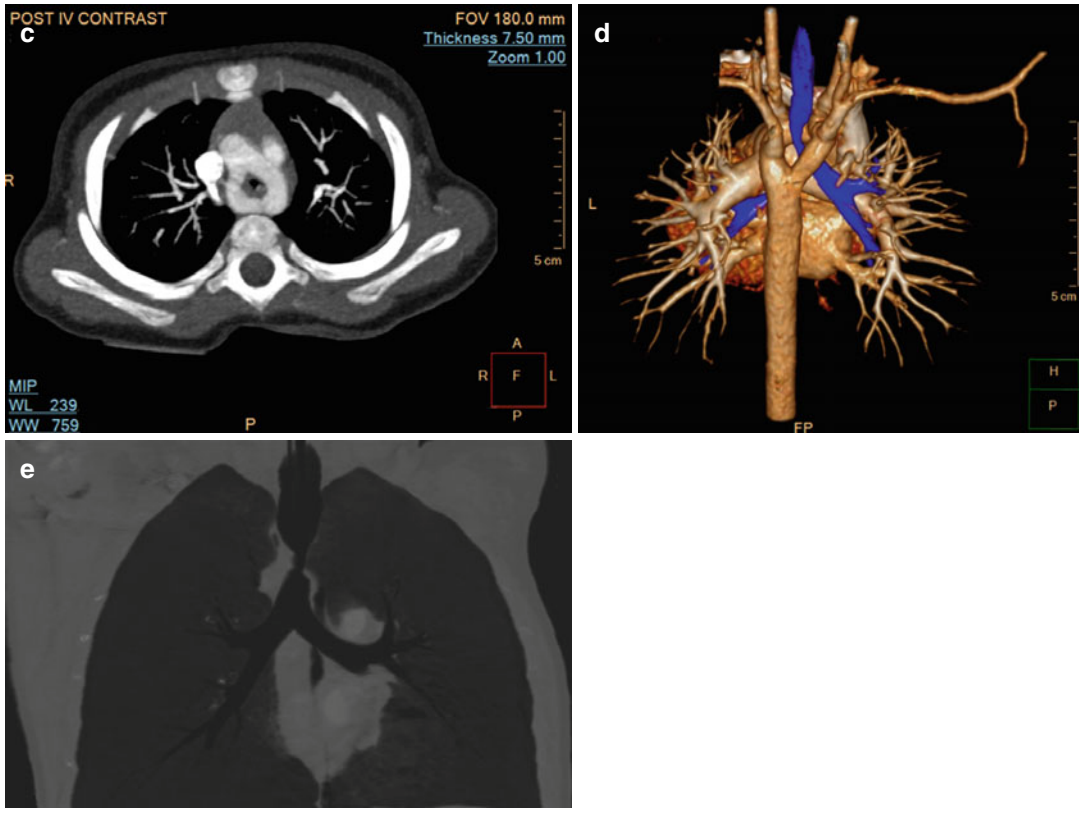


**Fig. 33** (continued)

esophagram does not reliably distinguish between the various other forms of vascular ring. Cross-sectional imaging, either with MR or enhanced MDCT, is most useful delineating the spatial anatomy to provide a preoperative roadmap for thoracoscopy or an open thoracotomy (Yedururi et al. 2008). MDCT is rapidly acquired over a few seconds without the need for sedation or anesthesia in most cases (Fig. 33c–e). MR typically would require sedation and immobilization for studies that can take between 45 and 60 min. Respiratory and EKG-navigator MRI with feeding and swaddling is feasible for the very young neonate to avoid sedation. The obvious disadvantage of MDCT is the radiation dose and pediatric-specific protocols are mandated. MDCT is still favored by many as the lungs and bronchi are exquisitely demonstrated. Diagnostic yield is further enhanced with multiplanar, maximum-intensity projection, minimum-intensity projection, and 3D volume-rendered reformations. High-resolution black blood, 3D FISP (fast imaging with steady precession), and magnetic resonance imaging (MRA) will accurately define vascular rings (Fig. 34). The choice of imaging modality varies with institutional preference.

### 4.6.2 Pulmonary Artery Sling

Pulmonary artery sling complex is a rare vascular anomaly in which the left pulmonary artery (LPA) arises from the right pulmonary artery, encircles the distal trachea and right main bronchus, and indents the anterior margin of the esophagus prior to entering the left lung hilum. The LPA ring-sling complex is defined as the association of an aberrant LPA with complete cartilaginous tracheal rings and tracheal stenosis. Symptoms are typically related to airway compression. Surgical repair requires relief of the sling compression with reimplantation of the LPA to the main pulmonary artery, while tracheal rings require major airway reconstruction with a slide tracheoplasty.

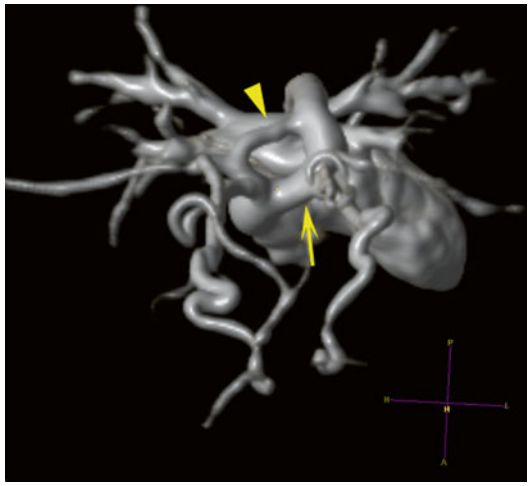

**Fig. 34** Double aortic arch. Contrast-enhanced MRA of the thorax in a child demonstrating a dominant left aortic arch (*arrow*) and smaller right arch (*arrowhead*)

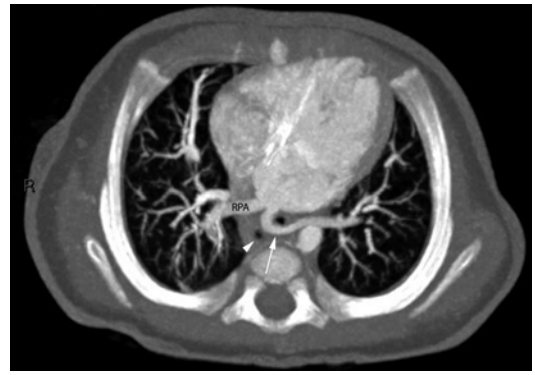


**Fig. 35** Anomalous left pulmonary artery origin. Axial contrast-enhanced CT maximum-intensity projection image showing anomalous origin of the left pulmonary artery (*arrow*) from the right pulmonary artery (*RPA*). The LPA passes behind the trachea and forms an anterior indentation upon the esophagus (*arrowhead*)

#### 4.6.2.1 Radiological Findings

Cross-sectional imaging with MDCT (Fig. 35) or MR is helpful in presurgical planning and post-surgical assessment. A barium esophagram is not usually performed but may reveal an abnormal anterior indentation upon the esophagus by the anomalous LPA.

## 5 Acquired Abnormalities

### 5.1 Gastroesophageal Reflux

Gastroesophageal reflux (GER) is defined by the retrograde passage of gastric content into the esophagus with or without vomiting or regurgitation. GER is very common in infants and children and may be physiologic in young infants. Gastroesophageal reflux disease (GERD) refers to those children with GER who develop troublesome symptoms and/or complications (Vakil et al. 2006).

The incidence of GER ranges from 25 to 60 % in all infants (Rosen 2014) and up to 70 % in children with underlying conditions such as tracheoesophageal fistula, neurological deficits, and anatomic abnormalities of the esophagus (McGuirt 2003). The clinical presentation of GER is variable. In infants it manifests as feeding difficulties including vomiting, regurgitation, and 'spitting up'. Other symptoms include arching, hoarseness, and cough. GER has a peak incidence at 4 months of age, decreasing by 6 months and falling sharply by around 12 months of age coinciding with the age at which children learn to sit up (Campanozzi et al. 2009). Epigastric pain is more common in older children. In young infants, the short length of the intra-abdominal esophagus and physiologic immaturity of the developing lower esophageal sphincter (LES) contribute to GER. A transient fall in LES pressure to a level at or below intragastric pressure results in GER. GER invariably improves with the introduction of solid food. Severe GERD can lead to growth disturbance and troublesome gastroesophageal symptoms such as "heartburn" and refusal to eat. GER is associated with asthma. Hyperinflation changes the pressure gradient across the LES, increases negative intra-thoracic pressure, and alters the relationship between the diaphragm and lower esophageal sphincter. This may be exacerbated by some asthma medications that decrease LES pressure. Pulmonary aspiration is a significant complication although seldom demonstrated by diagnostic imaging.

Clinical investigation of GER includes a 24-h continuous ambulatory esophageal pH-impedance test to document acid and non-acid reflux events. pH studies have a much higher

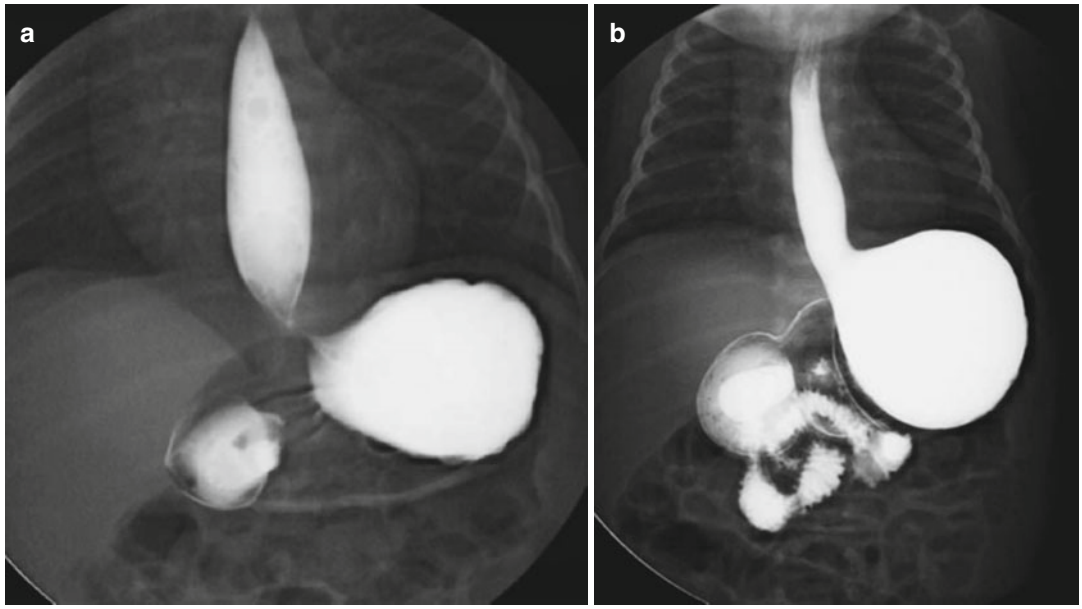


**Fig. 36** (**a**, **b**) Gastroesophageal reflux. (**a**) During swallowing, the gastroesophageal junction is closed. (**b**) The gastroesophageal junction is widely patent, and barium refluxes to the upper esophagus

sensitivity for GER than radiological investigations (Vandenplas et al. 2009). pH studies without impedance are more widely available but do not document significant non-acid reflux episodes and rely on the period of time pH falls below 4, referred to as the pH index. Endoscopy will confirm macroscopic features of GERD such as esophagitis, erosions, ulceration, and stricturing with the potential for biopsy. Esophageal manometry detects LES pressure and may diagnose achalasia of the cardia or transient relaxation of the LES implicated in GERD. All these techniques are highly invasive.

The initial treatment for GERD is conservative and most commonly involves a regime of offering smaller boluses of thickened feed and maintaining an upright position after feeding. Children with GERD refractory to medication may benefit from surgery. Laparoscopic fundoplication whereby the LES is augmented with a gastric fundal wrap is the surgical treatment of choice for GERD. In some children the wrap can be "too tight" leading to troublesome dysphagia and may require endoscopy +/− dilatation (Kubiak et al. 2011). Fundoplication failure requiring reoperation is uncommon but most common in children with neurological disability.

### 5.1.1 Radiological Findings

The (barium) esophagram and UGI series is frequently requested in children with suspected GER (Fig. 36) and is the least invasive routine diagnostic imaging test. Contrast studies have low sensitivity (43 %) and low negative predictive value (24 %) for detecting GER (Macharia 2012). The main role of the contrast examination is to exclude anatomic abnormalities of the esophagus such as hiatal hernia, to define the position of the duodenojejunal junction; document gastric emptying, the cephalad anatomical level of any reflux, evaluate for pulmonary aspiration and assess the effectiveness of a fundoplication procedure (Fig. 37). Late complications of GERD in childhood include esophagitis, stricture formation (Fig. 38), and Barrett's intestinal metaplasia.

Dilute barium is administered orally. Water-soluble contrast medium may be initially used if there is initial concern for aspiration. Ideally the stomach should be filled with the same volume as a normal feed. If barium intake is insufficient, the ingested volume can be supplemented with infant formula or fruit juice. Chilled barium and adding flavorings may improve palatability. Alternatively

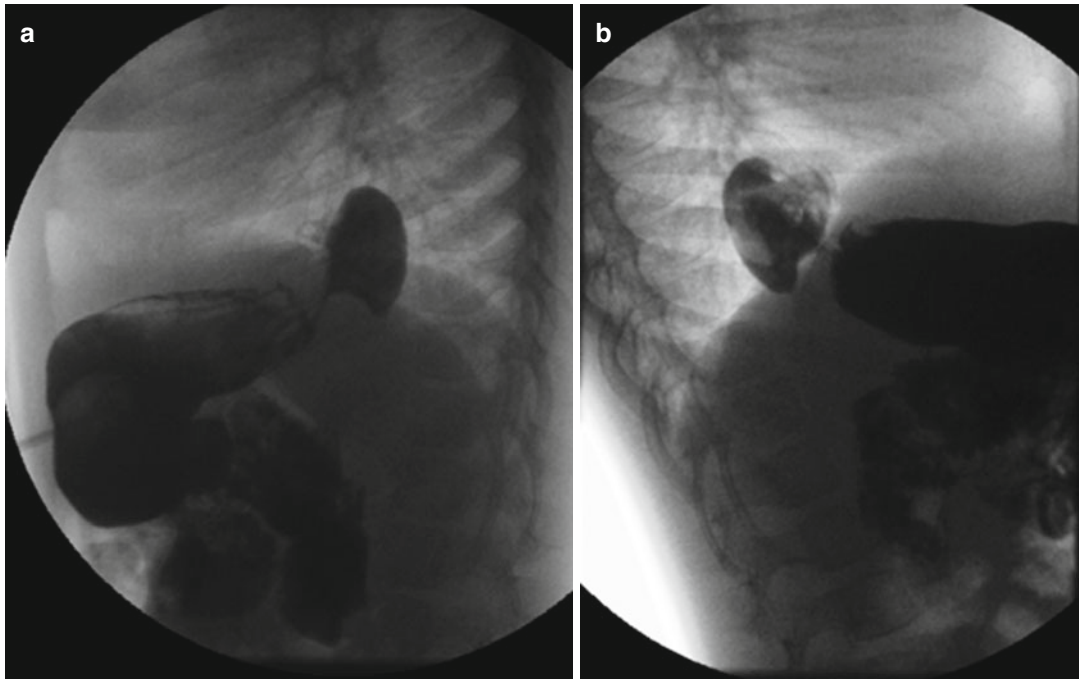


**Fig. 37** (**a**, **b**) Nissen fundoplication. (**a**) Lateral and (**b**) AP view of an esophagram showing the subdiaphragmatic wrap. Adequate passage of contrast through the fundoplasty into the stomach is demonstrated

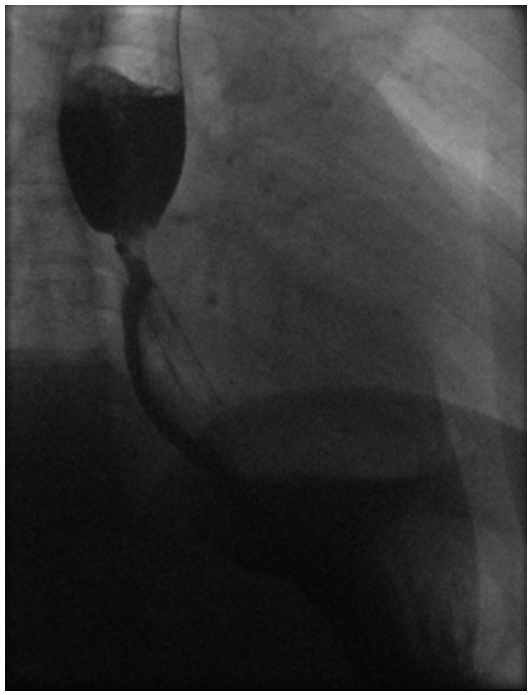

**Fig. 38** Reflux stricture. Tapered stricture of the distal esophagus in a teenager with GERD refractory to medical therapy

the feed may be administered via an indwelling percutaneous gastrostomy tube. The stomach can be filled via a nasogastric tube. As any enteric tube passing through the GEJ maintains patency of the lower esophageal sphincter and impairs its function, such tubes must be immediately removed when evaluating for GER. The presence of GER does not necessarily imply GERD nor does its absence exclude GERD (Rudolph et al. 2001). Imaging for GER could be construed as "objectifying the subjective." The estimated dose of an UGI series in a single center using 16 spot images and 40 s of fluoroscopy is of the order of around 1 mSv and almost equivalent to annual background radiation exposure (Macharia 2012).

The radionuclide "milk scan" is a sensitive test for diagnosing GER but is not routinely indicated for assessing GERD (Vandenplas et al. 2009). Milk, formula, or juice mixed with Tc 99 m sulfur colloid is administered to the child who is then scanned. Scintigraphy offers continuous dynamic assessment enabling documentation of the rate of gastric emptying, number of episodes of GER, and cephalad extent of each GER

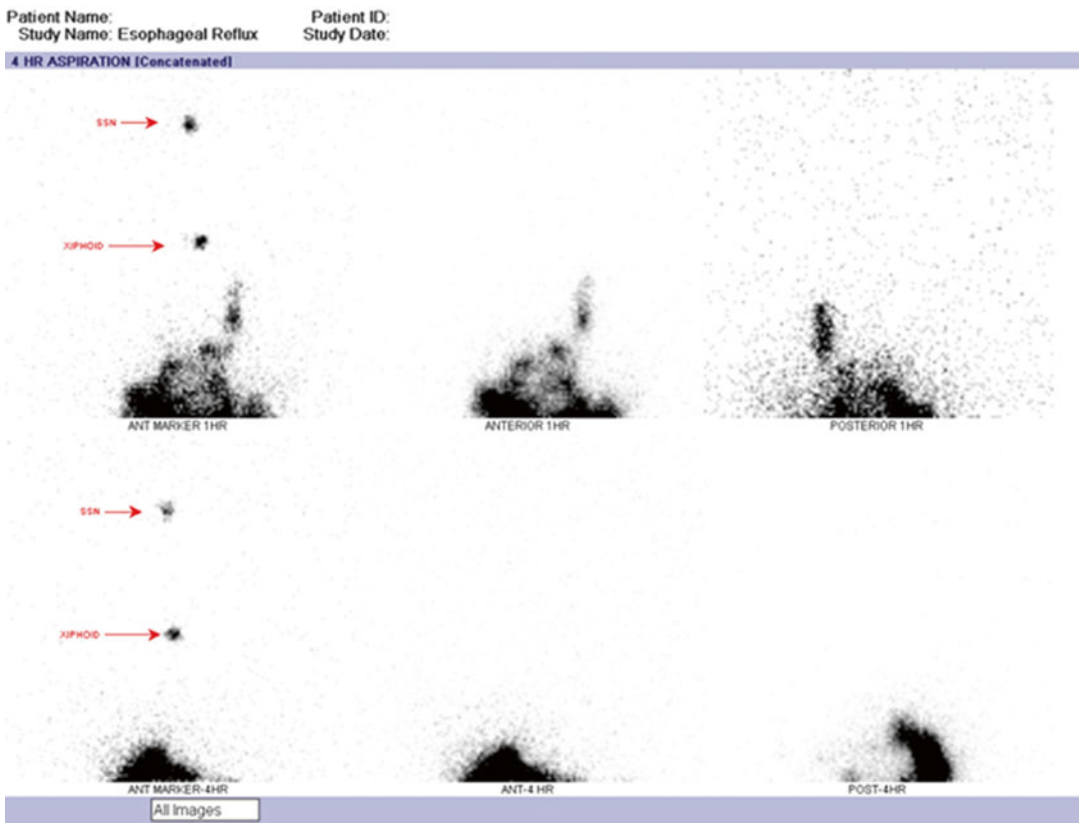


**Fig. 39** Gastroesophageal reflux. Tc99m gastric emptying (radionuclide milk) scan showing gastric reflux to the level of the upper esophagus. Delayed imaging at 4 h reveals no pulmonary aspiration

episode and confirms pulmonary aspiration (Fig. 39). Practice guidelines for pediatric gastric scintigraphy have recently been updated and describe current techniques in more detail (ACR 2014). Scintigraphy is still undertaken in some centers to document response to treatment and stratify those who merit surgical intervention.

Passive reflux into the distal esophagus can be demonstrated sonographically (Koumanidou et al. 2004). The technique is performed after a suitable fast of approximately 2–4 h. Initial assessment, especially if there is no correlative barium study, concentrates on excluding gastric outflow tract obstruction including hypertrophic pyloric stenosis. According to some authors malrotation may also be assessed sonographically (Yousefzadeh 2009). Assessment of both these conditions is hampered when there is excessive aerophagia from crying in the starving child and a liquid feed should be given up to the normal amount. Using an age-appropriate curvilinear, or high-resolution linear probe with virtual trapezoid mode enabled, imaging is obtained with gentle graded compression in the transverse oblique plane with approximately 45°cranial tilt. The intra-abdominal esophagus is assessed as it enters through the diaphragm to the gastric cardia. Intra-abdominal esophageal length and transmural wall thickness including the serosa as well as the gastroesophageal angle of "His" are recorded. The number of episodes of reflux is also recorded. Color Doppler may be used to determine flow direction of moving content across the GEJ. Approximate study time is of the order of 15 min. Savino et al. (2012) have summarized normal values in children for mean esophageal

transmural wall thickness of 2–5 mm, esophageal diameter of 10 mm, esophageal length of 20–25 mm, and gastroesophageal angle of 70–100°. A short intra-abdominal esophageal length and more obtuse gastroesophageal angle correlate with GER. Gastroesophageal angle varies with gastric distension. Esophageal wall thickness is a nonspecific marker of GERD. Technical limitations of gastroesophageal US include failure to accurately document the cephalad extent of reflux and incomplete assessment of the thoracic esophagus which is largely obscured by artifact from the lungs. Currently there is no consensus on the sonographic criteria for an abnormal GEJ. Routine use of sonography is not recommended (Vandenplas et al. 2009) but is advocated in some centers.

## 5.2 Achalasia

Achalasia is an esophageal motility disorder characterized by failure of lower esophageal sphincter (LES) relaxation at the gastric cardia and absence of esophageal peristalsis with normal pharyngeal and upper esophageal sphincter function. This results from degeneration of the inhibitory myenteric plexus at the LES. Achalasia is rare with an annual estimated incidence of approximately 1/1000,000 in children (Lee et al. 2010). The most common symptoms are vomiting, dysphagia, regurgitation, and weight loss. In the neonatal period presentations are similar to those of GERD. Achalasia has been associated with trisomy 21, eosinophilic esophagitis, glucocorticoid insufficiency, congenital hypoventilation syndrome, familial dysautonomia, Chagas disease, and AAA (achalasia, alacrima, and ACTH insensitivity) syndrome (Hallal et al. 2012).

Definitive diagnosis is made with (barium) swallow study and esophageal manometry.

Unlike in adults endoscopic biopsy of the distal esophagus is not indicated, as the risk of associated malignancy is very low. Medical therapy includes endoscopic botulinum toxin injection and dilatation but affords only temporary symptomatic relief. Definitive surgical treatment in children with achalasia is laparoscopic Heller myotomy with or without a fundoplication procedure. However, the underlying esophageal dysmotility will persist and lifelong clinical follow-up is required.

### 5.2.1 Radiological Findings

The chest radiograph may reveal a dilated esophagus with an air-fluid level, changes of chronic pulmonary aspiration, and tracheal displacement (Fig. 40a, b). The gastric bubble is not visualized in cases with high-grade obstruction. A barium or water-soluble esophagram is the initial diagnostic study of choice; retention of a small oral barium tablet may reveal subtle disorders of motility. This may be followed by esophageal manometry and endoscopy. Contrast studies reveal a dilated esophagus that smoothly tapers distally to a "bird's beak" (Fig. 40c). Chronic untreated achalasia may lead to marked distension of the esophagus (Fig. 41). Rarely, a leiomyoma (see Sect. 5.10) may mimic the symptoms and radiological appearance of achalasia (Hussain et al. 2002).

## 5.3 Foreign Body Ingestion

The vast majority of foreign body ingestions occur in the pediatric population with a peak incidence between the ages of 6 months and 6 years. Esophageal foreign bodies tend to lodge at the normal anatomic sites of narrowing. In the upper GI tract, these include the cricopharyngeus muscle, GEJ, aortic arch, and the crossing of the left mainstem bronchus. Objects which pass beyond the cricopharyngeus will typically pass freely into the stomach though persistent lodging of a foreign body in the esophagus beyond this level is usually indicative of esophageal pathology such as a vascular ring or stricture from prior esophageal repair (Fig. 42). In order of frequency, esophageal foreign bodies lodge at the level of the thoracic inlet (53 %), thoracic esophagus (32 %), and the cervical esophagus (15 %) (Harned et al. 1997).

Children typically present with dysphagia and chest pain. Salivation and drooling occur with

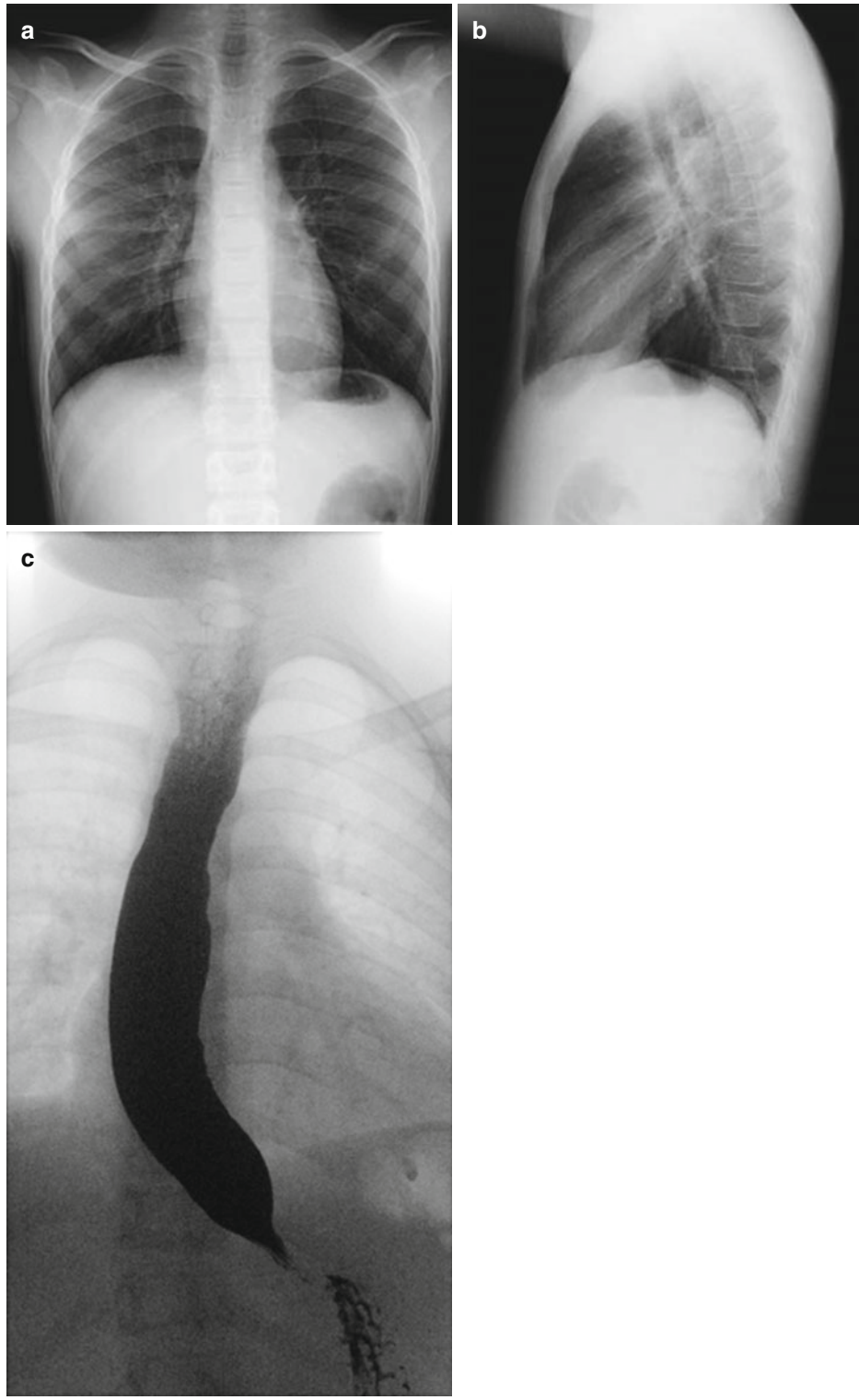


**Fig. 40** (**a**–**c**) Achalasia. (**a**) AP and (**b**) lateral chest radiographs reveal an air-fluid level in the distended esophagus. (**c**) Barium esophagram demonstrating a patulous and dilated esophagus with distal *beaking* deformity

esophageal obstruction. Swallowed objects may be partially chewed food (Fig. 43) or other foreign bodies, two-thirds of which are coins in children (Webb 1995). Occasionally more than one object may be ingested. Acute coin ingestion is rarely symptomatic unless the coin is above the thoracic inlet (Sharieff et al. 2003). The majority of asymptomatic esophageal coins will pass spontaneously. Blunt objects which are well tolerated, with the exception of lithium disk batteries (see below), can be followed for 16–24 h (Sharieff et al. 2003; Waltzman et al. 2005). A lodged radiopaque esophageal foreign body should be removed if repeat radiography reveals non-passage. Flexible endoscopy enables foreign body extraction and provides immediate information about state of the esophagus at the site of impaction.

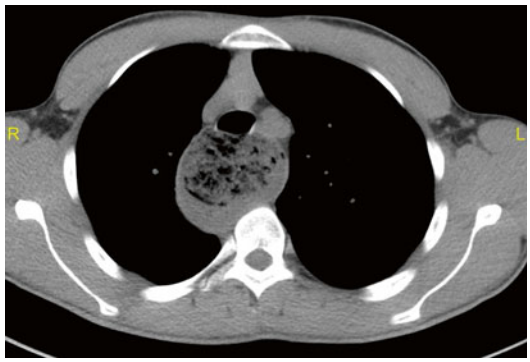


**Fig. 41** Achalasia. Axial CT showing marked distension of the upper thoracic esophagus with retained food debris

### 5.3.1 Radiological Findings

Children are not always reliable historians. If there is concern for an ingested foreign body, then a lateral soft tissue neck radiograph and frontal radiograph from the oropharynx to the pubic symphysis (mouth-to-anus view) should be obtained. Radiographic evaluation of foreign bodies in a single center pediatric case series revealed 100 % of metal objects, 86 % of glass, and only 26 % of fish bones (Cheng and Tam 1999). Commonly ingested foreign bodies such as organic matter, medication, or small plastic objects are not visible on plain radiography. Radiolucent foreign bodies may show on the bar-

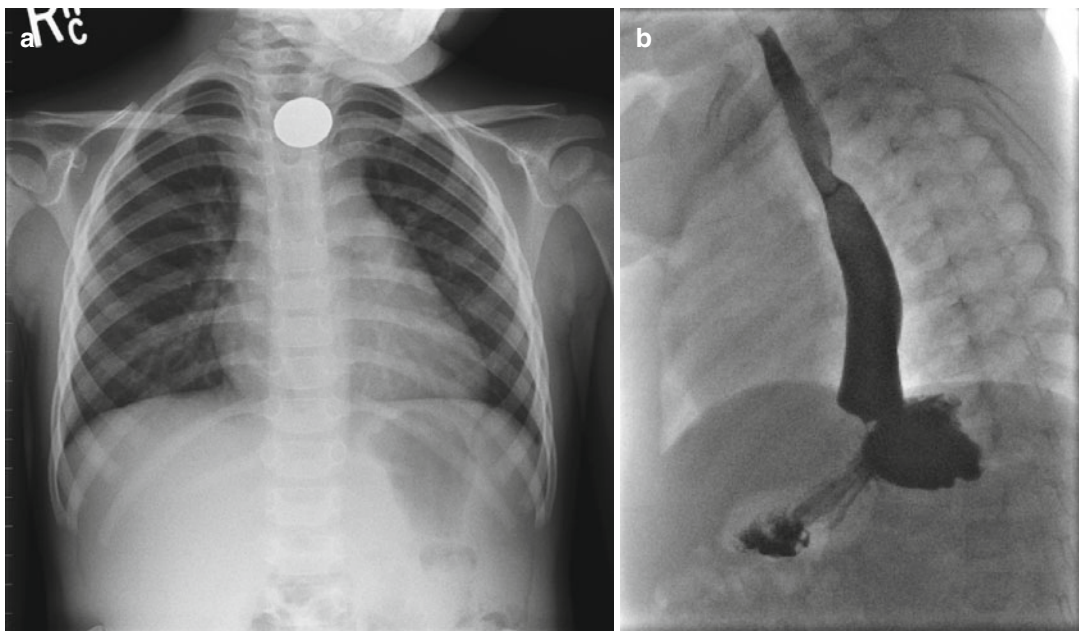


**Fig. 42** (**a**, **b**) Impacted foreign body above an unsuspected vascular ring. (**a**) Frontal chest radiograph shows a coin lodged in the esophagus proximal to the aortic arch. (**b**) Barium esophagram confirms an oblique posterior indentation upon the esophagus in keeping a left-sided aortic arch and aberrant right subclavian artery

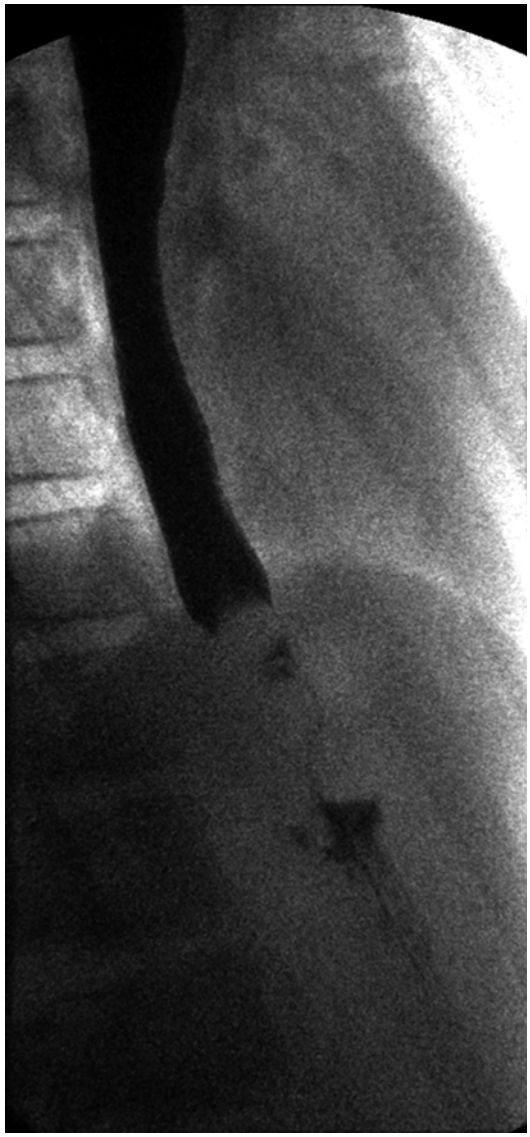

**Fig. 43** Obstructing foreign body. Barium esophagram reveals a filling defect impacted in the distal esophagus. This was a beef steak morsel and ultimately required endoscopic removal

ium esophagram as filling defects in the barium (Fig. 43). Contrast studies should be avoided with a high-grade obstruction because of the risk of aspiration and may make endoscopic retrieval more challenging. Chronically impacted foreign bodies cause inflammation, edema of the esophageal wall, and lumenal narrowing. Complications of foreign body ingestion include perforation and abscess formation. An otorhinolaryngology (ENT) opinion is recommended for foreign bodies at or above the level of the cricopharyngeus. Emergent removal of esophageal impacted food boluses and a foreign body with evidence of complete esophageal obstruction is necessary. Multiple small neodymium magnets found in toys may inadvertently be ingested and lodge in the hypopharynx or esophagus. These can rapidly cause mucosal pressure necrosis and merit emergent endoscopic management (Brown et al. 2014). Surgical consultation is required for non-progression through the GI tract.

Alkaline lithium disk batteries (Fig. 44) contain very high concentrations of potassium or sodium hydroxide. Mucosal damage due to leakage occurs within 1 h of ingestion. Perforation may ensue within 8–12 h of esophageal impaction. This scenario is a medical emergency and mandates immediate removal. Failure to act promptly may result in the impacted battery eroding through the esophagus and into the airway or worse gives rise to an aortoesophageal fistula resulting in a life-threatening sentinel bleed (Brumbaugh et al. 2011). Esophageal bleeding should raise the suspicion of an ingested foreign body in a child.

## 5.4 Caustic Injury

Ingestion of both alkali and acidic agents may cause significant trauma to the mucosa of the esophagus with concomitant injury to the lips, mouth, oropharynx, and upper airway. The ensuing damage can include superficial mucosal burns and deep ulceration, progressing to full thickness injury. Liquefactive necrosis with fat saponification, protein denaturation, and thrombosis is seen with alkali agents. The mid and distal thirds of the esophagus are most vulnerable to alkaline agents and typically the stomach is spared. Conversely acidic agents are usually liquids and pass through the esophagus rapidly

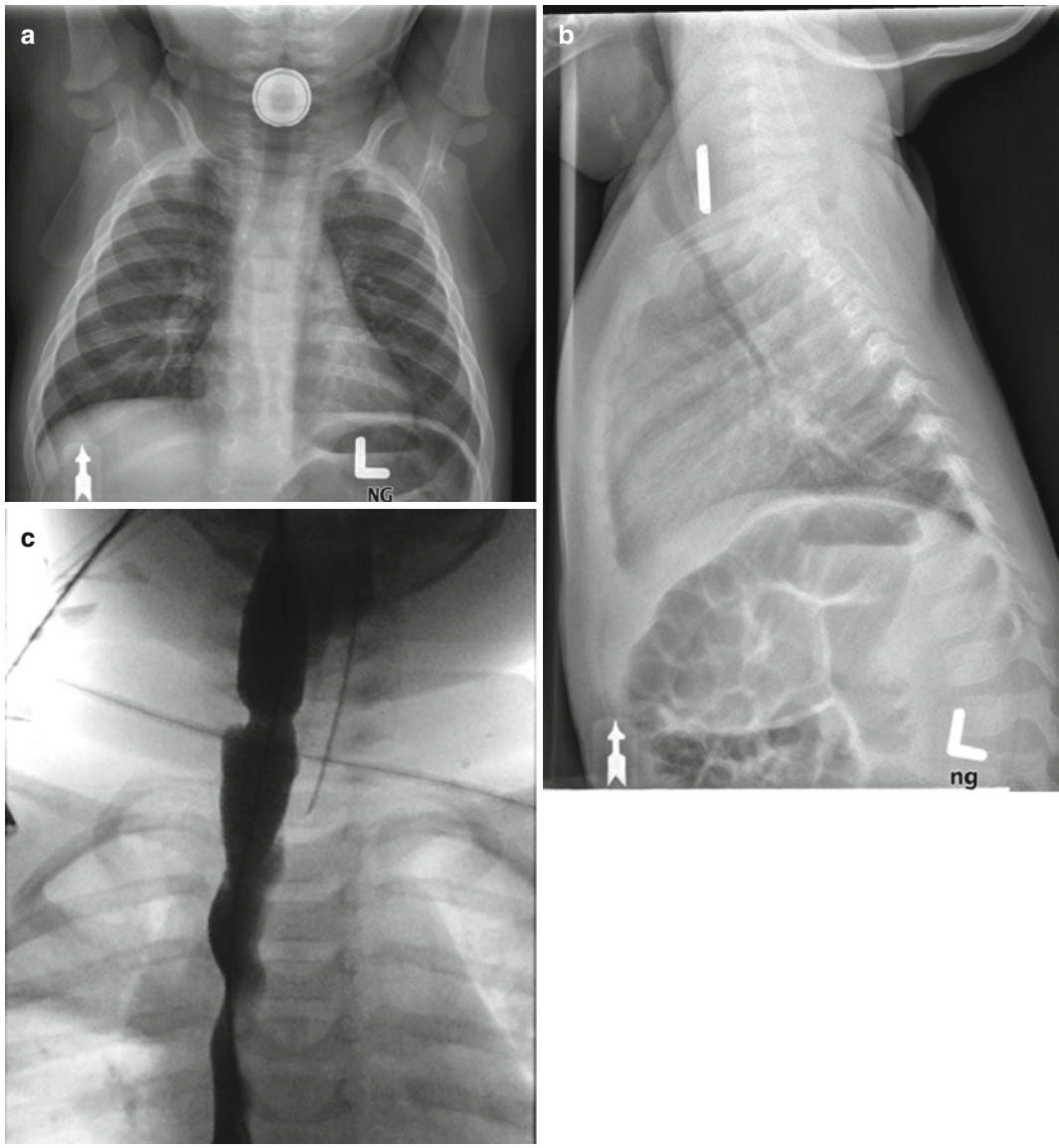


**Fig. 44** (**a**–**c**) Lithium battery ingestion. (**a**, **b**) Frontal and lateral chest radiographs showing a retained lithium button battery in the hypopharynx/proximal cervical esophagus. (**c**) AP esophagram showing an irregular proximal esophageal stricture secondary to prior lithium battery ingestion

and tend to preferentially injure the stomach more severely. The risk of esophageal injury depends on the type of agent, form, amount, concentration, and duration of exposure. Accidental injury with alkaline bleaching (lye) agents typically occurs in small children aged 1–3 years where relatively small quantities are consumed. Rarely this may represent non-accidental injury in this age group. At the other end of the spectrum, ingestion of large quantities is seen in cases of deliberate self-harm in the adolescent population. Signs and symptoms of caustic agent ingestion are typically nonspecific. They may include coughing,

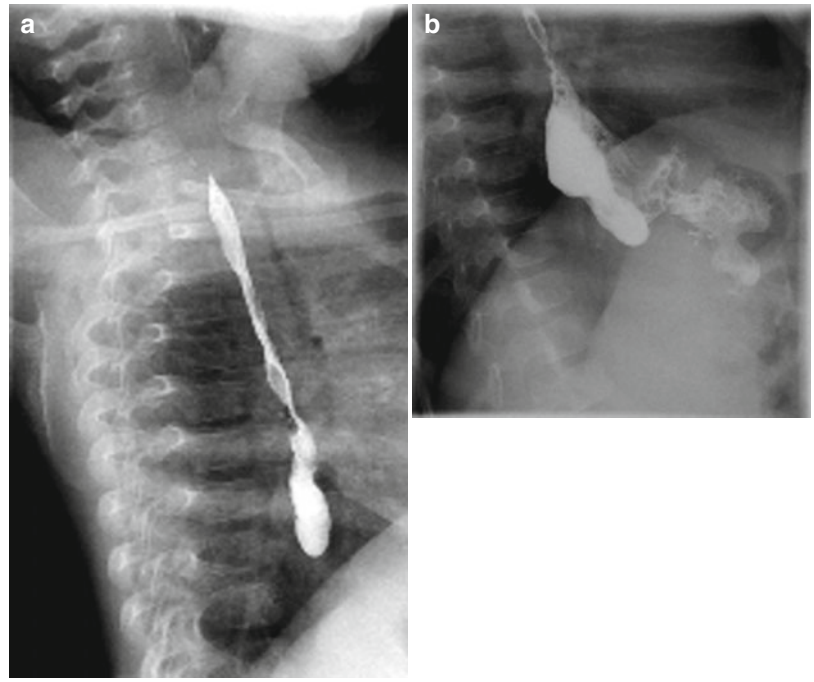


**Fig. 45** (**a**, **b**) Caustic stricture. (**a**) Barium swallow showing an irregular high-grade stricture affecting the mid and distal thirds of the esophagus secondary to ingestion of an unknown caustic agent. The stomach is relatively spared. (**b**) Follow-up study showing an acquired hiatus hernia due to esophageal shortening

dyspnea, stridor, dysphonia, emesis, dysphagia, odynophagia, drooling, and hematemesis. Endoscopy is mandated in symptomatic patients (Betalli et al. 2008). The presence of retrosternal chest discomfort with back pain may indicate mediastinitis, while epigastric pain with rigidity may reflect peritonitis. Initial treatment commences with airway management and fluid resuscitation. Sips of water are encouraged to dilute and displace the chemical ingestant. Neutralizing agents and emetics are contraindicated. Surgery is rarely required.

### 5.4.1 Radiological Findings

Chest and abdominal radiographs are obtained to look for signs of perforation. A water-soluble contrast series is the initial radiological investigation of choice. Signs of injury include epiglottic edema, mucosal edema and ulceration, and esophageal dysmotility (Fig. 45). Intramural contrast tracking and persistent gaseous dilatation of the esophagus reflect severe injury and may precede perforation (Fernbach 1994). CT is recommended when there is a strong suspicion for perforation. Deep esophageal burns are investigated by serial barium esophagrams to detect early stricture formation. These are typically elongated and follow a protracted clinical course requiring periodic dilatations to provide adequate symptomatic relief. Where conservative therapy and serial pneumatic dilatation do not provide adequate palliation, surgery with colonic interposition (Fig. 46) or gastric pull-up is performed.

## 5.5 Esophageal Strictures

The most common cause for an acquired esophageal stricture in children is the result of a surgical repair of EA and TEF (Fig. 26). Other causes include caustic agent ingestion (Fig. 45), reflux esophagitis (Fig. 38), and epidermolysis bullosa (see Sect. 5.7). Symptoms relate to the degree of stricture. These include dysphagia, chest pain, coughing, vomiting of retained liquid or food, and aspiration pneumonia. Refusal to eat and drooling may indicate complete obstruction of the stricture by a retained foreign body.

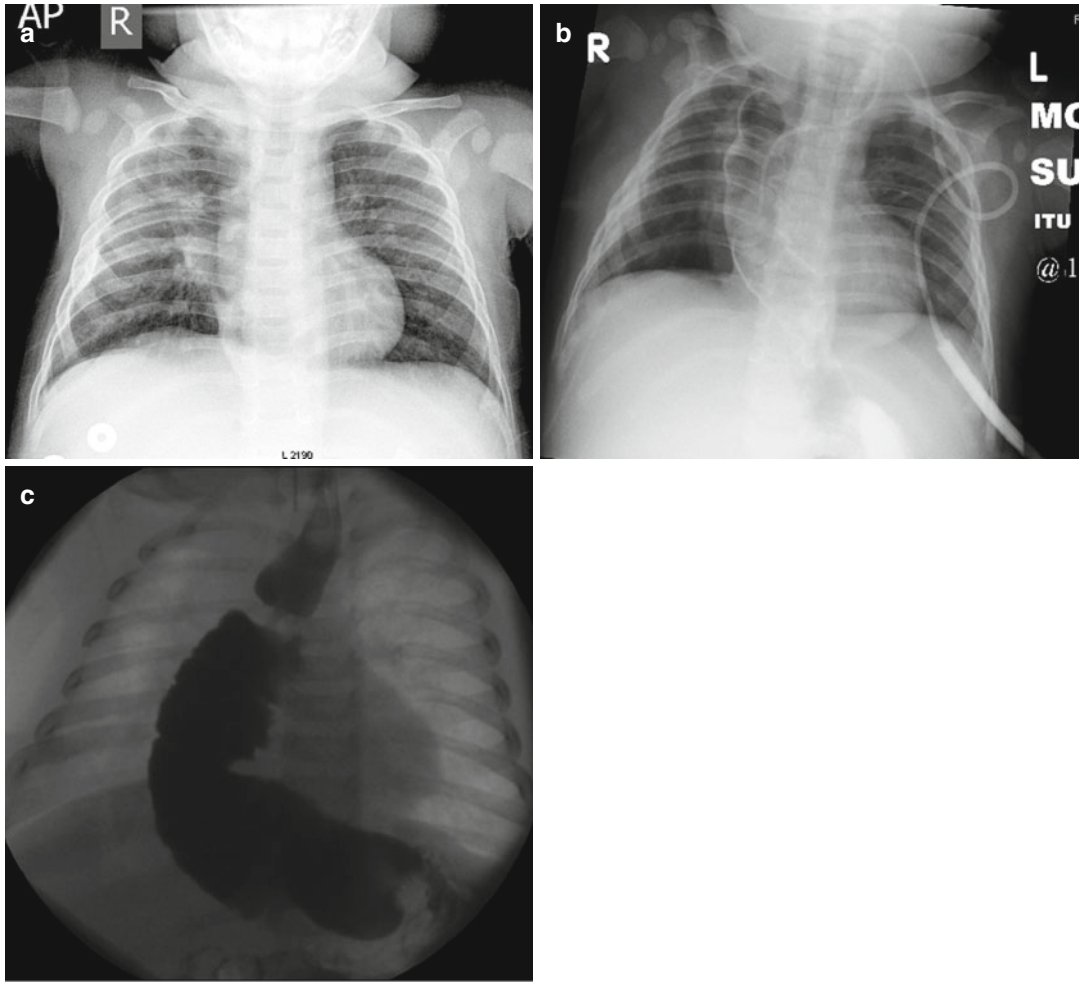


**Fig. 46** (**a**–**c**) Esophageal interposition graft. (**a**) AP chest radiograph showing a right paravertebral posterior mediastinal air-filled lucent structure, (**b**) correlative barium study showing the colonic interposition graft. (**c**) Barium swallow in another child with a capacious colonic esophageal interposition graft

### 5.5.1 Radiological Findings

Radiographs are usually normal, although rarely an intraesophageal air-fluid level may be seen above an esophageal obstruction on an erect chest x-ray. A chest x-ray is however mandated if the patient's symptoms deteriorate following endoscopic treatment of a structure. A (barium) esophagram is the most appropriate study. Non-gastrografin water-soluble contrast medium may initially be used if a leak is suspected. Contrast studies reveal strictures as localized or diffuse regions of esophageal lumen narrowing with lack of distensibility (Fig. 47a) (Karasick and Lev-Toaff 1995).

Fluoroscopically guided balloon dilatation is the preferred treatment for esophageal stricture (Fig. 47b). Bougienage is an alternative but is limited by the diameter of the nares or pharynx. The incidence of perforation with balloon dilatation is also much lower. Balloon insufflation applies uniform radial force that is less traumatic than the shearing force of bougienage at the level of a stricture (Fasulakis and Andronikou 2003). Fibrotic scar tissue with its altered blood supply impairs tissue elasticity. As a result, strictures will typically not resolve after balloon dilatation but treatment does provide adequate temporary

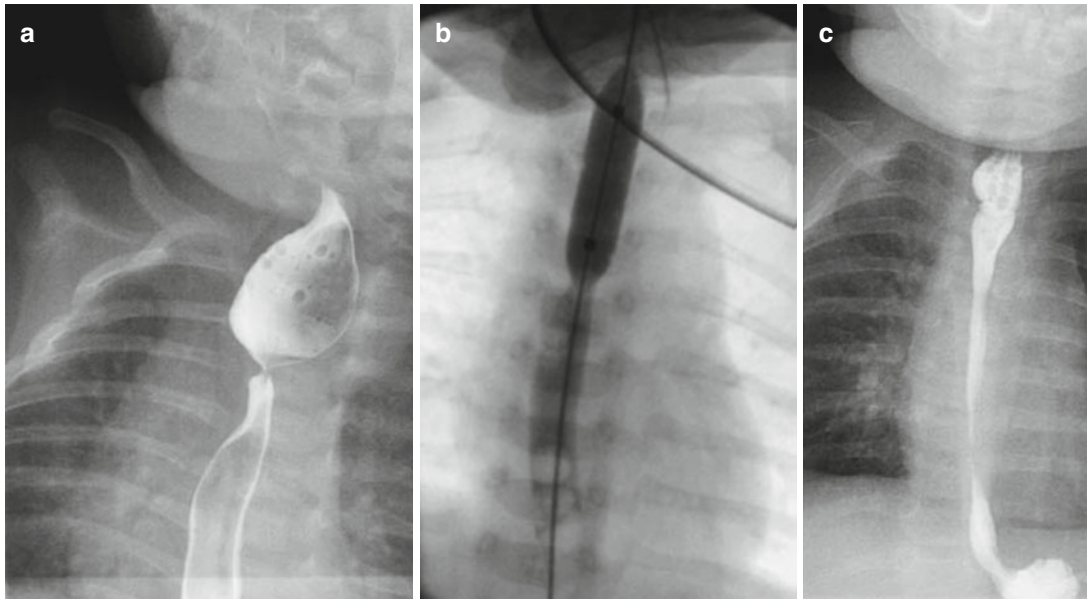


**Fig. 47** (**a**–**c**) Balloon dilation of an esophageal stricture. (**a**) Severe stenosis of the proximal esophagus 3 months post-surgical repair. (**b**) Dilatation balloon expanded across the narrowing, no extravasation. (**c**) Post-dilatation appearance

symptomatic relief (Fig. 47c). Interval balloon dilatations are indicated in repaired esophageal atresia, caustic stricture, and epidermolysis bullosa. Serial balloon dilatations aid progressive stretching of scar tissue and reduce the risk of iatrogenic tears or perforation. Fluoroscopy also allows the radiologist to check that the stricture is dilated to a suitable diameter. A post-procedural water-soluble contrast study is performed to assess esophageal caliber and to evaluate for a leak and state of the distal esophagus. Recalcitrant esophageal strictures have been successfully treated with intralesional triamcinolone acetonide steroid (Lévesque et al. 2013) and topical mitomycin-C (Heran et al. 2008). Commercially available removable pediatric covered esophageal stents have been used albeit rarely for refractory benign esophageal strictures (Kramer and Quiros 2010). Surgery is rarely indicated for complex or refractory strictures.

## 5.6 Esophageal Perforation

Esophageal perforation is rare in the pediatric population. Iatrogenic esophageal perforation is the cause in 33–75 % of cases (Martinez et al. 2003). The most frequent sources of iatrogenic injury in infants and children include nasogastric tube insertion (Fig. 5), stricture dilatation, and trauma related to inadvertent esophageal intubation with an endotracheal tube (Gander et al. 2009). The incidence of iatrogenic perforation is rising as more diagnostic and therapeutic endoscopies are performed. The incidence is low in upper gastrointestinal endoscopy and higher with use of rigid dilators. Esophageal perforations are more likely to occur if an intraluminal foreign body has been present more than 24 h and result from sustained pressure necrosis. Other etiologies include caustic agents, pill-induced damage, and infection (including candida, herpes, and tuberculosis). Spontaneous rupture of the esophagus following vomiting or Boerhaave syndrome is rare in children (Fig. 48).

Symptoms relate to the level of perforation. Pharyngoesophageal and cervical esophageal perforation may result from peroral penetrating trauma including lollipops and pencils; symptoms may include neck pain and drooling. Symptoms of thoracic perforation include chest pain, vomiting, and crepitus related to subcutaneous

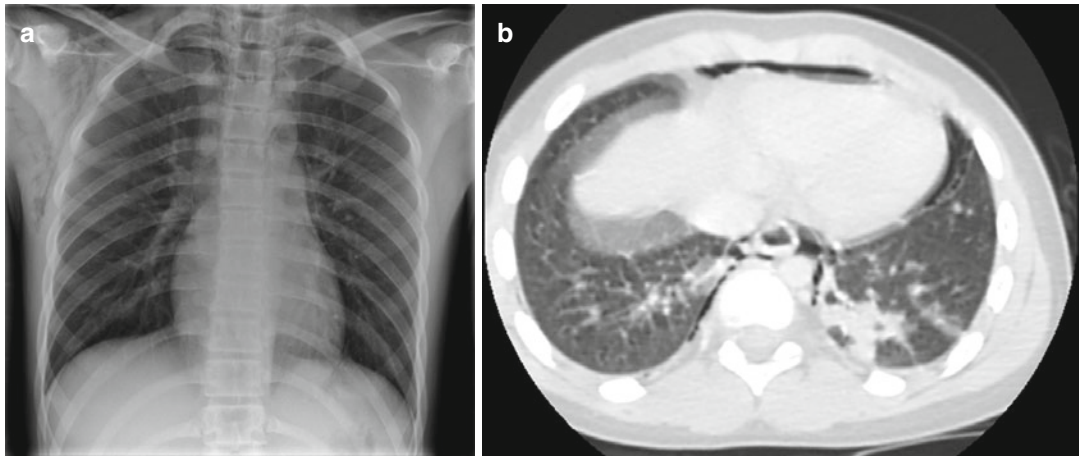


**Fig. 48** (**a**, **b**) Esophageal perforation. (**a**) Frontal chest radiograph showing a pneumomediastinum with subcutaneous emphysema in the root of the neck, axillae, and supraclavicular fossa in a teenager following a bout of forceful vomiting. (**b**) Corresponding axial contrast-enhanced CT of the thorax

emphysema also known as the Mackler triad. Thoracic esophageal perforation is associated high morbidity and if untreated mortality because it allows direct entry of gastrointestinal flora and digestive enzymes to soil the mediastinum, pleural and subphrenic spaces causing sepsis. Intra-abdominal esophageal perforation may lead to sepsis, shock and pneumoperitoneum. Treatment for esophageal perforation is preferably conservative and non-operative. If there is no evidence of contrast leak at esophagram therapy consists of broad-spectrum antibiotic coverage, drainage of pleural effusions, esophageal rest and total parenteral nutrition. Successful outcome depends on early diagnosis and treatment, young age and absence of underlying disease (Martinez et al. 2003). Operative treatment may be required in hemodynamically labile patients to manage gross extraluminal contamination. Direct surgical repair to maintain luminal patency in large perforations is rarely indicated (Gander et al. 2009).

### 5.6.1 Radiological Findings

In cervical esophageal perforation airway-soft tissue neck radiographs are required as chest radiography is typically non-contributory. Chest radiographic findings in thoracic esophageal perforation include pneumomediastinum, subcutaneous emphysema, pneumothorax, hydropneumothorax, and pleural effusions (Fig. 48). The false negative rate with contrast swallows is around 10 % (Gimenez et al. 2002). CT is recommended when the esophagram is negative and there is high suspicion of perforation or when a preoperative roadmap is required particularly for thoracic esophageal injury.

## 5.7 Epidermolysis Bullosa

Epidermolysis bullosa (EB) is a rare inherited disorder. It is characterized with mechanical fragility of the skin and mucous membranes with progressive development of recurrent blisters and non-healing open wounds as a consequence of minor trauma resulting in high nutritional demands. Recessive dystrophic epidermolysis bullosa (RDEB) is a rare severe autosomal recessive form resulting from abnormal production of type VII collagen secondary to mutation of the COL7A gene which presents in the neonatal period.

Overall, four major types of EB are recognized with multiple subtypes and related genetic mutations. The main types are epidermolytic type (EB simplex), junctional EB, a dermolytic type (dystrophic EB), and a mixed type (Kindler syndrome). The most common finding is skin blistering. Some types and subtypes of inherited EB may be at risk for developing specific gastrointestinal complications and typically present in

the first or second decade of life. Esophageal bullae, stricturing, scarring, and web formation are found predominantly in the junctional type. Other complications include poorly coordinated swallowing, dysphagia, esophageal perforation, dysmotility, vomiting of a cast, and hiatus hernia. GERD occurs mainly in the non-junctional types (Fine and Mellerio 2009). Scarring and fibrosis may result in esophageal shortening predisposing to GERD and secondary stricturing (Anderson et al. 2004). Esophageal squamous carcinoma is a recognized complication. Syndromic associations include pyloric, esophageal, and anal atresia (Cetinkurşun et al. 1995).

The mainstay of treating EB esophageal stricturing is repeat fluoroscopic dilatation (Demirogullari et al. 2001). Gastrostomy provides esophageal rest. Rarely resection and colonic interposition are indicated. Children with epidermolysis bullosa require gentle handling. Modifications of imaging and anesthetic and therapeutic techniques are required to prevent iatrogenic blistering. Use of soft padding, spontaneous oral intake of contrast medium, and avoidance of restraints and enteric intubation are necessary. Dilatation is ideally performed in the symptomatic child when the underlying disease is quiescent.

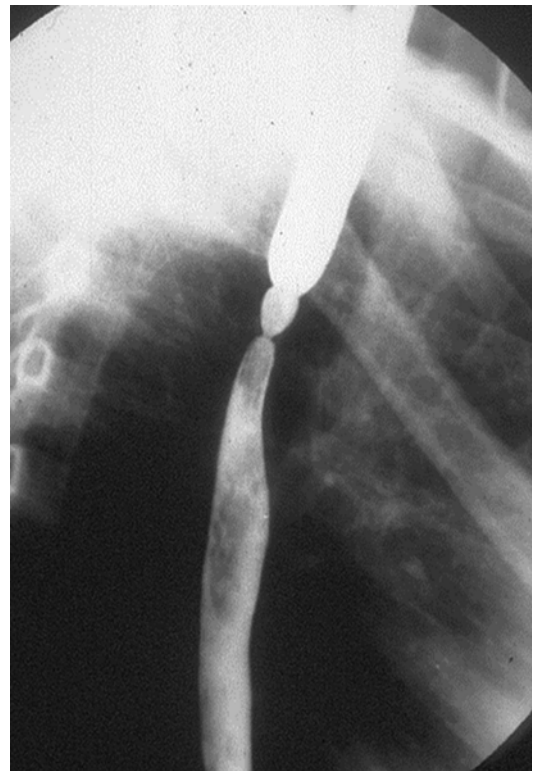

**Fig. 49** Epidermolysis bullosa. Barium esophagram showing an annular proximal esophageal stricture in a child with the dystrophic, recessive form of the disease (Image courtesy of Dr. C Buonomo MD, Boston Children's Hospital, Boston, MA, USA)

### 5.7.1 Radiological Findings

A barium esophagram should evaluate the oropharynx and entire esophagus to demonstrate strictures and GERD. Approximately half of strictures are in the proximal third of the esophagus near the cricopharyngeus muscle (Fig. 49), a quarter in the distal one-third, and the remainder at multiple sites (Kern et al. 1989a). Strictures vary in length from several centimeters to annular strictures, which are typically less than 3 cm in length.

## 5.8 Infectious and Inflammatory Esophagitis

### 5.8.1 Infectious Esophagitis

Infectious esophagitis is rare in children. The most common cause is candida and usually occurs in immunocompromised patients as a complication of bone marrow transplantation, chemotherapy, human immunodeficiency virus (HIV), corticosteroid therapy, or rarely diabetes. Candida esophagitis may frequently occur in the absence of oropharyngeal candida (thrush) and should be suspected in the immunocompromised child presenting with odynophagia. Barium esophagram demonstrates shallow ovoid ulcers, discrete linear ulceration, and shaggy cobblestoned mucosal pattern. The differential for esophageal candidiasis includes herpes simplex virus (HSV) and cytomegalovirus (CMV), both of which give rise to similar imaging appearances but are refractory to antifungal therapy. HIV infection itself can produce large penetrating esophageal ulcers. HSV esophagitis under the age of 13 years is considered an HIV defining illness. Candida, CMV, and HSV esophagitis are HIV defining illnesses above 13 years in the absence of other risk factors (Baker 2013).

### 5.8.2 Eosinophilic Esophagitis

Eosinophilic esophagitis (EoE) is a chronic antigen-mediated disorder of unknown etiology manifesting as esophageal dysfunction with histological evidence of an eosinophil-predominant infiltrate (Liacouras et al. 2011). Although by definition, EoE is confined to the esophagus, EoE may be found in over 10 % of cases of atypical croup implying wider involvement of the aerodigestive tract (Cooper et al. 2012). EoE is often associated with atopic conditions such as asthma and allergies.

Symptoms include dysphagia, odynophagia, chest pain, food impaction, GERD-like symptoms refractory to medical and surgical therapy, abdominal pain, vomiting, early satiety, and anorexia (Liacouras et al. 2011). The prevalence and annual incidence of EoE in children has increased over time and is highest in children with food impaction or dysphagia (Soon et al. 2013). Treatment includes topical corticosteroids; systemic therapy is reserved for all but the most severe cases. The radiological manifestations of EoE (Fig. 50) have been described in a pediatric case series at a single institution (Binkovitz et al. 2010). In 24 UGI studies performed in 17 children with histologically proven EoE, 12 studies were normal, including four children with five episodes of recently treated acute esophageal food impaction. In the remainder long-segment nonulcerative strictures with mild mucosal irregularity were found in five cases, two in the mid-esophagus, one in the distal esophagus, and two at the GEJ. Only one stricture was demonstrated at endoscopy highlighting the usefulness of the UGI in delineating strictures. The finding of a Schatzki ring raises the possibility of EoE (Fig. 51). A Schatzki ring is a symptomatic, intermittent or persistent, discrete circumferential submucosal narrowing which distorts the esophageal lumen at the level of the gastroesophageal junction. The Schatzki ring differs from an asymptomatic esophageal B-ring found up to 1 cm cephalad to the esophageal diaphragmatic hiatus. In a single center retrospective study of UGI series in a pediatric and adolescent population, the incidence of Schatzki ring was found to be 0.2 % and was associated with hiatus hernia, GERD, and EoE with the authors recommending endoscopic biopsy in all cases to exclude the latter (Towbin and Diniz 2012).

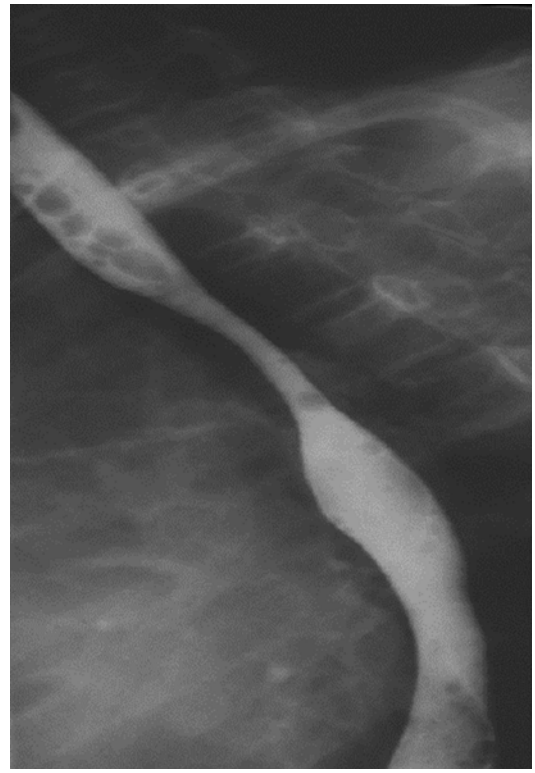

**Fig. 50** Eosinophilic esophagitis. Barium esophagram revealing a proximal long-segment nonulcerative stricture with mild mucosal irregularity (Image courtesy of Dr. C Buonomo MD, Boston Children's Hospital, Boston, MA, USA)

### 5.8.3 Crohn Disease

Although Crohn disease can affect any portion of the alimentary tract, esophageal involvement is rare. Radiological appearances are similar to those of adults and include aphthous ulceration, filiform polyposis, deep ulceration, fissuring, sinus tract formation, fistulae, and stricturing (Fig. 52).

### 5.8.4 Graft Versus Host Disease

Graft versus host disease (GVHD) is a multisystem complication following bone marrow transplantation, more commonly seen in allogenic rather than autologous transplants. In acute esophageal GVHD

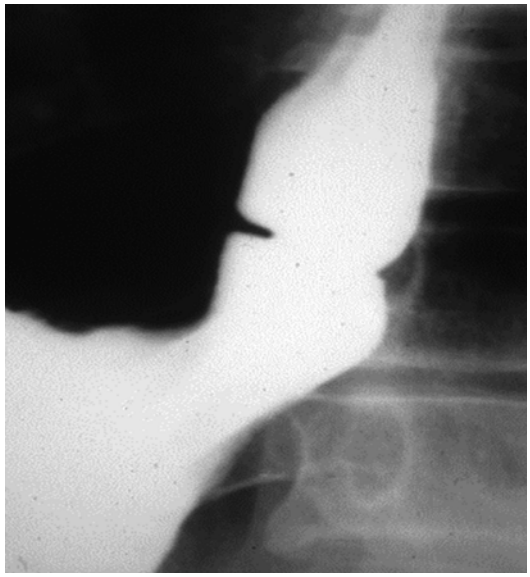

**Fig. 51** Schatzki ring. Barium esophagram showing a symptomatic circumferential B-ring in the distal esophagus (Image courtesy of Dr. C Buonomo MD, Boston Children's Hospital, Boston, MA, USA)

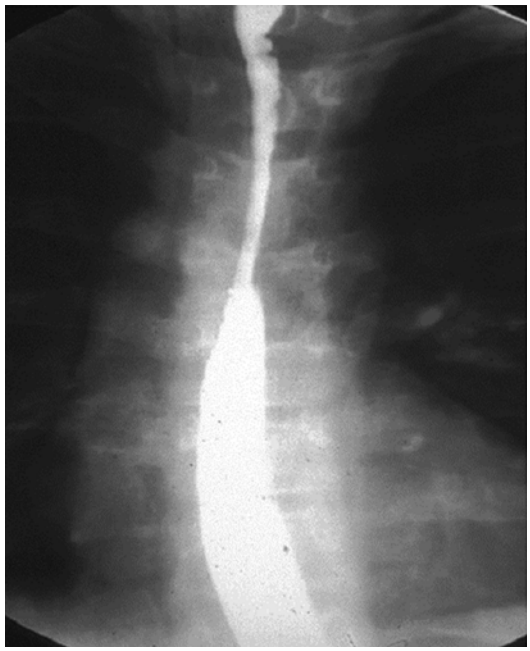

**Fig. 52** Esophageal Crohn disease. Barium esophagram showing an irregular long-segment stricture in the proximal esophagus. Esophageal involvement is rare in Crohn disease (Image courtesy of Dr. C Buonomo MD, Boston Children's Hospital, Boston, MA, USA)

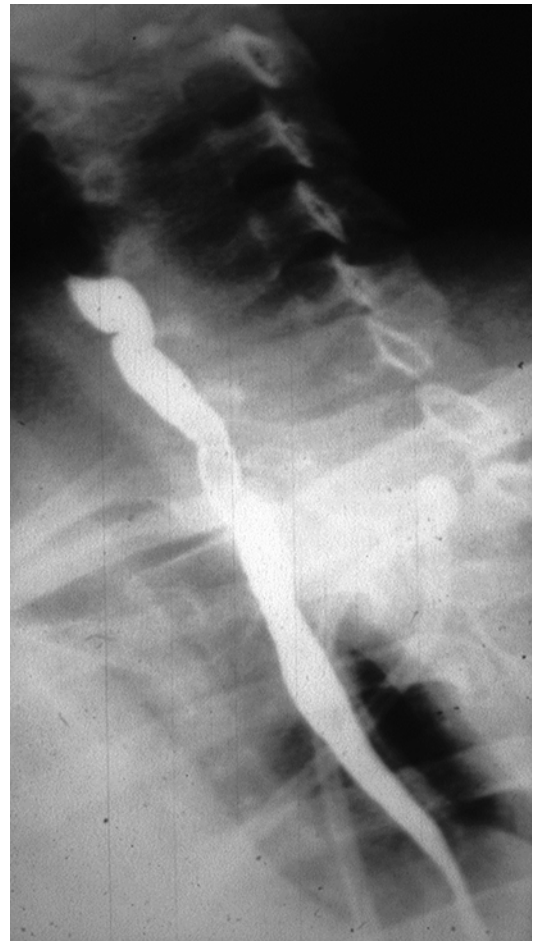

**Fig. 53** Esophageal graft versus host disease. Barium esophagram showing a chronic mid-upper esophageal web formation and stricturing (Image courtesy of Dr. C Buonomo MD, Boston Children's Hospital, Boston, MA, USA)

donor T lymphocytes and cytokines mediate an inflammatory superficial mucosal esophagitis. Chronic GVHD results in patchy submucosal fibrosis and focal stricturing. Radiological appearances at UGI include aperistalsis, webs, circumferential narrowing, and proximal and mid esophageal tapered strictures (Fig. 53).

## 5.9 Esophageal Varices

Esophageal varices are less common in children than in adults. Varices are a late complication of chronic pediatric liver disease. They typically

occur in the setting of portal hypertension secondary to umbilical venous catheterization, biliary atresia, alpha-1 antitrypsin deficiency, autosomal recessive polycystic renal disease, and cystic fibrosis. Flow through the variceal esophageal collateral veins is typically hepatofugal or "upstream" and toward the superior vena cava. At endoscopy these typically affect the distal esophagus. Downhill esophageal varices are extremely rare in children and occur in the setting of gradual superior vena cava (SVC) occlusion and may be suspected at endoscopy when the entire length of the esophagus is affected in the absence of portal hypertension. Upper esophageal involvement only implies SVC obstruction proximal to the inflow of a patent azygos vein.

### 5.9.1 Radiological Findings

On (barium) swallow, the normal parallel mucosal folds are interspersed by serpiginous variceal filling defects that are best appreciated on collapsed views of the esophagus. Doppler ultrasound, dynamic MR angiography, and MR cholangiography have largely supplanted barium studies in the diagnostic work-up of these children. Doppler ultrasonography (US) is the first-line imaging technique in children with liver cirrhosis and suspected varices. Portal vein diameter and flow velocity yield the congestion index. Splenic size, abnormal hepatic vein flow patterns, and presence of abdominal portosystemic collaterals are markers of portal hypertension. US has limited specificity for detecting large esophageal varices; alternatives include wireless capsule endoscopy and conventional endoscopy, the latter enables therapeutic intervention. Transient elastography (TE) is a noninvasive sonographic technique used to evaluate fibrosis in chronic liver disease. TE has been shown to be a useful noninvasive surrogate marker for the presence of esophageal and gastric varices in children following portoenterostomy for congenital biliary atresia (Chongsrisawat et al. 2011). Correlation with variceal size and bleeding risk was not documented. MR elastography (MRe) is an alternative to TE in children. A single study has depicted gastroesophageal variceal formation in two cases at MRe (Binkovitz et al. 2012).

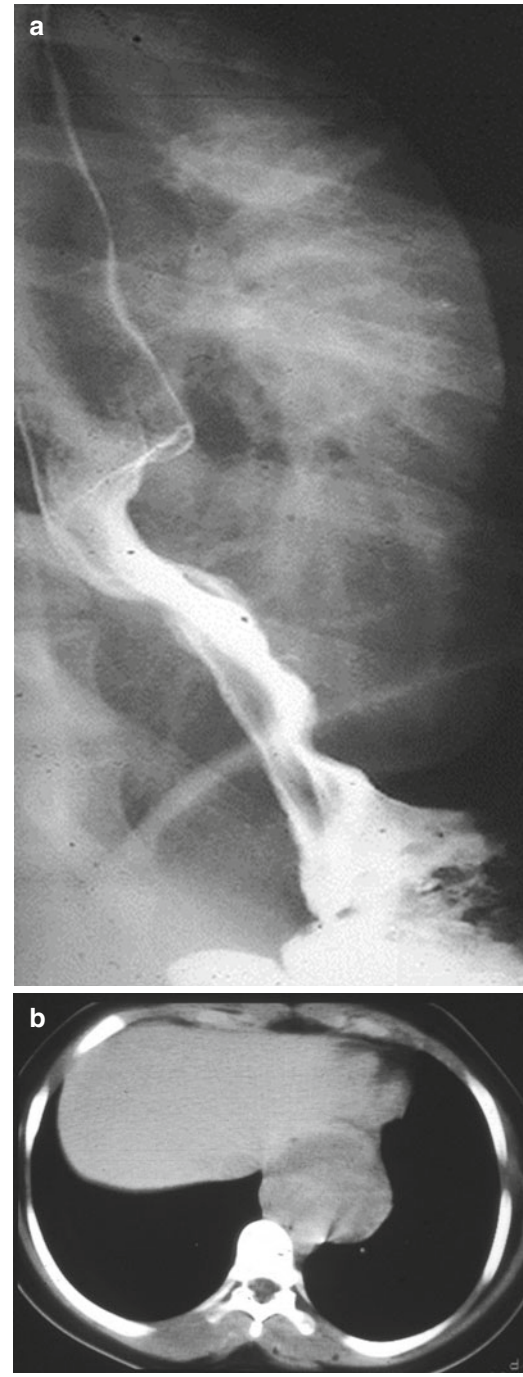


**Fig. 54** (**a**, **b**) Esophageal leiomyoma. (**a**) Barium esophagram demonstrating a submucosal filling defect within the distal third of the esophagus. (**b**) Corresponding axial contrast-enhanced CT showing a heterogeneous soft tissue mass centered on the esophagus and azygoesophageal recess (Images courtesy of Dr. C Buonomo MD, Boston Children's Hospital, Boston, MA, USA)

## 5.10 Esophageal Neoplasms

Pediatric esophageal neoplasia is rare. Symptoms are nonspecific but include dysphagia, odynophagia, chest pain, and weight loss. Leiomyomas (Fig. 54) are the most common benign esophageal neoplasm and are typically seen in teenage girls. Diffuse esophageal involvement is seen in 90 % of cases; in less than 10 % patients, they may present with a focal mass (Hryhorczuk et al. 2013). Leiomyoma is associated with Alport syndrome and familial leiomyoma syndromes. Lymphoma may involve the pediatric esophagus but rarely so. Esophageal carcinoma is extremely rare. Risk factors for adenocarcinoma include caustic ingestion, reflux disease, and Barrett esophagus. Risk factors for squamous cell carcinoma include caustic ingestion, inherited bone marrow failure syndromes, and epidermolysis bullosa. Owing to the rarity of pediatric esophageal neoplasia, there are no consensus guidelines in the approach to management and the prognosis is very poor for solid malignancies (Issaivanan et al. 2012).

## References


ACR (2014) ACR–SPR Practice parameter for the performance of contrast esophagrams and upper gastrointestinal examinations in infants and children. http://www.acr.org/~/media/A77716DEDE5C486EA73F2249D578FD39.pdf. Accessed 16 May 2015

ACR–SNM–SPR (2014) Practice parameter for the performance of gastrointestinal scintigraphy (2014) http://www.acr.org/~/media/26E5C0B4D8C2471FA7229E7B3B25DFF2.pdf. Accessed 18 Mar 2015

Al-Assiri A, Wiseman N, Bunge M (2005) Prenatal diagnosis of intrathoracic stomach (gastric herniation). J Pediatr Surg 40:E15–E17. doi:10.1016/j.jpedsurg.2004.10.006

Al-Bassam A, Saquib Mallick M, Al-Qahtani A et al (2007) Thoracoscopic division of vascular rings in infants and children. J Pediatr Surg 42:1357–1561

Alsenaidi K, Gurofsky R, Karamlou T et al (2006) Management and outcomes of double aortic arch in 81 patients. Pediatrics 118:e1336–e1341. doi:10.1542/peds.2006-1097

Amae S, Nio M, Kamiyama T (2003) Clinical characteristics and management of congenital esophageal stenosis:a report on 14 cases. J Pediatr Surg 38:565–570

Anderson SH, Meenan J, Williams KN, Eady RA et al (2004) Efficacy and safety of endoscopic dilation of esophageal strictures in epidermolysis bullosa. Gastrointest Endosc 59:28–32

Backer CL, Mavroudis C, Rigsby CK, Holinger LD (2005) Trends in vascular ring surgery. J Thorac Cardiovasc Surg 139:1339–1347

Baker CJ (2013) HIV infection. In: Red book atlas of pediatric infectious diseases, 2nd edn. American Academy of Pediatrics, Elk Grove Village, IL, pp 230–231

Bansal S, Rothenberg SS (2014) Evaluation of laparoscopic management of recurrent gastroesophageal reflux disease and hiatal hernia: long term results and evaluation of changing trends. J Pediatr Surg 49:72–75

Berrocal T, Torres I, Guttierrez J et al (1999) Congenital anomalies of the upper gastrointestinal tract. Radiographics 19:855–872

Betalli P, Falchetti D, Giuliani S et al (2008) Caustic ingestion in children: is endoscopy always indicated? The results of an Italian multicenter observational study. Gastrointest Endosc 68:434–439

Binkovitz LA, Lorenz EA, Di Lorenzo C, Kahwash S (2010) Pediatric eosinophilic esophagitis: radiologic findings with pathologic correlation. Pediatr Radiol 40:714–719

Binkovitz LA, El-Youssef M, Glaser KJ et al (2012) Pediatric MR elastography of hepatic fibrosis: principles, technique and early clinical experience. Pediatr Radiol 42:402–409

Bonnard A, Auber F, Fourcade L et al (2003) Vascular ring abnormalities: a retrospective study of 62 cases. J Pediatr Surg 38:539–543

Brown JC, Baik FM, Ou HC et al (2014) Upper aerodigestive magnetic foreign bodies in children. Laryngoscope 124:1481–1485

Brumbaugh DE, Colson SB, Sandoval JA et al (2011) Management of button battery-induced hemorrhage in children. J Pediatr Gastroenterol Nutr 52:585–589

Campanozzi A, Boccia G, Pensabene L et al (2009) Prevalence and natural history of gastroesophageal reflux. Pediatrics 123:779–783

Cetinkurşun OH, Celasun B et al (1995) Epidermolysis bullosa associated with pyloric, esophageal, and anal atresia: a case report. J Pediatr Surg 30:1477–1478

Cheng W, Tam PKH (1999) Foreign-body ingestion in children: experience with 1,265 cases. J Pediatr Surg 34:1472–1476

Chongsrisawat V, Vejapipat P, Siripon N et al (2011) Transient elastography for predicting esophageal/gastric varices in children with biliary atresia. BMC Gastroenterol 11:41–45

Cooper T, Kuruvilla G, Persad R, El-Hakim H (2012) Atypical croup: association with airway lesions, atopy, and esophagitis. Otolaryngol Head Neck Surg 147:209–214

Dantas RO, Dodds WJ, Massey BT, Kern MK (1989) The effect of high- vs low-density barium preparations on the quantitative features of swallowing. AJR Am J Roentgenol 153:1191–1195

DeMatteo C, Matovich D, Hjartarson A (2005) Comparison of clinical and video fluoroscopic evaluation of children with feeding and swallowing difficulties. Dev Med Child Neurol 47:149–157

Demirogullari B, Sonmez K, Turkyilmaz Z et al (2001) Colon interposition for esophageal stenosis in a patient with epidermolysis bullosa. J Pediatr Surg 36:1861–1863

Ethun CG, Fallon SC, Cassady C et al (2014) Fetal MRI improves diagnostic accuracy in patients referred to a fetal center for suspected esophageal atresia. J Pediatr Surg 49:712–715

Fasulakis S, Andronikou S (2003) Balloon dilatation in children for oesophageal strictures other than those due to primary repair of oesophageal atresia, interposition or restrictive fundoplication. Pediatr Radiol 33:682–687

Felix JF, Tibboel D, de Klein A (2007) Chromosomal anomalies in the aetiology of oesophageal atresia and tracheo-oesophageal fistula. Eur J Med Genet 50:163–175

Felix JF, de Jong EM, Torfs CP et al (2009) Genetic and environmental factors in the etiology of esophageal atresia and/or tracheoesophageal fistula: an overview of the current concepts. Birt Defects Res A Clin Mol Teratol 85:747–754

Fernbach SK (1994) In: Gore RM, Levine MS, Laufer I (eds). Esophagus. WB Saunders Company, Philadelphia, pp 1380–1497

Fine J, Mellerio JE (2009) Extracutaneous manifestations and complications of inherited epidermolysis bullosa. Part I. Epithelial associated tissues. J Am Acad Dermatol 61:367–384

Fraser CD Jr, Carberry KE (2012) Congenital heart disease. In: Townsend CM Jr, Beauchamp RD, Evers BM, Mattox KL (eds) Sabiston textbook of surgery, 19th edn. Saunders, Philadelphia, chap 59

Gander JW, Berdon WE, Cowles RA (2009) Iatrogenic esophageal perforation in children. Pediatr Surg Int 25:395–401

Gibbs JM, Chandrasekhar CA, Ferguson EC, Oldham SAA (2007) Lines and stripes: where did they go? — From conventional radiography to CT. RadioGraphics 27:33–48

Gimenez A, Franquet T, Erasmus JJ et al (2002) Thoracic complications of esophageal disorders. Radiographics Spec No: S247–258

Gross RE (1953) The surgery of infancy and childhood. WB Saunders, Philadelphia, pp 75–102

Hallal C, Kieling CO, Nunes DL et al (2012) Diagnosis, misdiagnosis, and associated diseases of achalasia in children and adolescents: a twelve-year single center experience. Pediatr Surg Int 28:1211–1217

Harned RK, Strain JD, Hay TC, Douglas MR (1997) Esophageal foreign bodies: safety and efficacy of Foley catheters extraction of coins. AJR Am J Roentgenol 168:443–446

Heran MK, Baird R, Blair GK et al (2008) Topical mitomycin-C for recalcitrant esophageal strictures: a novel endoscopic/fluoroscopic technique for safe endoluminal delivery. J Pediatr Surg 43:815–818

Herman TE, Oser AB, McAlister WH (1991) Tubular communicating duplications of esophagus and stomach. Pediatr Radiol 21:494–496

Hochart V, Verpillat P, Langlois C et al (2015) The contribution of fetal MR imaging to the assessment of oesophageal atresia. Eur Radiol 25:306–314

Holland AJA, Fitzgerald DA (2010) Oesophageal atresia and tracheo-oesophageal fistula: current management strategies and complications. Paediatr Respir Rev 11:100–107

Hryhorczuk AL, Lee EY, Eisenberg RL (2013) Esophageal abnormalities in pediatric patients. AJR Am J Roentgenol 201:W519–W532. doi:10.2214/AJR.12.9291

Hussain SZ, Thomas R, Tolia V (2002) A review of achalasia in 33 children. Dig Dis Sci 47:2538–2543

Issaivanan M, Redner A, Weinstein T et al (2012) Esophageal carcinoma in children and adolescents. J Pediatr Hematol Oncol 34:63–67

Jadcherla SR, Duong HK, Hofmann C et al (2005) Characteristics of upper esophageal sphincter and esophageal body during maturation in healthy human neonates compared with adults. Neurogastroenterol Motil 17:663–670

Kahrilas PJ, Kim HC, Pandolfino JE (2008) Approaches to the diagnosis and grading of hiatal hernia. Best Pract Res Clin Gastroenterol 22:601–616

Kalache KD, Chaoui R, Mau H (1998) The upper neck pouch sign: a prenatal sonographic marker for esophageal atresia. Ultrasound Obstet Gynecol 11:138–140

Karasick S, Lev-Toaff AS (1995) Esophageal strictures: findings on barium radiographs. AJR Am J Roentgenol 165:561–565

Kern IB, Eisenberg M, Willis S (1989) Management of oesophageal stenosis in epidermolysis bullosa dystrophica. Arch Dis Child 64:551–556

Koumanidou C, Vakaki M, Pitsoulakis G et al (2004) Sonographic measurement of the abdominal esophagus length in infancy: a diagnostic tool for gastroesophageal reflux. AJR Am J Roentgenol 183:801–807

Kovesi T, Rubin S (2004) Long-term complications of congenital esophageal atresia and/or tracheoesophageal fistula. Chest 126:915–925

Kramer SS (1989) Radiologic examination of the swallowing impaired child. Dysphagia 3:117–125

Kramer RE, Quiros JA (2010) Esophageal stents for severe strictures in young children: experience, benefits, and risks. Curr Gastroenterol Rep 12:203–210

Kubiak R, Andrews J, Grant HW (2011) Long-term outcome of laparoscopic Nissen fundoplication compared with laparoscopic Thal fundoplication in children: a prospective, randomized study. Ann Surg 253:44–49

Kulkarni B, Rao RS, Oak S, Upadhyaya MA (1997) 13 pairs of ribs – a predictor of long-gap atresia in tracheoesophageal fistula. J Pediatr Surg 32:1453–1454

Kuo B, Urma D (2006) Esophagus – anatomy and development. GI Motility online (2006). doi:10.1038/gimo6 Available online http://www.nature.com/gimo/contents/pt1/full/gimo6.html. Accessed 24 Jan 2015

Ladd WE (1944) The surgical treatment of esophageal atresia and tracheoesophageal fistulas. N Engl J Med 230:625–637

Lee CW, Kays DW, Chen MK et al (2010) Outcomes of treatment of childhood achalasia. Pediatr Surg 45:1173–1177
Lefton-Greif MA, Arvedson JC (2007) Pediatric feeding and swallowing disorders: state of health, population trends, and application of the international classification of functioning, disability, and health. Semin Speech Lang 28:161–165
Lévesque D, Baird R, Laberge JM (2013) Refractory strictures post-esophageal atresia repair: what are the alternatives? Dis Esophagus 26:382–387
Liacouras CA, Furuta GT, Hirano I (2011) Eosinophilic esophagitis: updated consensus recommendations for children and adults. J Allergy Clin Immunol 128:3–20
Macharia EW (2012) Comparison of upper gastrointestinal contrast studies and pH/impedance tests for the diagnosis of childhood gastro-oesophageal reflux. Ped Radiol 42:946–951
Martinez L, Rivas S, Hernandez F et al (2003) Aggressive conservative treatment of esophageal perforations in children. J Pediatr Surg 38:685–689
Matsuo K, Palmer JB (2008) Anatomy and physiology of swallowing. Phys Med Rehabil Clin N Am 19:691–707
McGuirt WF Jr (2003) Gastroesophageal reflux and the upper airway. Pediatr Clin North Am 50:487–502
Mercado-Deane MG, Burton EM, Harlow SA et al (2001) Swallowing dysfunction in infants less than 1 year of age. Pediatr Radiol 31:423–428
Michaud L, Coutenier F, Podevin G et al (2013) Characteristics and management of congenital esophageal stenosis: findings from a multicenter study. Orphanet J Rare Dis 8:186, Accessed December 12 2014
Miller JL, Kang SM (2007) Preliminary ultrasound observation of lingual movement patterns during nutritive versus non-nutritive sucking in a premature infant. Dysphagia 22:150–160
Newman B, Bender TM (1997) Esophageal atresia/tracheo- esophageal fistula and associated congenital esophageal stenosis. Pediatr Radiol 27:530–534
Newman LA, Keckley C, Petersen MC, Hammer A (2001) Swallowing function and medical diagnoses in infants suspected of dysphagia. Pediatrics 108, E106. doi:10.1542/peds.108.6.e106
Nihoul-Fekete C, DeBacker A, Lortat-Jacob S et al (1987) Congenital esophageal stenosis: a review of 20 cases. Pediatr Surg Int 2:86–92
Pedersen RN, Calzolari E, Husby S, Garne E (2012) EUROCAT Working group Oesophageal atresia: prevalence, prenatal diagnosis and associated anomalies in 23 European regions. Arch Dis Child 97:227–232
Prasse JE, Kikano GE (2009) An overview of pediatric dysphagia. Clin Pediatr 48:247–251
Rosen R (2014) Gastroesophageal reflux in infants more than just a pHenomenon. JAMA Pediatr 168:83–89
Rudolph CD, Mazur LJ, Liptak GS et al (2001) Guidelines for evaluation and treatment of gastroesophageal reflux in infants and children: recommendations of the North American Society for Pediatric Gastroenterology and Nutrition. J Pediatr Gastroenterol Nutr 32(Suppl 2):S1–S31
Sadler TW (2012) Ch 15: Digestive tract. In: Langmans medical embryology, 12th edn. Lippincott Williams & Wilkins, Philadelphia, PA, pp 208–210
Savino A, Cecamore C, Matronola MF et al (2012) US in the diagnosis of gastroesophageal reflux in children. Pediatr Radiol 42:515–524
Sharieff GQ, Brousseau TJ, Bradshaw JA, Shad JA (2003) Acute esophageal coin ingestion: is immediate removal necessary? Pediatr Radiol 33:859–863
Sharma S, Nezakatgoo N, Sreenivasan P et al (2009) Foregut cystic developmental malformation: new taxonomy and classification – Unifying embryopathological concepts. Indian J Pathol Microbiol 52:461–472
Shaw-Smith CJ (2006) Oesophageal atresia, tracheo-oesophageal fistula, and the VACTERL association: review of genetics and epidemiology. J Med Genet 43:545–554
Shinkawa T, Greenberg SB, Jaquiss RD, Imamura M (2012) Primary translocation of aberrant left subclavian artery for children with symptomatic vascular ring. Ann Thorac Surg 93:1262–1265
Soon IS, Butzner JD, Kaplan GG, deBruyn JC (2013) Incidence and prevalence of eosinophilic esophagitis in children. J Pediatr Gastroenterol Nutr 57:72–80
Spitz L (2007) Oesophageal atresia. Orphanet J Rare Dis 2:24. doi:10.1186/1750-1172-2-24 accessed May 9 2015
Srikanth MS, Ford EG, Stanley P et al (1992) Communicating bronchopulmonary foregut malformations: classification and embryogenesis. J Pediatr Surg 27:732–736
Stoll C, Alembik Y, Dott B, Roth MP (2009) Associated malformations in patients with esophageal atresia. Eur J Med Genet 52:287–290
Sugandhi N, Sharma P, Agarwala S et al (2011) Esophageal lung: presentation, management and review of literature. J Pediatr Surg 46:1634–1637
Takubo K (2009) Embryology and developmental disorders of the esophagus in pathology of the esophagus: an atlas and textbook. Springer, Tokyo, pp p1–p3
Towbin AJ, Diniz LO (2012) Schatzki ring in pediatric and young adult patients. Pediatr Radiol 42:1437–1440
Turner A, Gavel G, Coutts J (2005) Vascular rings-presentation, investigation and outcome. Eur J Pediatr 164:266–670
Vakil N, van Zanten SV, Kahrilas P et al (2006) Global Consensus Group. The Montreal definition and classification of gastroesophageal reflux disease: a global evidence- based consensus. Am J Gastroenterol 101:1900–1920
van Bokhoven H, Celli J, van Reeuwijk J et al (2005) MYCN haploinsufficiency is associated with reduced brain size and intestinal atresias in Feingold syndrome. Nat Genet 37:465–467
Vandenplas Y, Rudolph CD, Di Lorenzo C et al (2009) Pediatric gastroesophageal reflux clinical practice guidelines: joint recommendations of the North American Society for Pediatric Gastroenterology, Hepatology and Nutrition (NASPGHAN) and the European Society for Pediatric Gastroenterology,

Hepatology and Nutrition (ESPGHAN). J Pediatr Gastroenterol Nutr 49:498–547
Vasudevan SA, Kerendi F, Lee H et al (2002) Management of congenital esophageal stenosis. J Pediatr Surg 37:1024–1026
Vazquez JL, Buonomo C (1999) Feeding difficulties in the first days of life: findings on upper gastrointestinal series and the role of videofluoroscopic swallowing study. Pediatr Radiol 29:894–896
Vogt EC (1929) Congenital esophageal atresia. Am J Roentgenol 22:463–465
Walor D, Berdon W, Anderson N et al (2005) Gaseous distention of the cervical esophagus with nasal CPAP: mimicker of pharyngeal perforation and esophageal atresia. Pediatr Radiol 35:1196–1198
Waltzman ML, Baskin M, Wypij D et al (2005) A randomized clinical trial of the management of esophageal coins in children. Pediatrics 116:614–619
Webb WA (1995) Management of foreign bodies of the upper gastrointestinal tract: update. Gastrointest Endosc 41:39–51
Westra SJ, Wolf BH, Staalman CR (1990) Ultrasound diagnosis of gastroesophageal reflux and hiatal hernia in infants and young children. J Clin Ultrasound 18:477–485
Yedururi S, Guillerman RP, Chung T et al (2008) Multimodality imaging of tracheobronchial disorders in children. Radiographics 28, e29. doi:10.1148/rg.e29
Yoshida T, Fukahara T, Inoue A et al (2005) Congenital esophageal duplication. Gastrointest Endosc 61:350–352
Yousefzadeh DK (2009) The position of the duodenojejunal junction: the wrong horse to bet on in diagnosing or excluding malrotation. Ped Radiol 39:S172–S177

# The Stomach

Abdusamea G. Shabani, Deepak R. Kaura,
Aisha Rizvi, Gurdeep S. Mann, and Samuel Stafrace

## Contents



A.G. Shabani, MBBCh, FRCR (✉)
G.S. Mann, MBCHB, MRCP, FRCR
S. Stafrace, MD, MRCP, FRCR, FRCP Edin
Department of Radiology, Sidra Medical and Research Center, PO Box 26999, Doha, Qatar

Weill Cornell Medicine-Qatar, Doha, Qatar
e-mail: ashabani@sidra.org; gmann@sidra.org; sstafrace@sidra.org

D.R. Kaura, MD, FRCPC, DABR
Chair, Department of Radiology, Sidra Medical and Research Center, PO Box 26999, Doha, Qatar
e-mail: dkaura@sidra.org

A. Rizvi, MBBS
Doha, Qatar
e-mail: aisha.rizvi89@gmail.com

**Abstract**

The stomach is an essential organ in the first stages of digestion and also acts as a conduit between the esophagus and the small bowel. The pediatric stomach is subject to a number of congenital and acquired disorders. In this chapter we review the development of the stomach, the applied anatomy and the diagnostic imaging findings of gastric disorders.

## 1 Embryology and Anatomy

The abdominal portion of the foregut is visibly divided into the esophagus, stomach, and proximal duodenum by the fifth week of gestation (Larsen 2001). The stomach starts out as a straight tubular structure with a slight fusiform dilation. This area soon enlarges and broadens



S. Stafrace, J.G. (Hans) Blickman (eds.), *Radiological Imaging of the Digestive Tract in Infants and Children*, Medical Radiology, DOI 10.1007/978-3-319-18434-0_5

ventro-dorsally. During the sixth and seventh gestational weeks, the dorsal wall of the stomach grows faster than the ventral wall, resulting in the greater curvature becoming more elongated. Following this the fundus and cardiac incisures develop with continued differential expansion of the superior part of the greater curvature.

During the seventh and eighth weeks, the stomach rotates 90 degrees clockwise about its craniocaudal axis. With rotation the ventral wall (lesser curvature) moves to the right, while the dorsal wall moves to the left (greater curvature). Prior to the above rotation, the cranial and caudal ends of the stomach are in the median plane. With rotation and growth, the stomach's cranial half displaces to the left, while the more caudal component moves to the right (Fig. 1).

The stomach is the broadest part of the gastrointestinal tract. Its end lies in the left upper quadrant underneath the left dome of the diaphragm. It can be anatomically divided into four parts: the fundus, being the upper most portion; the body, which is the largest segment; the antrum; and the pylorus. Proximally it is continuous with the esophagus via the gastroesophageal junction, while distally it communicates with the duodenum through the pyloric canal.

The stomach is relatively fixed; achieved through four ligaments: the gastrohepatic ligament, the gastrophrenic ligament, the gastrosplenic ligament, and the gastrocolic ligament.

Gastric capacity varies greatly depending on the child's age. In the newborn the stomach capacity is only a few millilitres, but this increases rapidly with age (Silverman 1961).

The duodenum starts to develop early in the fourth week from the caudal portion of the foregut, the cranial portion of the midgut, and splanchnic mesenchyme. The junction of these two portions is just distal to the origin of the common bile duct. With rapid growth the developing duodenum forms a C-shaped loop projecting ventrally. Due to rotation of the stomach, the duodenum rotates to the right where it comes to lie retroperitoneally. The blood supply of the stomach and proximal duodenum, being derived from the foregut, arises from the branches of celiac axis. The distal portion of the third part and fourth part of the duodenum receive their blood supply from the superior mesenteric artery.

A system of digestive glands develops from the endodermal buds of the duodenum including the liver parenchyma, the gall bladder, as well as the pancreatic parenchyma and its ducts (the latter derived from the fusion of the dorsal and ventral pancreatic ducts) (Moore and Persaud 2011).

The gastrointestinal (GI) tract starts out as a short, straight tube (Larsen 2001). Through a complicated process, this primitive tube elongates and becomes fixed in the abdominal cavity. The proximal duodenojejunal loop and the distal cecocolic loop are able to pull adjacent bowel along with them. Before the tenth week of embryonic life, both loops independently rotate around the SMA by 270° in a counterclockwise direction returning to the abdominal cavity. This process results in the described end position of the duodenum with the duodenojejunal junction at the left side in the upper abdomen. The cecum comes to lie in the right lower quadrant. Through this process the bowel's position becomes fixed by the mesentery. The broad-based normal mesentery extends from the left upper quadrant (at the ligament of Treitz) to the cecum in the right lower quadrant.

Histologically, the gastric wall consists of the mucosa, muscularis mucosae, submucosa, muscularis externa, and serosa. Mucus produced by the surface cells protects the stomach lining from the hydrochloric acid and pepsin secreted by the gastric glands. The rugae or longitudinal folds of the empty stomach consist of the 2 superficial layers (mucosa and submucosa). The muscularis externa of the stomach is formed by three smooth muscle layers: an inner oblique, a middle circular, and an outer longitudinal. These muscle layers are responsible for the "gastric motility" propelling the gastric contents into the small intestine.

## 2 Examination of the Upper GI Tract

### 2.1 Abdominal X-Ray: Air as a Contrast Agent

The plain radiograph of the abdomen plays an important role in assessing upper GI anatomical and functional status in neonates and young

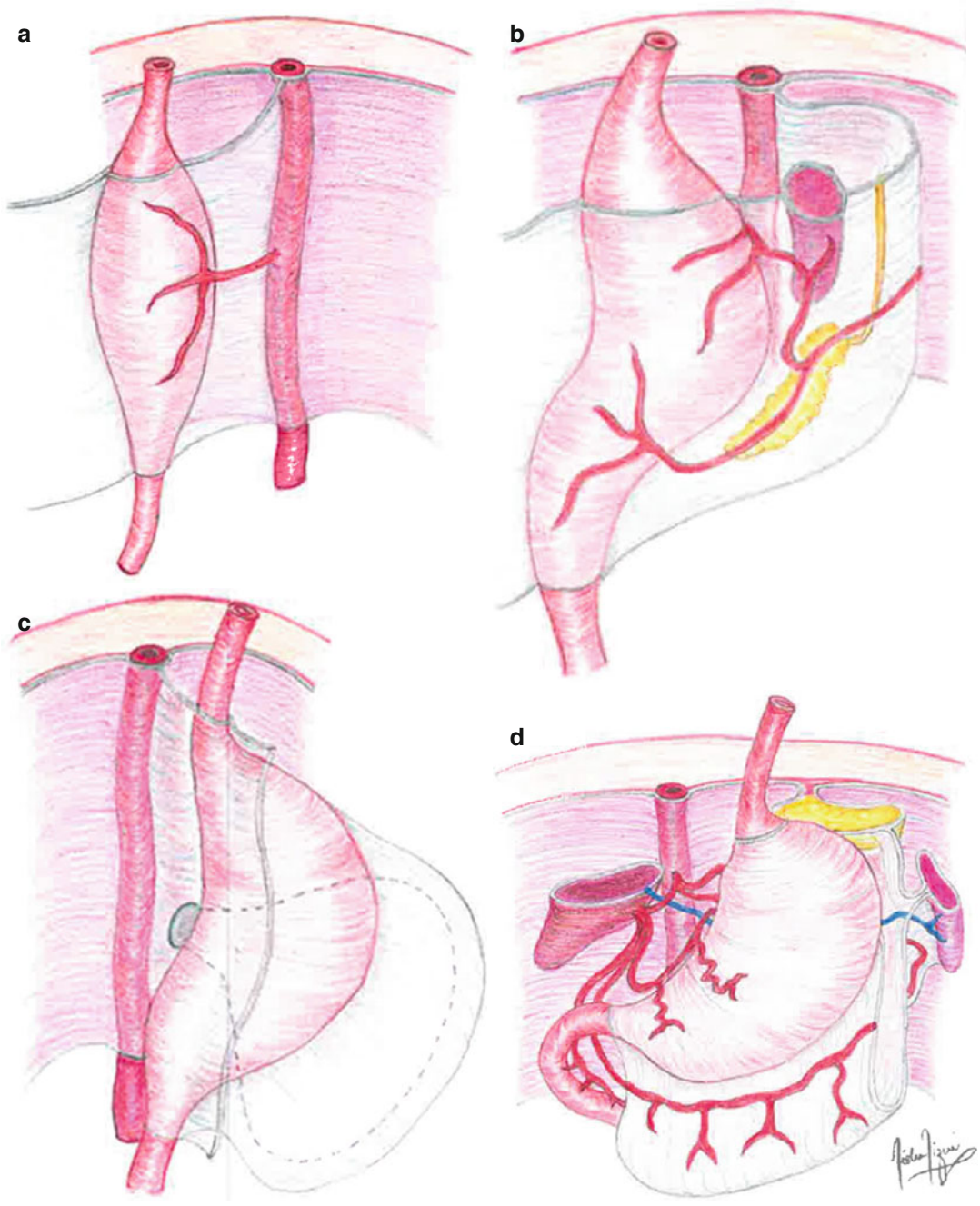


**Fig. 1** Normal embryology and anatomy of the foregut and organs of digestion (Drawings courtesy of Dr. Aisha Rizvi)

children. Air is swallowed immediately after birth. Air is expected to be present within the stomach 15 min from birth, and if no air is seen after 1 h, higher upper GI tract obstruction should be considered. After 3 h, air should be seen throughout the entire small bowel, while air in the sigmoid colon is seen after 8–9 h (Berrocal et al. 1999). Air is safe and can be used in children as a negative contrast agent in diagnosing upper GI obstruction, allowing some congenital anomalies (e.g., congenital duodenal obstruction) to be readily diagnosed without the need for other contrast media (Fig. 2).

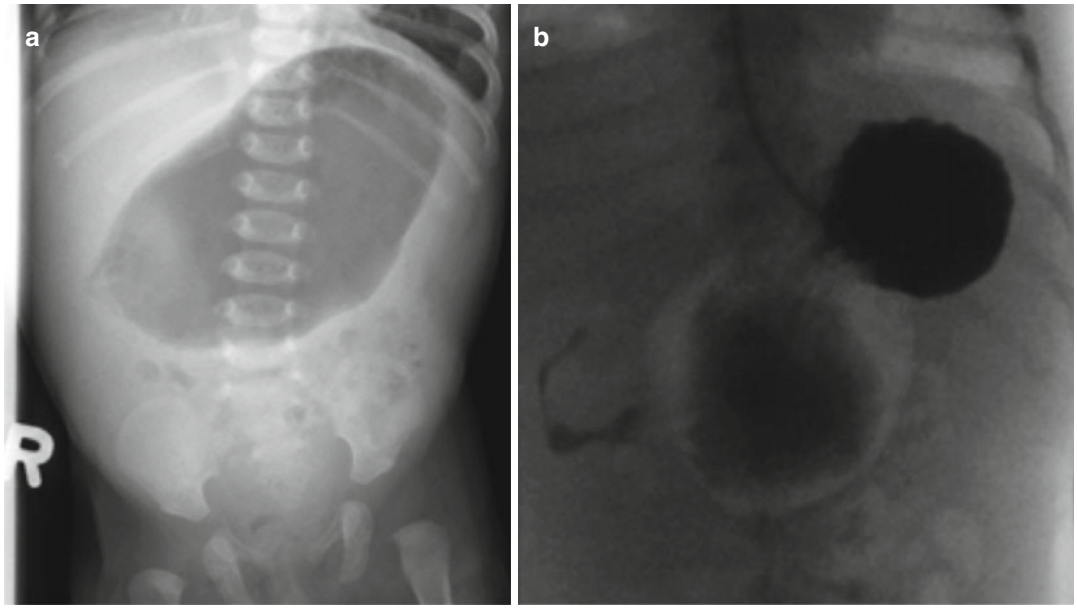


**Fig. 2** (**a**) Plain abdominal radiograph in a 30-day-old infant. Gastric distention with paucity of distal air in keeping with obstruction at the pylorus. (**b**) Repeat radiograph post-administration of water-soluble contrast through the NG tube confirms hypertrophic pyloric stenosis

## 2.2 Fluoroscopy/Upper GI Study

Despite the "upper GI contrast study" (UGI) having been utilized for nearly a century, this still has an essential role in the evaluation of the anatomical and functional status of the upper gastrointestinal tract. The UGI in children should be performed using as low a radiation dose as possible but without compromising the diagnostic quality of the study. This can be accomplished by using pulsed fluoroscopy together with careful collimation and gonadal shielding.

Barium sulfate is the most commonly used contrast medium in the assessment of gastrointestinal tract. Barium is considered to be relatively safe and a nontoxic contrast agent utilizable in children and infants. Contraindications to its use include the suspicion of perforation (risk of barium peritonitis) and high risk of aspiration (e.g., neurologically impaired children). In premature infants, a high-iodine-concentration, water-soluble contrast medium should be used instead of barium sulfate. The main advantages of the latter are the lack of large fluid shifts, absence of contrast dilution, lack of injury to the bowel mucosa, low absorption from the bowel, and a relatively low risk of pulmonary edema if aspirated (Hiorns 2011).

The recommended fasting time before the study is equal in length to the regular time between meals for the patient, hence being longer in adolescents than in newborn babies. Typically in children under 1 year of age, a 3-h fasting period is sufficient to empty the normal stomach. A longer fasting time bares the risk of dehydration. Older children are kept fasting overnight (Schlesinger and Parker 2004).

The technique for a UGI in newborns and small infants is different from studies performed in the older children. In the former group, the study is performed to evaluate a (known) congenital proximal obstruction or, more importantly, to evaluate the position of the duodenojejunal flexure (the ligament of Treitz) in suspected malposition/rotation.

The study is tailored to answer these specific questions and is performed as a single-contrast study. In older children, however, double-contrast studies may be required depending on the clinical question (e.g., in the assessment of polyps).

An UGI in children should always include the evaluation of the esophagus, stomach, and duodenum including the duodenojejunal flexure. On assessing with barium, the contour of the stomach typically appears smooth in newborns and young infants with normal gastric rugal folds visible in older children.

### 2.3 Ultrasound

Ultrasonography (US) plays a vital role in investigating gastrointestinal tract abnormalities particularly in infants and young children. As US is a radiation-free study, readily available, and inexpensive, this should be the first imaging modality of choice in the UGI. US is widely accepted as the diagnostic test for infantile hypertrophic pyloric stenosis (HPS) and is also used for the evaluation of the stomach wall thickness and the characterization of suspected duplication cysts. US is also useful in the localization and follow-up of radiolucent gastric foreign bodies. Contrast-enhanced Doppler ultrasound can be successfully used in the management of gastroesophageal reflux (GER) – both in the diagnosis and the subsequent monitoring of treatment response (Farina et al. 2008).

Pediatric US sector probes can be used for a good overview of the stomach, but linear high-frequency transducers are necessary for a more detailed examination. Typically, the patient is scanned in the supine position. A right posterior oblique position is used to evaluate the antrum and the pyloric region since fluid displaces air to the gastric body and fundus.

### 2.4 Cross-Sectional Imaging

Computed tomography (CT) and magnetic resonance (MR) imaging are not routinely used to evaluate the stomach in children, except for staging purposes in cases of a suspected or known malignancy, and to assess response to therapy, complex lesions (such as foregut malformations), and in the case of trauma.

### 2.5 Scintigraphic Studies

Several scintigraphic studies may be indicated to evaluate for gastric pathology in children. The radionuclide gastric emptying study is performed to evaluate for gastric motility and emptying. 99Tcm-pertechnetate scintigraphy can be performed to evaluate the presence and localization of functioning ectopic gastric mucosa. Technetium-99 m HMPAO-labeled leukocyte imaging can be used in the evaluation of inflammatory bowel disease.

## 3 Congenital Anomalies

### 3.1 Fetal Study (US and/or MR)

The stomach appears as a cystic structure in the left hypochondrium of the fetus and should be constantly visible on fetal US from around 11–12 weeks of gestation.

When the stomach is small or not visible in the second or third trimester, the US should be repeated to confirm or exclude these findings. The most common etiology presenting with this scenario is esophageal atresia. A dilated pharyngeal pouch is also seen detected at the same study. Fetal MR can more easily demonstrate the dilated pharyngeal pouch or can exclude the diagnosis by documenting fluid along a normal esophagus. A small or absent stomach is also seen in intrauterine growth retardation with associated oligohydramnios.

If a large (distended) stomach is seen in the third trimester, the most likely cause is duodenal atresia. This demonstrates the typical "double-bubble" appearance. Approximately 30 % of these patients will have trisomy 21 (Buonomo et al. 1998). There is an associated increased risk of esophageal atresia in which case the appearance of a "double bubble" is not seen unless there is an associated H-type tracheoesophageal fistula. The differential diagnosis for the double bubble appearance should include duodenal stenosis and an annular pancreas (Rathaus et al. 1992; Poki et al. 2005). Midgut volvulus rarely manifests as a

double bubble appearance and should also be considered.

When the stomach lies in the midline as opposed to its normal left upper quadrant location, the main suspicion is intestinal malposition/malrotation – with or without obstruction. A postnatal workup is indicated in these patients.

Further description of the above mentioned anomalies is given in the sections below.

## 3.2 Gastric Duplication

Gastrointestinal tract duplication is a rare congenital anomaly. It can be defined as a spherical or tubular structure occurring anywhere along the GI tract from the mouth to the anus, sharing both blood supply and muscle wall but having a separate mucosal lining. This can be seen as an isolated finding or in association with other anomalies including an aberrant pancreas, vertebral anomalies (Schlesinger and Parker 2004), and pulmonary sequestration (Chen et al. 2006; Granata et al. 2003).

Gastric duplication cysts (GDCs) account for 4–7 % of all gastrointestinal tract duplication anomalies, usually found in the region of the greater curvature of the antrum – here typically single and noncommunicating (Pruksapong et al. 1979; Macpherson 1993).

GDCs typically present in childhood, 67 % being diagnosed within the first year of life (Johnston et al. 2008). GDCs are more common in females. The symptoms vary depending on the size and age of the patients. Vomiting, abdominal pain, and failure to thrive are common symptoms; however, other complications such as ulceration, bleeding, and perforation may take center stage as presenting symptoms. Up to 10 % of GDCs contain ectopic pancreatic duplications and may present with pancreatitis and pseudocyst formation.

In adults the majority of cases are asymptomatic and discovered incidentally. An increased risk of malignancy has been reported; therefore, complete surgical resection is recommended. Once the GDCs become malignant, the outcome is usually very poor (Ma et al. 2012).

GDCs are usually detected at prenatal ultrasound. Characteristic appearances include a hyperechoic inner lining due to the mucosa and a hypoechoic outer layer from the musculature so called double-wall sign or gut signature (Fig. 3). The duplication is located intramurally and is filled with anechoic fluid. Less commonly this is filled with echogenic material secondary to hemorrhage, infection, or proteinaceous fluid.

Plain radiographs of the abdomen may demonstrate a soft tissue mass lying between the greater curvature of the stomach and superior to the transverse colon.

When the ultrasound findings are inconclusive, diagnosis of GDCs can be made by CT scan or MRI. Both modalities are helpful for anatomical localization and determination of the extent of the lesions.

On MRI GDCs are filled with low-attenuation fluid/low signal intensity on T1-weighted images and high signal intensity on T2-weighted images. Less commonly one identifies high-attenuation fluid/high signal intensity on T1-weighted images.

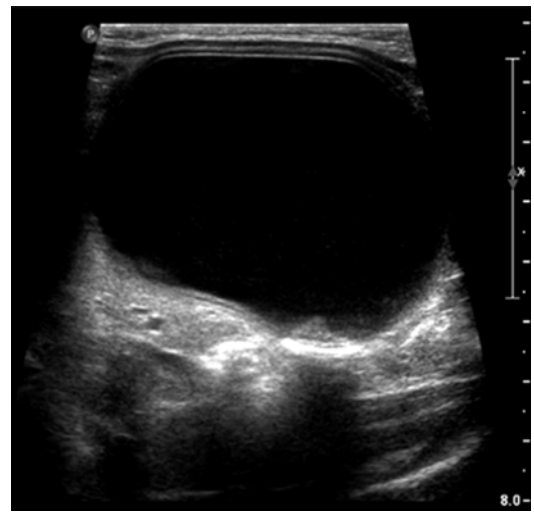


**Fig. 3** Postnatal US appearance of a duplication cyst of the greater curvature of the stomach demonstrating the characteristic double-echo pattern of the GI mucosa

## 3.3 Gastric Diverticula

Gastric diverticula (GD) are the least common type of diverticular disease of the gastrointestinal tract. The true incidence is variable and depends on the method used to detect the gastric diverticulum. For instance it has been described in 0.01–0.11 % of gastroscopies and 0.03–0.1 % of upper GI contrast studies. In the more recent literature, the incidence at CT abdomen is reported at 0.12 % (Schramm et al. 2014).

The congenital type of gastric diverticulum is the most common representing 72 % of all gastric diverticula, equally affecting males and females (Rodeberg et al. 2002). These are true diverticula which have all the components of gastric wall. The likely cause is weakness of the longitudinal muscular fibers (Cheng and Pavelong 1990). This is most commonly located about 2–3 cm distal to the gastroesophageal junction on the posterior wall of the stomach. In the majority of cases, GD are single and of variable size.

GD are rarely symptomatic; however, symptoms and signs such as upper abdominal pain, vomiting, and failure to thrive can occur, and these relate to the location and the size of the diverticulum. The most serious complications of GD are bleeding and perforation. Upper GI contrast studies show these diverticula to fill with contrast (Elliot et al. 2006). Cystic masses with air-fluid levels adjacent to the posterior stomach wall found in the CT scan should raise the possibility of GD (Schramm et al. 2014).

## 3.4 Microgastria

Congenital microgastria refers to a small poorly developed stomach and was first described in 1894 (Dide 1894). It is an extremely rare condition with around 60 reported cases in the literature (Shepherd et al. 2011). It is thought to be the result of an early gastric developmental arrest between the 4th and 5th week of gestation, with the absence of fetal gastric rotation and failure of the greater and lesser curvatures to develop. The spleen arises in the dorsal mesogastrium (by mesenchymal differentiation) at around the same time explaining the frequent association of microgastria with asplenia or polysplenia. Complete lack of gastric development or agastria (absent stomach) is the most extreme form of microgastria (Schlesinger and Parker 2004).

Presenting symptoms of microgastria are recurrent postprandial vomiting, respiratory distress/infection, recurrent aspiration pneumonia, failure to thrive, and malnutrition. These are all consequences of the small stomach and associated GER (Hoehner et al. 1994; Waasdorp et al. 2003).

Diagnosis is made by an UGI which demonstrates an abnormal midline small tubular or saccular stomach (Kroes and Festen 1998) (Fig. 4). Congenital Megaesophagus is almost always associated with microgastria, which may be secondary to the GER or caused by the esophagus taking over the reservoir capacity of the stomach (Moulton et al. 1994).

There is a very high incidence of other associated anomalies, such as a left-sided diaphragmatic hernia (Sharma and Menon 2005), right-sided diaphragmatic hernia (Velasco et al. 1990), growth hormone deficiency and diabetes

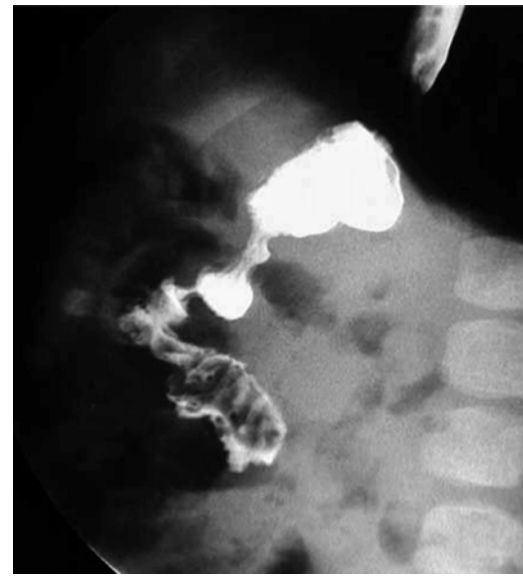

**Fig. 4** Upper GI barium study reveals a markedly small stomach in a case of microgastria (Courtesy of Dr. Carlo Buonomo, Boston, MA, USA)

insipidus (Herniaz Driever et al. 1997), intestinal malrotation, cardiopulmonary anomalies, central nervous system anomalies (hydrocephalus, arhinencephaly, microphthalmia) (Schlesinger and Parker 2004), renal anomalies (Kroes and Festen 1998), laryngo-tracheo-bronchial clefts (Ryan et al. 1991; Samuel et al. 1997), limb reduction defects (Cunniff et al. 1993), Pierre Robin sequence and partial trismus (Giurgea et al. 2000), radiohumeral synostosis, femoral deficiency, and other unusual findings (Roberts et al. 2014). Isolated congenital microgastria is extremely rare.

If no other life-threatening anomalies are present, the treatment of choice in patients with microgastria is gastric augmentation (Menon et al. 2003), classically a Hunt-Lawrence pouch (a double-lumen jejunal pouch anastomosed to the greater curvature of the stomach with a distal Roux-en-Y jejunostomy). Prolonged medical management of gastroesophageal reflux in these patients is not beneficial, since the stomach size will not increase significantly over time (Blank and Chisholm 1973). Operating at an early stage is indicated to allow normal growth and development. Life expectancy is determined mostly by the associated anomalies (Moulton et al. 1994).

## 3.5 Pyloric and Prepyloric/Antral Atresias, Stenosis, and Webs

Congenital (pre-) pyloric atresias, stenosis and webs are rare. These lesions are thought to be the consequence of an intrauterine vascular insult (Schlesinger and Parker 2004). The abundance of the gastric blood supply explains the relative rarity of this condition. There are three different types of pyloric atresia: (1) complete atresia and absence of a connection between the stomach and duodenum, (2) complete atresia with a fibrous band between stomach and duodenum, and (3) the presence of a gastric membrane or diaphragm (Gupta and Guglani 2005). An association between pyloric atresia and epidermolysis bullosa has been described and the responsible genetic mutation for this identified (Schlesinger and Parker 2004).

Symptoms vary among patients, depending on the degree of obstruction: true atresias result in a complete obstruction, while patients with stenosis or webs will only have obstruction depending on relative size of the orifice and bolus. This also effects the time of presentation: patients with complete gastric atresias present very early in life, while patients with stenosis or webs of the pylorus can present later in life, including in adulthood.

The findings described above correlate with the imaging findings. In patients with atresia, there may be no air distal to the body of the stomach, while the stomach is unusually dilated. With stenosis and webs, varying degrees of distal air may be seen. In cases of incomplete obstruction, webs are more common than stenosis. On upper GI studies, these can be seen as linear filling defects. Sometimes the diagnosis can also be made with US where, when the stomach is filled with clear liquid, a membrane can be seen in the antrum (Gupta and Guglani 2005).

## 3.6 Gastric Volvulus

Gastric volvulus can be defined as a pathological gastric rotation by more than 180° around its long (organo-axial) and/or short (mesentero-axial) axis, creating a closed loop obstruction that may result in incarceration, strangulation, and gastric perforation (due to ischemia and necrosis). This can lead to sepsis and cardiovascular collapse. It is rare in children. Acute gastric volvulus in neonates and infants is a life-threatening emergency. It was first described in children in the late 19th century. To date, 282 cases of acute gastric volvulus in the pediatric population have been recorded (Tillman et al. 2014). A gastric rotation of less than 180° can be defined as "gastric torsion" causing only partial obstruction (Porcaro et al. 2013).

The normal stomach is fixed in the peritoneal cavity by four different ligaments. Gastric volvulus is the result of the absence or laxity (e.g., postsurgical) of the gastrocolic and gastrosplenic ligaments (Dalgaard 1952) associated with congenital diaphragmatic hernia, paraesophageal hernia, or wandering spleen (Lin et al. 2005). Gastric volvulus may also be iatrogenic, e.g., after the placement of a percutaneous endoscopic gastrostomy (Sookpotarom et al. 2005).

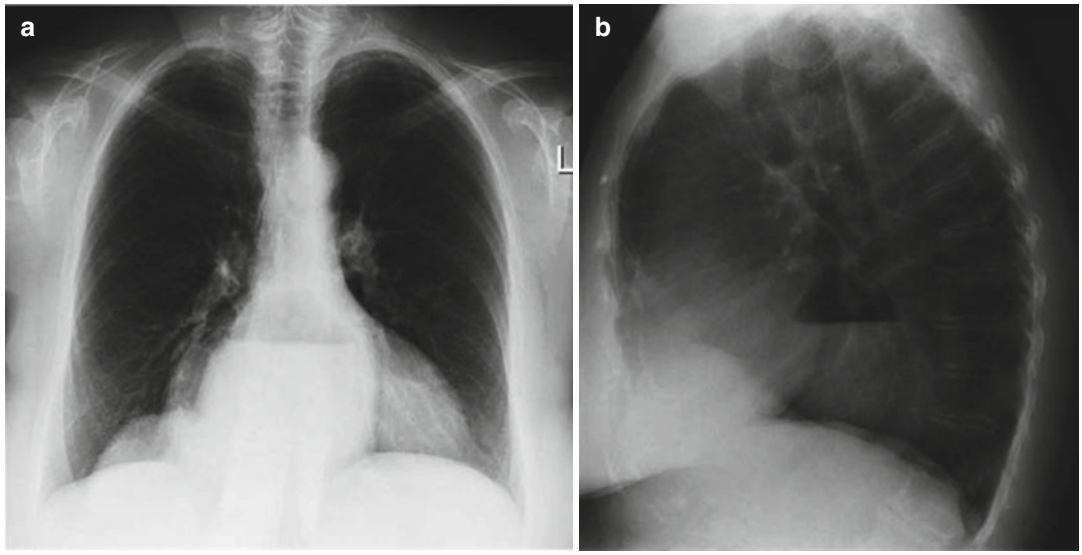


**Fig. 5** (**a**) PA and (**b**) lateral chest radiographs in a 14-year-old girl demonstrate a retrocardiac air-fluid level consistent with a diaphragmatic hiatus hernia (Courtesy of Dr. Carlo Buonomo, Boston, MA, USA)

Acute, recurrent subacute, or chronic forms of gastric volvulus have been described. The symptoms are related to the degree of rotation and gastric obstruction. In the acute form, patients present with sudden vomiting, intractable retching, and acute abdominal pain as well as hypotonia, pallor, and ocular revulsion. It is thought that during acute gastric volvulus, a vagal reflex is triggered by direct irritation of the parasympathetic nervous system. Prompt resuscitation in patients with acute vegetative symptoms is needed. In the subacute or chronic forms, only nonspecific symptoms will be apparent, including recurrent abdominal pain, vomiting, and gastric distension.

Plain X-ray studies may show suspicious signs for gastric volvulus. In organo-axial volvulus, a subtle inferiorly displaced gastroesophageal junction could be seen. More typically in mesentero-axial volvulus, the stomach appears spherical on supine films and a double air-fluid level can be seen in the upright position: a superior one in the antrum and an inferior one in the fundus. On chest radiography, a retrocardiac air-filled structure, consistent with a diaphragmatic hernia and/or an intrathoracic stomach, may be seen (Fig. 5).

The gold standard for the diagnosis of acute as well as the subacute or chronic forms of gastric volvulus is an upper GI study (Darani et al. 2005). The organo-axial type is characterized by the stomach lying in the horizontal position with the pylorus facing downward and with the greater curvature projecting higher than the lesser curvature in front of the distal portion of the esophagus. In this case the stomach rotates along its long axis, which connects the gastroesophageal junction and the pylorus. In contrast, the mesentero-axial type can be recognized by the stomach in a vertical position with the pylorus projecting above the gastroesophageal junction (Fig. 6). The inverted antrum, pylorus, and proximal duodenum can form a "beak" at the usual location of the gastroesophageal junction. In this type, the short axis bisects the lesser and greater curvatures and runs parallel to the hepatoduodenal ligament. The antrum then rotates anteriorly and superiorly so that the posterior surface of the stomach lies anteriorly (Fig. 6b, c). The diagnosis of gastric volvulus can sometimes be suggested on US, when this is performed in search of other diagnoses (Anagnostara et al. 2003).

Acute gastric volvulus requires immediate surgical intervention as a lifesaving procedure. The method of choice is laparoscopic gastropexy. Despite urgent surgical treatment, the diagnosis still has a 65 % mortality rate (Tillman et al. 2014). In some patients an anti-reflux procedure may be needed, as well as other nonsurgical

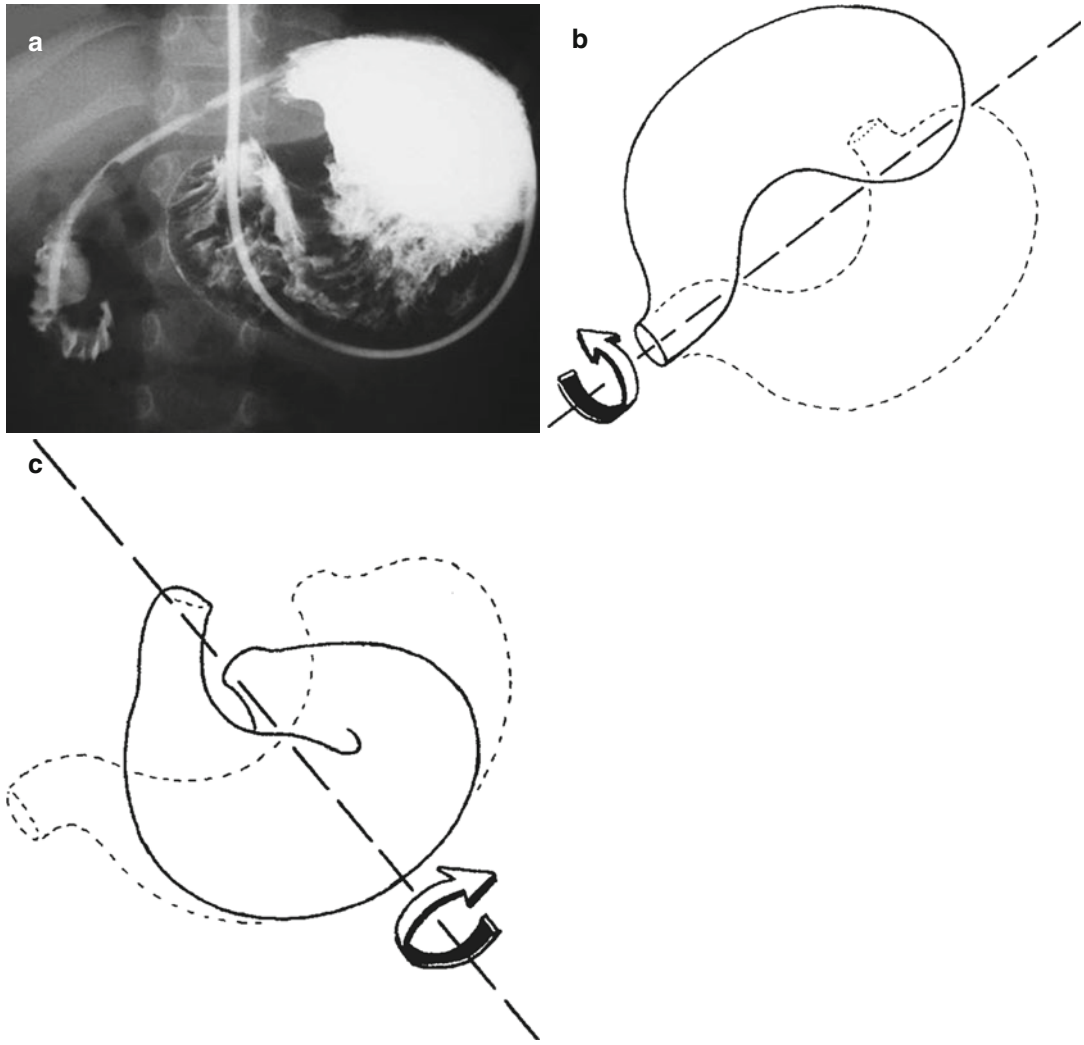


**Fig. 6** Volvulus of the stomach. (**a**) Mesentero-axial volvulus of the stomach; (**b**) organo-axial volvulus; (**c**) mesentero-axial volvulus

techniques like sleeping in prone position (Darani et al. 2005; Tillman et al. 2014).

## 3.7 Ectopic Gastric Mucosa

Meckel diverticulum is the most common congenital anomaly of the GI tract and is the most common site for ectopic gastric mucosa. GI duplications (noncommunicating or more rarely communicating) are less common and 20–30 % of these contain ectopic gastric mucosa. Ectopic mucosa is more commonly seen in tubular duplications in contrast to cystic.

Patients with functioning ectopic gastric mucosa present with pain, bleeding, and perforation. However, intrathoracic foregut duplication cysts that occur mainly in younger patients also present with respiratory distress caused by compression of the airway.

Kumar et al. (2005) described a series of 11 (male) children in which the diagnosis of ectopic gastric mucosa could be made by the use of 99Tcm-pertechnetate scintigraphy. Functioning ectopic gastric mucosa was found in Meckel diverticulum in three patients, in small bowel duplications in four patients, in a gastric duplication in one patient, and in intrathoracic foregut

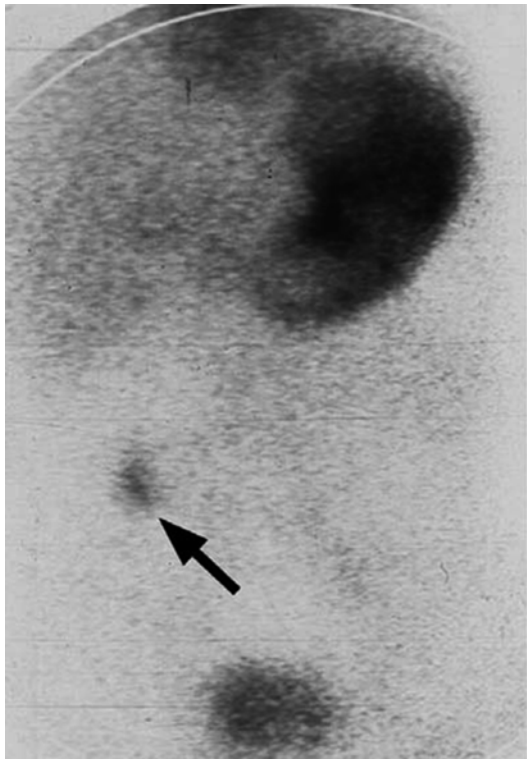

**Fig. 7** Technetium-99 m pertechnetate scan (Meckel's study). A 2-year-old boy with history of passage of bright red blood per rectum and a normal upper GI study. Uptake in ectopic gastric mucosa (*arrow*) is identified at the same time as the uptake in the stomach. This is in keeping with a Meckel diverticulum containing ectopic gastric mucosa

duplication cysts in three patients. The uptake of 99Tcm-pertechnetate in the ectopic gastric mucosa of Meckel diverticulum and gastric duplication is visualized simultaneously with the uptake in the stomach (Fig. 7).

### 3.8 Ectopic Pancreatic Tissue

Pancreatic tissue can be found in the antropyloric region of the stomach or less frequently in the duodenum. It is usually asymptomatic, but may present with pain, GI bleeding, or obstruction due to ulceration, inflammation (pancreatitis), and rarely with malignant degeneration. On barium studies, a rounded filling defect with a central niche can be seen, representing an attempt at duct formation (Fig. 8). This entity can also be identified on US and/or CT (Schlesinger and Parker 2004) (Fig. 9a–c).

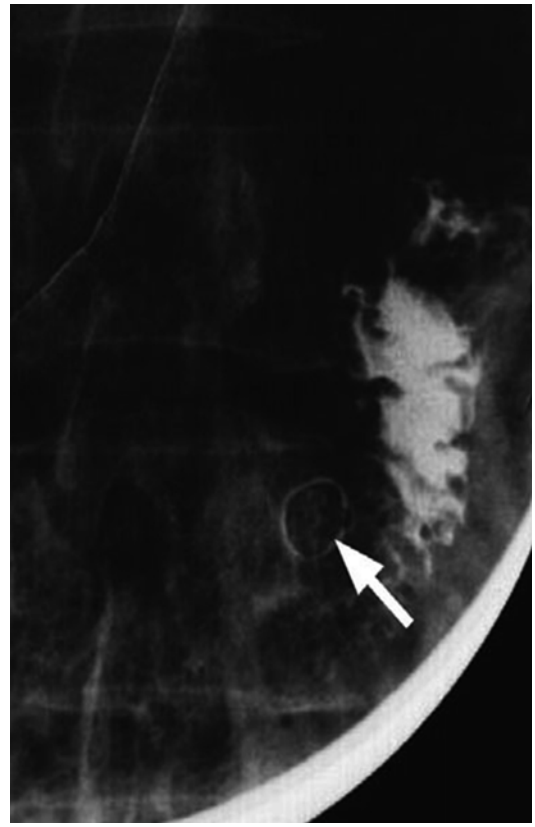

**Fig. 8** Double-contrast upper GI barium study – ectopic pancreatic tissue (*arrow*)

## 4 Acquired Gastric Disorders

### 4.1 Infantile Hypertrophic Pyloric Stenosis

Infantile hypertrophic pyloric stenosis (HPS) was first reported as an independent clinical condition by Hirschsprung in 1887 (Markowitz 2014). In 1912 Ramstedt performed the first successful pyloromyotomy.

HPS causes projectile non-bilious vomiting in infancy and usually affects children between 2 and 12 weeks. The vomit is sometimes blood stained as it may be associated with a degree of gastritis. The approximate incidence of HPS is 2–5/100 live births. This condition is more

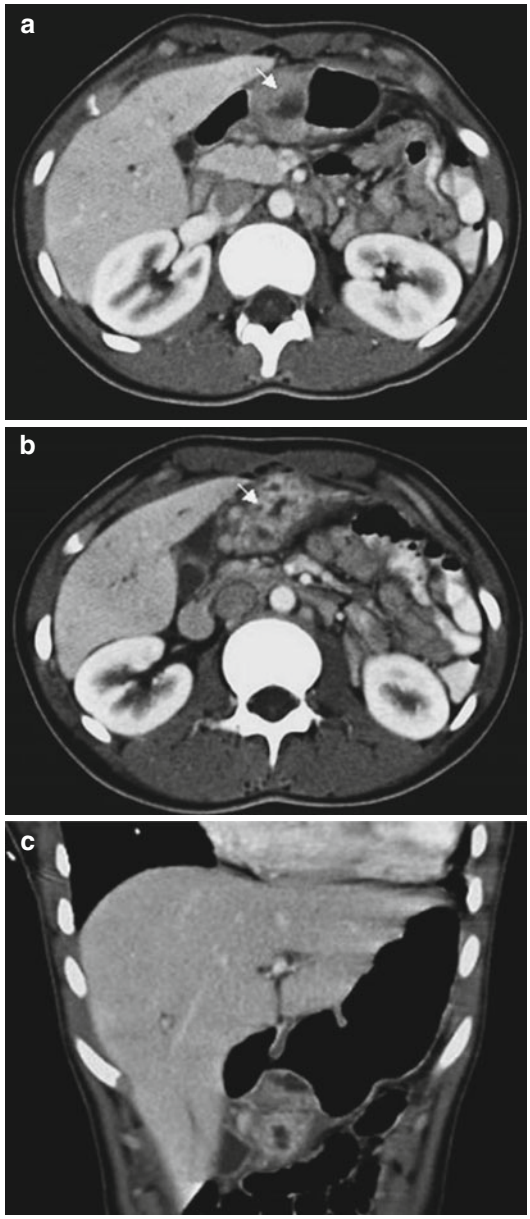


**Fig. 9** (**a**, **b**): Axial (**c**) coronal images from an abdominal contrast-enhanced CT scan in a 16-year-old with abdominal pain. This demonstrates an extrinsic mass in the greater curvature of the stomach from pancreatitis in ectopic pancreatic tissue located in the antropyloric region (*arrow*)

common in boys than girls with a ratio of 5:1 (Schechter et al. 1997).

The precise etiology of HPS remains elusive; however, recent reports have linked this condition with genetic and environmental factors (Panteli 2009).

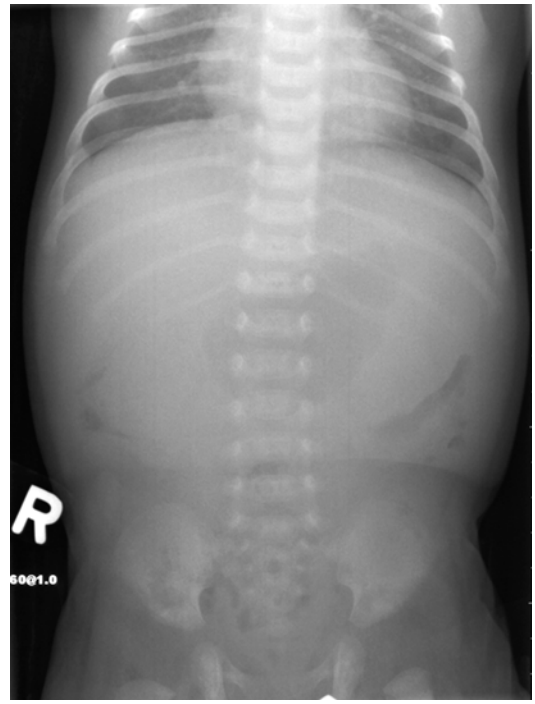


**Fig. 10** Plain abdominal radiograph showing a distended stomach with paucity of distal air in a case hypertrophic pyloric stenosis

Infants with HPS demonstrate (projectile) non-bilious vomiting after feeding. The diagnosis is often confirmed by palpating a small hard mass or "olive" representing the hypertrophied pyloric muscle in the epigastrium. In the right hands clinical examination has a 99 % positive predictive value (White et al. 1998).

An abdominal X-ray is often nonspecific. It may show a gaseously distended stomach with a little air distally (Fig. 10).

US has become the method of choice for evaluating children with suspected HPS. US is used to complement the physical examination and to confirm the clinical diagnosis with very high sensitivity and specificity approaching 100 % (Hernanz-Schulman et al. 1994). Ideally the study should use a high-frequency transducer, preferably, a linear transducer, that should be appropriate to the size of the baby and the position of the pylorus. Sometimes the stomach is filled with air; therefore, positioning the child in the right anterior oblique position facilitates fluid filling the antral region as an acoustic window.

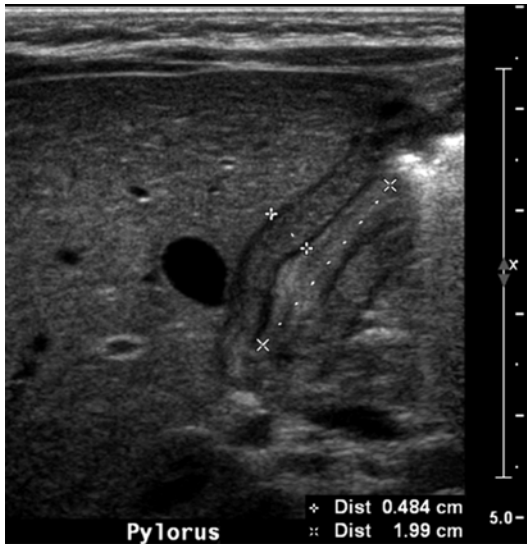


**Fig. 11** Longitudinal scan of the pyloric canal demonstrating the canal to be elongated with hypertrophied muscle wall in a classic case of infantile hypertrophic pyloric stenosis

Alternatively one may fill the stomach by giving water to the infant. The muscle thickness and the muscle length, pyloric canal length, pyloric muscle index (calculating using pyloric length, pyloric muscle thickness, and pyloric diameter), and the muscle volume have all been used as indicator of HPS (Westra et al. 1989). Recent literature reaffirms the established criterion for diagnosis of pyloric stenosis; the muscle wall thickness of 3 mm or higher was 100 % sensitive and 99 % specific, whereas the pyloric length of 15 mm or higher was 100 % sensitive and 97 % specific (Iqbal et al. 2012) (Fig. 11).

The UGI was the first imaging modality utilized for the diagnosis of HPS in children. It has been superseded by the use of US as fluoroscopy causes radiation exposure and can be a lengthy procedure, and it may result in vomiting and aspiration of the contrast. Upper GI contrast studies still have a role in equivocal cases and also in determining other causes of vomiting. Classically the contrast study is described to demonstrate the "string" sign with narrowing of the pyloric canal. This is almost always seen in conjunction with an elongated and upward curving pyloric canal. The "double track/string" sign is caused by contrast caught between folds of the underlying thickened wall. A similar sign can be seen in ultrasound, without being pathognomonic for HPS, since it can also be visualized in pylorospasm (Cohen et al. 2004). The "peak" sign is the result of the thickened muscle narrowing the contrast column as it enters the pyloric channel. The thickened and enlarged muscle mass resembles an "apple core lesion" with undercutting of the distal antrum and the proximal duodenum. The "pyloric tit" sign can be seen along the lesser curvature of the stomach, just proximal to the impression of the pyloric mass, and may be consistent with a blocked peristaltic wave. The "shoulder sign" is caused by the impression of the hypertrophied muscle of the antrum.

All of the above mentioned signs can be also seen transiently in normal children. Therefore, the study should be carefully performed with attention to persistence of these signs. Clear visualization of anterograde flow through the pylorus on ultrasound would go against the diagnosis.

Pyloromyotomy remains the surgical treatment of choice in HPS; however, some countries have a long experience in nonsurgical treatment with a success rate of 75 % (Asplund and Langer 2007). Medical treatment should be considered as an alternative in infants with contraindications to anesthesia or surgery.

## 4.2 Peptic Ulcer Disease

Peptic ulcer disease (PUD) is a common gastrointestinal problem affecting up to 10 % of the general population but is much less commonly seen in the pediatric population. The classification of peptic ulcer disease is based on the region of involvement (gastric versus duodenal ulcers) and on the presence or absence of a known etiology (primary or secondary due to an underlying disease). In 1983 Warren and Marshall established the link between *Helicobacter pylori* (*H. pylori*) infection and chronic gastritis (Hernandez et al. 2014). Gastric ulcers are seen in neonates (with or without the development of gastric perforation), while duodenal ulcers are much more common after the neonatal period.

The pathogenic effects of *H. pylori* as a causative agent of peptic ulcer disease, antral

atrophic gastritis, gastric adenocarcinoma, and gastric mucosa-associated lymphoid tissue (MALT) lymphoma are well known (Konturek et al. 2006). Although these diseases are much more common in adulthood, colonization with this pathogen occurs mostly during childhood. Prevalence rates vary from almost 10 % in children under the age of 10 years in industrialized countries to 57–83 % of children in the poorest Brazilian regions (Bittencourt et al. 2006). In theory, childhood is a good time to eradicate *H. pylori* because children are usually not infected long enough to develop gastric cancer (Bourke 2005). In this way, gastric cancers may be prevented. However, since the prevalence and incidence of gastric cancer are decreasing rapidly in developed nations, screening programs would be extremely expensive. A test and treat strategy can only be justified in high-risk areas or in families with a strong positive history (Bourke 2005; Graham and Shiotani 2005).

Drumm et al. (2004) demonstrated that single-contrast barium studies have a high false-negative rate for ulcer disease when compared with endoscopy. Double-contrast studies are indicated because of the higher sensitivity but cannot be performed in young children and imply a higher radiation dose in all. When perforation is suspected, a single-contrast study with a low osmolar nonionic contrast agent should be performed. As a general rule, endoscopy is the method of choice in the diagnosis of peptic ulcers. It has the highest sensitivity and allows the collection of fragments from the gastric mucosa for diagnosis of the underlying infection and histopathological analysis (Bittencourt et al. 2006).

An ulcer will be visible on an upper GI study as a round or ovoid collection of barium with radiating folds, consistent with edema/inflammation of surrounding mucosa. On US, thickening of the antropyloric mucosa can be seen as well as elongation of the antropyloric canal, persistent spasm, and delayed gastric emptying. US is not routinely used for the diagnosis of peptic ulcer disease. The presence or absence of intra-abdominal free air can be seen on plain film (upright, left lateral decubitus or with horizontal beam) radiographs in cases of a gastric perforation (Fig. 12).

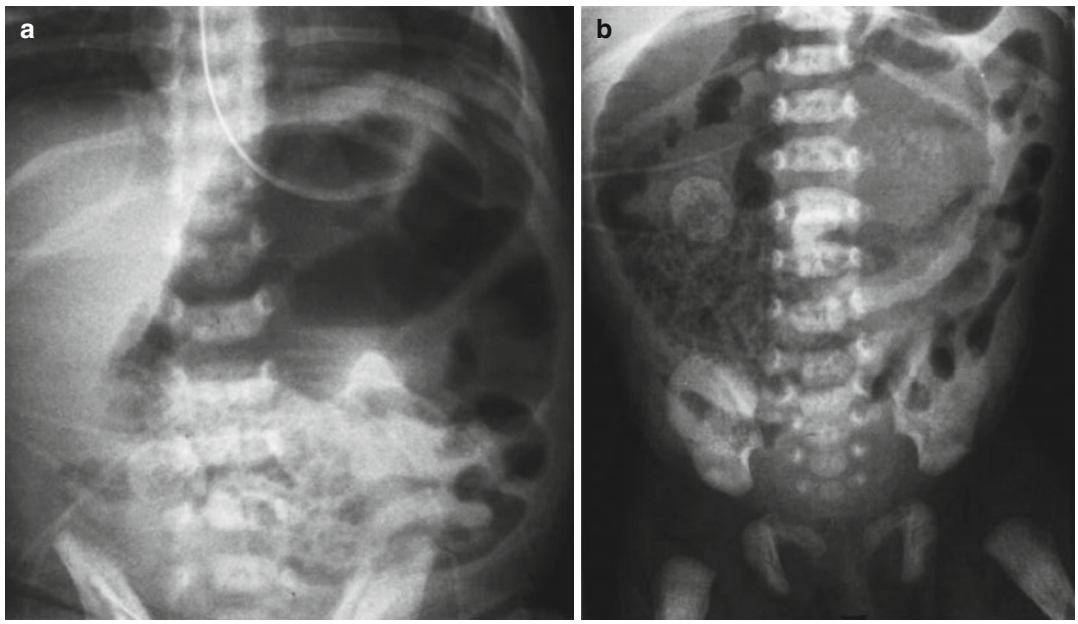


**Fig. 12** (**a**, **b**) Stress ulcer disease: supine radiographs reveal free air due to duodenal ulcer

## 4.3 Gastritis

### 4.3.1 Infectious Gastritis

*H. pylori* is a gram-negative bacterium with the ability to colonize gastric mucosa leading to chronic gastritis and peptic ulcer disease (see Sect. 4.2). Children rarely have symptoms; only a small minority will develop GI symptoms such as epigastric pain, nausea, vomiting, and diarrhea that are associated with *H. pylori*. Symptoms are often related to peptic ulcer disease (Iwańczak and Francavailla 2014; Dore et al. 2012).

On barium studies, the most frequent radiological finding is the presence of thickened gastric folds (Fig. 13). AIDS patients can develop infectious gastritis; the most common pathogens include cytomegalovirus (CMV), *Toxoplasma gondii*, and *Cryptosporidium*.

### 4.3.2 Caustic Ingestion with Chemical Gastritis

Ingestion of caustic agents may lead to severe damage of the gastrointestinal tract. The esophagus is the more common site of injury, but the stomach and duodenum may also be involved (Schlesinger and Parker 2004). Chemical esophagitis and/or gastritis can be caused by a variety of substances; strong alkaline agents (e.g., concentrated sodium hydroxide) typically affect the esophagus, while strong acid agents affect the stomach (e.g., calcium chloride, zinc chloride, iron sulfate tablets, and acids). An overlap certainly exists where acids can cause esophagitis and vice versa. Chemical gastritis can vary from mild antral gastritis to extensive necrosis of the stomach which can be lethal. Patients present with abdominal pain, vomiting, hematemesis, fever, and shock.

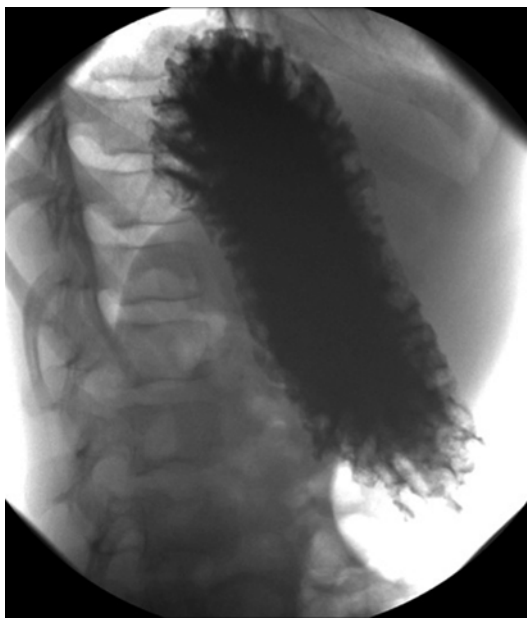

**Fig. 13** Lateral view from an upper GI barium study demonstrating marked thickening of the stomach mucosal folds

Contrast studies can be done for the evaluation of chemical gastritis. Imaging findings depend on the time interval between the acute ingestion and the contrast study. During the acute necrotic phase (1–4 days after the event), contrast studies should be performed with caution. Free air should be excluded before the start of the study. If perforation is suspected, barium is contraindicated and low osmolar nonionic contrast agents should be used instead. Thickened mucosal folds can be seen due to severe edema, ulceration, gastric atony, or mural defects. Intramural air can be sometimes seen in the stomach of patients with severe gastric necrosis; this can be due to either mechanical disruption of the gastric wall or to infection by air-forming organisms. In the former case, contrast leakage may be seen, almost always confined. Free leakage in the peritoneal cavity is rare.

At 5–28 days after the caustic ingestion, an ulceration-granulation phase takes place. By 3–4 weeks this is followed by scarring. Chemical gastritis can resolve with minor sequelae, or it can heal with gastric wall calcifications and cicatricial constrictions (Schlesinger and Parker 2004). In this phase, barium can be used as a contrast agent (Fig. 14). Typically, the scarring will take place in the antrum or body of the stomach since caustic agents tend to flow down the lesser curvature of the stomach into the antrum, causing severe pylorospasm delaying gastric emptying. Therefore, the duodenum may be unaffected. In other patients, however, severe duodenal injury may have occurred and can be seen as thickened folds, spasm, atony, and ulceration leading to

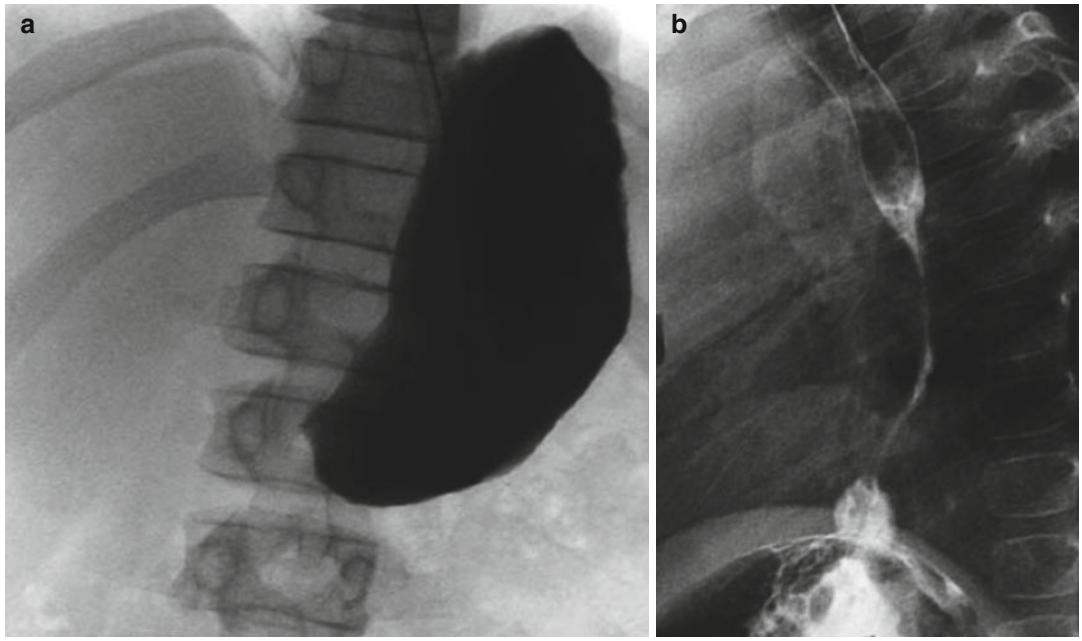


**Fig. 14** Caustic ingestion. (**a**) Gastric outlet obstruction post-ingestion of gasoline in a 9-year-old. (**b**) Esophageal stricture after alkaline ingestion in a 2-year-old

scarring, fibrosis, and strictures. Almost all of these patients will have associated gastric injury. Patients with chemical gastritis and/or duodenitis typically develop a gastric outlet obstruction after 3–4 weeks due to the scarring and stricture formation.

### 4.3.3 Ménétrier Disease

Ménétrier disease (MD) is a rare disorder in children, and the clinical course is different from adults. It is typically a self-limiting condition lasting few weeks usually requiring supportive care. Neonates, however, have a poor prognosis, with a mortality rate as high as 83 % (Konstantinidou et al. 2004). The etiology of Ménétrier disease remains uncertain. There are attributed triggering factors as causative agents like infection (*H. pylori* and CMV), allergy, and medications (prostaglandin $E_1$) (Park et al. 2013; Sferra et al. 1996; Kovacs et al. 1993; Eisenstat et al. 1995).

Children present with abdominal pain, nausea, and vomiting. Peripheral edema, ascites, and pleural effusions are commonly associated with MD due to an associated protein-losing enteropathy.

On UGI, markedly enlarged rugal folds are typically seen at the gastric fundus, along the greater curvature and the gastric body with sparing of the antral region (Fig. 15). US can also demonstrate the rugal hypertrophy with thickening of the mucosa. When the stomach is completely filled, these thickened folds collapse. CT can confirm these findings.

### 4.3.4 Eosinophilic Gastritis

Eosinophilic gastritis (EG) is rare. It is due to eosinophilic infiltration limited to the stomach, without known etiology for eosinophilia, such as drug reactions, parasitic infestation, IBD, and tumors. Peripheral eosinophilia can be normal – up to 50 % of children with EG have a normal peripheral eosinophilic count. EG can be part of diffuse involvement of the GI tract (Huaibin et al. 2013). A history of allergy can be obtained in half of patients. If patients only have eosinophilic gastritis, they present with epigastric pain, nausea, vomiting, hematemesis, and/or melena. Patients with eosinophilic enteritis will have diarrhea, malabsorption, or a protein-losing enteropathy.

On barium studies a strikingly nodular pattern in the gastric antrum can be seen with relative sparing of the body and fundus (Teele et al. 1979) (Fig. 16). Hummer-Ehret et al. (1998) reported

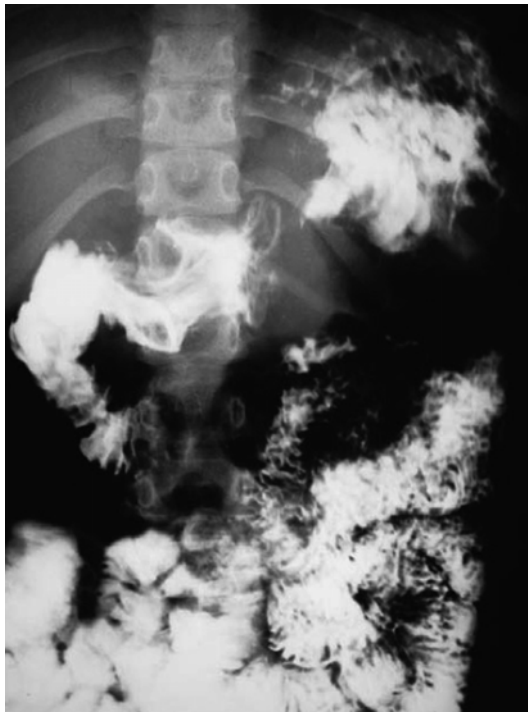

**Fig. 15** Ménétrier's disease: Thickened gastric rugae with no detectable peristalsis in an 8-year-old boy

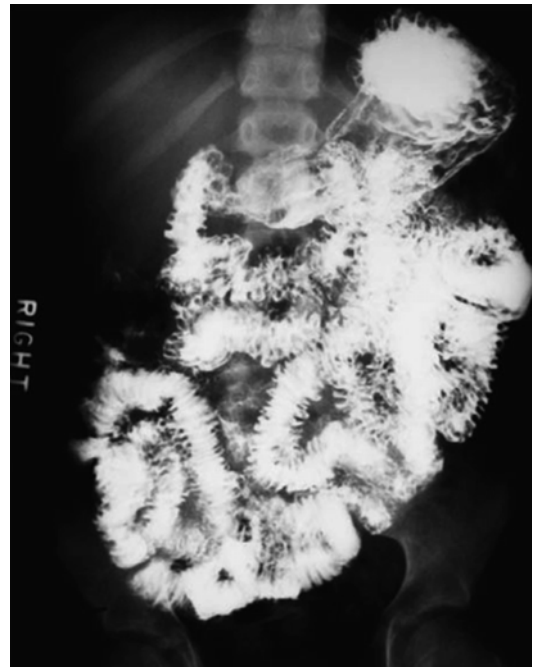


**Fig. 16** Eosinophilic gastritis: thickened mucosal folds and a suggestion of nodularity in a patient with diarrhea and eosinophilia

that eosinophilic gastroenteritis could mimic hypertrophic pyloric stenosis on US.

### 4.3.5 Chronic Granulomatous Disease of Childhood (CGDC)

Chronic granulomatous disease results from an inability of phagocytic cells to produce bactericidal superoxide anions caused by a defect in the nicotinamide adenine dinucleotide phosphate (reduced form) oxidase enzyme of phagocytes. This leads to recurrent life-threatening bacterial and fungal infections. About two thirds of patients inherit this condition through an X-linked defect, while one third inherit this disease in an autosomal recessive fashion. Over 75 % of patients present during the first 5 years of life. The most commonly involved organs are those that serve as barriers against the entry of microorganisms from the environment (e.g., lymph nodes, lungs, skin, GI tract, skeleton, upper respiratory tract, and central nervous system) (Movahedi et al. 2004; Garcia-Eulate et al. 2006).

Patients with GI tract involvement present with abdominal pain (periumbilical or diffuse), lower abdominal cramping, diarrhea (with or without blood in the stool), nausea and vomiting, constipation, growth delay, or hypoalbuminemia (Marciano et al. 2004).

A contrast study (Fig. 17a, b) will demonstrate narrowing of the antropyloric region (occurring in up to 16 % of patients) (Griscom et al. 1974) secondary to chronic inflammation and fibrosis, which can eventually lead to gastric outlet obstruction. In some cases, the proximal duodenum or even the esophagus will also be involved. US may also reveal thickening of the antropyloric wall, simulating HPS. Most patients, however, will be older than the typical HPS patient (Fig. 18).

### 4.3.6 Crohn Disease

Crohn disease (CD) is a chronic inflammatory disorder that may involve any part of the gastrointestinal tract. The exact etiology of CD is not clear; however, genetic, smoking, and environ-

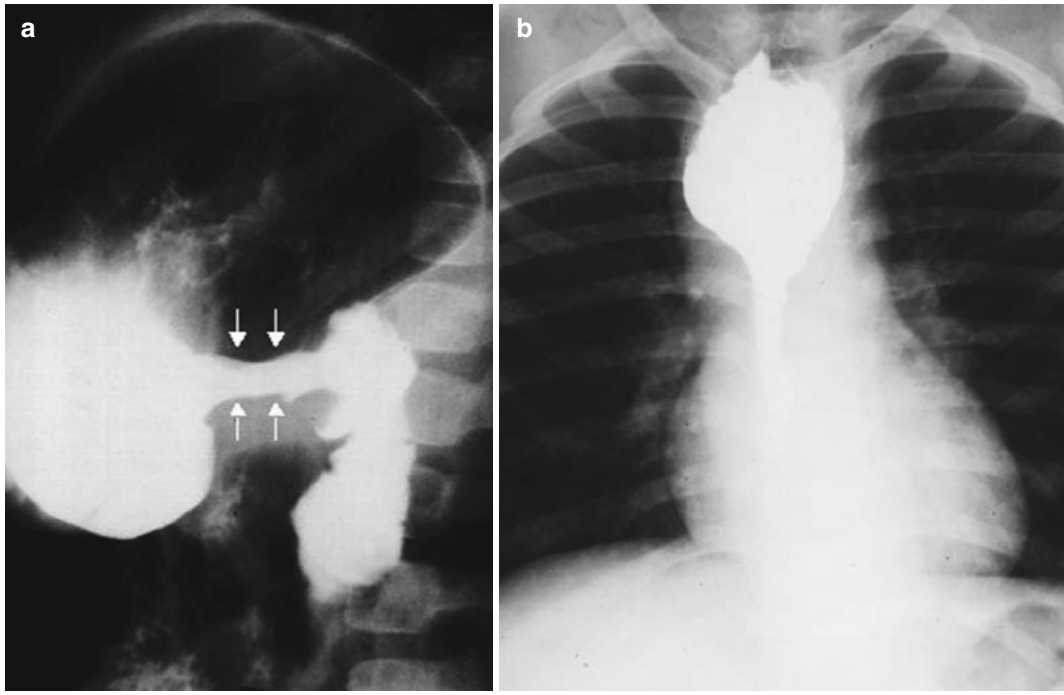


**Fig. 17** Chronic granulomatous disease of childhood (CGDC) involving the stomach in a 7-year-old girl. (**a**) Severe antral narrowing (*arrows*). (**b**) Mid-esophageal stenosis caused by enlarged mediastinal lymph nodes

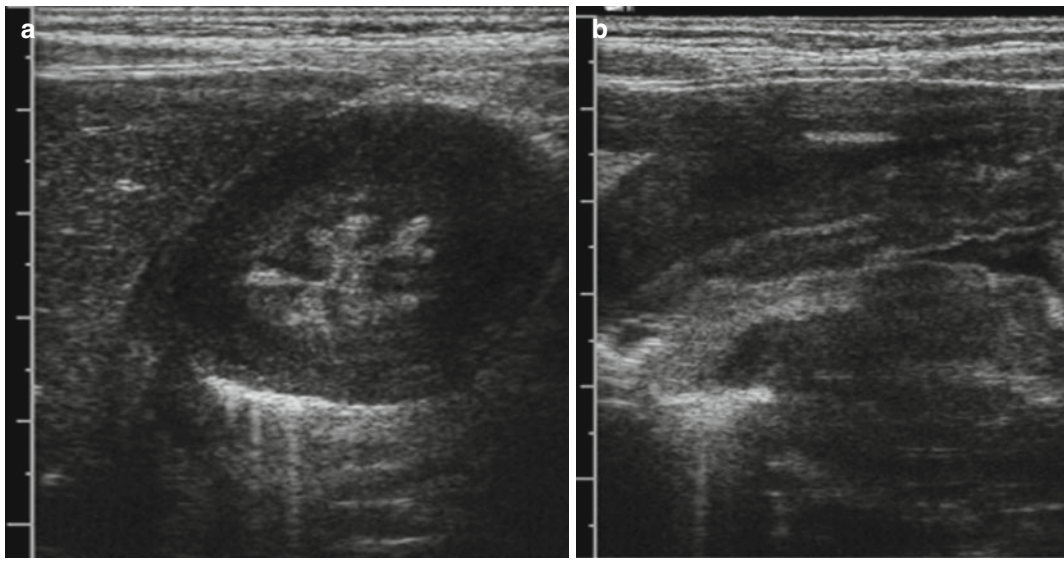


**Fig. 18** Chronic granulomatous disease of childhood on ultrasound. (**a**) Transverse and (**b**) longitudinal images of the pylorus demonstrating pyloric hypertrophy and luminal narrowing resembling the appearances of hypertrophic pyloric stenosis

mental causes are important factors that are likely to play some role. CD of the upper GI tract is more common than previously thought. Several studies confirm this (Lenaerts et al. 1989; Cameron 1991; Mashako et al. 1989; Ruuska et al. 1994; Oberhuber et al. 1998). In children with CD, the overall incidence of the upper GI tract involvement is 36 %. The most frequent location of CD is the terminal ileum and colon. More than 80 % of CD patients are diagnosed before the age of 40 years (Freeman 2014).

Upper gastrointestinal tract involvement may be asymptomatic, and the presentation can be from distal ileocolic CD (crampy abdominal pain, diarrhea). Alternatively patients can present with weight loss, epigastric pain, recurrent vomiting or hematemesis, and melena (Griffiths et al. 1989).

In the detection of CD of the upper GI tract, double-contrast studies are classically used to detect the aphthae (a punctate collection of barium surrounded by a radiolucent halo of edema), which are typical for onset of the disease. Other findings include larger ulcers, thickened folds, distorted, effaced, or rarely cobblestoned mucosa, fistula, sinus tracts, and the formation of pseudodiverticula (Fig. 19). Progressive antral narrowing will develop over the course of time due to scarring and fibrosis of the antrum, pylorus, or duodenum. Contrast studies can also be replaced by upper intestinal endoscopy and with MR enterography (Godefroy et al. 2005; Castellaneta et al. 2004). US is also used to follow CD in the terminal ileum and colon (Bremner et al. 2006).

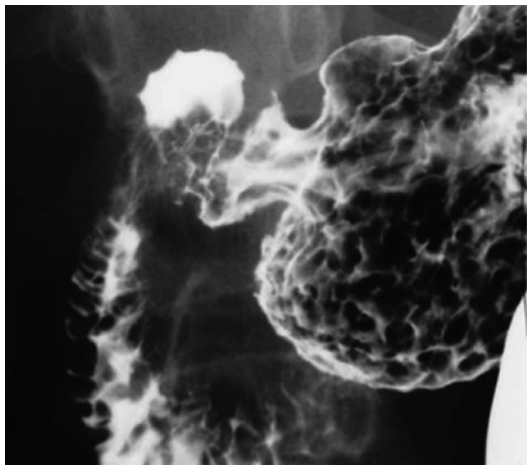

**Fig. 19** Spot image from upper GI study – gastritis and duodenitis in an 8-year-old child subsequently diagnosed with Crohn disease

## 4.4 Gastric Perforation

Gastric rupture is mainly seen in neonates due to acute distention of the stomach, ischemic necrosis associated with perinatal asphyxia, and distal obstruction such as annular pancreas or duodenal atresia/stenosis (Ibach and Inouye 1965). On the other hand, duodenal rupture in neonates is rare.

In the pediatric population, gastric perforation beyond infancy is also a rare occurrence. It can be seen in cases of iatrogenic trauma (tubes and catheters), after Nissen or other fundoplications, in patients with distal small bowel instruction, after caustic ingestion, or in patients with blunt trauma to a distended stomach. Gastric rupture can also be seen in patients with perforated peptic ulcer and dermatomyositis, although duodenal rupture is seen more frequently.

Abdominal X-ray will reveal free intraperitoneal air on upright or decubitus films (Fig. 20) – no gastric air-fluid level can be demonstrated.

## 4.5 Bezoar

Bezoar result from ingested indigestible materials that accumulate within the GI tract, most commonly the stomach. They are classified according to the composition of the ingested material: lactobezoar consisting of milk products, trichobezoar consisting of hair (Rapunzel syndrome), and phytobezoar consisting of fruit and vegetable fibers. Pharmacobezoar consists of long-acting medications. A trichobezoar is commonly seen in young females, and sometimes an

underlying psychiatric illness can be associated. Presenting symptoms may include nausea, emesis, epigastric pain, and an epigastric mass.

Ulceration, bleeding, obstruction, and perforation are the most common complications of bezoars (Sinzig et al. 1998); an intussusception may also be seen (Ben Cheikh et al. 2004).

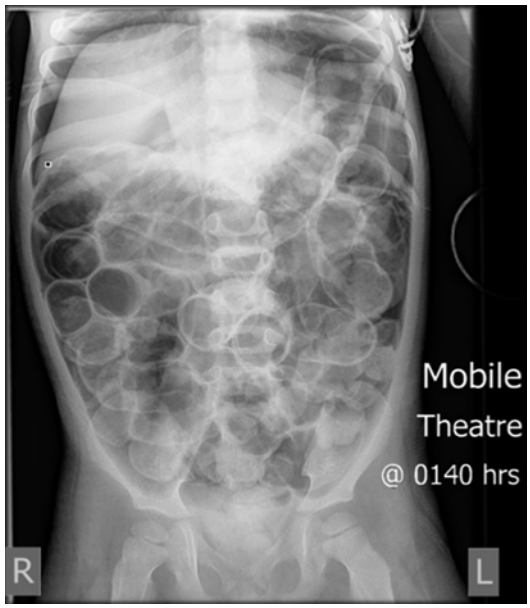


**Fig. 20** Plain radiograph demonstrating significant intraperitoneal air from a gastric perforation

Upper GI studies were the gold standard for the diagnosis of gastric bezoar in the past. This has now been replaced by other modalities mainly cross-sectional imaging – US, CT, and/or MR (Sinzig et al. 1998; Ben Cheikh et al. 2004; Ripollés et al. 2001) (Fig. 21).

On abdominal radiographs, a bezoar can be recognized as an area with a mottled air appearance similar to a food-filled stomach. This can be mistaken for an abdominal abscess or for feces in the colon (Ripollés et al. 2001). On US an intraluminal mass with a hyperechoic arc-like surface and a marked acoustic shadow can be detected. This must be differentiated from retained food products in the stomach. Small gastric bezoars are rounded or ovoid, tend to float, and have lower density than food particles on CT. Large gastric bezoars fill the gastric lumen and will demonstrate multiple small air bubbles throughout the mass on CT. On MR a gastric bezoar is characterized by very low signal intensity, similar to air, on T1- and T2-weighted sequences, which makes the diagnosis difficult to make on this modality. In most cases, giving water prior to the examination, in order to enhance contrast in the stomach contents, is not necessary (Ripollés et al. 2001).

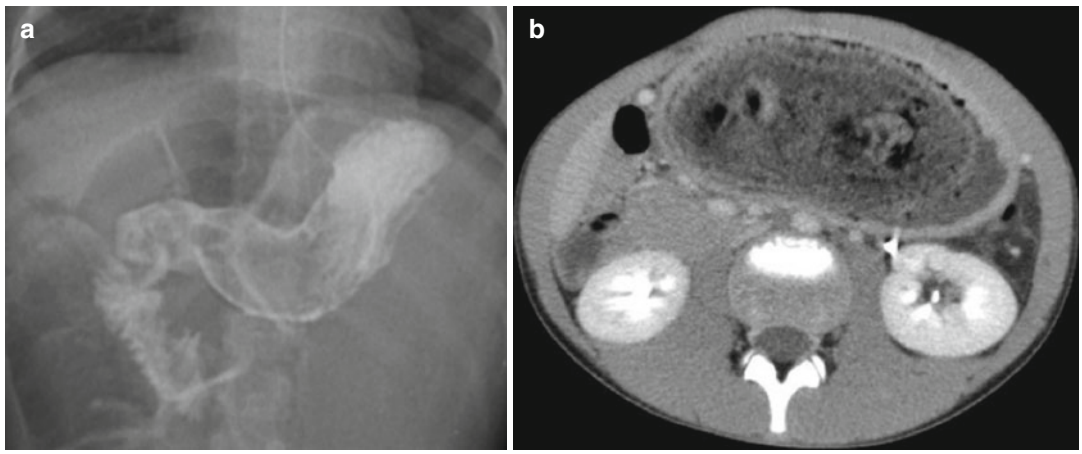


**Fig. 21** (**a**) Contrast study of the stomach showing a large intraluminal filling defect surgically confirmed to be a trichobezoar. (**b**) Axial CT scan of the abdomen at the level of the stomach shows a large low attenuated area with multiple layers of loculated air confirming the diagnosis

In the assessment of a gastric bezoar, it is important to evaluate the extent of the disease, as some patients will have multiple other bezoars in more distal intestinal locations.

## 4.6 Foreign Body Ingestion

Foreign body ingestion is frequently observed in children between the ages of 6 months and 3 years and almost always accidental. 80–90 % of swallowed foreign bodies will pass without problem. 10–20 % require endoscopic removal. Less than 1 % require surgical removal (Kay and Wyllie 2005). These include open safety pins, objects larger than 6 cm in the stomach (Welch et al. 1986), and button batteries (not because of their size but because of their content). Foreign bodies retained in the stomach or duodenum for more than 1 week also require intervention.

A "mouth-to-anus" image may be needed to find the foreign body in the upper gastrointestinal tract. Ultrasound is very useful for locating and identifying non-radiopaque foreign bodies (Fig. 22a, b).

## 4.7 Tumors and Tumorlike Conditions

### 4.7.1 Gastric Polyps

#### 4.7.1.1 Familial Adenomatous Polyposis Syndrome

Familial adenomatous polyposis (FAPS) is an autosomal dominant condition, caused by the mutation of an abnormal tumor suppressor adenomatous polyposis coli gene (APC) on chromosome 5. This condition includes Gardner syndrome (previously known as familial polyposis coli). FAPS is the most common adenomatous polyposis syndrome in the pediatric population.

Gastric involvement in patients with FAPS is common. Several types of gastric neoplasms, such as fundic gland polyp (65 %), gastric foveolar-type adenoma (23 %), and pyloric gland adenoma (6 %), have been described in the recent literature (Wood et al. 2014).

The fundic gland (hamartomatous) polyps are typically multiple and appear as small, sessile lesions ranging from 1 to 5 mm in size, located in the fundus and body of the stomach (Fig. 23). In general, there is no association

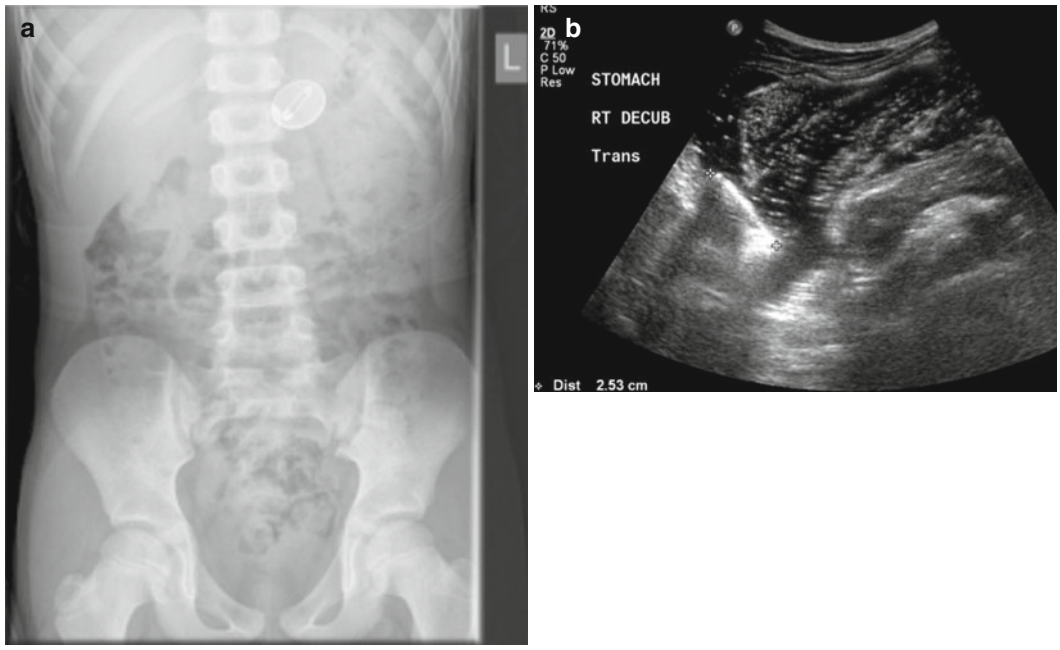


**Fig. 22** (**a**) AP radiograph demonstrating a swallowed "birthday badge" located in the stomach. (**b**) Nonopaque foreign body in the stomach confirmed by ultrasound (between calipers)

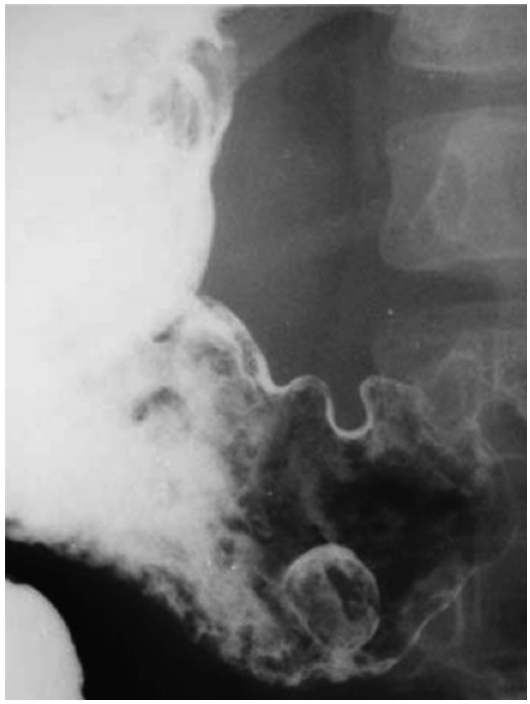

**Fig. 23** Juvenile polyposis: gastric polyps in a patient with peroral mucositis (Courtesy of Dr. Carlo Buonomo, Boston, MA, USA)

with chronic nonspecific gastritis, and these lesions are not precancerous. On the other hand, adenomas are premalignant lesions. The radiographic appearances are similar, but gastric adenomas are typically located in the antrum and are multiple in over half of the cases (Buck and Harned 2000).

#### 4.7.1.2 Hamartomatous Polyposis Syndrome

The hamartomatous syndromes are a heterogeneous group of disorders that have an autosomal dominant inheritance. These are less common than FAP and include Peutz-Jeghers syndrome, multiple hamartoma syndrome (Cowden disease), juvenile polyposis (Fig. 24a), Cronkhite-Canada syndrome, and Bannayan-Riley-Ruvalcaba syndrome.

Juvenile polyposis (JP) is the most common gastrointestinal hamartomatous syndrome. The diagnostic criteria for JP include any of the following: (a) five or more juvenile polyps in the large bowel, (b) juvenile polyps throughout the gastrointestinal tract, and (c) any number of juvenile polyps and one or more affected member of the family (Kevin et al. 2007).

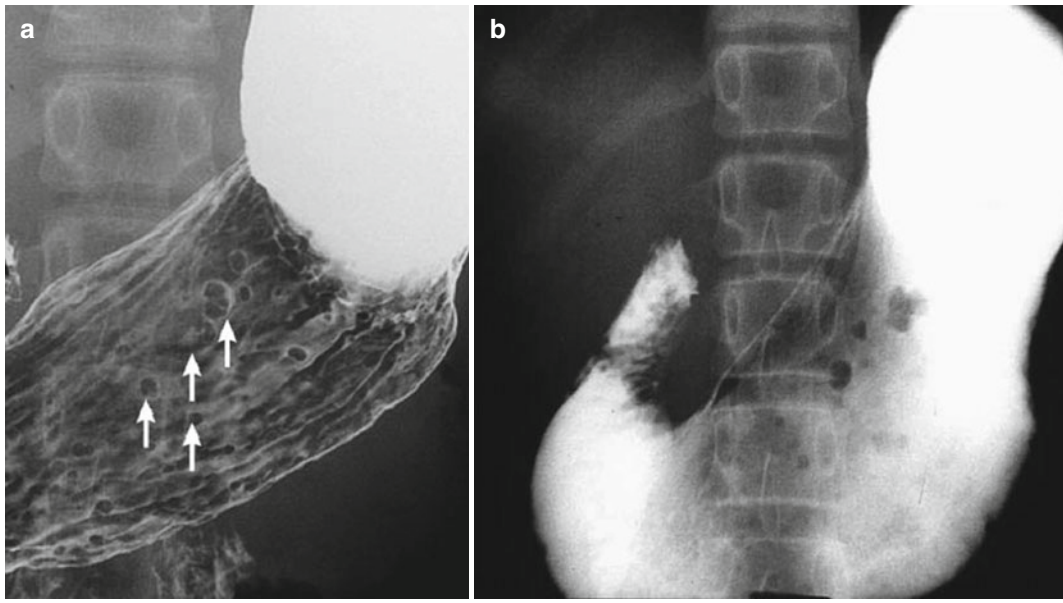


**Fig. 24** Polyposis syndromes: (**a**) Multiple polyps (*arrows*) in Peutz-Jeghers syndrome with malignant degeneration (adenocarcinoma). (**b**) This 12-year-old had a giant osteoma in the left frontal sinus: Gardner syndrome

Patients with Peutz-Jeghers syndrome have a unique type of gastrointestinal hamartoma, which can be found throughout the alimentary tract from the stomach to the rectum, most commonly in the jejunum and ileum (followed by duodenum, colon, and stomach). The polyps vary in size, tend to occur in clusters, may be sessile or pedunculated, and have a lobulated surface (larger lesions).

The common presenting symptom in patients with polyposis is rectal bleeding. Other presenting symptoms include abdominal pain, intussusception, diarrhea, and extraintestinal features such as anemia and hyperpigmentation. Patients are at increased risk of developing adenocarcinoma of the gastrointestinal tract. Increased risk of breast and gynecological malignancy also occurs (Kevin et al. 2007).

#### 4.7.1.3 Other Gastric Polyps

Gastric polyps and nodules can be seen in children receiving long-term omeprazole therapy. Pashankar and Israel (2002) suggested in their study of 31 pediatric patients that there is an association rather than a coincidental relationship between these two entities.

Other gastric polyps in children include the inflammatory fibroid polyp, solitary hyperplastic polyp, and polypoid focal foveolar hyperplasia (Teele and Share 2000).

### 4.7.2 Gastric Lymphoma

GI tumors represent no more than 5 % of all malignancies in children (Sasaki et al. 1999). GI malignancy in children is most frequently a lymphoma or sarcoma (Kurugoglu et al. 2002).

The primary extranodal non-Hodgkin's lymphoma applies to lymphoma arising from organ or tissue other than the lymph node, spleen, or bone marrow. The gastrointestinal tract is commonly involved and accounts for more than the one third of all non-Hodgkin's lymphoma. The stomach is the most common site for extranodal NHL of GI tract and represents more than 60 % of all cases (Zucca 2008; Psyrri et al. 2008).

Almost all gastric lymphomas (Figs. 25, 26a, b, and 27) are B-cell origin. These include extranodal marginal zone B-cell lymphoma (ENMZL) (previously known as marginal zone mucosa-associated lymphoid tissue – MALT) (Zullo et al. 2014) and diffuse large B-cell lymphoma (DLBL). T-cell gastric lymphoma is extremely rare. ENMZL is a low-grade B-cell lymphoma that is mainly found in the stomach and strongly associated with *H. pylori* infection (Lewis et al. 2014). Primary Burkitt lymphoma of the stomach is very rare (Moschovi et al. 2003).

Patients present with nonspecific signs and symptoms. On US hypoechoic thickening of the gastric wall or a mural mass can be seen. The presence or absence of adenopathy can also be evaluated. CT is used in the initial staging and is able to evaluate the extension of the primary tumor with or without invasion of adjacent structures as well as the coexistence of enlarged lymph nodes. On barium studies, mucosal nodularity, rugal thickening, shallow and/or deep ulceration(s), mass formation, or diffusely enlarged areae gastricae are seen either in isolation or as a combination of radiological signs.

### 4.7.3 Gastric Gastrointestinal Stromal Tumor

Gastrointestinal stromal tumors (GIST) are tumors of mesenchymal origin first recognized by Mazur and Clark in 1983. This newer tumor entity has characteristic histopathological features distinguishing it from what was previously known as leiomyoma and leiomyosarcoma by the presence of platelet-derived growth factor receptor alpha (PDGFRA) or KIT mutation proto-oncogene (Pappo et al. 2009). It originates from the interstitial cells of Cajal in the gastrointestinal stroma.

GIST neoplasm is very uncommon in children and exceedingly rare in newborns and neonates (Kurucu et al. 2014). They only represent 1.5–2.5 % of all non-rhabdomyosarcoma soft tissue sarcomas (Pappo et al. 2004). GIST are more common in girls. The stomach is the most commonly affected site, typically there is multifocal

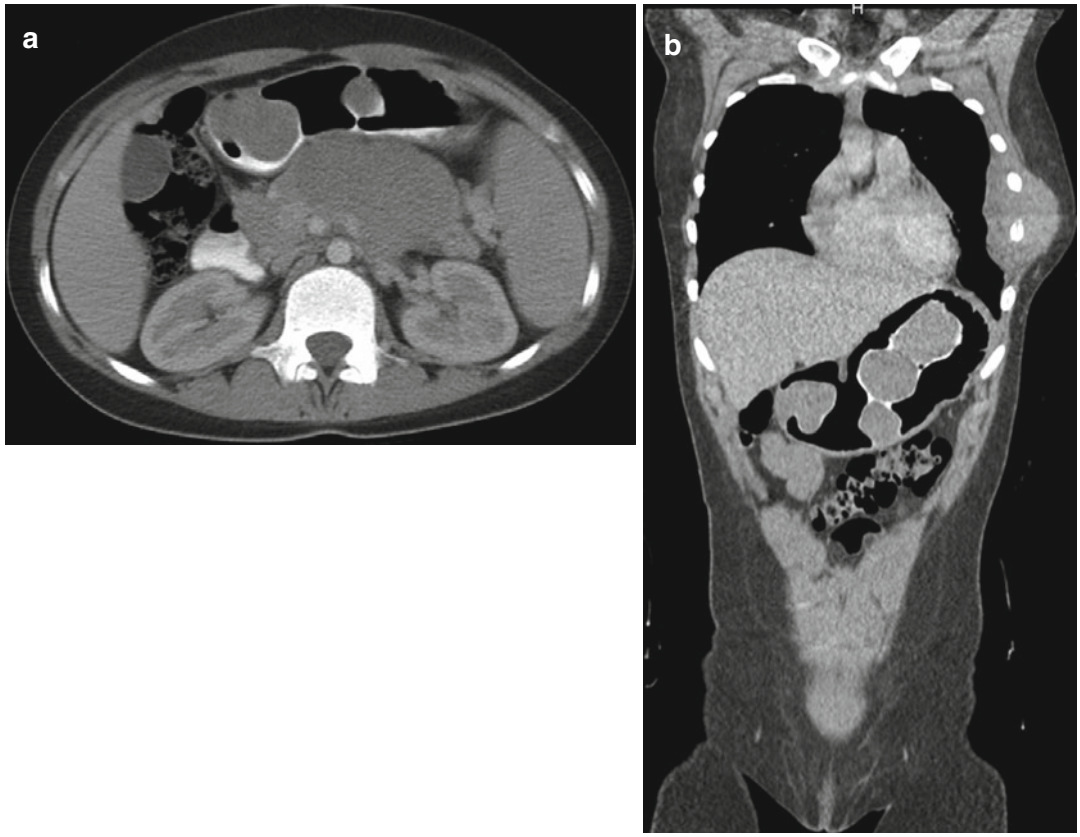


**Fig. 25** Contrast-enhanced axial (**a**) and coronal (**b**) CT scan of the abdomen demonstrating multiple gastric lesions with extensive retroperitoneal involvement

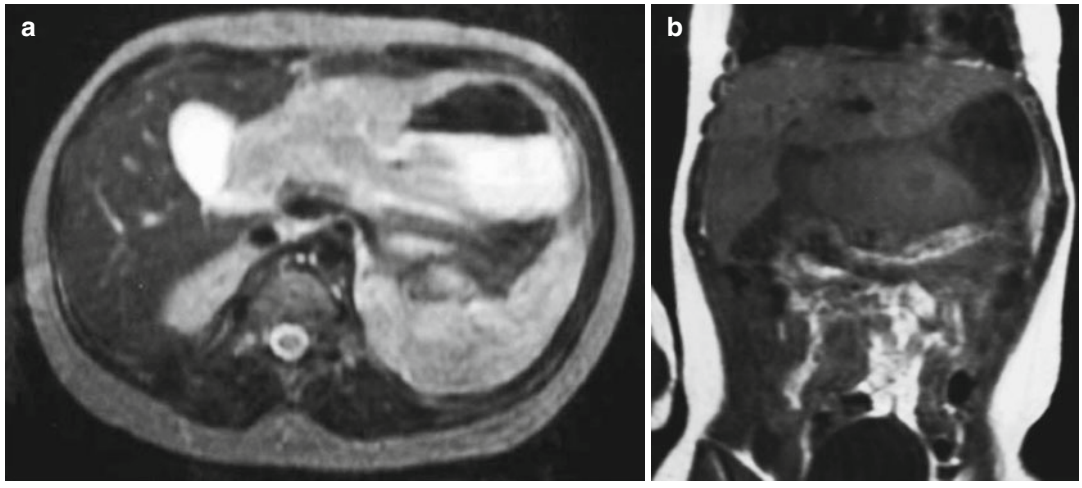


**Fig. 26** MRI of the abdomen in a 6-year-old with gastric lymphoma. (**a**) Axial T2 MRI and (**b**) coronal T1 of the abdomen demonstrating a predominantly antral lesion (Courtesy of Dr. Carlo Buonomo, Boston, MA, USA)

involvement. The affected children often present with anemia due to chronic insidious GI blood loss. Other symptoms such as abdominal pain and GI obstruction are uncommon (Pappo et al. 2011).

On imaging studies these tumors demonstrate well-defined solid or partially cystic masses; sometimes hemorrhage, necrosis, or calcification (extensive or in a mottled pattern) can be seen. Mucosal alteration, intracavitary air-fluid levels, and fistulas to the alimentary tract have been described (Figs. 27 and 28a–c).

### 4.7.4 Gastric Adenocarcinoma

Primary gastric adenocarcinoma is extremely rare in children; it represents only 0.05 % of all malignant pediatric gastrointestinal tumors (Sasaki et al. 1999). There are three different forms of presentation in the pediatric population: de novo, as part of a polyposis syndrome (e.g., Peutz-Jeghers syndrome, outlined above), and following treatment of a gastric lymphoma (Dokucu et al. 2002).

Imaging features on an UGI series may include loss of distensibility, distortion of the normal surface pattern of the stomach, thickened irregular folds, mucosal nodularity, irregular narrowing, and ulceration (the malignant ulcer is located intraluminally in contrast to a benign ulcer which is located beyond the expected border of the stomach) (Fig. 24).

Cross-sectional imaging will be used for staging purposes, to assess for lymphadenopathy and invasion of adjacent organs.

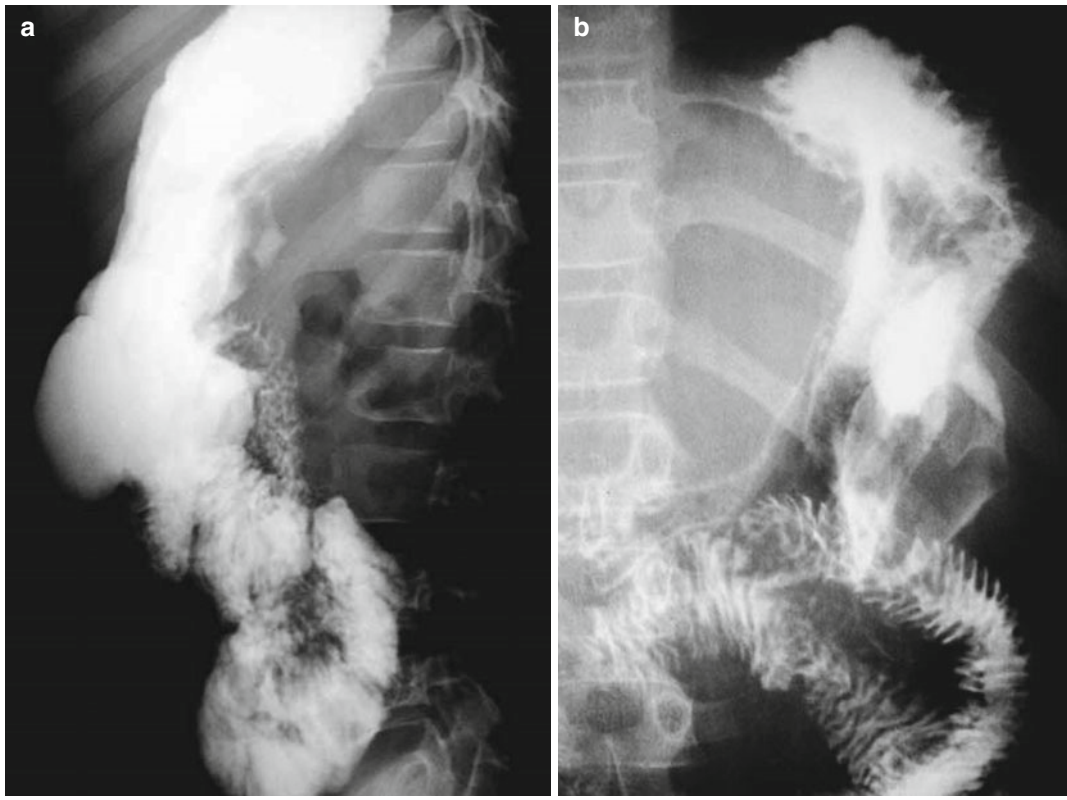


**Fig. 27** Upper GI study in a 12-year-old boy (**a**) lateral and (**b**) AP views demonstrating irregular mural thickening from B-cell lymphoma of the stomach

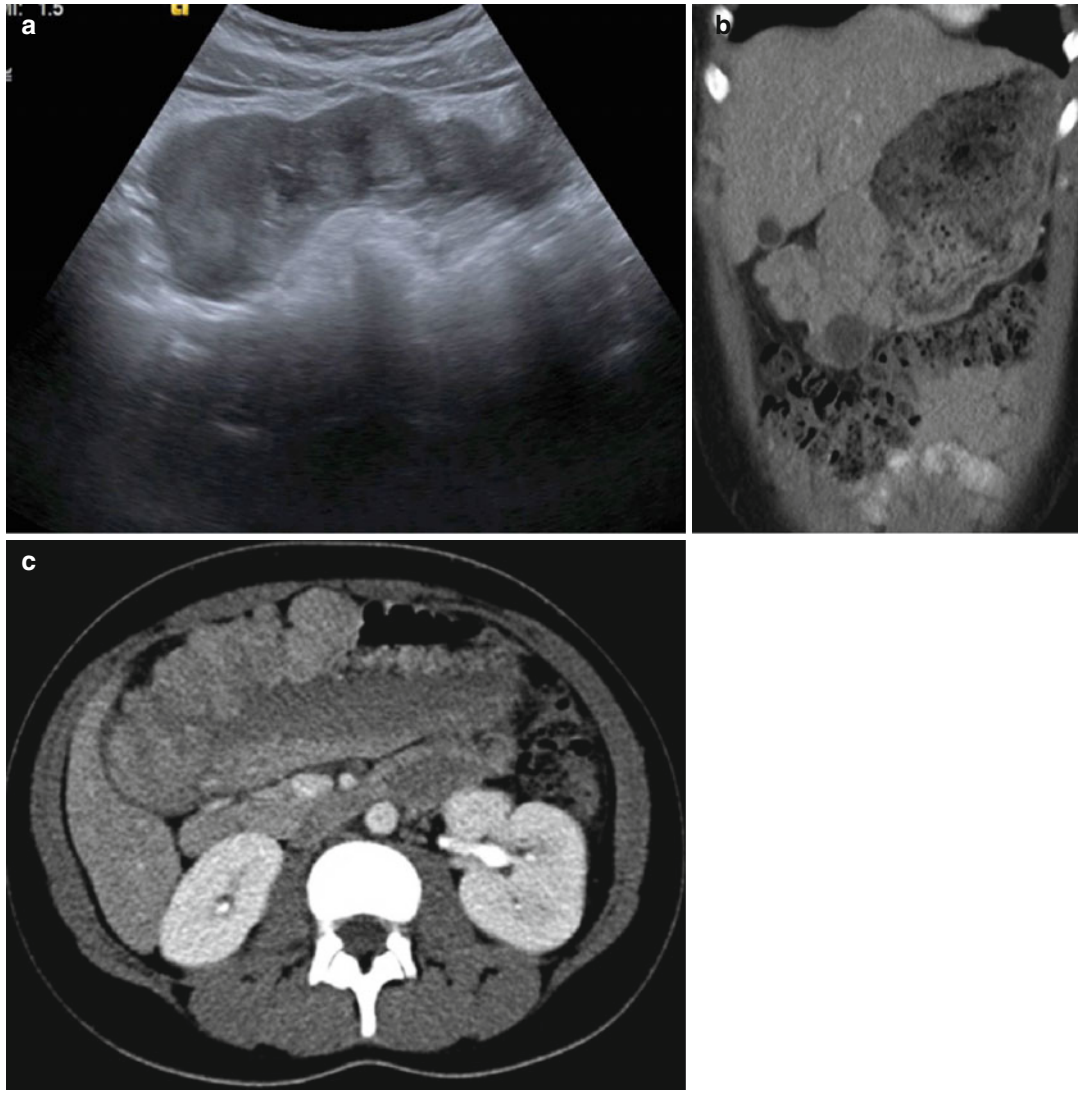


**Fig. 28** (**a**) Transverse ultrasound image of the upper abdomen in an 8-year-old girl shows a large mass in the epigastrium. (**b**, **c**) Axial and coronal contrast-enhanced CT of the abdomen confirms the gastric origin of the Gastrointestinal Stromal Tumor (GIST)

### 4.7.5 Gastric Teratoma

Gastric teratoma is an extremely rare tumor, comprising less than 1 % of all teratomas in children (Chandrasekharam et al. 2000; Kharga et al. 2014). Only 100 cases have been reported in the literature. Teratomas typically occur in infancy most commonly in boys. Patients present with an upper abdominal mass with evidence of proximal GI obstruction or GI hemorrhage. The treatment of choice is local resection. Gastric teratoma has an excellent prognosis (Wakhlu and Wakhlu 2002).

Radiographs may reveal the mass lesion displacing the stomach, and the mass may show calcifications. US, CT, and MR are helpful for characterization of these tumors. The majority of these tumors have mature components of endoderm, ectoderm, and mesoderm.

### 4.7.6 Gastric Inflammatory Pseudotumor

This entity can simulate a malignant tumor on radiographic studies and should be considered in children with other unusual problems such as retroperitoneal fibrosis, sclerosing cholangitis, and sclerosing peritonitis or in patients with Castleman's syndrome. It should be included in the differential diagnosis when a gastric mass contains an ulcer or where a confined perforation is seen.

## 4.8 Varices

Patients with portal hypertension will develop collateral pathways over time. Esophageal varices are very common, but gastric varices are also observed (Schlesinger and Parker 2004; Itha and Yachha 2006).

Barium studies reveal compressible serpentine filling defects, typically in the fundus and along the lesser curvature or less commonly in the antrum of the stomach or proximal duodenum. CT, MRI and US can demonstrate the different collaterals.

## 4.9 Gastrostomy

Percutaneous gastrostomy is a well-accepted, widely performed procedure in three main groups of patients. The first group includes children with anatomic disorders of the proximal upper GI tract, in which normal feeding is not possible. The second group consists of neurologically impaired children in whom normal swallowing is not possible or safe. The third group consists of patients who need more nutrition than normal feeding allows.

Imaging may be performed if a complication is suspected, such as duodenal obstruction by the balloon, leakage around the gastrostomy tube, malposition of the gastrostomy tube (Fig. 29), gastrocolic and gastrojejunal fistula, and duodenal hematoma. In most cases, water-soluble contrast agents or nonionic low osmolar contrast agents are used. Barium should not be used or used with caution (van Rijn et al. 2006).

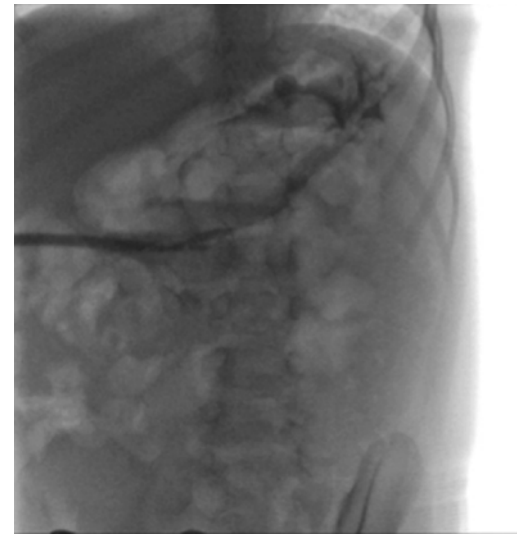

**Fig. 29** Single water-soluble contrast study through a gastrostomy tube demonstrating a misplaced gastrostomy catheter, with contrast agent spillage into the peritoneal cavity

## 4.10 Postoperative Appearances of the Stomach

One of the most commonly performed procedures on the stomach in children is pyloromyotomy for HPS. Postoperative UGI findings will depend on the time interval between the surgical procedure and the examination. In the immediate postoperative setting, the radiographic findings will tend to be the same as those preoperatively as discussed above. Gradually this will change over time with the persistence of asymmetry of the pyloric channel. After 6 weeks, in the majority of children, the pyloric channel appears normal again, although some patients will continue to have a degree of antropyloric dysfunction (may occasionally lead to the retention of foreign bodies) (Bramson et al. 1994).

Another frequently performed surgical procedure in the pediatric population is anti-reflux surgery or the Nissen fundoplication. Postoperative imaging is focused on demonstrating normal

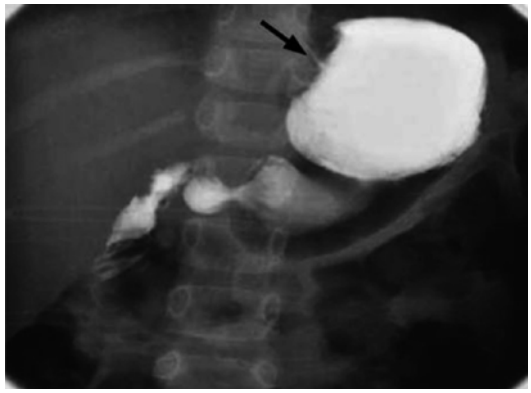

**Fig. 30** Typical indented appearance of a Nissen fundoplication at the neogastroesophageal junction (*arrow*)

antegrade flow and the surgically related cuff or "pseudotumor" (Fig. 30). Slippage leads to recurrence of gastroesophageal reflux.

## References


Asplund G, Langer JC (2007) Current management of hypertrophic pyloric stenosis. Semin Pediatric Surg 16:27–33

Anagnostara A, Koumanidou C, Vakaki M et al (2003) Chronic gastric volvulus and hypertrophic pyloric stenosis in an infant. J Clin Ultrasound 31:383–386

Ben Cheikh A, Gorincour G, Dugougeat-Pilleul F, Duipuis S, Basset T, Pracros JP (2004) Trichobézoard gastrique révélé par une anémie chez une adolescente: association échograpie-imagerie par résonance magnétique (IRM). J Radiol 85:411–413

Berrocal T, Lamas M, Gutieerrez J, Torres I, Prieto C, del Hoyo ML (1999) Congenital anomalies of the small intestine, colon and rectum. Radiographics 19:1219–1236

Bittencourt PF, Rocha GA, Penna FJ, Queiroz DM (2006) Gastroduodenal peptic ulcer and Helicobacter pylori infection in children and adolescents. J Pediatr (Rio J) 82:325–334

Blank E, Chisholm AJ (1973) Congenital microgastria; a case report with a 26-year follow-up. Pediatrics 51:1037–1041

Bourke B (2005) Will treatment of Helicobacter pylori infection in childhood alter the risk of developing gastric cancer? Can J Gastroenterol 19:409–411

Bramson RT, Buonomo C, Blickman JG (1994) Barium extravasation discovered some years after pyloromyotomy. Pediatr Radiol 24:216–217

Bremner AR, Griffiths M, Argent JD et al (2006) Sonographic evaluation of inflammatory bowel disease: a prospective, blinded, comparative study. Pediatr Radiol 36:947–953

Buck JL, Harned KH (2000) Polyposis syndromes. In: Textbook of gastrointestinal radiology, 2nd edn. WB Saunders Company, Philadelphia, pp 1075–1088

Buonomo C, Taylor GA, Share JC, Kirks DR (1998) Specific abnormalities of the abdomen. In: Kirks DR, Griscom NT (eds) Practical pediatric imaging: diagnostic radiology of infants and children, 3rd edn. Lippincott-Raven, Philadelphia, pp 838–953

Cameron DJ (1991) Upper and lower gastrointestinal endoscopy in children and adolescents with Crohn's disease: a prospective study. J Gastroenterol Hepatol 6:355–358

Castellaneta SP, Afzal NA, Greenberg M et al (2004) Diagnostic role of upper gastrointestinal endoscopy in pediatric inflammatory bowel disease. J Pediatr Gastroenterol Nutr 39:257–261

Chandrasekharam VV, Gupta AK, Bhatnagar V (2000) Infantile gastric teratoma. Trop Gastroenterol 21:192–193

Chen CP, Liu YP, Hsu CY, Lin SP, Wang W (2006) Prenatal sonography and magnetic resonance imaging of pulmonary sequestration associated with a gastric duplication cyst. Prenat Diagn 26:483–491

Cheng EH, Pavelong RR (1990) Multiple gastrointestinal tract diverticula. Gastrointest Radiol 15:282–284

Cohen HL, Blumer SL, Zucconi WB (2004) The sonographic double-track sign: not pathognomonic for hypertrophic pyloric stenosis; can be seen in pylorospasm. J Ultrasound Med 23:641–646

Cunniff C, Williamson-Kruse L, Olney AH (1993) Congenital microgastria and limb reduction defects. Pediatrics 91:1192–1194

Dalgaard JB (1952) Volvulus of the stomach. Acta Clin Scand 103:131–136

Darani A, Mendoza-Sagaon M, Reinberg O (2005) Gastric volvulus in children. J Ped Surg 40: 855–858

Dide M (1894) Sur en estomac d'adulte a type foetal. Bull Soc Anat (Paris) 69:669

Dokucu AU, Özturk H, Kilinç N, Önen A, Bukte Y, Soker M (2002) Primary gastric adenocarcinoma in a 2.5-year-old girl. Gastric Cancer 5:237–239

Dore MP, Franciulli G, Tomasi PA et al (2012) Gastrointestinal symptoms and Helicobacter pylori infection in school-age children residing in Porto Torres Sardinia, Italy. Helicobacter 17:369–373

Drumm B, Day AS, Gold B et al (European Society for Paediatric Gastroenterology, Hepatology and Nutrition) (2004) Helicobacter pylori and peptic ulcer: Working Group Report of the second World Congress of Pediatric Gastroenterology, Hepatology, and Nutrition. J Pediatr Gastroenterol Nutr 39(Suppl 2):S626–631

Eisenstat DD, Griffiths AM, Cutz E et al (1995) Acute cytomegalovirus infection in a child with Menetrier's disease. Gastroenterology 109:592–595

Elliot S, Sander AD, Meekan JJ et al (2006) Surgical treatment of a gastric diverticulum in an adolescent. J Ped Surg 41:1467–1469

Farina R, Pennisi F, La Rosa M et al (2008) Contrast-enhanced colour-Doppler sonography versus pH-metry in the diagnosis of gastro-oesophageal reflux in children. Radiol Med 113:591–598

Freeman HF (2014) Natural history and long-term clinical course of Crohn's disease. World J Gastroenterol 20(1):31–36

Garcia-Eulate R, Hussain N, Heller T et al (2006) CT and MRI of hepatic abscess in patients with chronic granulomatous disease. AJR Am J Roentgenol 187:482–490

Giurgea I, Raqbi F, Nihoul-Fekete C et al (2000) Congenital microgastria with Pierre Robin sequence and partial trismus. Clin Dysmorphol 9:307–308

Godefroy C, Pilleul F, Dugougeat F et al (2005) Value of contrast enhanced MR enterography in pediatric Crohn disease. J Radiol 86:1685–1692

Graham DY, Shiotani A (2005) The time to eradicate gastric cancer is now. Gut 54:735–738

Granata C, Dell'Acqua A, Lituania M et al (2003) Gastric duplication cyst: appearance on prenatal US and MRI. Pediatr Radiol 33:148–149

Griscom NT, Kirkpatrick JA Jr, Girdany BR, Berdon WE, Grand RJ, Mackie GG (1974) Gastric antral narrowing in chronic granulomatous disease of childhood. Pediatrics 54:456–460

Griffiths AM, Alemayehu E, Sherman P (1989) Clinical features of gastroduodenal Crohn's disease in adolescents. J Pediatr Gastroenterol Nutr 8:166–171

Gupta AK, Guglani B (2005) Imaging of congenital anomalies of the gastrointestinal tract. Indian J Ped 72:403–414

Hernandez C, Serrano C, Einisman H et al (2014) Peptic ulcer disease in helicobacter pylori–infected children: clinical findings and mucosal immune response. J Pediatr Gastroenterol Nutr 59(6):773–778

Hernanz-Schulman M, Sells LL, Ambrosino MM et al (1994) Hypertrophic pyloric stenosis in the infant without a palpable olive: accuracy of sonographic diagnosis. Radiology 193(3):771–776

Herniaz Driever P, Gohlich Ratmann G, Konig R (1997) Congenital microgastria, growth hormone deficiency and diabetes insipidus. Eur J Pediatr 156:37–40

Hiorns MP (2011) Gastrointestinal tract imaging in children: current techniques. Pediatr Radiol 41:42–54

Hoehner JC, Kimura K, Soper RT (1994) Congenital microgastria. J Pediatr Surg 29:1591–1593

Huaibin M, Morotti RA, Yershov O et al (2013) Eosinophilic gastritis in children: clinicopathological correlation, disease course and response to therapy. Am J Gastroenterol 109:1277–1285

Hummer-Ehret BH, Rohrschneider WK, Oleszczuk-Raschke K et al (1998) Eosinophilic gastroenteritis mimicking hypertrophic pyloric stenosis. Pediatr Radiol 28:711–713

Ibach JR, Inouye WY (1965) Neonatal gastric perforation secondary to annular pancreas. Am J Surg 110:985–987

Iqbal CW, Rivard DC, Mortellaro VE et al (2012) Evaluation of ultrasonographic parameters in the diagnosis of pyloric stenosis relative to patient age and size. J Pediatr Surg 47(8):1542–1547

Itha S, Yachha SK (2006) Endoscopic outcome beyond esophageal variceal eradication in children with extrahepatic portal venous obstruction. J Ped Gastroenterol Nutr 42:196–200

Iwańczak B, Francavailla R (2014) Helicobacter pylori infection in pediatrics. Helicobacter 19(Suppl 1):46–51

Johnston J, Wheatley GH, El Sayed HF, Marsh WB, Ellison EC, Bloomston M (2008) Gastric duplication cysts expressing carcinoembryonic antigen mimicking cystic pancreatic neoplasms in two adults. Am Surg 74:91–94

Kay M, Wyllie R (2005) Pediatric foreign bodies and their management. Curr Gastroenterol Rep 7:212–218

Kevin M Zbuk and Charis Eng (2007) Hamartomatous polyposis syndromes. Nature Clinical Practice Gastroenterology & Hepatology 4(9)

Kharga B, Kumar V, Prabhu PS, Surdeep PT, John SK (2014) Neonatal gastric teratoma: a rare entity. J Clin Diagn Res 8(1):185–186

Konstantinidou AE, Morphopoulos G, Korkolopoulou P et al (2004) Menetrier disease of early infancy: a separate entity? J Pediatr Gastroenterol Nutr 39: 177–182

Konturek PC, Konturek SJ, Brzozowski T (2006) Gastric cancer and Helicobacter pylori infection. J Physiol Pharmacol 57(Suppl 3):51–65

Kovacs AA, Churchill MA, Wood D, Mascola L, Zaia JA (1993) Molecular and epidemiologic evaluations of a cluster of cases of Menetrier's disease associated with cytomegalovirus. Pediatr Infect Dis J 12:1011–1014

Kroes EJ, Festen C (1998) Congenital microgastria: a case report and review of the literature. Pediatr Surg Int 13:416–418

Kumar R, Tripathi M, Chandrashekar N et al (2005) Diagnosis of ectopic gastric mucosa using 99Tc m-pertechnetate: spectrum of scintigraphic findings. Br J Radiol 78:714–720

Kurucu N, Sari N, Celasun B et al (2014) Gastrointestinal stromal tumor in a newborn diagnosed in prenatal period: a case report and review of literature. J Pediatr Hematol Oncol 36(8):649–652

Kurugoglu S, Mihmanli I, Celkan T, Aki H, Aksoy H, Korman U (2002) Radiological features in pediatric primary gastric MALT lymphoma and association with Helicobacter Pylori. Pediatr Radiol 32:82–87

Larsen WJ (2001) Development of the gastrointestinal tract. In: Larsen WJ (ed) Human embryology, 3rd edn. Churchill Livingstone, Philadelphia, pp 235–264

Lenaerts C, Roy CC, Vaillancourt M et al (1989) High incidence of upper gastrointestinal tract involvement in children with Crohn disease. Pediatrics 83: 777–781

Lewis RB, Mehrotra AK, Rodriguez P et al (2014) From the radiology archives: gastrointestinal lymphoma: radiologic and pathologic findings. Radiographics 34(7):1934–1953

Lin CH, Wu SF, Lin WC, Chen AC (2005) Wandering spleen with torsion and gastric volvulus. J Formos Med Assoc 104:755–758

Ma H, Xiao W, Li J et al (2012) Clinical and pathological analysis of malignancies arising from alimentary tract duplication. Surg Oncol 21(4):324–3

Macpherson RI (1993) Gastrointestinal tract duplications: clinical, pathologic, etiologic, and radiologic considerations. Radiographics 13:1063–1080

Marciano BE, Rosenzweig SD, Kleiner DE (2004) Gastrointestinal involvement in chronic granulomatous disease. Pediatrics 114:462–468

Markowitz RI (2014) Olive without a cause: the story of infantile hypertrophic pyloric stenosis. Pediatr Radiol 44:202–211

Mashako MN, Cezard JP, Navarro J et al (1989) Crohn's disease lesions in the upper gastrointestinal tract: correlation between clinical, radiological, endoscopic and histological features in adolescents and children. J Pediatr Gastroenterol 8:442–446

Mazur MT, Clark HB (1983) Gastric stromal tumors. Reappraisal of histogenesis. Am J Surg Pathol 7: 507–519

Menon P, Rao KLN, Cutinha HP et al (2003) Gastric augmentation in isolated congenital microgastria. J Ped Surg 38:4–6

Moore KL, Persaud TVN (2011) The developing human. 6th ed, Suanders, Philadelphia, pp 272–278

Moulton SL, Bouvet M, Lynch FP (1994) Congenital microgastria in a premature infant. J Pediatr Surg 29:1594–1595

Movahedi M, Aghamohammadi A, Rezaei N et al (2004) Chronic granulomatous disease: a clinical survey of 41 patients form the Iranian primary immunodeficiency registry. Int Arch Allergy Immunol 134:253–259

Moschovi M, Menegas D, Stefanaki K, Constantinidou CVV, Tzortzatou-Stathopoulou F (2003) Primary gastric Burkitt lymphoma in childhood: associated with Helicobacter Pylori? Med Pediatr Oncol 41:444–447

Micheal J. Rosen, Ashish Dhawan, Shehzad A Saeed September (2015) Inflamatory Bowel Disease in Children and Adolescents JAMA Pediatrics

Oberhuber G, Hirsch M, Stolte M (1998) High incidence of upper gastrointestinal tract involvement in Crohn's disease. Virchows Arch 432:49–52

Oltman H (1899) Inaugural discussion. Kiel

Panteli C (2009) New insights into the pathogenesis of infantile pyloric stenosis. Pediatr Sur Int 25:1043–1052

Pappo AS, Janeway KA (2009) Pediatric gastrointestinal stromal tumors. Hematol Oncol Clin North Am 23:15–34

Pappo AS, Janeway KA, LaQuaglia M, Kim SY (2011) Special considerations in pediatric gastrointestinal tumors. J Surg Oncol 104:928–932

Park S, Brown KB, Bishop PR et al (2013) Ménétrier disease in childhood: a reparative phenomenon. Clin Pediatr (Phila) 52(11):1059–1064

Pashankar DS, Israel DM (2002) Gastric polyps and nodules in children receiving long-term omeprazole therapy. J Pediatr Gastroenterol Nutr 35:658–662

Poki HO, Holland AJ, Pitkin J (2005) Double bubble, double trouble. Pediatr Surg Int 21(6):428–431

Porcaro F, Mattioli G, Romano C (2013) Pediatric gastric volvulus: diagnostic and clinical approach case. Rep Gastroenterol 7(1):63–68

Pruksapong C, Donovan RJ, Pinit A, Heldrich FJ (1979) Gastric duplication. J Pediatr Surg 14:83–85

Psyrri A, Papageorgiou S, Economopoulos T (2008) Primary extranodal lymphomas of stomach: clinical presentation, diagnostic pitfalls and management. Ann Oncol 19:1992–1999

Rathaus V, Grunebaum M, Ziv N et al (1992) The bubble sign in the gasless abdomen of the newborn. Pediatr Radiol 22(2):106–109

Ripollés T, Garcia-Aguayo J, Martinez MJ, Gil P (2001) Gastrointestinal bezoars: sonographic and CT characteristics. AJR Am J Roentgenol 177:65–69

Roberts J, Torres-Martinez W, Farrow E et al (2014) A case of Robin sequence, microgastria, radiohumeral synostosis, femoral deficiency, and other unusual findings: a newly recognized syndrome? Am J Med 164A(2):287–290

Rodeberg DA, Zaheer S, Moir CR et al (2002) Gastric diverticulum: a series of four pediatric patients. J Pediatr Gastroenterol Nutr 34:564–567

Rosen MJ, Ashish D, Saeed SA (2015) Inflammatory bowel disease in children and adolescents. JAMA Pediatr 169:1053–1060

Ruuska T, Vaajalahti P, Arajarvi P, Maki M (1994) Prospective evaluation of upper gastrointestinal mucosal lesions in children with ulcerative colitis and Crohn's disease. J Pediatr Gastroenterol Nutr 19: 181–186

Ryan DP, Muehrcke DD, Doody DP et al (1991) Laryngotracheo-esophageal cleft (type IV): management of lesions beyond the carina. J Pediatr Surg 26:962–970

Samuel M, Burge DM, Griffiths DM (1997) Prenatal diagnosis of laryngotracheoesophageal clefts. Fetal Diagn Ther 12:260–265

Sasaki H, Sasano H, Ohi R et al (1999) Adenocarcinoma at the esophageal gastric junction arising in an 11-year-old girl. Path Int 49:1109–1113

Schechter R, Torfs CP, Bateson TF (1997) The epidemiology of infantile hypertrophic pyloric stenosis. Paediatr Perinat Epidemiol 11:407–427

Schlesinger AE, Parker BR (2004) Abdomen and gastrointestinal tract. In: Kuhn JP, Slovis TL, Haller JO (eds) Caffey's pediatric diagnostic imaging. Mosby, Philadelphia, pp 1539–1583

Schramm D, Bach A, Zipprich A et al (2014) Imaging findings of gastric diverticula. Scientific World Journal. Article 923098. doi:10.1155/2014/923098

Sferra TJ, Pawel BR, Qualman SJ, Li BU (1996) Menetrier disease of childhood: role of cytomegalovirus and transforming growth factor alpha. J Pediatr 128:213–219

Sharma SC, Menon P (2005) Congenital microgastria with esophageal stenosis and diaphragmatic hernia. Pediatr Surg Int 21:292–294

Shepherd P, Smeulders N, Coleman AHL et al (2011) Congenital microgastria: a rare cause of failure to visualise the fetal stomach. Prenat Diagn 31:1010–1012

Silverman WA (ed) (1961) Dunham's premature infants, 3rd edn. Hoeber Inc., Medical Division of Harper and Brothers, New York, pp 143–144

Sinzig M, Umschaden HW, Haselbach H et al (1998) Gastric trichobezoar with gastric ulcer: MR findings. Pediatr Radiol 28:296

Sookpotarom P, Vejchapipat P, Chongsrisawat V et al (2005) Gastric volvulus caused by percutaneous endoscopic gastrostomy: a case report. J Ped Surg 40:E21–E23

Teele RL, Share JC (2000) Diseases of the pediatric stomach and duodenum. In: Textbook of gastrointestinal radiology, 2nd edn. WB Suanders Company, Philadelphia, pp 2029–2107

Teele RL, Katz AJ, Goldman H et al (1979) Radiographic features of eosinophilic gastroenteritis (allergic gastroenteropathy) of childhood. AJR Am J Roentgenol 132:575–580

Tillman BW, Merritt NH, Emmerton-Coughlin H et al (2014) Acute gastric volvulus in a six –year-old: a case report and review of the literature. J Emerg Med 46(2):191–196

Van Rijn RR, van Lienden KP, Fortuna TL et al (2006) Membranous duodenal stenosis: initial experience with balloon dilatation in four children. Eur J Radiol 59:29–32

Velasco A, Holcomb GW III, Templeton JM Jr, Ziegler MM (1990) Management of congenital microgastria. J Pediatr Surg 25:192–197

Waasdorp CE, Rooks V, Sullivan C (2003) Congenital microgastria presenting as stridor. Pediatr Radiol 33:662–663

Wakhlu A, Wakhlu AK (2002) Paediatric gastric teratoma. Eur J Pediatr Surg 12:375–378

Welch KJ, Randolph JG, Ravitch MM et al (eds) (1986) Pediatric surgery, 4th edn. Year Book Medical, Chicago, pp 907–908

Westra SJ, de Groot CJ, Smits NJ et al (1989) Hypertrophic pyloric stenosis: use of pyloric volume measurement in early US diagnosis. Radiology 172:615–619

White MC, Langer JC, Don S et al (1998) Sensitivity and cost minimization analysis of Radiology versus olive palpation for the diagnosis of pyloric stenosis. J Pediatr Surg 33(6):913–917

Wood LD, Salaria SN, Cruise MW et al (2014) Upper GI tract lesions in familial adenomatous polyposis (FAP). Am J Surg Pathol 38(3):389–393

Zbuk KM, Charis E (2007) Hamartomatous polyposis syndromes. Nat Clin Pract Gastroenterol Hepatol 4(9):492–502

Zucca E (2008) Extranodal lymphoma: a reappraisal. Ann Oncol Suppl 4:77–80

Zullo A, Hassan C, Ridola L et al (2014) Gastric MALT lymphoma: old and new insights. Ann Gastroenterol 27(1):27–33

# The Small Bowel

Nazanin Ahmadi and Johan G. (Hans) Blickman

## Contents




**Abstract**

The pediatric small bowel is subject to a number of congenital and acquired disorders. In this chapter we systematically review the imaging techniques and imaging findings of congenital and acquired conditions effecting this region of the bowel in newborns, infants and older children.



N. Ahmadi, MD (✉)
Pediatric Radiologist, Department of Radiology, Vrije Universiteit Medisch Centrum, De Boelelaan 1118 1081HZ, Amsterdam, The Netherlands
e-mail: nazaninahmadi60@yahoo.com

J.G. (Hans) Blickman, MD, PhD FACR, FAAP
Department of Radiology, Golisano Childrens Hospital, URMC, Rochester, NY, USA
e-mail: johan_blickman@urmc.rochester.edu


## 1 Introduction

The radiological approach to the pediatric upper and lower gastrointestinal (GI) tract varies according to the clinical condition of the child, the patient's age, and the differential diagnostic considerations.



S. Stafrace, J.G. (Hans) Blickman (eds.), *Radiological Imaging of the Digestive Tract in Infants and Children*, Medical Radiology, DOI 10.1007/978-3-319-18434-0_6

The imaging procedures should be performed in a problem-oriented fashion in order to minimize the risks and to maximize the diagnostic benefit.

All efforts must be made to reduce irradiation, the well known ALARA principle. Especially in young children with chronic disease, repeated imaging evaluation should be as streamlined as possible.

Special attention should be paid to reduce any psychological trauma in these young children (e.g., placement of gastric, duodenal, or other tubes), and the environment of the radiology room should be adapted to calm and be user friendly for neonates and young children (e.g., the ambient experience) (Devos and Meradji 2003).

One can simplify the approach to analyzing the causes of disorders of the small bowel in children as congenital anomalies are not as prevalent in later life, and the differential diagnosis is significantly affected by the age of the child. Thus, the entities affecting the pediatric small bowel will be categorized into three groups: neonatal, infantile, and childhood diseases, each subdivided into acute and non-acute conditions (Devos and Meradji 2003).

## 2 Imaging Techniques

### 2.1 The Abdominal, Plain (or Conventional) Film/Radiograph

An abdominal conventional plain film/radiograph (CR) is usually the first imaging procedure performed, especially in acute abdominal conditions. It can give worthwhile information and positively influence the choice of subsequent imaging techniques.

In acute clinical conditions, imaging in two directions (Fig. 1) helps. A supine and a cross-table horizontal beam radiograph (or more frequently in the very young a left lateral decubitus) would be the standard radiographs. In the patient who can stand, the lateral radiograph may be performed standing.

On a supine film, changes such as dilatation with or without obstruction, calcification, and displacement of normal structures can all be identified and localized. Multiple (distended) loops are indicative of distal pathology (Fig. 2), whereas a few (distended) loops suggest proximal intestinal pathology (Fig. 3).

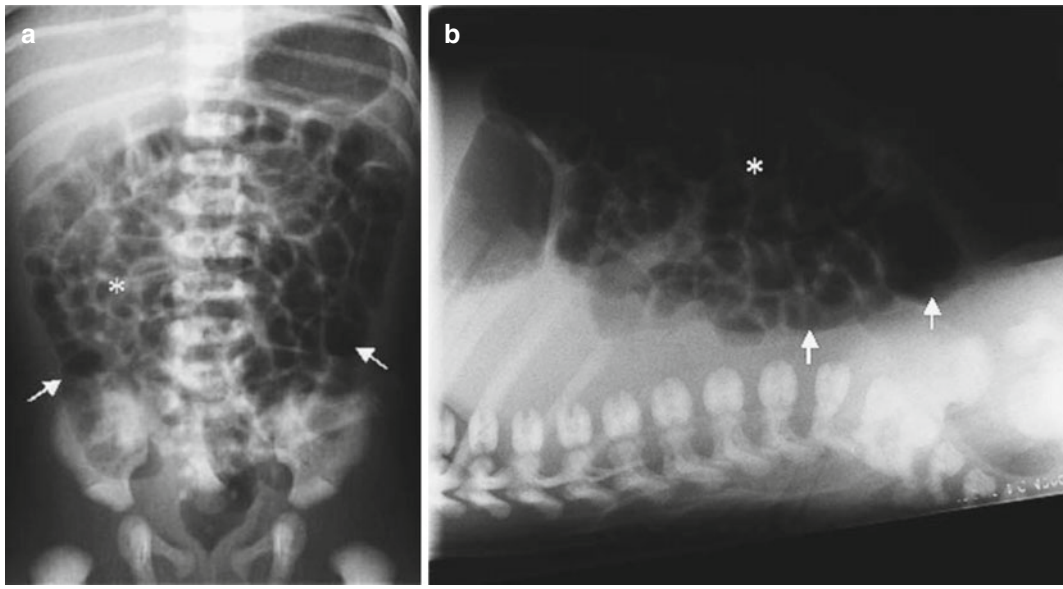


**Fig. 1** (**a**, **b**) Normal radiographs of abdomen in an infant with anatomic position and normal intestinal air distribution. Peripheral (AP) low (lateral) location (*single arrows*) depicts the colon; *asterisk* depicts the small bowel

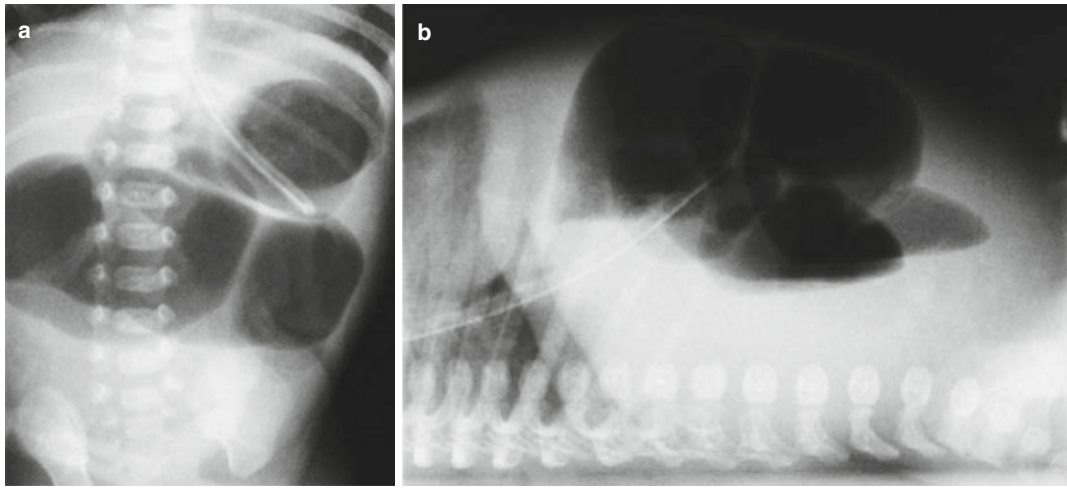


**Fig. 2** (**a**, **b**) Jejunal atresia with multiple distended loops and fluid levels on lateral film

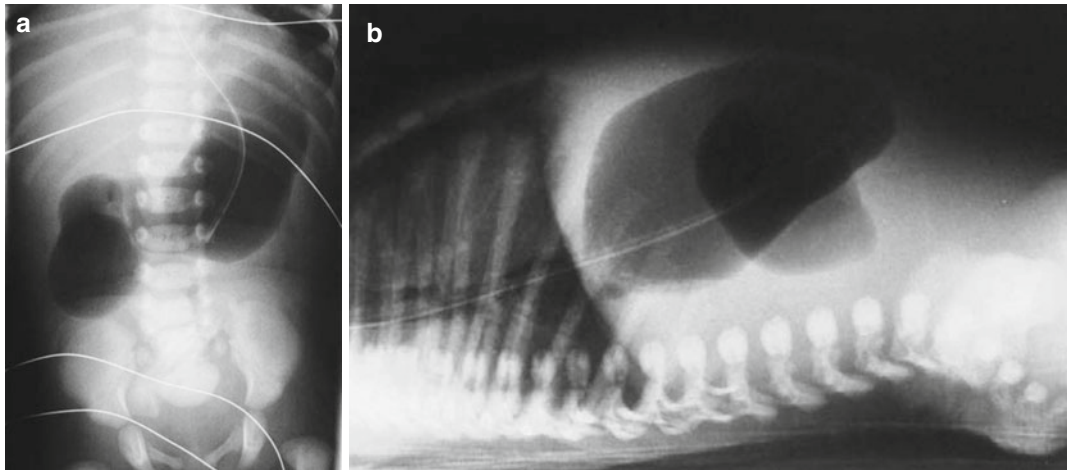


**Fig. 3** (**a**, **b**) A neonate with a highly distended duodenum and stomach due to duodenal atresia. No passage of air seen distally

On an upright, cross-table or a left lateral decubitus horizontal beam radiograph, the anatomic position of the small bowel (Fig. 1 asterisk) and colonic loops are easily recognized (Fig. 1, arrows). Because of the retroperitoneal (dorsal) positioning of ascending and descending colon as well as the rectum, these loops can be distinguished from the small bowel, which has an intraperitoneal (ventral) position. Fluid levels, as well as free intraperitoneal air collections (e.g., due to intestinal perforation) are also better appreciated on a horizontal beam lateral radiograph.

## 2.2 Contrast Examinations

In general, the contrast medium used to evaluate the upper GI tract and small bowel is a suspension of barium sulfate as this is cheap and easy to use. In patients at risk for aspiration, such as preterm neonates, a nonionic contrast agent is preferred because of the lower risk of dehydration. Ionic water-soluble contrast media are more commonly used when a larger amount of contrast medium is needed, such as in small bowel follow through (SBFT), although this is much less used today due to better small bowel visualization on MRE.

If bowel perforation or predisposition for pulmonary aspiration is suspected, barium is contraindicated because of the risk of granuloma formation in the lungs and in the peritoneal cavity with resulting peritonitis and adhesions. The reported side-effects of water-soluble contrast media such as hypothyroidism in neonates and allergic reaction in later life are rare.

In evaluating for abnormalities of the proximal digestive tract (where only few dilated loops are seen), contrast will be given orally or via a feeding tube placed in the stomach. For suspected abnormalities of the ileum or beyond (distal or many dilated loops seen) contrast is best administered rectally.

Contrast examinations will elucidate the anatomy and the motility pattern of the GI tract.

### 2.3 Ultrasound

As visualization with ultrasound (US) is limited by intraluminal intestinal air, it can be useful to prepare the bowel with a mild laxative. Fasting should be a minimum of 3 h to optimally visualize the gallbladder and minimize gaseous distension. This, however, is rarely achievable in today's fast workflow.

US is easy to perform, can be done at the bedside, does not use ionizing radiation, is not cumbersome for the child, and can be repeated as often as necessary.

US is the screening modality of choice in the child suspected of appendicitis, pyloric stenosis, and intussusception, and has already proven its utility in diagnosing other diseases both as a screening and as a follow-up modality (Pastore et al. 2014; Lioubashevsky et al. 2013). Other indications will be discussed in the appropriate sections.

### 2.4 Computed Tomography/ Positron Emission Tomography

Computed tomography (CT) has a superior contrast resolution compared with that achieved on conventional radiographs although in children interpretation can be challenging due to absence of intrabdominal fat. Optimal bowel filling and distension of the lumen with water or contrast media is helpful to better evaluate bowel loops and their surroundings. This is especially true in (follow-up) imaging of intra-abdominal neoplasm. On the other hand, oral contrast is not really needed when abdominal imaging is for trauma. One must keep in mind that CT implies an increased radiation exposure. The information gained must justify the increased radiation burden. Indications for CT use include trauma, intestinal wall and liver/spleen parenchymal evaluation, abscesses and in tumor staging (PET-CT) (Devos and Meradji 2003; Nicolaou et al. 2005; Boudiaf et al. 2001; Schöneberg et al. 2014; Kluge et al. 2013).

### 2.5 Magnetic Resonance Imaging (MRI)

The superior tissue resolution and the multiplanar imaging capabilities without using any ionizing radiation are all advantages of MRI. However, the long examination times, the need for sedation or general anesthesia in young children, and the high costs are limiting factors for this technique. MRI plays an important role in staging primarily retroperitoneal, intraspinal mass lesions and postoperatively in anorectal/cloacal malformations. It is becoming the standard in patients with inflammatory bowel disease, suspicion of acute appendicits, in the assesment of perianal abcesses, and in the staging and follow up in lymphoma patients (Frokjaer et al. 2005; Wiarda et al. 2013; Stéphane et al. 2013; Rosines et al. 2014; Orth et al. 2015).

## 3 Congenital Diseases in the Newborn

### 3.1 Duodenal Obstruction

Duodenal obstruction is the most common cause of proximal (high) intestinal obstruction in newborns. This may be complete (atresia) or incomplete (stenosis). Atresia is caused by failure of recanalisation. Approximately 30 % of patients with duodenal atresia have Down syndrome.

Duodenal stenosis can be the consequence of internal or external causes that narrow the lumen of the upper digestive tract such as malrotation with or without volvulus, a duodenal web, annular pancreas, and duplication cysts (Carty et al. 2005; Parker 2003; Grier 1999; Devos and Meradji 2003; Berrocal et al. 1999). Prenatal diagnosis of a "double bubble" as evidenced by polyhydramnios in 40 % of cases is more common today (Kucińska-Chahwan et al. 2015). Clinical manifestations are persistent (bilious) vomiting from the first hours of life, possibly complicated by dehydration. The abdomen is flat, scaphoid or minimally distended.

A conventional abdominal (plain) radiograph (CR) in two directions (including a horizontal beam) may show a (markedly) dilated stomach and proximal part of the duodenum.

The most important differential in these cases is to exclude conditions that are life-threatening for the patient: mainly midgut volvulus.

In the case of atresia, there will be no air in other parts of the intestinal tract, classically described as the "double bubble" sign (Fig. 3). No other imaging modality is then needed. However, the "double bubble" sign may be absent if the patient has vomited, has a feeding tube, or if there is intermittent passage of air.

In the case of duodenal obstruction with similar clinical signs as atresia but with air distal to the duodenum, intestinal malrotation should be ruled out first.

The sign of an intestinal malrotation is sometimes recognizable on an abdominal plain film in which the small bowel will be located in the right upper abdomen. When this is observed, color Doppler sonography shows in 85 % of the cases an abnormal position and course of the superior mesenteric artery with dextroposition to the superior mesenteric vein and the small bowel will lie in the right instead of the left upper quadrant (Figs. 4 and 5) (Carty et al. 2005; Parker 2003; Shah 2013). More difficult is the evaluation of the retroperitoneal position of the third part of duodenum by ultrasound as suggested by Yousefzadeh (2009, 2010).

An upper GI tract examination (with low osmolar water soluble contrast medium) (UGI)

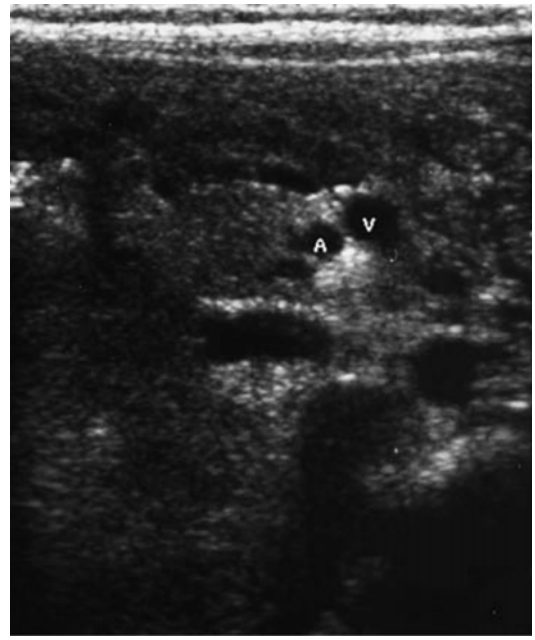


**Fig. 4** An infant with intestinal malrotation on US. Abnormal position of the superior mesenteric artery (**A**) to the right of the mesenteric vein (**V**)

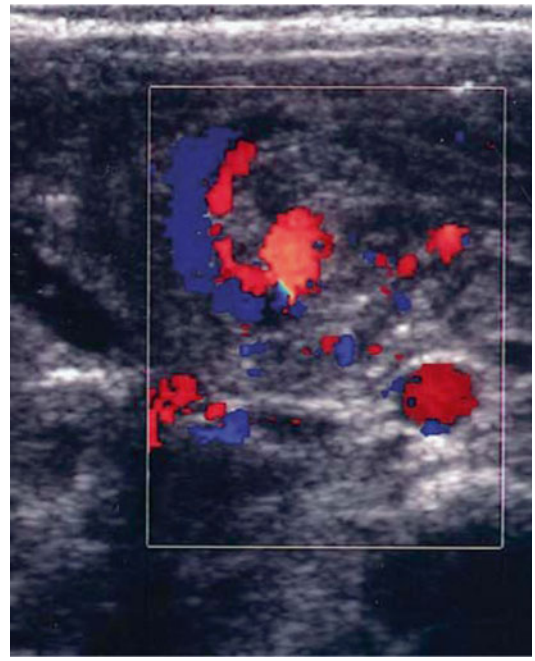

**Fig. 5** An infant with intestinal malrotation. Note the abnormal position and course of the superior mesenteric artery and vein imaged by color Doppler sonogram (the "whirlpool sign")

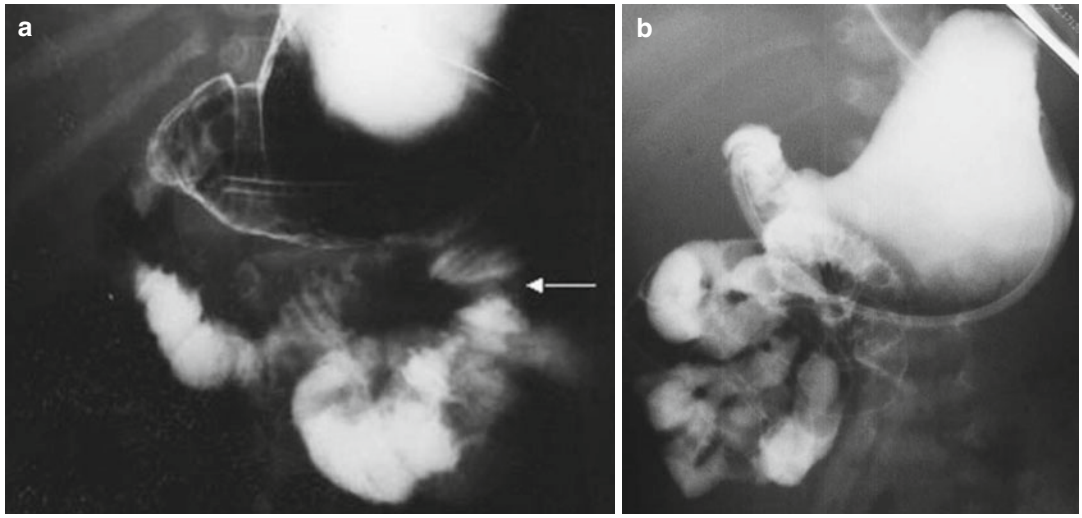


**Fig. 6** (**a**) UGI: determines normal rotation by identifying the normal location of the duodenojejunal junction (*arrow* – ligament of Treitz). (**b**) Intestinal malrotation demonstrated with a barium upper GI study. Localization of jejunum in right upper quadrant. The duodenal loop is abnormal and the duodenum does not cross the spine

is the optimal study to verify whether normal bowel rotation has occurred, and the imaging hallmark for this is to identify the position of the duodeno-jejunal junction (ligament of Treitz) (Fig. 6a). With an appropriate anteroposterior supine positioning of the patient, radiographically, this implies that the duodeno-jejunal junction is to the left of the vertebral column and at the same level or more superior than the duodenal bulb. In malrotation the above hallmarks are deficient (Fig. 6b) (Carty et al. 2005; Blickman et al. 2009).

A contrast enema cannot reliably exclude malrotation as in 15–20 % of normal neonates the caecum has not yet descended (which will occur in the subsequent 6–12 months).

A duodenal web or diaphragm is part of a spectrum; from an atretic duodenum to a fully recanalized duodenum with a central opening. The radiological findings are identical to any other type of duodenal stenosis. The so-called "windsock" appearance is easy to demonstrate as a curvilinear web that evacuates contrast medium through a tiny small central opening (Fig. 7a). The contrast medium is selectively administered through a feeding tube of which the tip is placed in the proximal duodenum.

An annular pancreas with complete or incomplete duodenal obstruction is another cause of duodenal obstruction. Its cause is persistence of the left lobe of the ventral pancreatic bud around the sixth week of gestation that then wraps around the duodenum causing a ring-like eccentric narrowing (Fig. 7b). The clinical and radiological findings are the same as other types of duodenal obstruction.

Duodenal duplication and diverticula are rare and incidentally cause a duodenal stenosis. A cystic non-communicating duplication is reliably detectable sonographically while a communicating duplication and diverticulum can be visualized by gastrointestinal contrast examinations, although often in retrospect.

## 3.2 Jejunal and Ileal Obstruction

Neonates with jejunal or ileal obstruction may also present with bilious vomiting depending on the level (most likely proximal) of obstruction. This clinical symptom is usually less severe than in duodenal obstruction.

A distended abdomen is virtually always present, more so the further distal the level of

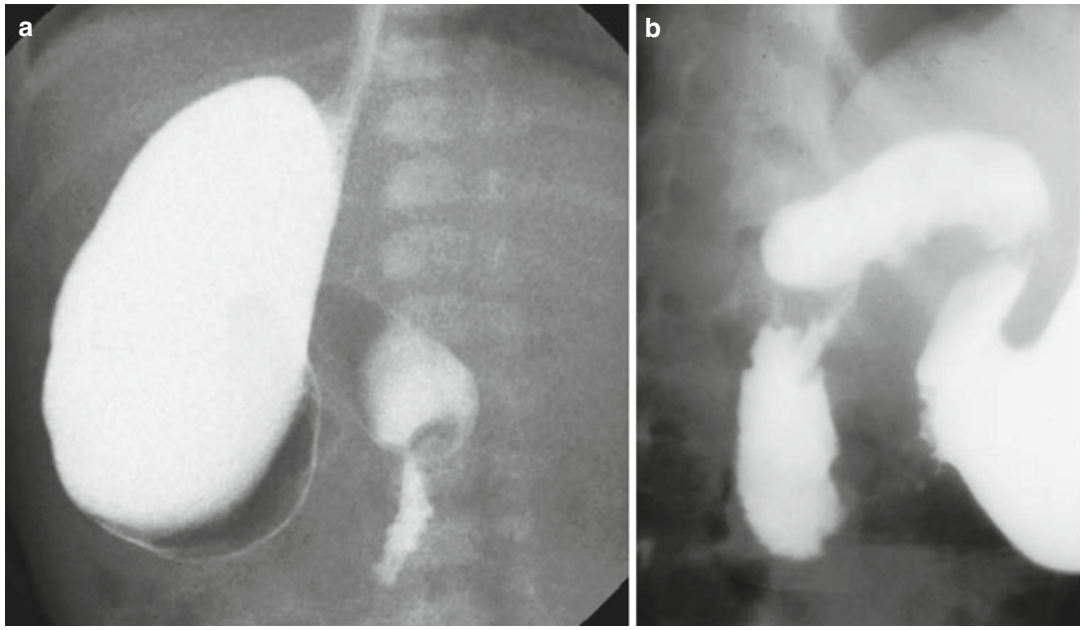


**Fig. 7** (**a**) Duodenal stenosis caused by a duodenal web with a "windsock" appearance. (**b**) Eccentric narrowing of the descending duodenum at the level of the sphincter of Oddi: annular pancreas

intestinal obstruction. Failure to pass meconium may be an additional early symptom. Atresia of the jejunum and ileum is twice as common as duodenal atresia, about equal in the jejunum and ileum, with an incidence of 1 in 400–500 live births. Multiple atresias occur in 10–20 % of cases. Intestinal vascular accidents, such a thromboembolic occlusion, hypoxia, or volvulus, are thought to be the cause of an atretic jejunum or ileum. This ischemic event may also cause perforation leading to meconium peritonitis. The atretic or stenotic intestinal segment is mostly monoloculated and rarely multiloculated.

The radiological diagnosis of obstruction is usually evident on the radiograph. In uncomplicated cases these radiographs of the abdomen are sufficient. The preatretic intestinal loops are dilated because of accumulation of large amounts of fluid and fluid levels are usually present on horizontal beam lateral films. In cases of jejunal atresia only a few loops of distended jejunum are present in the left upper abdomen while in ileal atresia more dilated loops are identified. In complicated cases, enema or US can be useful – particularly from the differential diagnostic point of view to exclude meconium ileus or meconium peritonitis. In cases of distal atresia, a microcolon without the presence of meconium is usually found.

## 3.3 Meconium Peritonitis

An ante- or peri-natal perforation of the intestinal tract results in an aseptic chemical peritonitis as the sterile bowel contents (such as desquamated cells, lanugo hairs, and vernix) escape into the peritoneal cavity causing an intense inflammatory reaction. This chemical peritonitis may lead to adhesions, granulomata, cystic changes and frequently to calcifications. The calcifications may extend into the scrotal cavity as the processus vaginalis may still be patent. Antenatal perforation due to meconium ileus in patients with cystic fibrosis is frequently the main cause of meconium peritonitis. A newborn with meconium peritonitis may have a distended, painful

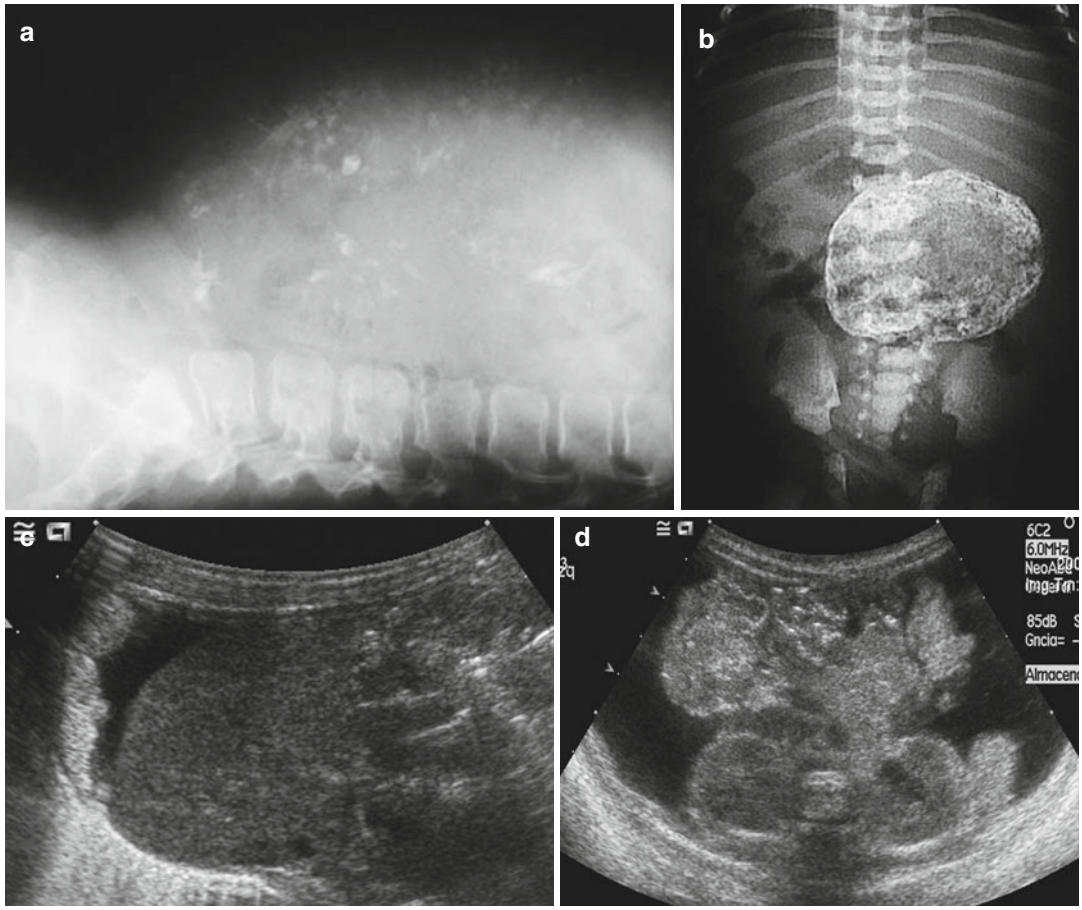


**Fig. 8** (**a**–**d**) Meconium peritonitis. (**a**) neonate with a distended, practically gasless abdomen characteristic for meconium peritonitis. The streaky and flocculent calcifications in the peritoneal cavity are characteristic. (**b**) A neonate with meconium peritonitis and a rounded cystic calcification located intraperitoneally. Distended abdomen with reduced intestinal air. (**c**) transverse US of the RUQ and (**d**) midline transverse US image in a further infant. Both US images demonstrate ascites and meconium deposits located subdiaphragmatically and next to the left kidney (Courtesy of G Del Pozo – image from Differential Diagnosis in Pediatric Imaging – Thieme 2011)

abdomen and may be lethargic. The child may have bilious vomiting and often produces no meconium.

Diagnosis is made by CR and US. The former reveals a swollen abdomen with a few or no air-containing bowel loops (Fig. 8). The bowel loops may be variably dilated. Often calcifications are visible. US shows not only the calcifications but also the extraluminal meconium and cystic fluid accumulations. The wall of the intestine is thickened (Fig. 9).

## 3.4 Megacystis-Microcolon-Malrotation-Intestinal-Hypoperistalsis Syndrome (MMMIHS)

The MMMIHS is a rare cause of intestinal obstruction and consists of a massively dilated bladder, malrotated microcolon, and absent or ineffective peristaltic activity of the bowel. The disease is more common in females. Clinical symptoms are vomiting, failure to pass

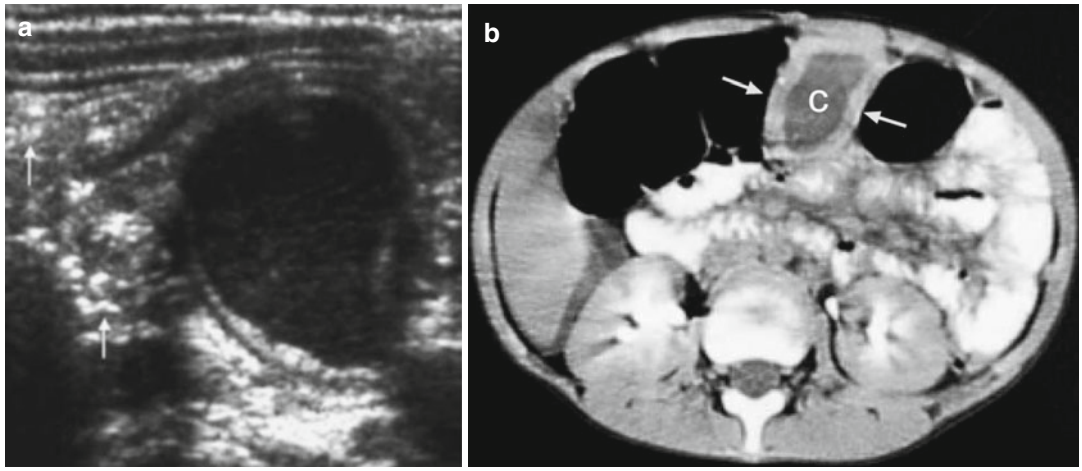


**Fig. 9** (**a**) Ileal duplication cyst in an infant with meconium peritonitis. Note the additional punctate calcifications and echogenic meconium intraperitoneally (*arrows*) (**b**) CT scan of the abdomen showing a further case with a large duplication cyst "C" between aerated bowel loops (*arrows*) – (Courtesy of G Del Pozo – image from Differential Diagnosis in Pediatric Imaging – Thieme 2011)

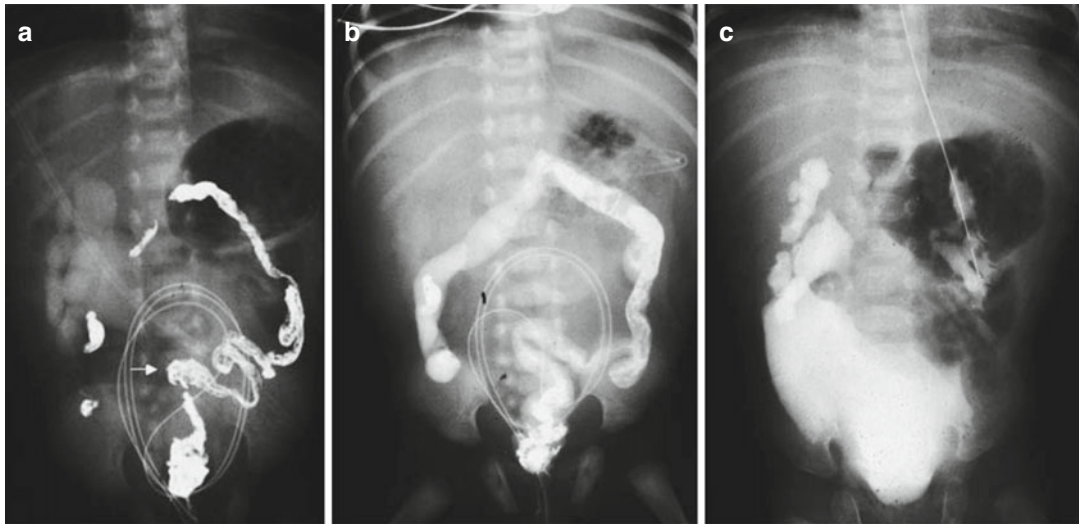


**Fig. 10** (**a**–**c**) MMMIHS: highly distended stomach on contrast study with slow passage of contrast. Very little peristaltic activity. (**a**, **b**) Note the unusual microcolon (*arrow*) and distended bladder (catheter). Secondary hydronephrosis because of dilated bladder. (**c**) Dilated system can be seen with the atonic, large bladder with dilatation of the pyelocaliceal system

meconium, absent spontaneous micturition, and a distended abdomen (Mc Laughlin and Puri 2013). On CR a distended abdomen (sometimes caused by a distended urinary bladder) may be identified.

A UGI may show dilated small bowel without peristaltic activity while on an enema, a microcolon will be identified (Fig. 10). US demonstrates a large urinary bladder with dilated ureters and pyelocaliceal systems.

### 3.5 Congenital Chloride Diarrhoea

Congenital chloride diarrhoea is a rare autosomal recessive disease with an often delayed diagnosis. The disease is most common in Saudi Arabia and Kuwait (1:3200–13,000 births), Finland (1:30,000–40,000), and Poland (1:200,000). Congenital chloride diarrhoea begins in fetal life. The main clinical sign is watery diarrhea that in utero leads to dilated bowel loops, polyhydramnios, and often premature birth. Newborns have a distended abdomen, absence of meconium, dilated bowel loops on ultrasonography, and watery diarrhea which can sometimes be mistaken for urine. The absence of meconium and the distended abdomen suggest meconium ileus or Hirschsprung disease and can lead to unnecessary surgical intervention.

Repetitive diarrhoea and severe electrolite disbalance may help in the differential diagnosis (Shamaly et al. 2013).

## 4 Acquired Diseases in the Newborn

### 4.1 Perforation

Perforation of the GI tract in newborns is mostly iatrogenic. Both stomach and esophagus can incidentally be perforated by feeding tubes. The treatment with prostaglandins in patent ductus can also be complicated with a gastrointestinal perforation. Rectal use of a thermometer may be followed by rectal perforation (Devos and Meradji 2003).

Sepsis, obstructions, and vascular accidents, especially necrotizing enterocolitis, are all non-iatrogenic causes of enteral perforation.

A distended and tender abdomen with or without respiratory problems are clinical signs of perforation.

Perforation is most reliably demonstrated on CR if taken in two projections. A supine film (Fig. 11) will demonstrate an abnormal lucency in the upper abdomen with air possibly outlining the right lobe of the liver, both sides of the wall of the stomach, and bowel loops. The falciform ligament may be visible in the upper abdomen (Football sign). In the newborn, a left-side down decubitus film will demonstrate free air between the liver and peritoneal wall, which is almost impossible to confuse with intraluminal air. In case of an unstable neonate, a cross-table lateral view is preferred, but it can mask free air behind intraluminal air, unless the so-called "triangle" sign (Fig. 12) is present.

### 4.2 Functional Intestinal Obstruction of the Premature Newborn

Functional intestinal obstruction of the premature newborn is also called "meconium ileus-like syndrome" because, as in the case of meconium ileus, an obstruction exists at the distal ileum and caecum but meconium has passed.

As in meconium ileus, there is a motility disturbance of the bowel. However, it can also be related to absorption problems if inadequate feeding formula is used (so-called milk curd syndrome). Clinical symptoms are similar to meconium plug syndrome or meconium ileus and are those of obstruction, such as progressive vomiting, progressive abdominal distension, and failure to pass stools. Sometimes a mass can be felt in the (right) side of the abdomen.

CR most frequently shows a dilated small bowel with only a few or even no fluid levels and an absence of air in the rectum. Because of air-trapping in stools, a mottled appearance can be seen in the right side of the abdomen (Fig. 13a, b). US will show dilated small bowel loops (ileum) fully filled with huge hypoechogenic masses (Fig. 13c). A contrast enema with nonionic media shows fecal impaction in upper colonic segment or higher ileum. This procedure may have a therapeutic effect.

Olive oil enema, which softens hard stools and induces smooth movement of these stools, is suggested as effective and safe first-line treatment in pre-term infants with milk curd syndrome (Watanabe et al. 2013).

## 5 Congenital Diseases in the Infant

Congenital diseases are encountered less often in infants but can manifest after the neonatal period.

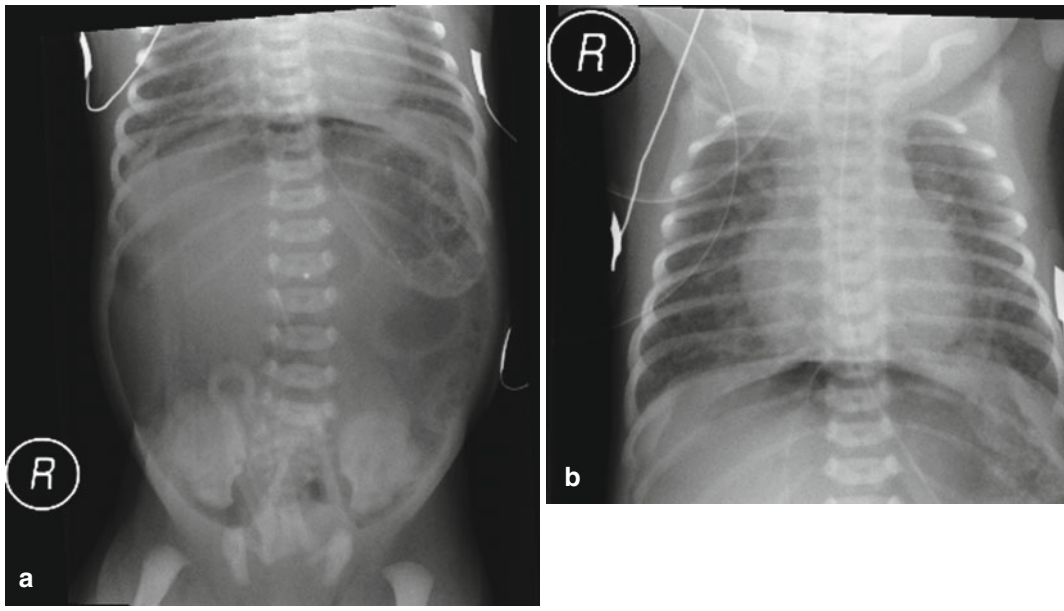


**Fig. 11** (**a**, **b**) Gross pneumoperitoneum in an infant with ileal perforation. Free air outlining the peritoneum (**b**) AP chest demonstrating the "cupula sign"; free air under the cardiac silhouette

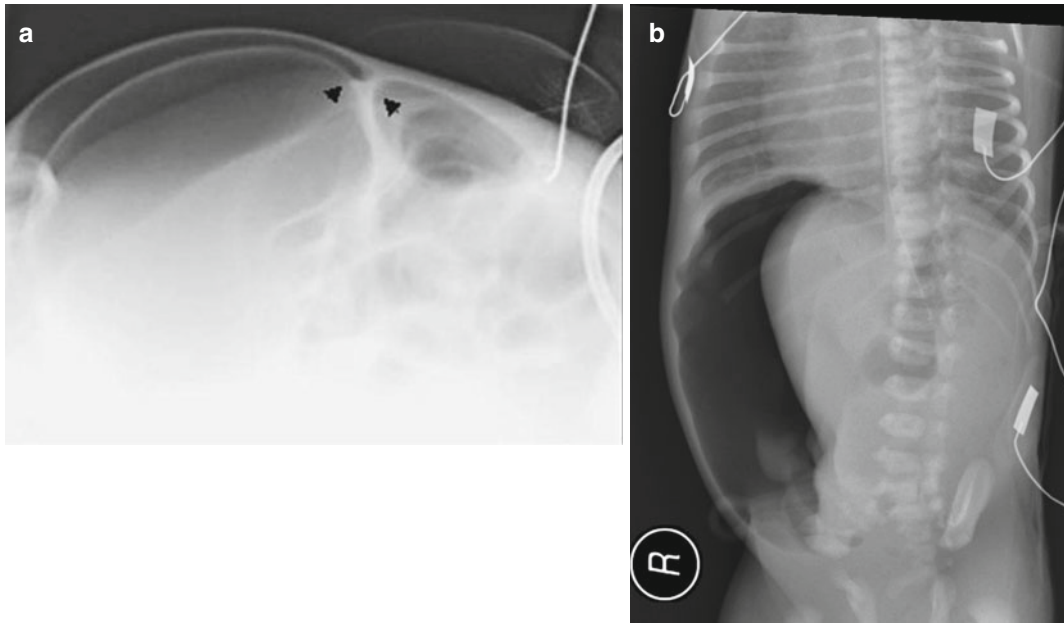


**Fig. 12** (**a**) Pneumoperitoneum with a "triangle sign" on the cross-table lateral film (*arrows*). (**b**) Left lateral decubitus image (presented as if an AP view). Free air is located in the "highest point": between the abdominal wall and the liver

## 5.1 Volvulus

Clinical manifestations and diagnostic procedures are mostly the same as in newborns.

## 5.2 Meckel Diverticulum

A Meckel diverticulum results from an incomplete obliteration of the vitelline duct and is situated near

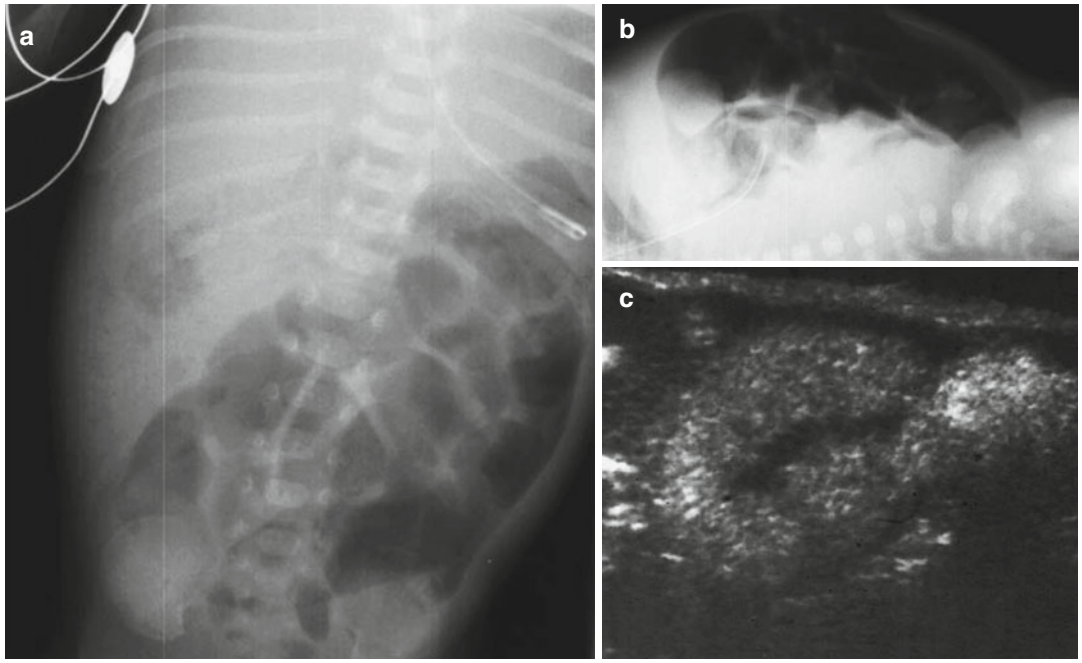


**Fig. 13** (**a**) A premature infant with intestinal dysfunction, so-called meconium ileus-like syndrome. The supine abdominal film shows dilated intestinal loops because of fecal impaction in ileum. (**b**) Cross-table radiograph. Meconium-like ileus with dilated intestinal loops without fluid levels. The whole colonic tract and rectum are gasless. (**c**) Ultrasound of the right lower quadrant of abdomen demonstrates the impacted and inspissated stool in the ileum

the ileocaecal valve on the antimesenteric border of the ileum. It is usually about 2 cm long, located about 2 cm from the ileocecal valve. It is the most common form of congenital abnormality of the small intestine, occurring in about 2 % of all infants, but mostly causes no clinical complaints. It contains all layers of the intestinal wall, but the mucosa is (ectopic) gastric in origin in about 15–20 % of cases (Carty et al. 2005; Parker 2003; Vali et al. 2015).

In half of the patients with complaints, clinical signs manifest in the first 2 years of life. Ulceration occurs only in those that contain ectopic gastric mucosa and thus is rare, but can cause occult fecal blood or frank blood in stool and anemia. Adhesions and formation of scar tissue can lead to obstructive ileus. The diverticulum can act as a lead point for ileocolic or ileoileal intussusception.

The visualization of a Meckel diverticulum is often unsuccessful. CR shows only the complications caused by a Meckel diverticulum.

CR is of course indicated if obstruction or perforation is suspected. A Meckel diverticulum may be incidentally found by US (Fig. 14), which may show cystic diverticula on the scan. Alternatively, it is diagnosed by enteroclysis. Small bowel or colon enemas can show the rather bigger diverticula. Cross sectional imaging can help confirm the findings. Scintigraphy may identify a Meckel diverticulum as a hot spot if it has gastric mucosa.

## 5.3 Duplication Cysts

A duplication cyst, the result of multiple twinning, persistent embryologic diverticula, or aberrant luminal recanalisation, is a spherical or tubular structure that contains mucosa of the intestinal type and is surrounded by a layer of smooth muscle. They all have the same anatomic structure as normal bowel wall and are mostly (35 %) located in the distal ileum on its mesenteric side, decreasing in frequency as one goes proximally. Sometimes there is a connection with adjoining bowel, but this exists in only a minority of cases. If they do communicate, its recognition as a tubular structure with intestinal content is

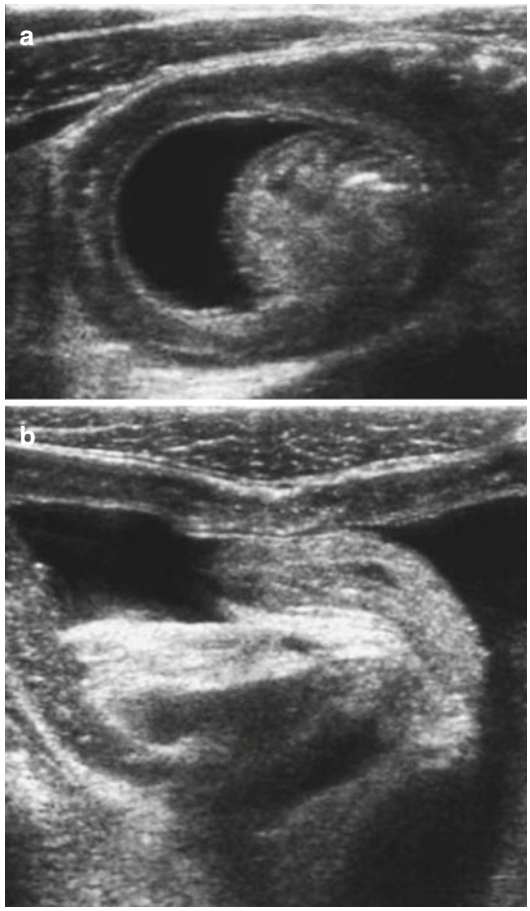


**Fig. 14** Meckel diverticulum as a lead point for an ileo-ileocolic intussusception. (**a**) Transverse and (**b**) longitudinal planes. Note the intraluminal intestinal fluid surrounding the diverticulum

more difficult. The non-communicating duplication cysts are cystic because of the mucosal secretions. The increasing number of prenatal and postnatal US examinations means that the noncommunicating duplication cysts are recognized earlier and more often (Berrocal et al. 1999). The clinical manifestation and diagnostic procedures depend on the localization and type of duplication cyst. These cysts are asymptomatic; however, they can manifest later in life because of complications. A duplication cyst can rarely contain ectopic gastric mucosa in which bleeding can occur.

Clinical symptoms are bleeding (melena and hematemesis can cause serious anemia), intermittent abdominal pain, vomiting, and sometimes

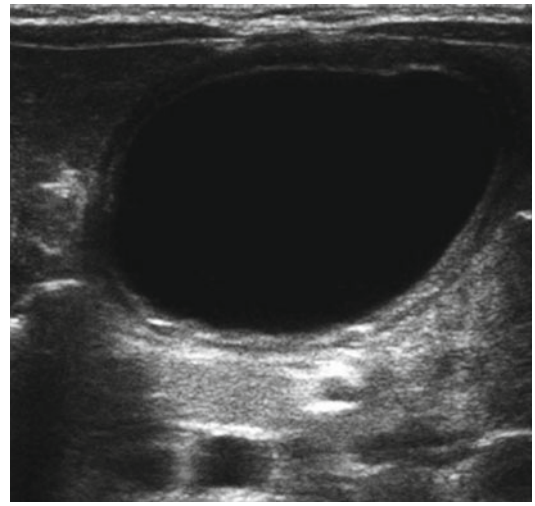

**Fig. 15** Typical US appearances of a duplication cyst (Courtesy of Dr. C. Buonomo, Boston, MA, USA)

a palpable mass. Obstruction, volvulus and intussusception are well known complications.

CR, US, contrast examination, scintigraphy, and even CT and MRI can be useful to diagnose a duplication cyst. CR may show obstruction. US may show the noncommunicating anechoic cystic duplication cysts with the clearly visible, characteristic bowel wall in which the mucosa is echogenic and the muscularis hypoechogenic (Figs. 9 and 15). The muscularis is typically shared with adjacent bowel wall, but the mucosal layer is separated. Although characteristic when seen, not all duplication cysts demonstrate the "gut signature" appearances. The cysts can be multilocular and can contain echogenic debris because of bleeding or mucosal secretions. The contrast follow-through exam can show an impression on the bowel wall and displacement of the bowel loops. In the case of communicating cysts the abnormal configuration of the bowel can be seen. CT and MRI show a cyst with an enhancing wall after contrast administration.

## 5.4 Intraperitoneal Cysts

There are three types of lymphangiomas: the simple (capillary), cavernous and cystic types. At least half have a haemangiomatous component. Most abdominal lymphangiomas are located in the mesentery and omentum, and are thus called mesenteric and

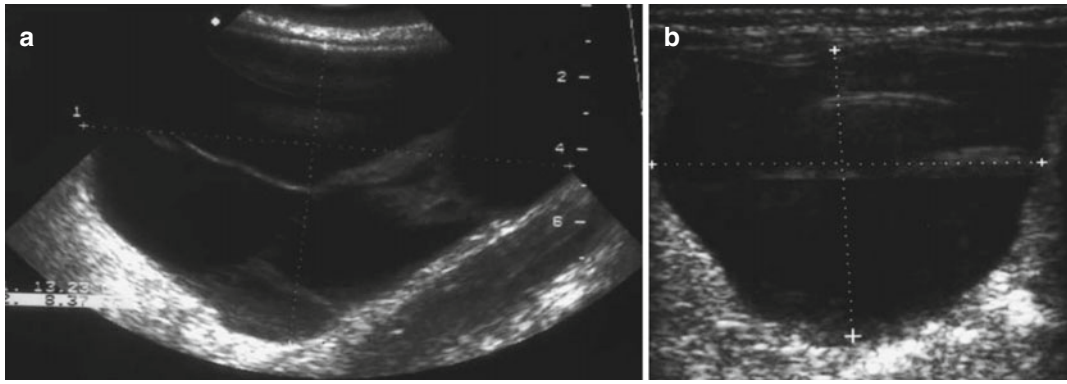


**Fig. 16** (**a**) A huge mesenterial cyst located intraperitoneally and sharply encapsulated. (**b**) An omental cyst in the upper abdomen which is unlayered. Note wall: no mucosal pattern

omental cysts, respectively. They are caused by sequestration (lack of involution) or obstruction of lymphatic vessels, are mono- or multilocular and can calcify in case of necrosis. The wall of a mesenteric or omental cyst is unilayered, which is in contrast to the multilayered aspect of the wall of the duplication cyst. Most cysts are asymptomatic, but because of bleeding or infection they can cause fever and pain and can necrose after torsion. Adherent cysts to the bowel can cause partial obstruction. Some cause a painless abdominal distension and palpable mass.

On CR, the cyst can be suspected by displacement of bowel loops and calcifications or by the signs of obstruction.

An upper GI tract examination may show displacement of bowel loops but is usually unremarkable.

On US, these mostly multilocular cysts have fine septations and can be anechoic or, after bleeding or infection, filled with echogenic debris (Fig. 16).

CT and MRI are rarely indicated but show wall and septal enhancement after contrast injection.

US guided percutaneous drainage and sclerotherapy is recommended in cystic retroperitoneal lymphangiomas (Shankar et al. 2011) (Fig. 17).

## 6 Acquired Diseases in infants

### 6.1 Enteritides

Worldwide viruses, bacteria and parasites can cause enteritis. Viral acute gastroenteritis and enterocolitis are most frequent in the first 2 years of life. Imaging is mostly not required but CR is sometimes useful to differentiate enteritis from other more serious diseases such as obstruction, intussusception, perforated appendix with peritonitis, neuroblastoma and Hirschsprung disease.

CR in two directions may show moderate dilatation of small bowel and colon. Both may contain air-fluid levels, and particularly in the colon air-fluid levels suggest disturbed resorptive activity. Either there is too much intraluminal fluid (diarrhea) or there is decreased peristaltic activity with resulting decreasing resorptive power. In cases with persistent vomiting a relatively gasless abdomen can be seen. US, performed to exclude intussusception for example, may show fluid in the small intestine and even colon, hyperperistalsis, large mesenteric lymph nodes and sometimes bowel wall thickening (Blickman et al. Ped Requisites 3rd ed.).

Eosinophilic gastroenteritis is a rare condition in children and discussed later in the chapter.

## 7 Diseases in Older Children

### 7.1 Small Bowel Intussusception

Small bowel intussusceptions are less frequently diagnosed than ileocolic intussusceptions, but if searched for carefully, are relatively frequently encountered. Most such small bowel intussusceptions are idiopathic and transient with no clinical importance. Pathologic entities that might predis-

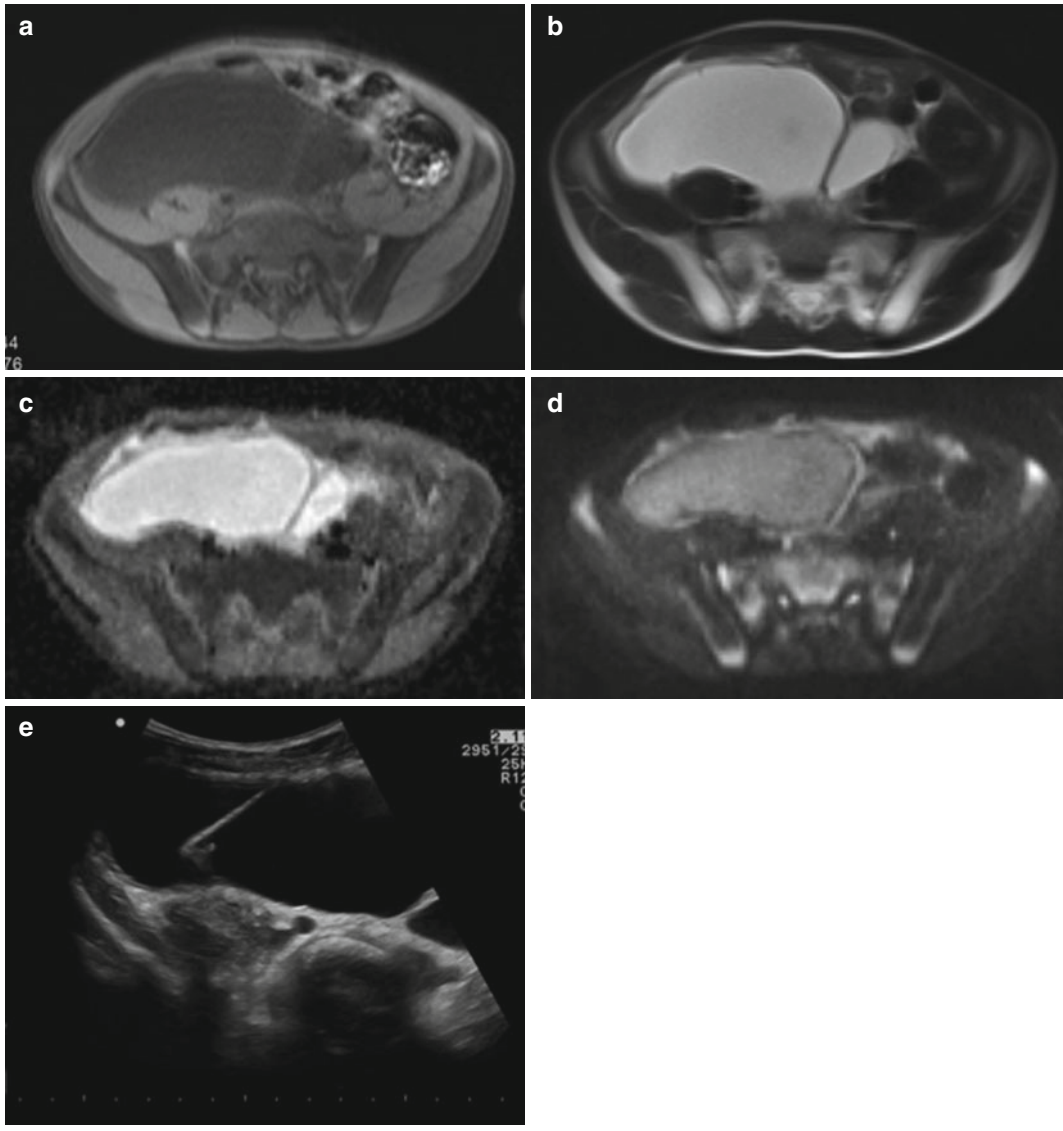


**Fig. 17** Retroperitoneal lymphangioma in a 13 year old boy (**a**) Axial T1 MRI (**b**) Axial T2 MRI (**c**) Axial DWI, (**d**) Axial ADC map demonstrate a well-defined thin-walled fluid-filled cystic leasion in the right retroperineum with displacement of the anterior structures. (**e**) Axial US image obtained during guided drainage of the lymphangioma with the needle identified within the centre oft he lesion

pose a child to small bowel intussusception that can be clinically significant are infection, malabsorption syndromes, gastroenteritis with increased peristaltic activity of small bowel, lymphoma, cystic fibrosis, intramural hematomata (Henoch-Schönlein, posttraumatic), polyps, Meckel diverticulum, duplication, foreign body and adhesions.

Small bowel intussusceptions can be found incidentally when searching for other pathology, in which case patients will have no complaints and no further imaging action is needed.

Otherwise patients can present with transient cramping abdominal pain or with persistent abdominal pain, or even with symptoms of obstruction.

On US (Fig. 18), an intraluminal mass with a layered appearance may be seen. It can be seen to intussuscept and de-intussuscept, can have the "pseudo-kidney" or "doughnut" appearance and occasionally the lead point can be determined.

CT findings correlate with the findings described for US but are usually incicentally noted as CT has no place in the search and/or therapeutic intervention for intussusception. A layered or target appearance of the mass, fat within the mass, particularly if in continuity with mesenteric fat and mesenteric vessels entering the mass, are features suggestive of intussusception. Both on US and CT a crescent of *air* or fluid may separate the mass (the intussusceptum) from the adjacent small bowel (the intussuscipiens).

Idiopathic, transient small bowel intussusceptions need no treatment. The transient nature of the small bowel intussusception will be confirmed by reinvestigation of the small bowel, preferably by sonography, after a few minutes or hours. The intussusception will in most cases have then disappeared (Mateen et al. 2006; Strouse et al. 2003).

## 7.2 Ileus

Acquired ileus, encountered in older children or even infants, is, like in adults, subdivided into paralytic (adynamic) or obstructive (mechanical).

Paralytic ileus, due to intrinsic abnormalities of the bowel wall, can be caused for example by drugs, after laparotomy, sepsis or peritonitis. Obstructive ileus is most often due to extrinsic causes, for example adhesions (in 70 % of cases),

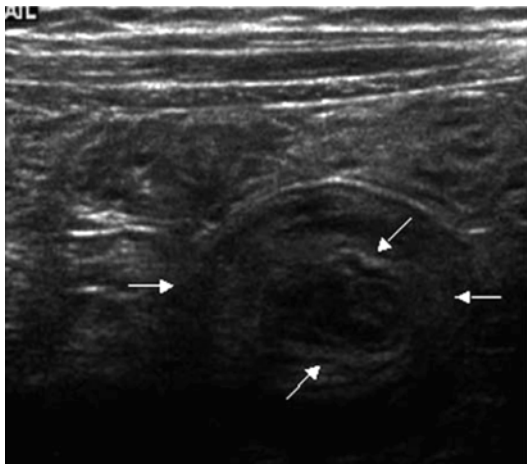

**Fig. 18** Transient small bowel intussusception. The intraluminal mass with layered appearance is the small bowel (*arrows*)

incarcerated hernia, post traumatic small bowel wall hematomas, neoplasms, Crohn disease and intussusception. Clinically the child has a distended and tender abdomen with failure to pass stools or no defecation and possibly (bilious) vomiting.

Imaging can indicate location, degree and cause of obstruction and assess for the presence of ischemia.

CR remains the first line of imaging. CT is used increasingly because it may provide essential diagnostic information not apparent on plain radiographs.

In paralytic ileus supine radiographs of the abdomen will show both dilated small bowel loops and colon, whereas in obstructive ileus usually only the loops proximal to the obstruction are dilated and those distal have a reduced caliber. The closer to the obstruction, the more the loops are dilated. Air-fluid levels on horizontal beam films can be seen in both types of ileus, but in case of obstructive ileus air-fluid levels are concentrated in the dilated loops (Figs. 19 and 20).

In the acute setting and with clinical symptoms such as (bilious) vomiting and the inability to drink contrast, studies such as an UGI are usually not indicated.

US may show dilated fluid-filled bowel loops. The obstructing cause can occasionally be visualized if it is a tumor or hernia. Absence of peristaltic movements, bowel wall thickening without perfusion on color Doppler imaging and dilated small bowel containing fluid can all indicate infarction in the appropriate clinical setting.

CT can be used to distinguish between paralytic (Fig. 20) and obstructive ileus or to localize the obstruction, but care needs to be taken to minimize total radiation dose. Other advantages of CT include the fact that no oral contrast material is needed as the retained intraluminal fluid serves as a natural (negative) contrast agent. It is a rapid, noninvasive, readily available technique with which also extraluminal pathology can be visualized. CT images of an obstructive ileus will identify dilated bowel loops proximally with normal caliber or collapsed loops distally. Sometimes the transition zone, which may resemble a beak, can be identified. This CT sign, among others, is well described by Nicolaou et al. (2005). Also described are the 'string-of-pearl' sign

and small-bowel-faeces sign. The string-of-pearl sign is caused by slow resorption of intraluminal air leaving small bubbles trapped between the folds of the valvulae conniventes. The small-bowel-faeces sign results from stasis and mixing of small bowel content. Signs associated with ischemia include thickened bowel wall, ascites, the 'target' sign which refers to the trilaminar appearance of the bowel wall after IV contrast injection, poor or absent contrast enhancement of the bowel wall after IV injection, pneumatosis intestinalis and air in mesenteric or portal veins, the 'whirl-pool' sign caused by twisting of the mesenteric vasculature around itself caused by a volvulus, tortuous engorged mesenteric

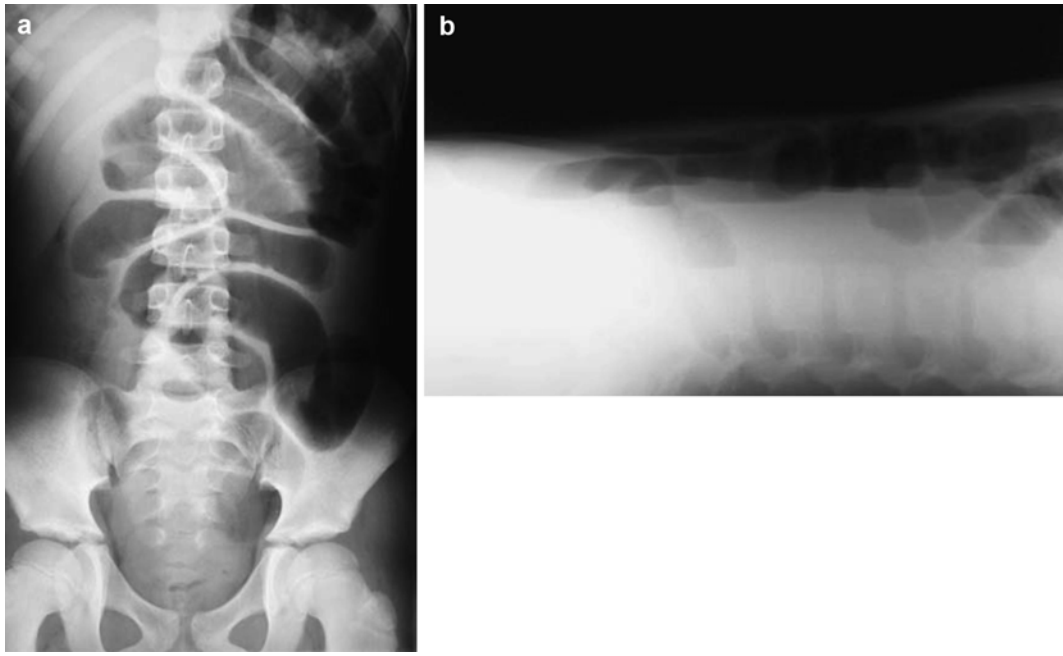


**Fig. 19** (**a**, **b**) Mechanical intestinal obstruction after complicated and perforated appendectomy in a girl. Note the dilated intestinal loops (**a**) and multiple fluid levels on lateral film (**b**)

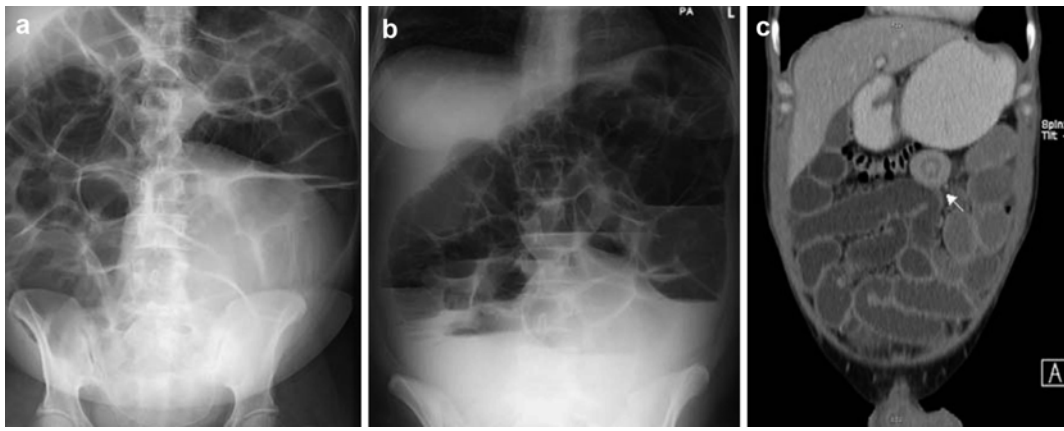


**Fig. 20** (**a**, **b**) Paralytic ileus. Note the extremely dilated small bowel loops and also the colonic loops containing air and fluid levels. (**c**) CT image shows multiple dilated loops of almost equal caliber: indicative of paralytic ileus. *Arrow* indicates small bowel intussusception (incidental)

vessels, mesenteric hemorrhage, and increased attenuation of bowel wall on noncontrast scans (Nicolaou et al. 2005; Boudiaf et al. 2001).

## 7.3 Tumors

Tumors of the small intestine are rare in children and with the exception of the premalignant polyposis syndromes (such as Gardner syndrome and Peutz-Jegher syndrome) a malignant lesion of the small bowel in children is extremely rare.

Benign small bowel neoplasms are often associated with multiorgan syndromes such as Osler-Weber-Rendu (telangiectatic arteriovenous fistulae), Klippel-Trenaunay-Weber (solitary or multiple haemangiomas) or neurofibromas.

Benign mesenchymal lesions such as lipomas, fibromas and leiomyomas also occur.

Any of these tend to present with symptoms of abdominal pain or obstruction, sometimes due to secondary intussusception (Carty et al. 2005; Parker 2003).

CR is usually unremarkable. Diagnosis may be made with contrast studies. These may reveal polypoid filling defects or a classic intussusceptum.

US distinguishes solid from cystic lesions, and may reveal the polyps as intraluminal, floating lesions that are hyperechogenic, due to the mucosal secretions, and may be nodular or tubular structures. The so-called "target" configuration on US is caused by the echogenic center that represents the polyp and the surrounding hypoechogenic region, which is the fluid collection in the dilated loops (Fig. 21).

CT and MRI can also reveal polyps, but the small bowel should then be filled with enough intraluminal contrast material that surrounds the polyps.

Pediatric malignant tumors of the small bowel are mostly secondary to non-Hodgkin lymphoma, usually B-cell Burkitt lymphoma. Burkitt lymphoma can develop at any age, but is most common in children under the age of 8 years and more predominant in boys. It is a very fast growing tumor and originates from B-lymphocytes with a predilection for abdominal organs, particularly the distal ileum. Large numbers of lymphoma cells may accumulate in mesenteric lymph nodes. Over the age of 4 years it is the most common lead point in children with ileocolic intussusception. Burkitt lymphoma metastasizes often to bone marrow, the blood stream and central nervous system (Parker 2003; Husband and Reznek 2004).

Patient complaints include loss of appetite, vomiting, abdominal pain, constipation, GI bleeding or a palpable mass in the right lower quadrant.

CR may be normal or show signs of obstruction. This may include so-called aneurysmal dilatation, better appreciated on contrast studies as polypoid enlargement/thickening of the mucosal folds. Sometimes a mass in the right lower quadrant can be detected.

Ultrasound may show a hypoechoic or anechoic mass, localized eccentrically in the ileum of which the lumen is frequently dilated (Fig. 22a). Enlarged mesenteric lymph nodes and ascites may be seen.

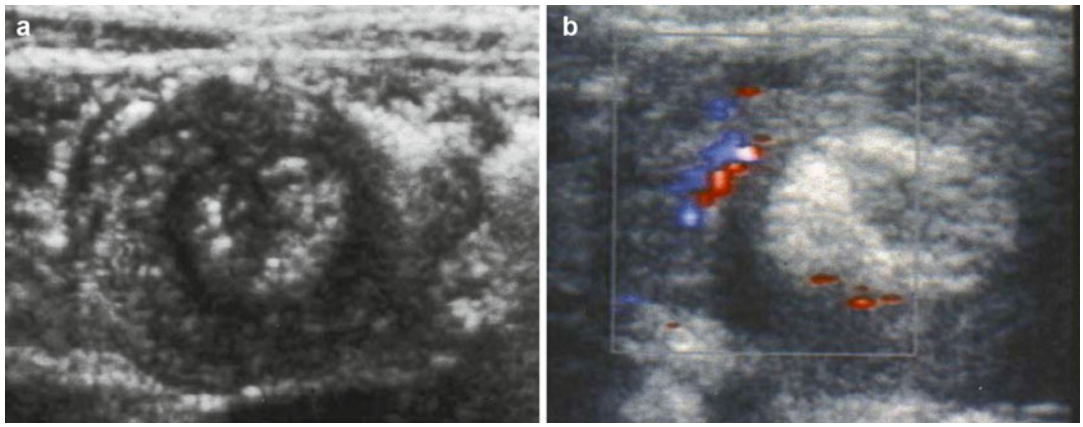


**Fig. 21** (**a**, **b**) A child with intussusception. The echogenic mass, characteristic for a polyp, is visible as a lead point

CT and MRI may show infiltration of the bowel wall, dilatation of the lumen, ascites and enlarged mesenteric lymph nodes (Fig. 22b).

PET- CT and Whole body MRI with DWI are used for the staging and evaluation of response after treatment in lymphoma (Littooij et al. 2014).

Unusual tumors in childhood also include the malignant counterparts of lipomas, fibromas, neurofibromas and leiomyomas (Parker 2003).

## 7.4 Protein-Losing Enteropathies

Many etiologies for protein-losing enteropathies (celiac disease, intestinal lymphangiectasis, allergic gastroenteritis, cow milk protein allergy, Crohn disease, cystic fibrosis, collagen vascular disease, short bowel, intestinal transplants and others) have been identified.

Celiac disease is the commonest cause of intestinal malabsorption in childhood. The etiology is an intolerance to the gliadin component of gluten. Most patients present early in childhood with failure to thrive, abdominal distension, diarrhea and stools that may be steatorrheic. Adolescents have delayed puberty, anorexia and clinical findings due to hypocalcemia and hypoproteinemia. It is distinctly unusual in people of Asian and African descent.

Diagnosis is made by clinical findings and jejunal biopsy that shows subtotal villous atrophy.

Imaging is done before diagnosis is made or to exclude other causes.

CR may be normal or show small bowel dilatation.

On US, hyperperistalsis, fluid-filled dilated small bowel loops, thickened bowel wall, enlarged mesenteric lymph nodes and ascites can be seen (Fig. 23).

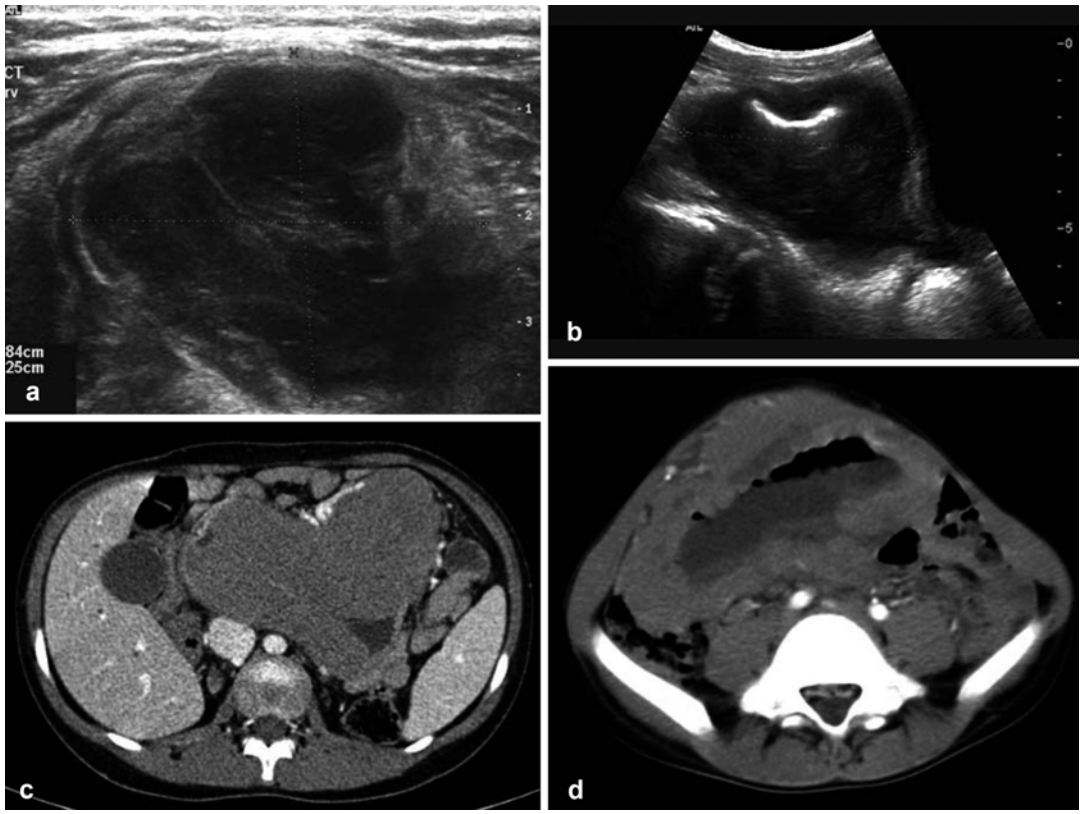


**Fig. 22** (**a**) Burkitt lymphoma. Note the hypoechoic mass located in the ileal wall. (**b**) Burkitt lymphoma of the small bowel wall with visualization of air (hyperechogenic band) containing small bowel loop. (**c**, **d**) Burkitt lymphoma depicted as a hypodense, contrast enhancing mass in the ileum on CT. Dilated neighboring loops from secondary obstruction

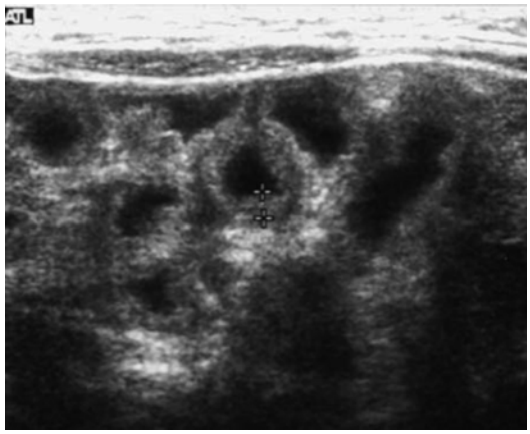

**Fig. 23** Ultrasound in a patient with celiac disease. Fluid-filled, dilated small bowel with a thickened wall is demonstrated

The upper GI tract examination may show dilated small bowel, thickened mucosal folds and rarely flocculation, as well as segmentation of the barium (Parker 2003).

Small intestinal lymphangiectasia is a primary or secondary protein-losing enteropathy. As a secondary disorder it is acquired as a result of surgical damage to the lymphatic vessels, chronic right-sided heart failure, ascites, constrictive pericarditis, retroperitoneal tumor, tuberculosis or inflammatory bowel disease. Primary intestinal lymphangiectasia is a rare congenital protein-losing enteropathy characterized by hypoplastic lymphatic vessels within the intestinal mucosa, submucosa and small bowel mesentery. Lymphatic flow is obstructed and small intestinal lymphatic channels will dilate, causing the small bowel wall to appear thickened. Rupture of these dilated lymphatics into the small bowel lumen and occasionally into the peritoneal cavity results in hypoproteinemia, steatorrhea, lymphopenia, ascites and even pleural effusions.

Findings on CR and contrast studies are similar to celiac disease, may be normal or show mild dilatation of the small bowel.

On US, hyperperistalsis, fluid-filled dilated small bowel loops, thickened bowel wall, hyperechogenic, edematous mesentery and ascites can be seen.

Abdominal CT images may show diffuse small intestinal wall thickening and dilatation, mesenteric edema, ascites and possibly relatively low density confluent mesenteric soft tissue masses that represent lymphangiomas (Parker 2003).

## 7.5 Inflammatory Disease (Crohn Disease)

In Crohn disease, the underlying etiology is a segmental transmural granulomatous inflammation that can be seen to extend from mouth to anus. It is the most common chronic inflammatory condition of the small bowel in children. While a total of 25 % of cases present during childhood, it is rare before the age of 5–8 years. Most affected are firstly the terminal ileum and secondly the colon. It is limited to the colon in 15 % of cases. The inflammation can be localized in one or more segments. In the case of multiple segments, normal intestine lies interdispersed between inflamed intestine. Edema and fibrotic thickening of the affected wall and spasms cause a narrowing of the intestinal lumen and resulting pre-stenotic dilatation. In cases of inflammatory bowel disease patients present not only with diarrhea, abdominal pain, anorexia, a palpable abdominal mass and, if of long-standing, anorectal fistulas, but also with a failure to thrive, delayed puberty, fever, aphthous stomatitis, arthralgia, arthritis, sacroiliitis and erythema nodosum.

CR may often be normal. Adynamic ileus, bowel wall thickening and occasionally focally abnormal dilated loops with thickened bowel wall can be seen in the case of acute exacerbation. Imaging the small bowel has always been difficult due to the long and winding shape of the lumen, overlapping segments and motility patterns. Small bowel lesions have traditionally been assessed on barium contrast follow-through exam or enteroclysis. Granularity, reflecting mucosal edema, mucosal fold thickening, effacement of the mucosal pattern, cobblestone pattern (because of linear and transverse ulceration), pseudopolyps, narrowed bowel loops, pre-stenotic dilatation, separation and retraction of bowel loops (inflamed, thickened, and fibrotic mesentery), as well as enteroenteric and enterocolic fistulas can be seen (Fig. 24a, b) (Parker 2003; Dillman et al. 2015).

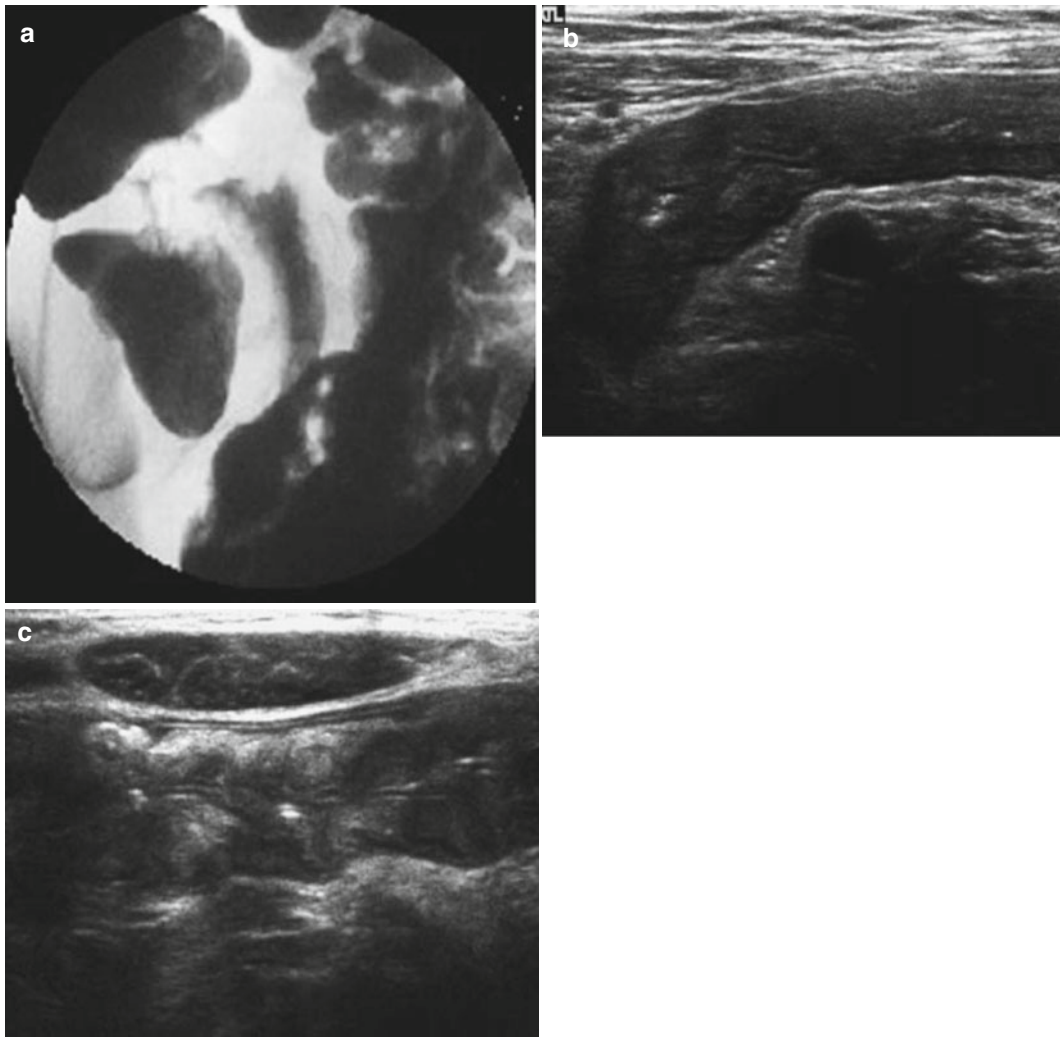


**Fig. 24** (**a**) Traditional small bowel study image of the terminal ileum in a boy with Crohn disease. The terminal ileum is affected and narrowed with prestenotic dilatation. There is effacement of the mucosal pattern and separation of the loops. Infiltration of the mesenteric fat causes isolation of the terminal ileum. (**b**-**c**) The US images show irregular bowel wall thickening and hyperechoic thickened mesentery

US is useful as a screening tool and in the follow-up to evaluate the therapeutic result, as well as complications such as abscesses.

US is able to show thickened bowel walls, separation of bowel loops because of thickened and edematous, hyperechogenic mesentery and absence of peristaltic movements. Color Doppler is useful to detect a higher flow velocity in the superior mesenteric artery and to identify areas of active inflammation in which an increased Doppler signal will be found in and around the thickened bowel wall (Fig. 24c).

CT is only used to evaluate complications, when US is inconclusive or percutaneous drainage is required (Parker 2003; Devos and Meradji 2003).

Recent developments in MR techniques allow much faster and higher quality image acquisition. Frokjaer et al. (2005) showed that high quality MR images can reliably identify stenosis, cobblestone pattern, fissures, wall thickening, wall enhancement upon intravenous gadolinium and exoenteric changes such as mesenterial inflammation, fibro-fatty proliferation, lymphadenopathy, hypervascularity, abscesses, and fistulae

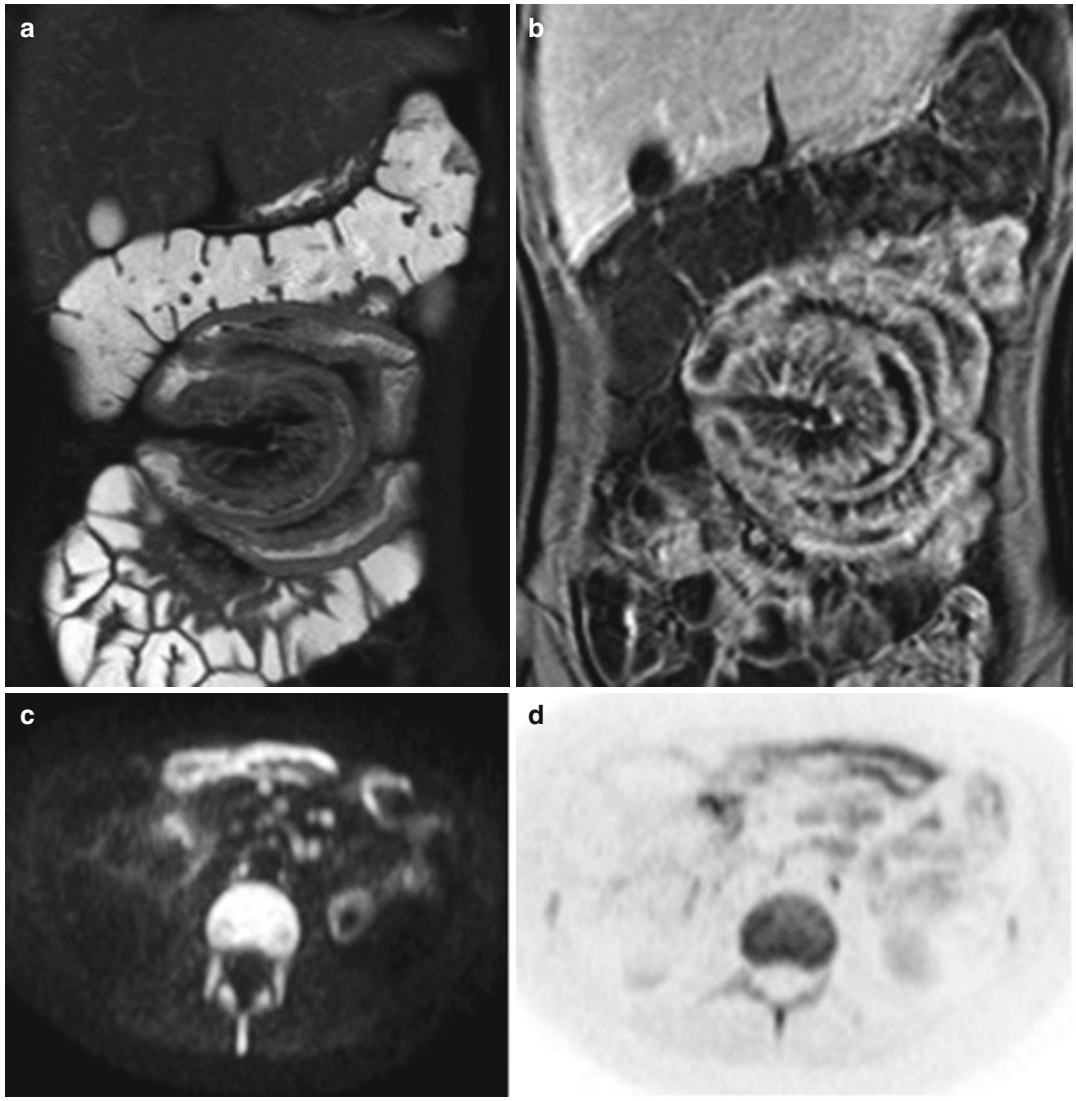


**Fig. 25** MR Enterography in Crohn disease in a 16-year-old male patient. (**a**) Coronal T2 image demonstrating long segment of thickened narrowed small bowel wall with hyperaemic mesenentry. (**b**) Coronal T1 FS image post IV contrast demonstrates diffuse mural enhancement in the involved segment. (**c**, **d**) DWI map demonstrating restricted diffusion in the involved small bowel segments. Note the presence of skip lesions. The mural inflammation is also appreciable on the DWI images

(Fig. 25). Luminal distension, achieved by oral or via the duodenal tube administration, is a necessity since collapsed bowel loops can conceal even large lesions, or the exact grade of obstruction can be underestimated. Certainly, in cases where repeat evaluation during treatment is necessary, and when US is inconclusive, MR has gained acceptance (Watson and Olsen 2015; Smolinski et al. 2014; Ziech et al. 2014).

Eosinophilic colitis (EC) is a rare condition with unknown etiology in children. The clinical and radiological findings may mimic Crohn disease. On US and CT scan, there is bowel wall thickening, mesenteric lymphadenopathy and rarely ascites. Caecal involvement in EC is very prominent, but the involvement of the terminal ileum ranges from mild to moderate (Savino et al. 2011; Brandon et al. 2013).

## 7.6 Superior Mesenteric Artery Syndrome

Superior mesenteric artery (SMA) syndrome is an uncommon but well-recognized clinical entity characterized by compression of the third, or transverse, portion of the duodenum against the aorta by the SMA, resulting in chronic, intermittent or acute complete or partial duodenal obstruction. Clinical symptoms are chronic upper abdominal symptoms such as epigastric pain, nausea, vomiting (bilious or partially digested food), postprandial discomfort and sometimes features of subacute small bowel obstruction. The stomach can be massively dilated and perforation has been described (Carty et al. 2005; Parker 2003).

An asthenic habitus is noted in about 80 % of cases. Other possible etiologic factors are exaggerated lumbar lordosis, depletion of the mesenteric fat caused by rapid severe weight loss, anorexia nervosa, spinal disease or deformity, anatomic anomalies such as abnormally high and fixed position of the ligament of Treitz with an upward displacement of the duodenum, and unusually low origin of the SMA and the familial SMA syndrome (Ortiz et al. 1990). An acute form of SMA syndrome is described following scoliosis treatment in which presumably the abrupt straightening of the spine changes the angle at which the SMA branches from the aorta causing duodenal compression.

CR may show gastric dilatation; however, the stomach may be decompressed by vomiting.

A UGI shows a high-grade partial obstruction of the third portion of the duodenum (Ortiz et al. 1990). US and CT may help measure the angle between the SMA and the Aorta.

## 7.7 Cystic Fibrosis

Cystic fibrosis (CF), with an incidence of 1 in 2500 white live births, is the most common lethal, autosomal recessive disorder in white children (Chaudry et al. 2006; Lardenoye et al. 2004; Agrons et al. 1996). This disorder is caused by mutations in the CF transmembrane regulator (CFTR) gene, which is located on the long arm of chromosome 7. Multiple different mutations of this gene exist.

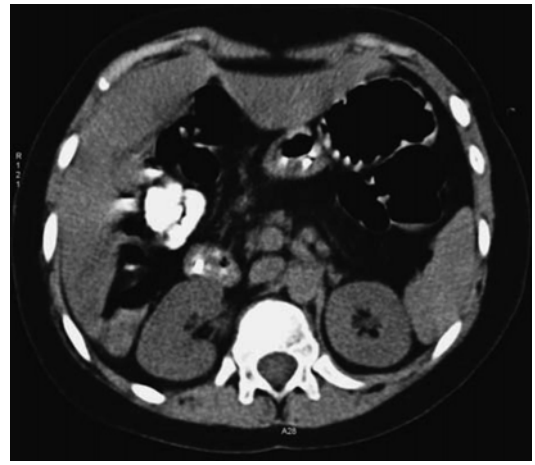

**Fig. 26** CT image depicts the virtual disappearance of the pancreas in a patient with CF

The gastrointestinal manifestations are seen throughout childhood, from infancy to adolescence. They result from abnormally viscous luminal secretions within hollow viscera and the ducts of solid organs.

Bowel obstruction may be present at birth due to meconium ileus. Older children might present with complications (Fig. 26), such as, distal intestinal obstruction syndrome (DIOS), colonic stricture(s) and, less commonly, intussusception, fecal impaction of the appendix, gastroesophageal reflux, or recurrent rectal prolapse.

### 7.7.1 Meconium Ileus

Between 10 and 15 % of newborns with CF are affected by meconium ileus resulting from inspissated intraluminal meconium at the terminal ileum, the narrowest portion of the GI tract (Carty et al. 2005).

Patients present with failure to pass meconium and a distended, painful abdomen.

CR will demonstrate a distended abdomen due to distal small bowel obstruction with many markedly dilated proximal small bowel loops and a bubbly appearance of the bowel in the right lower quadrant caused by mixing air with viscous impacted meconium in the terminal ileum (Fig. 27).

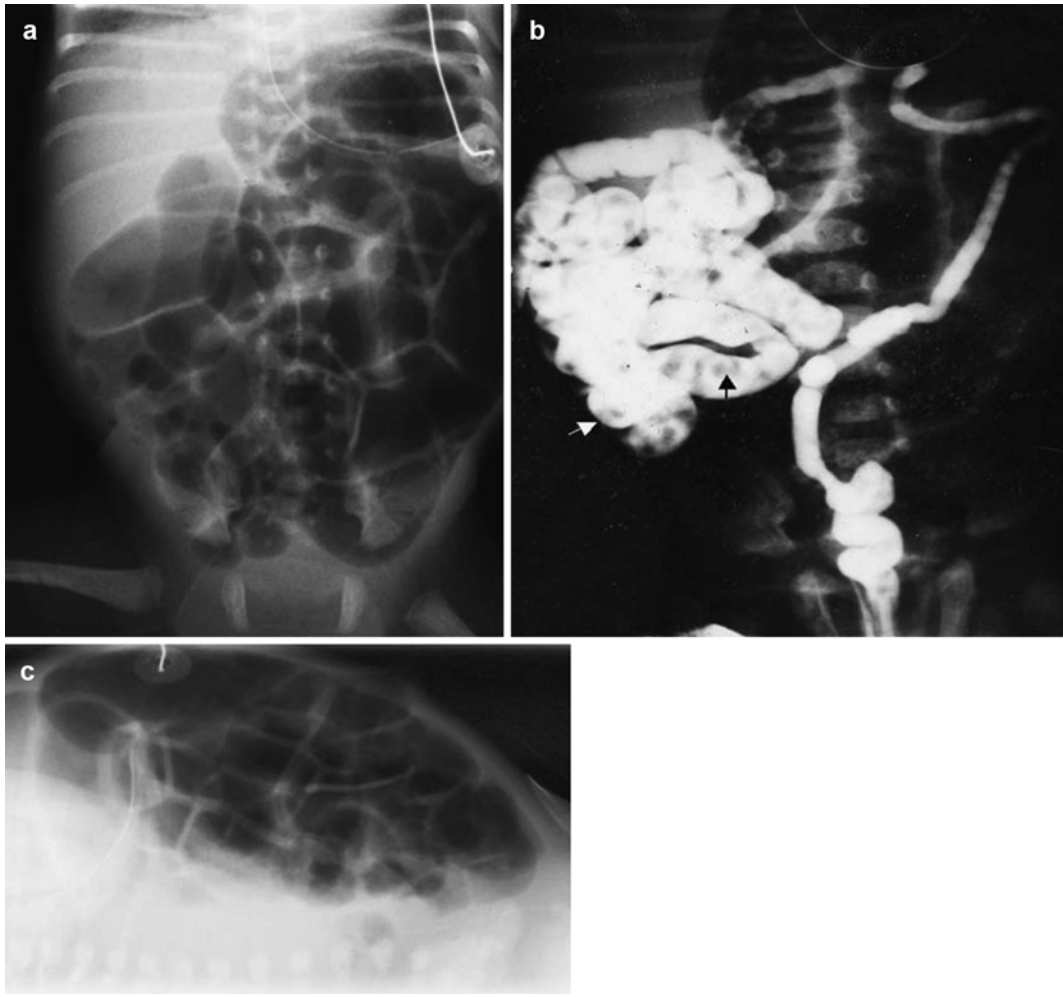


**Fig. 27** (**a**) Meconium ileus in a 3-day-old neonate. The small bowel is dilated and has a bubbly irregularity in the right lower quadrant. (**b**) Contrast enema shows "microcolon" as a result of meconium ileus. Meconium pellets demonstrated in the terminal ileum (*arrows*) (**c**) On the lateral film of the abdomen no colonic loops are visible. There are no air fluid levels

On US, this impacted meconium will be located in the ileum and has a distinctive appearance. Contrast enema will demonstrate a microcolon with visualization of the meconium pellets in the terminal ileum. The microcolon results from the failure of the meconium to pass into the colon, which would thereby allow the colon to assume its normal caliber (Fig. 28). In about 50 % of cases the enema will be curative.

Complications of meconium ileus are volvulus, perforation, small bowel atresia, and meconium peritonitis with abdominal calcifications.

### 7.7.2 Distal Intestinal Obstruction Syndrome (DIOS)

DIOS will develop in approximately 15 % of patients with CF (Maus et al. 2015; Carty et al. 2005).

Clinical symptoms are related to those caused by a varying severity of bowel obstruction with recurrent abdominal pain and a palpable right lower quadrant mass.

CR shows a proximal small bowel obstruction with faecal impaction in the terminal ileum and caecum (Fig. 29). The term "meconium ileus equivalent" should be discarded.

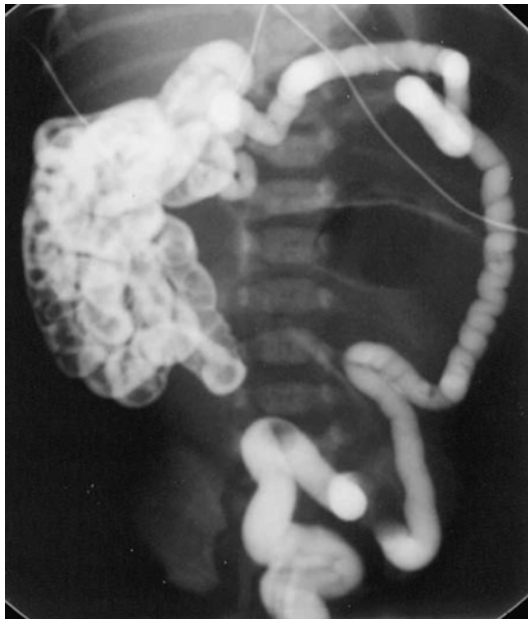

**Fig. 28** Contrast enema with water-soluble contrast medium which demonstrates a meconium ileus with impaction of meconium in the ileum and an unused colon

A contrast enema with a water-soluble contrast medium will show fecal impaction in the terminal ileum and proximal colon. This procedure may also have a therapeutic effect in 1/3 of patients (Devos and Meradji 2003).

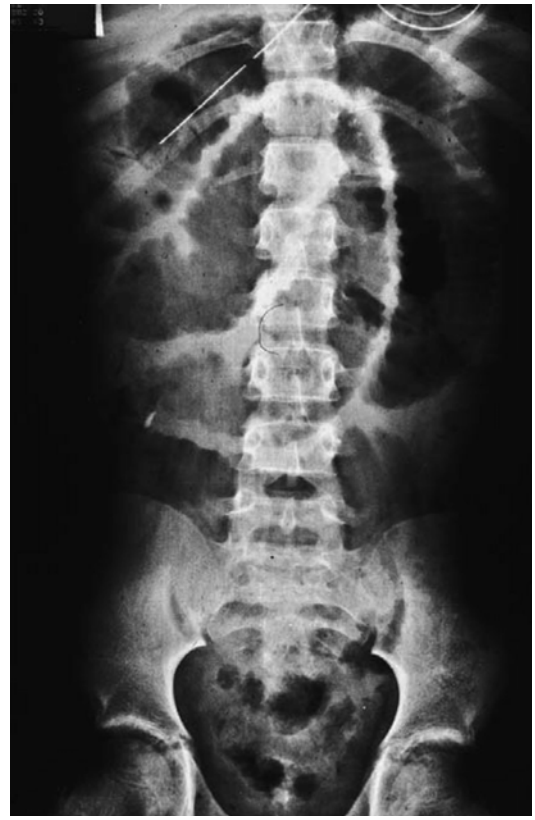

**Fig. 29** A boy with cystic fibrosis complicated with distal intestinal obstruction syndrome. Note the dilated intestinal loops and huge fecal impaction in the terminal ileum and caecum

## 7.8 Abdominal Tuberculosis

Abdominal tuberculosis (TB) is rare in childhood and usually a diagnostic challenge, particularly in the absence of active pulmonary infection. Clinical manifestations and results of laboratory studies are also nonspecific. Intestinal TB can involve any segment of the gastrointestinal tract, but has a predilection for the ileocecal valve and the adjacent ileum and cecum (Parker 2003; Engin and Balk 2005).

Clinical features suggestive of TB are a history of fever, abdominal pain and weight loss.

CR may show no abnormalities or show a few or multiple air-fluid levels in the small bowel loops due to the enteritis component.

A UGI reveals thickened folds, spasticity, irregular contours, and ulcers involving the cecum

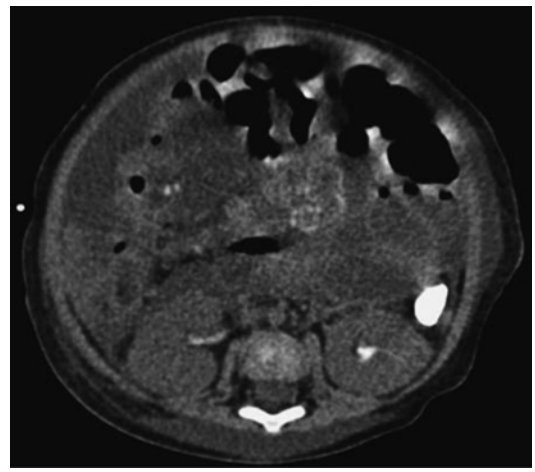

**Fig. 30** Intestinal tuberculosis. CT scan shows subtle central heterogenic, hypodense masses with peripheral ringlike calcifications (lymphadenitis) and ascites

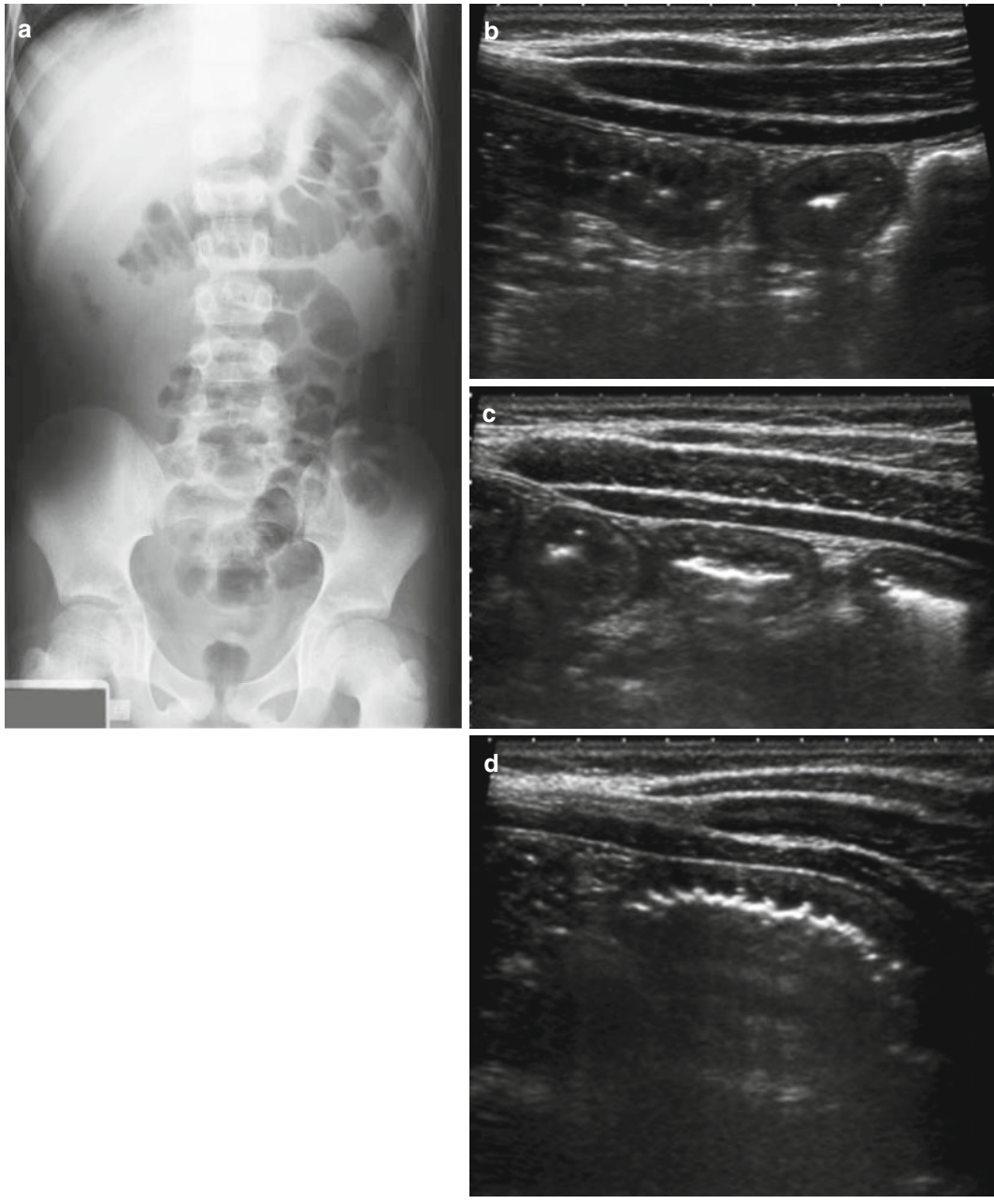


**Fig. 31** (**a**) Supine abdominal film of a child with Henoch-Schönlein purpura. (**b–d**) US images; Multiple thickened loops of small bowel are demonstrated

and terminal ileum. In the case of fibrosis, single or multiple short strictures that can be localized in a single segment or be present throughout the bowel will be found. Incidentally, fistulae formation can be recognized radiographically.

Sonographic evaluation may show thickening of the wall of the cecum and terminal ileum, an inflammatory mass, dilated small bowel loops, an increase of mesenteric thickness and echogenicity (due to fat deposition), mesenteric lymphadenopathy, and ascites. The lymph nodes are heterogeneous and can contain calcifications. Calcifications are virtually pathognomonic for TB (Jain et al. 1995).

Imaging with CT will show the same findings as with US, but is the preferred examination for obese children, children in which US is difficult because of heavy pain when touching the abdomen, or if biopsy is needed (Fig. 30).

MRI of abdominal TB lymphadenopathy shows a variety of signal intensities and patterns of contrast enhancement and is described by DeBacker et al. (2005). Signal intensities, in relation to abdominal wall muscle, are hyperintensity on T2-WI with, in some cases, a hypointense peripheral rim. There is internal heterogeneity with hypo-/iso-intensity on T1-WI, also occasionally demonstrating a peripheral rim on this sequence. Contrast-enhanced fat-suppressed T1-WI demonstrates predominantly peripheral enhancement.

Crohn disease and peri-appendiceal abscesses should be considered as differential diagnoses. Less frequently in the case of children, carcinoma and lymphoma.

## 7.9 Henoch-Schönlein Purpura

Henoch-Schönlein purpura is a type of hypersensitivity vasculitis and inflammatory response within the blood vessels. It is caused by an abnormal response of the immune system. The syndrome is usually seen in children and is more common in boys (Parker 2003).

Clinical symptoms are purple spots on the skin, joint pain, gastrointestinal symptoms and glomerulonephritis. Gastrointestinal symptoms include abdominal pain, nausea, vomiting, diarrhea, and bloody stools. Bleeding into the bowel wall occurs in about half of patients and may act as a lead point for intussusception.

Routine abdominal radiographs (Fig. 31a) give no significant information and are not recommended, unless perforation is clinically suspected.

US is the imaging modality of choice and will show thickened bowel wall, ascites, ileus of affected loops, bowel dilatation, and possible enteroenteric intussusceptions (Fig. 31b) (Connolly and O'Halpin 1994).

## References


Agrons GA, Corse WR, Markowitz RI et al (1996) Gastrointestinal manifestations of cystic fibrosis: radiologic-pathologic correlation. Radiographics 16:871–893

Berrocal T, Lamas M, Gutieerrez J et al (1999) Congenital anomalies of the small intestine, colon, and rectum. Radiographics 19:1219–1236

Blickman et al (2009) Pediatric Radiology: The Requisites, 3e (Requisites in Radiology) Mosby Elsevier, Philadelphia, pp 87–90

Boudiaf M, Soyer P, Terem C et al (2001) CT evaluation of small bowel obstruction. Radiographics 21:613–624 (review)

Brandon JL, Schroeder S, Furuta GT et al (2013) CT imaging features of eosinophilic colitis in children. Pediatr Radiol 43(6):697–702

Carty H, Brunelle F, Stringer D et al (2005) The gastrointestinal tract. In: Carty H, Brunelle F, Stringer D, Kao S (eds) Imaging children, vol 2, 2nd edn. Elsevier Churchill Livingston, Edinburgh, pp 1289–1545

Chaudry G, Navarro OM, Levine DS et al (2006) Abdominal manifestations of cystic fibrosis in children. PediatrRadiol 36:233–240

Connolly B, O'Halpin D (1994) Sonographic evaluation of the abdomen in Henoch-Schönleinpurpura. Clinradiol 49:320–323

De Backer AI1, Mortelé KJ, Deeren D, Vanschoubroeck IJ, De Keulenaer BL (2005) Abdominal tuberculous lymphadenopathy: MRI features. Eur Radiol. 15(10):2104–2109

Devos A, Meradji M (2003) Hoofdstuk VII: Maag-Darmkanaal. In: Werkboek Kinderradiologie. pp 72–99

Dillman JR, Smith EA, Sanchez R, DiPietro MA, Fazeli Dehkordy S, Adler J et al. (2015) Prospective cohort study of ultrasound-ultrasound and ultrasound-MR enterography agreement in the evaluation of pediatric small bowel Crohn disease. Pediatr Radiol. (Epub ahead of print)

Engin G, Balk E (2005) Imaging findings of intestinal tuberculosis. J Comput Assist Tomogr 29:37–41

Frokjaer JB, Larsen E, Steffensen E et al (2005) Magnetic resonance imaging of the small bowel in Crohn's disease. Scand J Gastroenterol 40:832–842

Grier D (1999) Radiology of pediatric gastrointestinal emergencies. In: Carty H (ed) Emergency pediatric radiology. Springer, Berlin/Heidelberg/New York, pp 117–182

Husband JE, Reznek RH (2004) Imaging in oncology, 2nd edn, parts III and IV. Taylor and Francis, London, pp 817–874 and pp 921–998

Jain R, Sawhney S, Bhargava DK et al (1995) Diagnosis of abdominal tuberculosis: sonographic findings in patients with early disease. AJR Am J Roentgenol 165:1391–1395

Kluge R, Kurch L, Montravers F et al (2013) FDG PET/CT in children and adolescents with lymphoma. Pediatr Radiol 43(4):406–417

Kucińska-Chahwan A, Posiewka A, Bijok J, Jakiel G, Roszkowski T (2015) Clinical significance of the prenatal double bubble sign – single institution experience. Prenat Diagn 35(11):1093–1096

Lardenoye SW, Puylaert JB, Smit MJ et al (2004) Appendix in children with cystic fibrosis: US features. Radiology 232:187–189

Lioubashevsky N, Hiller N, Rozovsky K et al (2013) Ileocolic versus small-bowel intussusception in children: can US enable reliable differentiation? Radiology 269(1):266–271

Littooij AS, Kwee TC, Barber I et al (2014) Whole-body MRI for initial staging of paediatric lymphoma: prospective comparison to an FDG-PET/CT-based reference standard. Eur Radiol 24(5):1153–1165

Mateen MA, Saleem S, Rao PC, Gangadhar V, Reddy DN (2006) Transient small bowel intussusceptions – ultrasound findings and clinical significance. Abdom Imaging 31(4):410–416

Maus J, Mana F, Reynaert H, Urbain D (2015) Distal intestinal obstruction in CF patients. Acta Gastroenterol Belg 78(1):49–52

Mc Laughlin D, Puri P (2013) Familial megacystic microcolon intestinal hyperperistalsis syndrome: a systematic review. Pediatr Surg Int 29(9):947–951

Nicolaou S, Kai B, Ho S et al (2005) Imaging of acute small bowel obstruction. AJR Am J Roentgenol 185:1036–1044 (review)

Orth RC, Guillerman RP, Zhang W, Masand P, Bisset GS 3rd (2015) Prospective comparison of MR imaging and US for the diagnosis of paediatric appendicitis. Radiology 277(3):927

Ortiz C, Cleveland RH, Blickman JG et al (1990) Familial superior mesenteric artery syndrome. PediatrRadiol 20:588–589

Parker BR (2003) Abdominal and gastrointestinal tract, small intestine. In: Kuhn J, Slovis T, Holler J (eds) Caffey's pediatric diagnostic imaging, 10th edn. Mosby, Philadelphia, pp 1616–1648

Pastore V, Cocomazzi R, Basile A et al (2014) Limits and advantages of abdominal ultrasonography in children with acute appendicitis syndrome. Afr J Paediatr Surg 11(4):293–296

Rosines LA, Chow DS, Lampl BS et al (2014) Value of gadolinium enhancing MRI in the detection of acute appendicitis in children and adoloscents. AJR Am J Roentgenol 203(5):W543–W548

Savino A, Salvatore R, Cafarotti A et al (2011) Role of ultrasonography in the diagnosis and follow-up of pediatric eosinophilic gastroenteritis: a case report and review of the literature. Ultraschall Med 32 Suppl 2:E57–E62

Schöneberg C, Schweiger B, Metzelder M et al (2014) The injured child - diagnostic work-up in the emergency room. Unfallchirurg 117(9):829–841

Shah S (2013) An update on common gastrointestinal emergencies. Emerg Med Clin North Am 31(3):775–793

Shamaly H, Jamalia J, Omari H et al (2013) Congenital chloride diarrhea presenting in newborn as a rare cause of meconium ileus. J Perinatol 33(2):154–156

Shankar KR, Roche CJ, Carty HM et al (2011) Cystic retroperitoneal lymphangioma: treatment by image-guided percutaneous catheter drainage and sclerotherapy. Eur Radiol 11(6):1021–1023

Smolinski S, George M, Dredar A et al (2014) Magnetic resonance enterography in evaluation and management of children with Crohn's disease. Semin Ultrasound CT MR 35(4):331–348

Stéphane V, Samuel B, Vincent D et al (2013) Comparison of PET-CT and magnetic resonance diffusion weighted imaging with body suppression (DWIBS) for initial staging of malignant lymphomas. Eur J Radiol 82(11):2011–2017

Strouse PJ, DiPietro MA, Saez F (2003) Transient small-bowel intussusception in children on CT. PediatrRadiol 33:316–320

Vali R, Daneman A, McQuattie S, Shammas A (2015) The value of repeat scintigraphy in patients with a high clinical suspicion for Meckel diverticulum after a negative or equivocal first Meckel scan. Pediatr Radiol 45(10):1506–1514

Watanabe T, Takahashi M, Amari S (2013) Olive oil enema in a pre-term infant with milk curd syndrome. Pediatr Int 55(4):e93–e96

Watson TA, Olsen ØE (2015) Fusion and subtraction post-processing in body MRI. Pediatr Radiol 45(2):273–282. doi: 10.1007/s00247-014-3129-3. Epub 2014 Sep 2. PMID: 25179564

Wiarda BM, Stolk M, Heine DG et al (2013) Patient burden and patient preference: comparing magnetic resonance enteroclysis, capsule endoscopy and balloon-assisted enteroscopy. J Gastroenterol Hepatol 28(3):464–471

Yousefzadeh DK (2009) The position of the duodenojejunal junction: the wrong horse to bet on in diagnosing or excluding malrotation. Pediatr Radiol 39 Suppl 2:S172–S177

Yousefzadeh DK, Kang L, Tessicini L (2010) Assessment of retromesenteric position of the third portion of the duodenum: an US feasibility study in 33 newborns. Pediatr Radiol 40(9):1476–1484

Ziech ML, Hummel TZ, Smets AM et al (2014) Accuracy of abdominal ultrasound and MRI for detection of Crohn disease and ulcerative colitis in children. Pediatr Radiol 44(11):1370–1378

# The Colon

Melanie P. Hiorns

## Contents




### Abstract

Pathology affecting the colon may be either congenital, or acquired during childhood. Congenital conditions are relatively uncommon but important to recognize, and frequently need diagnosis and immediate treatment in the perinatal period. Acquired conditions including appendicitis and intussusception also need prompt recognition, and possible treatment, by the pediatric radiologist who must be familiar with the radiological presentations and the management pathways. This chapter reviews the imaging of this broad spectrum of diseases with recommendations on imaging pathways and best practice.


M.P. Hiorns, MBBS, MRCP, FRCR
Department of Radiology, Great Ormond Street Hospital, London WC1N 3JH, UK
e-mail: melanie.hiorns@gosh.nhs.uk



S. Stafrace, J.G. (Hans) Blickman (eds.), *Radiological Imaging of the Digestive Tract in Infants and Children*, Medical Radiology, DOI 10.1007/978-3-319-18434-0_7

# 1 Appendicitis

## 1.1 Overview

Appendicitis most commonly occurs over the age of 5 years, is rare in those under 2 years, but may occur at any age and is the most common condition requiring emergency abdominal surgery in children (Janik and Firor 1979). Incidence in the paediatric age group shows wide geographical variation, but overall incidence is declining. Historic quoted incidence rates from the 1940s were approximately 1 in every 250 children, but a study in the late 1990s showed rates had been falling over the previous decades falling to 1 in 850 in children and young adults (Williams et al. 1998). Rates in the Western world have continued to decline and are now quoted at 1 in 900 or less. The aetiology is that of appendiceal luminal obstruction, most commonly by lymphoid hyperplasia (60 %) but also by hard concretions (faecoliths 33 %), faecal impaction or appendiceal calculi (appendicolith). Rarer causes in children include tumour, stricture, parasites and Crohn disease. Appendiceal obstruction is followed by luminal distension, ischaemia and bacterial invasion. Necrosis of the appendiceal wall then develops, resulting in perforation and abscess formation.

Clinical criteria are most often used to make the diagnosis of appendicitis, and the common clinical symptoms include cramping in the right iliac fossa and lower abdominal pain, vomiting, diarrhoea and sometimes dysuria. The signs are those of fever (56 %), a leucocytosis (88 %) of between 10,000 cells per millilitre and 20,000 cells per millilitre, guarding and tenderness in the right iliac fossa. However, the classic signs and symptoms are not present in up to 30 % of patients, and hence the clinical diagnosis is not always straightforward. Imaging plays an increasingly important role in the diagnostic pathway.

The main imaging technique in children with suspected appendicitis is compression-graded ultrasound. Much has been written and described about the findings on the plain abdominal radiograph (AXR), but the AXR is typically normal in the early stages of appendicitis and can remain normal in more than 50 % of cases. Plain films are insensitive and non-specific. Current practice is therefore either to make a clinical decision to go to appendectomy, or not, meaning to observe the child, or to proceed to imaging for diagnostic guidance and feel confident in sending the child home.

The sensitivity of ultrasound has ranged from 80 to 94 % and the specificity between 86 and 98 % in various published series (Abu-Yousef et al. 1987; Jeffrey et al. 1988; Puylaert 1986 Sivit et al. 1992; Vignault et al. 1990). Ultrasound has several advantages as a diagnostic tool in the setting of appendicitis, and these include its lower cost than other techniques, lack of ionising radiation and its ability to assess ovarian pathology that can often mimic acute appendicitis in young female patients. Furthermore, ultrasound is useful for excluding other differential diagnoses including intussusception. The disadvantages of ultrasound are a higher dependency on the skills of the operator and its reduced sensitivity in obese patients or in patients whose degree of abdominal pain prevents a thorough examination.

In the last decade computed tomography (CT) has become widely utilised in the adult population in the diagnosis of the acute abdomen, and this is increasingly common practice in children. The main advantages of CT include less operator dependency than sonography and a subsequent higher diagnostic accuracy and enhanced delineation of disease extent in perforated appendicitis. The significant disadvantages, particularly in children, are those of lack of intra-abdominal fat, a moderate to high radiation burden and, depending on the age of the child, the need for sedation or general anaesthesia (in US no sedation or anaesthesia is used preferentially). In a large series of 2763 patients from 2013, the sensitivity, specificity, positive predictive value and negative predictive value for ultrasonography were 99.1, 91.7, 96.5 and 97.7 %, respectively; for computed tomography 96.4, 95.4, 95.6

and 96.3 %, respectively; and for physical examination 99.0, 76.1, 88.1 and 97.6 %, respectively (Park et al. 2013). This suggests that if the physical examination is negative, then any imaging study may be unnecessary, but if imaging is performed, then, in the paediatric population, ultrasound matches CT for diagnostic performance and there is very little clinical justification for performing CT. Previously a meta-analysis from 2006 that included 9356 children demonstrated a higher sensitivity for CT over US (94 % versus 88 %) (Doria et al. 2006), but the authors specifically stated the associated risks from the radiation associated with CT might offset this advantage. A separate more recent prospective study of 2625 children found variation in the sensitivity and rate of visualisation of the appendix across sites but still concluded that assuming the appendix was demonstrated then US had a universally high sensitivity and specificity (Mittal et al. 2013). Nonvisualisation of the appendix, with an otherwise normal ultrasound scan, confers a significantly lower risk for appendicitis (either perforated or unperforated), and there is a strong argument for active clinical observation rather than proceeding to CT (Stewart et al. 2012). It has been further demonstrated that clinical outcomes do not suffer as a result of a transition to an ultrasound-first pathway from a previously CT-based pathway (Le et al. 2013).

The current suggested diagnostic approach in children is therefore to proceed directly to ultrasound as the first-line imaging tool (if the clinical findings suggest that imaging is necessary) particularly in girls. AXR is no longer routinely indicated (but if it is performed, it is not for the purpose of making the diagnosis of appendicitis, but is only to exclude complications such as free intraperitoneal air or to exclude other confounding diagnoses such as renal colic, small bowel obstruction or constipation). Following the results of the ultrasound, clinical examination and laboratory tests, CT should only then be considered depending on the degree of confidence in the diagnosis and the institution. Modern management is more towards clinical observation if the ultrasound is inconclusive (Stewart et al. 2012).

Going forward it is possible that MRI may supplant CT as the secondary modality to follow inconclusive appendix sonography. A recent study of 60 paediatric patients with inconclusive sonography for appendicitis has shown a sensitivity and specificity of 100 and 96 % (Herliczek et al. 2013). MRI is becoming a viable alternative to CT in this context, and a short four-sequence MRI consisting of coronal and axial single-shot turbo spin echo (SS-TSE) T2, coronal spectral adiabatic inversion recovery (SPAIR) and axial SS-TSE T2 with fat saturation has been proposed with good results (Moore et al. 2012).

## 1.2 Graded Compression Sonography for Appendicitis

Graded compression sonography for appendicitis was first described by Puylaert (Puylaert 1986). Normal bowel is readily compressible when light pressure is applied with an ultrasound transducer. Processes affecting the bowel wall such as oedema, inflammation, neoplasm or haemorrhage alter the compliance of the bowel wall and render it relatively noncompressible. The basic principle underlying graded compression in diagnosing appendicitis is to compress away the normal lumen of the terminal ileum and the caecum and to allow better visualisation of the noncompressible inflamed or obstructed appendix. A linear array transducer is used, typically a 6- to 8-MHz transducer depending on the patient's age and body habitus, although an 8- to 15-MHz transducer may be suitable in infants. The transducer must have sufficient penetration to image the iliac vessel and psoas muscles as visualisation of these structures is necessary for an adequate examination, the appendix lying anterior to these structures. It is often helpful with co-operative children to ask the patient to point to the site of maximal pain and tenderness. This can be particularly helpful if the appendix is in an atypical site. Initially the right flank is scanned with light pressure to identify the ascending colon, this being the largest luminal structure of the gastrointestinal tract (with little or no peristalsis), and is seen adjacent to the abdominal wall. The right

colon is then followed inferiorly to termination at the caecum. To avoid inducing pain, pressure is gradually increased over the tip of the caecum. Bowel air and fluid within the caecum and terminal ileum are gradually compressed away, allowing visualisation of the appendix. The study is performed in both longitudinal and transverse planes.

Criteria to be sought include: enlarged appendix, fluid in the appendiceal lumen, lack of compressibility of the appendix, colour in the appendiceal wall on colour Doppler ultrasound, inflammatory changes in the perienteric fat in the right lower quadrant, caecal wall thickening, right lower quadrant lymph nodes and peritoneal fluid (Kessler et al. 2004; Quigley and Stafrace 2013).

The inability to visualise a normal appendix has previously been considered a major weakness of ultrasound in assessing patients with suspected appendicitis. However, with technological advances in equipment and increasing operator experience, the normal appendix should be visualised in 64–82 % of healthy patients (Rioux 1992; Rettenbacher et al. 2001; Kessler et al. 2004). Inability to visualise the appendix, and in the context of an otherwise normal scan, is an indication for active clinical observation rather than direct referral for CT (Stewart et al. 2012).

### 1.2.1 Diagnostic Criteria

Sonographic criteria for acute appendicitis have conventionally included a noncompressible appendix with an outer AP diameter of at least 6 mm (Kessler et al. 2004), mural thickness of 3 mm or greater, or the presence of an appendicolith in an appendix of any size (Figs. 1 and 2). The two most useful ultrasound signs have been those of an appendiceal diameter of 6 mm (sensitivity 98 %, specificity 98 %, positive predictive value (PPV) 98 %, negative predictive values (NPV) 98 %) and non-compressibility (sensitivity 96 %, specificity 96 %, PPV 96 %, NPV 96 % (Kessler et al. 2004)). If the appendix measures less than 6 mm in diameter, particularly if compressible, this should be considered normal. The use of colour Doppler may be helpful in showing hyperaemia associated with appendiceal wall inflammation.

However, recent re-evaluation of these criteria suggests that using a maximal outer diameter of 7 mm, and a wall thickness of greater than 1.7 mm, improves diagnostic accuracy and compares favourably with CT (Goldin et al. 2011). Furthermore, the presence of echogenic periappendiceal fat is the most important diagnostic criterion for acute appendicitis in children, and strict application of other criteria such as diameter should be avoided (Trout et al. 2012)

Presence of a hypoechoic fluid collection containing an appendicolith or a fluid collection adjacent to a gangrenous appendix is diagnostic for a periappendiceal abscess (Fig. 3).

Appendicitis may occur at the tip of the appendix, and therefore the appendix must be visualised throughout its length to exclude a distal ‘tip

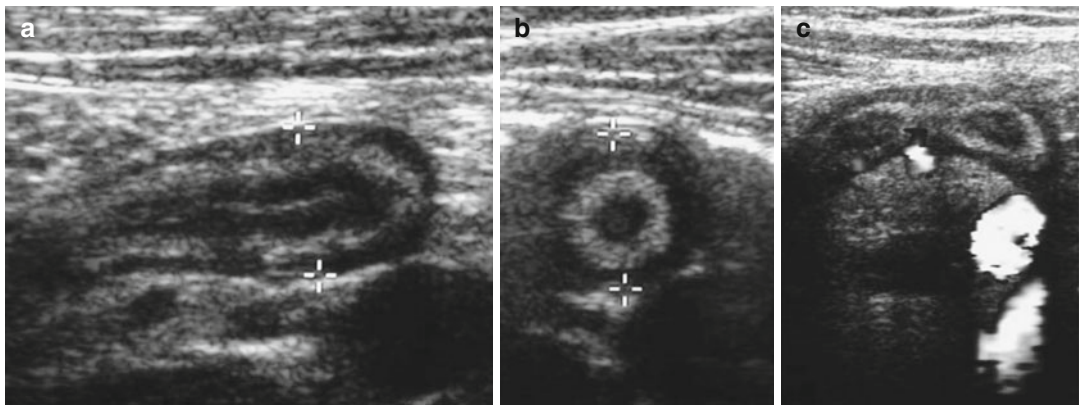


**Fig. 1** (**a**–**c**) Acute appendicitis in a 12-year-old boy. (**a**) Longitudinal ultrasound image showing a swollen appendix (*markers*) which measured 7 mm. Note the increased echogenicity in the wall. (**b**) Transverse image (TS) showing the concentric layers of the inflamed appendix. (**c**) TS image showing two sections of the curved appendix and its relationship to the iliac vessels

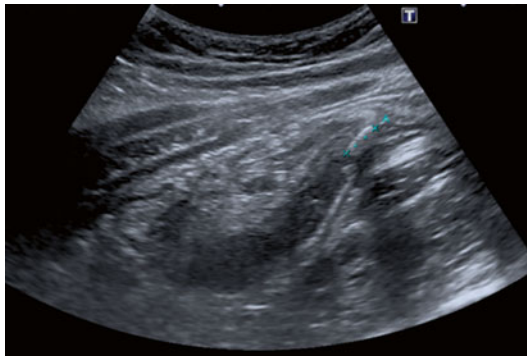

**Fig. 2** Acute appendicitis in a 14-year-old boy showing the presence of an appendicolith (*markers*) with posterior acoustic shadowing on ultrasound

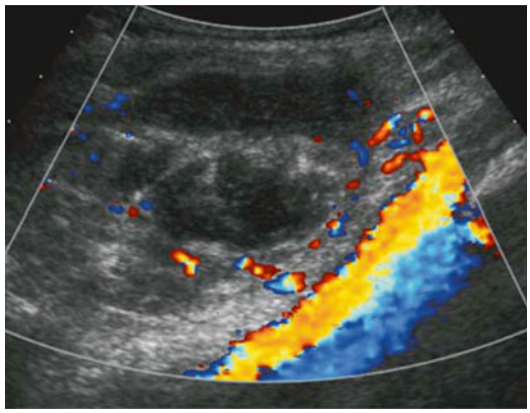

**Fig. 3** Ultrasound of a heterogenous appendix mass in a 12-year-old girl

appendicitis'. The normal appendix may be difficult to visualise due to its small luminal diameter and easy compressibility. However, with operator experience it should be identified in the majority of cases. Features of a normal appendix include: (1) a tubular structure with the typical normal sonographic appearance of bowel having an echogenic submucosal ring (2) which terminates with a blind tip and (3) which takes its origin from the caecal pole and (4) does not demonstrate peristalsis as it is part of the colon.

If the clinical signs and symptoms strongly suggest appendicitis, but it has not been possible to demonstrate the appendix, a retrocaecal appendix may be present. Various operator techniques can be employed to improve delineation of the retrocaecal appendix. These include manoeuvres to scan the patient in a left posterior oblique position. Ancillary techniques for demonstrating a 'hidden' appendix include the additional use of the posterior manual compression technique, upward graded compression technique (Lee et al. 2005), using a low-frequency contrast transducer or left/lateral decubitus change of body position.

It is reported that graded compression sonography with additional operator-dependent techniques can yield a sensitivity of up to 99 %, specificity of 99 % and an accuracy of 99 % for acute appendicitis (Lee et al. 2005).

The lack of visualisation of the appendix with US has a negative predictive value of 90 % in experienced hands (Kessler et al. 2004). The identification of an appendix measuring less than 6 mm in diameter is a very accurate indication to exclude appendicitis with a negative predictive value of between 98 and 100 % (Kessler et al. 2004; Rioux 1992; Rettenbacher et al. 2001).

Secondary signs may help the sonographer establish the diagnosis of appendicitis. These include prominent echogenic fat in the right lower quadrant suggestive of an inflammatory process, the presence of appendiceal mass, the presence of free fluid or of a collection or the presence of free air seen over the liver on ultrasound. However, the secondary signs alone are not specific for acute appendicitis because these may also be seen with other intra-abdominal pathology.

## 1.3 The Use of CT in Diagnosing Acute Appendicitis

CT is widely used to diagnose acute appendicitis in the adult population and to a lesser extent in the paediatric population. Ultrasound is still strongly advised as the first-line examination in children, but CT may be considered in difficult cases if clinical observation is considered inappropriate. Numerous studies have looked at the use of intravenous, oral or rectal contrast media for CT scan for appendicitis. Some centres prefer unenhanced scans and may do a focused CT scan of the lower abdomen, scanning from the lower pole of the right kidney inferiorly for approximately 15 cm. These scans are usually performed without intravenous contrast, but oral or rectal contrast is sometimes given. Other centres per-

form a standard CT of the abdomen following intravenous contrast. An unenhanced CT study in adult patients has shown no difference in sensitivity or specificity for appendicitis when using relatively low dose (30 effective mAs) against standard dose (100 effective mAs) (Keyzer et al. 2004), and a recent Korean study has again demonstrated this (Kim et al. 2012). A study looking at focused CT in children found no difference in the sensitivity and specificity of positive predicted value or negative predicted value of interpretation of images whether they were focused below the right lower pole or whether they include the whole abdomen (Fefferman et al. 2001). Whilst practice varies, it would seem a reasonable strategy when considering CT for appendicitis in children to only scan from the level of the lower pole of the right kidney, after intravenous contrast, and with a very low-dose technique.

Diagnostic signs on CT scan include the visualisation of the oedematous appendix, the presence of an appendicolith, periappendiceal fat stranding, increased caecal wall thickness and abscess formation (Figs. 4 and 5). Fat stranding may be difficult to visualise in children with little body fat. The diameter of the appendix would normally be measured and should be less than 6 mm.

Some authors have looked at the presence or absence of intraluminal air in the appendix as a discriminating sign for appendicitis. However, it has been shown that intraluminal air is frequently detected in both normal and abnormal appendices at CT and at ultrasound and is therefore a non-specific finding of little diagnostic value (Rao et al. 1997).

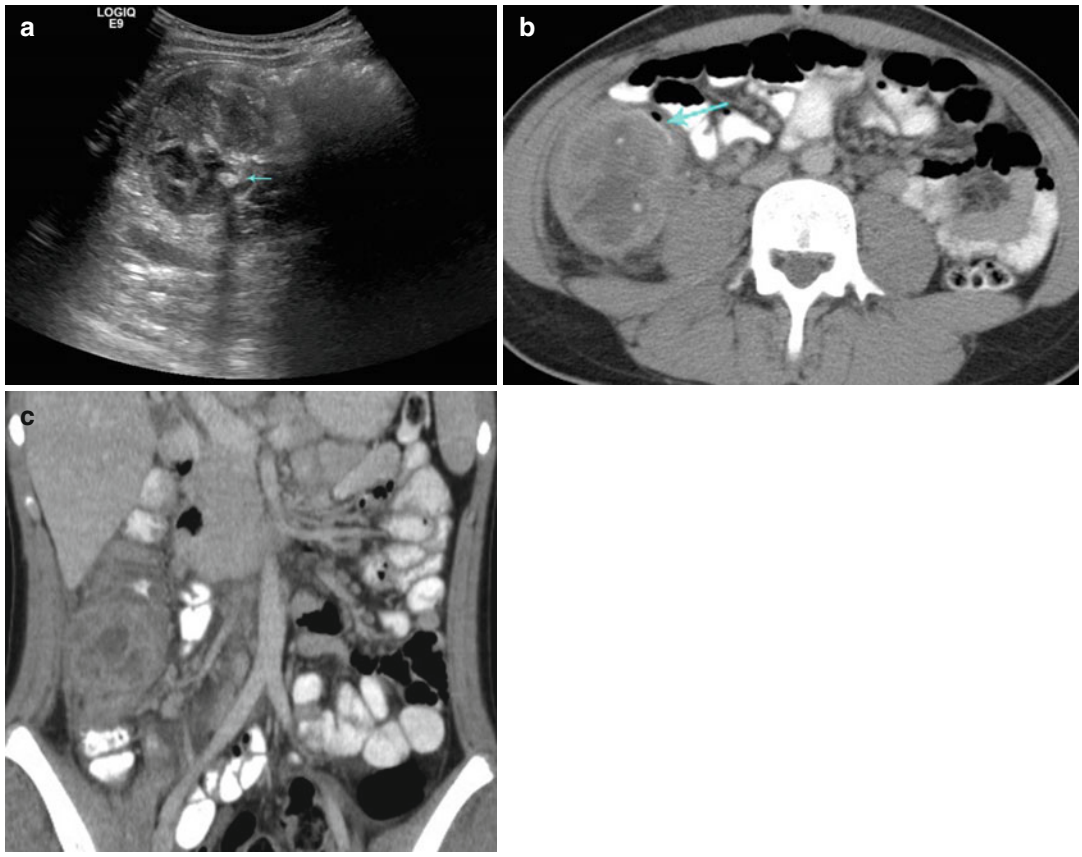


**Fig. 4** US (**a**) and CT images (axial, **b**, and coronal, **c**) of the lower abdomen showing an appendicular abscess containing an appendicolith (*arrow*; **a**) and extraluminal air adjacent to the abscess (*arrow*; **b**)

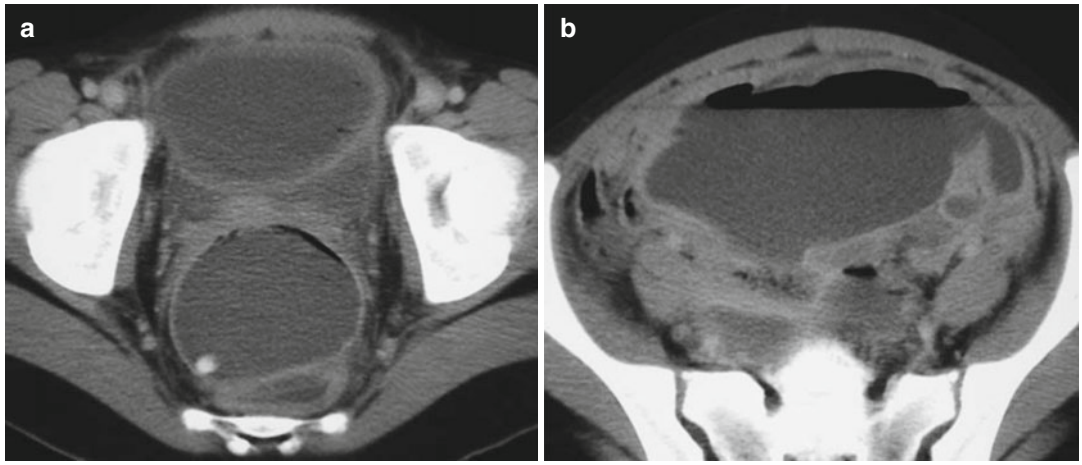


**Fig. 5** (**a**, **b**) CT of the abdomen in a 12-year-old girl with a perforated appendicitis. (**a**) A large collection of fluid in the abdomen with an appendicolith seen low in the pelvis. (**b**) Fluid extending throughout the abdomen with an associated air-fluid level

## 2 Intussusception

Intussusception occurs when a length of bowel, the 'intussusceptum', prolapses and invaginates (or telescopes) into an adjacent segment, the 'intussuscipiens'. Four types of intussusception are described: ileocolic, ileo-ileocolic, colocolic and ileoileal. Ileocolic is the most frequent and occurs in 90 % of cases. Intussusception is the most common cause of intestinal obstruction in infants and young children. Delayed diagnosis may lead to bowel necrosis and perforation.

The majority of symptomatic intussusceptions in children arise in the ileum due to mucosal oedema and lymphoid hyperplasia of Peyer's patches following viral gastroenteritis or upper respiratory tract infection. These so-called idiopathic intussusceptions occur predominantly at the ileocaecal valve (95 %). A 'lead point' (5 %) may be the cause of the intussusception. Typical lead points include a Meckel diverticulum, polyps, duplication cysts, suture granulomas, appendiceal inflammation, Henoch-Schönlein purpura or occasionally inspissated meconium. Symptomatic ileocolic and ileo-ileocolic intussusceptions are generally idiopathic, rather than secondary to a lead point. There is a reported association between intussusception and malrotation/malfixation (Waugh syndrome).

The peak incidence of idiopathic intussusception is between the ages of 3 and 9 months (40 %) with a range between 3 months and 2 years (Carty 2002). Approximately 75 % of cases are in children less than 2 years, and in children older than 2 years a cause for a secondary lead point should be sought. Idiopathic intussusceptions are more common in boys (male/female = 2:1). Incidence of idiopathic intussusception is often seasonal, being more common in late spring and autumn.

The clinical diagnosis of ileocolic and ileo-ileocolic intussusception is not always straightforward. The classical clinical triad of abdominal pain, red currant jelly stool and a palpable abdominal mass is present in fewer than 50 % of children with this condition. The child will typically draw up his/her legs to the abdomen during bouts of colic, which may be associated with facial pallor and the passage of red currant jelly stools. Clinical examination of the abdomen may be difficult in a distressed child. The child may be shocked and peripherally shut down at the time of presentation. However, conversely, some children may be pain free at the time of presentation with only a history of bloody stools to suggest the diagnosis.

### 2.1 Imaging

Historically, the AXR has been the first investigation in children presenting with suspected intussusception. The most frequent plain film findings are

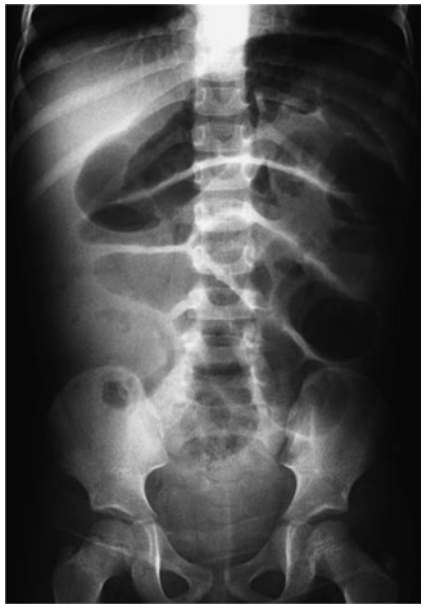

**Fig. 6** AXR of a patient with intussusception. Note the soft tissue mass of the intussusception in the right iliac fossa and the dilated small bowel loops of obstruction

those of reduced large bowel air and the presence of a mass (Fig. 6) (Ratcliffe et al. 1992). Other signs include the meniscus sign and the target sign (Sargent et al. 1994; Lee et al. 1994). Exclusion of an ileocolic intussusception on AXR is based on the presence of air and stool in the caecum (Sargent et al. 1994). However, in 45 % of children aged less than 5 years the sigmoid colon is in the right lower quadrant of the abdomen, and therefore sigmoid filled with air and stool can be misinterpreted for caecum. Also, sometimes loops of 'pulled-up' small bowel will project over the right lower quadrant as a result of the bowel shortening secondary to intussusception. It has been shown that intussusception was correctly identified on AXR in only 45 % of children with intussusception (Sargent et al. 1994). Hence, as the plain abdominal radiograph is unable to categorically confirm or refute the presence of intussusception in the majority of cases, although it may be helpful as part of the workup for investigation of an acute abdomen, an alternative investigation will still be necessary to confirm intussusception. The investigation of choice is ultrasound, and it is suggested that in cases of suspected intussusception the patient should proceed directly to ultrasound without an AXR.

## 2.2 Ultrasound in Intussusception

The use of sonography was first described in the late 1980s (Pracros et al. 1987) with a reported accuracy of 100 % for intussusception. This accuracy rate has since been verified in many reports, and the use of ultrasound for this indication has been validated (Daneman and Navarro 2003; Applegate 2009). Ultrasound is now the first line of investigation in a child with suspected intussusception.

### 2.2.1 Ultrasound Technique

The ultrasound is performed with the child supine and at rest. It is recommended that initially a general survey of the abdomen is undertaken using a curvilinear probe of typically 6–8 MHz. If an intussusception is present, this is most likely to be demonstrated in the right flank, but may also be demonstrated in the epigastrium, left flank or in the pelvis, depending on the extent of the intussusception. This general survey may also show the presence of other secondary signs such as small amounts of free fluid and the presence of lymphadenopathy both in the intussusception and elsewhere in the abdomen or, in the absence of an intussusception, may show an alternative underlying cause for the abdominal pain. It is then recommended that the operator switches to a higher-frequency linear probe (typically an 8- to 15-MHz probe) for further evaluation of the intussusception. Doppler examination of the intussusceptum can also be performed.

Ileocolic intussusception has a characteristic sonographic appearance (Pracros et al. 1987; del-Pozo et al. 1996, 1999) making the diagnosis straightforward. The intussusceptum typically shows as a 3- to 5-cm-diameter soft tissue concentric mass in transverse section and a sausage-like mass in longitudinal section. The characteristic appearances are of the circular wall of the intussuscipiens and the central echogenic mucosa of the intussusceptum, along with the appearance on transverse scans of the eccentric, semilunar, hyperechoic mesenteric fat that is pulled with vessels and lymph nodes into the intussusception by the intussusceptum, the so-called crescent and doughnut sign (Fig. 7) (del-Pozo et al. 1996). It can be difficult to distinguish a 'straightforward'

ileocolic intussusception from a small bowel intussusception; findings that favour a small bowel intussusception (ileo-ileo) on ultrasound include: the absence of an inner fatty core in the intussusception, reduced lesion diameter, reduced wall thickness, reduced ratio of fatty core thickness to outer wall thickness and the absence of lymph nodes (Lioubashevsky et al. 2013).

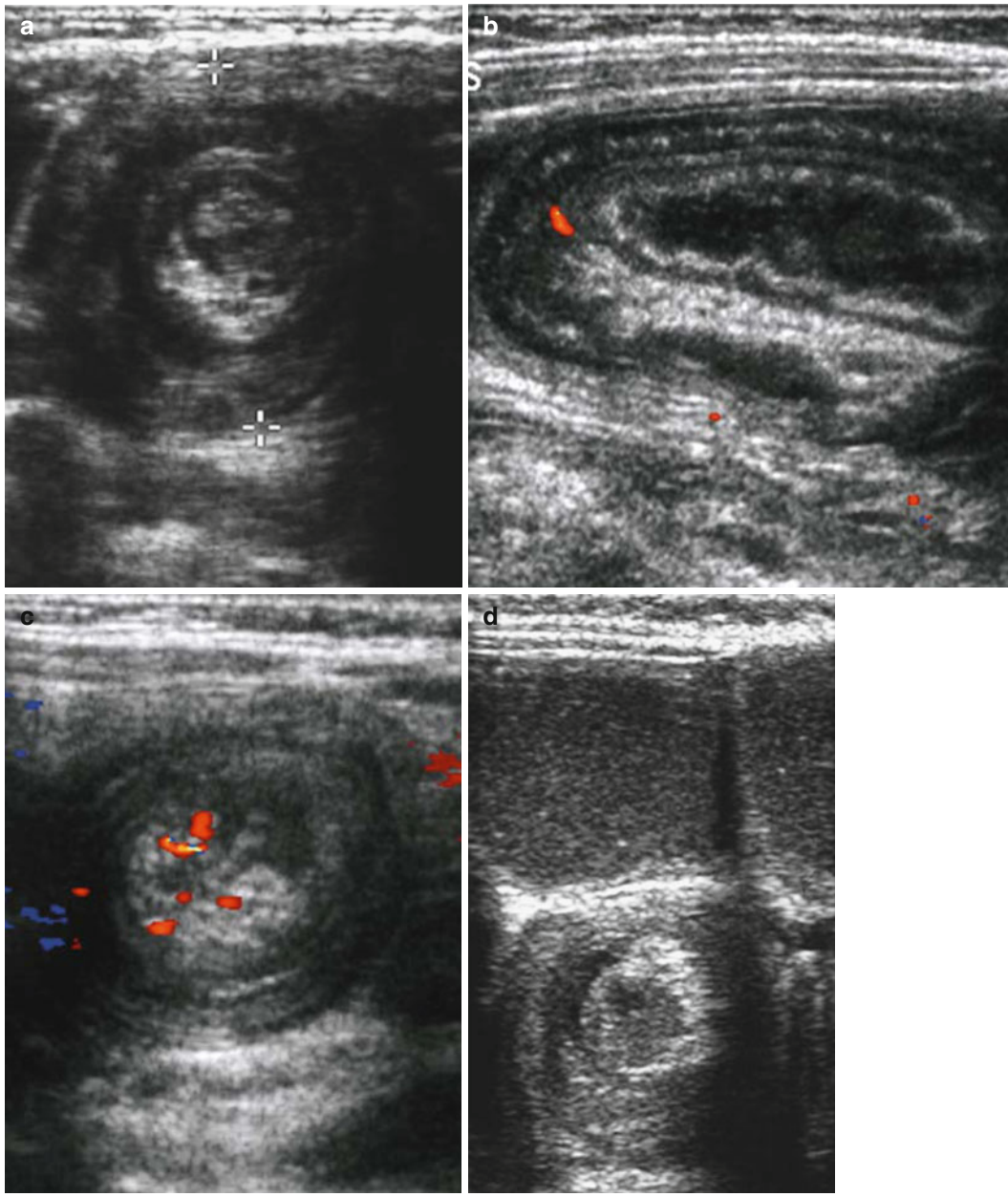


**Fig. 7** (**a**–**e**) Ultrasound appearances of intussusception. (**a**) Transverse (TS) image showing the 'crescent and doughnut sign' as hyperechoic mesenteric fat is pulled into the intussusception. (**b**) Longitudinal image showing the 'sausage' appearance of the intussusception. (**c**) TS image with Doppler showing some blood flow present within the intussusception. (**d**) TS image showing dilated fluid-filled loops of small bowel which should not be mistaken for the intussusception which lies deep to them. Note the absence of the echogenic layers in the small bowel loops. (**e**) TS image showing lymph nodes pulled into the intussusception

**Fig. 7** (continued)

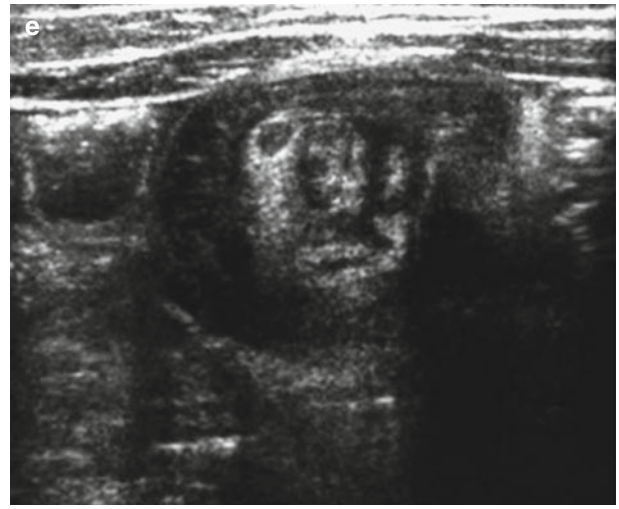


As with any ultrasound study the quality and diagnostic rate is determined by the operator. However, it has been shown that 100 % accuracy rate can be achieved for ileocolic intussusceptions by 3rd and 4th year radiology residents who had completed a 3- to 5-month training period in adult sonography (Verschelden et al. 1992).

Whilst the sonographic appearances of an intussusception are straightforward, care must still be taken not to confuse these appearances with other causes of bowel wall thickening such as inflammation, oedema, haematoma or any area of volvulus. Nevertheless these other conditions will not show the characteristic 'crescent and doughnut' sign.

Ultrasound is also extremely useful for demonstrating the presence or absence of pathological lead points, and these should be looked for in each examination. Ultrasound has been reported as demonstrating a lead point in up to 66 % of patients when a lead point is present (Navarro et al. 2000) and allowing specific pathological diagnosis in up to one third of these patients.

With sonography now being the tool of choice for identifying intussusception, the use of a water-soluble contrast enema or barium enema to make the diagnosis is no longer justified.

### 2.2.2 Assessment for Reducibility

Ultrasound may also be used to make some assessment as to whether the intussusception is suitable for non-surgical reduction and the likelihood of success. Various sonographic signs have been evaluated, including a thick peripheral hypoechoic rim of the intussusception, free intraperitoneal fluid, trapped fluid within the intussusception and the absence of blood flow in the intussusception on Doppler interrogation. There appears to be no relation between the reduction rate and thickness of the external hypoechoic rim (Verschelden et al. 1992), and free intraperitoneal fluid is commonly associated due to transudation of fluid from the congested intussusception which is present in at least 50 % of cases. Fluid trapped within the serosal layers of the entering and returning limbs of the intussusception has been shown to be associated with a lower reduction rate, but at least 26 % of these cases can still be reduced. Similarly the absence of flow on Doppler interrogation reduces the rate of successful reduction but does not preclude it, reduction still being successful in approximately 31 % of cases (Kong et al. 1997). The absence of visualised blood flow on Doppler interrogation is therefore not a contraindication for attempted air enema reduction. Similarly the identification of a pathological lead point does not necessarily mean that an intussusception will be irreducible (Navarro et al. 2000, Navarro and Daneman 2004).

Clinical factors are also useful for predicting the need for operative treatment of intussusception, and these include symptoms lasting for

more than 2 days, age less than 1 year, multiple ultrasound findings and failure of initial enema reduction (Fallon et al. 2013). However whilst it is a widely held belief that the length of the history influences the outcome of pneumatic reduction of intussusception in children, there is evidence to the contrary and air reduction should be the first-line treatment in all children with intussusception regardless of the length of the history (Tareen et al. 2011).

## 2.3 Nonoperative Reduction of Intussusception

Nonoperative reduction is the treatment of choice. Historically barium or water-soluble contrast media have been used for the hydrostatic reduction of intussusception. These techniques have been almost completely replaced by the use of the air enema under fluoroscopic guidance or ultrasound-guided hydrostatic or air reduction. The fluoroscopic guided air enema is currently the most universal procedure, but as experience grows, ultrasound-guided reduction is also used in several centres. The basic principal is to raise the intraluminal pressure in the distal colon to push the intussusceptum retrogradely along the colon, thereby reducing the intussusception, until it is completely resolved, usually through the ileocaecal valve. Complete reduction is achieved when either air or contrast media flood back into multiple loops of terminal ileum. Whilst hydrostatic or pneumatic reduction can be successful in ileoileal intussusception, this is more commonly treated by surgery.

Some authors have also recently described the external manual reduction of idiopathic ileocolic intussusceptions with ultrasound with the patients under deep sedation (Vazquez et al. 2012). At the time of writing it is uncertain if this will gain mainstream uptake.

### 2.3.1 Technique for Fluoroscopic Air Enema

Once the presence of an intussusception has been confirmed by ultrasound, the child is taken to the fluoroscopy room. Some centres administer pain relief and/or sedation in anticipation of the procedure, but this is by no means universal and there is some evidence that the use of sedation (or the use of smooth muscle relaxants) may prevent the patient from performing the Valsalva manoeuvre which might otherwise enhance the chance of reduction and possibly reduce the chance of perforation. Children should be well resuscitated before attempted reduction and should be monitored whilst the attempted reduction is in progress. This is particularly important in children who have received sedation, as signs of clinical deterioration may not be so apparent. Antibiotic prophylaxis has conventionally been given before starting the procedure. However there is some evidence that antibiotics confer little advantage (Al-Tokhais et al. 2012), and this remains at the discretion or practice of the institution.

A balloon catheter is placed per rectum (10–18 F). Many operators inflate the balloon on the Foley catheter, but this is not universal practice and caution should be used when inflating a balloon catheter in the rectum because of the reported risk of mucosal ischaemia. The buttocks are subsequently taped or gripped firmly to complete a good seal at the anus. Air is then introduced into the distal colon, with a manometer or other monitoring device present on the system to ensure safe and constant pressure of air. The progress of the air (and the reduction of the intussusceptum) is closely observed under fluoroscopic guidance (Fig. 8a–c). It is usual practice to include the whole abdomen within the field of view so as not to miss a perforation, which would necessitate the immediate termination of the procedure (Fig. 8d). In the case of a tension pneumoperitoneum, an 18-G needle should immediately be positioned in the midline to relieve the abdominal distension, thereby preventing respiratory collapse. Typically the pressure is raised to 80 mm of mercury (Hg) equivalent and sustained at this level for approximately 3 min. This may then be repeated either at the same pressure, or at 100 or 120 mmHg, until reduction is complete. Typically three attempts of 3 min each are made at each pressure. The whole procedure may be performed with the infant supine or prone at the

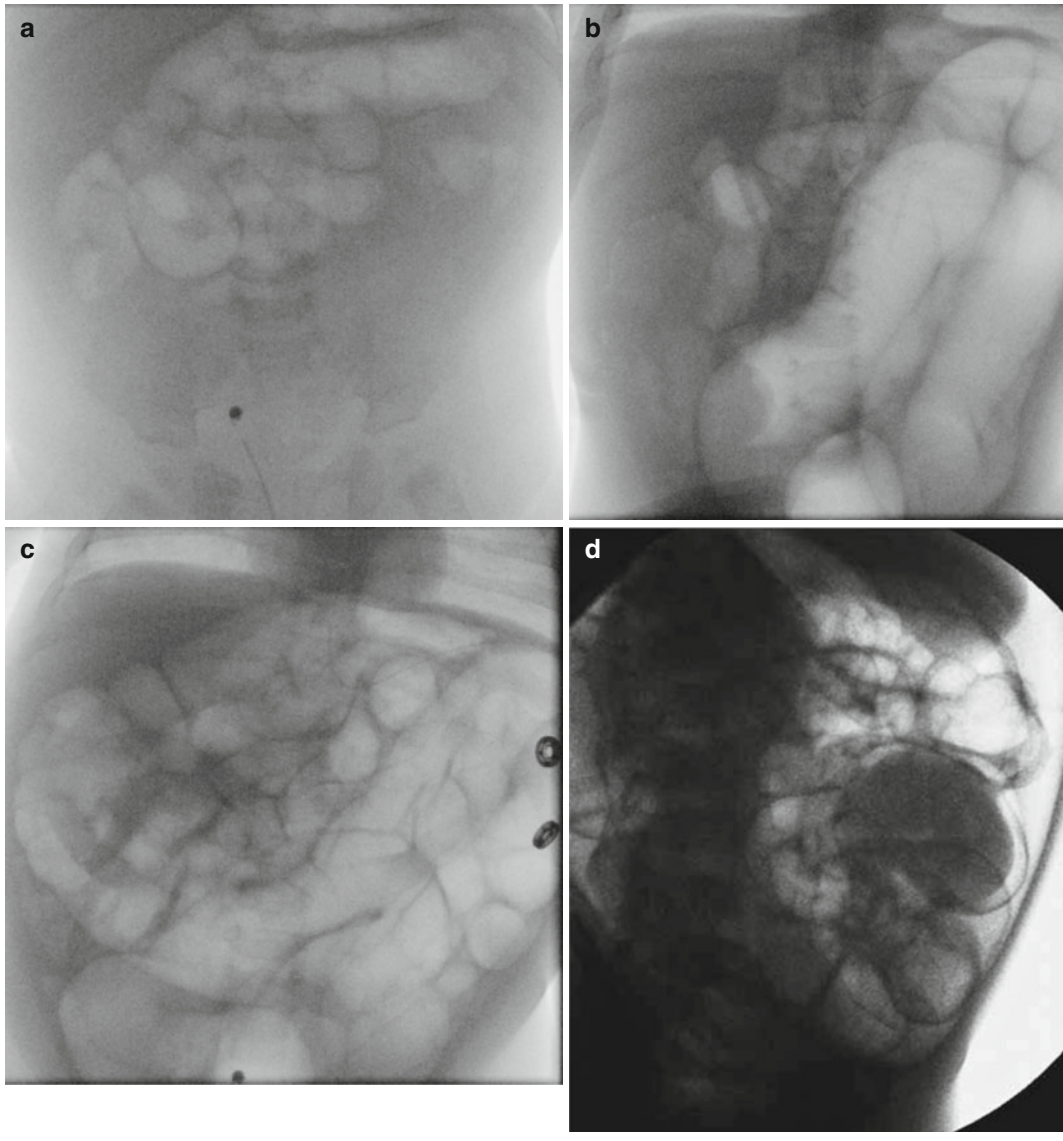


**Fig. 8** Appearance of intussusception during reduction by air enema. (**a**) Pre-reduction fluorograb image demonstrating mild gaseous distention of the small bowel. Rectal catheter in situ. (**b**) Fluorograb half way to the reduction – the left side of the colon is distended. The intussusception mass can be identified in the right lower quadrant. (**c**) Successful reduction with multiple small bowel loops distended with air dominating the abdomen. (**d**) Air enema in a different patient: the intussusception is shown as a soft tissue mass but perforation of the bowel has occurred

operator's discretion and preference. Advantages for the supine position include being able to observe the child more closely and for a normally orientated radiographic view. Advantages for the prone position include it being easier to obtain a complete seal on the child's buttocks if these are uppermost.

### 2.3.2 Ultrasound-Guided Hydrostatic or Air Reduction

Once the diagnosis of intussusception has been made by ultrasound a 10- to 18-F balloon catheter is placed per rectum as above. In the case of hydrostatic reduction this is normally performed with the child supine. The child may be placed on

a plastic enema ring approximately 50 cm in diameter, which allows a suction device to continuously remove fluid which has escaped per rectum during the procedure. Fluid is then introduced per rectum, which may be water, saline or isotonic Hartmann's solution, and a constant pressure of injection is maintained, typically 100 mm of mercury. During the reduction the intussusceptum is observed under continuous ultrasound guidance as it proceeds to the caecum and reduces across the ileocaecal valve (Khong et al. 2000). One advantage of ultrasound-guided hydrostatic reduction is that it may allow identification of an ileo-ileocolic intussusception. This has a characteristic complex fronded appearance, compared with the otherwise smooth appearance of an ileocolic intussusception. A disadvantage is that if perforation does occur, there is likely to be greater contamination of the peritoneal cavity by bowel contents than with an air procedure.

### 2.3.3 Ultrasound-Guided Pneumatic Reduction

Whilst this technique was described in 2001 and was reported to have similar success rates to the fluoroscopic air enema technique (Yoon et al. 2001), it does not seem to have been widely taken up since that time. Yoon et al. describe their technique as follows: A balloon catheter (10–18 F) is inserted per rectum, and 20–25 ml of air is injected to inflate the balloon. The Foley catheter is gently pulled as low as possible. Tape is applied to secure the catheter to the buttocks. By means of a pressure-monitoring device linked to a T connector and with ultrasound guidance, air is injected manually to the initial intracolonic pressure of approximately 60 mm of mercury and held for 30 s and then released. Ultrasound criteria for successful reduction after deflation of the air includes the disappearance of the intussusceptum with the presence of a single concentric echogenic ring representing the swollen terminal ileum instead of the multiple concentric rings of the intussusception and the abrupt transition of bowel wall thickness between the swollen terminal ileum and the proximal normal ileum when scanned along the axis of the ileum. If the intussusception is still visible, air is reintroduced by gradually increasing pressures up to a limit of 120 mm of mercury. Air is typically insufflated and deflated three times at each increment. If there is an abrupt decrease in pressure during air insufflation, sudden abdominal distension or clinical improvement, the air is then deflated to allow further ultrasound assessment. To detect free intraperitoneal air caused by bowel perforation, intermittent ultrasound of the epigastrium is performed to look for a 'ring-down' (or 'comet-tail') reverberation artefact in the subphrenic area obscuring the inferior hepatic margin.

Overall, using one of these techniques, a reduction rate of at least 70 % would be expected, with a perforation rate of approximately 1 % or less. However success rates vary wildly with geographical location and referral patterns. A recent suggestion of using the proportion of intussusceptions not requiring resection that are reduced successfully non-operatively, a 'composite reduction rate', would reduce bias and confounding factors by taking out of the statistics those intussusceptions that could never reasonably have been expected to be reduced and would allow better comparison between centres (Bekdash et al. 2013). This seems a supremely pragmatic approach to defining a better index for measuring 'success'.

Guidelines to the performance of intussusception reduction are published by various bodies including the American College of Radiology http://www.acr.org/~/media/ACR/Documents/PGTS/guidelines/Pediatric_Contrast_Enema.pdf, and the clinician should be aware of these pertaining to his/her region of practice.

## 2.4 Delayed Repeat Enema

If the attempted intussusception reduction has been partly successful, there is value in a delayed repeat enema if the child is clinically stable. It has been shown that a delayed repeated enema can be successful in reducing the intussusception in a further 50 % of those patients in whom it is used and thus has a place in the management of

the infant who remains clinically stable with no evidence of peritonitis, where there has been a partial reduction of the intussusception at the first attempt (Daneman and Navarro 2003; Navarro and Daneman 2004; Pazo et al. 2010). The best time interval between the two enemas remains uncertain, and the number of times a delayed enema can be reasonably repeated is also unproven. In published series (Navarro et al. 2004) the delay has varied between 15 min and 12 h (Gorenstein et al. 1998; Navarro et al. 2004). Some centres allow a planned delay of between 45 and 60 min between three consecutive air enema attempts (Gorenstein et al. 1998), but other centres wait between 4 and 6 h, to allow resolution of oedema. In any event, repeated delayed reduction attempts increase the overall success rate and should be advocated in a stable patient. Finally, the use of multiple delayed reduction attempts is not contraindicated in the presence of a pathological lead point as successful reduction may facilitate subsequent surgery for resection of the lead point. Multiple recurrences of intussusception in this context are not a contraindication to repeated reduction. A careful search for a pathological lead point is mandatory. Surgery should be reserved for irreducible recurrences or for a demonstrated pathological lead point (Daneman et al. 1998; Navarro et al. 2004; Pazo et al. 2010).

### 2.5 Summary

A diagnosis of intussusception is preferentially made by ultrasound. The plain abdominal radiograph has been shown to be of only limited value and may be omitted safely in the vast majority of children suspected of having an intussusception, provided sonography is available.

The preferred reduction technique is either that of the air enema under fluoroscopic guidance or of air or hydrostatic enema under ultrasound guidance. The only absolute contraindication to attempted enema reduction is full thickness bowel necrosis (which will present with features of shock and peritonitis) or if there is imaging evidence of perforation with free air.

## 3 Constipation

Constipation is a common problem in infants and children and accounts for approximately 3 % of visits to paediatric outpatients (Loening-Baucke 1993); it is also likely that constipation is the most common digestive complaint outnumbering all other chronic gastrointestinal conditions (Mezwa et al. 1993). Only 5 % of children with constipation have an underlying disease (Tabbers et al. 2011).

Constipation is defined clinically as an alteration in the frequency, size, consistency or ease of passage of stools (Seth and Heyman 1994). A common working definition for constipation in children is a stool frequency of less than 3 per week, but painful bowel movements and/or stool retention can be regarded as constipation even if the stool frequency is three or more per week (Loening-Baucke 1993; Seth and Heyman 1994). Encopresis is the voluntary or involuntary passage of a normal bowel movement into the underwear after the age of 4 years, and faecal soiling is defined as the involuntary seepage of faeces which is often associated with faecal impaction and is reflected in the staining of the underwear (Benninga et al. 1994; Partin et al. 1992).

Causes of constipation in infants and children include functional constipation, neurogenic constipation [aganglionosis, hypoganglionosis, neuronal intestinal dysplasia (NID)], chronic intestinal pseudo-obstruction, disorders of the spinal cord, cerebral palsy, constipation secondary to anal fissures and strictures, neonatal hypothyroidism and drug-induced constipation (Fotter 1998).

### 3.1 Functional Constipation

Approximately 90–95 % of cases of childhood constipation are likely to represent functional constipation. Rectal distension is present in nearly all cases, and failure of the external anal sphincter and/or puborectalis muscle to relax during defecation attempts has been found in the majority of these children. Whilst delayed colonic transit time may be part of the problem, pelvic floor dysfunction seems to be the

dominating factor (Loening-Baucke 1993). Frequently used tests in the diagnosis of childhood constipation are abdominal radiography with or without the use of radio-opaque markers to measure colonic transit time and abdominal ultrasonography. However recent guidelines have found insufficient evidence for a diagnostic association between clinical symptoms of constipation and imaging findings (AXR, AXR with markers or US), and as such these tests are not helpful in diagnosing childhood constipation and are no longer recommended in some national guidelines (Berger et al. 2012; Bardisa-Ezcurra et al. 2010).

## 3.2 Neurogenic Constipation

### 3.2.1 Hirschsprung Disease

Hirschsprung disease (HSCR) is a complex genetic disease with a low, sex-dependent penetrance and is the most common cause of neonatal obstruction of the colon, accounting for 33 % of all neonatal obstructions. It has an incidence of approximately 1 in 5000 with a strong male gender bias (up to 4:1, M:F) and has a strong correlation with a wide range of associated anomalies (Kenny et al. 2010), with medullary thyroid carcinoma as part of MEN2B being particularly deleterious and Down syndrome being one of the commonest associations which carries a 100-fold greater risk for HSCR than the normal population (Kenny et al. 2010). The enteric nervous system is of neural crest origin, and as such HSCR is regarded as a neurocristopathy, and some of the associated conditions are also of neural crest-derived cells.

It is characterised by congenital absence or deficiency of the ganglion cells in the myenteric and submucosal plexuses of the rectum and the distal, non-dilated part of the colon, together with a hyperplasia of cholinergic nerve fibres in the circular muscle layer, muscularis mucosae and mucosa with a high activity of acetylcholinesterase (Fotter 1998). This results from failure of neural crest cells to migrate into the wall of the colon during the fifth to seventh week of embryological life and subsequent failure of development of the parasympathetic ganglion cells. The absence of the intramural ganglion cells interferes with normal relaxation and peristalsis of the bowel wall and the internal anal sphincter. The abnormally innervated segment of colon becomes hypertonic and behaves as a functional stenosis leading to partial or complete colonic obstruction. Immediately proximal to the aganglionic segment, the intestine becomes markedly dilated with faeces and air. In most cases aganglionosis is limited to the rectum or the rectum and a short distal segment of the sigmoid colon. This so-called short segment disease occurs in approximately 80 % of cases, with long segment disease occurring in 15 % and total colonic aganglionosis (Zuelzer-Wilson syndrome) accounting for approximately 2–13 %. Ultrashort-segment Hirschsprung disease accounts for up to 10 % in some series. In ultrashort-segment Hirschsprung disease, the aganglionic segment is usually confined to the internal anal sphincter or up to 3–4 cm above the pectinate line (Meier-Ruge and Scharli 1986).

Presentation is most common in the full-term infant during the first 6 weeks of life (70–80 %) and is extremely rare in premature infants. In classic Hirschsprung disease and in ultrashort-segment disease, there is a male-to-female ratio of 4:1, but in total colonic aganglionosis the ratio is 1.8:1.

Complications of Hirschsprung disease include an enterocolitis with or without intraluminal air and intermittent dilatation after surgical treatment which may give a picture of pseudo-obstruction. Following a Duhamel procedure ('pull-through' procedure), there may be persistent narrowing at the anastomosis site.

Hirschsprung disease has now been shown to be one of several disorders in intestinal innervation due to an abnormal number of neurones. These disorders are known as dysganglionoses and include congenital intestinal aganglionosis (Hirschsprung disease), hypoganglionosis and hyperganglionosis (Kapur 2000). Hypoganglionosis is described histologically as a variable length of gut with abnormal numbers of ganglion cells. It is believed to be the primary cause of intestinal pseudo-obstruction (see Sect. 7.3.3) and may represent a *forme fruste* of Hirschsprung disease. The patient may present

with multiple loops of dilated bowel with an obstructive picture but with no cause of mechanical obstruction found.

Hyperganglionosis is described as having two distinct patterns: ganglioneuromas (nodular proliferations of ganglion cells often associated with multiple endocrine neoplasia type 2B and not seen in children) and intestinal neuronal dysplasia (NID). NID is a controversial entity, but a consistently described feature is of increased density of the submucosal ganglia. Patients may present with intestinal dysmotility clinically indistinguishable from Hirschsprung disease.

In view of these overlapping presentations these disorders should be considered in the differential diagnosis of Hirschsprung disease until histological confirmation has been made.

#### 3.2.2 Chronic Intestinal Pseudo-obstruction

Chronic intestinal pseudo-obstruction (CIPO) is a rare clinical disease/syndrome with an unknown prevalence and incidence. Approximately 100 infants a year are born in the United States with congenital forms of CIPO although this is likely to be an underestimate of the number of new cases per year. The term was introduced in the late 1950s and is used to describe a condition characterised by symptoms and signs (both clinical and radiological) of intestinal obstruction, but without evidence of any lesion occluding the lumen of the gut (De Giorgio et al. 2011). It has also been known as/includes chronic adynamic ileus, pseudo-Hirschsprung disease and adynamic bowel syndrome. Megacystis-microcolon-intestinal hypoperistalsis syndrome is the most severe form of chronic intestinal pseudo-obstruction.

Onset of CIPO can be at any age but tends to be more severe with the earlier presentation. In the neonatal period symptoms include failure to pass meconium, abdominal distention or bilious vomiting. Constipation may subsequently develop. In older children presentation may be abrupt or slowly progressive. Urinary tract involvement occurs in up to 50 % of patients. Histologically abnormalities are either seen in the myenteric plexus with an associated visceral myopathy or show argyophobic cells or argyrophilic cells on silver stains. The overall result is a lack of coordinated intestinal motility. Inheritance may be autosomal dominant, but the majority of cases are sporadic. There is an association with malrotation. Overall there is a high morbidity and high mortality (Heneyke et al. 1999).

### 3.3 Imaging in Constipation

In the newborn period the patient may present with a delay or failure to pass meconium, distension of the abdomen, bilious vomiting or signs of neonatal intestinal obstruction. An AXR will show evidence of low obstruction but will be non-specific; however, it may allow assessment of the lower spine, and in Hirschsprung disease a lack of air in the distal colon or rectum may be a sign of congenital aganglionosis (Fig. 9a).

In suspected neurogenic causes of constipation (Hirschsprung disease, NID and hypoganglionosis), a contrast enema is often performed. It is not advisable to prepare the bowel before this procedure because the narrow segment may be dilated up and therefore missed.

In the neonatal period water-soluble contrast is instilled preferentially as this may wash out the colonic contents and relieve obstruction in cases of neonatal small left colon syndrome or in meconium plug syndrome. In infants or older children either water-soluble contrast medium or barium can be used. It is not usually appropriate to inflate a balloon catheter as this may obscure visualisation of a narrow segment in congenital aganglionosis. The infant or child is usually placed in a lateral position at the beginning of the study to allow observation of the anorectal junction during filling, and in cases of aganglionosis, bowel filling should be limited to as far as the transitional zone. The transitional zone should be sought and is identified by change in calibre from relatively small or normal calibre/collapsed lower bowel to distended stool-filled proximal bowel (an ‘inverted cone’ appearance). In the case of Hirschsprung disease the most common site for the transitional zone is in the rectosigmoid (Fig. 9b, c). It should be noted that the aganglionic

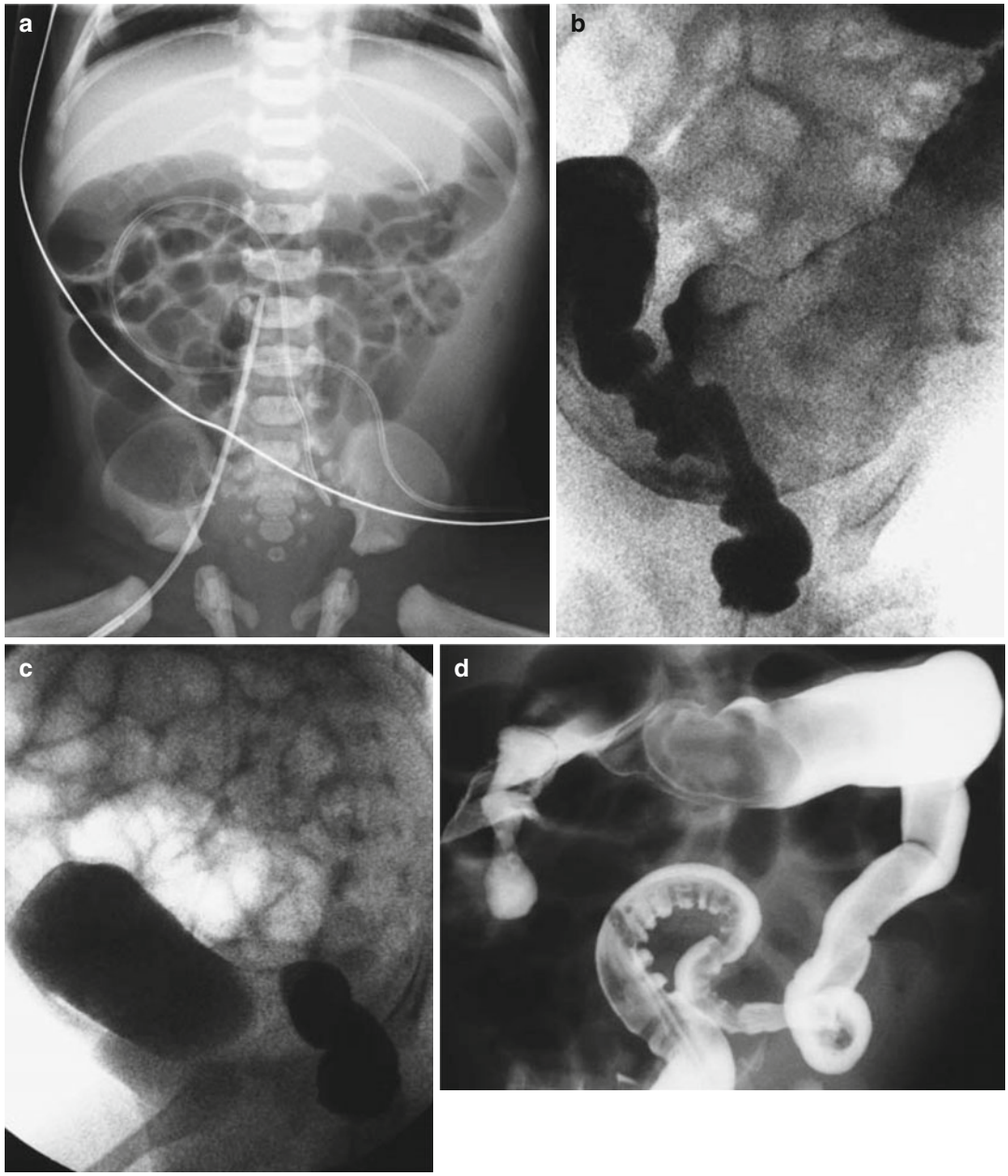


**Fig. 9** (**a**–**d**) Imaging of Hirschsprung disease. (**a**) AXR in total colonic Hirschsprung disease showing the absence of air in the large bowel but otherwise non-specific appearances. (**b**) Contrast enema showing an irregular and non-dilated rectum with a transition to a markedly dilated and stool-filled sigmoid colon. (**c**) Contrast enema showing a transition zone at the rectosigmoid junction. The rectosigmoid ratio is greater than 1. (**d**) Contrast enema in a neonate with Hirschsprung disease with a conical transition zone at the splenic flexure. There is also a long meconium plug in the distal colon, and the differential diagnosis would be functional immaturity of the colon. The final diagnosis was made by biopsy

segment appears normal in size. The rectosigmoid ratio may be used to assess the relative size of the rectum to the sigmoid. This should normally be 1:1 and if greater than this suggests a diagnosis of Hirschsprung disease (i.e. in normality the rectum may be larger than the

sigmoid, but the sigmoid should not be larger than the rectum).

Filling with contrast should continue slowly, leaving enough time for the bowel to adapt to the instilled volume. The aganglionic segment may need some time to contract to its former diameter. One suggested technique in infants and older children is to use barium, with secondary insufflation with air. As air does not expand a narrow segment as much as barium, the transition zone can be demonstrated more easily and more accurately. A 24-h delayed film can show a complete lack of evacuation of contrast medium especially in cases of total colonic aganglionosis (O'Donovan et al. 1996).

### 3.3.1 Imaging Findings in Hirschsprung Disease

The cardinal sign in Hirschsprung disease, shown on a contrast or barium enema, is the transitional zone between the narrow and dilated bowel segment, most often seen at the rectosigmoid junction (Fig. 9b, c). It may be represented by an abrupt change of calibre or may have a more conical appearance (Fig. 9d). The absence of a demonstrated transitional zone does not exclude the diagnosis of Hirschsprung disease. A classic aganglionic segment may not be visible before days 10–14 of life. A narrow segment refers to a segment of rectum where the relationship of the diameter of the rectum to the sigmoid colon is 1:1 or less. A transitional zone with a megacolon may be seen only after 4–6 weeks. The wall of the colon often has a 'saw-tooth' appearance as a result of non-peristaltic contractions. There may be marked retention of barium on delayed films after 24 h, and mixing of barium and stools after 24 h is a common finding.

The differential diagnosis in the neonatal period is that of small left colon syndrome. In this condition the left colon is a reduced calibre, typically, from the level of the splenic flexure distally, with an abrupt transitional zone between the dilated transverse colon and the narrow calibre descending colon. These findings are visible right from the first few days of life in small left colon syndrome but would not typically be present in Hirschsprung disease for some delayed period.

### 3.3.2 Imaging Findings in NID, Hypoganglionosis, Chronic Intestinal Pseudo-obstruction, Ultrashort-Segment Hirschsprung Disease and Total Colonic Aganglionosis

The appearances at contrast or barium enema in these remaining conditions are often non-specific. In ultrashort-segment Hirschsprung disease the barium enema may show a large megarectum but no other specific findings. In NID, chronic intestinal pseudo-obstruction and total colonic aganglionosis, the barium enema is often non-contributory. However, total colonic aganglionosis may sometimes have the appearance of a microcolon and therefore needs to be differentiated from ileal atresia and meconium ileus.

In all these conditions the final diagnosis is usually made by histology, most commonly following suction biopsy via the rectum. This technique is fast and simple and can be carried out in neonates without a general anaesthetic. In some cases full thickness biopsy will be required to obtain all layers of the intestinal wall, in which case a general anaesthetic is required. Complex enzyme histochemistry and immune histochemistry is frequently necessary. If contrast enema is required, it should be performed pre-biopsy or at least 24 h post biopsy.

### 3.3.3 Imaging in Functional Constipation

The plain abdominal radiograph is no longer indicated in cases of chronic functional constipation. Quantifying stool on the abdominal film is not reliable. Many have tried but a grading system has been elusive (Barr et al. 1979).

Barium or contrast enema may still occasionally be performed to assess the degree of bowel dilatation and the degree of colonic loading. However, a conclusive diagnosis is rarely reached by this method alone, and it is not recommended. Biopsies are routinely performed to exclude a previously missed diagnosis of Hirschsprung disease. Pellet studies may be performed for transit times: the patient is given a pellet containing tiny radio-opaque markers on each of the 3 days preceding a single AXR. The markers in the pellets

are different on each day allowing for estimation of transit time. Defecography is performed rarely in some children with chronic constipation and defecation disorders after the third to fourth year of life. Defecography allows assessment of the degree or relaxation of the internal anal sphincter during retrograde filling and during defecation. The anorectal angle can be assessed as can the degree of relaxation of the external anal sphincter during defecation. The combined function of the puborectalis muscle and the external sphincter can be demonstrated. A detailed description of the procedure of defecography and the range of findings is beyond the scope of this chapter.

## 4 Functional Immaturity of the Colon (Small Left Colon and Meconium Plug Syndrome)

Historically 'meconium plug syndrome' and small left colon syndrome have been considered as separate, if possibly overlapping, entities. The main finding in both entities is that of a narrow rectosigmoid and descending colon with a transition to normal size or dilated colon typically at the level of the splenic flexure. The term 'meconium plug syndrome' was used initially, reflecting the belief that the obstruction was probably due to 'an alteration in the character of the most distal portion of the meconium mass' (Clatworthy et al. 1956). Subsequent authors observed that a small left colon with proximal obstruction could be seen in the absence of the meconium plug and termed the syndrome 'neonatal small left colon syndrome', in the belief that the abnormality was due to the smallness of the colon rather than the abnormality of the meconium. Finally the term 'functional immaturity of the colon' has come into widespread use and reflects the overlapping or synonymous entities of 'small left colon syndrome' and 'meconium plug syndrome' (Berdon et al. 1977).

The underlying aetiology remains unknown but is likely due to impaired intestinal motility, leading to local inspissation of meconium and secondary low colonic obstruction. Presentation is in newborn infants, normally within the first 24 h of life. Approximately 50 % of infants have diabetic mothers (Ellis et al. 2009). The signs are those of abdominal distention, vomiting and failure to pass meconium. The AXR will show evidence of a low obstruction with multiple dilated loops of bowel. Occasionally there is a bubbly appearance in the colon which raises concern about the differential diagnosis of submucosal air including necrotising enterocolitis. Investigation is by water-soluble contrast enema. A catheter is passed per rectum and contrast introduced under fluoroscopic guidance. If a meconium plug is present, there may be a ribbon-like filling defect in the small left colon with a larger filling defect in an otherwise normal-appearing transverse colon (Fig. 10). The hyperosmolality of the contrast medium often causes the meconium plug to shell away from the bowel wall, and meconium is usually evacuated during or soon after the enema examination, resulting in relief of obstruction. If a meconium plug is not present, a small left colon will be seen usually with an abrupt change of calibre at the splenic flexure. The images confirm the diagnosis and usually no further treatment is necessary with the infant normally passing meco-

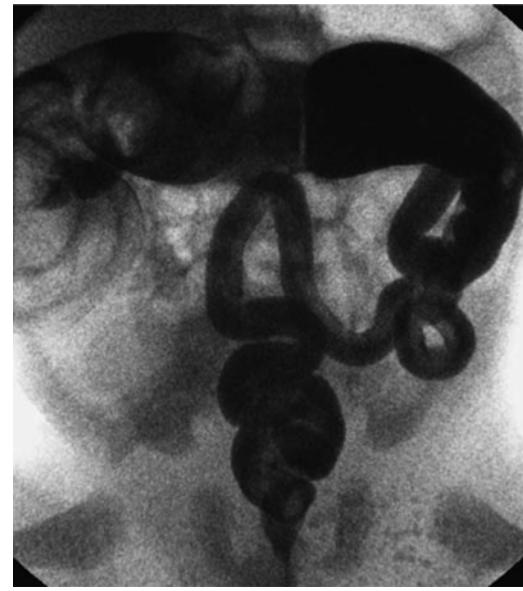

**Fig. 10** Contrast enema appearances in functional immaturity of the colon: a small left-sided colon filled with meconium

nium from the ascending and transverse colon soon after the study. Though infants with functional immaturity of the colon usually do well, a benign course is not invariable and perforation may occur.

A differential diagnosis in infants with these findings includes that of Hirschsprung disease. However, it is unusual for a case of Hirschsprung disease to have a transition zone at the splenic flexure; the transition zone in functional immaturity is often quite abrupt, whereas the transition zone in Hirschsprung disease may be cone shaped and gradual; and finally in Hirschsprung disease aganglionic colon is usually of near normal calibre, whereas in functional immaturity the left colon is usually small. In newborns with functional immaturity the rectum is usually quite distensible unlike in Hirschsprung disease when the aganglionic colon usually remains of uniform calibre to the anus. If any doubt about the diagnosis remains after treatment by contrast enema, a rectal biopsy should be obtained.

## 5 Colon Agenesis, Colonic Atresia and Stenosis

Complete absence of the colon and rectum is extremely rare. However, segmental atresias or stenosis of the colon are seen more often and are believed to be secondary to an intrauterine vascular insult. Nevertheless they are still quite unusual and are seen much less commonly than atresias in the small bowel. The colon typically accounts for only 5–15 % of total intestinal atresias (Powell and Raffensperger 1982). The atresia may be represented simply by a membrane across the lumen of the colon, by a fibrous band connecting the two ends of the large bowel, by a complete atresia with no fibrous connection or by multiple series of atresias.

In complete colonic agenesis or atresia, the child will present with failure to pass meconium in the first 24 h and with clinical features of obstruction. In colonic stenosis the degree of obstruction will be variable. The AXR will show features of a low intestinal obstruction. At contrast enema the distal colon is likely to be a microcolon, never having been used, and it will not be possible to pass contrast beyond the level of the atresia (Fig. 11a, b). In cases of stenosis, rather than complete atresia, the stenotic portion may be demonstrated with contrast material and the colon proximal to the stenosis is likely to be very dilated and filled with meconium or stool. The colon proximal to the obstruction can become overdistended and ischaemic secondary to compression by the massive intraluminal contents. Some authors have described an association between colonic atresia and Hirschsprung disease. However, it now seems likely that this anecdotal link is due to the vascular insult rendering the colon atretic and also rendering the involved segment aganglionic.

Acquired stenosis can also occur following necrotising enterocolitis, and this is described later in this chapter.

## 6 Duplication Cysts

A gastrointestinal tract duplication cyst represents a congenital anomaly found anywhere along the alimentary tract, with the colon being an uncommon site and representing only 13–30 % of cases. It shares a common muscle wall and blood supply but has a separate mucosal lining. The aetiology is unclear but the duplication is thought to occur early in embryological development, around the 6th week of fetal development, and probably as a result of abnormal recanalisation. Other hypotheses for the formation of gastrointestinal duplication cysts include the persistent embryologic diverticular theory, bronchopulmonary-foregut malformation, the intrauterine vascular accident theory and the abortive twinning theory (Hur et al. 2007; Macpherson 1993). There are two types of gastrointestinal duplication cysts: ‘cystic duplication’ which accounts for approximately 80 % of cases and is spherical in shape with no communication with the bowel lumen and ‘tubular duplication’ accounting for 20 % of cases and which parallels the normal gut, most commonly being on the mesenteric aspect of the alimentary canal, and which communicates directly with the bowel

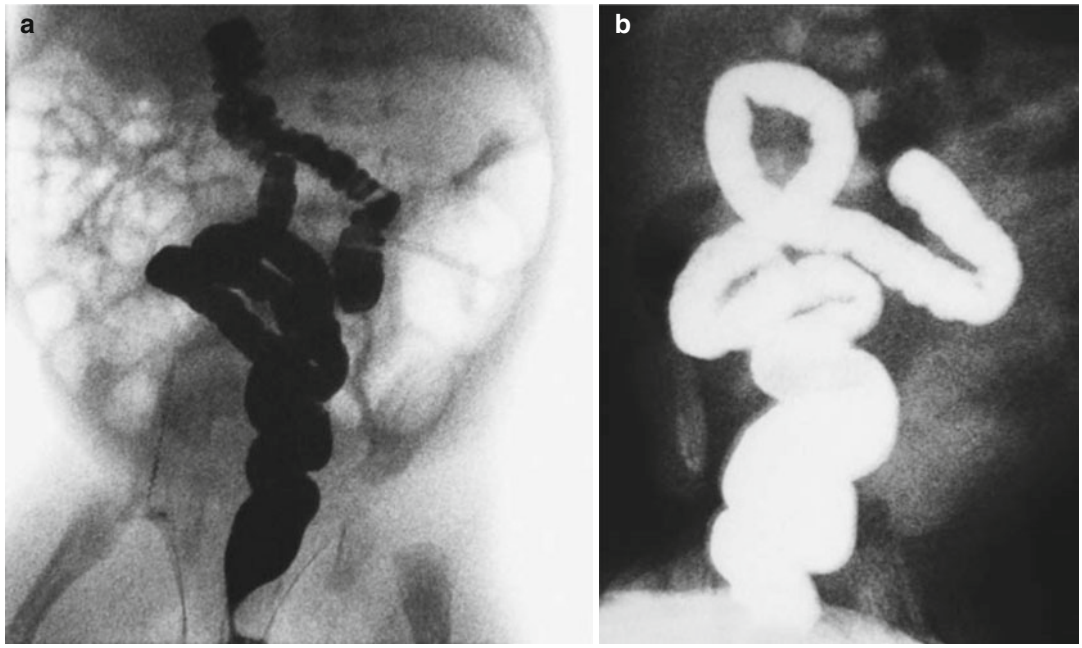


**Fig. 11** (**a**, **b**) Colonic atresia and stenosis. (**a**) Colonic atresia in a neonate with a small distal colon and a blind upper end. (**b**) Colonic atresia showing a lower bowel well distended with contrast but with no connection to the more proximal bowel

lumen (Lee et al. 2010). The colon is the least frequently involved site, and there is a gradient of decreasing frequency from the caecum to the rectum. Of the large bowel duplication cysts approximately 40 % are within the caecum. Their variation includes the colorectal tubular duplication cyst (duplication of the hind gut). This is a double-barrelled duplication involving part, or all, of the large bowel with a 'twin' segment on the mesenteric or ante-mesenteric side.

As such, these cysts are located in or adjacent to the wall of part of the gastrointestinal tract, have smooth muscle in their walls, and are lined by mucosa similar to that of some other portion of the alimentary tract. However, there may be ectopic squamous mucosa, transitional ciliated mucosa, lymphoid aggregates or ganglion cells. Gastric mucosa and pancreatic tissue are the only ectopic tissues of clinical importance. Technetium isotope studies may help demonstrate ectopic gastric mucosa.

Patients normally present in the neonatal period or in infancy, and there is a male-to-female ratio of 1:2. The patient may present with constipation, with obstruction if the cyst is of large size or with bleeding if the cyst communicates with the normal gut lumen and if there is ulceration of gastric mucosa within the duplication cyst. Duplication cysts may be associated with recto-genital or recto-urinary fistula, duplication of the internal or external genitalia, vertebral anomalies and multisystem congenital anomaly complexes. Female patients may present with the passage of faeces through the vagina. Approximately 20 % of rectal duplications communicate with the rectal lumen or may connect with the perineum as a chronic perianal fistula.

At contrast enema there may be simultaneous opacification of the true and the twin lumen. The cystic duplication may or may not contain air depending on whether it communicates with the lumen of the colon.

The most effective imaging is cross sectional, with ultrasound being the modality of choice although cysts may also be seen on fluoroscopy as filling defects (Fig. 12a). Ultrasound may show a sonolucent mass with through transmission if the cyst contains clear fluid con-

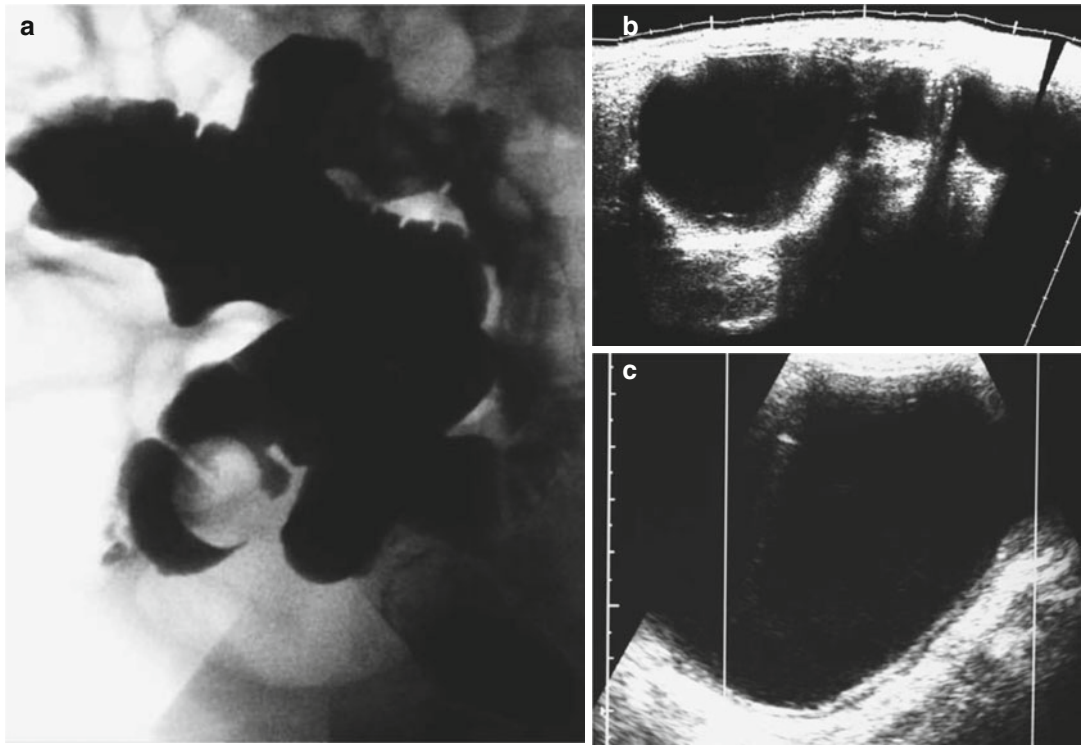


**Fig. 12** (**a**–**c**) Duplication cyst of the colon. (**a**) Contrast enema outlines the filling defect of a caecal duplication cyst. (**b**) Ultrasound of a duplication cyst at the hepatic flexure. (**c**) High-resolution ultrasound in the same patient shows the layers of the cyst wall and some echogenic debris within it

tents or may show an echogenic mass if the cyst contains haemorrhage or debris (Fig. 12b, c). Typically the inner echogenic mucosa and outer hypoechoic muscle layers are seen, a finding known as the 'double wall' or 'muscular rim'. Whilst this is very suggestive of a duplication cyst, this appearance can be seen with other cystic lesions and should therefore be interpreted with caution. The potential sonographic visualisation of the split hypoechoic muscularis propria layer or identification of all five layers of the bowel wall increases the specificity in making the sonographic diagnosis of duplication cyst (Cheng et al. 2005). CT or MRI can be used for greater clarification. MRI would be the investigation of preference given the absence of ionising radiation and the additional information that can be obtained about the cyst contents on different sequences. The intracystic fluid will be of mid-signal intensity on T1-weighted MR images and may be heterogeneous; it will return homogeneous high signal intensity on T2-weighted images.

## 7 Anorectal Anomalies

Anorectal anomalies occur in approximately 1 per 5000 live births and are more common in males.

The embryological development of the anorectal segment is complex, and as a result many anomalies are possible. The normal and abnormal development of the hindgut is still a matter of speculation, and our understanding is continually changing. However some aspects are better understood than previously: the process of maldevelopment starts very early in embryonic stages, the cloacal membrane is always too short in its dorsal part and as such the dorsal cloaca is missing, and as a result the hindgut remains attached to the sinus urogenitalis forming the rec-

tourethral fistula (Kluth 2010). It is only now becoming apparent that abnormal configurations of the hindgut/cloaca, which subsequently become manifest as an 'anorectal malformation', are not part of a normal development that has become 'arrested' but rather are an indicator of a fundamental error early in embryonic life.

Many clinical classification schemes have been proposed, and whilst one of the simplest and earliest outlines (Gans 1970) is still in use, it has largely been superseded. The 'Wingspread' classification (see below) was also been largely superseded by a classification described after the Krickenbeck conference of 2005 (Holschneider et al. 2005). More recently again, a classification by Levitt and Pena (2007) has come into use which aims to group together defects that share common diagnostic, therapeutic and prognostic features (below) (Levitt and Pena 2007).

| Classification of nonsyndromic anorectal malformations (ARM) |
|---|
| Males |
| Recto-perineal fistula |
| Rectourethral-bulbar fistula |
| Rectourethral-prostatic fistula |
| Recto-bladder neck fistula |
| Imperforated anus without fistula |
| Complex and unusual defects |
| Females |
| Recto-perineal fistula |
| Rectovestibular fistula |
| Cloaca with short common channel (<3 cm) |
| Cloaca with long common channel (>3 cm) |
| Imperforated anus without fistula |
| Complex and unusual defects |
| Cloacal exstrophy, covered cloacal extrophy |
| Posterior cloaca |
| Associated to presacral mass |
| Rectal atresia |

The Wingspread classification divides anorectal malformations into high, intermediate or low form, and although this terminology is still in widespread use, the assignment of a malformation to a particular category is somewhat arbitrary and inaccurate. The classification is/was based on the level of the rectal pouch relative to the levator ani muscle, i.e. above the levator ani is designated a supralevator or high, at the level of the levator ani is termed intermediate, and below the levator ani is termed translevator or low.

The majority of anorectal malformations are of the communicating type, in which the enteric component joins into the urinary or genital tract or to the perineum. This abnormally located opening to the exterior is usually termed 'fistula'; however, recent work suggests that embryologically this is not a fistula but an ectopic anal orifice (Nievelstein et al. 1994, 1998a, b).

Depending on the exact level of the distal end of the colon, it may have passed through the puborectal sling. In cases of a high ending colon, the colon ends at or above the puborectal sling which may be hypoplastic or absent. If the colon ends low, it will have passed through the puborectal sling, which will usually be well developed and functional. The level of the distal end of a colon will affect the imaging required and the subsequent surgical approach.

Anorectal malformations are frequently associated with other congenital anomalies, especially of the vertebra, kidney, oesophagus or trachea. Anorectal anomalies may present as part of the VACTERL pattern of anomalies (i.e. vertebral, anal, cardiac, tracheal, esophageal, renal and limb anomalies). The overall incidence of associated anomalies is approximately 50 %. Associated genitourinary tract abnormalities occur in 28–72 % of cases. The anomalies are twice as common with 'high' as opposed to 'low' anorectal malformations, although up to 30 % of patients with low imperforate anus have associated urologic anomalies which may still cause significant morbidity (Misra et al. 1996). Many of the associated anomalies are significant, and the long-term outcome for children with anorectal malformations is often dependent on the extent of the associated anomalies more than on the anorectal malformation itself.

When anorectal malformations are associated with several other congenital abnormalities, involving the spinal cord, spine and urogenital system, it is often called the caudal regression syndrome, which has an association with maternal diabetes. A further associated syndrome, Currarino's triad is the rare autosomal dominant genetic disorder characterised by the complex of

a congenital sacral bony abnormality with a 'sickle shape', anorectal malformation and a presacral mass (anterior meningocele, teratoma, dermoid cyst or enteric duplication cyst) (Currarino et al. 1981).

A separate, more complex group of anomalies is formed by the cloacal malformations, in which the urinary, genital and intestinal tracts converge to form a common channel with a single perineal orifice, i.e. the cloaca. These malformations are found exclusively in phenotypic females.

## 7.1 Imaging for Anorectal Anomalies

An anorectal anomaly is usually identified clinically. There may be an anal dimple present on the perineum, or there may be an apparently patent external orifice but with a digitally palpable membrane on examination. Meconium may be passed per urethra in boys or per vagina in girls.

It is still common that plain radiography is performed, and this will show a low obstruction early in the neonatal period (Fig. 13a) although this is no longer routinely advocated. A prone lateral shoot through radiograph may be helpful in determining the level of the atresia and allow assessment of the sacrum (Figs. 13b, c).

Ultrasound has been used to delineate the distance from the distal air-filled colon to the perineum although its use is not widespread (Donaldson et al. 1989); less than 10 mm indicates a low lesion, and 15 mm or greater indicates a high lesion that will require diversion with colostomy.

Given the high incidence of associated anomalies, all patients should have a renal ultrasound early in the newborn period. If this shows collecting system dilatation, dilatation of the ureter or other renal abnormality (Fig. 13d), a full urological workup should be performed before a colostomy is fashioned or immediately after (Pena 1993). It is appropriate to perform spinal ultrasound at the same examination to assess the integrity of the spinal cord and any associated dysraphic abnormalities (Fig. 13e). If this is normal, only plain radiographs of the lumbar spine will be required, but if any further anomalies are demonstrated, MRI of the lumbosacral spine should be obtained later when clinically appropriate (Fig. 13f). Possible associated intraspinal pathology includes caudal regression syndrome, cord tethering, hydromyelia or lipoma of the filum terminale. Newborn females with a cloaca may need drainage of a hydrocolpos.

Many centres make a clinical decision whether to proceed to definitive primary repair by perinealanoplasty (for low malformations) or to perform a colostomy only, deferring further imaging until definitive repair can be performed at a later date (in high malformations). Most centres routinely use a combination of a micturating cystogram (MCU) and a loopogram through the loop colostomy (high-pressure distal colostogram) to outline any associated connection or 'fistula' between the distal bowel and the urinary tract (Fig. 13g, h). The MCU/VCUG will also demonstrate the degree of any associated vesicoureteral reflux. An increasing number of centres are additionally using MR imaging, as it can help determine the presence of the puborectalis muscle and external sphincter as well as the rectal pouch prior to surgery. The definitive surgical approach for high malformations is dependent on the type of fistula demonstrated. The posterior sagittal anorectoplasty (PSARP) is most often used in this group, but in cases with an additional rectovesical fistula, a laparotomy is also required in addition to the posterior sagittal approach.

A PSARP is performed prone. A midline posterior sagittal incision is made extending from the mid level of the sacrum to the anterior edge of the external sphincter.

The sphincter mechanism is divided in the midline, hence preserving the nerve fibres and thus faecal continence. The gluteal muscles are opened like a book, and all internal structures including the 'fistula' are exposed. The rectum is then separated from the genitourinary tract, dissected and freed enough to reach its normal orifice without tension. The fistula site is then closed.

With the use of an electrical muscle stimulator, the limits of the sphincter mechanism are determined, and the rectum is placed in its optimal location to achieve the best functional results. Adequate placement of the neorectum in both the puborecta-

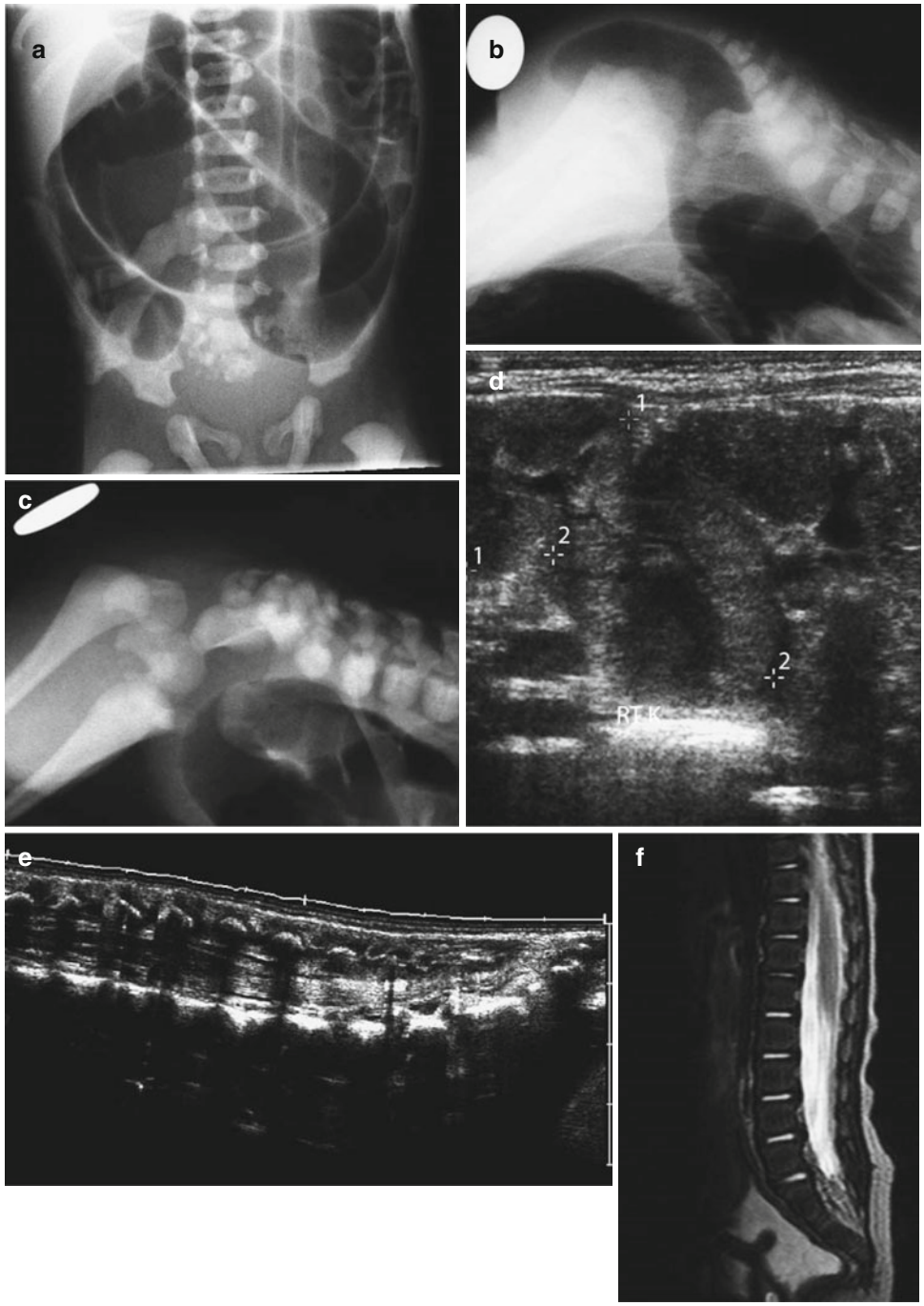


**Fig. 13** (**a**) Abdominal radiograph on day 1 of life. The bowel is distended with air but this comes to an abrupt end low in the pelvis. Note the associated deficient sacrum. (**b**) A prone lateral shoot through radiograph showing the lowest air-filled bowel which is near the radio-opaque marker place in the natal cleft. This is a 'low' anomaly. (**c**) A prone lateral shoot through radiograph showing the lowest air-filled bowel which is near the radio-opaque marker place in the natal cleft. This is a higher anomaly. (**d**) Renal US showing crossed fused ectopia in an infant with an anorectal malformation. The fused right and left kidneys are shown by the markers. (**e**) Spine ultrasound in the patient shown in (**a**) showing the deficient sacrum; the cord was normal. (**f**) T2-weighted sagittal sequence of the spine showing the partly absent sacrum. (**g**) A 'fistula' inserting into the posterior urethra of a male infant. (**h**) Loopogram study demonstrating distension of the distal colon with retrograde filling of the bladder via the very narrow fistula. (**i**) MR of the pelvic floor following surgery showing mesenteric fat that has inadvertently been brought down into the rectal complex

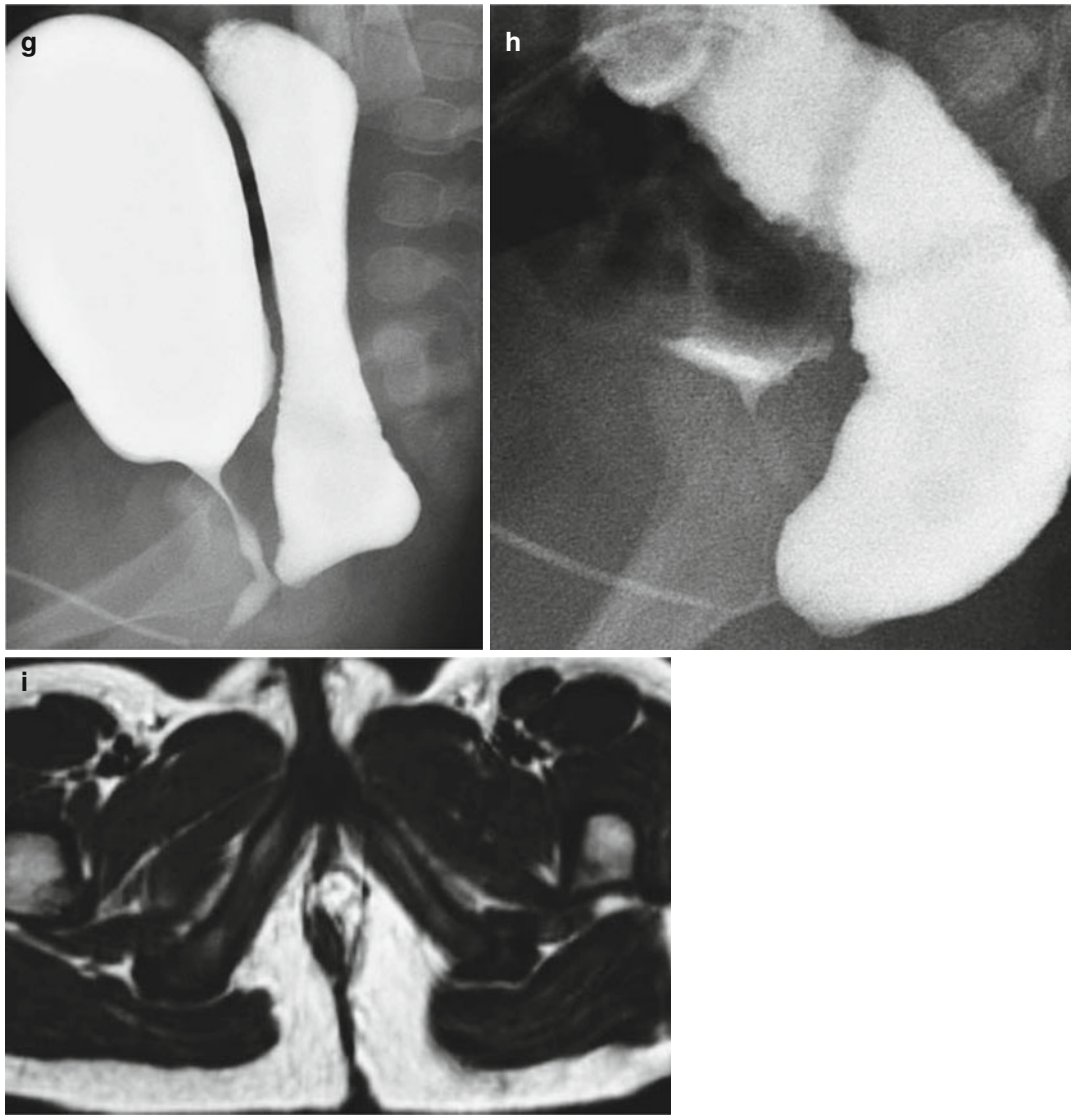


**Fig. 13** (continued)

lis muscle and the external anal sphincter is essential in achieving an acceptable functional outcome (Fig. 13i) (Nievelstein et al. 1998a, b).

### 7.1.1 MCU/VCUG and Loopogram Technique

The combined MCU/VCUG and loopogram is usually performed when the child is a few months old. An MCU/VCUG is performed first using a urethral catheter, and good distention of the bladder must be achieved. The 'fistula', if present, is often demonstrated at MCU when the child voids (raising bladder pressure) with retrograde filling of the fistula connecting to the distal bowel. The urethral catheter is then kept in place to demarcate the exact course of the urethra. The loopogram is then performed using water-soluble contrast, with a good seal being obtained at the stomal orifice by careful inflation of the catheter balloon. The hydrostatic pressure must be high enough (manual syringe injection) to overcome the muscle tone of the striated muscle mecha-

nism that surrounds the rectum and normally keeps it collapsed. With maximal filling of the distal pouch, and with refilling of the bladder so that the child voids a second time, the fistula may again be delineated, and the inferior limit of the distal pouch can be demonstrated. It is essential to get good pressure in the distal segment to be certain that any possible ectopic insertion of the bowel has been demonstrated. The final single image should show the sacrum, height of the rectum, perineum, fistula location, bladder, vesicoureteral reflux if present and urethra. This study is vital in determining the anatomy so that the definitive repair can be planned. In 10 % of patients the fistula is at the bladder neck. In this case, during the main repair, the surgeon knows that the rectum will only be found through the abdomen, and a combined posterior sagittal and abdominal or laparoscopic approach is employed (Levitt and Pena 2007).

### 7.1.2 MRI Imaging Technique in the Prenatal, Neonatal and Presurgical Periods

Fetal MR imaging for ARM is typically performed in the third trimester of pregnancy. It should not be performed before 20 weeks gestation because before this time meconium cannot be accurately demonstrated within the colon and rectum. Fetal MRI is routinely performed in a 1.5 T magnet with a standard phased-array body coil. Recommended sequences are obtained in all three planes relative to the fetus and without fat saturation: 1) T2-weighted single-shot fast spin echo, 2) two-dimensional (2D) balanced steady-state free precession (bSSFP) and 3) T1-weighted fast gradient recalled echo (Podberesky et al. 2013).

Baughman et al. described 'MR genitography' in 2007, and their protocol consisted of routine multiplanar high-resolution T1-weighted and T2-weighted sequences through the pelvis, followed by a 3D T1-weighted spoiled gradient recalled echo (SPGR) sequence with fat saturation acquired during active hand instillation of dilute gadolinium through balloon catheters via the common channel, mucous fistula/colonic stoma and urethra/vesicostomy (when present) (Podberesky, Towbin et al. 2013) (Baughman et al. 2007). This has been further refined by Jarboe and colleagues in 2012 describing a similar technique combining MRI with 3D rotational fluoroscopy (Jarboe et al. 2012). All of these techniques are summarised in an overview by Podberesky (Podberesky et al. 2013).

The level of the anorectal malformation can be adequately demonstrated on T1-weighted images, but the T2-weighted images are particularly helpful in the evaluation of intermediate and low malformation because the highest signal intensity of the anorectal mucosa allows better delineation of the anorectum with respect to this sphincter muscle complex and perineum (Nievelstein et al. 1998a, b). Reconstruction in sagittal and coronal planes allows accurate determination of the level of the malformation. The use of FSE T2-weighted sagittal and axial images allows detection of a fistula, although the exact level of connection to the urogenital system may still be difficult to ascertain unless appropriate fluid distension has been achieved. If MRI is performed in the immediate neonatal period, the hyperintense meconium inside the rectal pouch on T1-weighted images may serve as an excellent MRI contrast agent.

The advantages of MRI are its exquisite depiction of the malformation(s), the ability to reconstruct in 3D, the lack of ionising radiation and the opportunity to characterise the vast range of associated anomalies in one imaging session.

For further details of specialised MRI anatomy and techniques, the interested reader is referred to the cited literature (Pena 1993; Nievelstein et al. 1998a, b; Pringle et al. 1987; Vade et al. 1989; Taccone et al. 1992; Fukuya et al. 1993; Podberesky et al. 2013; Baughman et al. 2007; Jarboe et al. 2012).

## 8 Typhlitis

Typhlitis, also known as ileocaecal syndrome or neutropenic colitis, is an acute inflammation of the caecum, appendix and occasionally terminal ileum. It is primarily described in children

with leukaemia and a severe neutropenia. Histologically the changes are of oedema and ulceration of the entire bowel wall, with transmural necrosis and perforation possible. It is thought to be due to a leukaemia or lymphomatous infiltrate, ischaemia, focal pseudomembranous colitis and/or infection. The most common organisms found include cytomegalovirus virus, *Pseudomonas*, *Candida*, *Klebsiella*, *E. coli*, *B. fragilis* and *Enterobacter*. Whilst being most common in childhood leukaemia, it is also seen in aplastic anaemia, lymphoma and during immunosuppressive therapy. Children present with abdominal pain (which may be localised to the right iliac fossa), watery diarrhoea, a palpable mass in the right iliac fossa, fever in neutropenia or with bloody stools.

The caecum and ascending colon are the most common sites of involvement; the appendix and the terminal ileum may be secondarily involved. The plain abdominal radiograph may show distention of nearby small bowel loops, possibly a fluid-filled mass-like density in the right iliac fossa, representing the caecum, thumbprinting of the ascending colon and thickening of the caecal wall to greater than 4 mm. Typhlitis may be associated with pneumatosis coli which is a common finding in markedly immunosuppressed children. Ultrasound examination can be either by a curvilinear or a linear probe. The circumferential thickening of the caecal wall, and possibly the terminal ileum, will be seen. There may be adjacent oedema. Some centres advocate the use of CT where the main findings will again be of wall thickening of the caecum, decreased bowel wall attenuation due to oedema, streaking and stranding of the adjacent fat and thickening of the fascial planes, as well as fluid around the colon associated with intramural pneumatosis.

Contrast studies should not be attempted due to the risk of perforation. In the absence of perforation surgery is not indicated.

The differential diagnosis includes appendicitis with an appendicular abscess, inflammatory bowel disease or leukaemic deposit (in which case the wall thickening is likely to be eccentric) (Alexander et al. 1988) (Fig. 14).

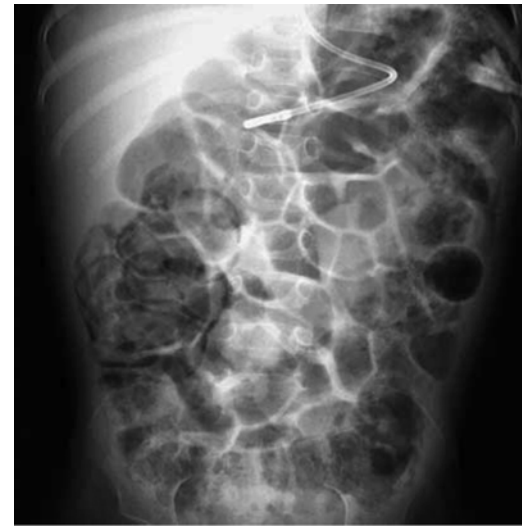

**Fig. 14** Abdominal radiograph showing thickening of the caecal wall and intramural air consistent with typhlitis in this immunocompromised patient

## 9 Volvulus

Volvulus of the colon is rare in children and infants, with only sporadic cases reported thus far, but when seen it most commonly involves the sigmoid colon, although caecal volvulus can also occur. The sigmoid colon in infants and children is often redundant, and therefore the extra length is believed to be prone to twisting. In a recent review of the literature (Salas et al. 2000) the median age at presentation was 7 years, ranging from 4 h to 18 years. Boys were more commonly affected than girls (ratio: 3.5 to 1) and presentation could be either acute or recurrent. In acute cases, the mean duration of symptoms, including severe pain that may escalate to shock and circulatory collapse, was 1.5 days. In recurrent cases, the chronic and intermittent episodes of pain had been present, on average, for 1 year. The most common symptoms are abdominal pain that is relieved by passage of stool or flatus, abdominal distention and vomiting.

A plain abdominal radiograph shows colonic dilatation. A sigmoid volvulus tends to point to the right upper quadrant and will be shown by enclosed loop of dilated bowel. As in adults, a caecal volvulus will tend to lie in the left upper quadrant. The diagnosis is usually made from the

plain abdominal film; however, if a contrast enema is performed, this may demonstrate a typical beak deformity showing the point of obstruction as a result of twisting by the volvulus. The volvulus may resolve spontaneously, but if persistent will need to be reduced surgically, although in some patients a contrast examination may reduce the volvulus (Mellor and Drake 1994).

## 10 Lymphoid Hyperplasia

Lymphoid hyperplasia affecting the colon in infants and children is well recognised and best seen on a double-contrast barium enema. The classical finding is a mucosa studded with innumerable 1- to 3-mm small uniform nodules. Some of these lesions may show an umbilicated centre, but this is not always seen. Whilst it is normal to find some lymphoid follicles in the paediatric gut, they are usually sparser and more diffuse.

Lymphoid hyperplasia is most commonly seen in children less than 2 years old but is also seen in older children and adults. The histology is that of hyperplastic lymph follicles in the lamina propria (Peyer's patches), and these follicles probably represent a compensatory attempt for immunoglobulin deficiency. In adults lymphoid hyperplasia is associated with late onset immunoglobulin deficiency (IgA, IgM). Occasionally lymphoid hyperplasia can take the form of large polypoid growths in the ileocaecal region. Clinical presentation may be indistinguishable from acute appendicitis. In this variant of lymphoid hyperplasia there is increased risk of bleeding and intussusception, with secondary obstruction. The condition may require surgical intervention.

## 11 Necrotising Enterocolitis

Necrotising enterocolitis (NEC) in modern paediatric practice refers to the idiopathic, often severe, enterocolitis that occurs in premature infants in neonatal intensive care units. The only definite risk factor for NEC is prematurity, and the majority of cases occur in infants who weigh less than 2000 g, with both the incidence and mortality

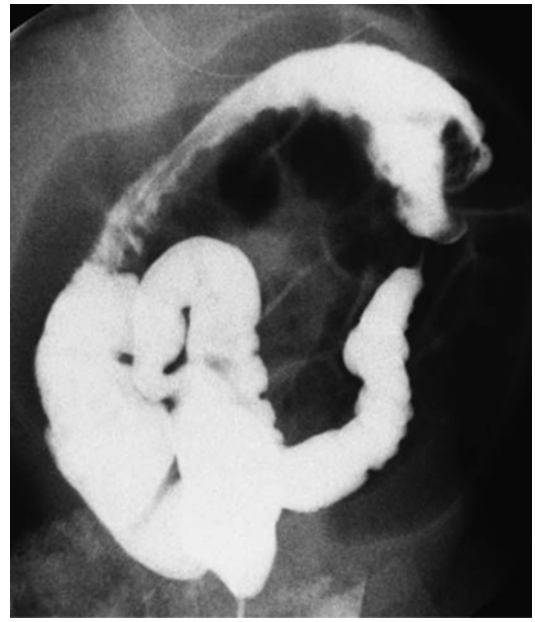

**Fig. 15** Contrast enema showing a stricture of the descending colon following necrotising enterocolitis

increasing with decreasing birth weight and gestational age (Holman et al. 1997). NEC may also occur in full-term infants with a predisposition, such as those who have had surgery for congenital heart disease or who have had abdominal surgery. An acute enteritis may be seen in Hirschsprung disease. Vascular lines and generalised sepsis have been loosely associated with NEC.

Inflammation begins in the mucosa of the bowel wall and then extends through the whole bowel wall. The terminal ileum and the proximal colon are the most commonly affected areas. The main ultrasound findings are of portal venous air, free air, peritoneal fluid, bowel wall thickness, echogenicity, perfusion and intramural air and are comprehensively described in the literature (Faingold et al. 2005; Epelman et al. 2007; Silva et al. 2007).

Details of the acute radiological findings are described elsewhere in the text, as they are not specific to the colon. However, the complications of NEC often do involve the colon with approximately 10–20 % of survivors developing strictures of the bowel that may be single or multiple. Despite NEC most commonly affecting the distal ileum and the ascending colon the majority of strictures affect the descending colon (Fig. 15).

Infants who have developed strictures may be asymptomatic, but most present clinically within weeks to months of the initial diagnosis of NEC, usually with a distended abdomen, intolerance of feeds or obstruction. In those infants who have had surgery to raise an ileostomy or colostomy, it is essential to assess the distal bowel using a loopogram or contrast enema before reversal of the stoma.

## 12 Inflammatory Bowel Disease Affecting the Colon

In infants and young children the majority of the colitides are thought to be infectious in origin, although ulcerative colitis (UC) and Crohn disease (CD) are also seen. In the neonatal period, inflammatory processes of the colon are often related to necrotising enterocolitis, but the enterocolitis of Hirschsprung disease and colitis associated with milk allergy are also well recognised. UC and CD are the main inflammatory diseases of the colon that come to the attention of the paediatric radiologist and hence are discussed below.

### 12.1 Chronic Inflammatory Bowel Disease

UC and CD are both considered 'idiopathic' types of inflammatory bowel disease (IBD). They are distinguished by their morphological, histological, clinical and epidemiological features and by their distribution in the gut. In some cases it is not possible to differentiate the two conditions by the standard criteria and in such patients the colitis is considered 'indeterminate'. Patients may present with abdominal symptoms such as pain, cramping, diarrhoea, bloody stools and weight loss, but also with associated symptoms including anorexia, arthritis, failure to thrive and other extra-intestinal symptoms. The aetiology is unclear but childhood infection, early diarrhoea, immunological hypersensitivity and vasculitis have all been linked to both CD and UC. Affected relatives or a family history is reported in up to 20 % of patients suggesting a genetic contribution in at least some cases. It is becoming increasingly apparent from prospective studies of international registries (EUROKIDS) that there are different phenotypes within paediatric CD at the point of diagnosis, and isolated colonic disease accounts for approximately 27 % of newly diagnosed CD (de Bie et al. 2013). Accurate phenotyping is essential in paediatric CD as this affects the management of individual patients; imaging plays a significant part in that phenotyping. There are significant differences in the location and activity of intestinal CD lesions between adult and paediatric patients which are detected with MRE: (1) the distal ileum is maximally involved in adults vs. the left colon in children, (2) the causes of the severe left colonic disease in children are unknown, and (3) the extensive colonic involvement in children has clinical-diagnostic implications (Maccioni et al. 2012).

### 12.2 Imaging in Inflammatory Bowel Disease of the Colon

Colonoscopy and biopsy has been the mainstay in the investigation of suspected IBD affecting the colon or terminal ileum. Capsule endoscopy is increasingly used for assessment of the small bowel lumen and also affords information regarding the colon; its use in children is now widely accepted. However, imaging can add important information during disease exacerbations and complications. Plain abdominal radiographs may demonstrate an acute colitis, bowel perforation or obstruction. The features of acute colitis include increased thickness of the colonic wall, irregularity of the mucosal surface, bowel dilatation and an abnormal stool distribution (stool being non-adherent to inflamed mucosa). Absence of any stool suggests significant and widespread inflammation, and associated spasm may result in the absence of any bowel contents (stool or air). Nuclear medicine examinations provide an adjunct to endoscopy and radiological techniques with technetium-leucocyte scans (white cell scans) useful for assessing the presence and location of active disease in children (Fig. 16a). Whilst

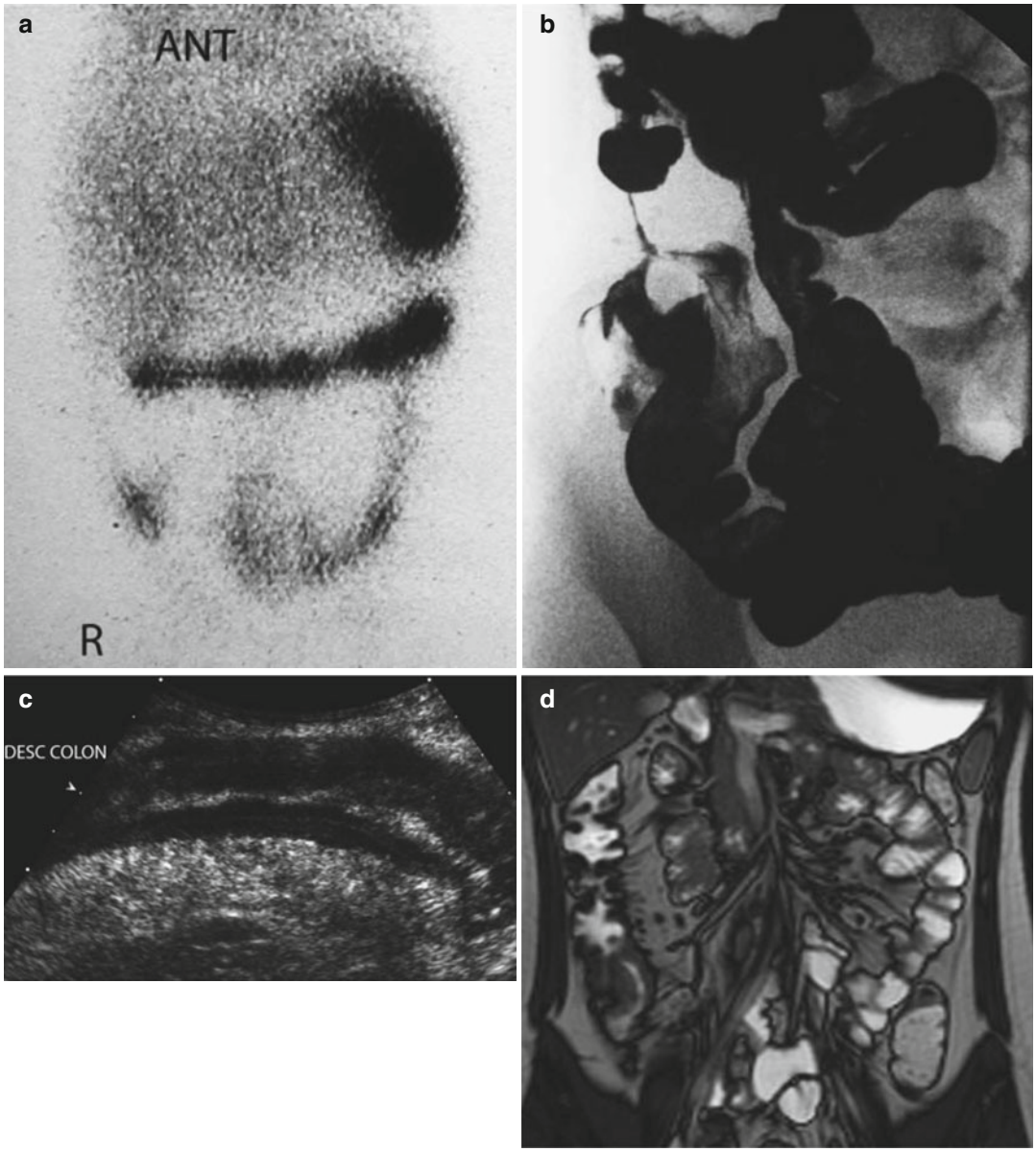


**Fig. 16** (**a**–**d**) Crohn disease of the colon. (**a**) Indium labelled white cell scan in active disease with widespread involvement of the caecum and transverse and descending colon. (**b**) Barium follow-through demonstrating stricture formation of the ascending colon with displaced adjacent bowel consistent with an inflammatory mass. (**c**) Ultrasound of the descending colon in a patient with active disease. Note the thickened bowel wall and the obliterated bowel lumen. (**d**) Coronal MRI showing marked wall thickening of the caecal pole with a narrowed lumen

this technique cannot give anatomical detail regarding strictures and fistulae, it is able to confirm active disease using a lower radiation dose than the barium follow through or barium enema.

Whilst the barium follow-through has historically been the main contrast examination for assessing the small bowel in IBD (Fig. 16b), it may still provide information on the colon if delayed views are obtained. However contrast studies have now been largely superseded by the use of MR enterography due to the high cumulative radiation burden (Sauer et al. 2011) and the

limited information that contrast studies can provide in the context of IBD. Consensus evidence-based guidelines have recently been produced (2013) by the ECCO and ESGAR scientific societies which clearly delineate an imaging strategy in the assessment of IBD (Panes et al. 2013).

There has been increasing use of MRI in the imaging of CD in children, and it has been shown that MR enterography (MRE) successfully identifies small bowel and colon segments affected by paediatric CD with an overall sensitivity of 94 % (Dillman et al. 2011). Specifically in the colon an MRI total colonic inflammation score (TCIS) has been developed for the assessment of patients with severe acute inflammatory colitis taking into account segmental haustral loss, mesenteric and mural oedema, mural thickness and small bowel and colonic dilatation (Hafeez et al. 2011). A recent study comparing MRE with endoscopy, histopathology and laboratory evaluation in paediatric CD has added to the growing body of evidence that MRE provides excellent assessment of inflammation and measures disease activity in CD (Sauer et al. 2012). CT enterography is an alternative (and gives excellent depiction of the paediatric bowel) but carries a high radiation burden, and MRE is used in preference wherever possible. As such CT enterography will not be discussed further.

## 12.3 MR Enterography (MRE) in Inflammatory Bowel Disease in Children

MRE is now considered the study of choice when evaluating paediatric IBD, especially at follow-up when the diagnosis has been established, although it mainly focuses on the small bowel (and is described elsewhere in the text). It has excellent contrast resolution and no radiation burden, allowing superb depiction of the bowel lumen, bowel wall and adjacent soft tissue structures and related pathologies (including abscesses and intra-abdominal and perianal sinus tracts and fistulae). The lack of ionising radiation allows for dynamic post-contrast imaging, assessment of areas of luminal narrowing over an extended period of time to confirm the presence of a stricture and repeat imaging if a series is of limited diagnostic quality. Further benefits of MRE include excellent contrast resolution, availability of cine imaging techniques to show bowel peristalsis/rigidity and the availability of qualitative and quantitative function techniques such as diffusion-weighted imaging (Hammer, Podberesky et al. 2013).

Dedicated MR colonography (MRC) specifically targeted at the colon is still being developed, but MRC would seem to offer great potential for the assessment of colonic inflammation in children/adolescents with IBD affecting the colon. Two different approaches can be used: bright lumen and dark lumen MRC. A dark lumen approach, using a water enema that produces low signal intensity on T1-weighted images, is preferred for the evaluation of IBD because it permits better evaluation of the bowel wall (Paolantonio et al. 2009). By giving barium before the MR examination, stool is rendered virtually indistinguishable from the administered water enema on heavily T1w GRE images. This technique is called faecal tagging and avoids the needs for large bowel cleansing prior to the procedure and yet gives high contrast resolution between the brightly enhancing colonic wall after intravenous gadolinium and the bowel lumen (and its contents).

MRE is generally well tolerated in the paediatric population and obtains images of similar quality to those of adults. It is feasible in patients of 9 years old and older without sedation, and younger children who are compliant may also be able to tolerate it without too much difficulty. Oral contrast ingestion regimes should be based on patient age (Absah et al. 2012).

Various protocols are in use and are well described in the literature (Towbin et al. 2013; Hammer et al. 2013; Panes et al. 2013; Horsthuis et al. 2005; Gourtsoyiannis et al. 2004; Kim and Ha 2003). Typically this may be performed using 1 l of 2.5 % mannitol solution as an oral preparation, taken over the hour leading up to the imaging, and following a 6-h fast. Hyoscine butylbromide (or glucagon) and gadolinium are given intravenously at the start of the scan, and

sequences typically including heavily T2-weighted (HASTE), true FISPs and VIBEs (3D volume acquisition) are obtained in a coronal plane and axial plane.

### 12.3.1 Imaging Finding in Ulcerative Colitis

Ulcerative colitis is well recognised in children, but tends to occur in older children, with a similar pattern to that seen in adults. The inflammatory process is confined to the mucosa and superficial mucosa of the colon, and the inflammation typically extends for a varying distance retrogradely from the rectum. Colonoscopy (and the facility for biopsy) is the investigation of choice for making the initial diagnosis, and the barium enema is considered virtually obsolete. If a double-contrast enema is obtained, the classic findings are those of superficial ulceration of the mucosa, often appearing as a fine mucosal granularity and loss of haustration. The presacral space may be widened with active disease in the rectum. As the disease progresses the ulceration will become more prominent with spicules and serrated bowel margins. Deeper ulcers are described as being 'collar button'. and there may be 'double tracking' representing longitudinal submucosal ulceration. 'Thumbprinting' demonstrates symmetric thickening of the colonic folds. As the disease progresses inflammatory polyps may be seen, the mucosa becomes coarsened, and eventually the colon becomes shortened, distensible and without haustral markings or a mucosal pattern.

On MR imaging the colon wall should normally measure less than 3 mm. On T2-weighted MRE or MRC images, normal bowel is of intermediate signal, whereas abnormal bowel is not well seen. The differential diagnosis between colonic CD, UC and indeterminate colitis is not always possible on imaging alone and will often require colonoscopy and biopsy. However, a common finding of UC on MRI is mural thickening due to oedema or fatty infiltration of the submucosa and hypertrophy of the muscularis mucosae. During UC inflammation does not involve the entire thickness of the colonic wall but is usually limited to the mucosa and submucosa.

### 12.3.2 Imaging Findings in Crohn Disease (CD) Affecting the Colon

In contrast, CD shows transmural inflammation and characteristically affects some areas of bowel and not others. Compared to ulcerative colitis, the colon is less affected in CD, but overall CD is more common than ulcerative colitis in children, and therefore inflammatory bowel disease affecting the colon in children is most commonly CD. CD particularly affects the right side of the colon with sparing of the rectum and sigmoid colon. In the early stages there will be nodular enlargement of lymphoid follicles and aphthous ulcers that can be seen directly by colonoscopy on a barium enema. As the disease progresses the findings are similar to those in adults, i.e. a cobblestone appearance to the bowel wall caused by longitudinal and transverse ulcers separated by areas of oedema, straightening and rigidity of the affected part of the colon, strictures and fistulae. Contrast studies have been largely replaced by a combination of capsule endoscopy, direct colonoscopy and MR examination; however, white cell studies (nuclear medicine) are useful for confirming acute exacerbation when anatomical detail is not required. Ultrasound is useful for showing thickening of the bowel wall, typically to 8 mm or more (Fig. 16c), and can also show the presence of abscesses and distended loops. MRI (as described in the section above) is now the investigation of choice to examine the bowel wall (Fig. 16d) and also to show the presence and configuration of fistulae, especially in the perianal region.

As both CD and ulcerative colitis are similar in adults and children, the reader is referred to the adult literature for further reading.

### 12.3.3 Imaging the Perianal and Perineal Region in Inflammatory Bowel Disease

Perianal and perineal cutaneous inflammatory involvement in the setting of IBD occurs almost exclusive with Crohn disease (CD) and has been reported to occur in 13–49 % of paediatric CD patients (Essary et al. 2007), manifesting as fistulae and fissures, associated abscesses, non-specific

skin inflammation and skin tags. Whilst MRE allows for superb examination of the affected bowel, high-resolution, small field of view imaging of the perineum (especially at 3 T field strength) gives precise information on the degree of perianal, labial and scrotal involvement. Typical sequences would include T2w without fat suppression (sagittal, coronal, transverse), T2w with fat suppression (transverse) and T1w fast spin echo with fat suppression +/- contrast (transverse) (Halligan and Stoker 2006) or with the addition of T1w 3-DSPGR pre- and post-contrast sequences (Hammer et al. 2013). A critical component of the MR technique is that the localiser needs to be aligned with the longitudinal axis of the anal canal and the other orthogonal planes then based relative to this. A comprehensive review of the current state of the art is given by Hammer and coinvestigators (Hammer et al. 2013) and in the adult literature on perianal CD.

## References


Absah I, Bruining DH, Matsumoto JM et al (2012) MR enterography in pediatric inflammatory bowel disease: retrospective assessment of patient tolerance, image quality, and initial performance estimates. AJR Am J Roentgenol 199(3):W367–W375

Abu-Yousef M, Bleicher JJ, Maher JM et al (1987) High-resolution sonography of acute appendicitis. AJR Am J Roentgenol 149(1):53–58

Alexander JE, Williamson SL, Seibert JJ et al (1988) The ultrasonographic diagnosis of typhlitis (neutropenic colitis). Pediatr Radiol 18(3):200–204

Al-Tokhais T, Hsieh H, Pemberton J et al (2012) Antibiotics administration before enema reduction of intussusception: is it necessary? J Pediatr Surg 47(5): 928–930

Applegate KE (2009) Intussusception in children: evidence-based diagnosis and treatment. Pediatr Radiol 39(Suppl 2):S140–S143

Bardisa-Ezcurra L, Ullman R, Gordon J (2010) Diagnosis and management of idiopathic childhood constipation: summary of NICE guidance. BMJ 340:c2585

Barr RG, Levine MD, Wilkinson RH, Mulvihill D (1979) Chronic and occult stool retention: a clinical tool for its evaluation in school-aged children. Clin Pediatr (Phila). 18(11):674, 676–679, passim.

Baughman SM, Richardson RR, Podberesky DJ et al (2007) 3-Dimensional magnetic resonance genitography: a different look at cloacal malformations. J Urol 178(4 Pt 2):1675–1678; discussion 1678–1679

Bekdash BSS, Marven SS, Sprigg A (2013) Reduction of intussusception: defining a better index of successful non-operative treatment. Pediatr Radiol 43(6):649–656

Benninga MA, Buller HA, Heymans HS et al (1994) Is encopresis always the result of constipation? Arch Dis Child 71(3):186–193

Berdon WE, Slovis TL, Campbell JB et al (1977) Neonatal small left colon syndrome: its relationship to aganglionosis and meconium plug syndrome. Radiology 125(2):457–462

Berger MY, Tabbers MM, Kurver MJ et al (2012) Value of abdominal radiography, colonic transit time, and rectal ultrasound scanning in the diagnosis of idiopathic constipation in children: a systematic review. J Pediatr 161(1):44–50.e41–42

Carty HM (2002) Paediatric emergencies: non-traumatic abdominal emergencies. Eur Radiol 12(12):2835–2848

Cheng G, Soboleski D, Daneman A et al (2005) Sonographic pitfalls in the diagnosis of enteric duplication cysts. AJR Am J Roentgenol 184(2):521–525

Clatworthy HW Jr, Howard WH, Lloyd J (1956) The meconium plug syndrome. Surgery 39(1):131–142

Currarino G, Coln D, Votteler T (1981) Triad of anorectal, sacral, and presacral anomalies. AJR Am J Roentgenol 137(2):395–398

Daneman A, Navarro O (2003) Intussusception. Part 1: a review of diagnostic approaches. Pediatr Radiol 33(2): 79–85

Daneman A, Alton DA, Lobo E et al (1998) Patterns of recurrence of intussusception in children: a 17-year review. Pediatr Radiol 28(12):913–919

De Bie CI, Paerregaard A, Kolacek S et al (2013) Disease phenotype at diagnosis in pediatric Crohn's disease: 5-year analyses of the EUROKIDS Registry. Inflamm Bowel Dis 19(2):378–385

De Giorgio R, Cogliandro RF, Barbara G et al (2011) Chronic intestinal pseudo-obstruction: clinical features, diagnosis, and therapy. Gastroenterol Clin North Am 40(4):787–807

Del-Pozo G, Albillos JC, Tejedor D (1996) Intussusception: US findings with pathologic correlation – the crescent-in-doughnut sign. Radiology 199(3):688–692

Del-Pozo G, Albillos JC, Tejedor D et al (1999) Intussusception in children: current concepts in diagnosis and enema reduction. Radiographics 19(2): 299–319

Dillman JR, Ladino-Torres MF, Adler J et al (2011) Comparison of MR enterography and histopathology in the evaluation of pediatric Crohn disease. Pediatr Radiol 41(12):1552–1558

Donaldson JS, Black CT, Reynolds M et al (1989) Ultrasound of the distal pouch in infants with imperforate anus. J Pediatr Surg 24(5):465–468

Doria AS, Moineddin R, Kellenberger CJ et al (2006) US or CT for diagnosis of appendicitis in children and adults? A meta-analysis. Radiology 241(1):83–94

Ellis H, Kumar R, Kostyrka B (2009) Neonatal small left colon syndrome in the offspring of diabetic mothers-an analysis of 105 children. J Pediatr Surg 44(12): 2343–2346

Epelman M, Daneman A, Navarro OM et al (2007) Necrotizing enterocolitis: review of state-of-the-art imaging findings with pathologic correlation. Radiographics 27(2):285–305

Essary B, Kim J, Anupindi S et al (2007) Pelvic MRI in children with Crohn disease and suspected perianal involvement. Pediatr Radiol 37(2):201–208

Faingold R, Daneman A, Tomlinson G et al (2005) Necrotizing enterocolitis: assessment of bowel viability with color doppler US. Radiology 235(2):587–594

Fallon SC, Lopez ME, Zhang W et al (2013) Risk factors for surgery in pediatric intussusception in the era of pneumatic reduction. J Pediatr Surg 48(5):1032–1036

Fefferman NR, Roche KJ, Pinkney LP et al (2001) Suspected appendicitis in children: focused CT technique for evaluation. Radiology 220(3):691–695

Fotter R (1998) Imaging of constipation in infants and children. Eur Radiol 8(2):248–258

Fukuya T, Honda H, Kubota M et al (1993) Postoperative MRI evaluation of anorectal malformations with clinical correlation. Pediatr Radiol 23(8):583–586

Gans SL (1970) Classification of anorectal anomalies: a critical analysis. J Pediatr Surg 5(5):511–513

Goldin AB, Khanna P, Thapa M et al (2011) Revised ultrasound criteria for appendicitis in children improve diagnostic accuracy. Pediatr Radiol 41(8):993–999

Gorenstein A, Raucher A, Serour F et al (1998) Intussusception in children: reduction with repeated, delayed air enema. Radiology 206(3):721–724

Gourtsoyiannis N, Papanikolaou N, Grammatikakis J et al (2004) Assessment of Crohn's disease activity in the small bowel with MR and conventional enteroclysis: preliminary results. Eur Radiol 14(6):1017–1024

Hafeez R, Punwani S, Pendse D et al (2011) Derivation of a T2-weighted MRI total colonic inflammation score (TCIS) for assessment of patients with severe acute inflammatory colitis-a preliminary study. Eur Radiol 21(2):366–377

Halligan S, Stoker J (2006) Imaging of fistula in ano. Radiology 239(1):18–33

Hammer MR, Podberesky DJ, Dillman JR (2013) Multidetector computed tomographic and magnetic resonance enterography in children: state of the art. Radiol Clin North Am 51(4):615–636

Heneyke S, Smith VV, Spitz L et al (1999) Chronic intestinal pseudo-obstruction: treatment and long term follow up of 44 patients. Arch Dis Child 81(1):21–27

Herliczek TW, Swenson DS, Mayo-Smith WW (2013) Utility of MRI after inconclusive ultrasound in pediatric patients with suspected appendicitis: retrospective review of 60 consecutive patients. AJR Am J Roentgenol 200(5):969–973

Holman RC, Stoll BJ, Clarke MJ et al (1997) The epidemiology of necrotizing enterocolitis infant mortality in the United States. Am J Public Health 87(12):2026–2031

Holschneider A, Hutson J, Pena A et al (2005) Preliminary report on the International Conference for the Development of Standards for the Treatment of Anorectal Malformations. J Pediatr Surg 40(10): 1521–1526

Horsthuis K, Lavini C, Stoker J (2005) MRI in Crohn's disease. J Magn Reson Imaging 22(1):1–12

Hur J, Yoon CS, Kim MJ et al (2007) Imaging features of gastrointestinal tract duplications in infants and children: from oesophagus to rectum. Pediatr Radiol 37(7):691–699

Janik JS, Firor HV (1979) Pediatric appendicitis. A 20-year study of 1,640 children at Cook County (Illinois) Hospital. Arch Surg 114(6):717–719

Jarboe MD, Teitelbaum DH, Dillman JR (2012) Combined 3D rotational fluoroscopic-MRI cloacagram procedure defines luminal and extraluminal pelvic anatomy prior to surgical reconstruction of cloacal and other complex pelvic malformations. Pediatr Surg Int 28(8): 757–763

Jeffrey RB Jr, Laing FC, Townsend RR (1988) Acute appendicitis: sonographic criteria based on 250 cases. Radiology 167(2):327–329

Kapur RP (2000) Developmental disorders of the enteric nervous system. Gut 47(Suppl 4):iv81–iv83; discussion iv87

Kenny SE, Tam PK, Garcia-Barcelo M (2010) Hirschsprung's disease. Semin Pediatr Surg 19(3):194–200

Kessler N, Cyteval C, Gallix B et al (2004) Appendicitis: evaluation of sensitivity, specificity, and predictive values of US, Doppler US, and laboratory findings. Radiology 230(2):472–478

Keyzer C, Tack D, de Maertelaer V et al (2004) Acute appendicitis: comparison of low-dose and standard-dose unenhanced multi-detector row CT. Radiology 232(1):164–172

Khong PL, Peh WC, Lam CH et al (2000) Ultrasound-guided hydrostatic reduction of childhood intussusception: technique and demonstration. Radiographics 20(5), E1

Kim KW, Ha HK (2003) MRI for small bowel diseases. Semin Ultrasound CT MR 24(5):387–402

Kim K, Kim YH, Kim SY (2012) Low-dose abdominal CT for evaluating suspected appendicitis. N Engl J Med 366(17):1596–1605

Kluth D (2010) Embryology of anorectal malformations. Semin Pediatr Surg 19(3):201–208

Kong MS, Wong HF, Lin SL et al (1997) Factors related to detection of blood flow by color Doppler ultrasonography in intussusception. J Ultrasound Med 16(2): 141–144

Le J, Kurian J, Cohen HW et al (2013) Do clinical outcomes suffer during transition to an ultrasound-first paradigm for the evaluation of acute appendicitis in children? AJR Am J Roentgenol 201(6):1348–1352

Lee JM, Kim H, Byun JY et al (1994) Intussusception: characteristic radiolucencies on the abdominal radiograph. Pediatr Radiol 24(4):293–295

Lee JH, Jeong YK, Park KB et al (2005) Operator-dependent techniques for graded compression sonography to detect the appendix and diagnose acute appendicitis. AJR Am J Roentgenol 184(1):91–97

Lee NK, Kim S, Jeon TY et al (2010) Complications of congenital and developmental abnormalities of the

gastrointestinal tract in adolescents and adults: evaluation with multimodality imaging. Radiographics 30(6):1489–1507
Levitt MA, Pena A (2007) Anorectal malformations. Orphanet J Rare Dis 2:33
Lioubashevsky N, Hiller N, Rozovsky K (2013) Ileocolic versus small-bowel intussusception in children: can US enable reliable differentiation? Radiology 269(1):266–271
Loening-Baucke V (1993) Chronic constipation in children. Gastroenterology 105(5):1557–1564
Maccioni F, Viola F, Carrozzo F et al (2012) Differences in the location and activity of intestinal Crohn's disease lesions between adult and paediatric patients detected with MRI. Eur Radiol 22(11): 2465–2477
Macpherson RI (1993) Gastrointestinal tract duplications: clinical, pathologic, etiologic, and radiologic considerations. Radiographics 13(5):1063–1080
Meier-Ruge W, Scharli AF (1986) The epidemiology and enzyme histotopochemical characterization of ultrashort-segment Hirschsprung's disease. Pediatr Surg Int 1(1):37–42
Mellor MF, Drake DG (1994) Colonic volvulus in children: value of barium enema for diagnosis and treatment in 14 children. AJR Am J Roentgenol 162(5): 1157–1159
Mezwa DG, Feczko PJ, Bosanko C (1993) Radiologic evaluation of constipation and anorectal disorders. Radiol Clin North Am 31(6):1375–1393
Misra D, Mushtaq I, Drake DP et al (1996) Associated urologic anomalies in low imperforate anus are capable of causing significant morbidity: a 15-year experience. Urology 48(2):281–283
Mittal MK, Dayan PS, Macias CG et al (2013) Performance of ultrasound in the diagnosis of appendicitis in children in a multicenter cohort. Acad Emerg Med 20(7):697–702
Moore MM, Gustas CN, Choudhary AK et al (2012) MRI for clinically suspected pediatric appendicitis: an implemented program. Pediatr Radiol 42(9): 1056–1063
Navarro O, Daneman A (2004) Intussusception. Part 3: diagnosis and management of those with an identifiable or predisposing cause and those that reduce spontaneously. Pediatr Radiol 34(4):305–312; quiz 369
Navarro O, Dugougeat F, Kornecki A et al (2000) The impact of imaging in the management of intussusception owing to pathologic lead points in children. A review of 43 cases. Pediatr Radiol 30(9):594–603
Navarro OM, Daneman A, Chae A (2004) Intussusception: the use of delayed, repeated reduction attempts and the management of intussusceptions due to pathologic lead points in pediatric patients. AJR Am J Roentgenol 182(5):1169–1176
Nievelstein RA, Valk J, Smit LM et al (1994) MR of the caudal regression syndrome: embryologic implications. AJNR Am J Neuroradiol 15(6):1021–1029
Nievelstein RA, van der Werff JF, Verbeek FJ et al (1998a) Normal and abnormal embryonic development of the anorectum in human embryos. Teratology 57(2):70–78
Nievelstein RA, Vos A, Valk J (1998b) MR imaging of anorectal malformations and associated anomalies. Eur Radiol 8(4):573–581
O'Donovan AN, Habra G, Somers S et al (1996) Diagnosis of Hirschsprung's disease. AJR Am J Roentgenol 167(2):517–520
Panes J, Bouhnik Y, Reinisch W et al (2013) Imaging techniques for assessment of inflammatory bowel disease: joint ECCO and ESGAR evidence-based consensus guidelines. J Crohns Colitis 7(7):556–585
Paolantonio P, Ferrari R, Vecchietti F et al (2009) Current status of MR imaging in the evaluation of IBD in a pediatric population of patients. Eur J Radiol 69(3):418–424
Park JS, Jeong JH, Lee JI et al (2013) Accuracies of diagnostic methods for acute appendicitis. Am Surg 79(1):101–106
Partin JC, Hamill SK, Fischel JE et al (1992) Painful defecation and fecal soiling in children. Pediatrics 89(6 Pt 1):1007–1009
Pazo A, Hill J, Losek JD (2010) Delayed repeat enema in the management of intussusception. Pediatr Emerg Care 26(9):640–645
Pena A (1993) Management of anorectal malformations during the newborn period.World. J Surg 17(3):385–392
Podberesky DJ, Towbin AJ, Eltomey MA et al (2013) Magnetic resonance imaging of anorectal malformations. Magn Reson Imaging Clin N Am 21(4):791–812
Powell RW, Raffensperger JG (1982) Congenital colonic atresia. J Pediatr Surg 17(2):166–170
Pracros JP, Tran-Minh VA, Morin de Finfe CH et al (1987) Acute intestinal intussusception in children. Contribution of ultrasonography (145 cases). Ann Radiol (Paris) 30(7):525–530
Pringle KC, Sato Y, Soper RT (1987) Magnetic resonance imaging as an adjunct to planning an anorectal pull-through. J Pediatr Surg 22(6):571–574
Puylaert JB (1986) Acute appendicitis: US evaluation using graded compression. Radiology 158(2):355–360
Quigley AJ, Stafrace S (2013) Ultrasound assessment of acute appendicitis in paediatric patients: methodology and pictorial overview of findings seen. Insights Imaging 4(6):741–751
Rao PM, Rhea JT, Novelline RA (1997) Appendiceal and peri-appendiceal air at CT: prevalence, appearance and clinical significance. Clin Radiol 52(10):750–754
Ratcliffe JF, Fong S, Cheong I et al (1992) The plain abdominal film in intussusception: the accuracy and incidence of radiographic signs. Pediatr Radiol 22(2):110–111
Rettenbacher T, Hollerweger A, Macheiner P et al (2001) Outer diameter of the vermiform appendix as a sign of acute appendicitis: evaluation at US. Radiology 218(3):757–762
Rioux M (1992) Sonographic detection of the normal and abnormal appendix. AJR Am J Roentgenol 158(4): 773–778

Salas S, Angel CA, Salas N et al (2000) Sigmoid volvulus in children and adolescents. J Am Coll Surg 190(6): 717–723

Sargent MA, Babyn P, Alton DJ (1994) Plain abdominal radiography in suspected intussusception: a reassessment. Pediatr Radiol 24(1):17–20

Sauer CG, Kugathasan S, Martin DR et al (2011) Medical radiation exposure in children with inflammatory bowel disease estimates high cumulative doses. Inflamm Bowel Dis 17(11):2326–2332

Sauer CG, Middleton JP, Alazraki A et al (2012) Comparison of magnetic resonance enterography with endoscopy, histopathology, and laboratory evaluation in pediatric Crohn disease. J Pediatr Gastroenterol Nutr 55(2):178–184

Seth R, Heyman MB (1994) Management of constipation and encopresis in infants and children. Gastroenterol Clin North Am 23(4):621–636

Silva CT, Daneman A, Navarro OM et al (2007) Correlation of sonographic findings and outcome in necrotizing enterocolitis. Pediatr Radiol 37(3):274–282

Sivit CJ, Newman KD, Boenning DA et al (1992) Appendicitis: usefulness of US in diagnosis in a pediatric population. Radiology 185(2):549–552

Stewart JK, Olcott EW, Jeffrey BR (2012) Sonography for appendicitis: nonvisualization of the appendix is an indication for active clinical observation rather than direct referral for computed tomography. J Clin Ultrasound 40(8):455–461

Tabbers M, Boluyt MN, Berger MY et al (2011) Clinical practice : diagnosis and treatment of functional constipation. Eur J Pediatr 170(8):955–963

Taccone A, Martucciello G, Dodero P et al (1992) New concepts in preoperative imaging of anorectal malformation. New concepts in imaging of ARM. Pediatr Radiol 22(3):196–199

Tareen F, Ryan S, Avanzini S et al (2011) Does the length of the history influence the outcome of pneumatic reduction of intussusception in children? Pediatr Surg Int 27(6):587–589

Towbin AJ, Sullivan J, Denson LA et al (2013) CT and MR enterography in children and adolescents with inflammatory bowel disease. Radiographics 33(7): 1843–1860

Trout AT, Sanchez R, Ladino-Torres MF (2012) Reevaluating the sonographic criteria for acute appendicitis in children: a review of the literature and a retrospective analysis of 246 cases. Acad Radiol 19(11):1382–1394

Vade A, Reyes H, Wilbur A et al (1989) The anorectal sphincter after rectal pull-through surgery for anorectal anomalies: MRI evaluation. Pediatr Radiol 19(3):179–183

Vazquez JL, Ortiz M, Doniz MC et al (2012) External manual reduction of paediatric idiopathic ileocolic intussusception with US assistance: a new, standardised, effective and safe manoeuvre. Pediatr Radiol 42(10):1197–1204

Verschelden P, Filiatrault D, Garel L et al (1992) Intussusception in children: reliability of US in diagnosis – a prospective study. Radiology 184(3): 741–744

Vignault F, Filiatrault D, Brandt ML et al (1990) Acute appendicitis in children: evaluation with US. Radiology 176(2):501–504

Williams NM, Jackson D et al (1998) Is the incidence of acute appendicitis really falling? Ann R Coll Surg Engl 80(2):122–124

Yoon CH, Kim HJ, Goo HW (2001) Intussusception in children: US-guided pneumatic reduction – initial experience. Radiology 218(1):85–88

# Accessory Organs of Digestion

Apeksha Chaturvedi

## Contents



A. Chaturvedi, MBBS, MD, DABR
Department of Radiology, Golisano Childrens Hospital, URMC, Rochester, NY, USA
e-mail: apeksha_chaturvedi@urmc.rochester.edu

**Abstract**

Congenital and acquired disorders of the accessory organs of digestion are encountered relatively commonly when imaging infants and young children. This chapter reviews the relevant embryology, anatomy and imaging findings of the spectrum of pathology affecting these organs.

## 1 The Liver

At birth, a normal liver can extend below the costal margin and occupies two-fifths of the abdominal cavity. As the child grows, these proportions transit to those of an adult.

Ultrasound (US) is an excellent screening and diagnostic tool in children (Siegel 2001). Magnetic resonance imaging (MRI), in particular magnetic resonance cholangiopancreatography (MRCP), is increasingly being used for noninvasive evaluation of biliary pathology. MRCP uses heavily T2-weighted sequences to highlight fluid-filled biliary structures. Improved signal-to-noise/contrast-to-noise ratios and diminished susceptibility and motion artifacts have been made possible by use of fast spin-echo sequences with long echo times (Griffin et al. 2013). MR imaging protocols can be tailored to answer specific clinical questions ranging from tumor assessment (including staging and resectability), biliary tract pathology, and vascular assessment (Tran and Vasanawala 2013).



S. Stafrace, J.G. (Hans) Blickman (eds.), *Radiological Imaging of the Digestive Tract in Infants and Children*, Medical Radiology, DOI 10.1007/978-3-319-18434-0_8

**Table 1** Longitudinal dimensions of right lobe of the liver in neonates, infants, and older children (Soyupak et al. 2002)

| Subjects | | Longitudinal dimensions of right liver lobe (mm) | |
|---|---|---|---|
| Body height (cm) | Age range (months) | Mean | SD |
| 47–64 | 1–3 | 64 | 10.4 |
| 54–73 | 4–6 | 73 | 10.8 |
| 65–78 | 7–9 | 79 | 8.0 |

Conventional radiology can only indirectly "image" the liver, and CT comes at the expense of ionizing radiation; therefore, both have a limited role in evaluation of hepatobiliary pathology.

Different liver measurements have been reported for normal neonates, infants, and older children (Table 1), and although such measurements can be a guideline, the diagnosis of hepatomegaly is usually done clinically. On US evaluation, a normal liver in a young infant should not be more than 1 cm beneath the costal margin and should be above the costal margin in older infants and children. In 50 % of neonates, renal cortical echogenicity is higher than that of the liver at birth (Sporcq et al. 2007). However, by 6 months of age, the echogenicity of the liver will be greater (more "adult") than that of the normal kidneys (Gubernick et al. 2000).

Evaluation of the intrahepatic and extrahepatic biliary ducts in order to rule out ductal dilatation is an integral part of US evaluation of the liver. In neonates, the normal common bile duct measures less than 1 mm, thus making it too small to be visualized. A normal measurement expected in an infant of less than 1 year of age is 2 mm and up to 4 mm in older children (Gubernick et al. 2000; Soyupak et al. 2002).

On the underside of the liver, a round, fluid-filled, teardrop-shaped structure seen by US corresponds to the gallbladder. A normal gallbladder should be smaller than the contiguous kidney, and a thin hyperechoic wall should be present. In the fasting state, the wall thickness can be up to 3 mm (Siegel 2001). The normal gallbladder length ranges from 1.5 to 3 cm (mean 2.5 cm) in infants (<1 year old) and 3–7 cm in older children (Gubernick et al. 2000) (Fig. 1).

## 1.1 Neonatal Jaundice

Shortly after birth, the sclerae and skin may acquire a yellow appearance secondary to the accumulation of bilirubin in these tissues. This is clinically referred to as neonatal jaundice.

Jaundice can be physiological or pathological. Physiological jaundice is a common condition that can be observed in 80 % of preterm newborns and in 60 % of normal newborns. It is a benign condition with increased levels of bilirubin at the end of the first week of life. Patients are active, and no signs of sepsis or anemia should be present (Gubernick et al. 2000).

Pathological bilirubinemia, on the other hand, is characterized by jaundice presenting within the first day of life or persistence of jaundice beyond the first week of life in term newborns and beyond

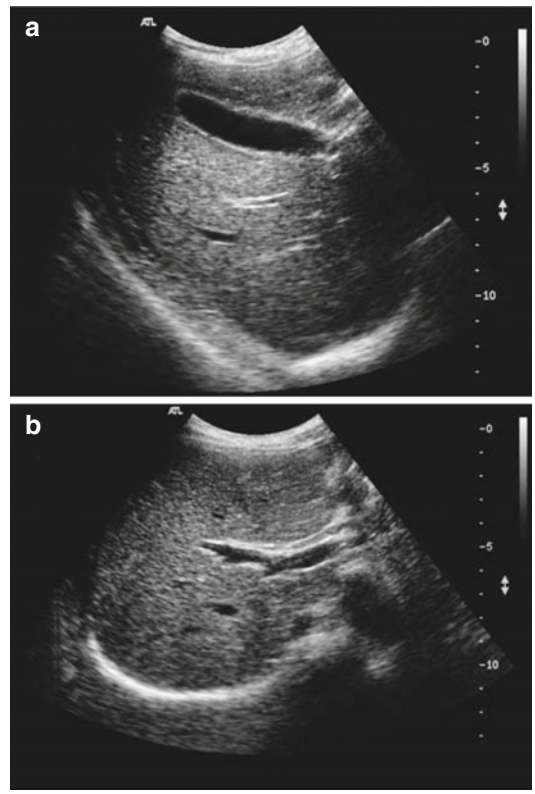


**Fig. 1** (**a**) Longitudinal US image shows the normal liver echo texture and a normal gallbladder. (**b**) Transverse US image reveals normal echo texture and a normal portal vein/common bile duct. (**c**) Illustration depicting normal anatomy of the pancreatobiliary system

**Fig. 1** (continued)

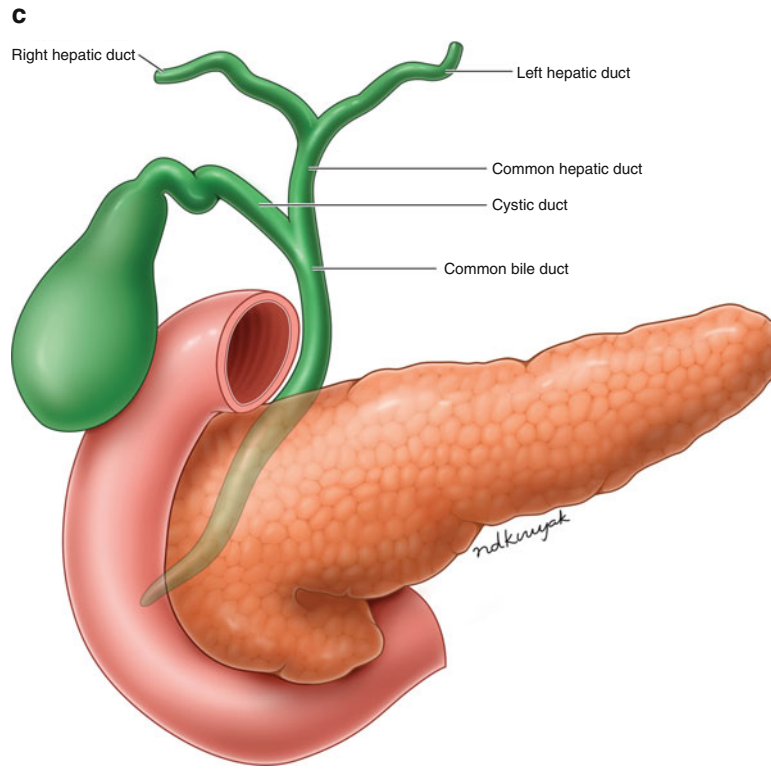


2 weeks in preterm infants. It is characterized by an increase of bilirubin levels greater than 5 mg/dl in 1 day, with levels of direct bilirubin greater than 2 mg/dl and total bilirubin greater than 15 mg/dl. The child is often lethargic.

Pathological jaundice is a consequence of increased bilirubin production, impaired bilirubin excretion, or a combination of these. Increased bilirubin turnover is caused by fetomaternal blood group incompatibilities, extravasation of blood in body tissues, polycythemia, hemoglobinopathies, or enzyme membrane defects. Impaired bilirubin excretion can be a consequence of breastfeeding, inborn errors of metabolism, cholestatic syndromes, and biliary tree obstruction. A combination of increased bilirubin production and impaired excretion is seen with sepsis, infection, and congenital cirrhosis (Rozel et al. 2011).

Biliary disorders constitute an important etiology for conjugated hyperbilirubinemia and encompass a variety of entities. US is a fast, safe, and inexpensive initial imaging tool for evaluation of these disorders. Lately, MRCP (magnetic resonance cholangiography) is being increasingly used as it provides exquisite detail of biliary-pancreatic ductal anatomy and lacks radiation potential. Hepatobiliary scintigraphy with 99m Tc-DISIDA is another useful imaging tool for differentiating between biliary atresia and neonatal hepatitis. Such a differentiation is important for management decisions (Gazelle 1998; Mortele et al. 2006).

## 1.2 Biliary Atresia

Biliary atresia (BA) accounts for the majority of chronic liver diseases without a genetic cause and is the primary indication for liver transplantation in children. Girls are more affected than boys with an incidence of 1:14,000 reported in the USA (Davenport 2005). This is most reliably diagnosed on biopsy and by direct visualization of obliterated intrahepatic ducts during intraoperative cholangiography (Rozel et al. 2011).

A macroscopic classification scheme for BA has been proposed, based on the level of obstruction. In type 1 BA (5 % cases) there is obstruction at the level of the common bile duct. Type 2 cases (3 %) are characterized by obstruction at the common hepatic duct. In type 3 (90 %) cases, there is obstruction at the porta hepatis. In 10 % of cases, biliary atresia occurs in the syndromic form and may be associated with polysplenia, cardiac and pulmonary malformations, situs inversus, preduodenal portal vein, interrupted inferior vena cava, and intestinal malrotation (Sokol et al. 2003; Varela-Fascinetto et al. 1998).

Patients with BA present with cholestatic jaundice, acholic stools, and dark urine. If not recognized promptly, cirrhosis and vitamin K coagulopathy may occur. A Kasai procedure (Roux-en-Y hepatoportoenterostomy) should be performed in the first 40–60 days of life, with liver transplantation often ultimately required (Suchy 2003).

US is a useful antenatal tool for detection of biliary malformations. The presence of a cystic structure localized at the hepatic hilum can occur in BA or may represent as a choledochal cyst. However, if this cyst is small and anechoic, it will be more suggestive of an atresia of the biliary canals, while the presence of an echoic cyst that gradually increases in size supports a choledochal cyst. The specificity of these US findings with BA, however, is not well known (Kim et al. 2000).

Postnatally, the parenchymal US pattern of the liver in a patient with BA may be normal or slightly heterogeneous. The vast majority of patients will have a small (length less than 1.5 cm) hyperechoic or beaded appearance or an absent gallbladder. The absence of the gallbladder is therefore highly suspicious of BA, while a normal-sized gallbladder or a change in its size after feeding will support neonatal hepatitis (Teele and Jane Chrestman 1991; Kirks and Griscom 1998; Kanegawa et al. 2003). Some studies have reported the presence of fibrous tissue close to the porta hepatis, and US may depict this tissue as a triangular or tubular echogenic structure. Although a positive predictive value of 95 % and a sensitivity between 84 and 93 % have been noted between the "triangular cord sign" and BA, inflammatory diseases and cirrhosis can mask this finding (Mowat et al. 1976; Jaw et al. 1999; Gubernick et al. 2000; Norton et al. 2002) (Fig. 2a, b). Other reported US signs for BA include a microcyst (98 % specificity and 20 % sensitivity) and a macrocyst without bile duct dilatation (100 % specificity and 6 % sensitivity) (Koob et al. 2015).

MRCP using T2-weighted turbo spin-echo sequences has been helpful in the diagnosis and visualization of choledochal cysts and dilated common bile ducts. However, in neonates and young infants, the intrahepatic ducts are very thin, and their visualization is challenging. The triangular cord sign may be seen on MRCP as a high-signal-intensity area on T2-weighted images, corresponding to inflammatory tissue and fluid (Jaw et al. 1999; Kim et al. 2000). MR cholangiography is of value toward excluding choledochal cysts or sclerosing cholangitis.

Hepatobiliary scintigraphy with Tc-DISIDA can also differentiate between BA and neonatal hepatitis. Phenobarbital must be administered for 3–5 days to "jump-start" hepatocellular function. If the tracer reaches the duodenum, biliary atresia can be excluded. However, some authors recommend imaging at 24 h to exclude delayed excretion. Scintigraphy has 50–75 % specificity and 90–100 % sensitivity for BA (Petersen and Ure 2003) (Fig. 2c, d).

Finally, an intraoperative cholangiogram will depict the anatomy of the biliary ducts and will assess whether the main right and left hepatic ducts have the caliber necessary to perform the Kasai hepatic portoenterostomy (Gazelle 1998) (Fig. 2e).

A percutaneous liver biopsy will clinch the diagnosis. Histological analysis demonstrates bile plugs, lymphocytic infiltration in the portal tracts, and proliferation of the small intrahepatic bile ducts. There may also be an absence of the extrahepatic biliary ducts and the presence of periportal fibrosis that will eventually progress to cirrhosis. The accuracy of this procedure is reported to be greater than 90 % (Gubernick et al. 2000). Surgical success depends on several factors, such as the time of operation, extent of fibrosis, and jaundice disappearance. Surgical

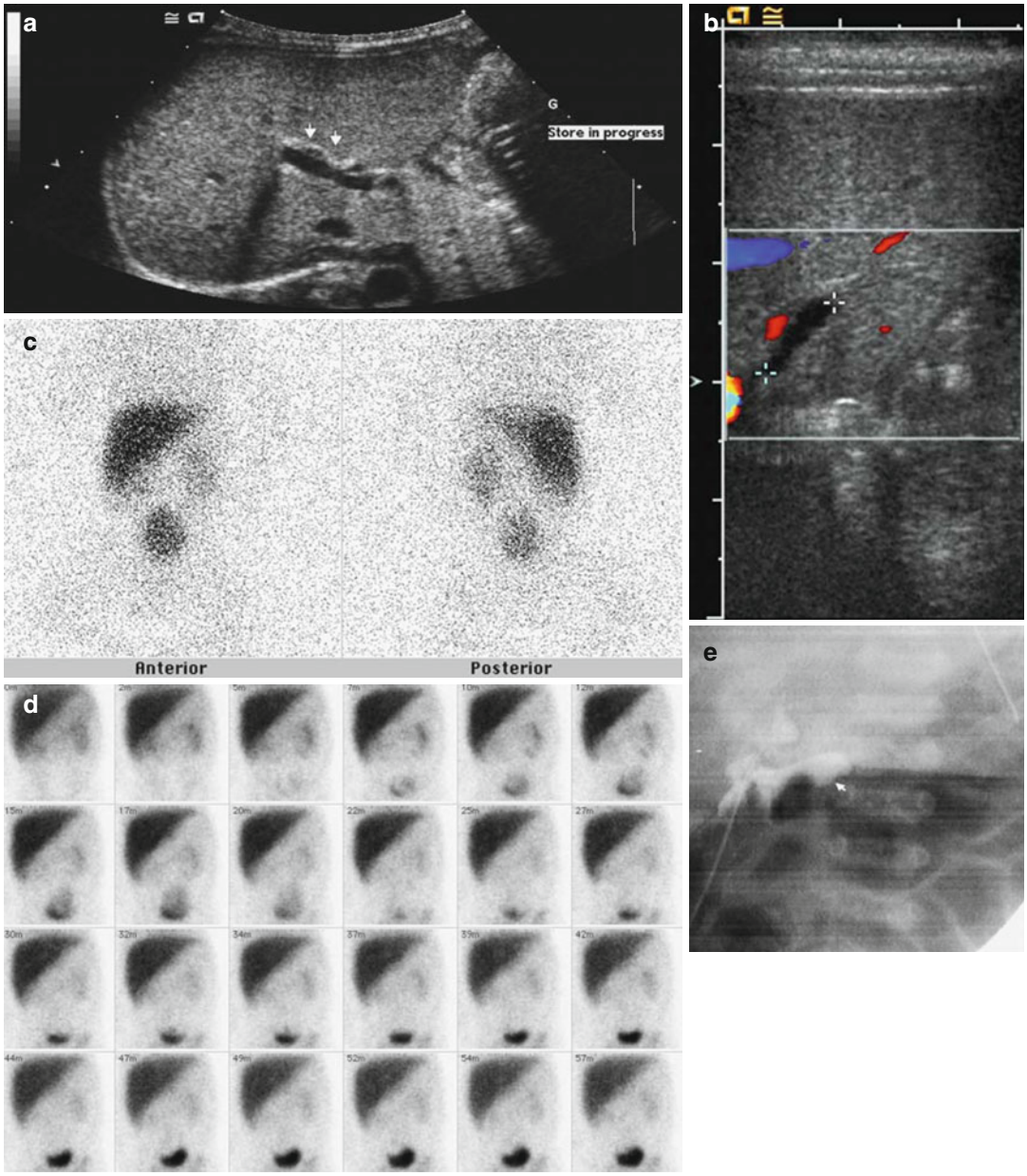


**Fig. 2** Biliary atresia (BA). (**a**) Slightly inhomogeneous echo texture of the liver, prominent wall of the common bile duct (CBD) (*arrows*). (**b**) Tiny gallbladder. (**c**, **d**) Tracer uptake in the liver, both kidneys, and bladder, but not in the gallbladder or duodenum. (**e**) Transhepatic cholangiography reveals atretic CBD (*arrow*)

timing of the Kasai procedure is one of the most important determinants of success showing a 17 % success rate when the surgery is done after 90 days of age and 91 % success rate if it is done before 60 days of age. Disappearance of the jaundice after surgery has been correlated with survival rates of between 73 and 92 % after 10 years; however, if the jaundice persists, the 3-year survival can be as low as 20 % (Sokol et al. 2003).

After surgery, approximately one-third of patients will require liver transplantation in the first year of life, another third by their teenage

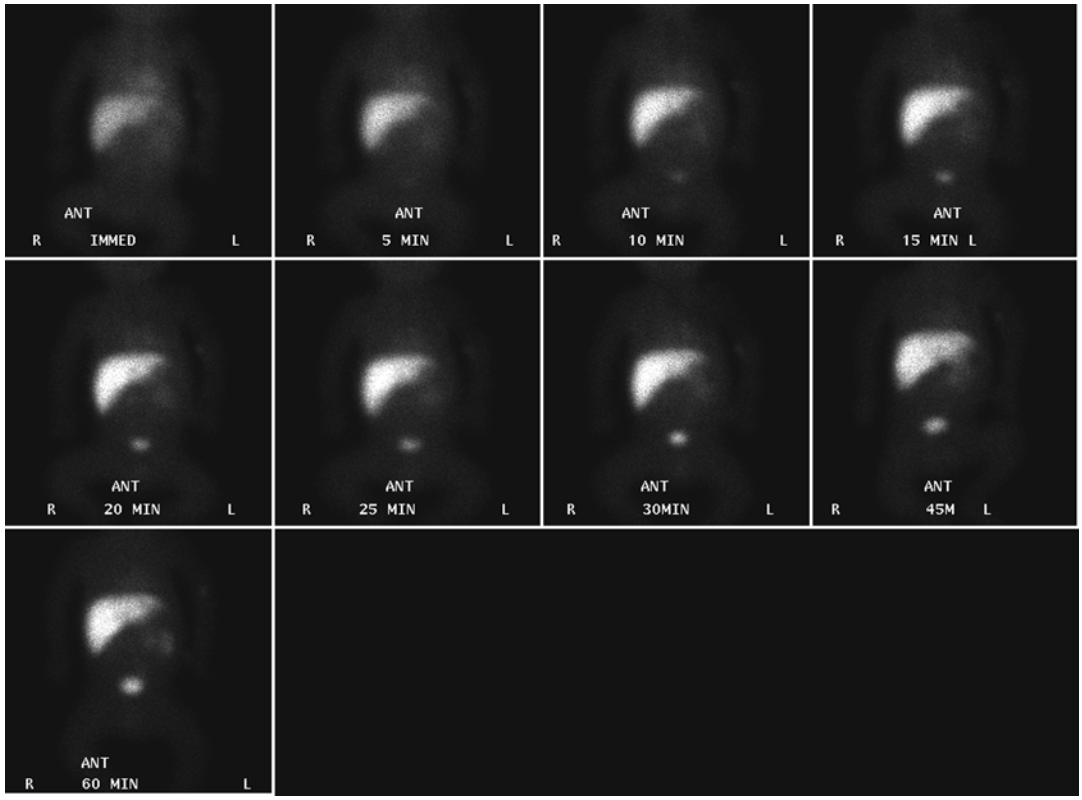


**Fig. 3** Neonatal hepatitis: HIDA scan on a preterm jaundiced neonate reveals slightly delayed blood pool clearance of radiotracer. There is, however, prompt and progressive accumulation of radiotracer in the small bowel (unlike in biliary atresia where tracer will not be seen in the small bowel even at 24 h)

years, and the remaining third will have a good outcome. Liver transplantation should be delayed as long as possible to permit maximal growth or deferred until progressive cholestasis, liver decompensation, or severe portal hypertension supervenes.

## 1.3 Idiopathic Neonatal Hepatitis

Idiopathic neonatal hepatitis is an inflammation of the liver parenchyma responsible for most cases of intrahepatic cholestasis and accounts for at least 25–40 % of patients with neonatal cholestasis. A multitude of etiologies can be the cause (Gubernick et al. 2000).

Treatment of these patients is medical with a good prognosis in 80 % of cases. However, up to 20 % of cases are progressive and have a mortality of between 13 and 25 %. Poor outcome predictors include familial occurrence, persistence of jaundice for more than 6 months, and evidence of severe inflammatory infiltration on histology (Gubernick et al. 2000).

The clinical presentation of a patient with idiopathic neonatal hepatitis can be similar to BA. Histologically, there is a transformation of hepatocytes into giant cells with lobular disarrangement. Although the bile ducts appear normal, the differentiation among idiopathic neonatal hepatitis and BA may be difficult.

US examination will show a normal or enlarged liver with hyperechogenicity of the parenchyma and poor delineation of the peripheral portal venous vasculature. Typically the gallbladder has a normal size, but in some cases it can become small after severe hepatocyte dam-

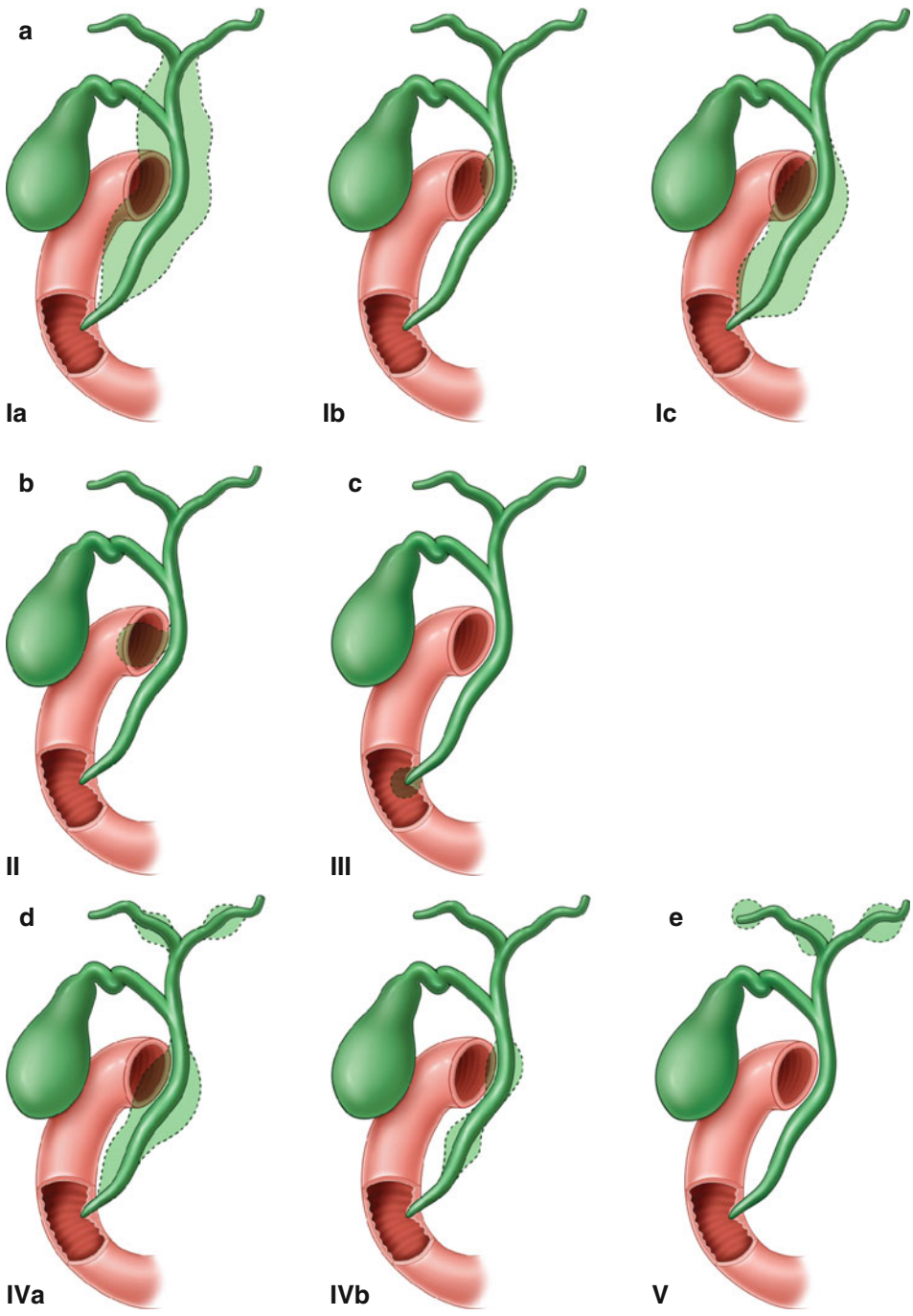


**Fig. 4** Choledochal cyst classification. (**a**) *Type I*, fusiform dilatation of the extrahepatic bile duct (EHD) (Ia, dilatation of the entire EHD; Ib, dilatation of a focal segment of EHD; and Ic, dilatation of the common bile duct portion of EHD). (**b**) *Type II*, "diverticulum" off the CBD. (**c**) *Type III*, intraduodenal choledochocele. (**d**) *Type IV*, intrahepatic and extrahepatic dilatation of the biliary tree. This is subclassified in 2 types **a** (*left*) with multiple intra- and extrahepatic cysts and **b** (*right*) involving multiple extrahepatic dilatations of the CBD. (**e**) *Type V*, multiple cystic dilatations (saccular) of the intrahepatic bile ducts – Caroli disease. (**f**, **g**) a 2-year-old with elevated direct bilirubin. Multiple cystic dilatations of the intrahepatic bile ducts were noted on the MRCP image (**f**) and subsequently the intraoperative cholangiogram (**g**). Findings in keeping with Caroli disease

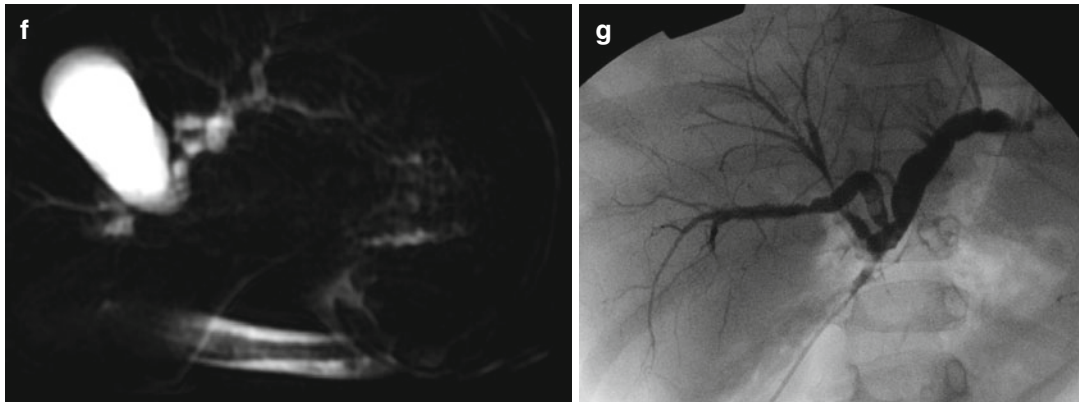


**Fig. 4** (continued)

age. A decrease in the length of the gallbladder after feeding will indicate a normal contraction and supports a diagnosis of idiopathic neonatal hepatitis.

Scintigraphy will show a decreased uptake of 99m Tc-IDA with excretion into the duodenum (Fig. 3). Nevertheless, patients with BA for more than 3 months may depict a scintigraphic pattern similar to those with idiopathic neonatal hepatitis.

## 1.4 Cystic Changes in the Liver and Biliary Tree

A choledochal cyst comprises a dilatation of the intra- or extrahepatic biliary system and is a rare cause of neonatal jaundice. These are four times more common in females than in males. This anomaly can result from an unusually long pancreaticobiliary duct, which allows reflux of activated pancreatic enzymes into the biliary duct (Rozel et al. 2011). Other possible etiologies include a deficient autonomic innervation with few ganglion cells in the distal common bile duct, a retroviral infection, and an immune or familial cause.

There are five types of choledochal cysts (Rozel et al. 2011) (Fig. 4):

- Type I (80 %): fusiform dilatation of the extrahepatic biliary system (subtypes A, B, and C, respectively).
- Type II (2 %): saccular diverticulum of the common bile duct.
- Type III (1.4–5 %): choledochocele emerges from the intraduodenal segment of the choledochal duct.
- Type IV-A: intrahepatic and extrahepatic dilatation of the biliary tree.
- Type IV-B: multiple extrahepatic cysts.
- Type V: nonobstructive multiple intrahepatic biliary dilatations, synonymous with Caroli disease.

Type V cyst is a rare congenital disease characterized by segmental-saccular ductal dilatation. Recurrent bacterial cholangitis and stone formation have been associated with "Caroli disease" (Fig. 4e–g) (Todani et al. 2003).

On US, a choledochal cyst is seen as a thin-walled cystic lesion located at the porta hepatis or under the liver. Typically the cyst is distinct from the gallbladder and communicates with the proximal biliary duct. Enlargement of proximal biliary ducts and dilated intrahepatic ducts may result due to cholestasis. As US has shown a specificity of 97 % for choledochal cysts, it is widely used as the first diagnostic tool (Teele and Jane Chrestman 1991; Gubernick et al. 2000).

Magnetic resonance cholangiography (MRCP) has, to a large extent, replaced percutaneous transhepatic cholangiography (PTC) for evaluation of choledochal cysts. The "central dot

sign" seen on MRCP represents the enhancing portal vein surrounded by cystic intrahepatic biliary ducts. Post-contrast T1 sequences provide fine detail on the periportal spaces, parenchyma, and blood vessels.

Interventional procedures including percutaneous cholangiogram (PTC) or endoscopic retrograde cholangiography (ERCP) have a role in preoperative assessment of anatomy and assist toward management of complications including cholangitis and stone formation (Rozel et al. 2011). In these cases, percutaneous biliary drainage and/or biliary stone manipulation into the duodenum may be performed prior to more definitive surgery.

Treatment varies based on the type of choledochal cyst. The most frequently occurring (type 1) cyst should be surgically excised, and a retrocolic, isoperistaltic, jejunal Roux-en-Y loop placed to reconstruct the extrahepatic biliary tree and anastomosis. For type 2 cysts, the diverticulum is excised and the common bile duct closed at the neck of the diverticulum. Type 3 cysts, depending on their size, should be treated either using endoscopy with sphincterotomy (for cysts <3 cm) or via a transduodenal approach (cysts >3 cm). Ultimately, for type IV and type V choledochal cysts, cholangiography may be required to define the full extent of intrahepatic involvement and surgical intervention planned accordingly. Complications in type V choledochal cysts may, on occasion, necessitate lobectomy and even hepatic transplantation (Rozel et al. 2011).

## 1.5 Polycystic Liver Disease

Two types of polycystic liver disease (PLD) have been identified: one is related to autosomal dominant polycystic kidney disease (ADPKD) linked to PKD 1 or PKD 2, while the second form is isolated, totally unlinked to PKD 1 or PKD 2. While ADPKD is usually a disease of adults, about 1–2 % of patients display an early presenting clinical course and may die perinatally.

Early manifesting cases of ADPKD may mimic the autosomal recessive form (ARPKD) that is usually an infantile disease and an important cause of renal- and liver-related morbidity and mortality in children. Most cases manifest peri-/neonatally with a high mortality rate in the first month of life, while the clinical spectrum of surviving patients is much more variable (Fig. 5a).

Patients with PLD can present with abdominal pain, hepatomegaly, and symptoms associated with renal involvement. Complications of hepatic cysts include compression of the biliary tree and fever secondary to cyst infection or abscess formation (Fig. 5b–d).

The hepatic cysts are thought to arise from dilatation of biliary microhamartomas (BMH). They demonstrate a cuboidal epithelial lining with the same histological appearance as that of the biliary epithelium and may contain fluid. These lesions are generally smaller than 10 cm, surrounded by fibrotic tissue, and localized close to the portal tracts (Suchy 2003).

On US, hepatic cysts will be seen as multiple anechoic lesions that do not communicate with the liver. Occasionally echogenic debris may be present inside the cyst corresponding to hemorrhage. Renal evaluation by US demonstrating enlarged hyperechoic kidneys will be obvious prenatally as well as later (Kuhn et al. 2004) (Fig. 5e, f).

On CT, the cyst has lower attenuation than the surrounding parenchyma.

On MRI, these cysts may show low signal intensity on T1-weighted images and high signal intensity on T2-weighted images. Heterogeneous signal inside the cyst suggests hemorrhage. Some patients with PLD may have portal hypertension and hepatic venous obstruction. In these cases MRI allows evaluation of flow direction and compression in the hepatic vein, portal vein, and inferior vena cava (Kuhn et al. 2004).

Treatment of PLD is very controversial. Ethanol injection has been used resulting in relief of symptoms for 10 years after serial needle aspiration. However, following this procedure, multiple small cysts might replace the treated cyst.

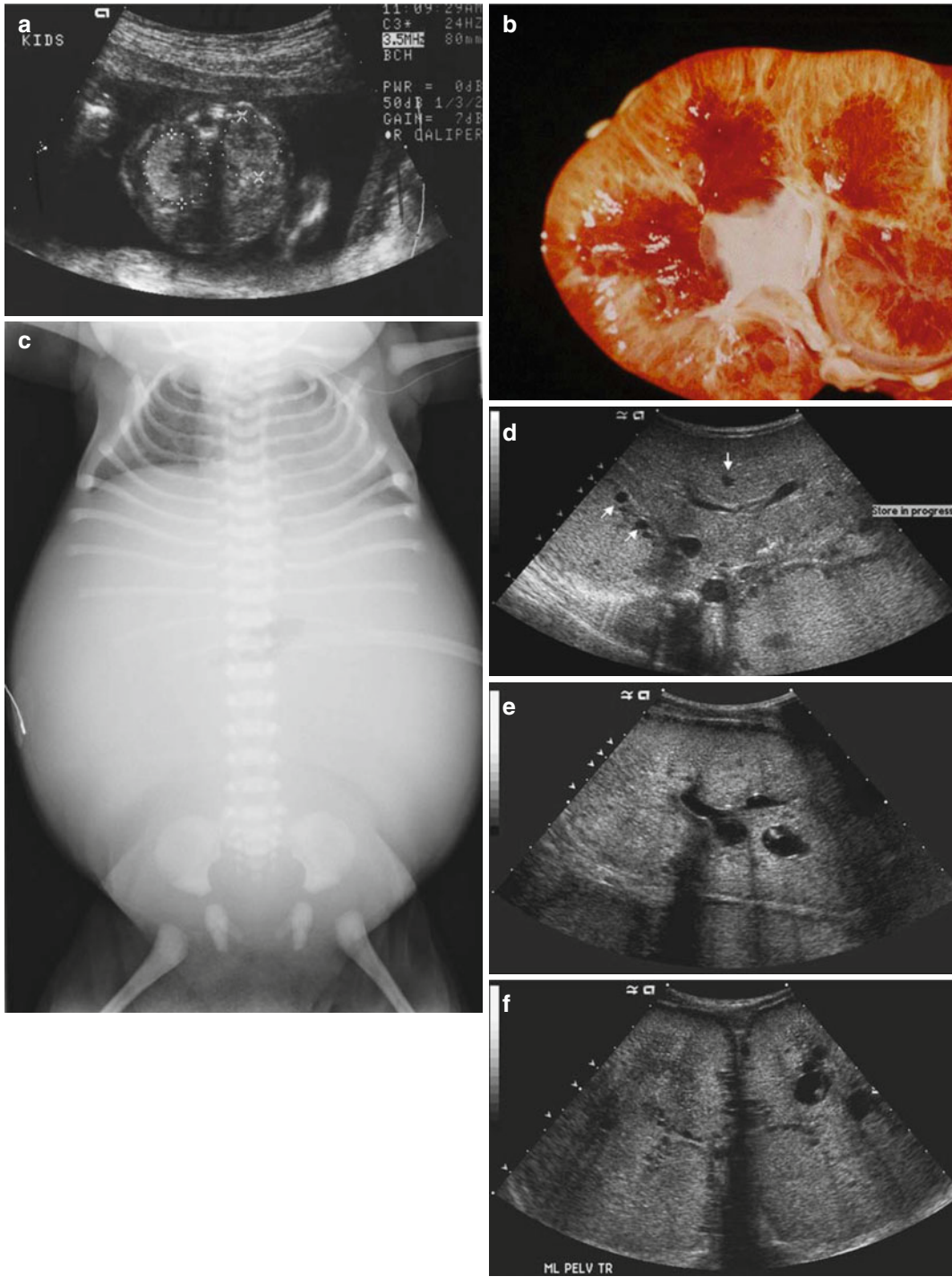


**Fig. 5** Autosomal dominant polycystic kidney disease ADPKD. (**a**) Prenatal depiction of ADPKD. (**b**) Gross pathology of cysts in ADPKD. (**c**) Hepatomegaly with ascites suggested on neonatal abdominal radiograph. (**d**) Echogenic liver with a few cysts (*arrows*). (**e**) Longitudinal left, (**f**) transverse image at the interpolar level of both kidneys. Echogenic, massively enlarged kidneys with "salt and pepper" pattern

Other alternative treatments used include stent placement, resection, or fenestration of the cyst wall. Liver transplantation, however, is the definitive treatment in a patient with end-stage PLD and portal hypertension (Chauveau et al. 2000; Arrive and Tubiana 2003).

## 1.6 Neoplasms

Roughly 6 % of all abdominal tumors in the pediatric age group occur in the liver, i.e., 30 % of all benign abdominal lesions and 0.5–2.0 % of all malignant abdominal lesions (Suchy 2003). An incidence of 1.6 cases/million has been reported (Darbari et al. 2003).

The malignant neoplasms of the liver most commonly seen in children are hepatoblastoma and hepatocellular carcinoma. Although the incidence of hepatoblastoma is higher and has been increasing over the last two decades compared with that of hepatocellular carcinoma, the survival rates for hepatocellular carcinoma are lower than those of hepatoblastoma (Darbari et al. 2003).

US, CT, and MR imaging are very useful tools in the evaluation of hepatic tumors. They can help in the differentiation between benign versus malignant neoplasms, extent of the tumor, resectability, and response to treatment (Pobiel and Bisset 1995; Helmberger et al. 1999).

### 1.6.1 Benign Neoplasms

#### 1.6.1.1 Infantile Hemangioendothelioma/ Infantile Hemangioma

There are two definable subtypes of hemangioendothelioma (HAE): types 1 and 2, of which type 1 is encountered in infancy (Makin and Davenport 2010). Type 1 HAE is composed of variably sized vascular spaces lined with immature endothelial cells and separated by fibrous stroma and scattered biliary ductules. These manifest the GLUT-1 transporter protein on their endothelial cells. There is a female predominance (2:1). Type 2 HAE harbors malignant potential and is seen in adults and will be excluded from the current discussion.

The typical age of presentation for type 1 HAE is in the first year of life with approximately 85 % of cases having presented by 6 months of age (Suchy 2003) (Fig. 6a). On the other hand, HAE may be diagnosed at 16 weeks of gestation using color-flow Doppler US (Makin and Davenport 2010). On ultrasound, the appearances are of a mixed solid-cystic, hypervascular tumor with punctate calcifications.

Clinical symptoms may vary but abdominal pain and nausea are common. Other symptoms such as hemorrhage, consumptive coagulopathy, thrombocytopenia (Kasabach-Merritt syndrome), and cardiac failure may be seen (Suchy 2003).

On histological examination, HAE of the liver will present with multiple vascular channels lined by a single layer of endothelial cells. Based on the endothelial layer and proliferation, hemangiomas have been subclassified into types I and II. In type I, multiple vascular spaces with immature endothelial cells will be seen, while in type II, the vascular spaces will be larger and the endothelial component will be predominant. Sometimes hemorrhage, fibrous tissue, and calcifications may be found inside the lesion.

HAE usually show as echogenic lesions on US; however, sometimes a lesion with heterogeneous echogenicity or a hypoechoic lesion may correspond to a hemangioma. This variable echogenicity depends on the extent of vessels and thrombi inside the structure (Siegel 2001). Besides the hepatic mass, a decrease in the aortic diameter distal to the hepatic artery with an increase in the diameter of the hepatic and celiac arteries will support the diagnosis. On color Doppler, the lesion will show mixed arterial and venous flow with a high-frequency peak of systolic shift and high diastolic flow (Swischuk 2005).

CT typically demonstrates a mass with lower attenuation than the adjacent liver. After contrast injection, it will show a peripheral enhancement followed by centripetal filling on late images. Some necrotic areas or calcifications might not enhance. More than 50 % of hemangiomas will contain calcifications on CT.

On MRI, HAE will have low signal intensity on T1-weighted sequences and high signal intensity on T2-weighted sequences (Fig. 6b). Hemorrhage and hemosiderin deposition may be responsible for a heterogeneous signal pattern.

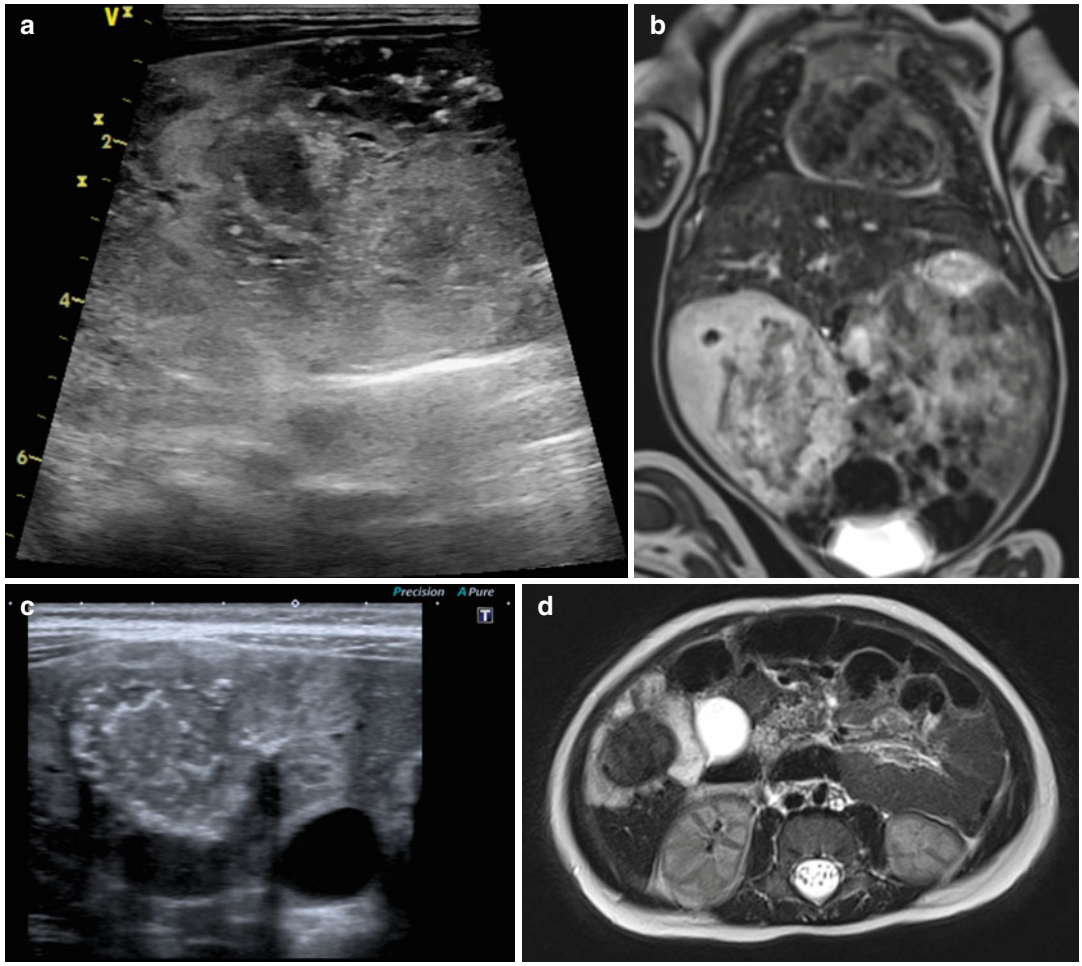


**Fig. 6** Infantile hemangioendothelioma: 7-day-old neonate presenting with recurrent vomiting. (**a**) High-resolution transverse US of the right lobe of the liver showing a mixed solid-cystic tumor with punctate calcifications. (**b**) Coronal MR outlining a mostly exophytic right hepatic tumor. The mass displaced the gallbladder, colon, and small bowel to the left. The central necrosis can be appreciated as a central high-signal irregular area outlined by low signal. (**c**) Transverse right hepatic US image at 5 months follow-up; the mass has significantly reduced in size with increase in the central punctate calcifications. The oval low echogenicity seen to the right of the image represents the gallbladder. (**d**) T2 axial image performed at the same time demonstrates the significantly reduced tumor size and the low signal related to the central calcified component. The gallbladder (high signal) once again helps identify the location of the mass (Courtesy of S Stafrace)

Acute hemorrhage will have high signal intensity on T1-weighted images, while hemosiderin will depict low signal intensity. After contrast injection, an enhancement pattern similar to that seen on enhanced CT occurs with central enhancement and uniform distribution to the periphery on delayed images. Other findings include a small infrahepatic aorta with increased caliber of the celiac and hepatic arteries (Mortele et al. 1998; Siegel 2001; Fulcher and Sterling 2002).

Angiographic evaluation can be performed if embolization is a consideration. On angiography, the hepatic arteries will show an increased diameter with early filling of hepatic veins (Mortele et al. 2002).

#### 1.6.1.2 Mesenchymal Hamartoma

Mesenchymal hamartoma of the liver (MHL) is another benign neoplasm in children. Boys are slightly more affected than girls. It is very unusual

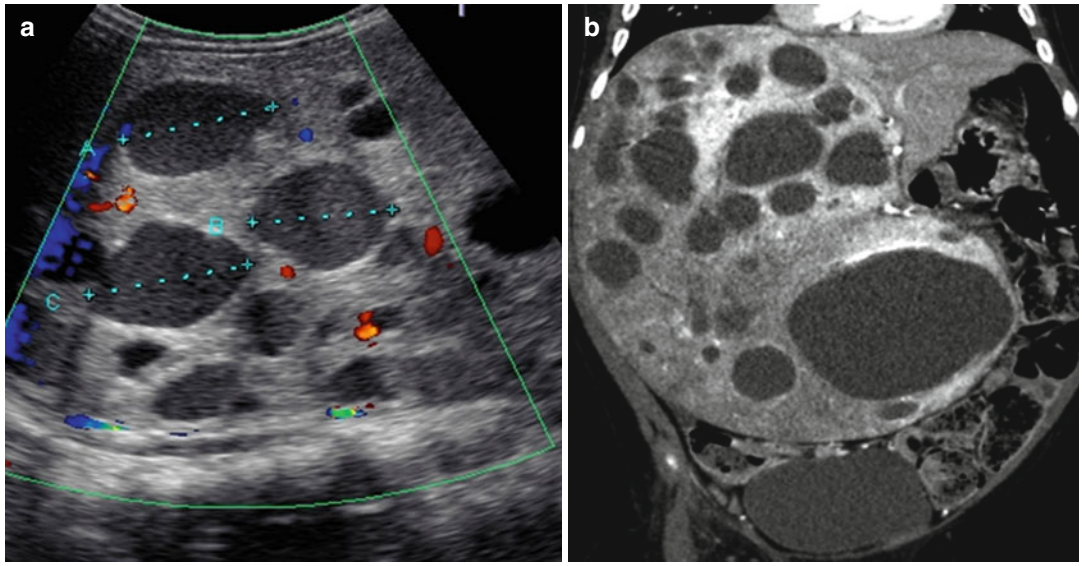


**Fig. 7** Mesenchymal hamartoma. (**a**) Ultrasound reveals multiple cystic areas within the right liver lobe, three of these marked by measuring calipers. (**b**) Enhanced coronal CT image confirms a large mass replacing the right liver lobe and containing multiple cystic areas of varying sizes within it. The mass extends down to the pelvis

to find an MHL after 5 years of age. The lesion usually has a good prognosis (Ramirez et al. 2003; Yen et al. 2003).

Typically, patients with MHL will present with a painless abdominal mass before the first year of life in 55 % of cases. Rapid increase in size may result in misdiagnosis as a malignancy (Orlowski and Breborowicz 2011). Other symptoms such as decreased appetite or cardiac heart failure due to arteriovenous shunting are very uncommon.

Mesenchymal hamartomas are considered to be a developmental anomaly more than a true neoplasm. A total of 75 % of cases are located in the right lobe of the liver. Histologically, MHL arise from the mesenchyma of the portal tract and will have connective tissue, blood vessels, lymphatic spaces, bile ducts, and normal hepatocytes (Konez et al. 2001; Cetin et al. 2002).

The characteristic appearance of MHL on US is a large multicystic mass surrounded by solid areas ("Swiss cheese" appearance) with internal septations within the cyst (Fig. 7). Another distinctive US finding is the presence of a large cystic space with thin, mobile septations. The cyst represents accumulation of fluid in bile ducts and degeneration of mesenchyma. Some echogenic material may be seen within the cyst and most likely represents blood. Some of these tumors may present with a high amount of solid tissue. Usually, these are the tumors with a high vascular component and can be depicted with Doppler. The hepatic origin of mesenchymal hamartomas of the liver can usually be determined by US; however, in some exophytic tumors, the origin and continuity are difficult to evaluate (Konez et al. 2001). On antenatal US, this can be seen as a hypoechoic mass in the liver with coexisting placental abnormalities such as thickening or multicystic placental enlargement (Cornette et al. 2009).

On CT, MHL will typically show a mass with multilocular elements and enhancement of the noncystic components. The imaging characteristics of MHL on CT will depend on the predominance of the cystic or mesenchymatous tissue (Cetin et al. 2002).

On MRI, the cystic component of the tumor will show low signal intensity on T1-weighted images and high signal intensity on T2-weighted images, while the stromal component of the mass will depict low signal intensity on T1-weighted

images due to fibrosis. However, heterogeneous signal intensity may be seen as well, secondary to protein or blood within the cyst (Somech et al. 2001; Cetin et al. 2002).

#### 1.6.1.3 Focal Nodular Hyperplasia

Focal nodular hyperplasia (FNH) arises in utero as an overgrowth of the hepatic parenchyma secondary to an arteriovenous malformation of the liver (Somech et al. 2001; Swischuk 2005). Although it commonly presents in the adult population, some children with FNH have also been reported with a pediatric presentation peak between 6 and 10 years of age (39 % of cases) (Somech et al. 2001).

Typically, these children will present with a painless abdominal right upper-quadrant mass on routine examination. Other symptoms include vomiting, diarrhea, and weight loss.

Histologically, a single mass involving the left lobe will be seen in 90 % of cases. Only 23 % of cases will present with multifocal disease. On histology, a lesion with abnormally organized hepatocytes, Kupffer cells, bile ductules, and well-defined margins is characteristic. All the bile ductules and arterial vessels will be dilated, and multiple fibrotic bands secondary to a central scar will separate the nodules of hepatocytes.

FNH will show a single slightly hypoechoic lesion on US; a central scar may be seen, as well as normal surrounding parenchyma (Carlson et al. 2000). The biliary tree may or may not be dilated.

On unenhanced CT, FNH may appear as isodense or hypodense compared to the liver parenchyma with the presence of a low-attenuation central scar. On contrast CT, this benign tumor may reveal an enhancement greater than that of the adjacent liver during the early phase (arterial and early portal venous) and may be indistinguishable from adjacent liver in delayed images, indicating rapid washout of contrast material from the lesion. Homogeneous enhancement, smooth surface, subcapsular location, and ill-defined margins may also be shown (Fig. 8).

As FNH is a tumor with normal hepatic elements, the signal on MRI will be similar to the surrounding liver, showing slightly low signal intensity or an isointense signal on T1-weighted images and a slightly high signal intensity or isointense signal on T2-weighted images. Usually, FNH will present with a central scar, which will be better depicted on T2-weighted images as a high-signal lesion. Post-gadolinium images will show an enhancement pattern that resembles that seen on CT (Carlson et al. 2000; Mortele et al. 2000) (Fig. 8).

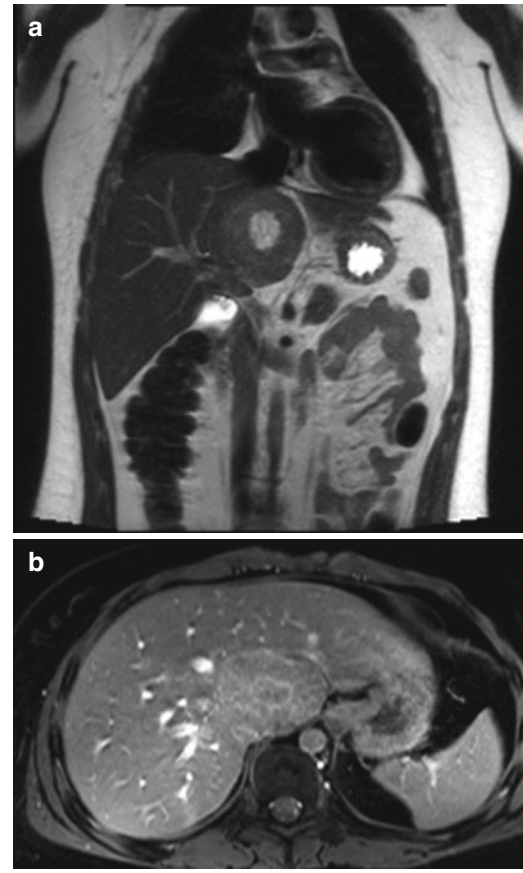


**Fig. 8** Focal nodular hyperplasia. (**a**) Coronal T2-weighted image of the liver reveals a well-circumscribed, somewhat oblong mass in the caudate lobe. The mass has a homogeneous, markedly hyperintense center. (**b**) 15-min delayed T1-W fat-suppressed axial image post-intravenous Eovist injection reveals near isointensity of the mass to the surrounding liver parenchyma

### 1.6.2 Malignant Neoplasms

#### 1.6.2.1 Hepatoblastoma

Hepatoblastoma is the third most common intra-abdominal malignancy (after neuroblastoma and

Wilms' tumor) in children. Almost all patients with hepatoblastoma are younger than 3 years at presentation with a peak presentation at between 18 and 24 months. Imaging features are nonspecific, but the history can provide important diagnostic clues. In a child with a liver mass and elevated alpha-fetoprotein, the presence of any of the following strongly suggests hepatoblastoma: family history of adenomatous polyposis, extremely low birth weight (<1.5 kg), or Beckwith-Wiedemann syndrome (McCarville and Roebuck 2012). Unlike hepatocellular carcinoma, hepatoblastoma has no association with cirrhosis (Dachman et al. 1987; Oue et al. 2003).

Typically, a hepatoblastoma will present with hepatomegaly. Increased levels of alpha-fetoprotein will be present in >90 % of cases and will be helpful in following up the patient. Weight loss, fever, and loss of appetite are other symptoms. When metastases occur, the lungs and regional lymph nodes are commonly involved, but the tumor can also metastasize to the skeleton, ovaries, brain, and eyes.

The two systems in widespread use for hepatoblastoma staging include the PRETEXT and Children's Oncology Group (COG) staging. A detailed discussion is beyond the scope of this chapter (McCarville and Roebuck 2012).

Abdominal radiography may show hepatomegaly as evidenced by elevation of the right hemidiaphragm and displacement of intraluminal air by an enlarged liver (Fig. 9a). Although not diagnostically specific, coarse, stippled, and solid hepatic calcifications may be present in the right upper quadrant. Chest radiography may demonstrate pulmonary metastases and can aid in the differential diagnosis. Plain films cannot localize the tumor to the liver definitively, distinguish between the solid and cystic nature of a neoplasm, or provide information regarding tumor vascularity (Kuhn et al. 2004).

A hepatoblastoma can present as a solitary mass, with or without satellite lesion, as multiple nodules throughout the liver (Roebuck 2006) or as a diffusely infiltrative mass (McCarville and Roebuck 2012). On US, hepatoblastoma presents as a mass with ill-defined borders and heterogeneous echogenicity, showing slightly more echogenic areas compared to the surrounding parenchyma and anechoic areas that correspond to necrosis or hemorrhage. Calcifications can also be present (McCarville and Roebuck 2012) (Fig. 9b).

Visualization and evaluation of intrahepatic vascular structures is important because hepatoblastomas can invade or compress the portal and the hepatic veins. The absence of a portal branch or the presence of a thrombus supports portal vein invasion. Although the inferior vena cava can be invaded, US examination overestimates the incidence of obliteration of this vessel (Siegel 2001; Kuhn et al. 2004).

On CT, the appearance of hepatoblastoma varies greatly based on the tumor's histologic composition (McCarville and Roebuck 2012). Fine calcifications may be observed in epithelial tumors and coarse, extensive calcifications in mixed mesenchymal-epithelial tumors (McCarville and Roebuck 2012). Prior to contrast administration, the tumor may appear as single or multiple, homogeneous, hypodense mass(es) (epithelial-type tumor); however, it may demonstrate a more heterogeneous appearance (mixed mesenchymal-epithelial tumor), corresponding to areas of necrosis or hemorrhage (Fig. 9c–e). Post-contrast, the enhancement is generally less than that of the surrounding liver, although a thin peripheral rim of enhancement may be observed if imaging is performed in the arterial phase. Vascular compression and tumor extension are also well assessed by CT. Although pediatric radiologists tend to favor MR over CT, the superior ability of CT to detect lung metastases makes it a useful modality in evaluation of patients with hepatoblastoma.

On MRI, hepatoblastoma will have low signal intensity on T1-weighted images and heterogeneous high signal intensity on T2. Mixed epithelial-mesenchymal tumors are typically more heterogeneous owing to internal hemorrhage, necrosis, fibrosis, calcification, cartilage, and septations. MRI is used more for evaluation of tumor extension, vascular compression, and complications than for diagnosis. Gradient-echo imaging and contrast-enhanced MR angiography (MRA) are useful for assessment of vascular invasion and detailed mapping of vascular anatomy which assists the surgeon in preoperative planning.

Newer techniques such as diffusion-weighted imaging (DWI) and the use of superparamagnetic iron oxide (SPIO) or liver cell-specific contrast agents are other potential techniques which can assist in liver tumor imaging. Experience in this area has, so far, been limited (McCarville and Roebuck 2012).

FDG-PET (positron emission tomography) is being increasingly used for diagnosis, staging, assessing therapeutic response, and recurrence. FDG avidity of hepatoblastoma depends on tumor subtype and biologic behavior. The pure fetal subtype, for example, demonstrates much lower FDG avidity than the more unfavorable

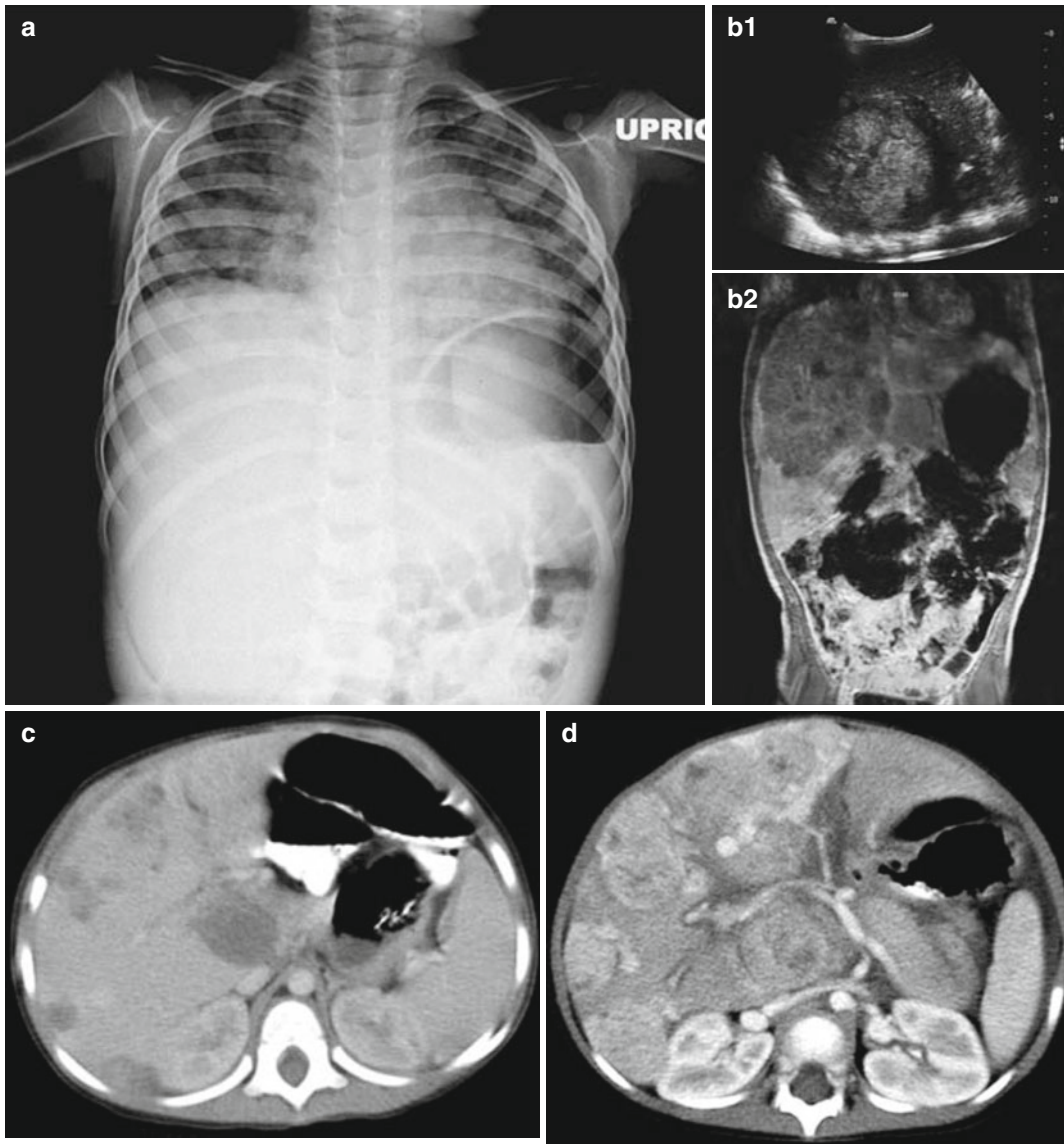


**Fig. 9** Hepatoblastoma. (**a**) Plain film demonstrates hepatomegaly and multiple round lesions in the chest. Patient with hepatoblastoma in which (**b1**) US shows a highly echogenic lesion located posteriorly in the right lobe liver, and (**b2**) coronal T2 MRI image of the same mass. (**c–e**) CT of the abdomen depicts heterogeneous enhancement of multiple lesions, with tumor extension into the IVC (*arrow*). (**f–g**) CT of chest demonstrating multiple metastatic lung lesions

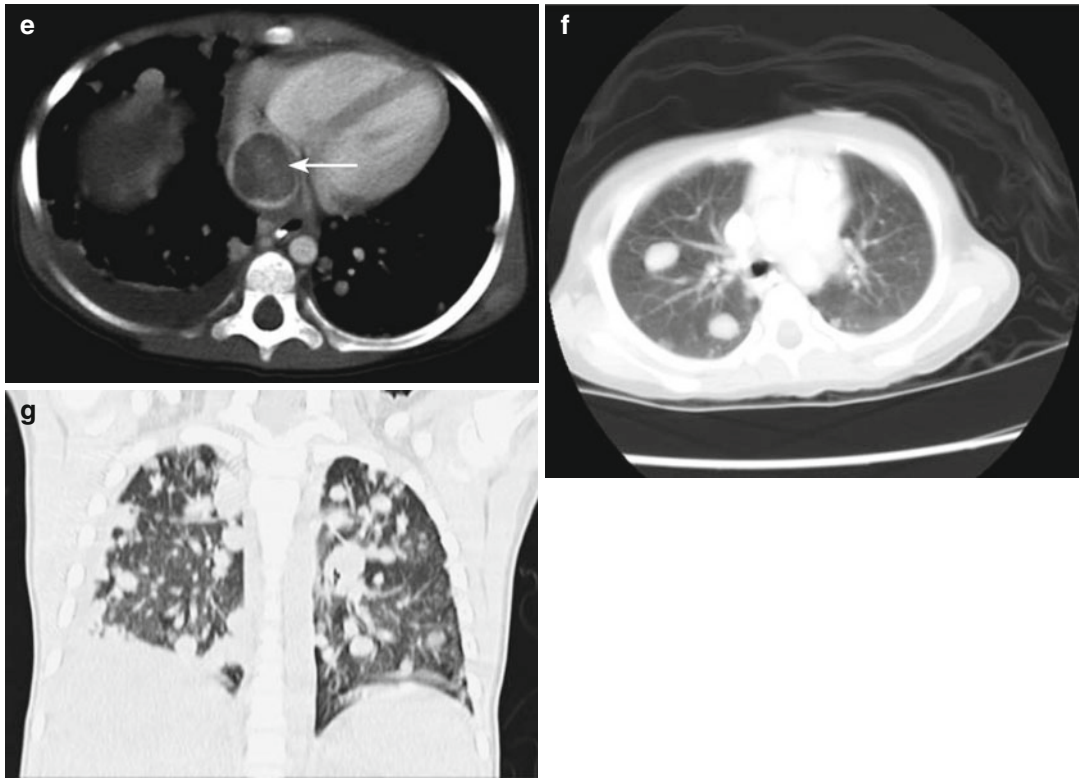


**Fig. 9** (continued)

histologic types which may limit the clinical utility of PET in assessment of this subtype. The ability of PET to image the entire patient provides a huge benefit toward assessment of bone metastases (McCarville and Roebuck 2012).

For postoperative patients, alpha-fetoprotein levels constitute a sensitive marker of recurrence, which limits the value of surveillance imaging. Relapses usually occur in the lungs, liver, or both (McCarville and Roebuck 2012).

#### 1.6.2.2 Hepatocellular Carcinoma

Hepatocellular carcinoma (HCC) accounts for approximately 35 % of primary malignant liver tumors. There are two age peaks in childhood: 2–4 years and 12–14 years (Das et al. 2009). Males are affected more than females, and 25 % of these patients will usually have an underlying liver condition such as cirrhosis, biliary atresia, hereditary tyrosinemia, glycogen storage disease, or chronic hepatitis. At diagnosis, half of the patients will have metastatic disease, and elevated levels of alpha-fetoprotein will be found. In the USA, HCC has a prevalence of 0.2–0.7 % of children, while in Asia and sub-Saharan Africa, a prevalence of 5.5 % has been reported (Katzenstein et al. 2003).

The typical presentation will be a child with an abdominal mass or abdominal distension on physical examination. Although not common, abdominal pain, anorexia, weight loss, or hemoperitoneum may also be present (Katzenstein et al. 2003).

Macroscopically, a mass that involves both the right and left lobes will be found in 70 % of cases. On histological analysis, HCC will show giant tumor cells with large trabeculae arranged in an acinar pattern. Necrosis and vascular involvement are commonly seen. Often there is vascular invasion of the portal system and less frequently that of the hepatic vein and IVC. A variant of HCC is fibrolamellar HCC, which will present

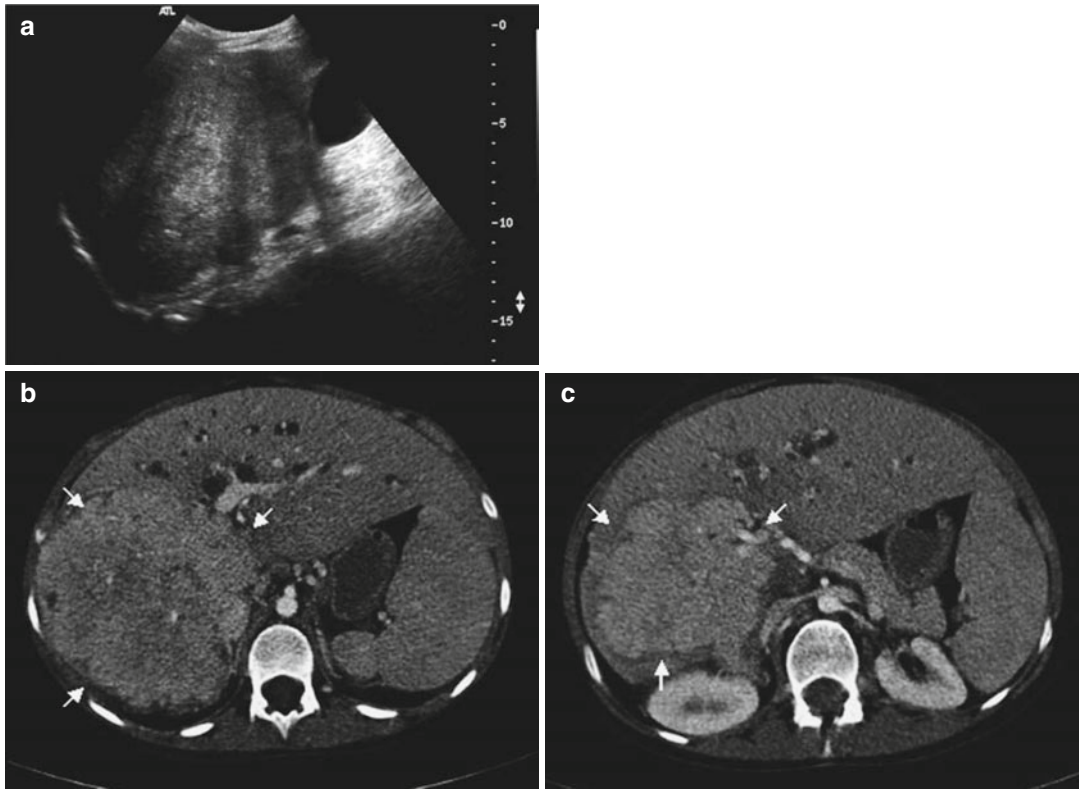


**Fig. 10** Hepatocellular carcinoma. (**a**) US of the right lobe of the liver demonstrates an irregular echo texture with areas of posterior acoustic shadowing. (**b–c**) Axial enhanced CT of the liver in arterial (**b**) and portal phases (**c**) show a moderately enhanced lesion (*arrows*) with a suggestion of a central scar

with a central scar in 76 % of patients on macroscopic examination.

HCC can be represented on US as a hypo- or hyperechoic mass depending on the amount of fat or even as a heterogeneous mass with ill-defined borders. It may look identical to a hepatoblastoma. The presence of foci with posterior acoustic shadowing within the tumor suggests intra-tumor calcifications. Evaluation of vascular invasion and dilatation of the portal vein with color Doppler and with conventional grayscale US should be performed (Siegel 2000) (Fig. 10a).

On unenhanced CT, HCC is shown as a low-attenuation heterogeneous mass. Heterogeneity in attenuation indicates either necrosis or hemorrhage. Lesions may be missed if early vascular imaging is not performed. On enhanced CT, heterogeneous hypervascularity may be seen. Tumors smaller than 3 cm tend to enhance on arterial phase, while in larger tumors this enhancement pattern is nonspecific. Fibrolamellar HCC has specific features on CT. It will be seen as a mass with well-defined borders, calcifications, central scar, and abdominal lymph node enlargement. The tumor will enhance in a heterogeneous pattern and show areas of hypervascularity (Ichikawa et al. 1999; Siegel 2000). The central scar does not enhance in the arterial phase but may do so in the portal or equilibrium phase (Fig. 10b, c).

On MRI, HCC will show low signal intensity on T1-weighted images and high signal or isointensity to the surrounding liver on T2-weighted images. Sometimes, hyperintense areas might be seen on T1-weighted images and will represent hemorrhage or steatosis. A central scar may be present and is characteristic of fibrolamellar HCC. The central scar of fibrolamellar HCC has low signal on both pulse sequences which constitutes an important differentiating factor from focal nodular hyperplasia (Das et al. 2009). Vascular evaluation for thrombus detection involving the portal vein can be carried out with MRI. If the

thrombus enhances, this indicates that it is composed of tumor and will contraindicate embolization or transplantation (Siegel 2000).

#### 1.6.2.3 Embryonal Rhabdomyosarcoma of the Biliary Tree

Embryonal rhabdomyosarcoma ("sarcoma botryoides") is responsible for only 1 % of rhabdomyosarcoma (RMS) in children. There is no difference between genders, and it occurs typically in children less than 5 years of age.

Since the tumor arises in the intrahepatic ducts, intrahepatic cysts, gallbladder, extrahepatic ducts, or in a choledochal cyst, jaundice will develop in 60–80 % of patients. Other manifestations include vomiting, fever, and abdominal distension (Roebuck et al. 1998).

US is used to evaluate the size of the tumor, vascular involvement, and biliary tract compromise. Usually, biliary dilatation and an echogenic intraductal mass with or without portal vein displacement may be seen. Necrosis might be present in these tumors, especially when they are extensive.

On CT, embryonal rhabdomyosarcoma will be seen as a variably enhancing intraductal mass (Das et al. 2009).

On MRI, embryonal RMS may show low signal intensity on T1-weighted sequences and high signal intensity on T2-weighted sequences. After contrast injection, a heterogeneous enhancement pattern will occur. Bile duct dilatation and bile duct irregularities are also easily noted. However, if the tumor arises in an intrahepatic duct, the diagnosis may be challenging (Gazelle 1998) (Fig. 11a–c).

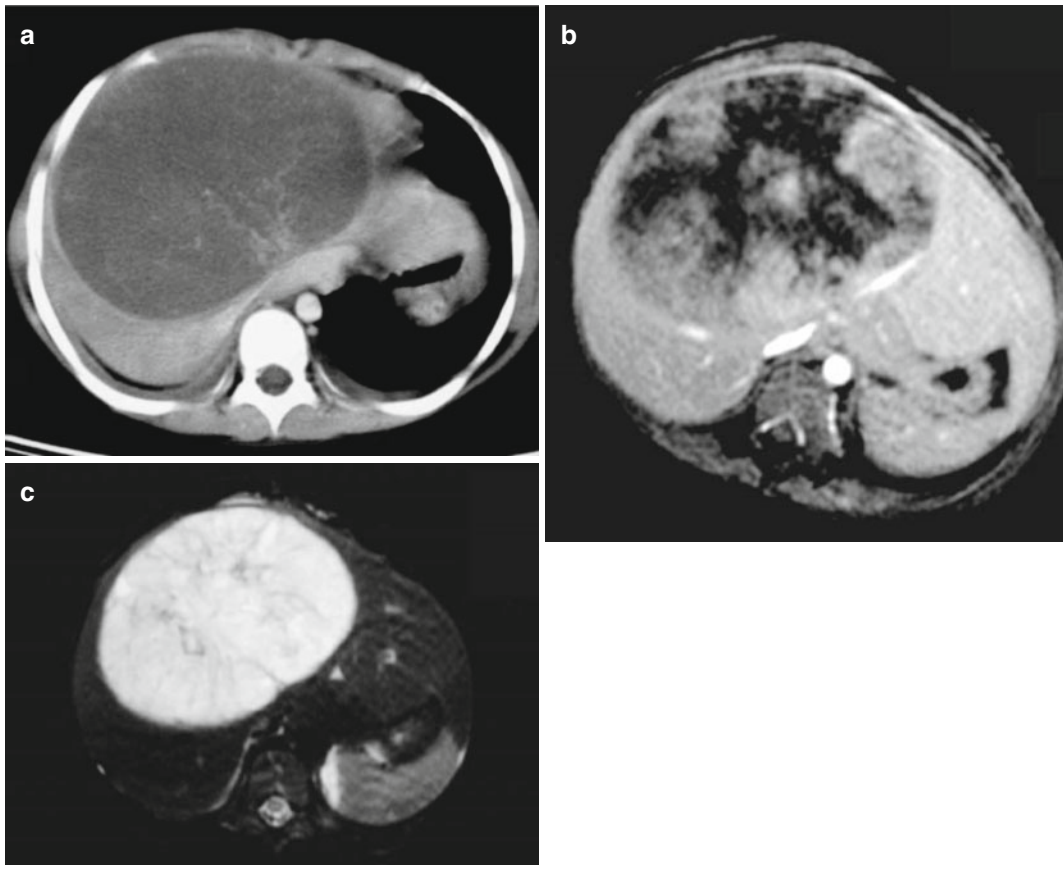


**Fig. 11** Embryonal rhabdomyosarcoma of the biliary tree. (**a**) Contrast CT image of the liver reveals a large, sharply circumscribed, mainly hypoattenuating intrahepatic mass. (**b**) Post-contrast MR image shows marked heterogeneous contrast enhancement. (**c**) T2W fat suppressed MR image of the liver shows the mass to be mostly hyperintense with thin internal septations

On percutaneous transhepatic cholangiography (PTC) extensive filling defects in the biliary tree may be seen with or without obstruction of the extrahepatic bile ducts. PTC can be performed in cases of RMS without biliary dilatation and is very useful if there is an obstructive jaundice (Gazelle 1998).

#### 1.6.2.4 Undifferentiated Embryonal Sarcoma

Undifferentiated embryonal sarcoma (UES) is a rare and highly malignant hepatic neoplasm, affecting almost exclusively the pediatric population. A total of 63 % of patients are between 6 and 10 years of age, and it commonly occurs in the first two decades of life. It has a survival rate of 40 % at 3 years (Lack et al. 1991; O'Sullivan et al. 2001).

Abdominal pain located in the right upper quadrant or epigastrium and an abdominal mass are the principal findings in the initial examination. Other manifestations such as jaundice, chest pain, fever, and a cardiac murmur (due to extension of the tumor into the right atrium and ventricle) are very rarely seen.

On imaging, UES manifests discrepant appearances on US compared to CT/MR. The solid nature of the tumor is best assessed by US on which it appears iso- to hyperechoic compared to the surrounding liver. On both CT and MR, the mass has a cystic appearance and multiple internal septations. Septa enhance with contrast. A pseudocapsule may also be seen (Das et al. 2009). Areas of high T1 signal may be seen within the tumor, which correspond to hemorrhagic tissue on pathologic analysis. If a pseudocapsule is present, it will be of low signal intensity on both T1- and T2-weighted images (Chowdhary et al. 2004).

On histological analysis, a mass with spindle-shaped cells surrounded by a mucopolysaccharide-rich stroma with necrosis or hemorrhagic tissue and surrounded by a fibrous pseudocapsule will be seen in a great number of cases.

#### 1.6.2.5 Metastatic Lesions

Neuroblastoma, Wilms' tumor, rhabdomyosarcoma, gastrointestinal tract cancer, and lymphoma (Fig. 12) are the major tumors of childhood that spread to the liver. Metastatic tumors can also be classified as hypervascular or non-hypervascular metastatic tumors. Hypervascular metastatic tumors include carcinoid tumors, pancreatic islet tumors, melanomas, choriocarcinomas, pheochromocytomas, thyroid carcinoma, and renal cell carcinomas. These tumors will show an intense arterial phase enhancement on CT and MR images with variable washout in the venous phase (Martin et al. 2005). There is low signal intensity on T1-weighted images and high signal intensity on T2-weighted images. Metastatic neuroblastoma will be seen on US as small hypoechoic lesions within the liver parenchyma (Brody et al. 1989; Lack et al. 1991; Kirks and Griscom 1998). Neuroblastoma 4S variant primarily involves the liver skin and bone marrow (Fig. 13a–d).

## 1.7 Hepatitis

Hepatitis is a general term that refers to acute or chronic inflammation of the liver. This condition may result from various infectious and noninfectious etiologies. Infectious etiologies include viral, bacterial, fungal, and parasitic organisms (Gazelle 1998; Kirks and Griscom 1998; Suchy 2003).

### 1.7.1 Viral Infection

Usually hepatitis is caused by a viral infection, mostly hepatitis virus types A and B. However, hepatitis virus types C, D, and E and other viruses such as CMV, Epstein-Barr, herpes, and AIDS-HIV may also be involved. The clinical manifestations depend on the insult with jaundice, nausea, vomiting, and pyrexia commonly seen.

On US, the liver will usually have a normal echo signal. However, in severe cases, the hepatocytes will swell, and fatty infiltration will occur, and this may appear as a hyperechoic liver with increased echoes in the portal vein radicles. The gallbladder wall may be thickened, and an increase in the size of the lymph nodes around the portal vein and around the cystic duct may be visualized.

Children with chronic hepatitis will initially have a hypoechoic liver that will advance to a

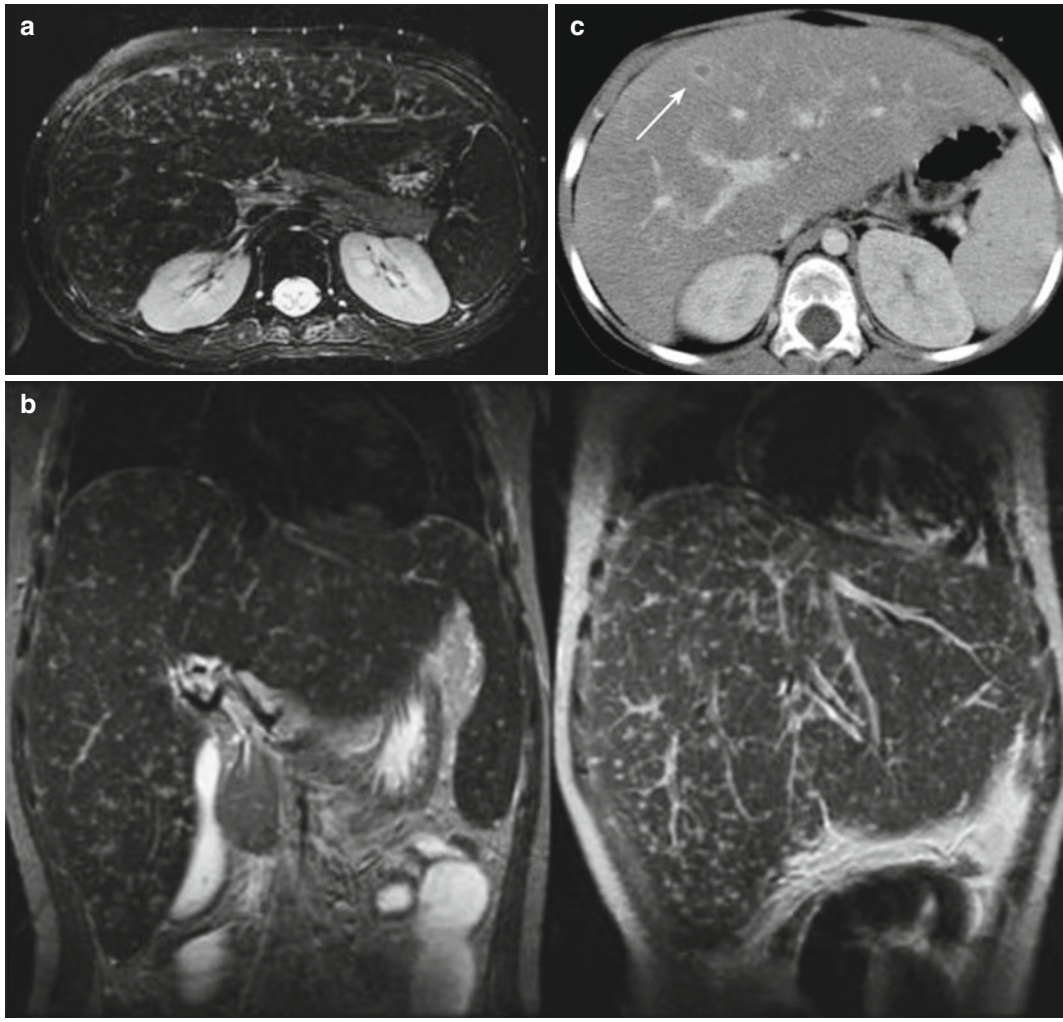


**Fig. 12** Metastatic lesions. (**a**, **b**) Axial and coronal T2 MRI images showing multiple hyperintense lesions in a patient with metastatic lymphoma and hepatomegaly. (**c**) Post-contrast axial CT image showing a metastatic ring-enhancing lesion in the right hepatic lobe (*arrow*)

heterogeneous liver and finally to a small liver with a hyperechoic signal.

On CT livers with acute hepatitis are usually heterogeneous in attenuation, with areas of low attenuation due to the presence of edema and lymphocytic portal infiltration. Areas of nodular regeneration will have high attenuation on unenhanced CT and low attenuation after contrast injection. Necrotic areas will be seen as low-attenuation areas on unenhanced CT and will show higher attenuation than surrounding parenchyma on contrast CT. Enlarged lymph nodes close to the hilum or hepatogastric ligament may also be present.

In 80 % of patients with acute hepatitis, MRI may demonstrate areas of high signal intensity close to the periportal region on T2-weighted images. Necrotic tissue may be seen in fulminant hepatitis and will have high signal intensity on T2-weighted images and low signal intensity on T1-weighted images. After an episode of fulminant hepatitis, peripheral regeneration in the liver will be seen as nodular areas of high signal intensity on T1-weighted images and low signal on T2-weighted images.

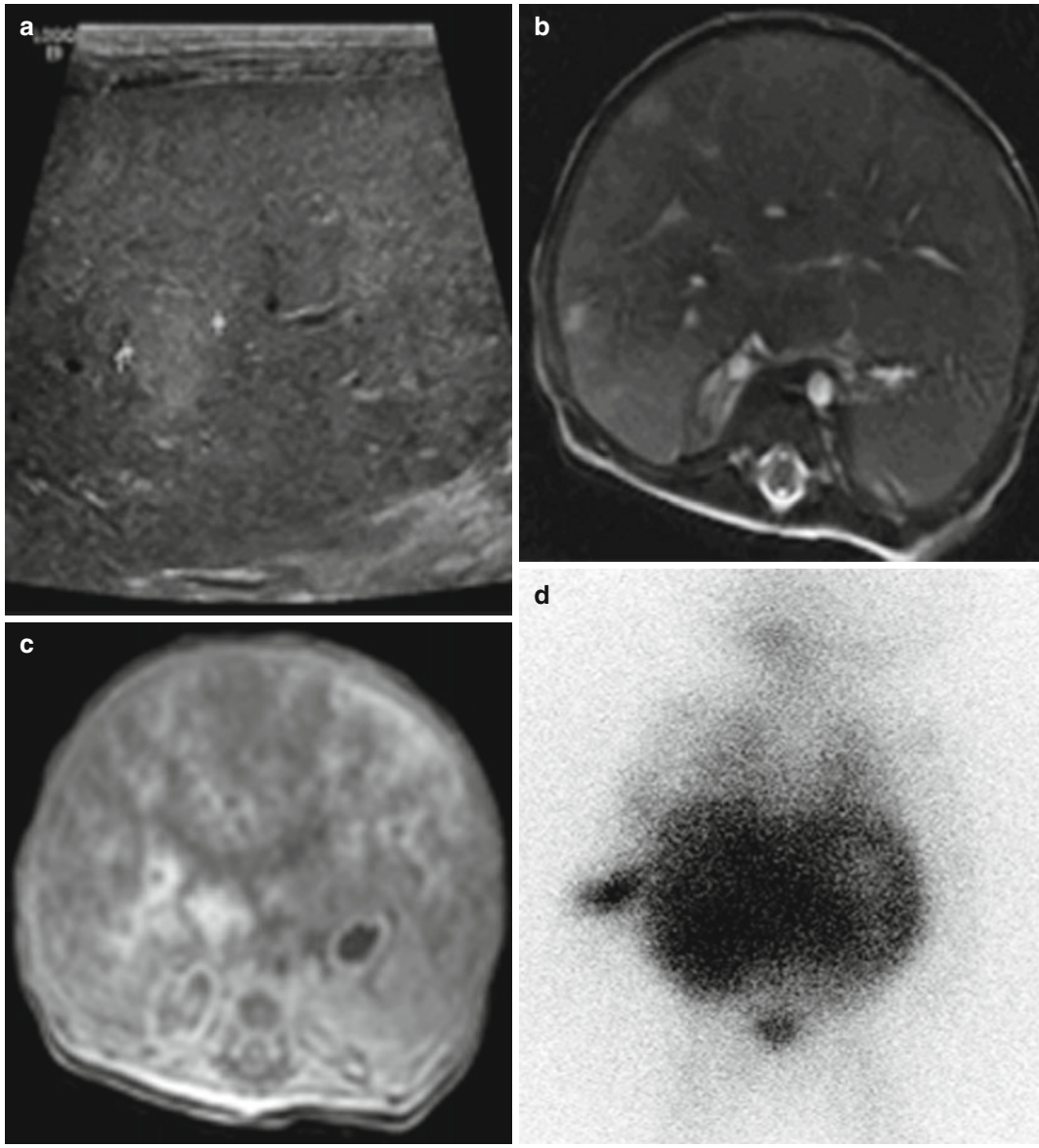


**Fig. 13** Neuroblastoma 4S. Newborn with hepatosplenomegaly and coagulopathy. (**a**) Ultrasound revealed an inhomogeneous hepatic echotexture. Few scattered ill-defined hyperechoic areas within the liver were seen, of which one is marked by calipers on the image. (**b**) T2-W fat-suppressed axial MR image reveals scattered intrahepatic hyperintensities. (**c**) Patchy contrast uptake within the liver on post-contrast axial T1-W image. (**d**) MIBG reveals marked diffuse hepatic uptake

### 1.7.2 Bacterial Infection

Pyogenic liver abscess is a rare disease in the pediatric patients with an incidence of 25 per 100,000 hospital admissions; however, it has a high mortality rate, especially in immunocompromised patients, patients with multiple (or ruptured) abscesses, and patients with chronic granulomatous disease.

Patients usually present with (spiking) fever, abdominal pain, right upper quadrant tenderness, and hepatomegaly. Although the principal etiologic agent involved is *Staphylococcus aureus* in

immunocompromised and immunocompetent patients, other organisms such as *Streptococcus*, *Escherichia coli*, *Klebsiella*, *Pseudomonas*, and *Proteus* anaerobic bacteria are also common. Diagnosis is by aspiration or biopsy.

Elevation of the right hemidiaphragm, infiltration, atelectasis, and pleural effusion is often seen on conventional radiography.

US examination is the primary imaging tool for evaluation of immunocompromised patients with intrahepatic or extrahepatic abscess. Usually, pyogenic liver abscesses are localized in the posterior right lobe and will be seen as hypoechoic lesions with ill-defined borders and good sound transmission in 75 % of cases. Image characteristics can vary from a sonolucent to an echogenic mass; the wall can be thick or thin and/or ill defined (containing fluid or gas/air).

CT will define the abscess cavity well and also allows for evaluation of the ductal system.

On MRI, a hepatic cyst will be evident if the lesion is greater than 5 mm. Usually MRI will demonstrate a low-signal-intensity lesion on T1-weighted images and high-signal-intensity lesion compared to the surrounding liver on T2-weighted images. The absence of signal inside the lesion will represent air, and low T2 signal intensity inside the abscess may correspond to protein debris. On post-contrast images, the abscess will be seen as a low-signal-intensity mass with a peripheral ring of high intensity signal. Some necrotic or cystic tumors may resemble a hepatic cyst. Diffusion-weighted MRI has been used to differentiate these lesions: liver abscesses will typically show hyperintensity on DW images and hypointensity on ADC maps, while cystic or necrotic tumors will show hypointensity on DW images and hyperintensity on ADC maps (Chan 2001).

### 1.7.3 Fungal Infections

Fungal infections of the liver are very rare in normal patients. They are more typically seen in immunocompromised patients secondary to chemotherapy or AIDS-HIV.

The clinical presentation will vary depending on the area of infection and the systems involved. Symptoms such as fever and abdominal pain and signs such as hepatomegaly or splenomegaly may be present but are very nonspecific. *Candida* is the most common etiologic agent isolated in these patients. Other etiologic agents include *Aspergillus*, *Cryptococcus*, and *Mucormycosis*.

US may demonstrate different patterns of hepatic lesions depending on the stage of the disease. In acute candidiasis, an echogenic lesion with a peripheral hypoechoic rim may be seen, while in the healing stage, the lesion will be pure echogenic with varying intensity of the posterior acoustic shadow, the so-called "wheel-within-wheel" appearance. Focal calcifications may be seen posttreatment (Fig. 14)

On CT, hepatic candidiasis may be seen as a non-enhancing low-attenuation lesion within both lobes of the liver and spleen. Sometimes central high attenuation foci may be seen and represent the candidal hyphae. Some of these lesions may also show rim enhancement (Fig. 14a).

MRI has replaced the liver biopsy in the evaluation and diagnosis of immunocompromised patients with a suspected fungal infection in the liver. Liver candidiasis will be encountered as discrete areas of high signal intensity on T2-weighted images with a progressive decrease in the signal intensity as the lesion is treated (Siegel 2001b).

### 1.7.4 Parasitic Disease

#### 1.7.4.1 Hydatid Cysts

The two most prevalent subtypes of hydatid disease are a unilocular cyst caused by *Echinococcus granulosus* (worldwide prevalence), which has right lobe predilection, and a multilocular cyst caused by *E. alveolaris* (Northern Hemisphere only). Children usually become infected through exposure to canine feces or by eating food contaminated with tapeworm eggs that hatch in the human small intestine under the influence of gastric and intestinal secretions.

An abdominal mass with pain is a common manifestation. Loss of appetite is a frequent symptom, and weight loss and weakness may occur. Approximately 80 % of hydatid cysts will be localized in the liver and may compress the porta and biliary ducts producing jaundice or cholangitis.

Hepatic echinococcal cysts have been classified into four groups based on US findings: type I

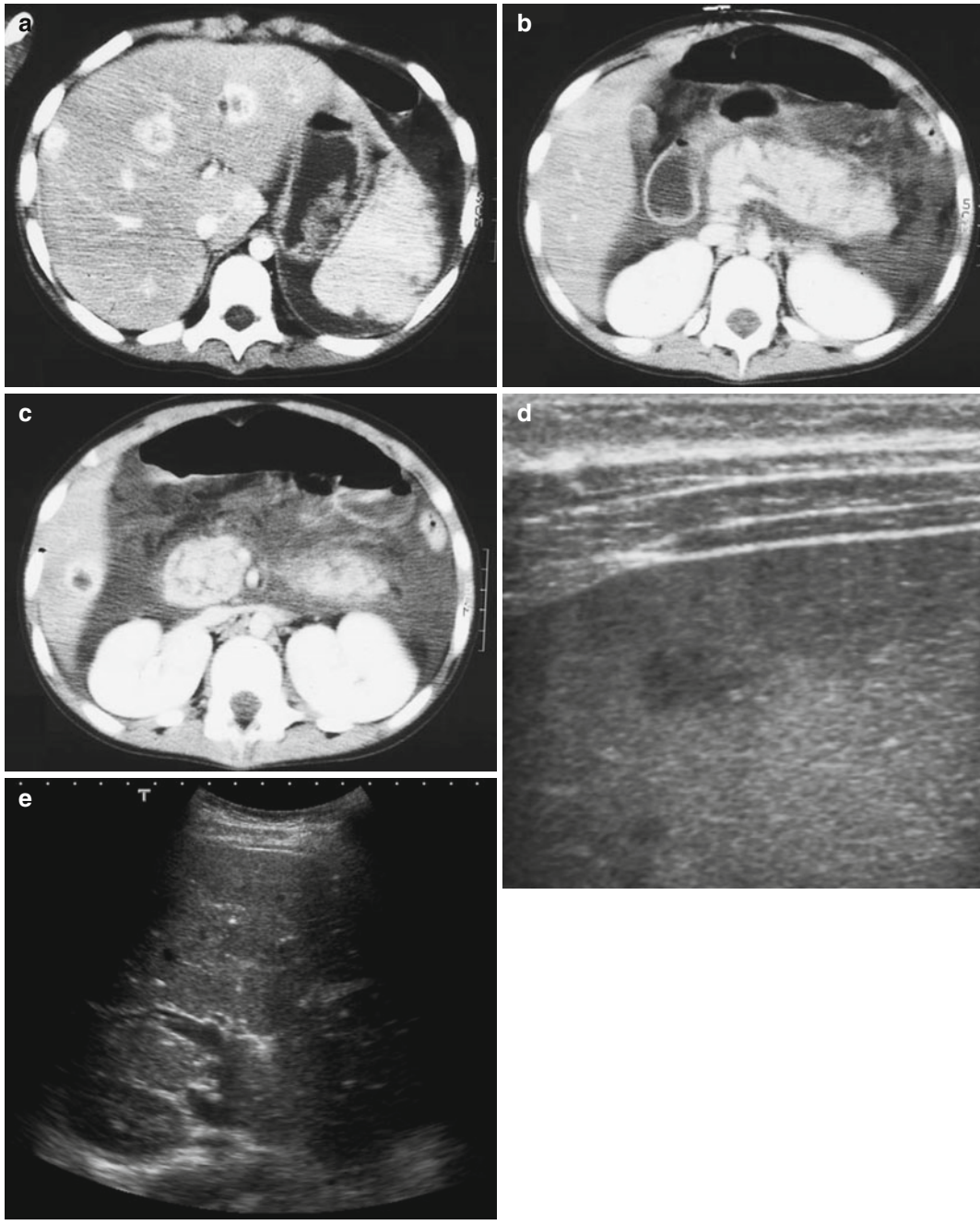


**Fig. 14** Transverse CT images of focal candidiasis. (**a**) Multiple ring-enhancing lesions in the liver with focal hypodensities in the spleen from *Candida* in an immunocompromised patient. (**b**, **c**) Demonstrate ascites, enhancing pancreatic tissue. (**d**) A 3-year-old immunocompromised child, targeted high-resolution US image of the surface of the right lobe of the liver demonstrating a focal hypoechoic lesion consistent with fungal infection. (**e**) An 11-year-old immunocompromised child with previous confirmed *Candida* infection. Transverse US of the liver demonstrates multiple focal residual calcifications posttreatment (Images **d** and **e** courtesy of S Stafrace)

is a simple anechoic fluid-filled cyst, type IR is a cyst with undulating membrane secondary to rupture, type II is a cyst with a daughter cyst, and type III is a densely calcified, echogenic cyst with shadowing. It has been proposed that the natural progression is from types I to III.

On CT, *E. granulosus* cysts appear as well-demarcated thin- or thick-walled hypoattenuating structures. CT can identify the small dissections of the parasitic fluid into the pericystic space with collapse of the parasitic membrane. This is pathognomonic of *E. granulosus* and has been called the "snake" sign because of the undulated membrane appearance. Peripheral calcifications may be seen in advanced stages.

Hydatid cyst can be identified on MRI as unilocular structures with low signal intensity inside the cyst on T1-weighted images. At the bottom of the cyst, a structure with intermediate signal intensity can be visualized, and it represents the hydatid sand. On T2 sequences, the cyst will have high signal intensity with a low-intensity rim surrounding the lesion. Typically, a mother cyst will have greater signal intensity than a daughter cyst. In some patients, the unilocular cyst will have an increased intensity inside the cyst on T1-weighted images which corresponds to signal from proteins and lipids (Kuhn et al. 2004).

#### 1.7.4.2 Amebiasis

Amebiasis is a parasitic infection caused by the protozoon *Entamoeba histolytica*. It is the third leading parasitic cause of death worldwide surpassed only by malaria and schistosomiasis. Amebiasis can localize in many different sites besides the bowel. One of the most common extraintestinal manifestations is the amebic liver abscess, which usually occurs in children less than 3 years of age, with a peak incidence in the first year of life (Elizondo et al. 1987; Giovagnoni et al. 1993).

The child will present with abdominal pain, fever, and hepatomegaly at the initial examination. An acute abdomen may be the initial manifestation of a ruptured amebic abscess in some patients; however, this is very uncommon.

US is preferred for the evaluation of amebic liver abscess because of its low cost, speed of image acquisition and lack of adverse effects (Kuhn et al. 2004). Amebic abscess can be identified on US as hypoechoic lesions with good sound transmission through the cyst. Sometimes it may be difficult to differentiate between amebic versus pyogenic abscesses by US. However, amebic abscesses are usually multiple and in very close proximity to one another. They have a central area of liquefaction that will be seen on US as a central hypoechoic area. Some are more likely to have a peripheral halo and better-defined borders compared to pyogenic abscesses.

CT may demonstrate multiple cysts with ill-defined margins adjacent to the liver capsule.

On MRI, a well-defined lesion with heterogeneous signal intensity on T1-weighted images and with high signal intensity on T2-weighted images can be identified. Some abscesses may show a perilesional rim with increased signal intensity that corresponds to edema. After treatment, the abscesses are typically seen as homogeneous lesions with low signal intensity on T1-weighted images and with concentric rims and decreased edema on T2-weighted images.

## 2 The Pancreas

### 2.1 Anatomy and Embryology

The normal pancreas forms at week 6 from the rotation and fusion of the ventral and dorsal buds which are derived from the foregut (Alexander 2012). The ventral bud constitutes the posterior and inferior part of the pancreatic head and the uncinate process, while the dorsal bud constitutes the body, tail, and anterior head. During the 7th week the duct of the ventral anlage fuses with the distal portion of the duct of the dorsal anlage to form the main pancreatic duct of Wirsung. This opens at the papilla of Vater close to the common bile duct (Nijs et al. 2005). The proximal portion of the dorsal duct either disappears or may persist as the accessory duct (Santorini).

Deviation of this process will result in different congenital anomalies of the pancreas. For instance, in some patients the pancreatic ducts will not connect. In these patients the duct of

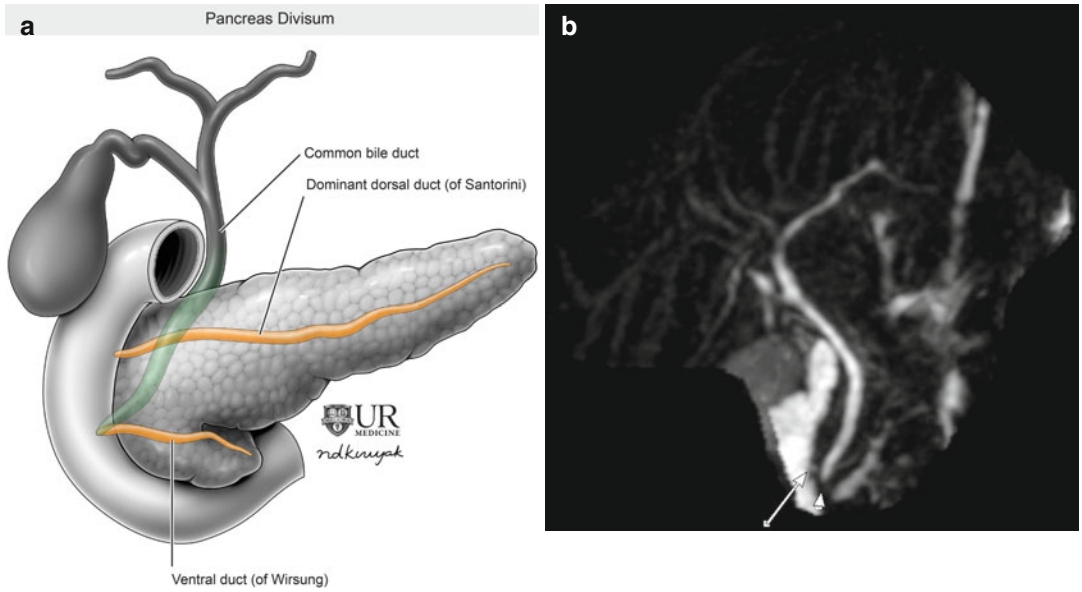


**Fig. 15** Pancreas divisum. (**a**) Illustration depicting pancreas divisum. (**b**) MRCP image documenting separate openings of the ducts of Wirsung (*arrowhead*) and Santorini (*arrow*) (Image courtesy: Deepa R Biyyam, Attending pediatric radiologist, Phoenix Children's Hospital, Phoenix, AZ)

Santorini will drain the main portion of the pancreas into the papilla minor, while the main pancreatic duct of Wirsung will drain only the posterior and inferior portion of the head and uncinate process in the duodenum through the papilla major after joining the common bile duct. This congenital anomaly is called a pancreas divisum (Fig. 15).

Pancreatic growth during the first year of life is substantial; it slows down between 1 and 18 years (Berrocal et al. 1995; Vaughn et al. 1998). The gland is relatively larger in children; the ratio of glandular size to patient body size decreases with age (Nijs et al. 2005). The pancreatic head is relatively more prominent in children than in adults. Pancreatic ductal caliber should be assessed in conjunction with other clinical and laboratory data. Upper limits of normal pancreatic duct in adolescents can run up to 2.2 mm (Nijs et al. 2005).

## 2.2 Congenital Anomalies

Congenital anomalies of the pancreas are typically incidental findings. Only in a few patients are these anomalies associated with important clinical symptoms.

### 2.2.1 Annular Pancreas

An annular pancreas is the result of an abnormal fusion of the ventral and dorsal buds during the 6th week of embryogenesis. These patients will have a "ringed" pancreas surrounding the duodenum that, with growth, may lead to narrowing of the descending duodenum. Two broad types exist, extramural and intramural. In the extramural type, the ventral pancreatic duct encircles the duodenum to join the main pancreatic duct. This clinically presents with high gastrointestinal obstruction. The intramural type has pancreatic tissue intermingled with muscle fibers in the duodenal wall, with small ducts draining directly into the duodenum. Clinically this presents with duodenal ulceration (Borghei et al. 2013).

Other symptoms include polyhydramnios in utero, feeding intolerance in newborns, vomiting, or recurrent pancreatitis. Anomalies such as esophageal atresia, tracheoesophageal fistula, duodenal stenosis, duodenal atresia, trisomy 21, and malrotation have been associated with annular pancreas (Gazelle 1998).

In annular pancreas, the duodenum is often compressed at a point distal to the ampulla of Vater, making bilious vomiting a hallmark symptom. Abdominal distension is typically not a feature because of the proximal location of the obstruction. Patients may not pass meconium, or bowel movements may cease abruptly. A more insidious form of chronic partial duodenal obstruction may also occur.

In neonates, plain radiographs may reveal a spectrum from a "double-bubble" sign with little or no air in the distal bowel to a normal plain film abdomen. This radiographic finding correlates with a high gastrointestinal obstruction such as malrotation/midgut volvulus, duodenal atresia, and duodenal web (Gazelle 1998) (Fig. 16a).

US may show an enlarged pancreatic head or a solid band of pancreatic tissue around the (possibly dilated) duodenum with gastric dilatation (Gazelle 1998).

On CT, an annular pancreas (with or without pancreatitis) may be seen as enlargement of the pancreatic head, surrounding the second portion of the duodenum. Follow-up CT may demonstrate calcifications limited to the annulus of the pancreas (Gazelle 1998).

On ERCP, various ductal configurations may be seen. A classification of six types of annular pancreas according to the site into which the duct of the annulus drains has been described (Gazelle 1998).

On MRI, the normal pancreatic tissue has higher signal intensity compared with other tissues on T1-weighted images with fat saturation. This signal is due to the high concentration of proteins inside the acini. An annular pancreas will be seen on MRI as a high-signal-intensity tissue encircling the second part of the duodenum (Fig. 16b). MRCP has been used to classify the annular pancreas according to the different duct subtypes and to evaluate the concomitant presence of pancreas divisum (Nijs et al. 2005).

### 2.2.2 Ectopic Pancreas

Ectopic pancreas is described as the presence of pancreatic tissue without an anatomic or vascular connection with the pancreatic body. This ectopic tissue may be localized anywhere in or outside of the gastrointestinal tract. Common sites in the gastrointestinal tract are the stomach, duodenum, and proximal jejunum and less commonly in the appendix, Meckel diverticulum (in 5 % of cases), or ileum in just 1 % of cases. Extraintestinal localization, such as in the wall of the gallbladder, the bile ducts in the liver, the hilum of the spleen, the omentum, and the perigastric or periduodenal area, may be seen in 4 % of cases (Gazelle 1998).

If the ectopic pancreatic tissue is localized in the stomach or duodenum, it may be detected on a barium study as a small broad-based submucosal mass with central umbilication. This central umbilication corresponds to remnants of pancreatic ducts. The "bull's eye" appearance represents barium accumulation inside these remnants (Gazelle 1998).

Better delineation of ectopic pancreas may be seen on CT as a round mass with a variation of borders in the antral wall of the stomach; localization in the fundus is very unusual. After contrast injection, the ectopic pancreatic tissue will enhance with a similar pattern to the normal pancreas. Cystic dilatation of an ectopic pancreatic duct, ectopic pancreatic tissue in the perigastric fat, or malignant transformation of ectopic pancreas has been described but is rarely seen (Cho et al. 2000).

### 2.2.3 Pancreas Divisum

Pancreas divisum is the most common congenital anomaly of the pancreatic duct system. It arises from an incomplete fusion of the dorsal and ventral pancreatic ducts. The ventral duct (Wirsung) only drains the ventral pancreatic anlage, and the remainder of the pancreas empties via the dorsal (Santorini) duct into the minor papilla (Borghei et al. 2013). The incidence of pancreas divisum at autopsy ranges between 4.7 and 11 %; 3–8 % are seen at endoscopic retrograde cholangiopancreatography (ERCP) and 9 % seen with magnetic resonance cholangiopancreatography (MRCP). In patients with unexplained pancreatitis, the incidence can be as high as 25.6 %. Multiple attacks of pancreatitis with severe and intermittent epigastric pain but with normal amylase levels are common manifestations of pancreas

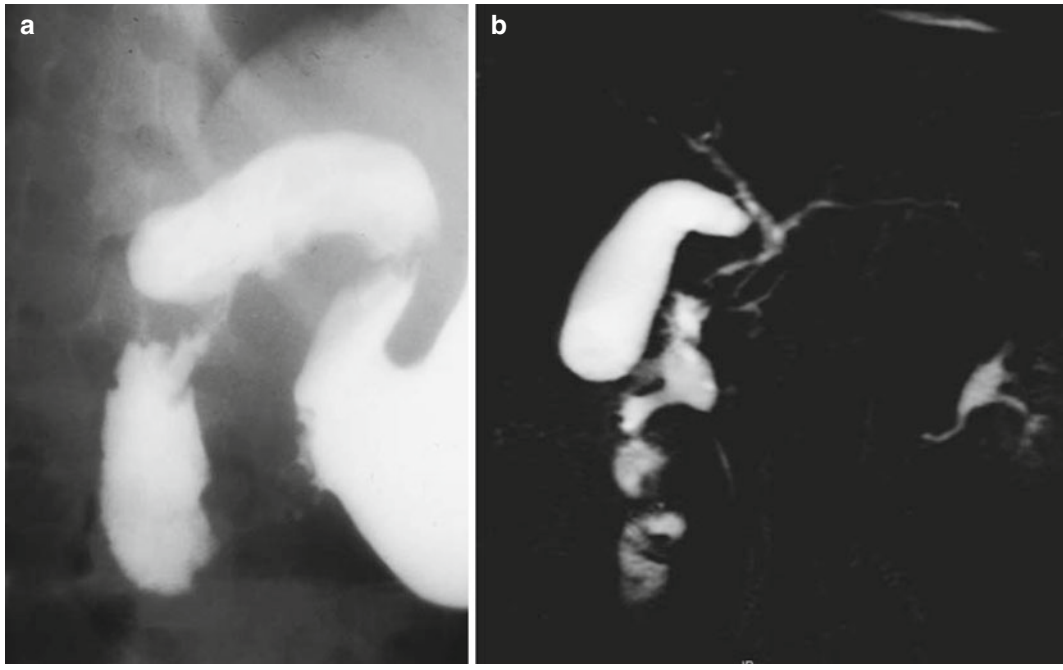


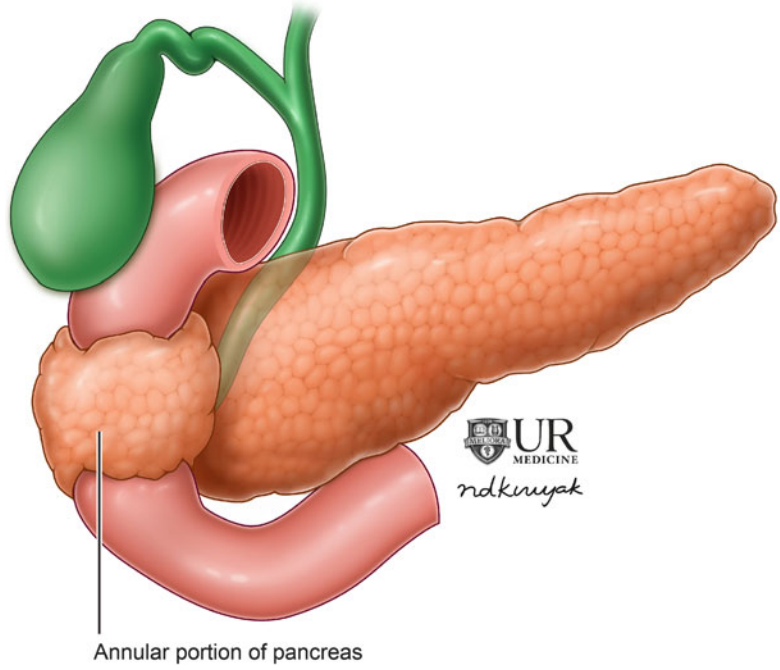


**Fig. 16** (**a**) Classic UGI image of annular pancreas with hold up in the second part of the duodenum. (**b**) MRCP image of an annular pancreas causing relative obstruction of the descending duodenum. (**c**) Illustration depicting the anatomical appearances of an annular pancreas

divisum. Affected children are usually between 5 and 18 years of age (Gazelle 1998).

ERCP has traditionally been considered a very useful tool for the evaluation of pancreas divisum, but with the advent of MRCP, noninvasive multiplanar visualization of the biliary tree and pancreatic duct is possible while also avoiding the risks associated with radiation, sedation, and ERCP-induced pancreatitis.

The absence of union between the dorsal and ventral ducts with a ventral duct directly entering the common bile duct will be encountered on thin-section CT (Fig. 16a).

Secretin administration during MRCP (S-MRCP) enhances visibility of the main pancreatic duct and its side branches (Fig. 16b, c). The duct of Santorini may be enlarged, and the pancreas may demonstrate the characteristic features of pancreatitis. However, the detection of pancreas divisum at S-MRCP might be more difficult when stones or strictures are present in the ventral or dorsal pancreatic ducts (Manfredi et al. 2000).

### 2.2.4 Pancreatic Agenesis, Hypoplasia, and Dysplasia

Complete agenesis of the pancreas is usually incompatible with life. Therefore, pancreatic aplasia or hypoplasia is uncommon in humans. Patients with pancreatic hypoplasia will have a normal development of the pancreas in size and shape but later in life will have a replacement of the glandular elements with fatty tissue. Some of these patients will present with an abnormal exocrine pancreatic insufficiency and normal endocrine function. Children with syndromes such as Shwachman-Diamond (Fig. 17), Beckwith-Wiedemann, polysplenia, bilobed lungs, and congenital heart disease have a higher relative risk of hypoplasia of the pancreas (Gazelle 1998).

### 2.2.5 Cystic Fibrosis

Cystic fibrosis (CF) is a common autosomal recessive disorder of the sodium and chloride channels, and it is characterized by dysfunction of exocrine glands and secondary failure to thrive, frequent foul stools, and pancreatic insufficiency. The damage to the pancreas starts in utero with a progressive dilatation of the acini and pancreatic ducts with secondary fibrosis and fatty replacement. Microscopic findings will include atrophy and cyst formation of the pancreatic stroma before the first year of life.

On US, the pancreas with CF is characteristically of echogenic texture secondary to fatty infiltration. An enlarged pancreas may be seen initially with subsequent atrophy later in life. Pancreatic duct dilatation and calcifications may be seen. Small cysts (anechoic areas) without vascular communication can be identified. Although a hyperechoic pancreas is very typical of CF, the differential diagnosis would include Shwachman-Diamond syndrome (above), hemosiderosis, chronic pancreatitis, and the administration of steroids, which may also demonstrate this feature (Feigelson et al. 2000).

CT may demonstrate an atrophic fatty pancreas with heterogeneous attenuation. Areas of low attenuation will correspond to cysts, while areas of high attenuation will represent calcifications. Partial or total fatty and fibrous replacement is also commonly seen in these patients. There may be a correlation between the degree of fatty infiltration and the pancreatic exocrine dysfunction (Feigelson et al. 2000).

MRI of CF can depict four different patterns. In the first pattern, diffuse high signal intensity with lobular features will be seen; the second will show a diffuse homogeneous hyperintensity without lobular features; in the third pattern the pancreas will have high signal intensity with focal areas of no change in signal intensity; while in the fourth, a normal pancreas is observed. In some cases the multiple cysts can be seen throughout the entire gland replacing the normal tissue. This feature has been called pancreatic cystosis (Feigelson et al. 2000).

### 2.2.6 Von Hippel-Lindau Disease

Von Hippel-Lindau disease (VHL) is an autosomal dominant condition secondary to an alteration in a tumor suppressor gene on chromosome 3. It has incomplete penetrance and is characterized by hemangioblastomas in the retina and CNS; renal cell carcinoma; endolymphatic sac

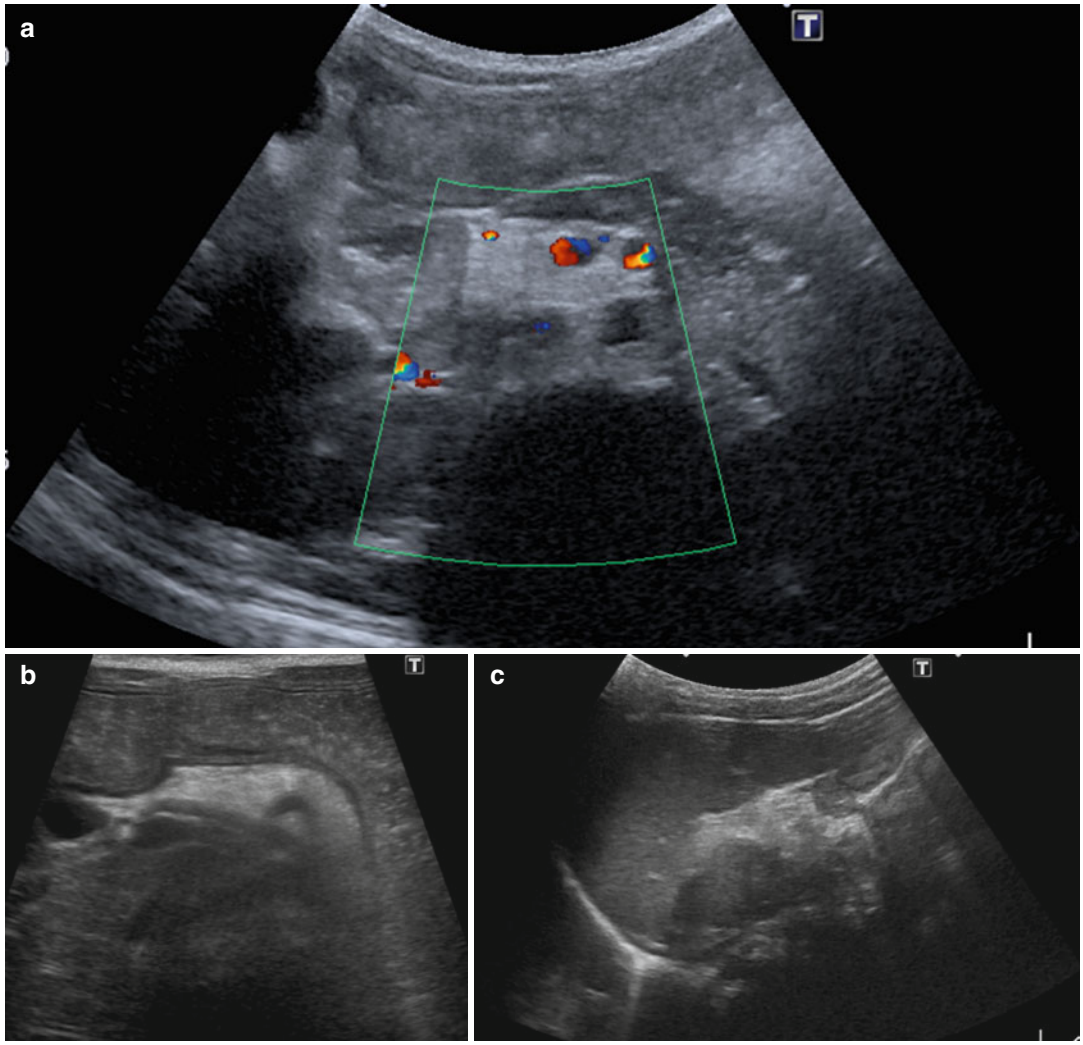


**Fig. 17** Shwachman-Diamond syndrome – US images demonstrating the pancreas as echogenic throughout its course. (**a**) Uncinate process (with color Doppler signal from the superior mesenteric vessels). (**b**) Body of the pancreas at the level of the celiac plexus (high-frequency transverse probe). (**c**) Tail of the pancreas in the splenic hilum (Images courtesy – Dr. Samuel Stafrace)

tumors; pheochromocytomas; papillary cystadenoma of the epididymis; angiomas of the liver and kidney; cysts of the liver, kidney, and epididymis; and pulmonary arteriovenous shunts (Fig. 18a–c). In the pancreas, VHL may have multiple presentations, the most common being the presence of multiple small pancreatic cysts with calcifications in 40 % of cases. Serous cystadenomas, solid nonfunctional islet cell tumors and adenocarcinoma are less common manifestations (Richard et al. 2004).

US typically demonstrates pancreatic cysts. On CT these cysts will have lower attenuation than the normal pancreatic parenchyma, and calcifications might be seen with unenhanced and enhanced CT (Choyke et al. 1990; Hough et al. 1994).

On MRI clusters of cysts may resemble microcystic adenoma of the pancreas; however, this lesion is most commonly found in adult patients. Microcystic adenomas show high signal intensity on T2-weighted images; cysts are typically lobu-

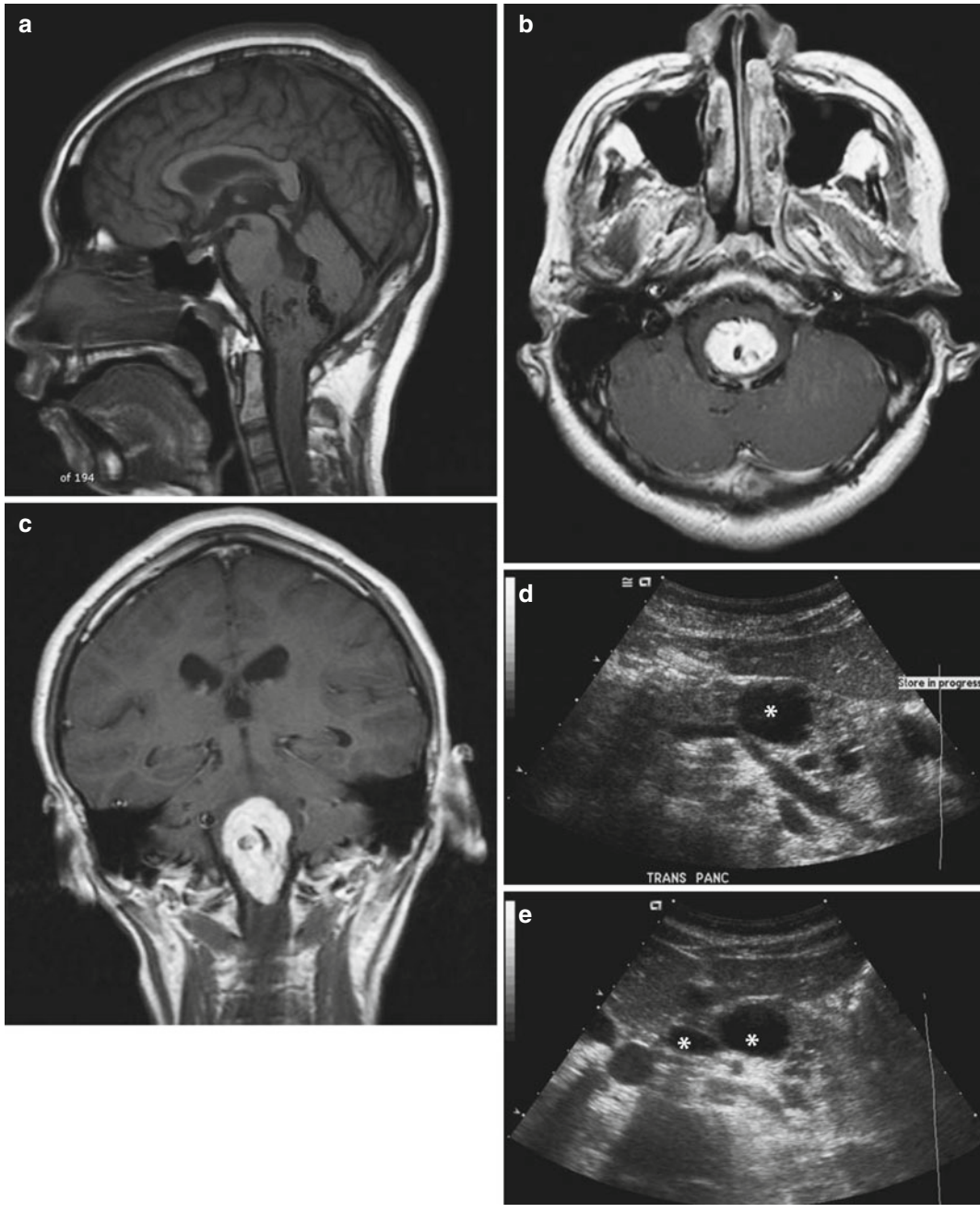


**Fig. 18** Von Hippel-Lindau. (**a**–**c**) MRI images of the brain showing inhomogeneous hemangioblastomas in the pons. (**d**, **e**) Transverse midline US images demonstrating multiple anechoic cysts of varying sizes in the pancreas (*asterisks*)

lated with internal septations. Blood inside the cyst may be seen on T1-weighted images as high signal intensity. Post-gadolinium images will show enhancement of the septations (Tattersall and Moore 2002).

### 2.2.7 Pancreatic Cysts

The pancreatic cyst can be congenital or acquired and can be subclassified depending on the epithelium lining the cyst. Congenital pancreatic cysts may present as solitary, multiple, or alimentary

tract duplications. Von Hippel-Lindau syndrome, trisomy 9, tuberous sclerosis, Meckel-Gruber syndrome, and polycystic kidney disease have been associated with multiple congenital cysts. These cysts may be numerous and can transform the pancreas into a cystic mass (Baker et al. 1990; Gazelle 1998) (Fig. 18d, e).

Solitary congenital cysts may be the least common cystic pancreatic lesion, with only 25 documented cases having been reported. Two additional patients were identified on prenatal US scan. Patients with pancreatic cysts may present with an asymptomatic mass upon physical examination or a symptomatic mass with abdominal distension.

CT and US may demonstrate a low attenuating lesion or an anechoic defect typically located in the tail of the pancreas. This lesion can be unilocular or multilocular with multiple septa. The differential diagnosis includes cysts of renal origin as well as choledochal, mesenteric, ovarian, and urachal cysts. ERCP and HIDA scans can be used to identify communication with the pancreatic duct or biliary tree.

On the other hand, pancreatic pseudocysts represent the most common cystic masses in the pancreas. Pseudocysts are usually fluid collections with a thick wall that arise secondary to infection or trauma. Differentiation between a true cyst and a pseudocyst by imaging is very difficult.

## 2.3 Pancreatic Neoplasia

In the pediatric population, pancreatic tumors are very unusual entities. They account for less than 5 % of all malignancies in children. These tumors may arise from the exocrine or endocrine pancreas. Exocrine neoplasias include ductal adenocarcinoma, acinar adenocarcinoma, pancreatoblastoma, or infantile adenocarcinoma. Endocrine tumors or islet cell tumors are named after the hormone produced, insulinoma being the most common in children.

### 2.3.1 Carcinoma of the Exocrine Pancreas

#### 2.3.1.1 Adenocarcinoma

Adenocarcinoma of the pancreas in childhood is exceedingly rare with the majority of patients diagnosed between 3 and 18 years. Abdominal pain and mass are the most common manifestations in the initial exam. This tumor has a bad prognosis in children, and patients with Peutz-Jeghers syndrome have been associated with a higher risk (×100-fold) of pancreatic adenocarcinoma.

On US, pancreatic adenocarcinoma will be seen as a heterogeneous mass with hyperechoic and anechoic areas. Involvement of the vessels can be identified on US.

CT may demonstrate a mass with heterogeneous density due to cystic elements, hemorrhagic tissue, loss of fat planes, and dilatation of bile and pancreatic ducts.

ERCP is useful in the evaluation of a small mass causing obstruction of the ductal system. MRCP is as sensitive as ERCP and may prevent inappropriate explorations of the pancreatic and bile ducts in patients with suspected pancreatic carcinoma in whom interventional endoscopic therapy is unlikely (Gazelle 1998; Chung 2006).

#### 2.3.1.2 Pancreatoblastoma

Pancreatoblastoma, or infantile adenocarcinoma, although rare (Montemarano et al. 2000; Roebuck et al. 2001), is the most common pancreatic tumor in young children (Ladino-Torres and Strouse 2011). It usually presents in the fourth year of life with males being more commonly affected than females. This tumor commonly arises from the head or tail of the gland and has been associated with Beckwith-Wiedemann syndrome. Microscopic analysis will show proliferation of poorly differentiated squamous cells surrounded by a fibrous capsule. Although it has a better prognosis than adult adenocarcinoma, approximately one-third of children present with metastases at the time of diagnosis (Rojas et al. 2012). Common sites for metastases include the liver and lymph nodes. Lung and brain metastases are rarely seen. Alpha-fetoprotein is elevated in 25–55 % patients; tumor may also secrete adrenocorticotrophic hormone (ACTH) (Nijs et al. 2005).

US evaluation may show a large mass with hemorrhage, necrosis, and degeneration within the tumor.

On CT a well-defined mass with multiple lobules and septal enhancement after contrast injec-

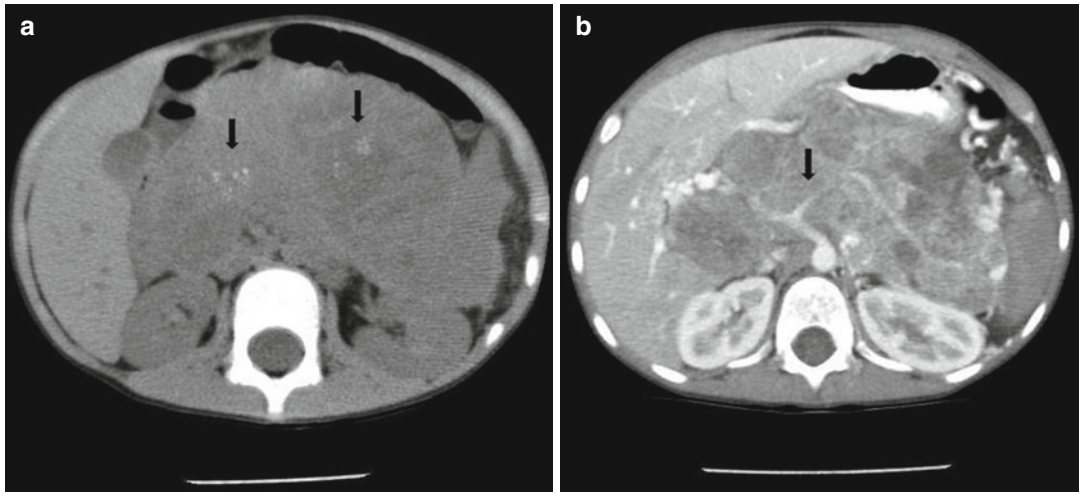


**Fig. 19** Pancreatoblastoma. A 5-year-old boy presenting with abdominal distension and pain. (**a**) Unenhanced axial CT image reveals numerous tiny calcifications (*arrows*) within a large abdominal mass which extends to either side of the midline. (**b**) Contrast-enhanced image reveals patchy enhancement throughout the mass which encases the celiac artery/vascular structures (*arrow*) (Image courtesy - Patricia Cornejo, Scott Jorgensen, Alexander J. Towbin, and Richard Towbin. Diagnostic and Interventional Radiology Department, Phoenix Children's Hospital, Phoenix, AZ, and Department of Radiology, Cincinnati Children's Hospital, Cincinnati, OH)

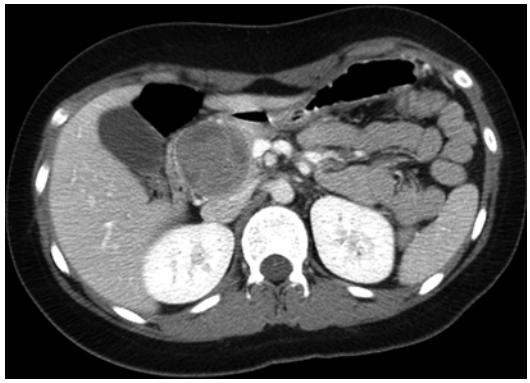

**Fig. 20** Frantz Tumor. A 13-year-old female presenting with abdominal pain. Axial image from contrast-enhanced CT reveals a well-demarcated, hypoattenuating mass in the pancreatic head (Image courtesy - Deepa R Biyyam, Attending Pediatric Radiologist, Phoenix Children's Hospital. Phoenix, AZ)

tion may be found. Either rim-like or clustered calcifications are seen intralesionally (Papaioannou et al. 2009). The tumor may encase mesenteric vessels and the inferior vena cava (Fig. 19a, b).

On MRI, pancreatoblastomas are heterogeneous lesions with predominant low signal intensity on T1-weighted images and high signal intensity on T2-weighted images. After contrast injection, the tumor will reveal intermediate signal intensity (Papaioannou et al. 2009). In some patients, MRCP has been used to define and determine the level of obstruction of the biliary system.

#### 2.3.1.3 Frantz Tumor

Solid pseudopapillary tumor of the pancreas (SPT), the so-called Frantz tumor, is an exceptionally rare neoplasm in children almost exclusively seen in adolescent girls (Fig. 20). Its origin remains enigmatic.

Although solid pseudopapillary tumors can present as large invasive tumors with metastases, they are remarkably indolent when compared to other malignant pancreatic tumors (Klimstra et al. 2000). In SPT, metastases are uncommon with only 10–15 % of patients with advanced disease at diagnosis (Klimstra et al. 2000). Despite metastases, the prognosis is excellent (Shorter et al. 2002; Papavramidis and Papavramidis 2005).

### 2.3.2 Endocrine Pancreatic Neoplasia

Neoplasias that arise from the endocrine portion of the pancreas can be classified as secretory or nonsecretory (Gouya et al. 2003). When secretory, the endocrine tumor will be subclassified

according to the type of hormone produced (insulin, gastrin, or active peptides). Insulinomas are the most common endocrine tumors, while glucagonomas or somatostatinomas have not been reported in children.

Nesidioblastosis is a hyperplasia of primitive pancreatic islet cells, i.e., B cells secreting insulin, and may be responsible for 5 % of cases of hyperinsulinism and hypoglycemia in pediatric patients.

The clinical presentation varies according to the type of hormone released. Hyperinsulinism manifests with diarrhea, abdominal pain, and low levels of glucose. Hunger, jitteriness, lethargy, apnea, and seizures are common manifestations in newborns with nesidioblastosis, while older children may show diaphoresis, confusion, or unusual behavior. Zollinger-Ellison syndrome presents with intractable peptic ulcers. Patients with VIPomas have watery diarrhea, hypokalemia, and achlorhydria, while multiple endocrine neoplasias have been reported with multiple endocrine neoplasia type 1 (MEN I).

Islet cell tumors are very difficult to visualize on US. Sometimes small and well-defined hypoechoic round lesions with a hyperechoic capsule may be found.

On CT, an area of low attenuation with calcifications and disruption of the normal contour can be identified. On enhanced CT, the tumor will show a momentary enhancement that will be higher in the arterial phase compared with the portal venous phase.

On MRI, a low-signal-intensity mass compared to a high-signal pancreas will be seen on T1-weighted fat-suppressed spin-echo images. Because of the high vascular component of these tumors, they will appear on dynamic or contrast-enhanced MR more hyperintense and with greater conspicuity than the normal pancreas.

## 2.4 Pancreatitis

Pancreatitis is defined as an inflammation of the pancreas, which can be classified as acute or chronic (Gazelle 1998). Acute pancreatitis can be subclassified in acute interstitial (edematous) or acute hemorrhagic form. Typically, patients with pancreatitis will present with abdominal pain, nausea, vomiting, and elevation of the pancreatic enzymes in the acute form.

### 2.4.1 Acute Pancreatitis

The pediatric incidence of acute pancreatitis is 2.7 cases per 100,000 children younger than 15 years. Many etiologic factors have been associated with pancreatitis in childhood, with the most common cause being blunt trauma. Other etiologies such as organ transplantation, malignancies, drug induced (valproic acid), biliary tract disease, and viral infections have been described. These etiologies are different from those seen in adults.

On US, an acute inflammation may show an increase in the duct calibers, with a diffuse swollen hypoechoic gland (Chao et al. 2000). Extrapancreatic fluid collections occur in about 50 % of patients, mostly in the anterior pararenal space, and this may be the only finding. Some studies have found a correlation between the diameter of the pancreatic duct and the serum lipase level. Early US is a helpful tool for the identification of stones in the biliary tract in jaundice patients, and Doppler US may diagnose secondary splenic vein thrombosis.

CT may demonstrate duct dilatation and focal areas of low attenuation in the pancreatic parenchyma that correspond to fluid collections (King et al. 1995). Necrosis is recognized as a focal or diffuse area of non-enhancing pancreatic tissue. The pancreas can be enlarged or normal. Other findings include extrapancreatic fluid collections located in the anterior pararenal space, lesser sac, lesser omentum, and transverse mesocolon. Peripancreatic fat stranding and pancreatic pseudocyst are sometimes encountered.

It is not uncommon to find pancreatic pseudocysts after an episode of traumatic pancreatitis or chronic pancreatitis, and some pseudocysts complicating hemolytic uremic syndrome or mediastinal pseudocysts have been reported. CT will reveal a round hypodense structure with a thin or thick wall that may enhance after contrast injection. Some of these pseudocysts can cause complications, presenting with obstruction of the common bile duct, infection, abscess formation, and rupture of the pseudocyst, and

can be responsible for splenic vein thrombosis or splenic hemorrhage. CT is the primary imaging tool to visualize and identify these complications.

MRCP is a very useful imaging tool used to identify possible etiologies of pancreatitis such as abnormal union of the pancreatobiliary junction, choledochal cyst, or pancreas divisum (Hirohashi et al. 1997; Arcement et al. 2001) (see earlier sections dedicated to these pathologies).

### 2.4.2 Chronic Pancreatitis

Chronic pancreatitis is a rare entity in children. Among the principal causes of chronic pancreatitis are hereditary pancreatitis, autoimmune conditions (sclerosing cholangitis), and CF. CT features of chronic pancreatitis include focal or diffuse increase in pancreatic size, dilatation of the main pancreatic duct (almost always present), intraductal calcifications, or pseudocyst formation. MRCP should be performed first, but ERCP can be used in children with unknown pancreatitis to identify and treat cases of biliary obstruction and structural cases of chronic pancreatitis.

### 2.4.3 Hereditary Pancreatitis

Hereditary pancreatitis is an autosomal dominant disorder that presents as a dysfunction of the pancreas (inflammation) during the first decade of life. Usually, each episode will last between 2 days and 2 weeks. US reveals a shrunken fibrotic pancreas with calcifications. CT shows dilatation of the ductal system, pancreatic stones, or pancreatic complications (Fig. 21). Approximately 15 % of patients with hereditary pancreatitis may have pancreatic carcinoma in adulthood.

### 2.4.4 Autoimmune Pancreatitis

This is a rare entity with unknown etiology in pediatrics (Blejter et al. 2008). Autoimmune pancreatitis is characterized by cholestasis secondary to obstruction of the common bile duct. On US, the pancreas is enlarged, heterogeneous, and hypoechoic. Intra- and extrahepatic biliary ductal dilatation with thickened walls is present. CT shows similar findings with irregularities in Wirsung ductal diameter. Delayed contrast enhancement and spherical hypodensities within the pancreatic parenchyma may be seen (Blejter et al. 2008). MR shows similar findings with better definition.

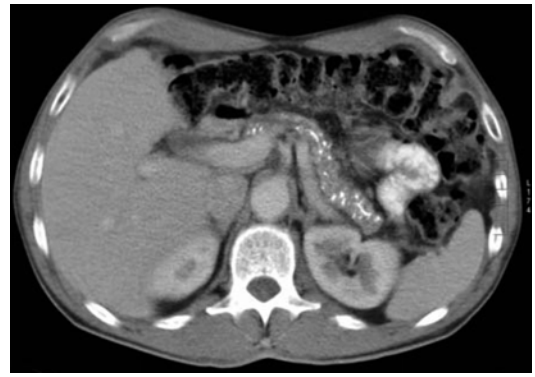

**Fig. 21** Hereditary pancreatitis. Transverse CT image of a shrunken pancreas with multiple focal calcifications. The patient's father had a similar CT appearance

Nodular lesions within the renal cortex may be an accompaniment of autoimmune pancreatitis; these could be secondary to vasculitis or inflammatory pseudotumor (Takahashi et al. 2007; Khalili et al. 2008).

**Acknowledgments** The author acknowledges the work of the illustrators Gwen Mack, MFA, and Nadezhda Kiriyak, BFA, who contributed original artwork in this chapter.

## References

Alexander LF (2012) Congenital pancreatic anomalies, variants and conditions. Radiol Clin North Am 50(3):487–498

Arcement CM et al (2001) MRCP in the evaluation of pancreaticobiliary disease in children. Pediatr Radiol 31(2):92–97

Arrive L, Tubiana JM (2003) Serial needle aspiration in polycystic liver disease. AJR Am J Roentgenol 181(6):1717

Baker LL et al (1990) Sonographic detection of congenital pancreatic cysts in the newborn: report of a case and review of the literature. Pediatr Radiol 20(6):488–490

Berrocal T et al (1995) Sonography of pancreatic disease in infants and children. Radiographics 15(2):301–313

Blejter J et al (2008) Autoimmune pancreatitis: an adolescent case and review of literature. J Pediatr Surg 43(7):1368–1372

Borghei P et al (2013) Anomalies, anatomic variants and sources of diagnostic pitfalls in pancreatic imaging. Radiology 266(1):28–36

Brody AS et al (1989) Metastatic Wilms' tumor to the liver with MR findings simulating cysts: case report emphasizing need for integrated imaging. Pediatr Radiol 19(5):337–338

Carlson SK et al (2000) CT of focal nodular hyperplasia of the liver. AJR Am J Roentgenol 174(3):705–712

Cetin M et al (2002) Stromal predominant type mesenchymal hamartoma of liver: CT and MR features. Comput Med Imaging Graph 26(3):167–169

Chan JH (2001) Diffusion-weighted MR imaging of the liver: distinguishing hepatic abscess from cystic or necrotic tumor. Abdom Imaging 26(2):161–165

Chao HC et al (2000) Sonographic evaluation of the pancreatic duct in normal children and children with pancreatitis. J Ultrasound Med 19(11):757–763

Chauveau D et al (2000) Liver involvement in autosomal-dominant polycystic kidney disease: therapeutic dilemma. J Am Soc Nephrol 11(9):1767–1775

Cho JS et al (2000) Heterotopic pancreas in the stomach: CT findings. Radiology 217(1):139–144

Chowdhary SK et al (2004) Undifferentiated embryonal sarcoma in children: beware of the solitary liver cyst. J Pediatr Surg 39(1):E9–E12

Choyke PL et al (1990) von Hippel-Lindau disease: radiologic screening for visceral manifestations. Radiology 174(3 Pt 1):815–820

Chung EM (2006) Pancreatic tumors in children: radiologic-pathologic correlation. Radiographics 26(4):1211–1238

Cornette J et al (2009) Mesenchymal hamartoma of the liver: a benign tumor with deceptive prognosis in the perinatal period. Case report and review of the literature. Fetal Diagn Ther 25(2):196–202

Dachman AH et al (1987) Hepatoblastoma: radiologic-pathologic correlation in 50 cases. Radiology 164(1):15–19

Darbari A et al (2003) Epidemiology of primary hepatic malignancies in U.S. children. Hepatology 38(3): 560–566

Das CJ et al (2009) Imaging of paediatric liver tumours with pathological correlation. Clin Radiol 64(10):1015–1025

Davenport M (2005) Biliary atresia. Semin Pediatr Surg 14(1):42–48

Elizondo G et al (1987) Amebic liver abscess: diagnosis and treatment evaluation with MR imaging. Radiology 165(3):795–800

Feigelson J et al (2000) Imaging changes in the pancreas in cystic fibrosis: a retrospective evaluation of 55 cases seen over a period of 9 years. J Pediatr Gastroenterol Nutr 30(2):145–151

Fulcher AS, Sterling RK (2002) Hepatic neoplasms: computed tomography and magnetic resonance features. J Clin Gastroenterol 34(4):463–471

Gazelle GS (1998) Hepatobiliary and pancreatic radiology imaging and intervention. Thieme, New York

Giovagnoni A et al (1993) MRI appearances in amoebic granulomatous hepatitis: a case report. Pediatr Radiol 23(7):536–537

Gouya H et al (2003) CT, endoscopic sonography and a combined protocol for preoperative evaluation of pancreatic insulinomas. AJR Am J Roentgenol 181(4):987–992

Griffin N et al (2013) Magnetic resonance cholangiopancreatography: pearls, pitfalls and pathology. Semin Ultrasound CT MR 34(1):32–43

Gubernick JA et al (2000) US approach to jaundice in infants and children. Radiographics 20(1):173–195

Helmberger TK et al (1999) Pediatric liver neoplasms: a radiologic-pathologic correlation. Eur Radiol 9(7):1339–1347

Hirohashi S et al (1997) Pancreatitis: evaluation with MR cholangiopancreatography in children. Radiology 203(2):411–415

Hough DM et al (1994) Pancreatic lesions in von Hippel-Lindau disease: prevalence, clinical significance and CT findings. AJR Am J Roentgenol 162(5):1091–1094

Ichikawa T et al (1999) Fibrolamellar hepatocellular carcinoma: imaging and pathologic findings in 31 recent cases. Radiology 213(2):352–361

Jaw TS et al (1999) MR cholangiography in the evaluation of neonatal cholestasis. Radiology 212(1):249–256

Kanegawa K et al (2003) Sonographic diagnosis of biliary atresia in pediatric patients using the "triangular cord" sign versus gallbladder length and contraction. AJR Am J Roentgenol 181(5):1387–1390

Katzenstein HM et al (2003) Fibrolamellar hepatocellular carcinoma in children and adolescents. Cancer 97(8):2006–2012

Khalili K, Doyle DJ et al (2008) Renal cortical lesions in patients with autoimmune pancreatitis: a clue to differentiation from pancreatic malignancy. Eur J Radiol 67(2):329–335

Kim MJ et al (2000) Biliary atresia in neonates and infants: triangular area of high signal intensity in the porta hepatis at T2-weighted MR cholangiography with US and histopathologic correlation. Radiology 215(2):395–401

King LR et al (1995) Acute pancreatitis in children: CT findings of intra- and extrapancreatic fluid collections. Radiology 195(1):196–200

Kirks DR, Griscom N (1998) Practical pediatric imaging: diagnostic radiology of infants and children. Lippincott-Raven, Philadelphia

Klimstra DS et al (2000) Solid-pseudopapillary tumor of the pancreas: a typically cystic carcinoma of low malignant potential. Semin Diagn Pathol 17(1):66–80

Konez O et al (2001) Mesenchymal hamartoma of the liver. Comput Med Imaging Graph 25(1):61–65

Koob M et al (2015) Porta hepatis micocyst: an additional reliable ultrasonographic (US) sign of biliary atresia (BS). Pediat Radiol 45 (Suppl 2):S247–S368 (abstract)

Kuhn JP, Slovis T, Haller JO, Caffey J (2004) Caffey's pediatric diagnostic imaging. Mosby/Elsevier Science, St. Louis

Lack EE et al (1991) Undifferentiated (embryonal) sarcoma of the liver. Clinical and pathologic study of 16

cases with emphasis on immunohistochemical features. Am J Surg Pathol 15(1):1–16
Ladino-Torres MF, Strouse PJ (2011) Gastrointestinal tumors in children. Radiol Clin North Am 49(4):665–677, v–vi
Makin E, Davenport M (2010) Fetal and neonatal liver tumours. Early Hum Dev 86(10):637–642
Manfredi R et al (2000) Pancreas divisum and "santorinicele: diagnosis with dynamic MR cholangiopancreatography with secretin stimulation.". Radiology 217(2):403–408
Martin DR et al (2005) MR imaging of the liver. Radiol Clin North Am 43(5):861–886, viii
McCarville MB, Roebuck DJ (2012) Diagnosis and staging of hepatoblastoma: imaging aspects. Pediatr Blood Cancer 59(5):793–799
Montemarano H et al (2000) Pancreatoblastoma: imaging findings in 10 patients and review of the literature. Radiology 214(2):476–482
Mortele KJ et al (1998) Dynamic gadolinium-enhanced MR findings in infantile hepatic hemangioendothelioma. J Comput Assist Tomogr 22(5):714–717
Mortele KJ et al (2000) CT and MR imaging findings in focal nodular hyperplasia of the liver: radiologic-pathologic correlation. AJR Am J Roentgenol 175(3):687–692
Mortele KJ et al (2002) Solitary hepatic infantile hemangioendothelioma: dynamic gadolinium-enhanced MR imaging findings. Eur Radiol 12(4):862–865
Mortele KJ et al (2006) Multimodality imaging of pancreatic and biliary congenital anomalies. Radiographics 26(3):715–731
Mowat AP et al (1976) Extrahepatic biliary atresia versus neonatal hepatitis. Review of 137 prospectively investigated infants. Arch Dis Child 51(10):763–770
Nijs E et al (2005) Disorders of the pediatric pancreas: imaging features. Pediatr Radiol 35(4):358–373, quiz 457
Norton KI et al (2002) MR cholangiography in the evaluation of neonatal cholestasis: initial results. Radiology 222(3):687–691
O'Sullivan MJ et al (2001) Undifferentiated embryonal sarcoma with unusual features arising within mesenchymal hamartoma of the liver: report of a case and review of the literature. Pediatr Dev Pathol 4(5):482–489
Orlowski A, Breborowicz D (2011) Mesenchymal hamartoma of the liver – case report and short literature overview. Pol J Pathol 62(2):108–112
Oue T et al (2003) Hepatoblastoma in children of extremely low birth weight: a report from a single perinatal center. J Pediatr Surg 38(1):134–137; discussion 134–137
Papaioannou G et al (2009) Imaging of the unusual pediatric 'blastomas'. Cancer Imaging 9:1–11
Papavramidis T, Papavramidis S (2005) Solid pseudopapillary tumors of the pancreas: review of 718 patients reported in English literature. J Am Coll Surg 200(6):965–972
Petersen C, Ure BM (2003) What's new in biliary atresia? Eur J Pediatr Surg 13(1):1–6
Pobiel RS, Bisset GS 3rd (1995) Pictorial essay: imaging of liver tumors in the infant and child. Pediatr Radiol 25(7):495–506
Ramirez GB et al (2003) Tagum study II: follow-up study at two years of age after prenatal exposure to mercury. Pediatrics 111(3):e289–e295
Richard S et al (2004) Von Hippel-Lindau disease. Lancet 363(9416):1231–1234
Roebuck DJ et al (1998) Hepatobiliary rhabdomyosarcoma in children: diagnostic radiology. Pediatr Radiol 28(2):101–108
Roebuck DJ et al (2001) Imaging features of pancreatoblastoma. Pediatr Radiol 31(7):501–506
Roebuck DJ et al (2006) Radiological staging in children with hepatoblastoma. Pediatr Radiol 36(3): 176–182
Rojas Y et al (2012) Primary malignant pancreatic neoplasms in children and adolescents: a 20 year experience. J Pediatr Surg 47(12):2199–2204
Rozel C et al (2011) Imaging of biliary disorders in children. Pediatr Radiol 41(2):208–220
Shorter NA et al (2002) Malignant pancreatic tumors in childhood and adolescence: the Memorial Sloan-Kettering experience, 1967 to present. J Pediatr Surg 37(6):887–892
Siegel MJ (2000) MR imaging of pediatric abdominal neoplasms. Magn Reson Imaging Clin N Am 8(4):837–851
Siegel MJ (2001) Pediatric sonography. Lippincott Williams and Wilkins, Philadelphia
Sokol RJ et al (2003) Pathogenesis and outcome of biliary atresia: current concepts. J Pediatr Gastroenterol Nutr 37(1):4–21
Somech R et al (2001) Focal nodular hyperplasia in children. J Pediatr Gastroenterol Nutr 32(4): 480–483
Soyupak SK et al (2002) Sonographic measurements of the liver, spleen and kidney dimensions in the healthy term and preterm newborns. Eur J Radiol 43(1) :73–78
Sporcq C, Avni F et al (2007) Reappraisal of the sonographic characteristics of the fetal and newborn kidney: introducing the cortico-medullary ratio. European society of paediatric radiology 44th annual meeting, Barcelona, 3rd–7th June 2007
Suchy FJ (2003) Clinical problems with developmental anomalies of the biliary tract. Semin Gastrointest Dis 14(4):156–164
Swischuk L (2005) Imaging of the newborn, infant and young child, 5th edn. Lippincott, Williams and Wilkins, Philadelphia
Takahashi N et al (2007) Renal involvement in patients with autoimmune pancreatitis: CT and MR imaging findings. Radiology 242(3):791–801
Tattersall DJ, Moore NR (2002) von Hippel-Lindau disease: MRI of abdominal manifestations. Clin Radiol 57(2):85–92
Teele RL, Jane Chrestman MS (1991) Ultrasonography of infants and children. Saunders, Philadelphia

Todani T et al (2003) Classification of congenital biliary cystic disease: special reference to type Ic and IVA cysts with primary ductal stricture. J Hepatobiliary Pancreat Surg 10(5):340–344

Tran VT, Vasanawala S (2013) Pediatric hepatobiliary magnetic resonance imaging. Radiol Clin North Am 51(4):599–614

Varela-Fascinetto G et al (1998) Biliary atresia-polysplenia syndrome: surgical and clinical relevance in liver transplantation. Ann Surg 227(4):583–589

Vaughn DD et al (1998) Pancreatic disease in children and young adults: evaluation with CT. Radiographics 18(5):1171–1187

Weinreb JC et al (1984) Magnetic resonance imaging of hepatic lymphoma. AJR Am J Roentgenol 143(6):1211–1214

Yen JB et al (2003) Hepatic mesenchymal hamartoma. J Paediatr Child Health 39(8):632–634

# Radiological Gastrointestinal Interventions in Childhood; A Review

K.P. van Lienden and R.R. van Rijn

## Contents



K.P. van Lienden, MD, PhD (✉) • R.R. van Rijn
Department of Radiology, Academic Medical Centre/Emma Children's Hospital Amsterdam, Amsterdam Zuid-Oost, The Netherlands
e-mail: k.p.vanlienden@amc.uva.nl

**Abstract**

Interventional radiology in children has expanded progressively over the recent years. This chapter outlines the more commonly performed procedures, describing the indications, imaging highlights and technical aspects of such pediatric gastrointestinal interventions.

## 1 Introduction

During the past decades, image guided interventions have become daily routine in radiology departments worldwide. Radiologists and clinicians alike clearly see the advantages of image-guided interventions, as it is minimally invasive, well tolerated by patients and has shown to have a low level of complications.

In paediatrics, interventional radiological techniques are widely accepted although they are mostly performed in specialized paediatric hospitals or hospitals with a large department of paediatrics and experienced interventional radiologists. As we all know, and should appreciate, children are not miniature adults, a fact reflected by age specific pathology and psychological development. This means that when a paediatric interventional program is initiated one should keep in mind specific problems when dealing with children. Generally speaking, one should plan ample time and be prepared to do fewer interventions in a given time



S. Stafrace, J.G. (Hans) Blickman (eds.), *Radiological Imaging of the Digestive Tract in Infants and Children*, Medical Radiology, DOI 10.1007/978-3-319-18434-0_9

frame compared to an adult setting. If one is prepared to go the proverbial extra mile, one will be rewarded by satisfied patients and parents alike.

In this chapter we will discuss sedation and interventional procedures related to the gastrointestinal tract.

## 2 Sedation

One of the hallmarks of paediatric radiological interventions is the need for sedation in combination with analgesia. Where as in the adult population local anaesthesia will mostly suffice, this will almost never be the case in children. This aspect of the interventional procedure may be one of the reasons for the lower level of acceptance of interventional radiology in children.

Although the situation will differ from country to country and most likely even from hospital to hospital, we would like to present a number of guidelines for running a sedation program in a radiology department.

It is very important to cooperate with your anaesthesiologists in order to develop a set of guidelines along which the decision can be made whether to perform the procedure under conscious sedation or under general anaesthesia.

Secondly, talk with the parents and where possible with the child. Explain the procedure extensively and try to assess if it will be possible to perform the procedure under sedation or that general anaesthesia is necessary.

It is also very important to discuss the risks and benefits of the procedure and the possible alternatives.

Finally, when in doubt do not use sedation but consult the appropriate experts, for after all, we are first and foremost radiologists.

What is sedation? For this we refer to the guidelines as stated by the American Society of Anaesthesiologists (ASA) and the American College of Radiology (ACR) (American Society of Anesthesiologists Task Force on Sedation and Analgesia by Non-Anesthesiologists 2002). Sedation can be classified into three different levels. Level I is light sedation or anxiolysis. This category is defined as 'the administration of oral medications for the reduction of anxiety' and 'a drug induced state during which the patient responds normally to verbal commands'. The ASA further states that 'although cognitive function and coordination may be impaired, ventilator and cardiovascular functions are unaffected. Level II is moderate or conscious sedation, which is defined as 'a minimally depressed level of consciousness induced by the administration of pharmacological agents in which the patient retains conscious and independent ability to maintain protective reflexes and a patent airway and to be aroused by physical or verbal stimulation'. Level II sedation is actually quite difficult to achieve and maintain as it may easily lead to the next level (level III), i.e. deep sedation which is 'a controlled state of depressed consciousness or unconsciousness from which the patient is not easily aroused' (American Society of Anesthesiologists Task Force on Sedation and Analgesia by Non-Anesthesiologists 2002). Sedation level IV is general anaesthesia, which is beyond the scope of this article.

Sedation should always be performed by or under the supervision of a trained physician. This is especially so in case of a radiological intervention as both sedation and analgesia are necessary. The latter combination makes it all the more difficult to adequately monitor the patient in question, thus it is essential that all persons responsible for the administration of medication and/or monitoring of the patient should be fully knowledgeable of the equipment in use and the medication. Furthermore they should possess basic life support skills in order to intervene in case of complications.

The current situation in Europe is that in many centres anaesthesia resources are limited, which has led to the situation that more and more non-anaesthesiologists are administering sedation. A possible solution to this problem in paediatric interventional radiology could be the use of a nurse-led sedation program.

Several publications show excellent results of these programs for MRI units (Sury et al. 1999; Beebe et al. 2000). Sury et al. report on a total of 1155 sedations for MRI with a failure rate of only 5 %, without cases of adverse reactions (Sury et al. 1999). Woodthorpe et al. published an article in which sedation was attempted in 455 cases

with chloral hydrate, and 325 with Temazepam and Droperidol (Woodthorpe et al. 2007). The success rate was 97.4 % and 92.6 % respectively. Top-up sedation was used in 10 % and 29 % respectively. There were seven minor incidents but none required admission. Approximately 20 % of children were drowsy the following day.

Finally, which patients are eligible for sedation? According to the ASA only class I and II patients (healthy patient and patient with mild systemic disease, respectively) are eligible (see Table 1). ASA Class III and higher require general anaesthesia (American Society of Anesthesiologists Task Force on Sedation and Analgesia by Non-Anesthesiologists 2002). Therefore patients, managed by the anaesthesiology or critical care service, patients on mechanical ventilation and patients who are ASA class V should not be sedated by non-anaesthesiologists.

When an interventional procedure is performed under sedation, the radiologist is also responsible for the pre-procedural management as this is an integral part of patient care. In neonates the last feeding should be withheld, while in older children the policy is nil-by-mouth for at least 6 h prior to sedation.

The facilities should include a large enough interventional suite to facilitate not only the procedure, but also resuscitation trollies and the personnel in case of a resuscitation event. Furthermore, there should be dedicated personnel to monitor the patient during the procedure and there should be an equipped recovery room with sufficiently trained personnel to monitor the patients after the procedure.

**Table 1** ASA physical status classification

| | |
|---|---|
| Class I | A normal, healthy patient |
| Class II | A patient with mild systemic disease |
| Class III | A patient with severe systemic disease |
| Class IV | A patient with severe systemic disease that is a constant threat to life |
| Class V | A moribund patient who is not expected to survive without the operation |
| Class VI | A brain-dead patient whose organs are being removed for donor purposes |

Several drugs can be used for sedation (Table 2). However, the choice of drugs will depend on the experience of the radiologist, availability of the drugs and hospital policy. In an excellent review article by Towbin et al. they describe a strategy that in their hands has a 98 % success rate (Towbin and Ball 1988). In children less than 2 years of age, oral chloral hydrate, at a dose of 50 mg/kg, is their drug of first choice. If more sedation is needed, for instance in case of a painful procedure, intravenous Fentanyl can be given albeit in small dosages of 1 mcg/kg. In children aged 2 years and above, oral chloral hydrate will generally not suffice. Intravenous Nembutal (Pentobarbital sodium), 2 mg/kg, is then preferred. Nembutal is a quick acting drug with relatively few side effects. When using Nembutal in interventional radiology, Fentanyl should be added, as Nembutal tends to make children hypersensitive to stimulation. Nembutal should be given in 2–3 mg/kg boluses, titrated to the preferred level of sedation. Rubin et al. presented their experience with oral or intravenous caffeine for the treatment of post-sedation paradoxical hyperactivity (Rubin et al. 2004). Of the children treated, 63 % showed a positive effect and returned to baseline behavioural status significantly sooner than untreated children.

The use of intranasal Midazolam as premedication has been described in several publications (Weber et al. 2003; Kogan et al. 2002; Ljungman et al. 2000). Its use reduces anxiety, induces amnesia in a significant number of patients and also has a sedative effect. The latter, however, is hardly ever satisfactory to allow an interventional procedure to be performed, but it will facilitate insertion of a venous access (Kaye et al. 2000). The most common adverse reaction is nasal discomfort,

**Table 2** Drugs used in sedation

| Drug | Dose | Range | Administration |
|---|---|---|---|
| Chloral hydrate | 50 mg/kg | 50–75 mg/kg | Oral |
| Nembutal | 2 mg/kg | 2–8 mg/kg | Intravenous |
| Fentanyl | 1 µg/kg | 1–5 µg/kg | Intravenous |
| Midazolam | | 0.1–0.3 mg/kg | Intranasally |

reported to be as high as 45 % of the cases; one case of an allergic reaction has also been published (McIlwain et al. 2004; Ljungman et al. 2000).

In a recent publication, Reeves et al. reported that conscious sedation using Propofol actually amounted to deep sedation (Reeves et al. 2004). The use of this medicine should therefore be restricted to personnel trained in anaesthesia and airway management.

Following an interventional procedure, the children should be observed and, depending on the intervention, feeding can be started but only if the child has regained full consciousness.

## 3 Esophageal Balloon Dilatation

### 3.1 Esophageal Strictures

Esophageal strictures in childhood can be the result of esophageal surgery performed in case of congenital esophageal atresia (with strictures occurring in up to 40 % of patients (Chittmittrapap et al. 1990)), or as a complication of ingestion of caustic agents, severe gastroesophageal reflux or oesophagitis and in rare cases of epidermolysis bullosa (Huang et al. 2004; Fasulakis and Andronikou 2003; Sato et al. 1988; Naehrlich et al. 2000; Said et al. 2003; Erdogan et al. 2003; Jayakrishnan and Wilkinson 2001; Antoniou et al. 2010; Youn et al. 2010; Temiz et al. 2010; Doo et al. 2009; Thyoka et al. 2013). Prior to the London et al. publication in 1981 on the use of a balloon catheter in order to treat esophageal strictures (London et al. 1981), these strictures were treated with serial bougienage, under general anaesthesia. Balloon dilatation has now become the initial choice of treatment in cases of esophageal stricture.

In this fluoroscopy guided procedure, a balloon catheter is passed over a guidewire after which dilation is performed (Fig. 1) (Fasulakis and Andronikou 2003). Prior to the procedure the patient is kept nil-by-mouth and an oesophagram is performed for precise localization of the stricture. Thereafter, a small feeding tube is placed just cranial of the stricture, through which a guidewire is passed, negotiated beyond the stric-

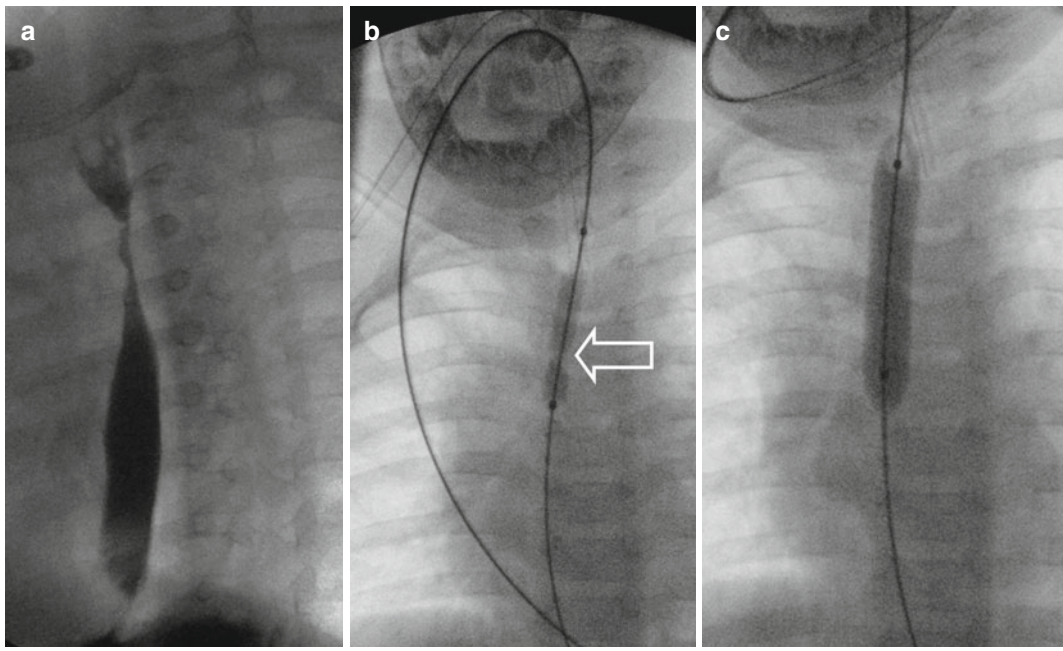


**Fig. 1** (**a**) One year old boy with a previous history of esophageal atresia. The child presented with difficulty of swallowing: barium meal study shows a clear stenosis at the level of the anastomosis. (**b**) A guidewire is passed beyond the stricture into the stomach and a balloon catheter is advanced and inflated. Note the waist in the balloon at the level of the anastomosis (*arrow*). (**c**) After full inflation the balloon shows no more waist

ture, and finally placed within the stomach for the duration of the procedure. The feeding tube is exchanged for a balloon catheter, of which the markers on the balloon are placed across the stricture. The size of the balloon can be measured on a calibrated oesophagram however, the 'rule of thumb' is as effective (Hamza et al. 2003). According to this latter rule, the calibre of the balloon is equal to the diameter of the patient's thumb. The balloon is inflated using a water-soluble contrast medium, enabling visual inspection during the procedure. Some authors recommend the use of serial dilatations in one session whereas others claim that a prolonged inflation of the balloon is as effective. In a study by Gideon et al. the influence of duration of balloon inflation, 15 versus 60 s, was investigated in an adult population (Gideon et al. 1999). In a prospective study in 24 patients the authors found no significant difference on clinical outcome, between inflation durations of either 15 or 60 s up till 6 months after intervention. After the procedure has been completed, a repeat oesophagram, using water-soluble contrast medium is performed to rule out perforation.

The success rate of balloon dilatation is reported to range from 62.5 to 100 %. This procedure has shown to be most effective in cases of post-surgical stenosis and gastroesophageal reflux induced stenosis (Lisy et al. 1998; Sandgren and Malmfors 1998; Thyoka et al. 2013). Lang et al. compared balloon dilatation with bougienage in a paediatric population, and found that in the balloon group 1 to 7 procedures (median 2) were required while in the bougienage group 1 to 60 (median 9, $p=0.002$) (Lang et al. 2001).

Balloon dilation should be seen as a multi-session procedure. Serial dilation has the advantage that it minimizes the risk for tears and perforation. The advantage of balloon dilation over bougienage is that when the balloon is inflated it exerts a radial force on the stricture opposed to the shearing forces induced by bougienage (McLean and LeVeen 1989; Yeming et al. 2002; Kim et al. 1993). This leads to a decreased risk in perforation, which in balloon dilation has been reported to be as low as 0–1.8 % compared to a 5.8 % risk in bougienage (Fasulakis and Andronikou 2003; McLean and LeVeen 1989; Kim et al. 1993; Sato et al. 1988; Said et al. 2003; Jayakrishnan and Wilkinson 2001; Sandgren and Malmfors 1998). Thyoka et al. performed a meta-analysis on balloon dilatation of anastomotic strictures after surgical repair of esophageal atresia which included 139 children who underwent a total of 401 balloon dilatations (Thyoka et al. 2013). In this meta-analysis a rate of 0.02 perforations per dilatation session was reported. The majority of the perforations could be treated conservatively, and based on this review the authors concluded that it is a safe procedure.

One of the often reported down-sides of balloon dilatation is the significant recurrence rate (Youn et al. 2010; Doo et al. 2009; Weintraub and Eubig 2006). Given the fact that it is a safe procedure, repeat balloon dilatation is advocated, with one publication stating that dilatation should be repeated up to 2 years before a decision of failed therapy should be taken (Temiz et al. 2010). Two Japanese papers have proposed, and showed a successful use of systemic or intralesional corticosteroids in case of refractory anastomotic strictures (Hishiki et al. 2009; Morikawa et al. 2008).

Although a safe procedure, contra-indications for balloon dilation do exist. These are considered to be multiple (>3) strictures, long strictures (>5 cm), tortuous strictures, or patients with tracheoesophageal fistulas (Hamza et al. 2003).

## 3.2 Achalasia

Achalasia is a rare disorder, with a reported incidence of 1:100,000 in adults (Spechler 2013; Alderliesten et al. 2011). Although it is mostly encountered in the adult age group, it can also be seen in children. Experience is mostly derived from adult studies where balloon dilatation is seen as the primary choice of treatment. This technique has been shown to be effective in up to 90 % and equal to a laparoscopic Heller's myotomy (Boeckxstaens et al. 2011). In achalasia-balloon dilatation of the lower esophageal sphincter (LES) is applied in order to allow for passage of food. The procedure is technically identical to balloon dilatation of esophageal strictures. In many cases the introduction of the

balloon is achieved via endoscopy, most of the time by gastroenterologists but there are interventional radiologists who also have been trained in the use of the endoscope.

In children there are only a limited number of publications on balloon dilatation for achalasia (Di et al. 2012; Khan et al. 2002; Hammond et al. 1997; Lee et al. 2010; Pastor et al. 2009; Upadhyaya et al. 2002). Although in some publications a shift from balloon dilatation to laparoscopic Heller's myotomy has been presented, the majority of the studies report high success rates of 45–90 %.

## 4 Percutaneous Gastrostomy

The use of percutaneous feeding techniques is well appreciated by clinicians and patients alike, and in most instances will be the preferred technique for nutritional supplementation. Percutaneous techniques surpass surgical procedures as in most cases they can be performed under IV sedation in combination with local anaesthesia. Chait et al. reported on 505 children in which 77.5 % of all procedures were done successfully under IV sedation in combination with local anaesthesia (Chait et al. 1996). Additionally, the percutaneous procedure is less time consuming, has a lower complication rate and is less expensive (Cory et al. 1988; Kaye and Towbin 2002). Compared to endoscopic techniques it has the advantage of visualizing the liver, the transverse colon and small bowel loops prior to puncture of the abdominal wall thus reducing the risk of passing the tube through the left liver lobe or perforating a bowel wall (Stellato and Gauderer 1987). Due to the relative ease of the procedure the number of indications has increased over the years. One can state that each child that needs nutritional support for a period of more than 6–8 weeks is a candidate for this procedure.

Currently there are two different approaches to percutaneous gastrostomy (PEG) placement: the retrograde or 'push' technique, and the antegrade or 'pull' technique (Kaye and Towbin 2002; Towbin and Ball 1988). Both techniques have a high reported success rate (84–100 %) and a low rate of complications (major 0.5–5 % and minor 12–16 %). In the largest retrospective study to date, by Dewald et al., of 701 adult cases only 3 (0.4 %) experienced major complications occurred (2 cases of peritonitis and 1 case of external leakage requiring removal of the catheter) (Dewald et al. 1999). However, in more recent literature, the occurrence of complications is more common (24.5 %) (McSweeney et al. 2015). Certain patient factors, including age (<6 months), neurologic status, and American Society of Anesthesiologists class, may be protective and the presence of a ventriculoperitoneal shunt may be associated with an increased risk of complications. The most important minor complications include superficial skin infection, parastomal granuloma formation and tube dislodgement. Infections requiring hospitalization, peritonitis and colon perforation are considered the most important major complications.

Occasionally the transverse colon or the splenic flexure can be interposed between the stomach and abdominal wall. Usually inflation of the stomach will displace the colon caudally. However, if this does not occur, safe access cannot be obtained. Wiebe et al. recently described a safe technique in which a 27 or 25 gauge needle can be used to deflate the colonic loop so as to obtain a safe entrance into the stomach (Wiebe et al. 2005).

Preprocedural preparation is relatively simple and consists of withholding the last feeding in children younger than 4 months and nil-by-mouth for older children. Antibiotic prophylaxis prior to percutaneous endoscopic gastrostomy insertion reduces both percutaneous endoscopic gastrostomy site and systemic infections. In children with a depressed immunological system or with a ventriculoperitoneal drain there is an absolute indication for prophylactic antibiotics (Saadeddin et al. 2005). In cases of perforation during the procedure or detection of free air after the procedure, antibiotics should also be administered. In a novel approach to antibiotic prophylaxis, Blomberg concluded that the deposition of 20 ml of co-trimoxazole solution in a newly inserted PEG catheter is at least as effective as cefuroxime prophylaxis given intravenously before PEG at preventing wound infections (Blomberg et al. 2010).

As both procedures are safe to perform, the number of contraindications is relatively low. However, in children with a severe non-correctable coagulopathy, severe respiratory or cardiac problems, a surgical approach would be more advisable. In some children their inherent anatomy, i.e. the absence of a good percutaneous route, or previous gastric surgery, will preclude a percutaneous approach. Dewald et al. reported this to occur in 4.4 % of their patients (Dewald et al. 1999). For the 'pull' technique the oesophagus should be sufficient in diameter (>12 mm) to pass the tube. If this is not the case, a push approach should be chosen.

### 4.1 Retrograde Gastrostomy 'Push'

The retrograde or 'push' technique is the most widely used technique for both the adult and paediatric populations. One should start by performing an upper abdominal ultrasound scan to assess and mark the position of the liver and transverse colon. The colon can be opacified using contrast medium to better delineate its position and thereby decrease the risk of inadvertently puncturing it during the procedure.

A nasogastric tube is inserted and the stomach inflated. Thereafter it is punctured under fluoroscopic guidance and a T-fastener is inserted (Fig. 2). Some radiologists will place up to three T-fasteners in order to secure the gastric wall to the anterior abdominal wall. The advantage of using only one T-fastener is that the procedure can be done with a single puncture of the stomach.

The position of the needle tip is checked by injection of contrast after which a guidewire is inserted. Using dilators the needle tract is dilated and a gastrostomy tube is placed within the stomach. The retention balloon is inflated and the gastrostomy tube is fixed to the abdominal wall using the supplied external stabilizer.

At the end of the procedure a cross table radiograph should be taken to rule out free intraperitoneal air. Post procedure the patient is kept nil-by-mouth and the tube is not used for at least 6 h after the procedure. In practice this will mean that the first feeding over the gastrostomy tube will occur the morning after the procedure. Medication and fluid should be given intravenously during this period. Both the patient and his/hers parents should be carefully instructed on the use of the gastrostomy tube. The external part of the T-fasteners can be removed after 10 days as the stomach wall will be adequately fixed to the anterior abdominal wall.

### 4.2 Antegrade Gastrostomy 'Pull'

The intervention starts with an ultrasound exam of the upper abdomen to assess and mark the position of the liver and transverse colon. Thereafter a nasogastric and an orogastric feeding tube are inserted into the stomach. A snare is passed through the orogastric tube and positioned in the stomach. With the snare in place, the stomach is inflated, displacing the transverse colon inferiorly, and punctured with a needle. Through the needle a long guidewire (260 cm) is inserted into the stomach and, under fluoroscopic guidance, grasped by the snare to be subsequently pulled up the oesophagus and out of the mouth. This now means that the guidewire runs through the mouth into the stomach and out via the puncture site. Over this guidewire a gastrostomy tube with a fixed terminal retention disk is fitted and fed until the tip of the dilator is visible at the puncture site. It is important to keep in mind that the collapsed retention disk has a diameter of approximately 12 mm. The calibre of the oesophagus should be large enough to capacitate its passage. The tip of the gastrostomy tube dilator is grasped and pulled through the anterior abdominal wall. Care should be taken not to cause damage to teeth at the time when the retention disk enters the mouth. The gastrostomy tube is fixed using the external stabilizer, which comes with the set. One should not place too much pressure on the abdominal wall when fixing the stabilizer, because pressure necrosis of gastric mucosa could occur. The post procedural approach is identical to the 'push' technique.

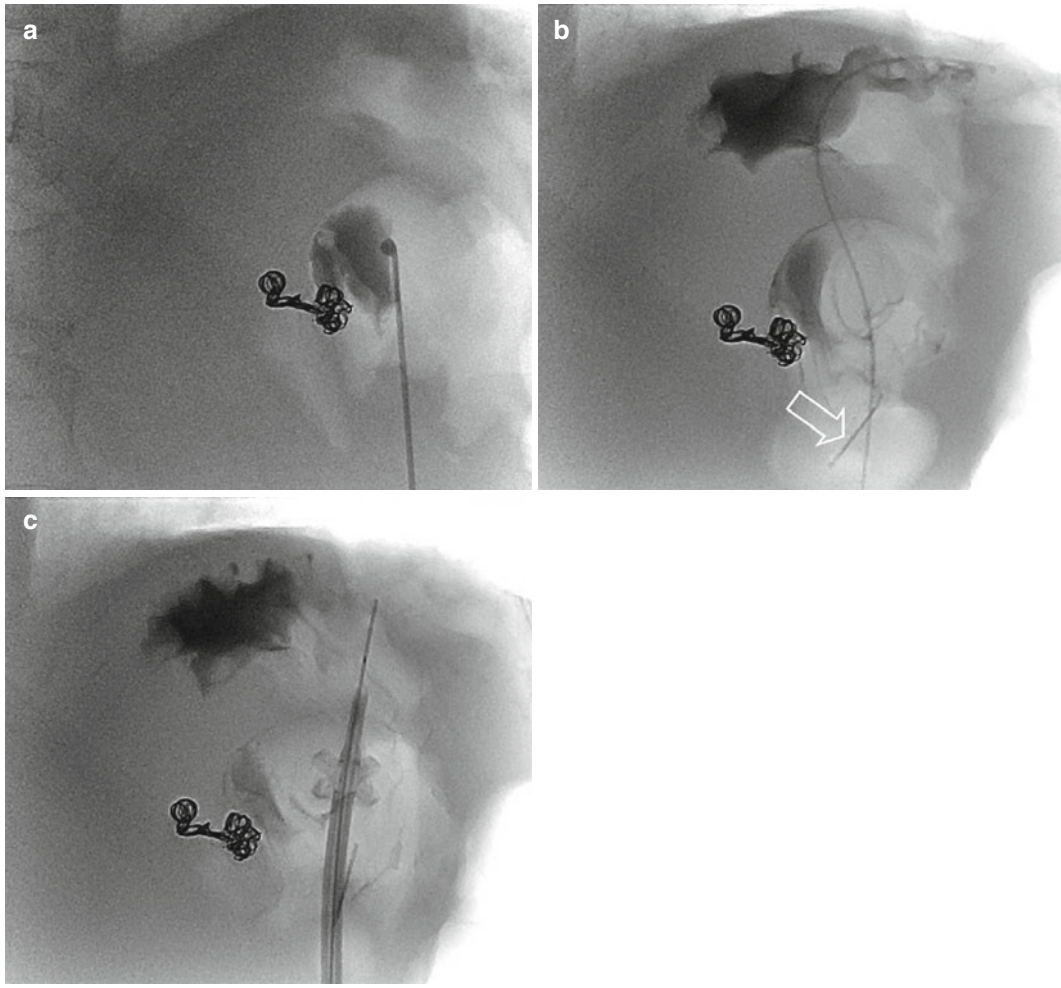


**Fig. 2** (**a**) Transcutaneous PEG placement. The first step is a puncture of the inflated stomach with a needle. A minor amount of contrast is used to certify that the tip of the needle is indeed in the stomach. (**b**) Through the needle an anchor is positioned within the stomach (*arrow*) and a guide wire is advanced into the stomach. With the anchor, the gastric wall is pulled and fixed against the abdominal wall. (**c**) After dilatation of the puncture tract, a gastrostomy tube is inserted

The advantage of the 'pull' technique is the use of fixed retention disks allowing for a lower number of cases of gastrostomy tube dislodgement. Most authors state that when the time has arrived to remove the gastrostomy tube it suffices to cut the gastrostomy tube and push the retention disk into the stomach. This way it will leave the patient's body via the natural route. However, Kaye et al. describe two complications of this approach and advocate the retrieval of the retention disk (Kaye et al. 2000). The procedure entails passing a snare through the gastrostomy tube and a guidewire down the oesophagus, the guidewire is grasped under fluoroscopy and pulled out of the stomach via the gastrostomy tube. A dilatation (PTA) balloon, with a sufficient balloon diameter is passed antegrade and inflated when it has passed the gastrostomy tube. The PTA balloon and gastrostomy tube are pulled into the stomach, where the PTA balloon is inflated further, and both the PTA balloon and gastrostomy tube are retrieved via the mouth.

## 5 Gastrojejunostomy

The indications for placement of a gastrojejunostomy tube in children are severe gastro-esophageal reflux, intestinal dysmotility, feeding intolerance and vomiting or gastric emptying abnormalities. A gastrojejunostomy tube is placed coaxially via a gastrostomy tube. This can be done either in the same session as the gastrostomy placement or at a later moment in time. The procedure itself is relatively simple. A catheter is placed into the stomach and directed towards the pylorus. Using a guidewire the catheter is advanced into the duodenum beyond the ligament of Treitz after which the catheter is exchanged for a gastrojejunostomy tube (Kaye et al. 2000; Norman 2001).

The gastrojejunostomy procedure knows virtually no major complications, besides those related to the placement of the gastrostomy tube. Minor complications consist of leakage of feeding from the puncture site and dislocation of the gastrojejunostomy tube. G-J feeding tubes are associated with the frequent need for tube maintenance and replacement and may not be the most feasible clinical option in providing long-term (>1 month) enteral access in children intolerant to gastrostomy tube feeds. Fortunato et al. describe the follow-up of 102 patients (Fortunato et al. 2005). The mean (range) number of tube replacements was 2.2 (1–14) over a median (range) follow up duration of 39 (2–474) days. The indication for replacement included: tube displacement (58), a clogged tube (41), a cracked tube or ruptured balloon (35). A rare complication has been described by Connolly et al. in five patients in whom small bowel intussusception was seen around the gastrojejunostomy tube (Connolly et al. 1998). We experienced the same rare complication in the case of a surgically placed jejunostomy tube (Fig. 3). Reduction of these intussusceptions can be achieved by bolus injection of air or water-soluble contrast medium through the gastrojejunostomy tube or by exchanging the jejunostomy tube over a guidewire.

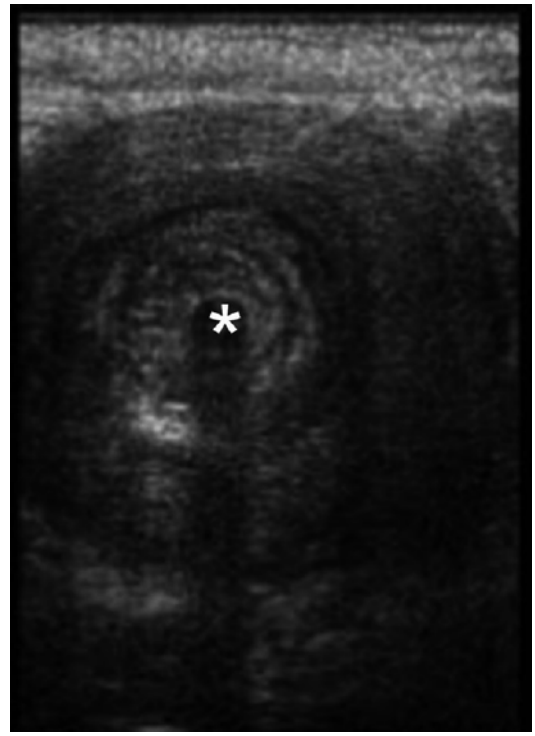


**Fig. 3** Case of a 7-years-old girl with Hereditary Sensory and Autonomic Neuropathy (HSAN) type II. A jejunostomy was placed because of feeding problems. Despite her condition she complained of cramping abdominal pain. The ultrasound image shows an ileo-ileal intussusception around the jejunostomy tube (*asterisk*). The abdominal pain was relieved after changing the jejunostomy catheter

## 6 Caecostomy

In children, the term faecal incontinence encompasses both encopresis and soiling (Rajindrajith et al. 2013). Encopresis is defined as the repeated expulsion of a normal bowel movement, whether involuntary or intentional in inappropriate places by a child aged 4 years or over. Soiling is defined as the involuntary leakage of small amounts of stool resulting in staining of underwear. Faecal incontinence is a serious problem in the paediatric population. The prevalence of faecal incontinence ranges from 0.8 to 7.8 % internationally, with boys outnumbering girls by 3:1–6:1 (Rajindrajith et al. 2013).

Children with faecal incontinence can be classified into four main groups: children with functional faecal retention and overflow soiling; children with functional non-retentive faecal soiling; children with anorectal malformations; and children with spinal deformities. The caecostomy technique described below is primarily aimed at the last two categories.

To date the most effective therapeutic method is the use of high volume enema, as this ensures complete evacuation of the colonic tract. This approach minimizes the risk of unwanted bowel evacuation, which is not only cumbersome but also humiliating for both patient as well as carers. The major disadvantage is the level of acceptance in patients, especially during puberty. In patients with paresis or paralysis of limbs it is impossible to perform the procedure without aid, lowering the level of compliance in this population.

In order to overcome the above mentioned problems, Malone et al. introduced an operation to perform an antegrade colonic enema (ACE) (Malone et al. 1990). The advantage of ACE above retrograde colonic enemas is that there is less mess and patients are more independent as they can easily perform the procedure themselves (Malone et al. 1990). In this operation, Malone et al. used the appendix as a conduit to irrigate the colon (Graf et al. 1998; Griffiths and Malone 1995; Malone et al. 1990; Squire et al. 1993). Although the procedure is effective, well tolerated and the level of acceptance in patients is high, complications have been described in a significant number of patients (Griffiths and Malone 1995; Squire et al. 1993; Ekmark and Adams 2000; Searles et al. 2000; Cascio et al. 2004; Hoekstra et al. 2011; Bani-Hani et al. 2008; Tiryaki et al. 2010). These complications consist of stoma prolapse, stenosis of the fistula, accidental perforation of the conduit, need for revision surgery and faecal soiling at the stoma site. In a retrospective literature study Graf et al. report a prevalence of 27 % of necrosis/stenosis of the stoma, 6.6 % catheter leak, 3.7 % difficulty in catheterization, 3 % pain with enema administration and 2.9 % wound infection (Graf et al. 1998). Besides the surgical approach, endoscopic approaches to the ACE procedure have also been described (Rivera et al. 2001; Becmeur et al. 2008; Lendvay et al. 2008; Yagmurlu et al. 2006).

In 1996, Shandling and Chait were the first to describe a percutaneous approach to caecostomy placement in 15 patients (Shandling et al. 1996). Kaye et al. and Chait et al. have described the percutaneous ACE procedure in detail (Chait et al. 2003; Kaye et al. 2000; Kaye and Towbin 2002). The patient is placed on a 2-day clear fluid diet pre-admission and a sodium phosphate oral solution is administered the night before the procedure. This regimen should completely clear the bowels of stools. Within 30 min prior to the procedure an antibiotic regimen should be started, this regimen can differ from hospital to hospital and it is advised to discuss this with the local pharmacologists.

Ultrasound is used to identify the liver, right kidney and bladder, and possibly other masses. The procedure is quite similar to the 'push' gastrostomy technique. The colon is inflated and after confirmation of its location, the cecum is punctured and transfixed using T-fasteners (Fig. 4a–d). A stiff guidewire is inserted into the ascending colon through the puncture needle. The puncture site can be dilated over the guidewire in order to capacitate the placement of an 8 F pigtail catheter. The position of the catheter is confirmed and secured in place.

After approximately 8 days antegrade enemas can commence. To prevent clogging of the pigtail, a daily flush with 10–15 ml. of saline is performed. After 6–12 weeks, the pigtail can be exchanged for a caecostomy button.

In 1997, Chait et al. presented an improved caecostomy button that protrudes no more than 1 cm from the abdominal wall, which constitutes an enormous cosmetic improvement as the button or trapdoor can easily be hidden under garments (Fig. 5) (Chait et al. 1997a).

As in all procedures complications have been described (Chait et al. 1997b). Minor complications consist of nausea, constipation, granulation of the puncture site, soiling and accidental dislodgement of the caecostomy tube. Chait et al. reported results of their 7 year experience with this technique, achieving a 100 % success rate for the procedure (Chait et al. 2003). The majority of

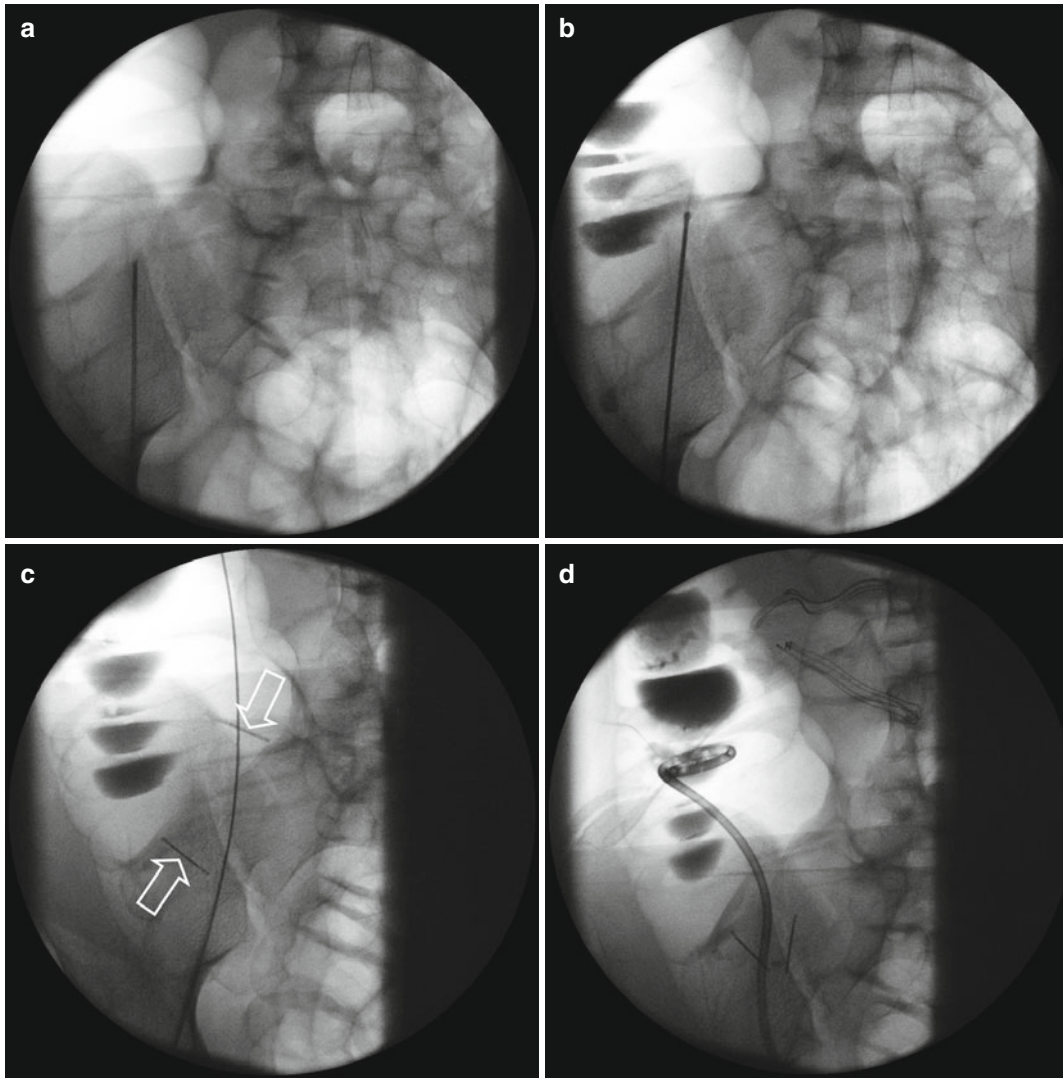


**Fig. 4** (**a**) Case of a 15-year-old boy with therapy resistant constipation. An antegrade percutaneous caecostomy was indicated. A needle is advanced into the inflated colon. (**b**) After puncture the position of the needle tip within the colonic lumen is identified using contrast. (**c**) Two T-Fastners are inserted (*arrows*) and pulled back, fixing the colon against the abdominal wall. With a third puncture a guidewire is positioned in the ascending colon. (**d**) A 10 F pigtail catheter is inserted and fastened using sutures. In a second stage this catheter will be exchanged over a guidewire for a Chait Trapdoor

patients (79 %) reported that the number of soiling accidents had decreased and, additionally, their independence had increased by being able to perform the antegrade enema themselves. In four cases the caecostomy tube had to be removed twice due to problems with tube maintenance and twice because of aesthetic reasons. The most impressive result in their study was that 97 % of respondents stated that they would recommend the procedure to others in the same position (Chait et al. 2003). Other studies also reported a high patient satisfaction rates (Dey et al. 2003; Sierre et al. 2007; Tiryaki et al. 2010).

The advantage of the percutaneous ACE procedure over the surgical approach is the fact that it can be performed without general anaesthesia.

**Fig. 5** The low-profile Chait Trapdoor (Chait, Cook, Bloomington, In, USA) catheter has a pigtail configuration for internal retention

An additional advantage is that with a surgical ACE procedure, in most cases, the appendix is used thus precluding its use in urinary incontinence, which these patients also frequently face.

## 7 Drainage

### 7.1 Abscesses

Percutaneous abscess drainage is a relatively straight forward technique with a wide field of indications, the most common being periappendiceal abscesses and Crohn abscesses (Hubbard and Fellows 1993; Norman 2001). The aim of the procedure is either to gain time in order to reduce surgery related morbidity and to be able to perform a one-stage operation or to obtain complete cure. The latter has been described in patients with Crohn disease, making surgery at the time unnecessary (Safrit et al. 1987). The only contraindications for percutaneous drainage are uncorrectable coagulopathy and the inability to approach the collection without transgressing major vessels, bowel loops, solid organs or the pleural cavity (Gervais et al. 2004). Studies performed in adult patients show a high success rate of up to 90 % and low mortality rates (Duszak et al. 2000).

Complications occur in less than 5 % of paediatric patients, and major complications occur in less than 1 %. In the English-language literature, the largest study of abscess drainage in children is that by Jamieson et al., who reported 59 drainage procedures (34 percutaneous, 25 transrectal) and five needle aspirations for treatment of appendiceal abscesses in 46 children (Jamieson et al. 1997). Only 4 of the 46 (9 %) experienced no improvement after abscess drainage and intravenous administration of antibiotics.

Depending on the location of the abscess the intervention can be performed using ultrasound, sometimes in combination with fluoroscopy or CT guidance. Ultrasound will be used for larger and superficial abscesses whereas CT will be used for smaller and more deeply located collections (Maher et al. 2004). In cases of multiple abscesses or loculated abscesses, more than one drain should be placed ensuring complete drainage of all locations. In cases of deep pelvic abscesses, a transrectal or transgluteal approach has been advocated. In children this procedure has been reported to be as effective as a percutaneous or a surgical approach and better tolerated (McDaniel et al. 2015).

Although some radiologists will use the trocar technique, which encompasses placing a catheter mounted on a sharp trocar into the abscess, a safer and more elegant way is the use of the Seldinger technique (Norman 2001). The Seldinger technique entails puncturing the skin with a thin (22–20 G) or thick (18–19 G) needle and placing the tip of the needle within the collection. When a thin needle is used one will need to upgrade to a system capable of accepting a 0.038-in. guidewire. Commercial kits are available for this purpose, one of which is the Neff-set® (Cook) (Fig. 6). Once the needle is in place, a stiff guidewire is placed within the collection and a catheter is advanced into the collection. Smaller calibre catheters (7–8.5 F) will only be used in liquefied collections, whereas thicker more viscous collections will require a 12–14 French catheter. In general, self-retaining pigtail catheters (Cook) will be used, as they have a lower risk of inadvertent dislocation (Fig. 7). We also always secure the drain to the skin, either by using a suture or by the supplied retention device. Decompression of the abscess

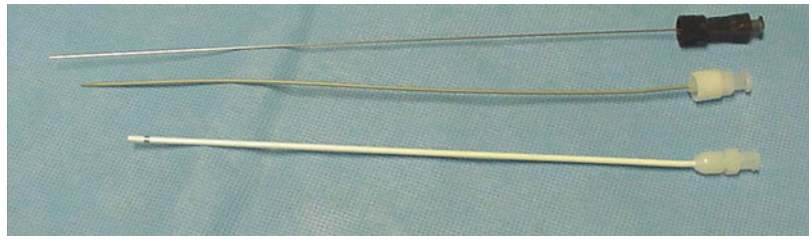

**Fig. 6** Neff set (Cook, Bloomington, In, USA)

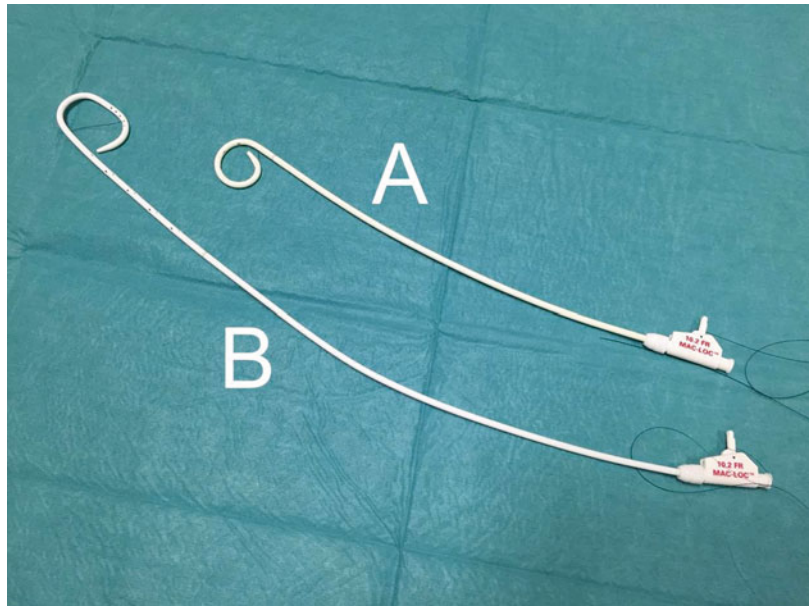


**Fig. 7** Internal/External draining catheter (*A*) and pigtail catheter for external drainage (*B*) (Cook, Bloomington, In, USA)

is generally attained using a syringe attached to the catheter. Some radiologists advocate flushing the abscess cavity with saline. However, care should be taken to use less fluid than was drained, as an increased pressure within the cavity can result in bacteraemia and sepsis. Towbin et al. report the use of contrast medium to identify catheter position and possible connections between the abscess and surrounding structures (Towbin 1991).

In case of a perirectal abscess, a transrectal approach can be chosen, using transabdominal ultrasonography to visualize the abscess (Fig. 8). Under ultrasound guidance a finger is placed within the rectum up to the level of the abscess. A trocar is guided upwards along this finger and the abscess is punctured. With the trocar in place, a guidewire and subsequently a pigtail can be inserted into the abscess. Another technique which has been advocated is the transgluteal approach, Cahill et al. described their experience in 54 patients (Cahill et al. 2005). Mostly all cases were performed under

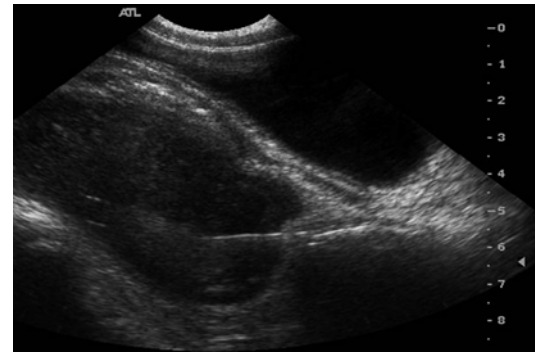

**Fig. 8** Case of an 8-year-old boy with a perirectal appendiceal abscess. The image shows the needle positioned, using ultrasound guidance, through the posterior rectal wall within the abscess (Courtesy of Dr. L. Fontalva, Hospital for Sick Children, Toronto, Canada)

CT guidance, in their study a successful drainage was achieved 98 % of cases without any serious complications.

Irrespective of the abscess location and the chosen technique, the drain is attached to a bag and left to drain by gravity. Ward nurses are supplied with a written instruction by the radiologist responsible for the intervention on how to care for the catheter. The drain is removed once the patient's symptoms have resolved and no drain production is noted. In case of a complex abscess a control study, CT (or in superficial collections ultrasound) should be performed prior to removal of the drain. Lang et al. reported that in 12 out of 136 patients (8.8 %) premature withdrawal of the catheter resulted in failure of the intervention (Lang et al. 1986).

## 7.2 Biliary System

The need for biliary drainage in children is less frequent than in adults; however, there are a number of indications for performing a percutaneous transhepatic cholangiogram (PTC) (Diament et al. 1985). The most common indications for PTC is obstructive jaundice resulting from either a malignancy (most commonly rhabdomyosarcoma of the bile ducts or pancreas and neuroblastoma) or post liver transplantation. More uncommon causes of extrahepatic biliary obstruction are idiopathic benign non-traumatic inflammatory stricture, and idiopathic fibrosing chronic pancreatitis (Krishna et al. 2008). Cholithiasis is less frequently a causative agent (Lorenz et al. 2001; Roebuck and Stanley 2000; Rose et al. 2001). Cholangitis, which is a relatively common indication for PTC in adults, is rarely seen in children.

As in all percutaneous procedures, an uncorrectable coagulopathy is a definite contraindication for PTC. In children the procedure should be performed under general anaesthesia. Prophylactic antibiotic therapy should be administered at least 1 hour before the procedure. A cephalosporin is typically administered. In case of allergy for cephalosporins, Ciprofloxacin can be used instead. Access to the biliary tree is gained by needle puncture; this can be done using fluoroscopy guidance, ultrasonography or a combination of both. We routinely use ultrasonography to access the biliary tree after which a small amount of contrast is injected to confirm appropriate position of the tip of the 22-gauge Chiba needle in the bile duct. This stage of the procedure is usually performed using a Neff set® (Cook), thus reducing the risk of bile spillage into the abdominal cavity. Using a guide wire the sheath is exchanged for a 6 or 8 F catheter. At this stage in the procedure one can either proceed for external biliary drainage or internal-external biliary drainage (Figs. 9a–f and 10a–d) (Roebuck and Stanley 2000). In the latter a modified pigtail catheter is used: the modification consists of the presence of additional holes in the catheter along the intrahepatic tract of the catheter. The decision of performing external biliary drainage or internal-external biliary drainage is dependent on the findings on the cholangiogram. If passage into the duodenum is deemed possible, one should choose internal-external biliary drainage. If it is not possible in the first procedure it may be possible to convert external biliary drainage into internal-external biliary drainage at a later stage.

The advantage of internal-external biliary drainage over external biliary drainage is first of all that it re-establishes the flow of bile into the

**Fig. 9** (**a**) Case of a 4-year-old boy with a history of hepatoblastoma. A hemihepatectomy with a hepatico-jejunostomy was performed. He presented with jaundice. US showed intrahepatic bile duct dilatation (*arrow*). A PTC was advised. (**b**) The PTC is performed in a sterile environment under US guidance using a Neff set (Cook, Bloomington, In, USA). (**c**) After percutaneous access of the intrahepatic bile ducts has been obtained, the system is opacified. An occluding stenosis of the hepatico-jejunostomy is visible (*arrow*). (**d**) A guidewire is advanced over the stenosis and positioned in the jejunum. Contrast spill into the jejunum, during the procedure, is visible. (**e**) A balloon catheter is advanced over the guidewire and a dilation of the stenosis is performed (*arrow*). (**f**) After dilatation an internal draining pigtail catheter is positioned over the stenosis in order to stent the stenosis. This procedure may have to be repeated several times to be successful

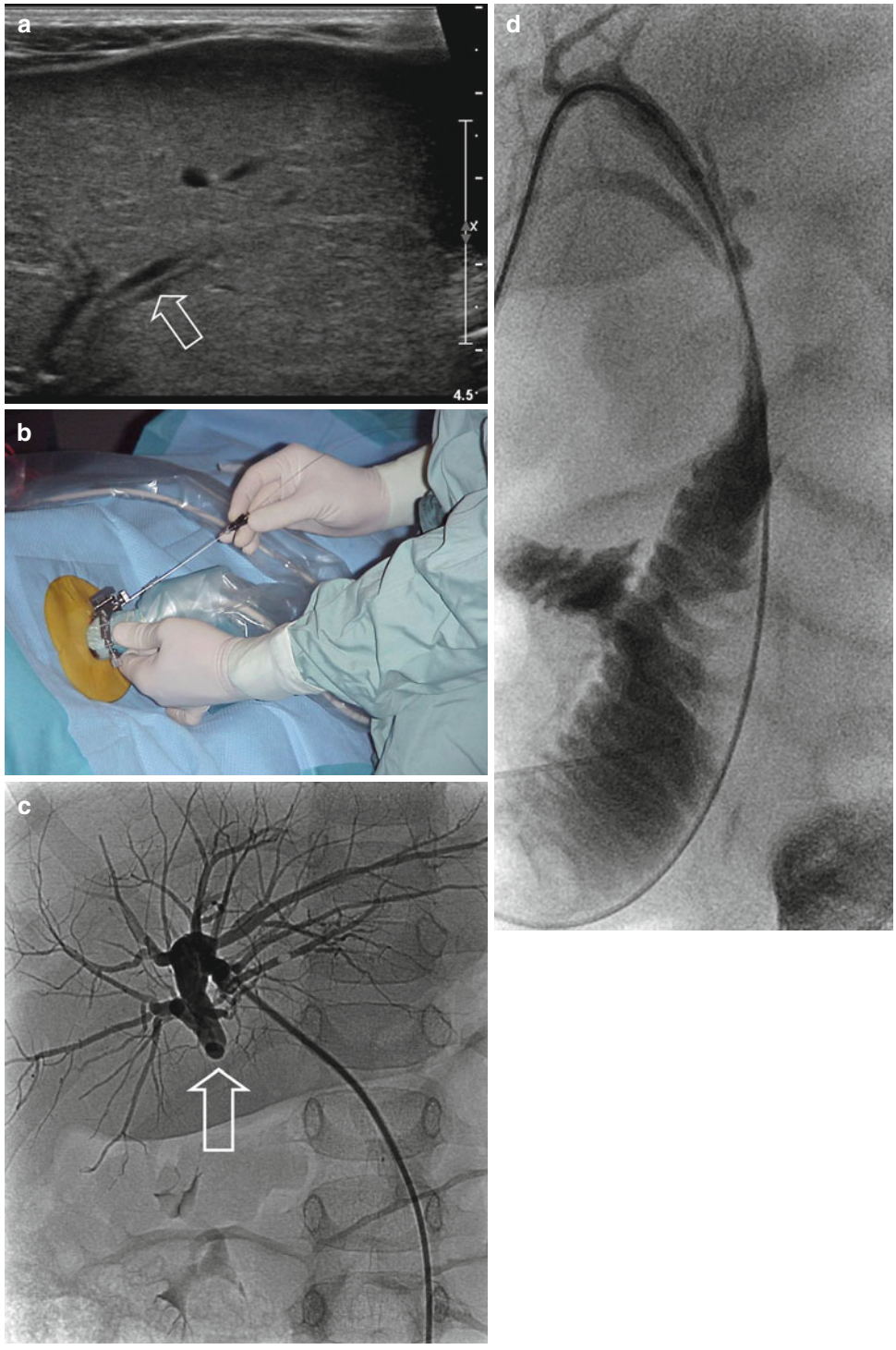
a
4.5
b
c
d

**Fig. 9** (continued)

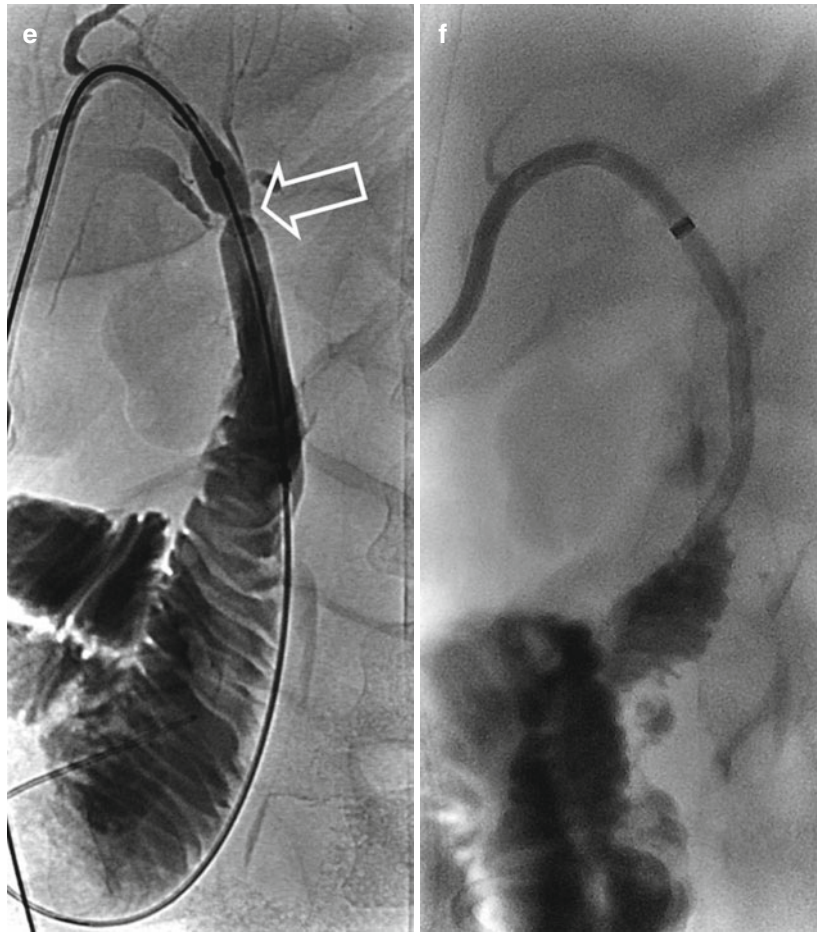


duodenum thus enhancing the absorption of dietary fats. An additional advantage is that positioning of the catheter into the duodenum increases catheter stability, which of course is advantageous in smaller children.

PTC is not only used for catheter drainage but it also allows for dilatation of strictures of the biliary tree, which in children is mostly in cases of biliary-enteric anastomoses (Sze and Esquivel 2002). The advantage of balloon dilatation of strictures is the relatively minimal invasive approach and that if dilatation fails surgical options remain viable. Lee et al. reported their experience in 34 children over a 15 year period (Lee et al. 2012). Balloon dilation of biliary-enteric anastomotic strictures was clinically successful in 21 of 32 patients (66 %). Anastomotic stricture recurred in one of 21 patients (5 %) after an average of 13.1 years of follow-up.

Complications of PTC can be mild, such as haemobilia, pancreatitis, and bacteraemia, or severe, such as haemoperitoneum and sepsis (Lorenz et al. 2001). There is, however, insufficient data to calculate the risk of the procedure in children.

If it is difficult to identify the bile duct, as can be the case in very young children, an alternative approach is to drain the biliary system via the gallbladder. This can of course only be done in cases of a distal obstruction (Fig. 11a–c).

Another approach to the treatment of biliary obstructive jaundice is the use of endoscopic antegrade cholangiography (ERC). The main advantage of PTC over ERC is that it is a percutaneous technique that allows for easier access to the

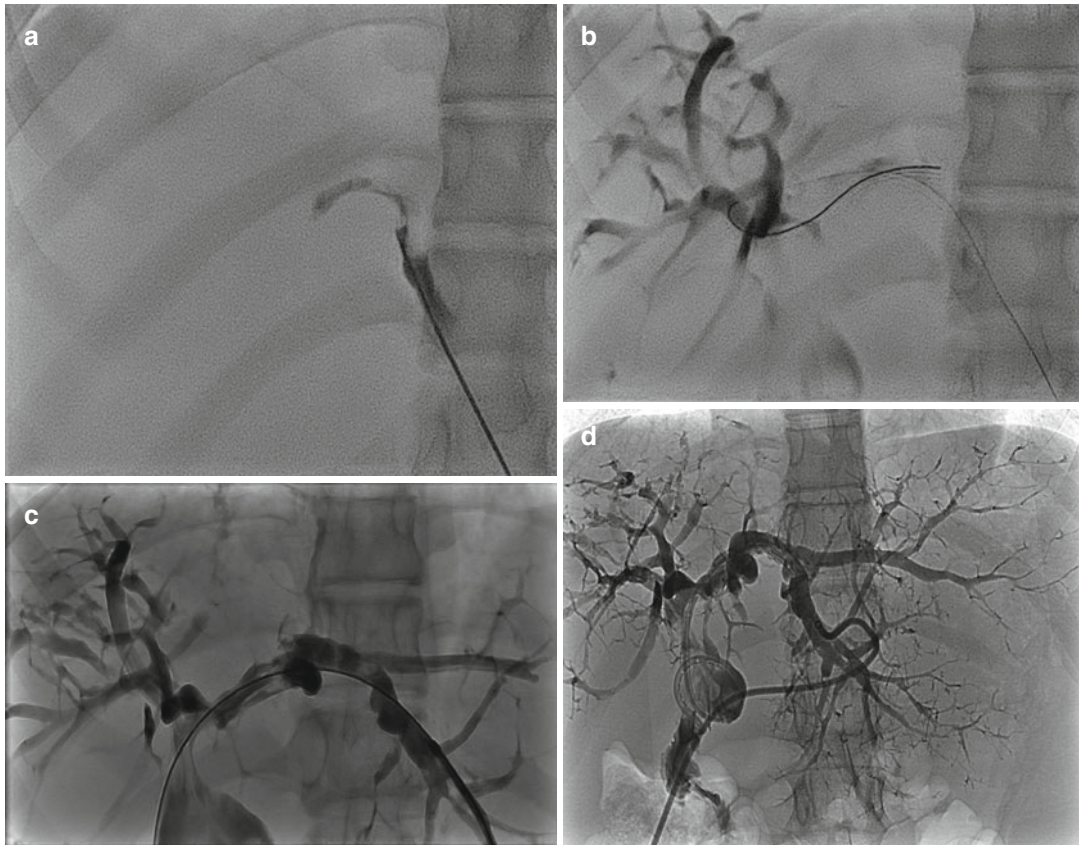


**Fig. 10** (**a**) A 14-year-old girl with recurrent cholangitis due to underlying Caroli disease. The dilated intrahepatic bile ducts are punctured using a Neff set (Cook, Bloomington, In, USA). (**b**) A copemandril 0.014 in. guidewire is advanced into the dilated system. (**c**) After exchanging the Neff set for a larger port a guidewire is advanced into the jejunum. (**d**) An internal draining catheter is positioned in the proximal jejunum

catheter in case of obstruction or infection. Secondly, PTC will be successful in cases of complete obstruction of the common bile duct because then external biliary drainage can be performed. Finally, ERC has a higher number of complications, such as pancreatitis and perforation, especially when the operator does not do the procedure on a regular basis. This is even more the case in children were special scopes are needed to perform a successful ERC. This procedure will therefore only be performed in specialized centres. The advantage of ERC over PTC lies mainly in treating cholelithiasis induced jaundice, as stone removal using a dormia basket and sphincterotomy can be performed (Guelrud et al. 1992).

## 8 Transjugular Intrahepatic Portosystemic Shunt (TIPS)

Portal hypertension is a relatively rare disorder in childhood compared to adults, where the majority of cases are caused by alcohol abuse (in the western parts of the world), and viral hepatitis and cirrhosis (in Africa and Asia). In children the cause of portal hypertension lies in extra hepatic biliary atresia, portal vein thrombosis, hepatitis and toxic liver injury (Cwikiel 2002; Cwikiel et al. 2003; Huppert et al. 1998). Clinical manifestations of portal hypertension consist of ascites production and the development of esophageal varices. Esophageal varices have a tendency to

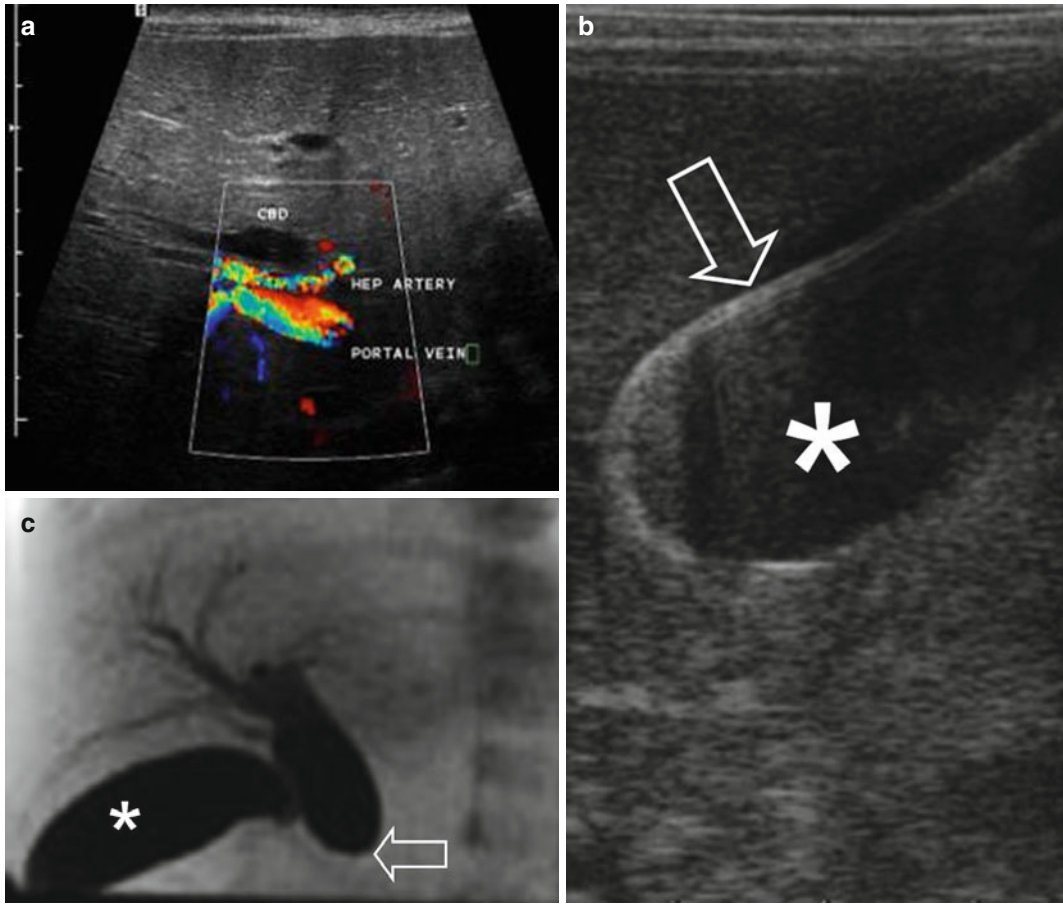


**Fig. 11** (**a**) Case of a 3-weeks-old boy with a history of urethral valves and obstructive ureters (diagnosed on prenatal ultrasound). After urological intervention (bilateral sober stoma) the baby developed progressive jaundice. The ultrasound exam reveals dilation of the intrahepatic bile ducts, gallbladder, and the common bile duct (*CBD*). Based on these findings the diagnosis of a choledochal cyst was made. (**b**) Biliary drainage via the dilated gallbladder. The oblique-coronal image shows an Amplatz guidewire (*arrow*) placed within the gallbladder (*asterisk*). (**c**) Post-intervention fluoroscopy image shows the dilated intrahepatic bile ducts, gallbladder (*asterisk*) and the dilated common bile duct (*arrow*). The latter is blind ending at the level of the pancreatic head. At surgery the presence a choledochal cyst was proven

bleed and this can cause a life-threatening situation. The first line of treatment is repeated paracentesis for the reduction of ascites and endoscopic sclerotherapy or rubber banding for esophageal variceal haemorrhage. In case of repeated haemorrhage from esophageal varices, shunting of blood away from the portal system thereby reducing the pressure in the collateral vessels, is necessary. Initially porto-systemic shunts consisted of surgical spleno-renal, porto-caval or meso-caval shunts. These surgical procedures, however, carry a high morbidity and mortality rate. As far back as 1969, Rösch et al. suggested creating an intrahepatic shunt. However it was not until the development of endovascular stents that this gained momentum (Rosch et al. 1969). In 1994, The United States National Digestive Diseases Advisory Board established the following clinical indications for TIPS: first, acute variceal bleeding that cannot be successfully controlled with medical treatment, including sclerotherapy. Second, recurrent and refractory variceal bleeding or recurrent variceal bleeding in patients who cannot tolerate

conventional medical treatment, including sclerotherapy and pharmacologic therapy (Shiffman et al. 1995). Other indications consist of medically refractory ascites, refractory hepatic hydrothorax, Budd-Chiari syndrome, veno-occlusive disease, hepatorenal syndrome and hypersplenism.

There are several contraindications for TIPS: absolute contraindications consist of right-sided heart failure with elevated central venous pressure, polycystic liver disease, and severe hepatic failure (Shiffman et al. 1995). The latter is based on the fact that the TIPS shunts blood away from the liver thus further compromising liver function. Relative contraindications consist of active or systemic infection, as TIPS makes use of a foreign device that could act as a colonization site for bacteria, severe hepatic encephalopathy poorly controlled by medical therapy and portal vein thrombosis.

Due to the nature of the procedure TIPS will always be performed under general anaesthesia. The right jugular vein is punctured and a sheath is inserted. A catheter and a guidewire are advanced into the inferior caval vein and from there into preferably the right middle hepatic vein. A special TIPS stainless steel angled catheter is exchanged over the guidewire and positioned in the right or middle hepatic vein. Under ultrasonic guidance or a wedged venogram an intrahepatic portal vein is punctured transhepatically using a special needle. Performing TIPS requires a thorough knowledge of the venous hepatic anatomy and its variations. After confirmation of intrahepatic portal venous position by use of contrast medium, a needle catheter is passed into the portal vein. When intrahepatic portal vein location is proven, the parenchymal tract is dilated and lined with a dedicated Viatorr covered stent (W. L. Gore, Flagstaff, AZ) (Fig. 12a–c). The diameter of the stent is chosen according to the age of the patient and the diameter of the portal vein (in our experience – 6–10 mm). A TIPS is considered to be successful if the pressure gradient is less than 15 mmHg. Care should be taken in placing the stent. It should not protrude into the inferior vena cava, since most children will at some point in time require a liver transplant. A stent placed into the inferior vena cava can complicate transplantation surgery (Lorenz 2008).

TIPS has shown to be a safe and effective treatment for portal hypertension, and compared to endoscopic sclerotherapy it has proven to be a more effective and safer technique (Garcia-Villarreal et al. 1999). In primary cases, endoscopic band ligation has shown to be as effective as TIPS in a randomized control study (Pomier-Layrargues et al. 2001). In a long term follow up study in adult TIPS patients, rates of rebleed from esophageal varices after 1, 2 and 5 years were 21 %, 21 % and 27 %, respectively (ter Borg et al. 2004).

A major concern of TIPS has been the development of encephalopathy. In a study by Pomier-Layrargues, 47 % of the TIPS patients developed encephalopathy versus 44 % in the endoscopic band ligation population, however this difference was not significant (Pomier-Layrargues et al. 2001). Of note is that encephalopathy does occur less frequently in children than in adults, although there is no clear reason for this observed difference (Heyman and LaBerge 1999).

As with all interventional procedures, TIPS has its complications. The main complication is procedure-related mortality, which has been reported to be 2 % (Freedman et al. 1993). The 30-day mortality of emergency surgical shunts ranges from 40–100 % compared to 7–45 % for TIPS (Heyman et al. 1997). In TIPS the majority of cases of mortality and morbidity are related to severity of disease, with death occurring in those with the worst Child-Pugh classification. Complications related to the TIPS itself are shunt occlusion and stenosis. Intimal hyperplasia is the most common cause of stenosis and subsequent occlusion, although the use of covered stents should largely overcome this problem. In cases of stenosis, restenting or balloon dilatation will, for the majority, successfully solve the problem (Heyman et al. 1997).

In adults the initial technical success rate of TIPS is reported to be over 95 %.

A Dutch study on long term outcome of TIPS in adult patients showed that the risk of definitive

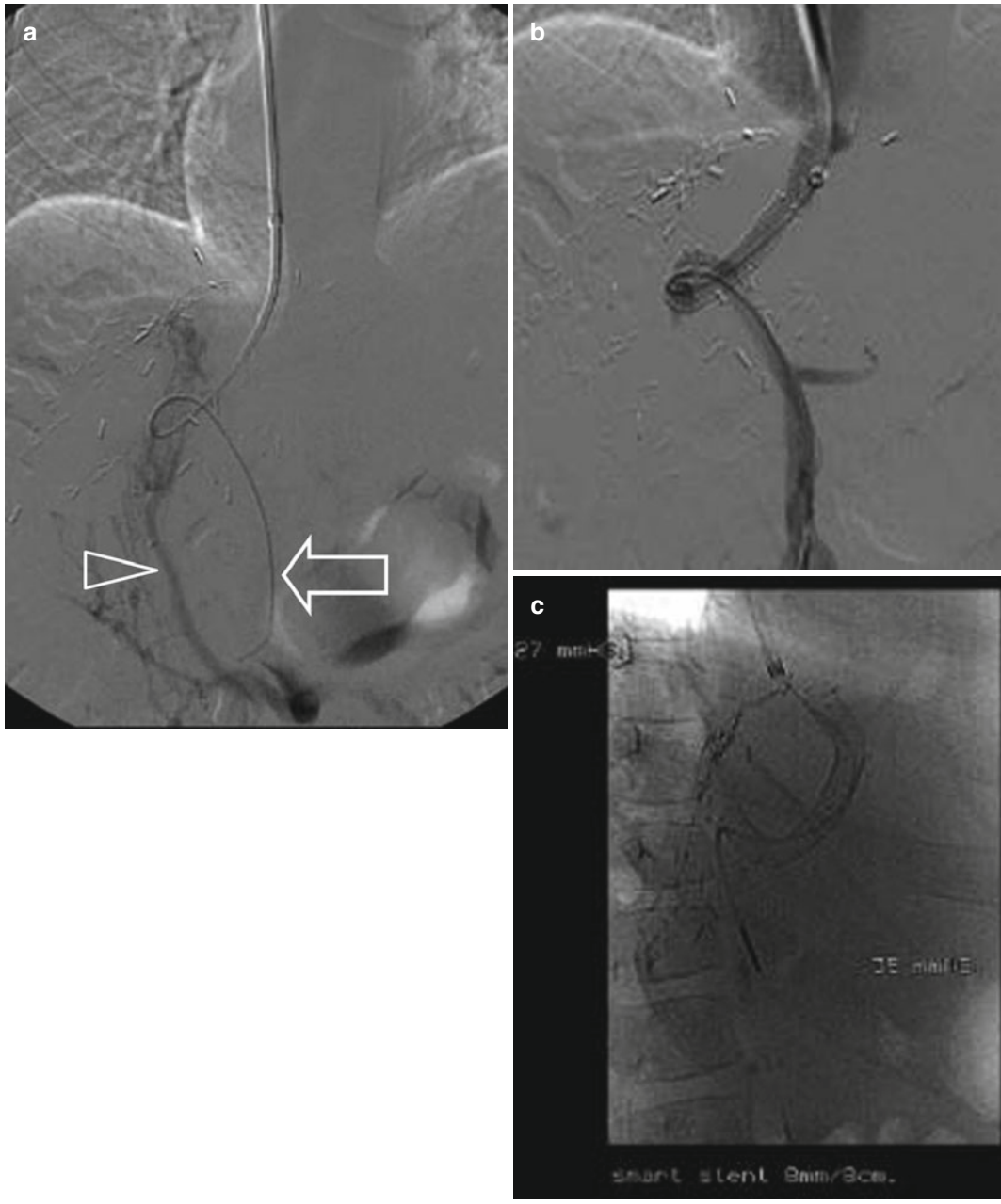


**Fig. 12** (**a**) Case of a 9-year-old boy with a split liver transplant. (segments II and III). The patient was admitted to the paediatric intensive care because of life threatening haematemesis. The fluoroscopy image shows the TIPS catheter (*arrow*) placed within the portal vein. Multiple collateral vessels are shown (*arrowhead*). (**b**) After dilation of the puncture tract, two self-expandable 9 mm diameter stents (Smart, Cordis, Johnson & Johnson Medical N.V., Belgium) were placed. Angiography shows that the collaterals have collapsed and that the primary flow direction is through the TIPS. (**c**) Measurements of intravascular pressures shows the gradient to be 8 mmHg, well below the threshold level of 15 mmHg

loss of shunt function was 17 % at 5 years follow up (ter Borg et al. 2004).

Di Girgio et al. presented their results on 13 TIPS procedures in children (Di Giorgio et al. 2012). With a median follow-up period of 1.2 years (0.2–5.7), seven patients had a patent shunt after a median of 20.4 months (range 7–67 months); 4 patients eventually underwent transplantation after a median of 6 months (1.5–33 months), with a patent shunt at transplant surgery. No patient had technical complications related to the procedure in the long term nor clinical events after TIPS placement.

## 9 Biopsy

The use and effectiveness of image guided percutaneous biopsy, either by fine needle aspiration (FNA) or core needle biopsy (CNB), has been well documented. The obvious advantage of percutaneous over surgical excision biopsies is that it can be done under local anaesthesia and mild sedation, although in some cases deep sedation will still be necessary. Indications for biopsies are e.g. obtaining pathologic information on a mass which can modify patient treatment or confirmation of metastatic disease (Norman 2001; Hoffer 1997).

The advantage of CNB over FNA is the fact that a larger specimen is obtained making it possible to perform histological studies, showing not only the absence or presence of malignant cells but also the architectural composition of the mass (Cheung et al. 2000). Therefore, whenever possible, CNB should be the biopsy method of choice (Fig. 13). The relative drawback of CNB over FNA is that it is somewhat more invasive. An advantage of FNA is that the procedure is relatively easy to perform and that the material can be screened on-site. In our hospital we always have a pathology technician in the room for immediate assessment of the quality of the aspirated material. The choice for FNA depends largely on the availability of an experienced cytologist and the type of lesion to be assessed. Especially deeper located lesions, such as pancreatic lesions, will be more approachable for FNA than CNB, for example using a transgastric or an endoscopic ultrasound-guided approach.

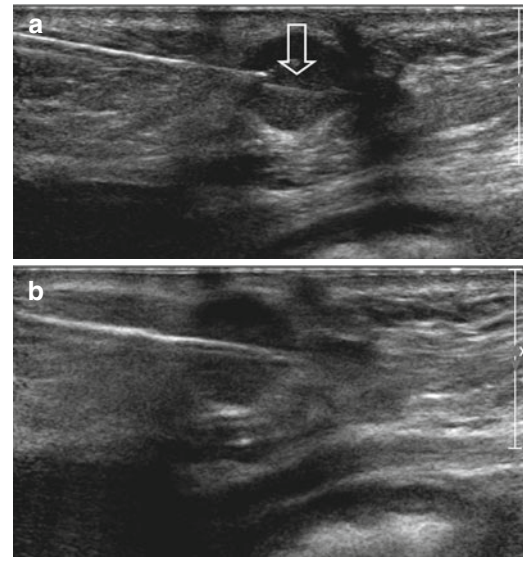


**Fig. 13** (**a**) Case of a 16-year-old boy with an enlarged lymph node seen in the subcutaneous fat in the left chest. The biopsy was performed using freehand technique with a 16G through-cut biopsy needle. The needle is shown here in an open position (*arrow*). (**b**) In this image the needle is shown is a closed position

For CNB one can choose either a cutting-edge or a so called 'tru-cut' needle with or without an automated biopsy device. Numerous variants of both devices are on the market, with personal experience usually guiding the choice for a specific device. The same applies for the use of a biopsy adaptor, which guides the needle, attached to the head of the ultrasound probe or the use of a freehand technique. When the biopsy adaptor is used the needle follows the path that is overlain over the ultrasound image by special biopsy software, thus allowing for a highly accurate biopsy. A much-used technique is using a coaxial approach. Using this technique a needle is advanced into or near to the lesion, the biopsy needle is inserted and biopsies are taken. Using this technique multiple passes are possible with a low risk of spill and avoiding potential complications of the procedure. A second advantage is that due to the coaxial needle configuration haemostatic material can be deposited into the needle tract. This has been reported to be a very effective technique for reducing the risk of CNB-induced haemorrhage, especially in liver lesions (Hoffer 2000; Kaye and Towbin 2002).

Several studies into the effectiveness of FNA and CNB in children have been published (Cheung et al. 2000; Guo et al. 2002; Hoffer 2000; Lieberman et al. 2003; Muraca et al. 2001; Nobili et al. 2003; Saarinen et al. 1991; Scheimann et al. 2000; Sklair-Levy et al. 2001; Yu et al. 2001; Sebire and Roebuck 2006). The diagnostic yield ranged from 83 to 100 %. The rate of complications depends largely on the biopsy site, with the highest number of complications found in hepatic biopsies (up to 14 % post procedural haemorrhage).

Although one would expect a significant difference in complication rates of blind versus image guided biopsies, relatively few studies have been performed to demonstrate this. Nobili et al. reported a retrospective analysis on 140 biopsies (64 blind versus 76 ultrasound guided), in which 95 % of the blind biopsies and 100 % of the ultrasound guided biopsies were of diagnostic quality (Nobili et al. 2003). Moreover, in the blind biopsy population three patients developed significant haemorrhage versus none in the ultrasound guided population.

A special approach to biopsies is that for liver biopsy in children with a coagulopathy or a significant amount of ascites. If in this category of patients, a liver biopsy is needed, a transjugular approach should be used. The right jugular vein is punctured under ultrasound guidance. Using guidewires and catheters the middle or right hepatic vein is catheterised. Subsequently, a stainless steel trocar is placed over the guidewire. Up to this stage the procedure is in effect identical to TIPS. Using a spring-loaded transjugular biopsy needle biopsies of hepatic tissue can be obtained. Drawbacks of the transjugular approach are the use of a more invasive technique, higher costs and smaller (18 gauge) histological samples.

## 10 Abdominal Trauma

Interventional radiology has evolved into a 24-7 service and as such it has acquired a role within the field of emergency medicine. Classically, angiography in the trauma setting was used to identify the site of haemorrhage in order to direct subsequent surgical approach. Nowadays, invasive techniques as angiography for diagnostic purpose, became obsolete due to the role of contrast enhanced CT scans. Although radiation exposure in paediatric patients should be as low as possible, a step-up diagnostic imaging strategy is advised (van Schuppen et al. 2014).

Patients with instable vital signs or with intra-abdominal fluid seen on the Focused Assessment with Sonography for Trauma (FAST) must undergo a CE-CT scan to detect abdominal/pelvic trauma and select patients for angiography and embolization.

Patients with blunt traumatic abdominal trauma can become caught up in the cycle of coagulopathy, acidosis and hypothermia (Kushimoto et al. 2003). The first priority in these patients is to control haemorrhage, for which transcatheter arterial embolization (TAE) has been shown to be rapid and highly effective (Kushimoto et al. 2003; Christensen 2001). In abdominal trauma four sites, the pelvis, liver, spleen, and kidneys, are of main importance in controlling haemorrhage.

On CT-scan and during angiography several signs of vascular injury can be found. Most commonly arterial blushes are seen, progressing in time. Irregular vascular contours, dissections and acute cut-offs should also be treated as they can cause severe haemorrhage in a later phase.

Pelvic injuries accompanied by either arterial, venous or bone haemorrhage are associated with high mortality rates. Unfortunately, surgical exploration is hindered by the often-associated haematoma and the surgical procedure itself can release the tamponade effect of the haematoma leading to a subsequent increase in haemorrhage. TAE results in haemostatic control in 85–94 % of cases of traumatic pelvic haemorrhage (Dondelinger et al. 2002).

Due to the dual blood supply to the liver, patients with blunt hepatic injuries (BHI) are ideal candidates for TAE, with success percentages of TAE reported to be as high as 98 % (Fig. 14a–c). Complication rates of hepatic TAE are low although one must keep in mind that necrosis can occur if portal venous supply is also disrupted due to trauma. In a retrospective study of 21 paediatric trauma patients with BHI, 18 patients could be managed conservatively, two of whom successfully underwent TAE in order to stop haemorrhage (Ohtsuka et al. 2003).

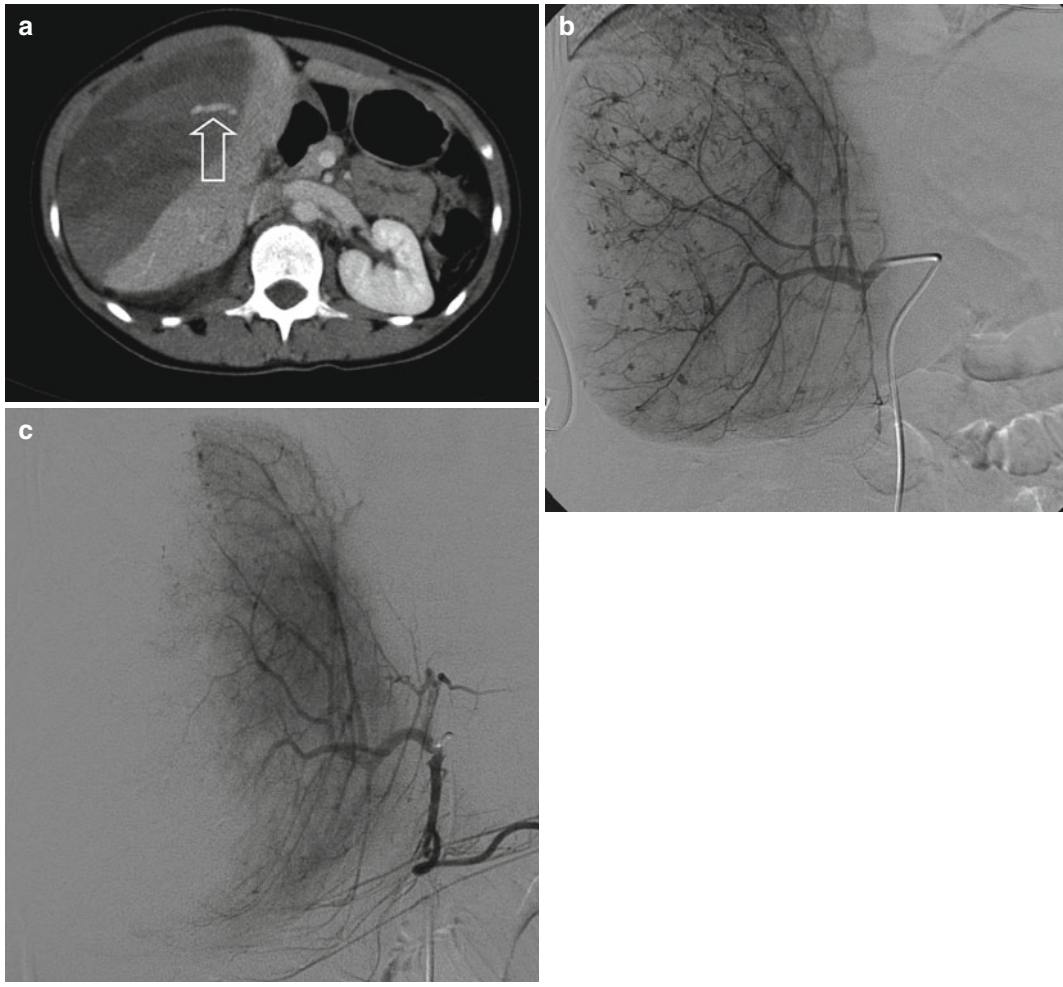


**Fig. 14** (**a**) A 15-year-old girl presented at the ER after a fall from a horse. FAST ultrasound scan was positive for free fluid and consequently a contrast enhanced CT of the abdomen was performed. A large subcapsular hepatic hematoma with active contrast extravasation (*arrow*) was noted. (**b**) Angiography of the hepatic artery shows diffuse contrast extravasation (small blushes) along a large area of the liver capsule. (**c**) Due to the extensive haemorrhage the use of gelfoam was chosen to close the peripheral branches without occluding the hepatic segmental main branches allowing perfusion of the liver. After intervention the patient became haemodynamically stable and no contrast extravasation was visible

In splenic trauma, with a life-long increased risk of sepsis after splenectomy, non operative management (NOM) is the option of choice. Although a contrast blush is often seen on CT-scan in children, invasive treatment is often not necessary (Bansal et al. 2015). In cases of haemodynamic instability TAE is the treatment of choice. In several studies the efficacy of TAE has been shown to be over 90 % (Hagiwara et al. 2005; Lee et al. 2014; Miller et al. 2014; van der Vlies et al. 2012). The preferred method in focal splenic injury is superselective peripheral embolization using a microcatheter. In diffuse splenic injury, central embolization of the splenic artery, distal to the pancreatic artery, has a high success rate in controlling the haemorrhage and can lead to splenic preservation resulting from collaterization by pancreatic and gastric branches.

The majority of renal injuries are a result of blunt abdominal trauma (Fig. 15a–f). In severe blunt renal injury controversy exists on treatment, with some advocating surgical exploration, accompanied with a significant increase in nephrectomy rates, whereas others advocate

conservative treatment. Selective TAE has a high success rate without significant complications; post-procedural hypertension can occur but is generally temporary in nature (Dondelinger et al. 2002).

TAE is achieved by using co-axial microcatheters in order to be able to achieve selective embolization. Most radiologists will use either coils (permanent) or gelfoam (temporary) to embolize vessels. The advantage of coils is their

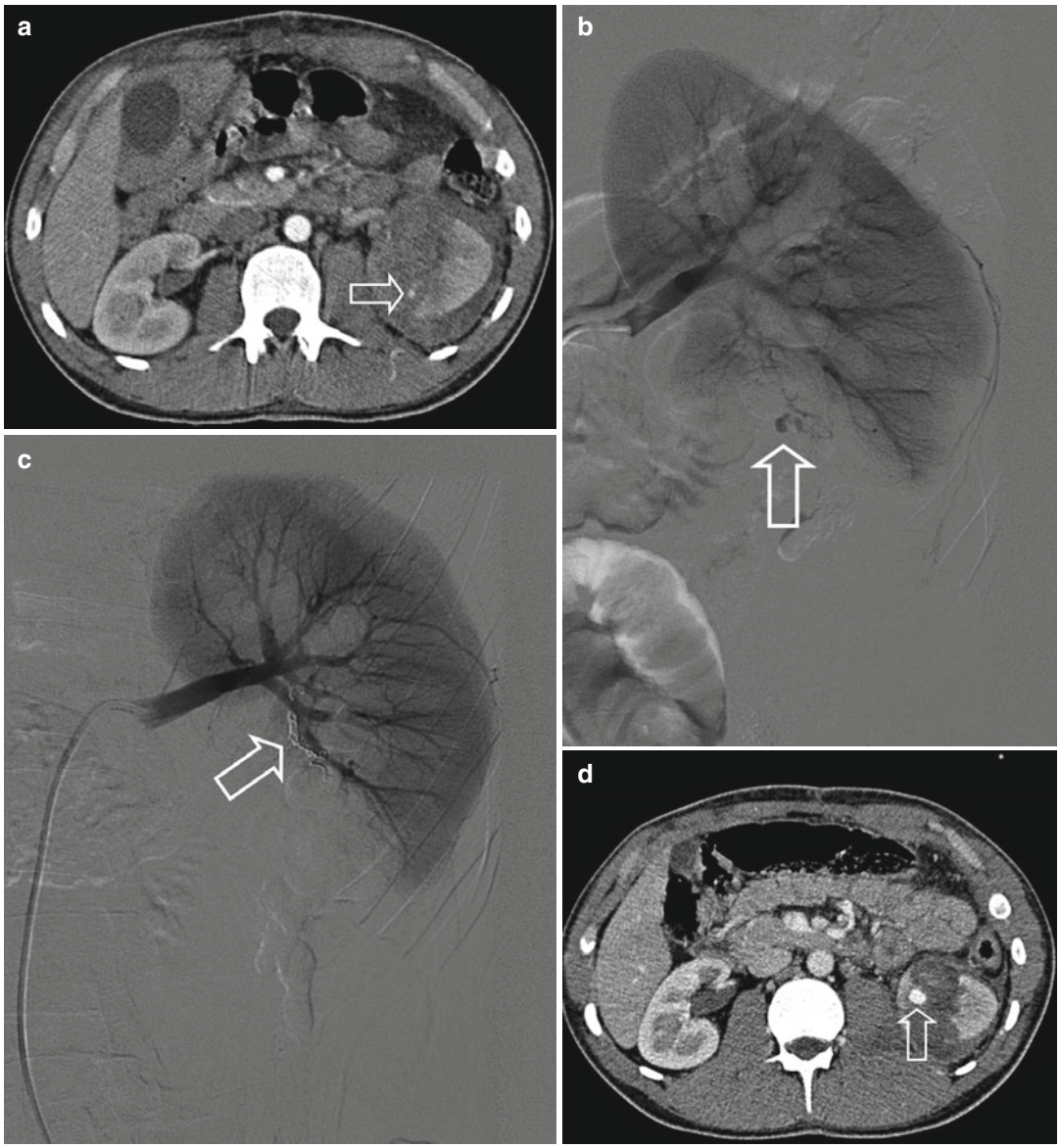


**Fig. 15** (**a**) An 18-year-old male was shot in his left upper abdomen. CT of the abdomen shows a renal laceration with active contrast extravasation (*arrow*). (**b**) Selective angiography of the left renal artery shows contrast extravasation (*arrow*). (**c**) Using multiple selective coils the haemorrhage wass treated and the patient was transferred to the intensive care. (**d**) Twenty days after initial treatment the patient showed a drop in haemoglobin levels and complained of left sided upper abdominal pain. A CT scan shows a renal hematoma with a pseudoaneurysm (*arrow*). (**e**) A second angiography shows the presence of an accessory lower pole renal artery and confirms the presence of a pseudoaneurysm (*arrow*). (**f**) Using 4 mm. coils the pseudoaneurysm was successfully treated

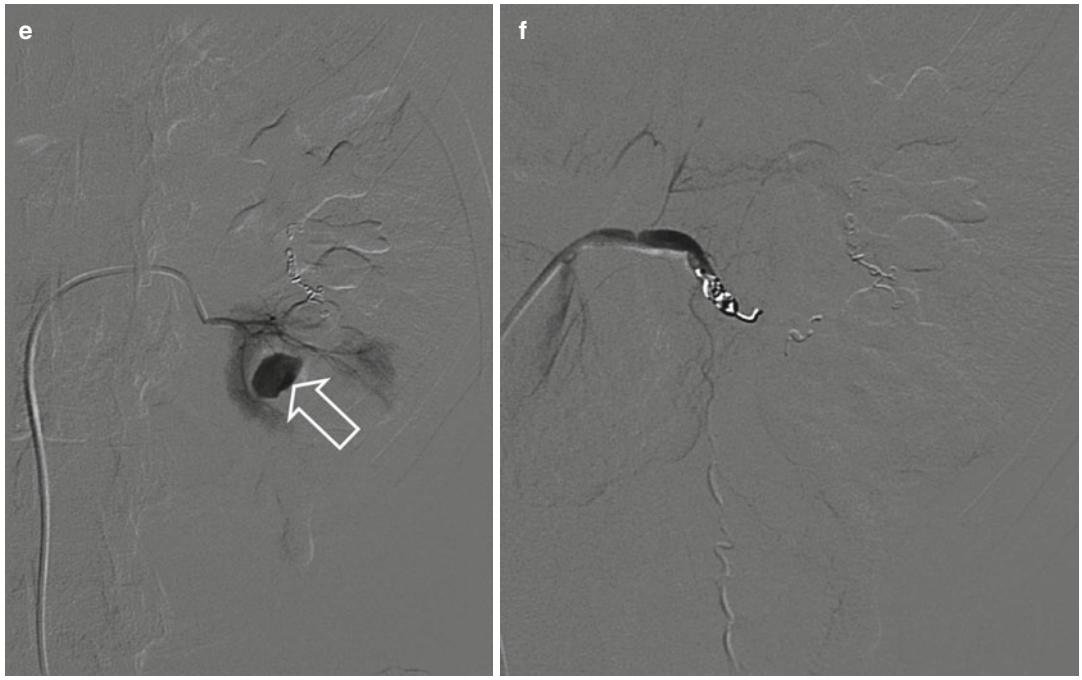


**Fig. 15** (continued)

relative ease of use and the capacity to be placed accurately. Gelfoam has only a temporary effect, lasting up to 3 weeks, and can be used in cases where haemostasis will normalize within this time frame. Other embolization materials, such as poly-vinyl-alcohol particles and bovine collagen are not normally used for this specific indication.

Vo et al. described the role of TAE in paediatric patients after blunt abdominal trauma (Vo et al. 2014). Of 97 paediatric patients who underwent angiography for acute abdominal or pelvic trauma, 54 (56 %) required embolization involving 62 separate sites. Injury severity score greater than 15 was present in 94 % of patients. Targets of embolization included the pelvis ($n=39$), liver ($n=8$), kidney ($n=7$), spleen ($n=6$), and retroperitoneum ($n=2$). Effective haemorrhage control was achieved in 47 patients (87 %). Overall mortality rate was 22 % (12 of 54), with most deaths related to traumatic brain injury. Five complications occurred in four patients (7 %), including three major complications (hepatic abscess, bile leak, and urinary incontinence). Therefore angiography with embolization should be considered in the treatment algorithm for this patient population.

With the increasing use of NOM in trauma patients an increase in late complications can be expected. These late complications in children are reported to be up to 10 %. As treatment of these late complications is outside the scope of this chapter we refer the interested reader to the exquisite review article by Gofette and Laterre (Goffette and Laterre 2002).

## Conclusion

The aim of this chapter is to highlight the importance of image guided interventions in children. The ever increasing capabilities of interventional radiology combined with the increasing awareness amongst paediatricians and paediatric surgeons has led to an increase in the number and level of image guided interventions and will continue to do so in the future. In addition, we strove to convey clearly that only close cooperation between attending paediatrician, paediatric surgeon, paediatric radiologist, interventional radiologist and, whenever necessary, paediatric anaesthesiologist is mandatory for a successful image guided intervention program.

## References


Alderliesten J, Conchillo JM, Leeuwenburgh I, Steyerberg EW, Kuipers EJ (2011) Predictors for outcome of failure of balloon dilatation in patients with achalasia. Gut 60(1):10–16

American Society of Anesthesiologists Task Force on Sedation and Analgesia by Non-Anesthesiologists (2002) Practice guidelines for sedation and analgesia by non-anesthesiologists. Anesthesiology 96(4):1004–1017

Antoniou D, Soutis M, Christopoulos-Geroulanos G (2010) Anastomotic strictures following esophageal atresia repair: a 20-year experience with endoscopic balloon dilatation. J Pediatr Gastroenterol Nutr 51(4):464–467

Bani-Hani AH, Cain MP, Kaefer M, Meldrum KK, King S, Johnson CS, Rink RC (2008) The Malone antegrade continence enema: single institutional review. J Urol 180(3):1106–1110

Bansal S, Karrer FM, Hansen K, Partrick DA (2015) Contrast blush in pediatric blunt splenic trauma does not warrant the routine use of angiography and embolization. Am J Surg. doi:10.1016/j.amjsurg.2014.09.028

Becmeur F, Demarche M, Lacreuse I, Molinaro F, Kauffmann I, Moog R, Donnars F, Rebeuh J (2008) Cecostomy button for antegrade enemas: survey of 29 patients. J Pediatr Surg 43(10):1853–1857

Beebe DS, Tran P, Bragg M, Stillman A, Truwitt C, Belani KG (2000) Trained nurses can provide safe and effective sedation for MRI in pediatric patients. Can J Anaesth 47(3):205–210

Blomberg J, Lagergren P, Martin L, Mattsson F, Lagergren J (2010) Novel approach to antibiotic prophylaxis in percutaneous endoscopic gastrostomy (PEG): randomised controlled trial. BMJ 341:c3115. doi:10.1136/bmj.c3115

Boeckxstaens GE, Annese V, des Varannes SB, Chaussade S, Costantini M, Cuttitta A, Elizalde JI, Fumagalli U, Gaudric M, Rohof WO, Smout AJ, Tack J, Zwinderman AH, Zaninotto G, Busch OR (2011) Pneumatic dilation versus laparoscopic Heller's myotomy for idiopathic achalasia. N Engl J Med 364(19):1807–1816

Cahill AM, Baskin KM, Kaye RD, Fitz CR, Towbin RB (2005) Transgluteal approach for draining pelvic fluid collections in pediatric patients. Radiology 234(3):893–898. doi:10.1148/radiol.2343031804

Cascio S, Flett ME, De la Hunt M, Barrett AM, Jaffray B (2004) MACE or caecostomy button for idiopathic constipation in children: a comparison of complications and outcomes. Pediatr Surg Int 20(7):484–487

Chait PG, Weinberg J, Connolly BL, Pencharz P, Richards H, Clift JE, Savoie S, Harrison D (1996) Retrograde percutaneous gastrostomy and gastrojejunostomy in 505 children: a 4 1/2-year experience. Radiology 201(3):691–695. doi:10.1148/radiology.201.3.8939217

Chait PG, Shandling B, Richards HF (1997a) The cecostomy button. J Pediatr Surg 32(6):849–851

Chait PG, Shandling B, Richards HM, Connolly BL (1997b) Fecal incontinence in children: treatment with percutaneous cecostomy tube placement – a prospective study. Radiology 203(3):621–624

Chait PG, Shlomovitz E, Connolly BL, Temple MJ, Restrepo R, Amaral JG, Muraca S, Richards HF, Ein SH (2003) Percutaneous cecostomy: updates in technique and patient care. Radiology 227(1):246–250

Cheung YC, Wan YL, Lui KW, Lee KF (2000) Sonographically guided core-needle biopsy in the diagnosis of superficial lymphadenopathy. J Clin Ultrasound 28(6):283–289

Chittmittrapap S, Spitz L, Kiely EM, Brereton RJ (1990) Anastomotic stricture following repair of esophageal atresia. J Pediatr Surg 25(5):508–511

Christensen R (2001) Invasive radiology for pediatric trauma. Semin Pediatr Surg 10(1):7–11

Connolly BL, Chait PG, Siva-Nandan R, Duncan D, Peer M (1998) Recognition of intussusception around gastrojejunostomy tubes in children. AJR Am J Roentgenol 170(2):467–470

Cory DA, Fitzgerald JF, Cohen MD (1988) Percutaneous nonendoscopic gastrostomy in children. AJR Am J Roentgenol 151(5):995–997

Cwikiel W (2002) Transjugular intrahepatic portosystemic shunt. Acta Paediatr 91(4):374–375

Cwikiel W, Keussen I, Larsson L, Solvig J, Kullendorff CM (2003) Interventional treatment of children with portal hypertension secondary to portal vein occlusion. Eur J Pediatr Surg 13(5):312–318

Dewald CL, Hiette PO, Sewall LE, Fredenberg PG, Palestrant AM (1999) Percutaneous gastrostomy and gastrojejunostomy with gastropexy: experience in 701 procedures. Radiology 211(3):651–656

Dey R, Ferguson C, Kenny SE, Shankar KR, Coldicutt P, Baillie CT, Lamont GL, Lloyd DA, Losty PD, Turnock RR (2003) After the honeymoon – medium-term outcome of antegrade continence enema procedure. J Pediatr Surg 38(1):65–68

Di Giorgio A, Agazzi R, Alberti D, Colledan M, D'Antiga L (2012) Feasibility and efficacy of transjugular intrahepatic portosystemic shunt (TIPS) in children. J Pediatr Gastroenterol Nutr 54(5):594–600. doi:10.1097/MPG.0b013e3182490c05

Di NG, Rossi P, Oliva S, Aloi M, Cozzi DA, Frediani S, Redler A, Mallardo S, Ferrari F, Cucchiara S (2012) Pneumatic balloon dilation in pediatric achalasia: efficacy and factors predicting outcome at a single tertiary pediatric gastroenterology center. Gastrointest Endosc 76(5):927–932

Diament MJ, Boechat MI, Kangarloo H (1985) Interventional radiology in infants and children: clinical and technical aspects. Radiology 154(2):359–361

Dondelinger RF, Trotteur G, Ghaye B, Szapiro D (2002) Traumatic injuries: radiological hemostatic intervention at admission. Eur Radiol 12(5):979–993. doi:10.1007/s00330-002-1427-x

Doo EY, Shin JH, Kim JH, Song HY (2009) Oesophageal strictures caused by the ingestion of corrosive agents: effectiveness of balloon dilatation in children. Clin Radiol 64(3):265–271

Duszak RL Jr, Levy JM, Akins EW, Bakal CW, Denny DD Jr, Martin LG, Van Moore A Jr, Pentecost MJ, Roberts AC, Vogelzang RL, Kent KC, Perler BA, Resnick MI, Richie J, Priest E 2nd (2000) Percutaneous catheter drainage of infected intra-abdominal fluid collections. American College of Radiology. ACR appropriateness criteria. Radiology 215 Suppl:1067–1075

Ekmark E, Adams RC (2000) The antegrade continence enema (ACE) surgical procedure: patient selection, outcomes, long-term patient management. Eur J Pediatr Surg 10(Suppl 1):49–51

Erdogan E, Eroglu E, Tekant G, Yeker Y, Emir H, Sarimurat N, Yeker D (2003) Management of esophagogastric corrosive injuries in children. Eur J Pediatr Surg 13(5):289–293

Fasulakis S, Andronikou S (2003) Balloon dilatation in children for oesophageal strictures other than those due to primary repair of oesophageal atresia, interposition or restrictive fundoplication. Pediatr Radiol 33(10):682–687

Fortunato JE, Darbari A, Mitchell SE, Thompson RE, Cuffari C (2005) The limitations of gastro-jejunal (G-J) feeding tubes in children: a 9-year pediatric hospital database analysis. Am J Gastroenterol 100(1):186–189. doi:10.1111/j.1572-0241.2005.40893.x

Freedman AM, Sanyal AJ, Tisnado J, Cole PE, Shiffman ML, Luketic VA, Purdum PP, Darcy MD, Posner MP (1993) Complications of transjugular intrahepatic portosystemic shunt: a comprehensive review. Radiographics 13(6):1185–1210

Garcia-Villarreal L, Martinez-Lagares F, Sierra A, Guevara C, Marrero JM, Jimenez E, Monescillo A, Hernandez-Cabrero T, Alonso JM, Fuentes R (1999) Transjugular intrahepatic portosystemic shunt versus endoscopic sclerotherapy for the prevention of variceal rebleeding after recent variceal hemorrhage. Hepatology 29(1):27–32

Gervais DA, Brown SD, Connolly SA, Brec SL, Harisinghani MG, Mueller PR (2004) Percutaneous imaging-guided abdominal and pelvic abscess drainage in children. Radiographics 24(3):737–754. doi:10.1148/rg.243035107

Gideon RM, Castell DO, Yarze J (1999) Prospective randomized comparison of pneumatic dilatation technique in patients with idiopathic achalasia. Dig Dis Sci 44(9):1853–1857

Goffette PP, Laterre PF (2002) Traumatic injuries: imaging and intervention in post-traumatic complications (delayed intervention). Eur Radiol 12(5):994–1021. doi:10.1007/s00330-002-1396-0

Graf JL, Strear C, Bratton B, Housley HT, Jennings RW, Harrison MR, Albanese CT (1998) The antegrade continence enema procedure: a review of the literature. J Pediatr Surg 33(8):1294–1296

Griffiths DM, Malone PS (1995) The Malone antegrade continence enema. J Pediatr Surg 30(1):68–71

Guelrud M, Mendoza S, Jaen D, Plaz J, Machuca J, Torres P (1992) ERCP and endoscopic sphincterotomy in infants and children with jaundice due to common bile duct stones. Gastrointest Endosc 38(4):450–453

Guo Z, Kurtycz DF, Salem R, De Las Casas LE, Caya JG, Hoerl HD (2002) Radiologically guided percutaneous fine-needle aspiration biopsy of the liver: retrospective study of 119 cases evaluating diagnostic effectiveness and clinical complications. Diagn Cytopathol 26(5):283–289

Hagiwara A, Fukushima H, Murata A, Matsuda H, Shimazaki S (2005) Blunt splenic injury: usefulness of transcatheter arterial embolization in patients with a transient response to fluid resuscitation. Radiology 235(1):57–64. doi:10.1148/radiol.2351031132

Hammond PD, Moore DJ, Davidson GP, Davies RP (1997) Tandem balloon dilatation for childhood achalasia. Pediatr Radiol 27(7):609–613

Hamza AF, Abdelhay S, Sherif H, Hasan T, Soliman H, Kabesh A, Bassiouny I, Bahnassy AF (2003) Caustic esophageal strictures in children: 30 years' experience. J Pediatr Surg 38(6):828–833

Heyman MB, LaBerge JM (1999) Role of transjugular intrahepatic portosystemic shunt in the treatment of portal hypertension in pediatric patients. J Pediatr Gastroenterol Nutr 29(3):240–249

Heyman MB, LaBerge JM, Somberg KA, Rosenthal P, Mudge C, Ring EJ, Snyder JD (1997) Transjugular intrahepatic portosystemic shunts (TIPS) in children. J Pediatr 131(6):914–919

Hishiki T, Kouchi K, Saito T, Terui K, Sato Y, Mitsunaga T, Nakata M, Yoshida H (2009) Successful treatment of severe refractory anastomotic stricture in an infant after esophageal atresia repair by endoscopic balloon dilation combined with systemic administration of dexamethasone. Pediatr Surg Int 25(6):531–533

Hoekstra LT, Kuijper CF, Bakx R, Heij HA, Aronson DC, Benninga MA (2011) The Malone antegrade continence enema procedure: the Amsterdam experience. J Pediatr Surg 46(8):1603–1608

Hoffer FA (1997) Interventional radiology in the acute pediatric abdomen. Radiol Clin North Am 35(4):977–987

Hoffer FA (2000) Liver biopsy methods for pediatric oncology patients. Pediatr Radiol 30(7):481–488

Huang YC, Ni YH, Lai HS, Chang MH (2004) Corrosive esophagitis in children. Pediatr Surg Int 20(3):207–210

Hubbard AM, Fellows KE (1993) Pediatric interventional radiology: current practice and innovations. Cardiovasc Intervent Radiol 16(5):267–274

Huppert PE, Astfalk W, Brambs HJ, Schweizer P, Schott U, Pereira P, Duda SH, Dopfer RE, Claussen CD (1998) Transjugular intrahepatic portosystemic shunt in children. Initial clinical experiences and literature review. Rofo 168(6):595–603

Jamieson DH, Chait PG, Filler R (1997) Interventional drainage of appendiceal abscesses in children. AJR Am J Roentgenol 169(6):1619–1622. doi:10.2214/ajr.169.6.9393176

Jayakrishnan VK, Wilkinson AG (2001) Treatment of oesophageal strictures in children: a comparison of fluoroscopically guided balloon dilatation with surgical bouginage. Pediatr Radiol 31(2):98–101

Kaye RD, Towbin RB (2002) Imaging and intervention in the gastrointestinal tract in children. Gastroenterol Clin North Am 31(3):897–923, viii

Kaye RD, Sane SS, Towbin RB (2000) Pediatric intervention: an update – part I. J Vasc Interv Radiol 11(6): 683–697

Khan AA, Shah SW, Alam A, Butt AK, Shafqat F (2002) Efficacy of Rigiflex balloon dilatation in 12 children with achalasia: a 6-month prospective study showing weight gain and symptomatic improvement. Dis Esophagus 15(2):167–170

Kim IO, Yeon KM, Kim WS, Park KW, Kim JH, Han MC (1993) Perforation complicating balloon dilation of esophageal strictures in infants and children. Radiology 189(3):741–744

Kogan A, Katz J, Efrat R, Eidelman LA (2002) Premedication with midazolam in young children: a comparison of four routes of administration. Paediatr Anaesth 12(8):685–689

Krishna RP, Lal R, Sikora SS, Yachha SK, Pal L (2008) Unusual causes of extrahepatic biliary obstruction in children: a case series with review of literature. Pediatr Surg Int 24(2):183–190. doi:10.1007/s00383-007-2087-3

Kushimoto S, Arai M, Aiboshi J, Harada N, Tosaka N, Koido Y, Yoshida R, Yamamoto Y, Kumazaki T (2003) The role of interventional radiology in patients requiring damage control laparotomy. J Trauma 54(1):171–176

Lang EK, Springer RM, Glorioso LW III, Cammarata CA (1986) Abdominal abscess drainage under radiologic guidance: causes of failure. Radiology 159(2):329–336

Lang T, Hummer HP, Behrens R (2001) Balloon dilation is preferable to bougienage in children with esophageal atresia. Endoscopy 33(4):329–335

Lee CW, Kays DW, Chen MK, Islam S (2010) Outcomes of treatment of childhood achalasia. J Pediatr Surg 45(6):1173–1177

Lee AY, Gregorius J, Kerlan RK Jr, Gordon RL, Fidelman N (2012) Percutaneous transhepatic balloon dilation of biliary-enteric anastomotic strictures after surgical repair of iatrogenic bile duct injuries. PLoS One 7(10):e46478. doi:10.1371/journal.pone.0046478

Lee YH, Wu CH, Wang LJ, Wong YC, Chen HW, Wang CJ, Lin BC, Hsu YP (2014) Predictive factors for early failure of transarterial embolization in blunt hepatic injury patients. Clin Radiol 69(12):e505–e511. doi:10.1016/j.crad.2014.08.013

Lendvay TS, Shnorhavorian M, Grady RW (2008) Robotic-assisted laparoscopic mitrofanoff appendicovesicostomy and antegrade continent enema colon tube creation in a pediatric spina bifida patient. J Laparoendosc Adv Surg Tech A 18(2):310–312

Lieberman S, Libson E, Maly B, Lebensart P, Ben-Yehuda D, Bloom AI (2003) Imaging-guided percutaneous splenic biopsy using a 20- or 22-gauge cutting-edge core biopsy needle for the diagnosis of malignant lymphoma. AJR Am J Roentgenol 181(4):1025–1027

Lisy J, Hetkova M, Snajdauf J, Vyhnanek M, Tuma S (1998) Long-term outcomes of balloon dilation of esophageal strictures in children. Acad Radiol 5(12): 832–835

Ljungman G, Kreuger A, Andreasson S, Gordh T, Sorensen S (2000) Midazolam nasal spray reduces procedural anxiety in children. Pediatrics 105(1 Pt 1):73–78

London RL, Trotman BW, DiMarino AJ Jr, Oleaga JA, Freiman DB, Ring EJ, Rosato EF (1981) Dilatation of severe esophageal strictures by an inflatable balloon catheter. Gastroenterology 80(1):173–175

Lorenz JM (2008) Placement of transjugular intrahepatic portosystemic shunts in children. Tech Vasc Interv Radiol 11(4):235–240. doi:10.1053/j.tvir.2009.04.007

Lorenz JM, Leef JA, Chou CH, Funaki B, Straus CM, Rosenblum JD (2001) Sonographic needle guidance in cholangiography in children. J Vasc Interv Radiol 12(3):342–346

Maher MM, Gervais DA, Kalra MK, Lucey B, Sahani DV, Arellano R, Hahn PF, Mueller PR (2004) The inaccessible or undrainable abscess: how to drain it. Radiographics 24(3):717–735

Malone PS, Ransley PG, Kiely EM (1990) Preliminary report: the antegrade continence enema. Lancet 336(8725):1217–1218

McDaniel JD, Warren MT, Pence JC, Ey EH (2015) Ultrasound-guided transrectal drainage of deep pelvic abscesses in children: a modified and simplified technique. Pediatr Radiol 45(3):435–438. doi:10.1007/s00247-014-3154-2

McIlwain M, Primosch R, Bimstein E (2004) Allergic reaction to intranasal midazolam HCl: a case report. Pediatr Dent 26(4):359–361

McLean GK, LeVeen RF (1989) Shear stress in the performance of esophageal dilation: comparison of balloon dilation and bougienage. Radiology 172(3 Pt 2):983–986

McSweeney ME, Kerr J, Jiang H, Lightdale JR (2015) Risk factors for complications in infants and children with percutaneous endoscopic gastrostomy tubes. J Pediatr 166(6):1514–1519. doi:10.1016/j.jpeds.2015.03.009, e1511

Miller PR, Chang MC, Hoth JJ, Mowery NT, Hildreth AN, Martin RS, Holmes JH, Meredith JW, Requarth JA (2014) Prospective trial of angiography and embolization for all grade III to V blunt splenic injuries: nonoperative management success rate is significantly improved. J Am Coll Surg 218(4):644–648. doi:10.1016/j.jamcollsurg.2014.01.040

Morikawa N, Honna T, Kuroda T, Watanabe K, Tanaka H, Takayasu H, Fujino A, Tanemura H, Matsukubo M (2008) High dose intravenous methylprednisolone resolves esophageal stricture resistant to balloon dilatation with intralesional injection of dexamethasone. Pediatr Surg Int 24(10):1161–1164

Muraca S, Chait PG, Connolly BL, Baskin KM, Temple MJ (2001) US-guided core biopsy of the spleen in children. Radiology 218(1):200–206

Naehrlich L, Lang T, Schamberger U, Behrens R (2000) Balloon dilation of an esophageal stenosis in a patient with recessive dystrophic epidermolysis bullosa. Pediatr Dermatol 17(6):477–479

Nobili V, Comparcola D, Sartorelli MR, Natali G, Monti L, Falappa P, Marcellini M (2003) Blind and

ultrasound-guided percutaneous liver biopsy in children. Pediatr Radiol 33(11):772–775
Norman J (2001) Practical pediatric interventional radiology. Curr Probl Diagn Radiol 30(3):61–86
Ohtsuka Y, Iwasaki K, Okazumi S, Yoshida H, Matsunaga T, Kouchi K, Okada T, Ohnuma N (2003) Management of blunt hepatic injury in children: usefulness of emergency transcatheter arterial embolization. Pediatr Surg Int 19(1–2):29–34
Pastor AC, Pastor AC, Mills J, Marcon MA, Himidan S, Kim PC (2009) A single center 26-year experience with treatment of esophageal achalasia: is there an optimal method? J Pediatr Surg 44(7):1349–1354
Pomier-Layrargues G, Villeneuve JP, Deschenes M, Bui B, Perreault P, Fenyves D, Willems B, Marleau D, Bilodeau M, Lafortune M, Dufresne MP (2001) Transjugular intrahepatic portosystemic shunt (TIPS) versus endoscopic variceal ligation in the prevention of variceal rebleeding in patients with cirrhosis: a randomised trial. Gut 48(3):390–396
Rajindrajith S, Devanarayana NM, Benninga MA (2013) Review article: faecal incontinence in children: epidemiology, pathophysiology, clinical evaluation and management. Aliment Pharmacol Ther 37(1):37–48
Reeves ST, Havidich JE, Tobin DP (2004) Conscious sedation of children with propofol is anything but conscious. Pediatrics 114(1):e74–e76
Rivera MT, Kugathasan S, Berger W, Werlin SL (2001) Percutaneous colonoscopic cecostomy for management of chronic constipation in children. Gastrointest Endosc 53(2):225–228
Roebuck DJ, Stanley P (2000) External and internal-external biliary drainage in children with malignant obstructive jaundice. Pediatr Radiol 30(10):659–664
Rosch J, Hanafee WN, Snow H (1969) Transjugular portal venography and radiologic portacaval shunt: an experimental study. Radiology 92(5):1112–1114
Rose SC, Andre MP, Roberts AC, Kinney TB, Valji K, Ronaghi AH, Hassanein TI, Lavine JE, Hart ME, Khanna A (2001) Integral role of interventional radiology in the development of a pediatric liver transplantation program. Pediatr Transplant 5(5): 331–338
Rubin JT, Towbin RB, Bartko M, Baskin KM, Cahill AM, Kaye RD (2004) Oral and intravenous caffeine for treatment of children with post-sedation paradoxical hyperactivity. Pediatr Radiol 34(12):980–984
Saadeddin A, Freshwater DA, Fisher NC, Jones BJ (2005) Antibiotic prophylaxis for percutaneous endoscopic gastrostomy for non-malignant conditions: a double-blind prospective randomized controlled trial. Aliment Pharmacol Ther 22(6):565–570. doi:10.1111/j.1365-2036.2005.02578.x
Saarinen UM, Wikstrom S, Koskimies O, Sariola H (1991) Percutaneous needle biopsy preceding preoperative chemotherapy in the management of massive renal tumors in children. J Clin Oncol 9(3):406–415
Safrit HD, Mauro MA, Jaques PF (1987) Percutaneous abscess drainage in Crohn's disease. AJR Am J Roentgenol 148(5):859–862
Said M, Mekki M, Golli M, Memmi F, Hafsa C, Braham R, Belguith M, Letaief M, Gahbiche M, Nouri A, Ganouni A (2003) Balloon dilatation of anastomotic strictures secondary to surgical repair of oesophageal atresia. Br J Radiol 76(901):26–31
Sandgren K, Malmfors G (1998) Balloon dilatation of oesophageal strictures in children. Eur J Pediatr Surg 8(1):9–11
Sato Y, Frey EE, Smith WL, Pringle KC, Soper RT, Franken EA Jr (1988) Balloon dilatation of esophageal stenosis in children. AJR Am J Roentgenol 150(3):639–642
Scheimann AO, Barrios JM, Al-Tawil YS, Gray KM, Gilger MA (2000) Percutaneous liver biopsy in children: impact of ultrasonography and spring-loaded biopsy needles. J Pediatr Gastroenterol Nutr 31(5):536–539
Searles JM, Roberts JP, MacKinnon AE (2000) The ACE procedure – problems behind the success. Eur J Pediatr Surg 10(Suppl 1):51–52
Sebire NJ, Roebuck DJ (2006) Pathological diagnosis of paediatric tumours from image-guided needle core biopsies: a systematic review. Pediatr Radiol 36(5): 426–431. doi:10.1007/s00247-006-0123-4
Shandling B, Chait PG, Richards HF (1996) Percutaneous cecostomy: a new technique in the management of fecal incontinence. J Pediatr Surg 31(4):534–537
Shiffman ML, Jeffers L, Hoofnagle JH, Tralka TS (1995) The role of transjugular intrahepatic portosystemic shunt for treatment of portal hypertension and its complications: a conference sponsored by the National Digestive Diseases Advisory Board. Hepatology 22(5):1591–1597
Sierre S, Lipsich J, Questa H, Bailez M, Solana J (2007) Percutaneous cecostomy for management of fecal incontinence in pediatric patients. J Vasc Interv Radiol 18(8):982–985
Sklair-Levy M, Lebensart PD, Applbaum YH, Ramu N, Freeman A, Gozal D, Gross E, Sherman Y, Bar-Ziv J, Libson E (2001) Percutaneous image-guided needle biopsy in children – summary of our experience with 57 children. Pediatr Radiol 31(10):732–736
Spechler SJ (2013) Achalasia. Waltham, MA. (Accessed on February 25, 2015.)
Squire R, Kiely EM, Carr B, Ransley PG, Duffy PG (1993) The clinical application of the Malone antegrade colonic enema. J Pediatr Surg 28(8):1012–1015
Stellato TA, Gauderer MW (1987) Percutaneous endoscopic gastrostomy for gastrointestinal decompression. Ann Surg 205(2):119–122
Sury MR, Hatch DJ, Deeley T, Dicks-Mireaux C, Chong WK (1999) Development of a nurse-led sedation service for paediatric magnetic resonance imaging. Lancet 353(9165):1667–1671
Sze DY, Esquivel CO (2002) The role of interventional radiology in a pediatric liver transplant program. Pediatr Transplant 6(1):1–4
Temiz A, Oguzkurt P, Ezer SS, Ince E, Hicsonmez A (2010) Long-term management of corrosive esophageal stricture with balloon dilation in children. Surg Endosc 24(9):2287–2292
ter Borg PC, Hollemans M, Van Buuren HR, Vleggaar FP, Groeneweg M, Hop WC, Lameris JS (2004)

Transjugular intrahepatic portosystemic shunts: long-term patency and clinical results in a patient cohort observed for 3-9 years. Radiology 231(2):537–545

Thyoka M, Timmis A, Mhango T, Roebuck DJ (2013) Balloon dilatation of anastomotic strictures secondary to surgical repair of oesophageal atresia: a systematic review. Pediatr Radiol 43(8):898–901

Tiryaki S, Ergun O, Celik A, Ulman I, Avanoglu A (2010) Success of Malone's antegrade continence enema (MACE) from the patients' perspective. Eur J Pediatr Surg 20(6):405–407

Towbin RB (1991) Pediatric interventional radiology. Curr Opin Radiol 3(6):931–935

Towbin RB, Ball WS Jr (1988) Pediatric interventional radiology. Radiol Clin North Am 26(2):419–440

Upadhyaya M, Fataar S, Sajwany MJ, Upadhyaya M, Fataar S, Sajwany MJ (2002) Achalasia of the cardia: experience with hydrostatic balloon dilatation in children. Pediatr Radiol 32(6):409–412

van der Vlies CH, Hoekstra J, Ponsen KJ, Reekers JA, van Delden OM, Goslings JC (2012) Impact of splenic artery embolization on the success rate of nonoperative management for blunt splenic injury. Cardiovasc Intervent Radiol 35(1):76–81. doi:10.1007/s00270-011-0132-z

van Schuppen J, Olthof DC, Wilde JC, Beenen LF, van Rijn RR, Goslings JC (2014) Diagnostic accuracy of a step-up imaging strategy in pediatric patients with blunt abdominal trauma. Eur J Radiol 83(1): 206–211

Vo NJ, Althoen M, Hippe DS, Prabhu SJ, Valji K, Padia SA (2014) Pediatric abdominal and pelvic trauma: safety and efficacy of arterial embolization. J Vasc Interv Radiol 25(2):215–220. doi:10.1016/j.jvir.2013.09.014

Weber F, Wulf H, el Saeidi G (2003) Premedication with nasal s-ketamine and midazolam provides good conditions for induction of anesthesia in preschool children. Can J Anaesth 50(5):470–475

Weintraub JL, Eubig J (2006) Balloon catheter dilatation of benign esophageal strictures in children. J Vasc Interv Radiol 17(5):831–835

Wiebe S, Cohen J, Connolly B, Chait P (2005) Percutaneous decompression of the bowel with a small-caliber needle: a method to facilitate percutaneous abdominal access. AJR Am J Roentgenol 184(1): 227–229

Woodthorpe C, Trigg A, Alison G, Sury M (2007) Nurse led sedation for paediatric MRI: progress and issues. Paediatr Nurs 19(2):14–18

Yagmurlu A, Harmon CM, Georgeson KE (2006) Laparoscopic cecostomy button placement for the management of fecal incontinence in children with Hirschsprung's disease and anorectal anomalies. Surg Endosc 20(4):624–627

Yeming W, Somme S, Chenren S, Huiming J, Ming Z, Liu DC (2002) Balloon catheter dilatation in children with congenital and acquired esophageal anomalies. J Pediatr Surg 37(3):398–402

Youn BJ, Kim WS, Cheon JE, Kim WY, Shin SM, Kim IO, Yeon KM (2010) Balloon dilatation for corrosive esophageal strictures in children: radiologic and clinical outcomes. Korean J Radiol 11(2):203–210

Yu SC, Liew CT, Lau WY, Leung TW, Metreweli C (2001) US-guided percutaneous biopsy of small (< or = 1-cm) hepatic lesions. Radiology 218(1):195–199

# Index





S. Stafrace, J.G. (Hans) Blickman (eds.), *Radiological Imaging of the Digestive Tract in Infants and Children*, Medical Radiology, DOI 10.1007/978-3-319-18434-0